The establishment of an infectivity assay for human parvovirus B19 to investigate the efficacy of protocols for the inactiviation of pathogens from plasma products

Thesis

UNRESTRICTED

The establishment of an infectivity assay for human parvovirus B19 to investigate the efficacy of protocols for the inactivation of pathogens from plasma products

Cécile Claire Chaput

The Open University

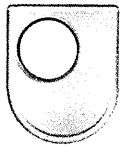

Sponsored by

NIBSC | National Institute for Biological Standards and Control

A thesis submitted for the degree of Doctor of Philosophy in the year 2006

DATE of SUBMISSION: 1 JULY 2005
DATE of AWARD: 25 OCTOBER 2006

ProQuest LLC.
789 East Eisenhower Parkway
P.O. Box 1346
Ann Arbor, MI 48106 – 1346

بسم الله الرحمن الرحيم

Preface

My research work was supervised by Dr J. Saldanha and Dr B. Cohen.

This thesis is the result of my own work except where explicitly stated in the text. The contents have not been previously submitted for any degree, diploma or any qualification at the Open University or any other university.

Acknowledgements

I am very grateful to my sponsoring establishment, the National Institute for Biological Standards and Controls, for allowing me to work in such an inspiring place, surrounded by talented scientists.

Thank you to Dr J. Blümel (Paul Erhlich Institut, Germany) for welcoming me into his laboratory, for his advice on immunofluorescence and for providing some virus stock (JB isolate) and some anti-B19 antibodies. I am also grateful to Mrs P. Pipkin (NIBSC) for her useful recommendations for the immunofluorescence technique. Thank you to Dr. S. Doyle (National University of Ireland, Republic of Ireland) for his kind donation of rabbit polyclonal antibody against NS1 protein. Many thanks to Dr L. Peddada (University of California, USA) for her kind gift of some virus stock (isolate LP) and to both Dr J. Clewley and Dr B. Cohen for providing some baculovirus expressing parvovirus VP1 and VP2 proteins.

I would like to thank Dr M. Watts (UCH, UK) for giving a regular supply of mobilized peripheral blood and apheresis cells. For supplying the KU812 cell line, I would like to thank Dr Nakazawa (Niigata University, Japan). For providing the KU812Ep6 cell line and the mouse monoclonal antibody against VP1 and VP2 proteins, many thanks to Dr Miyagawa (Fujirebo, Japan). Thank you to Dr Komatsu (Jichi Medical School, Japan) for proving some UT-7/EPO cells and to Dr Morita (Tohoku University, Japan) for supplying the UT-7/EPO-S1 cell line.

I am grateful to Ms H. Appleton and Mr B. Megson (HPA, UK), for performing electron microscopy on parvovirus B19 stock and taking photographs, as well as to Dr R. Fleck (Department of Cell Biology and Imaging, NIBSC) for the photographs of the

UT-7/EPO-S1 cells. Thank you to Dr R. Stebbings (Department of Immunobiology, NIBSC) for performing the FACS.

Many thanks to Mr A. Heath (Department of Informatics, NIBSC) for kindly doing all the statistical analyses of my results, and always with a smile.

I would like to thank Dr S. Satoh (Asahi Kasei Pharma Coropration, Japan) and Mr T. Sato (Asahi Kasei Deutchland, Germany) for coming to NIBSC and performing the nanofiltration experiments for removal of parvovirus B19. I am very grateful to Dr P. Roberts (BPL, UK) for his collaboration and for performing the dry heat inactivation studies. A big thank you to Dr T. Castor for inviting me to present my infectivity assay results at Aphios Inc. (USA) and to all his colleagues for performing the virus inactivation studies using SuperFluids™. Thank you to Dr. J. Chapman and his team (Vitex, USA) for carrying out the INACTINE™ treatment on human parvovirus B19 for inactivation studies. Many thanks to Dr K. Dupuis and Dr L. Sawyer (Cerus Corporation, USA) for performing the inactivation experiments using the Helinx® technology and for long and helpful conversation via the e-mail.

A big thank you to all my colleagues at NIBSC, too many to name, for their kindness and for sharing their scientific knowledge, with special thanks to Mr D. Padley, Mrs N. Shah and Dr. S. Baylis for their patience and help. Thanks to Dr P. Minor (Department of Virology, NIBSC) for his support and to Dr A. Bristow for his great help regarding administrative matters.

I am so grateful to Dr Bernard Cohen, my external supervisor, for whom I have great respect. Thank you for your kindness, invaluable advice and support! Thank you also for training me in your lab and for kindly providing some B19-antibody negative serum.

Dr John Saldanha, my director of studies... you have been my mentor and always will be! You are truly a brilliant scientist and I have learnt so much from you. I do apologise

for not always doing what you asked me to and would like to thank you for your patience and constant help! Thanks for always believing in me and pushing me! Thank you John!

Papa et Maman, je ne sais pas comment vous remercier! Non seulement pour votre soutien financier constant, mais aussi et surtout pour vos encouragements, vos paroles tendres, votre présence si proche malgré les kilomètres qui nous séparent... MILLE FOIS MERCI!!! Je vous aime... Merci aussi à mes amies et ma famille, surtout à Agnès, ma grande soeur que j'aime tendrement. "Shukran bzaaf" à ma belle-famille!

To my husband Hani, I would like to address a special thank you for making me realise what's really important in life and for his patience and love. I will be there for you every step of the way for your PhD and for life, God willing.

À Marie-Madeleine Richard et à son arrière-petite-fille Houssna

Abstract

Erythrovirus B19 is the only parvovirus known to cause disease in humans and represents a concern in transfusion medicine since several blood products were shown to contain B19 despite various inactivation steps and some products have even transmitted viral infection. The aim of the study was to establish a reliable and reproducible infectivity assay that could be used to evaluate the efficiency of viral removal/inactivation methods. This assay was based on the detection of B19-specific mRNA transcripts from susceptible cells inoculated with virus: the human leukaemic cell line UT-7/EPO-S1. B19 DNA concentrations were also determined using an optimised quantitative real-time PCR assay. Both assays were used to assess the efficacy of one virus removal method, nanofiltration, and four virus inactivation techniques, dry heating treatment, supercritical fluids, INACTINE™ system and Helinx® technology. Nanofiltration of a spiked solution of 0.5% albumin with 15N and 20N filters resulted in the removal of more than $\log_{10}$ 5 and $\log_{10}$ 6 of infectious B19, respectively. Dry heat treatment of factor VIII showed a reduction of infectivity greater than $\log_{10}$ 2 after 24 hours and below the limit of detection of the assay after 72 hours. The treatment of plasma with the *SuperFluids*™ system removed more than $\log_{10}$ 5 infectious viruses. Two chemicals methods used novel small molecules which target and crosslink nucleic acids: PEN 110 (INACTINE™ system) and Psoralen S-59 (Helinx® technology). Treatment of red cells with PEN 110 showed a reduction of infectivity below the detection limit while platelet concentrates treated with S-59 resulted in a reduction greater than $\log_{10}$ 5. Although chemical methods can be used on cells which do not have a nucleus (red cells and platelets), they also introduce potential toxicity. In contrast, physical methods of removal and inactivation are less toxic but would damage

red cells and platelets. Overall, this research work allowed the establishment of a reproducible infectivity assay that was successfully used to perform preliminary studies on the efficacy of various viral removal/inactivation methods.

Contents

Index of figures

Chapter I: General introduction

Chapter II: Materials and methods

Chapter III: Results

Appendix 3:

Index of tables

Chapter I: General introduction

Chapter II: Materials and methods

Chapter III: Results

Chapter IV: General discussion

Appendix 1: BFU-E reduction assay results

Appendix 2: Cell counts for continuous cell lines growth curves

Abbreviations

Å	Angstrom
AABB	American Association of Blood Banks
AAV	Adeno-Associated Virus
ACS	Acute Chest Syndrome
ADV	Aleutan mink Disease Virus
AFLF	Acute Fulminant Liver Failure
AIDS	Acquired Immuno Deficiency Syndrome
ALF	Acute Liver Failure
ANA	Anti Nuclear Antibodies
aPL	Anti-phospholipid
apoA-I	Human Apolipoprotein A-I
ATP	Adenosine Trisphosphate
B19	Human parvovirus B19
BFU-E	Burst-Forming Unit-Erythroid
β-ME	β-mercaptoethanol
BMT	Bone Marrow Transplant
BPL	Bioproducts Laboratory
BPV	Bovine Parvovirus
CAT	Chloramphenicol acetyltransferase
CD	Cluster of Differentiation
CE	European Community
CFU-E	Colony-forming unit-Erythroid
CHD	Congenital Heat Disease
CIE	Counte-immunoelectrophoresis
CMV	Cytomegalovirus
CNS	Central Nervous System
CPV	Canine Parvovirus
CSF	Cerebrospinal fluid
C_T	Crossing point
CXCR4	Human CXC chemokine receptor 4
DID	Double Immunodiffusion
DNA	Deoxyribonucleic Acid
ds	double-stranded
EBV	Epstein Barr virus
EDTA	Ethylenediamine tetraacetic acid
EI	Erythema Infectiosum
EIA	Enzyme Immunoassay
ELISA	Enzyme Linked Immunosorbent Assay
ELISpot	Enzyme Linked Immunosorbent spot Assay
EM	Electron Microscopy
EPO	Erythropoietin
EtBr	Ethidium bromide

EtOH	Ethanol
FACS	Fluorescence Activated Cell Sorter
FCH	Fibrosing Cholestatic Hepatitis
FCS	Fetal calf serum
FDA	Food and Drug Administration
FITC	Fluorescein Isothiocyanate
FPV	Feline Parvovirus
FSGS	Focal and Segmental Glomerulosclerosis
G-CSF	Granulocyte-Colony Stimulating Factor
GM-CSF	Granulocyte Macrophage-Colony Stimulating Factor
Grb2	Growth factor receptor-binding protein 2
H BsAg	Hepatitis B surface Antigen
HAART	Highly Active Antiretroviral Therapy
HAV	Hepatitis A Virus
HBV	Hepatitis B Virus
HCV	Hepatitis C Virus
HGV	Hepatitis G Virus
HIV	Human Immunodeficiency Virus
HLA	Human Leukocyte Antigen
HPA	Health Protection Agency
HPV	Human papilloma virus
HSV	Herpes Symplex Virus
IA-PCR	Immune Adherence PCR
ICTV	International Committee on Taxonomy of Viruses
ID	Immunodiffusion
IEM	Immune Electron Microscopy
IFA	Immunofluorescence assay
IFN-γ	Interferon gamma
Ig	Immunoglobulin
IL	Interleukin
ILD	Interstitial Lung Disease
IS	International Standard
ISH	*In Situ* Hybridisation assay
ITP	Idiopathic Thrombocytopenic Purpura
IU	International Units
IUFD	Intrauterine Fetal Death
IVIG	Intravenous Immunoglobulin
JCA	Juvenile Chronic Arthritis
JRA	Juvenile Rheumatoid Arthritis
LPV	Lapine Parvovirus
m.u	Map unit
MACRIA	IgM Antibody Capture Radioimmunuassay
MACS	Magnetic cell sorting
MB	Methylene Blue

M-CSF	Macrophage-Colony Stimulating Factor
MDS	Myelodysplastic syndrome
mRNA	Messenger ribonucleic acid
MsAFP	Maternal Serum Alpha-fetoprotein
MVM	Minute Virus of Mice
N	Nanometre
NAT	Nucleic acid amplification testing
NHS	National Health Service
NIRCA™	Non-Isotopic RNase Cleavage Assay™
NK	Natural Killer
NLS	Nuclear Localisation Signal
NS	Non Structural
nt	Nucleotide
NTP	Nucleotide Trisphosphate
OA	Osteoarthritis
OCD	Dilution buffer for mRNA extraction (Appendix 1)
OCL	Lysis buffer for mRNA extraction (Appendix 1)
ODB	Dilution buffer of the Oligotex direct mRNA kit (Qiagen)
OEB	Elution buffer of the Oligotex direct mRNA kit (Qiagen)
OL1	Lysis buffer of the Oligotex direct mRNA kit (Qiagen)
ORF	Open Reading Frame
OW1	Wash buffer 1 of the Oligotex direct mRNA kit (Qiagen)
OW2	Wash buffer 2 of the Oligotex direct mRNA kit (Qiagen)
PBMC	Peripheral Blood Mononuclear cells
PBS	Phosphate buffered saline
PCR	Polymerase Chain Reaction
PCT	Photochemical treatment
PHLS	Public Health Laboratory Services
PPGSS	Papular purpuric "gloves-and-socks" syndrome
PPV	Porcine Parvovirus
PRCA	Pure Red blood Cell Aplasia
PRP	Platelet-rich plasma
RA	Rheumatoid Arthiritis
RBC	Red Blood Cell
RBCC	Red Blood Cell Concentrates
RE	Restriction Enzyme
RF	Replicative Form
RHA	Receptor-mediated haemagglutination assay
RIA	Radioimmuno-assay
RNA	Ribonucleic Acid
RPE	R. Phycoerythrin
rRNA	Ribosomal ribonucleic acid
RSP	Restriction Site Polymorphism
RSV	Respiratory Syncytial Virus

RT-PCR	Reverse Transcriptase PCR
RV	Rat Virus
S/D	Solvent Detergent
SARS	Severe Acute Respiratory Syndrome
SDS	Sodium dodecyl sulfate
SH3	Src Homology 3
SIV	Simian Immunodeficiency Virus
SLE	Systemic Lupus Erythematosus
Spl	Promoter-specific transcription factor
SPLV	Serum parvovirus-like virus
SPV	Simian Parvovirus
ss	Single-stranded
SSCP	Single-Stranded Conformational Polymorphism
TAC	Transient Aplastic Crisis
TAE	Tris-HCl, glacial acetic acid, EDTA
TE	Tris-HCl, EDTA
TEC	Transient Erythroblastopenia of Childhood
T_H	T helper cell
T_H 1	T helper cell type 1
T_H 2	T helper cell type 2
TNBP	Tri(n-butyl) phosphate
TNF-α	Tumour Necrosis Factor alpha
TSA	Tyramide signal amplification
UCH	University College Hospital
UTR	Untranslated region
UV	Ultraviolet
VAHS	Virus-Associated Hemophagocytic Syndrome
VLP	Virus-like particles
VP	Viral Protein
VZV	Varicella Zoster Virus
WHO	World Health Organisation
WNV	West Nile Virus

Chapter I: Introduction

I.1. Human parvovirus B19

I.1.1. Discovery, classification and structure of human parvovirus B19

I.1.1.1. Discovery

In 1975, during routine screening for hepatitis B surface antigen (HBsAg) of sera from healthy blood donors, Dr Y. Cossart and coworkers noticed abnormal results in the counterimmunoelectrophoresis (CIE) assay of several samples that tested negative for hepatitis B by confirmatory methods (radioimmunoassay and haemagglutination) (Cossart *et al.*, 1975). The precipitin line from the CIE was cut out and electron microscopy showed the presence of spherical particles, with a diameter varying from 20.5nm to 25nm (mean 23nm). Their characteristic features included disrupted fragments and empty shells. Cossart *et al.* observed a resemblance with animal parvoviruses on account of the similar size and morphology of the particles, and because the antigen bands in cæsium chloride were at a density within the parvovirus range (1.36 to 1.40) (Cossart *et al.*, 1975; Siegl *et al.*, 1985). Similar observations were later made in France in 1982, where the "Aurillac" virus (named after the town in which it originated) was described (Courcoucé *et al.*, 1984a; Courcoucé *et al.*, 1984b). Subsequently, both "Aurillac" and "Nakatani" (from Japan) viruses were shown to be identical to the "serum parvovirus-like virus" (SPLV) discovered by Cossart and colleagues (Cossart *et al.*, 1975; Courcoucé *et al.*, 1984a; Courcoucé *et al.*, 1984b; Okochi *et al.*, 1984).

For some time, the isolates could not be related to naturally occurring diseases (Harley and Rotbart, 1990). However, in 1980, a brief publication reported the detection by electron microscopy (EM) of human parvovirus in the sera of two soldiers from the same unit, who presented with an uneventful and self-limited febrile episode (Shneerson *et al.*, 1980). In 1981, B19 was also detected in two children with sickle cell anemia

hospitalised for aplastic crisis (Pattison *et al.*, 1981). A few years later, B19 was reported in association with an outbreak of erythema infectiosum (EI) in a London school, UK (Anderson *et al.*, 1983). Moreover, the fetal damage in animals known to result from in utero infection with parvoviruses encouraged research, which led to the first report of B19 as a cause of human hydrops fetalis (Brown *et al*, 1984). Additionally, investigations on the link between B19 and arthritis started in 1985 (White *et al.*, 1985; Reid *et al.*, 1985; Lefrère *et al.*, 1985a). In the last twenty years, human parvovirus has been associated with a wide range of clinical diseases, from EI to hydrops fetalis and new links between this infectious agent and various conditions are still being found.

I.1.1.2. Taxonomy

Since parvoviruses are among the smallest DNA-containing viruses (18-26nm) able to infect mammalian cells, the Latin word for small, "parvum", was used to designate this group of linear, single-stranded DNA viruses related by their morphology and functional characteristics (Berns, 1996). The International Committee on Taxonomy of Viruses (ICTV) has divided the family *Parvoviridae* into two sub-families, the *Parvovirinae* and *Densovirinae*, according to their ability to infect vertebrate or invertebrate cells, respectively (ICTV, 2005). *Parvovirinae* is further divided into five genera, including *Parvovirus*, *Dependovirus*, *Erythrovirus*, *Amdovirus* and *Bocavirus*. The genus *Parvovirus* comprises all animal parvoviruses able to replicate autonomously in susceptible cells. These viruses do not require the presence of a helper virus (adenovirus, herpesvirus or even vaccinia virus) to undergo a complete cycle of replication. Most vertebrate disease-causing parvoviruses belong to the *Parvovirus* genus, including rat virus (RV): H-1 virus, minute virus of mice (MVM), porcine

(PPV), feline (FPV) and lapine (LPV) paroviruses (Siegl *et al.*, 1985). The second genus, *Dependovirus,* consists of parvoviruses that cannot replicate efficiently under standard *in vitro* culture conditions whereas they can multiply successfully when target cells are co-infected by either adenovirus or herpesvirus. Viruses in this genus have never been shown to cause disease, either in their natural host or under experimental conditions. The only member of the *Amdovirus* genus is Aleutian mink disease virus (ADV), which has been detected in most mustelids, skunks and racoons (ICTV, 2005). The *Bocavirus* genus includes bovine parvovirus (BPV) and canine minute virus species. Finally, several members of the *Densovirinae*, the so-called densonucleosis viruses, have been isolated from a variety of insect host species and are autonomously replicating pathogenic parvoviruses of insects. The organisation of the *parvoviridae* family is shown on figure 1.1.

Figure 1.1: Organisation chart of the *Parvoviridae* family (constructed using data from the ICTV 8th report of virus taxonomy, 2005)

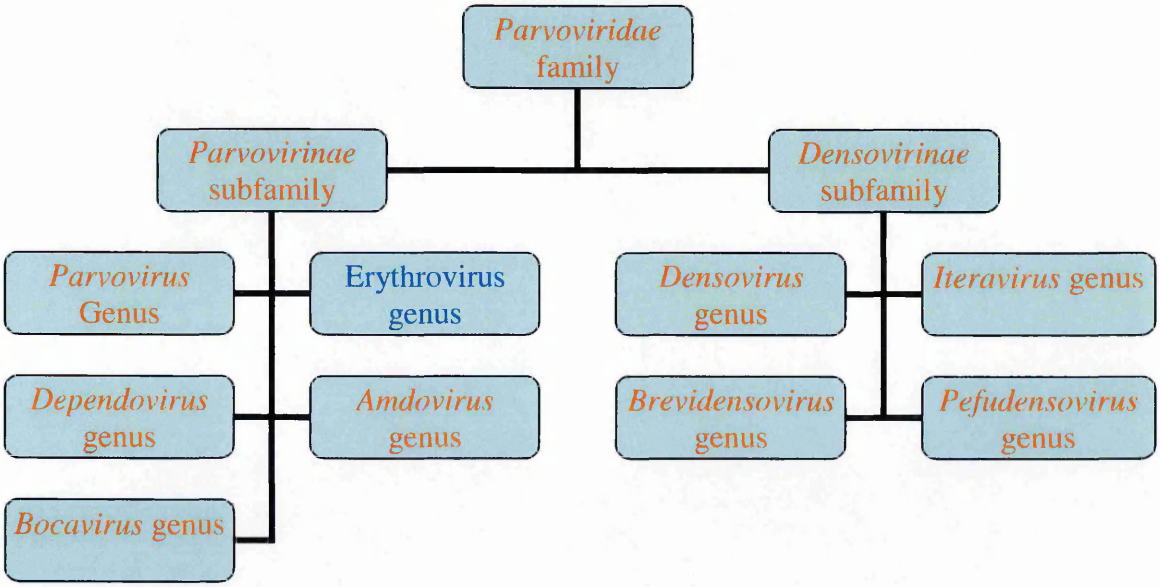

In 1985, when human parvovirus B19 was officially recognised as a member of the *Parvoviridae* family, it was classified in the *Parvovirus* genus (Siegl *et al.*, 1985). Although the acronym "HPV" for human parvovirus would have been in accordance with long-standing practice of the naming of autonomous parvoviruses, the acronym was already in use for human papillomavirus. Therefore, in order to avoid confusion, the ICTV recommended the use of the name "B19", which refers to the coding of this first isolate, number 19 in panel B (Cossart *et al.*, 1975; Siegl *et al.*, 1985). Since parvovirus B19 has a high erythroid tropism, it was reclassified in the genus *Erythrovirus* (ICTV, 2000). The other species recently classified in this genus are pig-tailed macaque parvovirus, rhesus macaque parvovirus and simian parvovirus (SPV) (ICTV, 2005) due to their predilection for host bone marrow *in vitro* and capacity to cause serious anaemia in infected animals, namely pig-tailed and rhesus macaques (Green *et al.*, 2000) and cynomolgus monkeys (O'Sullivan *et al.*, 1994; O'Sullivan *et al.*, 1997), respectively. Moreover, a Korean group identified a parvovirus in Manchurian chipmunks highly similar to B19 and SPV on the molecular level (Yoo *et al.*, 1999). This virus has thus been proposed as an additional member of the *Erythrovirus* genus.

I.1.1.3. Morphology

Parvovirus B19 has a simple structure made of only two capsid proteins, VP1 (~5%) and VP2 (~95%), and a linear, 5.5 kb single-stranded DNA molecule. Equal numbers of complementary DNA strands (positive and negative sense DNA) are packaged into separate virions (Summers *et al.*, 1983). In contrast, most other autonomous parvoviruses, such as LuIII (Muller and Siegl, 1983), and members of the Dependovirus genus (Berns and Adler, 1972), package only one type of complementary single-

stranded DNA, preferentially of negative polarity, in different types of particles. The B19 virus particles are non-enveloped and measure between 22 and 24 nm in diameter (Cossart *et al.*, 1975). Negative staining and EM revealed that often both empty and full capsids are present in the host's serum. The molecular weights of the mature virion and of empty particles are 5.5-6.2x10^6 and 4.2x10^6 Da, respectively (Agbandje *et al.*, 1994). Moreover, the buoyant density of a full particle in a cæsium chloride gradient is 1.43 g/mL (Clewley, 1984). Empty B19 capsids have been expressed from genetically engineered Chinese hamster ovary cell line (Kajigaya *et al.*, 1989), as well as in baculovirus expression systems (Kajigaya *et al.*, 1991; Brown CS *et al.*, 1991; Kaufmann *et al.*, 2004), and have been used as antigens for diagnosis assays, to develop a vaccine and for use in X-ray crystallographic analyses. A few years after successfully crystallising B19 empty capsids in a baculovirus expression system, Agbandje and coworkers established the structure of parvovirus B19 at 8Å resolution (Agbandje *et al.*, 1991; Agbandje *et al.*, 1994). More recently, the structure of B19-like particles was determined to about 3.5Å resolution (Kaufmann *et al.*, 2004).

The three-dimensional X-ray crystal structures of canine parvovirus (CPV) and FPV had already been determined to the atomic resolution (Tsao *et al.*, 1991; Agbandje *et al.*, 1993). Although CPV and FPV have similar antigenic properties, there is no cross-reactivity of antibodies to CPV or FPV with B19, indicating different surface structures (Agbandje *et al.*, 1994). However, sequence alignments suggest a distant, yet common origin of CPV, FPV and B19 (Chapman and Rossmann, 1993). Electron density maps of these viruses were therefore compared, keeping in mind that the resolution of the B19 map was lower than that of CPV and FPV (Agbandje *et al.*, 1994). All three viruses consist of 60 copies of the capsid protein arranged in icosahedral symmetry. Although the polypeptide folds of CPV and FPV contain 8 anti-parallel β-barrel structural motifs

("jelly roll"), most of their structure is made of insertions between the strands of the β-barrel. These insertions form elaborate loops on the viral surface that are important as antigen recognition sites. The most prominent of these insertions forms a spike on the icosahedral threefold axes. A 15Å canyon-like depression circulates around the fivefold axis.

As far as parvovirus B19 is concerned, the central β-barrel structural motif is easily recognisable in the same region as that of FPV (Agbandje *et al.*, 1994). However, the surface of B19 seems significantly different from the other parvoviruses since the prominent spikes on the icosahedral threefold axes are lacking. These two findings were in agreement with the amino acid sequence analyses by Chapman and Rossmann, showing a greater conservation in the central β-barrel structure of parvoviruses than in the surface insertions (Chapman and Rossmann, 1993). Another region of density in B19 that was very similar to that of FPV and Adeno-Associated Virus (AAV) (Xie *et al.*, 2002) was a hollow cylindrical structure about the fivefold icosahedral axis, which appears to penetrate inside the virion (Agbandje *et al.*, 1994). It is formed by the DE loop (amino acids 129-148) shown on figure 1.2, but in B19, the tip of the loop is bent towards the central axis of the channel (Kaufmann *et al.*, 2004). It was suggested that the unique region of the larger protein VP1 might extend through this cylinder to outside the virion. This hypothesis might be plausible since Bansal *et al.* had already suggested that at least part of the unique region of VP1 is exposed at the surface of the virion (Bansal *et al.*, 1993). This proposition originated from an experiment performed using altered concentrations of VP1 and VP2 proteins in baculovirus-produced empty capsids. The authors showed that antisera specific for the unique region of VP1 was able to precipitate both plasma-derived virions and these recombinant empty capsids. It is also important to note that VP1 alone cannot form empty capsids whereas severely

shortened VP1 did not seem to alter the capsid formation (Wong *et al.*, 1994). Although longer versions of VP1 also formed capsids, they did so less efficiently and the capsids were less ordered in appearance than the native empty capsids, recombinant empty capsids, VP2 only capsids and capsids formed by the truncated versions of VP1.

When the structure of recombinant B19 particles was investigated at 3.5Å resolution, it was found to be most similar to that of AAV-2 (Kaufmann *et al.*, 2004; Xie *et al.*, 2002). Moreover, both viruses require an integrin as a coreceptor: αVβ1 integrin for AAV-2 (Summerford *et al.*, 1999) and α5β1 for B19 (Weigel-Kelley *et al.*, 2003). However, the degree of similarity between these two viruses (26% identity between major structural proteins) is much less than between B19 and other human parvoviruses, such as LaLi (97%) and V9 (98%) -which will be detailed in section I.1.6-, and SPV (67%) (Servant *et al.*, 2002). Although AAV-2 and B19 share a common host (vertebrates), this low sequence similarity suggests a host-independent evolution (Kaufmann *et al.*, 2004).

Figure 1.2 shows the ribbon diagram of VP2 (a) and the surface topography of parvovirus B19 (Kaufmann *et al.*, 2004).

Figure 1.2: Secondary structure of parvovirus B19 (from Kaufmann *et al.*, 2004)

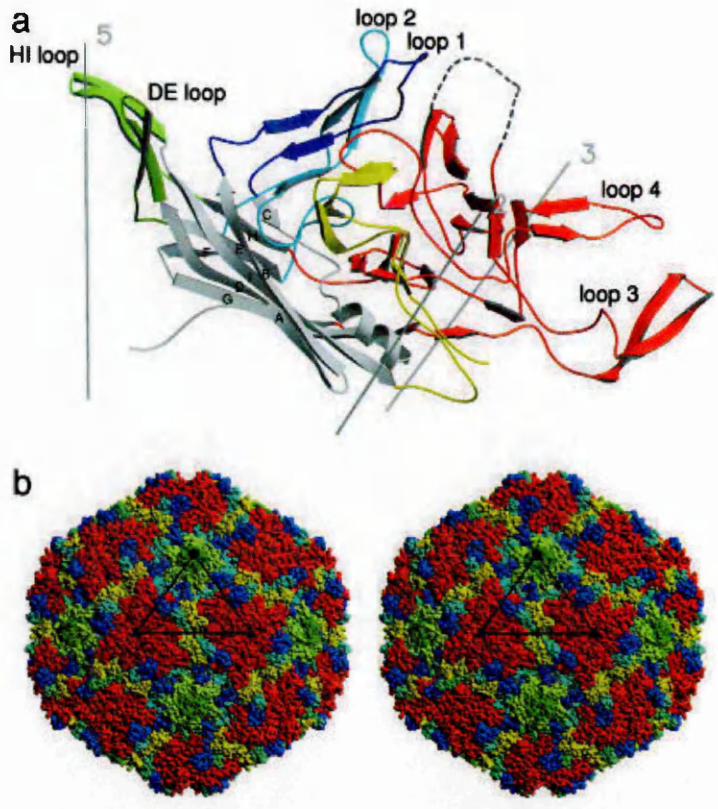

(*a*) **Ribbon diagram of VP2**. The strands of the β-barrel (grey) are labelled sequentially A through I. The surface loops connecting the strands of the β-barrel are labelled by colour: dark blue, BC loop; dark green, DE loop; light blue, EF loop; red, GH loop; light green, HI loop; yellow, C-terminal amino acids. The position of the disordered loop (amino acids 301–313) (dashed line) was modelled based on the corresponding AAV-2 loop.
(*b*) **Surface topography of B19.** The surface loops are colour-coded according to the ribbon diagram. The disordered loop has been omitted.

I.1.1.4. Genomic organisation

Particles found in viremic plasma contain single-stranded DNA, either positive or negative sense, each of which being fully capable of infection and replication (Summers *et al.*, 1983, Cotmore and Tattersall, 1984). MVM DNA is known for its terminal palindromic sequences, which allows the formation of hairpin structures at both ends of single-stranded DNA (Bourguignon *et al.,* 1976). The hairpin situated at the 3' end of each DNA molecule could serve as a primer for various prokaryotic and eukaryotic

DNA polymerases, resulting in the synthesis of the complementary strand *in vitro*. Similar 3' terminal hairpin structures have been demonstrated in parvovirus B19, making cloning of the complete genome into plasmid vectors difficult (Cotmore and Tattersall, 1984). An incomplete clone was obtained from the serum of a child with homozygous sickle cell disease who was in the early phase of reticulocytopenic aplastic crisis (isolate Au) (Shade *et al.*, 1986).

The clone, named pYT103, was lacking the extreme left and right ends known as terminal hairpin structures. The nucleotide sequence of pYT103 suggested that the organisation of the B19 transcription units is similar, although not identical, to that of other parvoviruses. The Au isolate was also cloned using two expression constructs containing B19 sequences from different halves of the viral genome (Cotmore *et al.*, 1986). These clones allowed the identification of the two major capsid proteins, VP1 and VP2, with apparent molecular weights of 83 kDa and 58kDa, respectively. These capsid sequences were located in a major stretch of open reading frame on the right-hand half of the viral genome. The next step in discovering the genomic structure of B19 was made by Mori and colleagues, who examined the virus by electron microscopy and observed double-stranded molecules with characteristic "fold-back" or forked ends, as shown in figure 1.3 (Mori *et al.*, 1987; Anderson and Young, 1997). The latter were assumed to be due to the terminal hairpin structures which had previously been predicted to be substantially longer than those of AAV (125 nucleotides) (Shade *et al.*, 1986; Lusby *et al.*, 1980). This large size was therefore thought to account for the ability to visualise the "fold-back" termini by EM whereas this phenomenon cannot be observed with other parvoviruses.

The exact measurement and the structural analysis of the palindromic termini were only possible in 1990, when the instability of these termini in bacterial cells was overcome

and the entire B19 genome cloned in plasmids (Deiss *et al.*, 1990). The 383 terminal nucleotides at each end of the genome were found to be identical inverted repeats, the distal 365 nucleotides being an almost perfect palindrome that can fold over to give a hairpin structure. Due to some mismatching between nucleotides 147 and 217, it is typical for terminal hairpins to occur in two distinct sequence configurations, which have been referred to as "flip" and "flop". These configurations, which are related since one is the inverted complement of the other, have been described in all parvoviruses analysed to date and are essential for viral replication. Thus the B19 genome consists of a linear, 5,596 nucleotides long, single-stranded DNA molecule that includes an internal coding sequence of 4830 nucleotides and flanked, on either ends, by inverted repeats of 383 nucleotides each (Deiss *et al.*, 1990).

Figure 1.3: B19 viral DNA showing terminal hairpin structures (published by Anderson and Young, 1997)

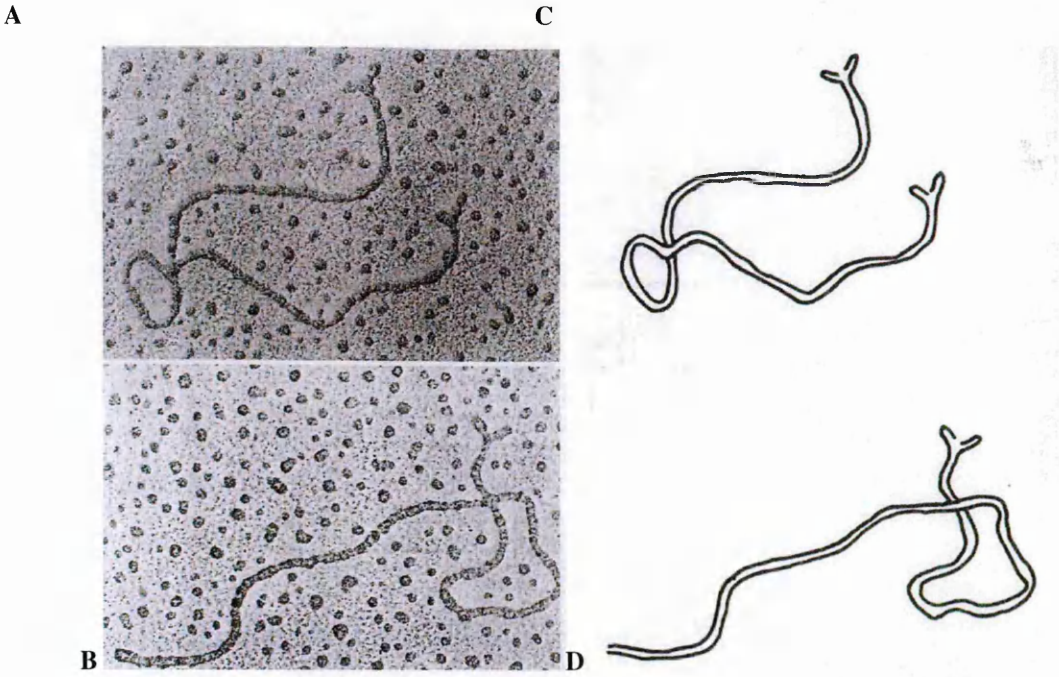

A and B are electron microscopic views. A Both ends of the molecule are folded back to form hairpins (x57,000). B One end of the molecule is folded back and the other end is annealed in an extended form (x68,000). C and D are drawings of the plus and minus strands with terminal hairpin structures.

I.1.1.5. Proteins

I.1.1.5.1. Protein synthesis

The genome of human parvovirus B19 encodes only three proteins of known function, namely the capsid proteins VP1 (83 kDa) and VP2 (58 kDa) and the nonstructural protein NS1 (77 kDa). The VP1 and VP2 open reading frames (ORFs) overlap completely, with approximately 990 extra nucleotides included in the VP1 ORF.

The sizes of these proteins, which were identified in various cell expression systems, are summarised in table 1.1 (Astell *et al.*, 1997), while figure 1.4 shows the transcription map described by Ozawa and colleagues (Ozawa *et al.*, 1987a).

Table 1.1: Summary of B19 NS1 and VP1, VP2 proteins identified in different expression systems (Astell *et al.*, 1997)

NS1 (kDa)	VP1 (minor) and VP2 (major) (kDa)	Cell system	Authors, year
71, 63, 52	83 (minor), 58 (major)	Clinical isolate	Cotmore *et al.*, 1986
77, 52, 34	84 (minor), 58 (major)	B19-infected human erythroid bone marrow	Ozawa and Young, 1987
77, 68	N/A	HeLa cells transfected with B19 expression plasmid	Ozawa *et al.*, 1988a
71, 63	83 (minor), 58 (major)	COS cells transfected with B19 expression plasmid	Beard *et al.*, 1989
71, 55, 34	84 (minor), 58 (major)	COS cells transfected with B19 expresssion plasmid	Astell *et al.*, 1997

Although the sizes for the VP1 and VP2 proteins were reasonably consistent (83 kDa and 58 kDa respectively), those of the NS1 protein were considerably different, ranging

in size from 77 kDa to 71 kDa. It is probable that these are the same protein and the difference in molecular weight is due to the use of different protein markers and/or gel composition. In addition, several smaller proteins were detected (ranging in size from 34 kDa to 68 kDa). These smaller NS proteins might arise due to post-translational cleavage or, less likely, internal initiation. It is also possible that they are degradation products of NS1. However, in other parvoviruses (MVM and AAV), alternate splicing generates mRNAs, which encode smaller NS or Rep proteins (Berns, 1990). Nevertheless, the transcription map suggests that these splicing sites do not exist in B19.

Figure 1.4: Human parvovirus B19 transcription map showing open reading frames and viral proteins (proposed by Ozawa *et al.*, 1987a)

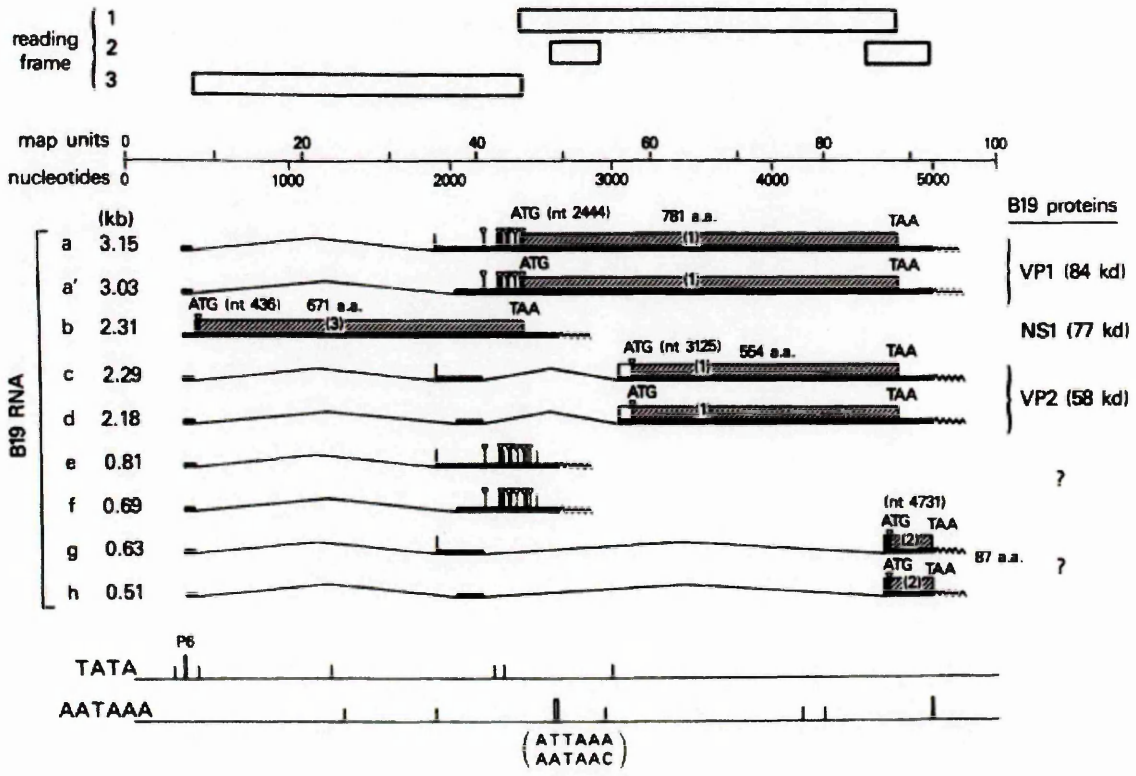

Shown is the location of the P6 promoter, functional polyadenylation signals, splice donor and acceptor sites, ORF (boxes), ATG sequences (vertical lines).

In addition to structural and nonstructural proteins, some smaller proteins (11- and 7.5kDa) are translated from the small abundant mRNAs, which are unique among parvoviruses (Astell *et al.,* 1995). Both size classes are polyadenylated RNAs with a small ORF (St Amand *et al.*, 1991). The 700- to 800-nt class includes an 807- and 687-nt RNA while the 500- to 600-nt class includes the 638- and 518-nt RNAs. These last two RNAs express a family of three 11-kDa proteins (St Amand *et al.*, 1991; St Amand and Astell, 1993) while the 807-nt RNAs express a 7.5kDa protein (Luo and Astell, 1993). Although the latter is within the NS coding region of the genome, it is in a different ORF to that of the NS protein. When transfected COS cells and infected human leukemic or peripheral blood mononuclear cells were investigated, the 11kDa proteins were found mainly in the nucleus, but also associated to a reticular network of the cytoplasm of COS cells (Luo and Astell, 1993). The 7.5kDa protein was both nuclear and cytoplasmic in COS cells whereas it was predominantly cytoplasmic in infected human peripheral blood mononuclear cells.

I.1.1.5.2. Role of structural proteins

Structural proteins have three important functions: to interact with the cellular receptor, to translocate the genetic material to appropriate sites of transcription and replication and to permit the assembly of infectious particles. The full B19 capsid is icosahedral and composed of 60 copies of the capsid proteins, 96% of which being VP2 and the remainder VP1 (Cotmore *et al.*, 1986; Ozawa and Young, 1987). This difference in the relative percentages of VP1 and VP2 is thought to be due to a translational regulation of capsid protein production (Ozawa *et al.,* 1988b). After translation of its mRNA in the cytoplasm, VP2 has to reach the nucleus where new B19 capsids are assembled (Pillet

et al., 2003). Due to its molecular weight (58kDa), VP2 is unlikely to diffuse passively into the nucleus and is thus probably transported by specific cellular transporters called karyopherins. This kind of transport was described previously for many cellular and viral proteins (Macara, 2001). The karyopherins recognise the proteins to be transported through specific peptides present on the proteins surface called nuclear localisation signals (NLS) (Pillet *et al.*, 2003). The latter have been found in the capsid proteins of several parvoviruses: within the N-terminal of the VP1 capsid protein of CPV (Vihinen-Ranta *et al.*, 1997), in VP2 of AAV-2 (Hoque *et al.*, 1999) and in both VP1 and VP2 of MVM, which are involved in cooperative cytoplasmic interactions for nuclear cotransport (Lombardo *et al.*, 2000; Lombardo *et al.*, 2002). The VP1 NLS was therefore shown to play a role in transport into the nucleus. However, no data has been reported to date regarding NLS in B19 VP1. A nonconsensus basic motif, KLGPRKATGRW, located in the C-terminal region of VP2, has been proposed as the main NLS of B19 VP2 capsid protein (Pillet *et al.*, 2003). This conserved sequence was shown to be necessary for the nuclear localisation of VP2 and is exposed on the surface of an isolated VP2 subunit where it can be recognised by the cellular import (Kaufmann *et al.*, 2004). Once in the nucleus, VP2 proteins are able to self-assemble alone or with VP1, whereas VP1 alone cannot self-assemble (Kajigaya *et al.*, 1991). After assembly, the NLS is hidden because it is on the inner capsid surface (Kaufmann *et al.*, 2004). In addition, the 226-amino acid unique terminal region of VP1 interferes progressively with particle assembly when more than 70 amino acids of that region are present (Wong *et al.*, 1994). As far as the small 11-kDa proteins are concerned, they were shown not to affect the self-assembly of the viral particles (Cohen CS *et al.*, 1991).

Although predictions concerning the surface structure of B19 could be made from the resolution at the atomic level of canine parvovirus capsid, B19 VP proteins expressed in

insect cells using recombinant baculovirus expression vectors were crystallised and the three-dimensional structure was elucidated (Agbandje *et al.*, 1991; Agbandje *et al.*, 1994; Chapman and Rossmann, 1993).

Several studies have been carried out to identify neutralising epitopes on the virus capsid. Heamagglutination was inhibited by means of a monoclonal antibody directed against amino acids 57-77 of the VP2 protein. This epitope was found to contribute to the spike on the three-fold axes of the capsid (Brown *et al.*, 1992). It is still not clear whether these regions represent viral attachment sites or whether deep canyons around the five-fold axes are the best candidates for interaction with the P receptor (Agbandje *et al.*, 1994). The 226-amino acid unique amino-terminal region of VP1 is known to be on the surface of the virus particles (Rosenfeld *et al.*, 1992) and antibodies to the capsid are directed predominantly against this region (Kurtzman *et al.*, 1989a; Schwarz *et al.*, 1988). Although neutralisation epitopes were also mapped to regions within VP2 protein, the latter is less immunodominant than VP1 (Sato *et al.*, 1991a; Sato *et al.*, 1991b; Yoshimoto *et al.*, 1991). The influence of B19 virus structure on antibody responses is not well defined. A strongly cross-linking antigen can activate B cells in the absence of T-cell help, whereas poorly cross-linking antigens need T-cell help for B-cell activation. A CD4+ T-cell response was found to be directed against B19 capsid proteins (Von Poblotzki *et al.*, 1996). This cellular immune response was restricted by HLA II molecules and might support specific B-cells in producing antibodies.

I.1.1.5.3. Role of non-structural proteins

Few functions for B19 NS1 have been directly demonstrated and a number of reports have suggested the important role of NS1 in the replication of viral DNA, as well as in the transactivation of promoter P6 and in cytotoxicity.

I.1.1.5.3.1. Role in DNA replication

Viral DNA replication is initiated from short double-stranded regions provided by self-annealed, terminal hairpin structures. DNA synthesis then proceeds from these palindromes to produce high molecular weight intermediates through a rolling hairpin model (Berns, 1990). By analogy with the major NS1 protein of MVM (Wilson *et al.*, 1991; Jindal *et al.*, 1994) and the nonstructural proteins Rep of AAV-2 (Im and Muzyczka, 1990; Synder *et al.*, 1990), it is likely that the nucleotide binding fold domain is involved in ATP hydrolysis. The energy derived from it might be used to drive an intrinsic helicase activity. In addition, resolution of terminal (and internal dimer bridge) hairpin structures during MVM (Cotmore *et al.*, 1992; Cotmore *et al.*, 1993; Liu *et al.*, 1994) and AAV (Snyder *et al.*, 1990) replication was found to be dependent on the NS1 and Rep68 and 78 proteins. This resolution has been predicted to reside in a protein motif found in enzymes functional in rolling circle replication (Ilyina and Koonin, 1992). This motif is located within the first third of the NS proteins.

Overall, it seems that parvovirus NS1 has a direct role in viral replication by providing the activities required for the resolution of covalently joined B19 termini, namely endonuclease and helicase activities. In the work of Jindal *et al.*, some of the mutants tested appeared to retain ATP-binding and ATPase activities but not helicase activities and some mutations in the NTP-binding site decreased viral replication but did not affect trans-activating activity (Jindal *et al.*, 1994).

I.1.1.5.3.2. Transactivation of the P6 promoter

When the B19 P6 promoter was used to drive expression of a reporter CAT gene in transfected Hela cells, promoter activity was upregulated by the B19 NS1 protein (Doerig *et al.*, 1990). In addition, *in vitro* translated B19 NS1 was shown to stimulate

transcription from the same promoter. Although studies to map the transactivational domain of the B19 NS protein have not been reported, the same activity in MVM NS1 protein was found in the C-terminal region (Legendre and Rommelaere, 1994). More recent studies showed that transcriptional regulation by the NS1 protein was likely to involve both the interaction with Sp1/Sp3 that can bind to the promoter region and direct binding of NS1 to the promoter DNA (Raab *et al.*, 2002).

The roles of NS1 in replication and transcription seem to be consistent with the nuclear localisation of this protein in infected cells. In addition, a nuclear localisation signal (NLS) (i.e. KKPR) was described at amino acid positions 177-180 (Cotmore *et al.*, 1986). However, the localisation of NS1 during the cell cycle may also be cytoplasmic, suggesting that it may be a shuttle protein (Morinet *et al.*, 2000).

I.1.1.5.3.3. Cytotoxicity

Between 1988 and 1998, several papers were published regarding NS1 cytotoxicity. During an attempt to obtain stable transfected HeLa cell lines containing the B19 genome, transformation occurred only when NS1 protein expression was blocked by mutation (Ozawa *et al.*, 1988a). Other studies using recombinant AAV-B19 particles showed that growth of megakaryocytic cells and erythroid progenitors was inhibited by NS1 (Srivastava *et al.*, 1990). Thus, NS-1 cytotoxicity was suggested in both erythroid and non-erythroid cells. Additionally, viral replication did not seem necessary since no DNA replicative forms were detected in megakaryocytic cells. The link between cytotoxicity and apoptosis was suggested in erythroid lineage cells transfected with the NS1 gene (Moffatt *et al.*, 1998). Caspase 3 participates in this process. In addition, the induction of erythroid cells apoptosis by human parvovirus B19 may involve the tumour necrosis factor alpha (TNF-α) receptor signalling pathway (Sol *et al.*, 1999). Moreover,

infected cells showed ultrastructural features typical of apoptosis (Morey *et al.,* 1993). Computer analysis allowed the identification of a NTP-binding motif in the middle of the B19 parvovirus nonstructural protein (Gorbalenya and Koonin, 1989). Studies have shown that mutations within this motif seem to moderate the cytotoxicity of NS1 (Momoeda *et al.*, 1994a). Lysine 334 in this domain was shown particularly critical for cell killing. Similar results had already been observed for homologous NS1 protein of parvovirus H-1, also responsible for cytotoxicity of rat host cells (Li and Rhode, 1990) and in the MVM NS1 protein (Legendre and Rommelaere, 1992). However, the effects of the latter on cellular transformation, as an indirect measure of cytotoxicity, were found not only on the nucleotide binding fold motif but also localised within the amino- and carboxyl-terminal domains.

Some authors suggested that the functions of transactivation of the P6 promoter and cytotoxicity are not localised in the same protein domain (Moffatt *et al.*, 1996; Moffatt *et al.*, 1998). These results concern B19-infected and NS1-transfected erythoid cells. Until now, B19-induced apoptosis in HeLa cells and megakaryocytic progenitors, where cytotoxicity was also observed (Srivastava *et al.*, 1990; Ozawa *et al.,* 1988a; Leruez-Vill *et al.*, 1997), has not been documented. NS1 mutants with a disruption of the NTP-binding domain have a dramatically suppressed cytotoxic activity, although complete abrogation of cell death was not observed (Moffat *et al.*, 1998).

I.1.1.5.4. Role of small 11-kDa proteins

The function of both the 11- and 7.5-kDa proteins still remains to be determined. However, a recent study showed that the amino acid sequence of the 11-kDa proteins present an unusually high proportion (15%) of proline residues (Fan *et al.,* 2001). Some of these residues can be grouped into three regions that share similarity with sequences

known to bind to Src homology 3 (SH3) domains in a variety of signal-transducing molecules. In addition, the B19 11-kDa proteins were shown to interact *in vitro* with the growth factor receptor-binding protein 2 (Grb2), an adaptor protein implicated in receptor tyrosine kinase-mediated signalling of mitogenic and stress stimuli. Consequently, it was suggested that the 11-kDa proteins could be involved in viral pathogenesis through perturbation of normal cellular signalling pathways by binding Grb2 or another as yet unidentified SH3 domain-containing protein.

I.1.1.6. Sequence variability

Unlike other parvoviruses such as ADV, human parvovirus B19 was first thought to have a highly conserved genome (Gottschalck *et al.*, 1991). One of the first attempts to explore the genetic variability of B19 virus was made in 1986 using restriction enzyme (RE) analysis to compare 17 isolates collected over a 12 year-period in France and Great Britain (Morinet *et al.*, 1986). Variant patterns characterised by altered sites for at least one RE, were observed in only 5 of the 17 isolates. However, the remaining 12 isolates had the same map, suggesting a high genetic stability of the parvovirus B19 genome. Shortly after these findings, the DNAs of over 40 isolates were mapped with 13 REs and a classification into several genome types was proposed (Mori *et al.*, 1987). Group I comprised blood donations collected between 1973 in Great Britain and 1979 in France and included the first published isolate (Cossart *et al.*, 1975), as well as the Wi isolate (Cotmore and Tattersall, 1984). Some isolates in circulation from 1978 in France to 1986 in the UK were classified in group II genome type (Mori *et al.*, 1987). A third restriction pattern was present in the UK from 1979 to 1986, namely group IIIa, while group IIIb genome type was first observed in a French blood donor in 1978 and from a case of aplastic crisis in Scotland in 1986. Only strains from Japan were included in group IV genome type while many strains remained unassigned. This classification of

genotypes suggested a possible epidemiological relationship among strains, which was investigated further with the study of 12 strains of parvovirus B19 isolated in Japan at two different time periods: 1981 and between 1981 and 1986 (Umene and Nunoue, 1990). The former were similar to that of the group IV genome type whereas the latter were related to that of group II, indicating a correlation between the genome type and the time of isolation, or prevalence.

A later publication reported a single-stranded conformational polymorphism (SSCP) assay, which was able to detect a mutated nucleotide sequence as a change of mobility in polyacrylamide gel electrophoresis caused by an altered folded structure (Kerr *et al.*, 1995a). These findings were consistent with those of Umene and Nunoue, since there was a correlation between the SSCP type and the country of origin, as well as time of isolation (Kerr *et al.*, 1995a; Umene and Nunoue, 1990). Within the Japanese group, strains isolated from 1981 to 1987 consisted of SSCP types 1 (~13%), 2 (~7%), 3 (~53%) and 4 (~27%), whereas strains isolated from 1990 to 1994 were mostly of type 3 (~91%) (Kerr *et al.*, 1995a). Type 3 strains were therefore predominantly found in Japan (~69%) but also in the UK (75%), whereas SSCP type 4 was mostly present in the USA (75%). Moreover, sequence analysis of the VP1/VP2 gene implied that the sequence variation was minimal among isolates obtained from a single community-wide B19 outbreak (Erdman *et al.*, 1996). Investigations of the VP1 unique sequence and of the C terminal region of NS1 of Japanese isolates, both by direct nucleotide sequencing and a mismatch detection method using the Non-Isotopic RNase Cleavage Assay™ (NIRCA™) and by amino acid polymorphism, also indicated a correlation between genome type and prevalence (Haseyama *et al.*, 1998, Fukada *et al.*, 2000).

However, although restriction site polymorphism (RSP) analysis may prove useful to define such epidemiological correlations between viral isolates, it does not give much

information about the degree of variation of the B19 genome. Indeed, sequencing of the region of viral genome coding for structural proteins of isolates collected in Italy between 1989 and 1994 showed that this region was stably conserved (Gallinella *et al.*, 1995a).

The first isolate of a divergent B19 sequence was reported in 1998 (Nguyen *et al.*, 1998). This variant was isolated from a French child with transient aplastic anaemia and found to have greater than 11% nucleotide divergence in the VP1 unique region compared with other B19 virus isolates (compared with <6% divergence between B19 isolates). When the almost full-length sequence of this new isolate, termed V9, was determined, the genome variability was found to extend outside the VP1 unique region with more than 12% nucleotide divergence between the entire genomes of V9 and B19 virus isolates (Heegaard *et al.*, 2001). Only one other V9-related isolate has been reported to date, namely the R1 isolate, which has sequence homology to the V9 isolate in a 346bp fragment of the VP1 unique region (Nguyen *et al.*, 1999).

A second B19 variant, K71, was identified in skin biopsies in Finland and found to differ, within the protein-coding region, by 10.8% and 8.6% from the B19 reference sequences and the V9 variant respectively. The variation in the noncoding region (covering nucleotides 189-435 of the promoter region), was 26.5% and 17.2%, respectively (Hokynar *et al.*, 2002). A further isolate found persistently in human skin was named LaLi (Hokynar *et al.*, 2002).

In a search for additional parvovirus variants, 225 serum and bone marrow samples and 62 plasma pools were screened, resulting in the identification of a new atypical parvovirus sequence, A6, from an anaemic HIV-positive patient (Nguyen *et al.*, 2002).

The A6 isolate exhibited 88% and 92% similarity to B19 and V9 respectively, compared with >98% overall similarity between reported B19 isolates.

Another variant, termed D91.1, was recovered in France from a child with transient aplastic crisis and, although related to V9 sequence, was found to be notably divergent (5.3% divergence) (Servant *et al.*, 2002). A Phylogenetic tree for erythroviruses proposed by Servant and colleagues (figure 1.5) shows the isolates distributed into three very distinct clusters corresponding to genotype 1 (prototype strain Pvbaua), genotype 2 (prototype strain LaLi) and genotype 3 (prototype strain V9). Although the isolation of V9 revealed the need for specific and differential screening techniques, serologic cross-reactivity between V9 and B19 was demonstrated, suggesting that antibody response from both genotypes can be diagnosed equally well by ELISA using either V9 or B19 recombinant capsids as antigen source (Heegaard *et al.*, 2002). As far as DNA of the variant erythroviruses is concerned, the commercial assay RealArt™ Parvo B19 LC PCR was found suitable for detection, quantification, and differentiation of all three B19 virus genotypes classified by Servant *et al.* (Hokynar *et al.*, 2004; Servant *et al.*, 2002).

Figure 1.5: Phylogenetic tree for erythroviruses (proposed by Servant *et al.*, 2002)

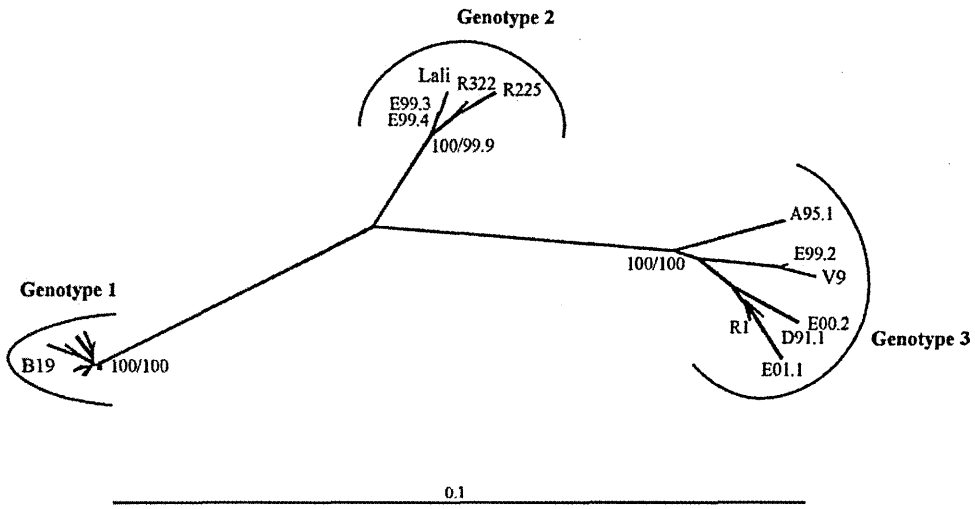

The other important issue discussed over the years has been the possible association of B19 variants with distinct clinical manifestations (Umene and Nunoue, 2002). Several groups failed to demonstrate a correlation between genome type and clinical illness (Morinet *et al.*, 1986; Mori *et al.*, 1987; Kerr *et al.*, 1995a; Erdman *et al.*, 1996). However, six of nine strains isolated from patients with hereditary spherocytosis and aplastic crisis were associated with skin rashes (Nunoue *et al.*, 1987). An examination of the B19 genome from human fetal organs and fluids, as well as sera from leukaemia patients, showed that these genome types were similar to those from patients suffering from aplastic crisis and from an asymptomatic individual (Umene and Nunoue, 1993). However, the number of substitutions in the nucleotide sequence from the damaged fetuses was higher (6 to 11 substitutions) than that found in patients with leukaemia, aplastic crisis or in the asymptomatic person (none to 4 substitutions). Although these findings do not indicate a link between a specific B19 variant and any particular clinical outcome, they suggested a wider diversity of B19 virus in the fetus, perhaps due to the persistence of the infection. Comparisons between different virus isolates at the DNA and protein levels revealed that isolates from patients with persistent parvovirus B19 infection showed a tendency towards higher sequence variability (up to 4 and 8%) when compared to isolates derived from individuals with acute B19 infection (Hemauer *et al.*, 1996). In addition, the genome type of three B19 isolates from patients with encephalopathy revealed two strains assigned to a new genome type, namely group V (Umene and Nunoue, 1995). A recent case study of children suffering from Henoch-Schönlein purpura could not find any link between this condition and either B19 or V9 (Heegaard and Taaning, 2002). While all these observations can serve as clues regarding connection between B19 genome types and clinical manifestations, further studies are needed in this field.

I.1.2. Infection and cell tropism

I.1.2.1. Life cycle

I.1.2.1.1. Receptor and viral entry

The receptor for human parvovirus B19 was first identified in 1993 as the blood group P antigen, or globoside (Brown *et al.,* 1993). Target cells were indeed found to be protected from infection by preincubation with monoclonal antibodies to globoside. The very small proportion of the general population who does not bear the P antigen was shown to be naturally resistant to B19 infection (Brown *et al.*, 1994).

Globoside is distributed on erythrocytes and erythroblasts, but also on endothelial cells, placenta, fetal liver and heart cells (Rouger *et al.*, 1987), which is consistent with the clinical outcomes of B19 infection. However, other nonerythroid cells presenting the P antigen are nonpermissive for the productive infection by B19 (Heegaard and Brown, 2002). Moreover, the high levels of globoside present on mature red blood cells (RBCs) would theoretically render them ideal targets for the virus, providing they had nuclei. Thanks to recombinant B19 vectors, the role of P antigen as the primary receptor for binding of B19 was confirmed (Weigel-Kelley *et al.*, 2001). The level of P antigen expression did not correlate with the efficiency of viral binding, as seen in erythrocytes. Additionally, P antigen was shown to be necessary but not sufficient for parvovirus B19 entry into cells, suggesting that a cell surface coreceptor might be needed for entry. Soon after, parvovirus B19 entry was shown to be mediated by $\alpha5\beta1$ integrins (Weigel-Kelley *et al.*, 2003). This crucial role was demonstrated by inhibition of B19 entry into purified human erythroid progenitor cells following blocking of $\beta1$ integrin function by antibodies. The model shown on figure 1.6 was proposed by Weigel-Kelley and coworkers (Weigel-Kelley *et al.*, 2003). On panel A, mature RBCs, which express high levels of P antigen but no $\alpha5\beta1$ integrin coreceptor, are only able to bind parvovirus

B19, without internalisation. On the other hand, panel B shows that erythroid progenitor cells, which express both P antigen and α5β1 integrin coreceptor, are permissive for parvovirus entry.

Figure 1.6: A model for parvovirus B19 binding and entry into primary human erythroid cells (Weigel-Kelley *et al.*, 2003)

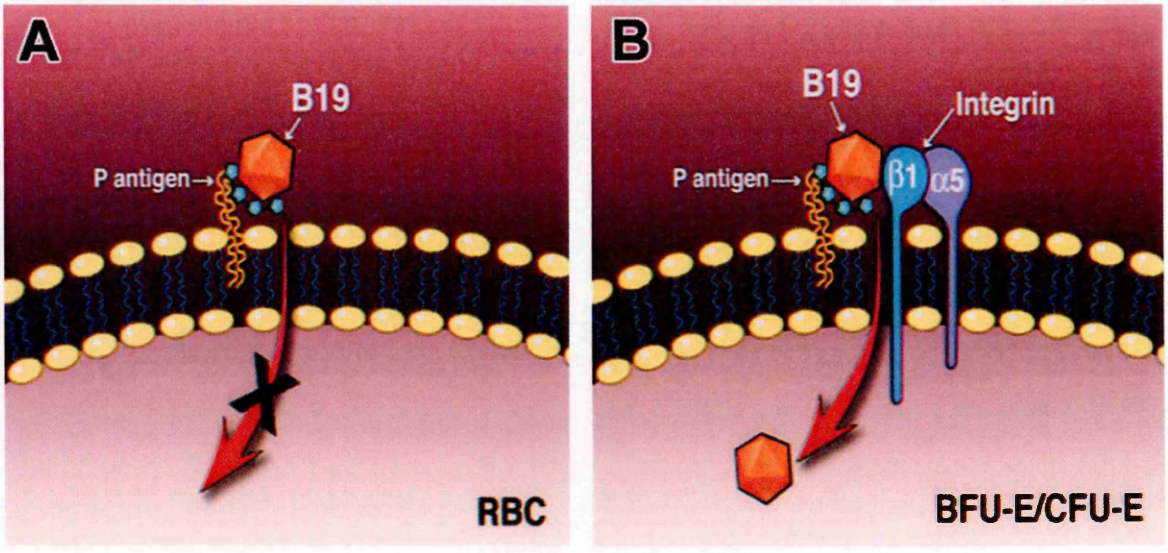

Moreover, Ku80 autoantigen was recently suggested to be a novel coreceptor for B19 infection B19 (Munakata *et al.*, 2005). This protein can be found on the surface of human bone marrow erythroid cells with glycophorin A or CD36, B cells with CD20, or T cells with CD3. When the Ku80 gene was transfected into HeLa cells, both binding of B19 and its entry into the cells were possible. Additionally, when the cell-surface expression of Ku80 was reduced in KU812Ep6 cells, a noticeable inhibition of B19 binding was observed (Munakata *et al.*, 2005).

I.1.2.1.2. Replication

After infection of the target cell, the viral DNA is liberated in the nucleus. The precise mechanisms involved in nuclear delivery of the viral DNA still remain undefined. The

phospholipase A2 activity, which has been associated with a domain of the viral capsid protein, may play a role in decapsidation and liberation of the viral genomic DNA (Zádori *et al.*, 2001).

Studies on the replication of B19 in human erythroid bone marrow cells isolated from individuals with haemolytic anemias suggested that B19 replicated through high molecular weight intermediate forms, linked through a terminal hairpin structure (Ozawa *et al.*, 1986; Ozawa *et al.*, 1987a). These replicative forms (RFs), both monomeric and dimeric, were found in the nuclear DNA of infected bone marrow cells, indicating a nuclear replication site. In addition, replication of B19 was shown to occur from both positive and negative strands. The fact that viral single-stranded DNA was converted to double-stranded RFs by host DNA polymerases has also been suggested (Astell *et al.*, 1997) (figure 1.7).

The monomer length molecules are converted to a double-stranded dimer intermediate, which is resolved into two monomer RF molecules by a mechanism still to be elucidated. These structures are used to synthesise single-stranded plus and minus strands, which are packaged into viral particles. The dotted line on the right side of figure 1.7 implies that dimeric molecules, although detected during B19 replication (Ozawa *et al.*, 1987b), are not absolutely required to explain replication (Astell *et al.*, 1997). Since replication of the viral genome of animal parvoviruses such as AAV-2 and MVM was shown to require viral non-structural proteins (Berns, 1996), it is likely that these proteins are also required for replication of human parvovirus B19.

Figure 1.7: General replication model for parvovirus genomes (proposed by Astell *et al.*, 1997)

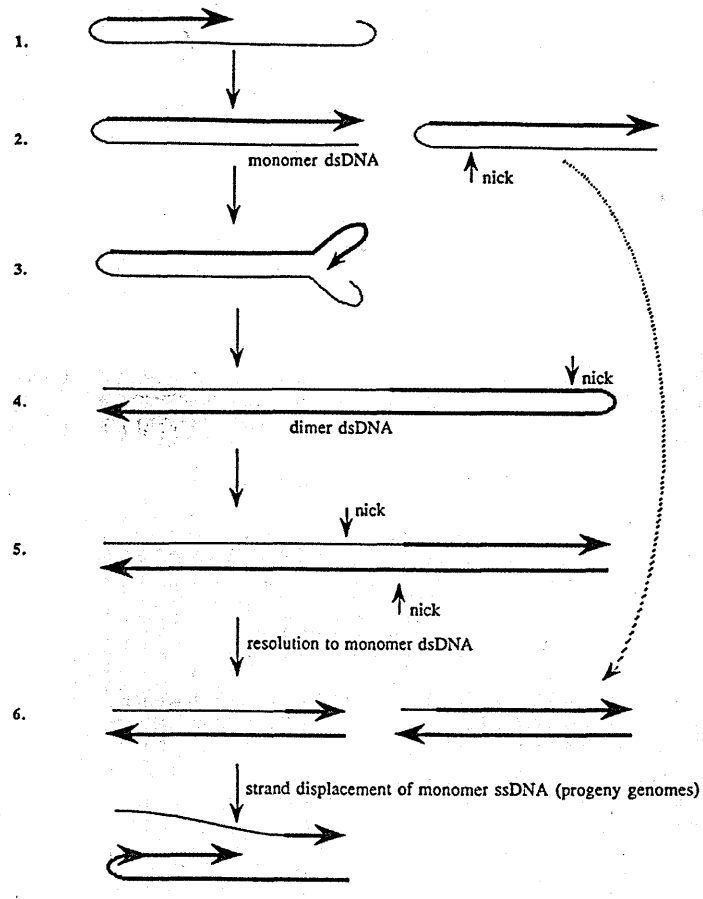

I.1.2.1.3. Transcription

I.1.2.1.3.1. RNA transcripts

One strand of parvovirus B19 DNA, by definition the plus strand, contains two large ORFs extending throughout almost the entire genome (Cotmore *et al.*, 1986; Ozawa *et al.*, 1988c). By comparison with the gene organisation of other members of the *Parvovirinae* subfamily, the major right hand ORF encodes the VP1 protein (3.1 and 2.9 kb mRNAs) and the smaller VP2 protein (2.2 and 2.1 kb mRNAs) while only one mRNA (2.3 kb mRNA) is derived from the left-hand side of the genome and encodes the NS protein. The proposed transcript map is shown in figure 1.4 (Ozawa *et al.*,

1987a). The splice junctions were predicted from careful mapping. In contrast to other parvoviruses, B19 utilises a variant middle polyadenylation signal (ATTAAA at nucleotide (nt) 2639 or AATAAC at nt 2645) and hence its transcripts can terminate at either the middle or the extreme right side of the genome. However, it is likely that the polyadenylation signal at nt 2639, in the middle of the genome, may be the major processing signal (Liu *et al.*, 1992). The main difference between B19 and other parvoviruses is the production by B19 of abundant smaller size RNA species during infection (Ozawa *et al.*, 1987a; Beard *et al.*, 1989). These small RNA transcripts can be categorised in two classes: the first containing RNA transcripts ranging from 700 to 800 nt in length and terminating at the middle polyadenylation signal and the second class containing RNA transcripts ranging from 500 to 600 nt in length and terminating at the extreme right-side of the genome (Ozawa *et al.*, 1987a). At least nine of these polyadenylated RNAs have been identified and the proteins encoded by five of them have been described. All but one of the nine transcripts are alternatively spliced and all transcripts contained a 57 nt leader sequence. The only non-spliced mRNA encodes NS1 and could be categorised in the first class described above since the sequence corresponding to this transcript polyadenylation site is located in the middle of the genome. In contrast, the polyadenylation site of the two mRNAs encoding for each of the capsid proteins VP1 and VP2, is situated on the far right side of the genome (Ozawa *et al.*, 1987a).

Libraries of cDNA clones from B19 infected CML cells (obtained from a chronic myelogenous leukemia patient) and COS-7 cells transfected with hybrid B19/SV40 plasmids were isolated and sequenced to establish unambiguously the splice junctions (St Amand and Astell, 1993). Two species of 11kDa proteins were identified and showed to be encoded by an ORF contained within the 500 to 600 nt RNAs class. On

the other hand, the 700 to 800 nt class was not detected in the COS-7 cell library, suggesting that the middle polyadenylation signal was not recognised in these cells (St Amand *et al.*, 1991). However, later studies showed that the translation product of at least one of these RNAs, a 7.5kDa protein, was made in transfected COS-7 cells (Luo and Astell, 1993). It is therefore likely these mRNAs were present but of low abundance. The biological functions of these small RNAs and 7.5 and 11kDa proteins in the viral cycle remain undefined.

I.1.2.1.3.2. Identification of promoter elements

Studies of MVM and AAV-2 have shown that these viruses have separate promoters used to express the nonstructural and capsid proteins (Berns, 1996). In MVM, the RNAs are transcribed from two promoters, located at 4 (P4) and 39 (P39) map units (m.u.) on the viral genome (Pintel *et al.*, 1983). Since the latter is 5,104 nt long, 1 m.u. corresponds to 51 nt. Transcripts overlap and all undergo 3' end processing at the most distal polyadenylation signal at the far right side of the genome (Clemens and Pintel, 1987). Alternate splicing generates mRNAs that encode NS and VP proteins (Pintel *et al.*, 1983; Cotmore *et al.*, 1983; Morgan and Ward, 1986; Jongeneel *et al.*, 1986). On the other hand, AAV-2 has three promoters at P5, P19 and P40 (Morinet *et al.*, 2000). This virus also uses alternate splicing and a polyadenylation signal at the far right side of the genome. While the P5 and P19 promoters trigger the expression of mRNAs that encode the NS proteins, the P40 promoter is used for VP expression.

In contrast, early studies of human parvovirus B19 transcription done by computer analysis of the virus sequence suggested that there could be a number of potential promoters able to express NS and VP proteins (Shade *et al.*, 1986). However, a transcription assay using HeLa cell nuclear extracts allowed the identification of a

region between nt 258 and 321 that was necessary for *in vitro* transcriptional activity (Blundell *et al.*, 1987). Moreover, RNA protection analysis of the 5' ends of transcripts indicated that all transcripts were initiated at a single strong left-hand promoter near m.u. 6, thus named P6 (Ozawa *et al.*, 1988a). In addition, primer extension studies identified the start site of transcription at nt 350-351, 31-32 nt downstream of the TATATATA sequence at position 319 (Blundell *et al.*, 1987). Although the presence of a second promoter at m.u. 44 (B19P44) was reported (Doerig *et al.*, 1990), other investigations failed to establish its function as a promoter (Blundell *et al.*, 1987; Doerig *et al.*, 1987; Liu *et al.*, 1991a). Nevertheless, both B19 P6 and P44 promoters may be transactivated by the adenovirus type 2 E1A protein in nonpermissive human cells, although the extent of transactivation of the P44 promoter was significantly lower than that of the P6 promoter (Ponnazhagan *et al.*, 1995).

I.1.2.1.3.3. Regulation of RNA processing

Similar to other parvoviruses, B19 nonstructural protein NS1 plays the role of a *trans*-activator protein that can up-regulate the P6 promoter (Doerig *et al.*, 1990). Further studies revealed that the region from nt 100 to 160 was essential for NS-1-mediated transcriptional activation (Gareus *et al.*, 1998). The P6 promoter region has been studied to establish the *cis*-acting signals required for its activity and their possible roles in limiting replication of this virus to human erythroid progenitor cells. Footprinting experiments showed that B19 promoter P6 includes a complex regulatory region containing multiple sequences which affect promoter strength and that the GC-box motif (nt 292 to 301) is a major controlling sequence for *in vitro,* and likely *in vivo,* transcription (Blundell and Astell, 1989). Analysis of sequences upstream of known promoters in MVM (Astell *et al.*, 1983), H-1 virus (Rhode and Paradiso, 1983), AAV-2

and B19 (Shade *et al.*, 1986) indicated sequences closely related to high-affinity transcription factor Sp1 sites. Blundell and Astell suggested that the HeLa cell nuclear factor that binds to the B19 virus GC-box might be Sp1 (Blundell and Astell, 1989).

Additionally, transient reporter gene assays allowed the identification of a minimal promoter extending to –96 upstream of the transcription start and containing two tandem GC-boxes and TATA box (Liu *et al.*, 1991b). The distal GC-box at –59 has the consensus binding sequence for Sp1, which would also suggest that this motif may be an important element in the minimal promoter *in vivo* and might bind Sp1. This minimal promoter lies within the terminal hairpin (from –249 to –157) and contains an area of tight protein binding with a 14 nt sequence that is protected by DNAaseI footprinting. This protein complex may be involved in the regulation of the promoter *in vivo* but it is probably not Sp1 that binds to this site (Liu *et al.*, 1991b). However, fixation of the Sp1 factor to a GC-box placed just downstream of the transcription factor Ets binding site was demonstrated, suggesting the Sp1 does play a role in the regulation of transcription (Vassias *et al.*, 1998). The palindromic terminal repeats of parvoviruses were also shown to be required for viral DNA replication since they constitute the replication origin and are almost completely protected from Dnase I digestion by proteins (Im and Muzyczka, 1990).

Furthermore, NS-1-mediated transactivation was found to be dependent on the presence of two GC-rich elements arranged in tandem upstream of the TATA box (Gareus *et al.*, 1998). Gareus and colleagues thus proposed a model of NS1-mediated P6 transactivation (figure 1.8) dependent on a multicomponent complex combining NS1 with ATF, NF-κB/c-Rel, and GC-box (Sp1) binding cellular factors.

In AAV, YY1, a multifunctional transcription factor, was found to act as a repressor of transcription from the AAV P5 promoter, which is relieved by E1A protein (Shi *et al.*,

1991). YY1 was also found to be prominently bound to three different motifs in the terminal repeat region of parvovirus B19 (Momoeda *et al.*, 1994b). However, in contrast to AAV, YY1 was shown to be a positive regulator of viral transcription in HeLa cells, although very weak (1.3-1.9-fold above basal transcription). When a different cell type was used, namely *Drosophila* SL2 cells, YY1 had no effect on the P6 promoter, suggesting that this transcription factor might be dependent on the cells transfected (Vassias *et al.*, 1998). In the same study, the binding of the transcription factor hGABP (also named E4TF1) to the Ets binding site resulted in the regulation of the P6 promoter. A "3-fold sequence" containing YY1, Ets and Sp1 binding sites was defined and Sp1 and hGHBP were shown to activate transcription synergistically throughout this sequence (Vassias *et al.*, 1998).

Figure 1.8: Model of the transactivating complex (proposed by Gareus *et al.*, 1998)

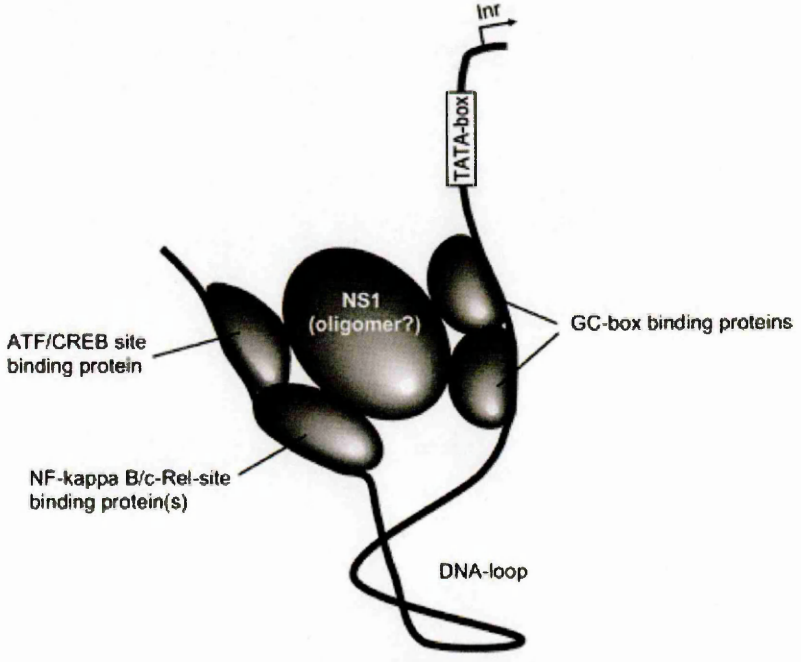

Inr: transcription start site. The DNA segment in between could easily be lopped out.

I.1.2.1.4. Translation regulation

Translational regulation may also be a way of controlling the expression of B19 genes. Immediately upstream from the VP1 translation initiation site is an unusual sequence containing multiple ATG triplets (Shade *et al.,* 1986; Ozawa *et al.*, 1987a). During RNA processing, this sequence, from nt 2,184 to nt 3,044/3,050, is spliced out of VP2 RNA. It has also been noted that the upstream nontranslated region of both VP1 mRNAs has multiple AUG codons. These codons are apparently bypassed by ribosomes to allow initiation of VP1 at the AUG at nt 2,444. Since capsid proteins are produced in strikingly different quantities (VP1<4%; VP2>96%), the role of this AUG-rich region in translational control was studied (Ozawa *et al.*, 1988b). Its removal from VP1 RNA greatly increased the efficiency of translation while the addition of the same AUG-rich sequence upstream of the initiation site of VP2 decreased its translation. Therefore, it seems likely that this upstream AUG-rich region acts as a negative regulatory element in the translational control of B19 capsid protein production. In addition, a noticeable fact is that all of the B19 mRNAs (except the unspliced NS1 messenger) exist as two related transcripts (Astell *et al.,* 1997). Thus the selection of the splice acceptor site at nt 1,910 versus nt 2,030 might plays some subtle, although currently not well understood, role in the regulation of expression of both structural proteins and 11kDa proteins.

I.1.2.2 Cell tropism

Early *in vitro* studies indicated that parvovirus B19 can cause clonal inhibition of erythroid progenitor cells in methylcellulose cultures (Mortimer *et al.,* 1983) and can productively infect progenitor cells from bone marrow (Ozawa *et al.*, 1986). Further reports detected infection of cells from peripheral blood (Kurtzman et al., 1988; Schwarz *et al.*, 1992), fetal liver (Yaegashi *et al.,* 1989; Brown KE *et al.*, 1991),

umbilical cord blood (Srivastava *et al.*, 1992; Sosa *et al.*, 1992), bone marrow cells from *M. fascicularis* (Gallinella *et al.,* 1995b), as well as in myocardial cells (Porter *et al.*, 1988) and megakaryocyte-enriched bone marrow fractions (Srivastava *et al.*, 1990). However, most of these cells are very difficult to obtain due to ethics issues and/or availability. The suitability of apheresis cells for *in vitro* infection with B19 has also been shown (Hemauer *et al.*, 1999). Apheresis is a technique that allows more of one particular part of the blood (platelets, granulocytes, etc.) to be collected than could be separated from a unit of whole blood. Using a special apheresis centrifuge, the blood can be fed into the system continually. As it spins, the components separate and the granulocytes (white blood cells) are drawn off. The plasma, erythrocytes and platelets are then recombined and returned to the donor. The whole procedure lasts about one hour. Apheresis may be therapeutically useful in cases of glomerulonephritides associated with antibody deposition, lupus erythematosus, antibody-mediated transplant rejection and in lowering the levels of preformed cytotoxic antibodies which may preclude transplantation (Smith *et al.*, 2003; Kaplan, 2003).

Although the target cells for B19 virus are in the erythroid lineage from Burst-Forming Unit-Erythroid (BFU-E) to erythroblasts, with susceptibility to the virus increasing along with differentiation (Takahashi *et al.*, 1990), some nonerythroid cells can also become infected. In addition, a number of human blast cell lines have also been infected with B19 virus, (either productively or non productively), namely TF-1 (Kitamura *et al.,* 1989), UT-7 (Komatsu *et al.*, 1991; Shimomura *et al.*, 1992; Nicolis *et al.,* 1993; Shimomura *et al.*, 1993), UT-7/EPO (Komatsu *et al.,* 1992; Erickson-Miller *et al.*, 2000), KU812 (Nakazawa *et al.*, 1989), KU812Ep6 (Miyagawa *et al.*, 1999), MB-02 (Munchi *et al.*, 1993), and JK-1 (Okuno *et al.*, 1990; Takahashi *et al.*, 1993). These cells have in common the fact that they all depend on the erythroid-specific hormone

erythropoietin (EPO) for growth or differentiation. EPO is necessary for viral replication, but it is not clear whether it represents a direct requirement. However, no system has been established that could be suitable for the large-scale production of infectious virus.

Studies of hypoxic culture conditions in France have suggested an enhancement of the B19 capsid protein synthesis, virus replication and virus production when human primary erythroid progenitor cells were exposed to severe hypoxia (1%) (Pillet *et al.*, 2004). Caillet-Fauquet and coworkers also suggested that B19 infection of the cell line KU812F cultured in mild hypoxia (6%) might result in higher yields of infectious B19 progeny and to enhanced viral transcription compared to normal oxygen concentration (20%) (Caillet-Fauquet *et al.*, 2004a). Severe hypoxia (1%) had previously been shown to have some positive effects on the maintenance and cloning efficiency of BFU-E, while inhibiting the terminal expansion and maturation of these clones (Cipolleschi *et al.*, 1997). Moreover, the differentiation and amplification of the CFU-E pool observed in a mouse model during hypoxia might be due to an increase in EPO levels (Mide *et al.*, 2001). These conditions might thus be sufficient for a more productive B19 infection.

At the transcriptional level, when a 100bp fragment containing the B19 P6 promoter replaced the authentic AAV promoter at m.u. 5 (AAV P5) in an infectious clone of AAV-2, this recombinant virus was able to replicate autonomously in primary human hematopoietic progenitor cells (Wang *et al.*, 1995). It was therefore proposed that the promoter P6 might play a role in erythroid specificity. In contrast, using plasmid-mediated transfection of established human cell lines, the B19 P6 promoter was shown to be very active in nonpermissive cells including Hela, K562, Raji and Jurkat, and

highly active CEM cells, a T-lymphoblastoid cell line (Liu *et al.*, 1991b). Because of this indiscriminate activity from the P6 promoter, the latter seemed unlikely to play a role in tropism of human parvovirus B19.

The different cellular permissiveness and regulation of B19 virus gene expression was assumed to lead to two different types of infection, according to a balance of production of NS or VP proteins, as shown on figure 1.9 (Liu *et al.*, 1992). In the case of fully permissive cells such as erythroid precursor cells (Ozawa *et al.*, 1987b), a full set of nonstructural and capsid proteins would be produced, leading to a productive infection. On the other hand, in the case of infection of nonpermissive cells, such as megakaryocytic precursor cells (Srivastava *et al.*, 1990), the NS1 protein would be mainly produced, leading to an abortive infection and to cell death by reason of its cytotoxic and/or apoptosis-inducing characteristics (Moffatt *et al.*, 1998; Ozawa *et al.*, 1988a). Furthermore, when the 3' processing signals located in the middle of the viral genome were removed, expression of the VP gene transcripts increased in nonpermissive cells. Therefore, Liu and colleagues proposed that "differential transcript accumulation might be controlled not at the level of promoter initiation but by RNA processing events or by recognition of variant termination signals" (Liu *et al.*, 1992).

Figure 1.9: Schematic model of NS gene expression in nonpermissive cells (NSP: NS protein) (proposed by Liu *et al.*, 1992)

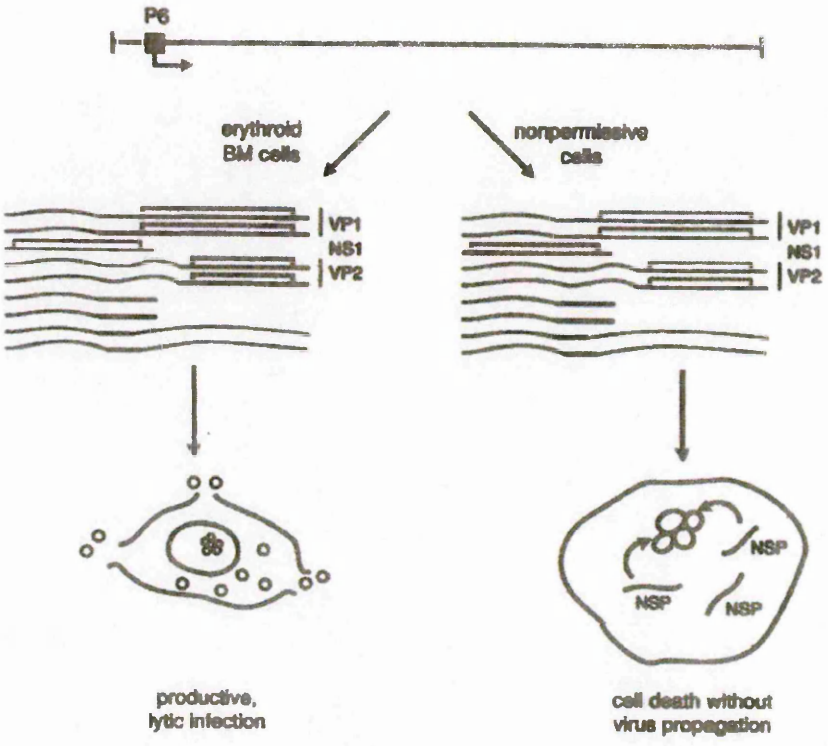

An obstacle at the translational level was first proposed by Leruez and colleagues (Leruez *et al.*, 1994). In addition, in nonpermissive cells, it was suggested that the 3' untranslated region (UTR) of the capsid protein mRNAs repressed capsid protein synthesis by inhibiting ribosome loading (Pallier *et al.*, 1997). Confirmation came from further studies comparing the infection of bone marrow cells and of different human blast cell lines with erythroblastoid (TF-1) and megakaryoblastoid (UT-7, M-07, B1647) phenotypic characteristics (Gallinella *et al.*, 2000; Avanzi *et al.*, 1990; Komatsu *et al.*, 1993; Kitamura *et al.*, 1989; Bonsi *et al.*, 1997). Two patterns of restriction to replication were observed in those cells (Gallinella *et al.*, 2000). In the first instance found in UT-7 cells, the ss viral DNA was converted into ds replicative intermediates similar to those found in bone marrow cells. In addition, a full set of viral transcripts

was produced. However, only a small proportion of cells supported replication and transcription, with no production of capsid proteins. In the second restriction pattern, which was observed in TF-1, M-07 and B1647, the ss viral DNA was not converted to ds replicative intermediates. In another study using the megakarycytic cell line MB-02, a novel splicing pattern was observed which lead to the fusion of the two first amino acid of NS1 with those of the small 7.5 kDa protein (Brunstein *et al.,* 2000). This novel splicing pattern resulted in the functional inactivation of the viral structural genes and effectively blocked production of progeny virions. According to Brunstein and coworkers, this mechanism is "the crucial one in restricting viral tropism among bone-marrow-derived cells" (Brunstein *et al.,* 2000).

In conclusion, since the susceptibility to infection and the permissiveness for infection are not directly linked, the spectrum of target cells may be wider than expected. Therefore, the presence of viral receptors on the cell surface and of intracellular permissiveness factors should be fully determined in various cell types.

I.1.3. Epidemiology

I.1.3.1. Seroprevalence

The prevalence of anti-B19 immunoglobulin G (IgG) antibodies in the general population ranges from 2 to 15% in children aged 1 to 5 years old, 15 to 60% in children aged 5 to 19 years old and from 30 to 78% in adults (Török, 1992; Kelly *et al.*, 2000; Abraham *et al.*, 2002).

When comparing prevalence in England, Wales and Australia to that in Singapore and South Africa, a variation among countries was observed, with B19 being more prevalent in temperate countries rather than tropical ones (Kelly *et al.*, 2000). Kelly and

colleagues, who reported serology data in Australia from 1992 to 1998, also suggested that parvovirus tended to occur in 4-year cycles, with 2 epidemic years followed by 2 endemic years. In addition, infection might be season-related since it was often found associated with outbreaks of EI in schools in the late winter and spring (Anderson and Török, 1989). However, it can also occur any time of the year in either the presence or absence of an EI outbreak.

I.1.3.2. Transmission

I.1.3.2.1. Route of transmission

In a B19 school outbreak, parvovirus DNA was detected in the throat swap of the teacher of several of the affected children, indicating that transmission of the virus might occur via the respiratory tract (Plummer *et al.*, 1985). In the same year, the respiratory route of transmission was confirmed by intranasal infection of volunteers (Anderson LJ *et al.*, 1985). Moreover, at the same time as viremia, parvovirus B19 was detected in nasal washes and gargle specimens from 3 of the 4 infected individuals, identifying the upper respiratory tract, and most probably the pharynx, as the site of viral shedding. Vertical transmission may also occur from mother to foetus in about one third of cases with serologically confirmed maternal infection (Török, 1992).

I.1.3.2.2. Household infections

In a study of intrafamilial associations of B19 infection, no link was found between seropositivity of the parents and their children, neither between one spouse and the cospouse (Koch and Adler, 1989). However, when considering only the first and second siblings in the family, 50% of the younger siblings were infected if the older siblings were seropositive. Therefore, household infections represent a very high percentage of

B19 infections among children but also were found to be significant in adults, especially women. The transmission rate for susceptible household contacts of persons with EI or B19-associated aplastic crisis was found to be approximately 50%, regardless of age (Plummer *et al.*, 1985; Chorba *et al.*, 1986). The infection rate amongst susceptible pregnant housewives was 8.7%, (4 of 46) (Cartter *et al.*, 1991). For pregnant women whose serological status is unknown, the chance of suffering fetal loss after household exposure is lower than 2.5% (Anderson *et al.*, 1990).

I.1.3.2.3. Nosocomial and occupational infections

The risk associated with nosocomial infections that can involve both patients attending the hospital and hospital staff members themselves have been well documented (Bell *et al.*, 1989, Dowell *et al.*, 1995, Pillay *et al.*, 1992, Koziol *et al.*, 1992, Miyamoto *et al.*, 2000, Lui *et al.*, 2001). The first report of a probable spread of B19 infection in hospital involved two paediatric patients with hereditary spherocytosis and sickle cell anemia, respectively (Evans *et al.*, 1984). The spread of aplastic crisis to the patient with sickle cell disease occurred when she was exposed to the patient with hereditary spherocytosis, thereby emphasising the danger of contacts between patients with known haemolytic anemia.

Although a prospective survey reported no increase in annual seroconversion rates in childcare providers (1.5%) compared to the women of childbearing age control group (1.5%) (Koch and Alder, 1989), many other reports show an increase risk of B19 infection in women working outside the home in school or day care settings (Cartter *et al.*, 1991; Valeur-Jensen *et al.*, 1999; Cordell, 2001; Schwarz *et al.*, 1990).

Taken together, these studies indicated that the highest risk for B19 infection is found in households and selected occupational settings where workers can be exposed to infected

patients or staff in hospital wards, or to infected children in schools and day care centres.

I.1.3.2.5. Parenteral transmission

Although much less likely than the respiratory route, parenteral transmission may occur by transfusion of contaminated blood products and will be discussed in section II.

I.1.4. Immune response

In immunocompetent individuals, clearance of human parvovirus B19 from blood appears to be achieved almost entirely through the humoral immune response of the individual. Moreover, this response is mainly directed against the structural proteins VP1 and VP2. The important role of neutralising antibodies in clearing the virus is suggested by the fact that intravenous immunoglobulin can cure chronic B19 infections in immunosuppressed patients.

I.1.4.1. Antibody response in acute and past B19 infections

Experimental infection of healthy volunteers has shown that the predominant immune response is humoral (Anderson *et al.*, 1985a; Kurtzman *et al.*, 1989a). Figure 1.10 summarises the time course of B19 serology, which will be detailed below (Heegaard and Brown, 2002).

Figure 1.10: Time course of B19 viraemia and antibody response following B19 infection (Heegaard and Brown, 2002)

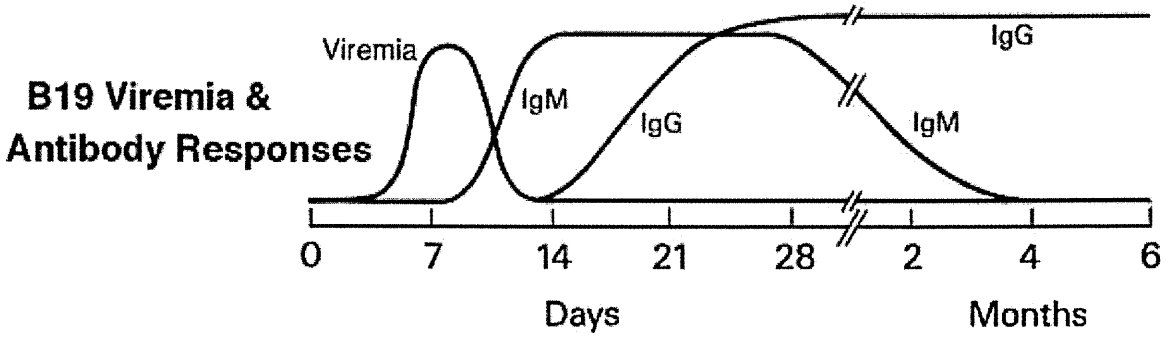

I.1.4.1.1. IgM response

The IgM immune response was examined by Anderson and coworkers, who inoculated healthy adult volunteers intranasally with parvovirus B19 obtained from an asymptomatic blood donor (Anderson LJ *et al.*, 1985). High-titre IgM antibodies to B19 developed during the second week (9 to 10 days) after inoculation and represented the first detectable immune reaction indicating an acute B19 infection. IgM antibodies may be found in serum for 3 to 6 months, although in some cases the IgM antibodies may decline very rapidly resulting in negative values already after 2 to 3 weeks.

In order to study the immune response to B19 infection without having to inoculate volunteers, scientists had to overcome the shortage of B19 antigens by expressing recombinant B19 proteins in several systems, both prokaryotic and eukaryotic (Sisk and Berman, 1987; Brown *et al.*, 1990a; Kajigaya *et al.*, 1991; Söderlund *et al.*, 1992; Saikawa *et al.*, 1993; Palmer *et al*, 1996; Manaresi *et al.*, 1999a).

Whether they are undenatured or denatured, recombinant VP1 and VP2 proteins can be used to detect immune response against conformational or linear epitopes respectively. Hence an Enzyme Linked Immunosorbent Assay (ELISA) with intact antigens can

detect antibodies against conformational epitopes whereas a Western blot assay with denatured antigens can be used to identify immunity against linear epitopes (Kerr *et al.*, 1999). However, data available on IgM reactivity against linear and conformational epitopes of VP1 and VP2 is limited and rather controversial. While some studies indicate that in patients with primary B19 infection, the IgM response to linear VP1 epitopes was more frequent, intense and persistent than the response to linear VP2 epitopes (Palmer *et al.*, 1996, Manaresi *et al.*, 2001; Manaresi *et al.*, 2002a), other studies found no difference in the IgM responses to VP1 and VP2 linear epitopes (Kerr *et al.*, 1999). It has also been reported that in the active phase of infection, IgM antibodies against conformational epitopes of both VP1 and VP2 appeared at the same time and with the same frequency but those against VP1 epitopes were longer lasting than the other epitope specific IgM (Manaresi *et al.*, 2001).

I.1.4.1.2. IgA response

A significant rise in specific IgG and IgA antibodies in 87% and 77%, respectively, of persons from whom acute and convalescent phase serum specimens were available has been reported (Erdman *et al.*, 1991). Specific IgA antibodies were found in 93% of persons with EI. However, these antibodies were also present in half of normal blood donors with prior B19 exposure, as indicated by specific IgG antibodies (Erdman *et al.*, 1991). This high prevalence of IgA antibodies among normal individuals indicates their long persistence. Moreover, breast milk has also been shown to contain IgA antibodies (Heegaard *et al.*, 2000).

I.1.4.1.3. IgG response

Studies in infected volunteers have shown that IgG antibodies to B19 began to develop at the end of the second week after inoculation and early in the third week,

simultaneously with the decrease of IgM antibodies and the observation of the rash typical for parvovirus B19 infection (Anderson *et al.*, 1985a).

During the acute and early convalescent phases of B19 infection, the majority of IgG antibodies are thought to be directed against both conformational and linear epitopes present in the VP2 protein and against linear epitopes of the VP1-unique region (Söderlund *et al.*, 1995a). However, another report suggests that antibodies from some individuals do not react against linear epitopes on both denatured B19 VP1 and VP2 antigens (Kerr *et al.*, 1999). The discrepancy might be due to the fact that the two studies used different proteins (the unique region of VP1 or a VP1/2 capsid combination compared with the whole proteins). In an attempt to further define the different phases in IgG response to B19 infection, it has been reported that in the active or very recent stage of infection, IgG against VP1 linear epitopes were detectable concomitantly, and with the same frequency, as IgG against VP2 conformational epitopes but in the convalescent phase, IgG against VP2 linear epitopes were detectable with the same frequency as IgG against VP2 conformational epitopes (Manaresi *et al.*, 1999a). However, other reports suggest that antibodies against VP2 are detectable prior to IgG against VP1 (Schwartz *et al*, 1988; Kurtzman *et al.*, 1989a) but this may reflect the 19-fold higher amount of VP2 antigen compared with VP1 antigen found in preparations using native virus as the antigen source (Manaresi *et al.*, 1999a). Finally, the persistence of antibodies to conformational but not linear epitopes of VP2 during late convalescence is also unclear (Söderlund *et al.*, 1995a; Manaresi *et al.* 1999a). The long term IgG antibody response is directed mainly against VP1, and in particular the aminoterminal half of the VP1-unique region, which has been shown to be immunodominant (Musiani *et al.*, 2000). A summary of IgG immune response in active and convalescent phases of B19 infection is shown in table 1.2.

Table 1.2: Summary of IgG antibody response in active and convalescent phases of parvovirus B19 infection

Stage of infection	VP1 epitope		VP2 epitope	
	Linear	Conformational	Linear	Conformational
Active phase	+	-	-	+
Convalescent phase	Unknown	Unknown	+	+

The predominant subclass of IgG antibodies involved in the binding to VP1 and VP2 capsid proteins is IgG1 during the acute phase and early convalescence while subclass IgG3 peaks 2 weeks after infection but stabilises to low levels over 6 months (Franssila *et al.*, 1996). Both IgG1 and IgG3 decline to background levels during the recovery period. At the same time, a dramatic increase in VP1-specific IgG4 activity is observed, although that subclass is barely detectable for the first three months after infection. This subclass of antibodies may also become prominent upon chronic antigenic stimulation (Aalberse *et al.*, 1983; Iskander *et al.*, 1981). This antigenic stimulation could arise from repeated subclinical exposure to the virus, which is highly probable in epidemic periods, persistence of the virus at low concentrations in immunocompetent individuals or repeated exposure to antigens as part of immune complexes (Franssila *et al.*, 1996).

I.1.4.2. Characteristics of the linear and conformational epitopes of VP1/VP2 and the VP1-unique region

I.1.4.2.1. Major capsid protein VP2

Studies using monoclonal antibodies binding to synthetic peptides show that the neutralising epitopes are located at the carboxy terminal half of VP2 (amino acids 328-344 from the amino terminus), with recognisation sites at amino acids 253-272, 309-

330, 325-346, 359-382, 449-468 and 491-515 (Sato *et al.*, 1991a; 1991b; Brown *et al.*, 1992). A comparison with CPV suggests that this region is probably on the surface of the native virion. The viral surface of CPV is composed of a "spike" on each of the threefold axes, consisting of four loops (Tsao *et al*, 1991; Chapman and Rossmann, 1993). Superimposition of the largest loops (loops 3 and 4) of CPV on a map of the B19 VP2 epitopes indicated that all the B19 epitopes lay between the projected surface loops of CPV, suggesting that the immunodominant domain on the VP2 capsids correlates with the surface spike of CPV (Brown *et al.*, 1992; Sato *et al.*, 1991b). Studies have shown that the CPV loops 1 and 3 are immunogenic and have surface exposed residues (Langeveld *et al.*, 1993). These loops might be possible sites for attachment of neutralising antibodies, which could interfere with binding between CPV virion and cell surface receptor. Similarly, in parvovirus B19, the proximity of the antigenic epitopes to the receptor site, suggests that virus neutralisation may be caused by preventing attachment of viruses to the cells (Chipman *et al.*, 1996).

Several studies have suggested that the VP1/VP2 junction and the VP2 capsid protein (amino acids 57-77) may be linear neutralising epitopes (Saikawa *et al.*, 1993; Yoshimoto *et al.*, 1991). It is clear that conformational epitopes are also present. In contrast, other studies have shown that recombinant VP2 capsids on their own do not elicit a neutralising antibody response in rabbits and require the presence of VP1 which may modulate the antigenicity of the native virus particles or, alternatively, may affect the conformational structure of the neutralising epitopes (Kajigaya *et al.*, 1991; Yoshimoto *et al.*, 1991).

Additionally, when B cell memory was induced after B19 infection, B cell memory was strongly maintained against VP2 conformational epitopes and against VP1 linear

epitopes, whereas it was not maintained against VP2 linear epitopes (Corcoran *et al.*, 2004).

I.1.4.2.2. VP1 and its unique region

Studies have shown that the most amino-terminal quarter of the unique region of VP1 is the most immunogenic region and that the immune recognition of the unique portion of VP1 is similar to reactivity against a soluble, conformationally free globular protein, while immune recognition of VP2 epitopes is much more conformationally fixed by the capsomere structure (Saikawa *et al.*, 1993). This region contains numerous neutralising linear epitopes, clustered in particular at the amino-terminus (between amino acids 1 and 80) and in the centre (amino acids 148-205) (Anderson *et al*, 1995; Gigler *et al.*, 1999; Zuffi *et al.*, 2001). All these data indicate that the unique region of VP1 is located on the virion surface and thus accessible to antibody binding but its precise relationship to the rest of the capsid is still unknown (Kawase *et al.*, 1995). An investigation of the genomic variability and the antigenic stability of the VP1 unique region confirmed that there was very little variation in amino acid sequence, between 0-3.2% or 8 amino acids (Dorsch *et al.*, 2001; Hemauer *et al.*, 1996; Erdman *et al.*, 1996). These results confirmed that the amino-terminal part (amino acids 1 to 80) must be surface exposed and highly stable, and suggest that it could be folded in a loop-like structure.

I.1.4.3. Antibody response in persistent B19 infection and implication of immune response against the non-structural protein NS1

After the onset of neutralising antibody production, the virus is rapidly cleared from the circulation but in some cases of parovovirus B19 infection, persistence of the virus for

up to a decade has been reported (Kurtzman *et al.*, 1989a; Pont *et al.*, 1992). Chronic infection has been observed in four populations of patients: those with congenital immunodeficiency, with HIV infection, those receiving immunosuppressive chemotherapy for treatment of cancer, acute lymphocytic leukaemia and tissue transplantation, and lastly in the developing fetus (Anderson and Young, 1997; Kurtzman *et al.*, 1989b).

Early studies indicated that sera from patients with acute or past infection without complications did not contain detectable levels of anti-NS1 antibodies but NS1-specific antibodies were present in sera from patients suffering from severe B19-associated arthritis, perhaps reflecting persistent viral infection (von Poblotzki *et al.*, 1995a; 1995b). It is possible that these specific antibodies might indicate an elevated production of the non-structural protein in particular individuals or that prolonged viral presence might lead to the infection of non-erythroid cells bearing the B19 receptor, which would not normally be susceptible to the virus. Thus the expression pattern of the parvovirus B19 genome in these non-permissive cells may be shifted to the preferential production of NS1 protein (Liu *et al.*, 1992). In addition, the elevated synthesis and release of NS1 protein after cell death might result in initiation of an NS1-specific humoral response (von Poblotzki *et al.*, 1995b). In contrast, later studies indicated that anti-NS1 antibodies were present in a proportion of patients with recent (12.5% to 45%) and past (36%) B19 infections (Searle *et al.*, 1998; Jones *et al.*, 1999). The discrepancy between these studies could be partly explained by three factors: the difference in the sizes of the patient groups investigated, the relative sensitivities of the assays used to detect the NS1 antibodies and the time of sampling after onset of infection as a number of studies have shown that NS1-specific IgG became detectable about four weeks after infection and about two weeks after VP1/VP2-specific immune response (Searle *et al.*,

1998; von Poblotzki *et al.*, 1995b; von Poblotzki *et al.*, 1996; Hemauer *et al.*, 2000). Finally, as only low amounts of NS1 are synthesised during replication in the erythroid progenitor cells, there may be insufficient antigen to prime a strong and long-lasting immune response detectable in persons with past parvovirus infection (Ozawa and Young, 1987; Tolfvenstam *et al.*, 2000). Other studies have also shown the presence of anti-NS1 antibodies in 22 to 30% of B19 infected individuals, of which 13 to 27% had recent infections and the remainder past infections (Venturoli *et al.*, 1998; Hemauer *et al.*, 2000). These studies confirm that the development of anti-NS antibodies is not limited to persistently infected patients or to those patients with B19 arthritis (Kerr and Cunniffe, 2000). The percentage of persons with NS1-specific IgG has been found to decline with increasing age, whereas IgG against capsid proteins are as prevalent in younger as in elderly individuals (Hemauer *et al.*, 1999; Searle *et al.*, 1998).

Three NS1-specific linear epitopes in the carboxy terminal region of NS1 (amino acids 191 to 206, 271 to 286 and 371 to 386) have been identified, with the highest seroreactivity being against amino acids 271 to 286 (Tolfvenstam *et al.*, 2000). These antibodies are unlikely to be protective as persistence of the virus in the serum at relatively high levels is possible despite the presence of NS1-specific immunoglobulins (Von Poblotzki *et al.*, 1995b). However, other reports have suggested a weak but significant neutralising ability of anti-NS1 antibodies (Gigler *et al*, 1999; Kurtzman *et al.*, 1989b), thus the role of NS1 in the persistence of B19 infection remains unclear and controversial.

I.1.4.4. Cellular immunity

Despite early, unsuccessful attempts at demonstrating a proliferative cellular response to B19 using peripheral blood mononuclear cells (PBMC) from individuals with serologic evidence of exposure to virus (Kurtzman *et al.*, 1989b), there is evidence now from

several studies of a cellular response to B19 infection (von Poblotzki *et al.*, 1996, Franssila *et al.*, 2001, Mitchell et al., 2001). A lymphoproliferative response against B19 recombinant capsid proteins VP1 and VP2 was reported, although not in the form of empty capsids (von Poblotzki *et al.*, 1996). These groups demonstrated that CD4+ T cells, also called T helper (T_H) cells, make up the major population of reactive cells and that viral determinants were presented to them by HLA class II molecules and observed lymphocyte proliferation in response to stimulation with a recombinant B19 NS-1 protein *in vitro*.

It appears that the cellular response to B19 mainly involves differentiated CD4+ cells in late convalescence as an immunoglobulin class switch to IgG4, normally triggered by interleukin-4 (IL-4) and interleukin-13 (IL-13), which in turn are produced specifically by T_H type 2 (T_H2) (Franssila *et al.*, 1996; Roitt *et al.*, 1998). However, other reports suggest that the cellular immune response could be more T_H1 oriented in the acute phase of infection as an increase in interferon gamma (IFN-γ), which is produced by T_H1 cells, as well as by natural killer (NK) cells (Roitt *et al.*, 1998), was detected in these studies (Wagner *et al.*, 1995). These authors also identified a rise in the production of IL-1 and IL-6 mRNA. The former is produced by many cells in response to infection and activates NK cells cytocidal activity, T_H cell proliferation as well as B-cell proliferation (Roitt *et al.*, 1998). Both IL-1 and IL-6 are released by some B-cells and enhance expression of IL-2 on T lymphocytes. In turn, IL-2 activates B-cells and NK cells and promotes division of T cells with release of IFN-γ. Although there are signs that the immune response is T_H1 oriented during the acute phase of infection, leading to macrophage activation, it is clear that the humoral response is also activated by a series of cytokines, which activate B-cell proliferation and subsequently antibody production.

Other findings showing a significant T cell immunity elicited by B19, have been reviewed (Klenerman *et al.*, 2002). The first B19-derived CD8+ T-lymphocyte epitope has been mapped and shown to be derived from the amino acids 391 to 399 of the non-structural protein NS-1 (Tolfvenstam *et al.*, 2001a). This peptide was able to stimulate *ex-vivo* CD8+ T-lymphocyte responses in B19-seropositive donors. Moreover, using ELISpot responses to peptides spanning the whole NS-1 sequence, multiple further responses were identified in seropositive individuals, thus pointing to the presence of a persistent memory population (Klenerman *et al.*, 2002). In conclusion, the CD8+ T-lymphocyte responses might indicate an ongoing stimulation by persistent antigen and might involve a simultaneous maintenance role of CD4+ T cells (Wagner *et al.*, 1995; von Poblotzki *et al.*, 1996; Franssila *et al.*, 2001).

I.1.5. Diagnosis

The symptoms of parvovirus B19 infection are often non-specific and could theoretically be confused with various other infectious agents, such as rubella, cytomegalovirus (CMV), varicella zoster virus (VZV), mumps or rubeola. Therefore, differential laboratory diagnosis of B19 infection is essential, as a recent study showed, when 123 out of 344 samples (35.7%) collected during an epidemic of B19 from children with rashes presented neither B19 DNA, IgM nor IgG (Gallinella *et al.*, 2003). Detection of B19 infection relies on a range of laboratory tests summarised in table 1.3. While serum samples are the most commonly tested specimens, bone marrow aspirates, cord blood samples, amniotic fluid samples and biopsy specimens of placenta and fetal tissues are also used to detect B19 infection (Zerbini *et al.*, 2002).

Table 1.3: Summary of diagnostic and detection assays for B19

Diagnosis by	Diagnostic laboratory tests
Cellular factors	• Numeration of reticulocytes, neutrophils, lymphocytes and platelets • Titration of haemoglobin • Microscopic examination of bone marrow aspirates (giant pronormoblasts) • Immunohistochemistry of skin lesions
Antibody detection IgM	• Immunoblot assay • Enzyme immunoassay (EIA) • Immunofluorescence assay (IFA)
IgG	• Immunoblot assay • EIA • IFA
B19 virus detection	• EM • Immune electron microscopy (IEM)
B19 antigen detection	• Counter- immunoelectrophoresis (CIE) • Radioimmuno-assays (RIA) • EIA • Blot immunoassays • Receptor-mediated haemagglutination assay (RHA)
B19 DNA detection	• Dot blot hybridisation • In situ hybridisation assay (ISH) • Polymerase chain reaction (PCR)

I.1.5.1. Diagnosis by cellular and blood markers

When natural infection developed in volunteers infected by B19 virus, reticulocytes were not detected from day 8 and 10 for a period of at least one week (Anderson *et al.*,

1985a). This finding demonstrated that erythropoiesis is prone to interruption following B19 infection in normal individuals. Moreover, a simultaneous significant decrease- as low as 30% of baseline values- in levels of neutrophils, lymphocytes and platelets were observed. In the normal host, the hemoglobin may fall by 2 to 3g/dL (Török, 1992). However, in patients who are already suffering from hematological disorders, characterised by decreased red cell production or increased red cell destruction, B19 infection may result in a dramatic decrease in hemoglobin. All these cellular and blood markers can sometimes prove useful in the diagnosis of recent B19 infection.

Furthermore, examination of bone marrow aspirates by light microscopy can reveal histopathologic changes of erythoid precursor cells, suggestive of parvovirus B19, such as abnormal giant pronormoblasts or "lantern" cells (Török, 1992; Brown and Young, 1995). These cells have a markedly enlarged size and basophilic cytoplasm, fine nuclear chromatin, prominent irregular nucleoli, or viral inclusions. Occasionally, vacuoles and pseudopods can also be seen. In addition to pronormoblasts, in a paediatric patient with acute anemia, some "lantern" cells, which contained a central clear area and reacted strongly in the presence of a parvovirus-specific monoclonal antibody, have been described (Jordan and Penchansky, 1995). Hence, a morphologic description of the bone marrow aspirate could lead the pathologist to the diagnosis of B19 infection, and thus is of major importance, especially when other tests, such as PCR, are not available.

Lastly, skin lesions can also be examined by light microscopy and using immunohistochemistry with anti-human B19 monoclonal antibodies in order to locate virus particles in the cytoplasm of endothelial cells (Takahashi *et al.*, 1995). B19 should be considered as part of a differential diagnosis in any patient presenting anaemia associated with low or absent reticulocytes, especially for those immunosuppressed individuals (Brown, 2000). The detection of morphologic changes may be

complementary to a variety of methods which are used to detect anti-B19 antibodies, B19 virus and viral antigens, as well as B19 genome.

I.1.5.2. Diagnosis by antibody detection

In immunocompetent hosts, B19-specific IgM are the first antibodies to be produced, thus assays for IgM detection can be used to diagnose acute or recent infection. IgM can indeed be detected in more than 90% of cases by the third day of transient aplastic crisis (TAC), or at the time of rash in EI, and can remain for up to 3 months (Anderson and Young, 1997). On the other hand, IgG antibodies become detectable several days after IgM and persist for years and are thus regarded as indicative of a past infection, either resolved or chronic. At present, only IgM and IgG directed against the capsid proteins VP1 and VP2 are used for diagnosis. In immunocompromised patients, B19 specific immune response may be normal, altered and even absent. Therefore, serological investigation is not the main tool to diagnose B19 in these subjects.

Antibodies to the non-structural protein NS1 may also be of interest as a supplementary assay in routine testing, since they may be related with persistent B19 infection or B19-associated arthritis (Von Poblotzki *et al.*, 1995a; 1995b). As these antibodies usually become detectable at least 6 weeks after infection, their detection in pregnant women with borderline or weakly positive IgM results may be fairly common during pregnancy (Searle *et al.*, 1998). However, only 30% of women in childbearing age were shown to produce anti-NS1 antibodies, thus limiting the potential use of anti-NS1 antibodies for diagnosis. IgA antibodies are too persistent to be a useful indicator of recent B19 infection (Erdman *et al.*, 1991) and the usual assays used are various assays for detection of IgM and IgG antibodies.

I.1.5.2.1. Immunoblot assays

Immunoblot assays have been used extensively to measure both B19 IgM and IgG antibody responses and although these assays have problems with sensitivity and specificity and are labour-intensive, they allow the characterisation of antibody response to discrete B19 proteins (Schwarz *et al.*, 1988; Anderson and Young, 1997). Immunoblots, also called Western blot assays, are now commercially available. The technique uses either recombinant or native B19 antigens, which are electrophoresed in denaturing gels and then transferred onto nitocellulose membranes. The immobilised antigens are exposed to patients' sera, followed by enzyme-linked secondary antibody and, finally, a colorimetric substrate to visualise the immunoreactive bands (Palmer *et al.*, 1996). The sensitivity of the assay may be improved by developing a chemiluminescent Western blot assay with a high-performance, video camera-based system (Manaresi *et al.*, 1999b). While Western blot assays are able to detect immune response against B19 VP1 and VP2 linear epitopes, ELISA is used to determine the immune status against conformational epitopes (Kerr *et al.*, 1999; Söderlund *et al.*, 1995a).

I.1.5.2.2. Enzyme immunoassays (EIA)

The early IgM immunoassay was based on an IgM antibody capture radioimmunoassay (MACRIA) and used to diagnose infection in children with sickle cell anaemia recovering from aplastic crisis (Anderson *et al.*, 1982a). At the time, sources of antigen were sera or blood units obtained while in the phase of viraemia. In this assay, IgM from a dilution of patients' serum is "captured" onto a solid phase coated with anti-human IgM. B19 antigen is then added, followed by a detection system. This method is easier to perform and more sensitive than CIE testing of gradient separated IgM fractions of serum (Kelleher *et al.*, 1983). However, one of the disadvantages of

MACRIA is that it uses large amounts of antigen. Development of an antibody-capture assay, based on monoclonal antibodies to B19, for B19-specific IgM and IgG resulted in improved sensitivity (Cohen *et al.*, 1983). Further improvements in sensitivity were obtained by use of a detection system that included a mouse monoclonal antibody to B19 and a ^{125}I-labelled anti-mouse antibody (Cohen, 1997). This assay is used to detect IgM antibodies and can thus be valuable for the diagnosis of recent acute B19 infection. Other groups have developed sensitive ELISA assays, one of which was shown to have comparable sensitivity to DNA spot hybridisation using crude plasma (Anderson *et al.*, 1986, Schwarz *et al.*, 1988). ELISA assays are easier to perform, can be used for mass screening to detect B19 positive plasma and are good non-isotopic alternatives to RIA.

Due to the limited availability of B19 native antigens, several authors have reported attempts to develop diagnostic tests based on renewable sources of B19 antigens using synthetic peptides or recombinant antigens expressed in a baculovirus system (VP2 alone or VP1 and VP2) (Brown *et al.*, 1990a; Schwartz *et al.*, 1991a; Fridell *et al.*, 1991; Kajagaya *et al.*, 1991; Salimans *et al.*, 1992; Jordan, 2000). Compared with an IgM assay using native B19 viral antigen, one of the peptide antigen assays was 92% sensitive and 87% specific (Fridell *et al.*, 1991). This assay showed good correlation with a RIA which used native B19 virus, confirming the importance of recombinant B19 antigens as a substitute for native virus. Lastly, a study showed that a Baculovirus-expressed VP2 EIA produced fewer equivocal results and proved to be the most accurate test to detect B19 antibodies in pregnant women compared with an *E.coli*-based VP1 EIA for the detection of both IgM and IgG in sera (Jordan, 2000).

In EIA commercial kits for B19 diagnosis, IgM antibodies are mainly detected in capture-EIA format, whereas IgG antibodies are usually revealed using indirect ELISA format with antigen coated onto a solid phase (Zerbini *et al.*, 2002). A comparison of

four commercially available IgM EIA to indirect immunofluorescence and PCR assays showed that the relative sensitivities and specificities of the ELISA assays ranged from 97 to 100% and from 81 to 99%, respectively (Sloots and Devine, 1996). Moreover, rubella IgM cross-reactivity was found as particularly problematic in several commercial assays. A similar study of a number of commercial assays showed specificities for B19 IgM antibody detection between 88 and 96% and again a tendency for cross-reactivity with IgM against rubella, as well as Epstein Barr virus (EBV) and CMV was noted (Tolfvenstam *et al.*, 1996). Other comparative studies of commercial EIA assays for IgM found specificities ranging from 70.1% to 93.5% and sensitivities in the range 97.4% to 97.5% (Bruu and Nordbø, 1995; Pickering *et al.*, 1998). However, it is likely that these comparative studies have little value in deciding which test format to use for B19 diagnosis because of the lack of data on the absolute assay performance and reproducibility (Doyle *et al.*, 2000). In addition, external regulatory bodies rarely control in-house assays, resulting in poor standardisation. The first parvovirus IgM EIA to be cleared by the US Food and Drug Administration (FDA) was reported in 2000 (Doyle *et al.*, 2000). There was no cross-reactivity with sera from patients with rubella, CMV, VZV, mumps or rubeola, all of which could theoretically be confused with parvovirus B19 infection.

EIA have also been used to measure IgG avidity to discriminate primary and secondary infections. In the avidity assay, the patients' antibodies are first allowed to bind to an immobilised antigen, then low-avidity antibodies, characteristic of primary infections, are eluted with a denaturing agent. The remaining antigen-bound IgG is quantified immunoenzymatically (Söderlund *et al.*, 1995b; Manaresi *et al.*, 2001). This assay can be used as a complement to IgM antibody assay.

I.1.5.2.3. Immunofluorescence assay (IFA)

Indirect IFA for serum B19-specific IgG and IgM antibodies can be used with recombinant baculovirus expressing either VP1 or VP2 antigen. Insect cells infected with this recombinant baculovirus expression system are then spotted and fixed onto glass slides. A series of incubations and washes are then carried out: first with dilutions of the serum to be tested, followed by goat-anti-human IgG or IgM conjugated with fluorescein isothiocyanate (FITC). Slides are mounted and examined under the fluorescence microscope and the IFA titres determined. A good correlation between IFA results and those obtained with solid-phase capture RIA have been reported although IFA has the advantage of being based on a renewable source of antigen (Brown *et al.*, 1990b; Cohen *et al.*, 1983). Moreover, a later study showed comparable sensitivity of IgG detection by indirect enzyme immunoassay and IFA, with more than 95% acute infection confirmed by the latter (Pereira *et al.*, 2001). In conclusion, although determination of antibody responses can be useful tools for the diagnosis of B19 infection, these assays can also be inconvenient because of the requirement for two serum specimens, resulting in diagnostic delays.

I.1.5.3. Diagnosis by B19 virus and viral antigens detection

I.1.5.3.1. B19 virus

EM and IEM are sometimes used to confirm positive results obtained by other assays and have also proven useful for antenatal diagnosis and in adult cases to examine erythematous skin lesions and confirm B19 infection (Naides and Weiner, 1989; Takahashi *et al.*, 1995). In IEM, B19-specific antibodies are added to the serum samples in order to aggregate viral particles, if present. These aggregates are easier to see than single particles would be by direct EM. Both EM and IEM require technical expertise and costly specialised equipment and cannot be applied to the diagnosis of a large

number of samples (Zerbini *et al.*, 2002). Moreover, serum specimens have to be collected during the early phase of infection when the virus titre is high.

I.1.5.3.2. B19 antigens

I.1.5.3.2.1. Counter-immunoelectrophoresis (CIE)

In early B19 studies, CIE was widely used to detect B19 antigens in serum samples and thus determine acute infection. In this method, wells punched in agarose gel near the cathode are filled with test serum while the opposite wells, near the anode, are filled with B19 antibody positive serum. When the antigens and antibodies meet and form immunocomplexes, a visible line of precipitate appears on the gel (Zerbini *et al.*, 2002). CIE can only detect B19 in blood samples containing 10^6 particles/ml or more and can thus diagnose primary B19 infection only when the virus titre is at a peak. Since CIE is quite insensitive, it has now been replaced by other techniques.

I.1.5.3.2.2. Radioimmunoassays (RIA) and enzyme immuno-assays (EIA)

The development and use of RIA and EIA for the detection of B19 antigens has improved sensitivities and specificities with respect to CIE and IEM. In these assays, a human reference immune serum is absorbed to a solid phase and captures B19 antigens present in serum sample. The immune complexes can then be detected by either I^{125} or enzyme labelled anti-mouse immunoglobulin for RIA and EIA, respectively (Anderson *et al.*, 1986; Cohen *et al.*, 1983). However, virus in immune complexes with early specific host antibodies may be masked from detection, as with CIE.

I.1.5.3.2.3. Blot immunoassays

Blot immunoassays have been developed in two formats: Western blot and dot-blot. In Western blot, human serum is electrophoresed and transferred onto a nitrocellulose membrane, which is then treated with B19-specific monoclonal antibodies. Immunocomplexes formed are visualised by addition of enzyme-conjugated anti-mouse antibody, followed by a colorimetric substrate. The dot-blot format can be used to test both serum samples and amniotic fluids, which are treated to expose the antigenic sites on the virions and to avoid the masking of the antigens by early specific host antibody. These samples are then directly placed onto a nylon membrane as a drop. This dot-blot immunoassay is performed in only four hours and is particularly suitable for large-scale screening of samples (Gentilomi *et al.*, 1997). Moreover, the assay has a comparable, or slightly higher, sensitivity than that achieved by dot-blot hybridisation technique but less than that achieved by nested PCR.

I.1.5.3.2.4. Receptor-mediated haemagglutination assay (RHA)

RHA is a detection assay based on the agglutination of RBCs when mixed with serum containing parvovirus B19 (Sato *et al.*, 1995). This reaction is pH-dependent and inhibited by purified globoside-B19 receptor, as well as by neutralising antibodies. The sensitivity of this method is between 10^5 and 10^6 genome copies/ml, which is almost as sensitive as RIA but much lower than PCR. However, it is simple and rapid to perform (the results are available in one day), can be suitable for large-scale screening and has the advantage of detecting only the virus particles that can bind to the receptor. A similar assay was developed in the UK (Cohen *et al.*, 1995).

I.1.5.4. Diagnosis by B19 DNA detection

The limitations of RIA assays can be avoided by an assay based on detection of the viral genome, rather than the capsid antigen, by dot-blot hybridisation, microwell hybridisation, *in situ* hybridisation and by amplification.

I.1.5.4.1. Dot-blot hybridisation assays

A dot-blot hybridisation assay for detecting viral DNA uses serum specimens, which are filtered and spotted onto a nylon membrane. Different types of probes are then used, including single and double stranded DNA (Prato *et al.*, 1991; Clewley, 1985). A single stranded RNA probe that eliminates the risk of contaminating plasmid sequences has been described but extra caution is needed in handling such RNA probes (Cunningham *et al.*, 1988; Zerbini *et al.*, 1993). DNA probes have been reported to be about ten-fold more sensitive than RNA probes (Salimans *et al.*, 1989a). Most hybridisation probes are obtained from cloned B19 DNA fragments (Clewley, 1985; Azzi *et al.*, 1990; Prato *et al.*, 1991; Zerbini *et al.*, 1993), but can also be prepared by PCR amplification (Hicks *et al.*, 1995; Zerbini *et al.*, 2000; Zerbini *et al.*, 2001) or synthetic oligonucleotides (Cubie *et al.*, 1995). Initial detection methods used hybridisation to ^{32}P-labelled probes (Anderson *et al.*, 1985b; Clewley, 1985). These were replaced with biotin probes which eliminated the disadvantages associated with radioactivity (Cunningham *et al.*, 1988). At present, digoxigenin is widely used since it is as sensitive as radioisotopes and more specific than biotin (Azzi *et al.*, 1990; Prato *et al.*, 1991; Hicks *et al.*, 1995; Zerbini *et al.*, 2001). Both digoxigenin-labelled probes and biotinylated probes can be stored at -20°C for months without loss of activity (Cunningham *et al.*, 1988; Azzi *et al.*, 1990).

The detection system for hybridisation assays can be an immuno-enzymatic or a chemiluminescent reaction. In the former, antibodies against the probe are conjugated

with alkaline phosphatase, which generates a colorimetric reaction. A variation of this technique uses a tyramide signal amplification for biotinylated probes (Zerbini *et al.*, 2000). This method uses a horseradish peroxidase-streptavidin complex to catalyse the deposition of biotinyl-tyramide conjugate and streptavidin coupled to alkaline phosphatase to amplify the signal. A 10 to 50 times increase was observed when compared to detection with alkaline phosphatase (~10^5 genome copies). Improved sensitivities are obtained using a chemiluminescent substrate (Zerbini *et al.*, 1993; Zerbini *et al.*, 2001). An initial study showed that the chemiluminescent reaction had a sensitivity of $6x10^3$ virus particles compared with an immuno-enzymatic reaction which was able to detect $1.5x10^4$ virus particles (Zerbini *et al.*, 1993). A second study in 2001 showed improved sensitivities for both methods of detection, although that of chemiluminescence (~$6x10^2$ genome copies) was higher than that of immuno-enzymatic reaction (~$3x10^3$ genome copies) (Zerbini *et al.*, 2001). Chemiluminescence detection offers the advantage of a permanent record of the reactions, whereas membranes stained with a colorimetric substrate can lose colour over time. Moreover, the latter often present a strong background, resulting in difficulty in interpreting results.

Unlike CIE and RIA, dot-blot hybridisation assay is not affected by the presence of B19-specific antibodies in host serum and allows testing of large numbers of specimens since 1,000 blood donor plasma samples can be tested per day. Moreover, in terms of virus particles detected, the dot-blot assay is more than 300 times more sensitive than RIA, partly because the assay uses a much smaller volume (Anderson *et al.*, 1985b). On the other hand, the detection of DNA by dot-blot hybridisation has limited value for the diagnosis of past B19 infections since the virus is detectable for only one week during viraemia.

I.1.5.4.2. *In situ* hybridisation assays (ISH)

ISH is an important tool for localisation of B19 DNA within individual cells and has been used in bone marrow cells, amniotic fluid cells, cord blood cells and fetal cells (Zerbini *et al*, 2002). The probes for *in situ* hybridisation have been made either from cloned DNA fragments or from synthetic oligonucleotides (Cubie *et al.*, 1995). ISH with cloned probes can be labelled with radioisotopes, biotin (Porter *et al.*, 1988), acetyl-aminofluorene (Salimans *et al.*, 1989b) or digoxigenin (Morey *et al.*, 1992). Non-radiolabelled probes have been reported to be more sensitive than radiolabelled probes for *in situ* hybridisation on fixed tissues from a hydropic fetus (Salimans *et al.*, 1989b). However, while biotinylated probes offered advantages over radioactive probes, positive results should be confirmed by other methods (Cubie *et al.*, 1995). Since individual, infected cells can be examined, the apparent sensitivity of ISH is greater than with DNA amplification applied to a tissue sample consisting of many cells only a few of which are infected. Detection by ISH has the advantage of identifying the virus and relating its distribution to tissue morphology.

I.1.5.4.3. DNA amplification

The technique of DNA amplification, commonly known as PCR (Mullis *et al.*, 1986; Mullis and Faloona, 1987), has vastly improved the sensitivity of detection of B19 DNA compared with other methods. Studies have shown that B19 DNA is detectable longer by PCR than was earlier suggested by nucleic acid hybridisation studies (Anderson *et al.*, 1985a; 1985b). It has been reported that the sensitivity can be improved by transfer of the DNA to a nylon membrane and hybridisation with a radioactive labelled probe (Salimans *et al.*, 1989a; Salimans, 1990). Compared with conventional gel electrophoresis of the amplified DNA, hybridisation of the PCR products increased the

sensitivity from 10^3-10^4 particles/ml to as few as 100 particles/ml. Various studies, using modification such as nested PCR, PCR alone with subsequent hybridisation and dot-blot hybridisation to detect B19-specific products, have reported even greater sensitivity of B19 DNA detection down to a single copy (Clewley, 1989; Koch and Adler, 1990; Frickhofen and Young, 1990; Cassinotti *et al.*, 1993a).

The most important drawback associated with this technique is the risk of contamination due to carry-over between samples from the first to the second PCR round, resulting in false positive results. In order to overcome these contamination problems extensive and extremely strict precautions should be taken during the handling of materials (Kwok and Higuchi, 1989). Additionally, only trained personnel should perform the assays in three separate laboratories, ideally equipped with a laminar flow cabinet and without cross-traffic of staff. Lastly, each sample should be tested in duplicate and several negative controls should be included in each PCR reaction. Another disadvantage of this technique is the high cost of screening a large number of samples. On the other hand, this method is highly specific and the most sensitive assay available at present. It can also be applied to a large variety of clinical materials, such as blood, bone marrow, urine, ascites and leukocyte extracts, as well as synovial and amniotic fluids, fetal and maternal blood (Koch and Adler, 1990; Cassinotti *et al.*, 1993a; Dieck *et al.*, 1999). Parvovirus DNA was also amplified from a cutaneous biopsy specimen during the acute phase of the disease in a case of popular purpuric "gloves-and-socks" syndrome (Grilli *et al.*, 1999). Lastly, results can be reported, depending on laboratories, within 1.5 to 2 days, making PCR an important tool for the early diagnosis of B19 infection.

Studies have shown circulating virus may present with IgM but can only be detected by PCR (Musiani *et al.*, 1993). This is a very important aspect of B19 detection, particularly in immunocompromised patients who often have a low-titre viraemia undetectable by conventional nucleic acid hybridisation techniques. PCR is thus the most suitable, and possibly the only, method of detection of B19 in such patients.

Sensitivity of detection being the major focus of any assay, further research has been undertaken recently to develop very sensitive detection methods for B19 DNA, especially useful for blood products testing. A PCR assay coupled with a hybridisation protection assay, using acridinium ester-labelled DNA probes to detect the amplified products claimed a sensitivity of a single copy in 10µl (100 copies/ml) (Sato *et al.*, 2000). In laboratory diagnostics, PCR assays are usually performed with qualitative methods but several semi-quantitative or quantitative methods have also been reported. These include competitive PCR assays and hybridisation of PCR products to probes in microtitre plates, with either chromogenic or chemiluminescent reaction as a detection system (Gallinella *et al.*, 1997; Gruber *et al.*, 1998; Fini *et al.*, 1999). However, these established methods are time-consuming, labour intensive and require post-PCR handling steps, which may lead to contamination, and lack of standardisation. On the contrary, the recently developed real-time PCR offers rapidity, monitoring of PCR activity as it happens, the potential to eliminate carry-over contamination due to the combination of amplification and detection in closed tube systems, and a quantitative analysis. Two different instruments can be used for this fluorescence-based assay: the ABI PRISM SD7700 system (PE Biosystems), otherwise known as TaqMan, and the LightCycler system (Roche Molecular Biochemicals). The latter (figures 1.11 and 1.12) has recently been used to detect PPV and to quantify the virus load in tested specimens (Krumbholz *et al.*, 2003). The ABI PRISM SD7700 system has been used for the

development of a real-time PCR method that included duplex amplification, internal standardisation and two-colour fluorescence detection (Gruber *et al.*, 2001). It has also been used to screen and identify blood donations containing high titres of B19, thereby improving the safety margin of plasma and plasma products (Aberham *et al.*, 2001) while the LightCycler technology has been useful to evaluate large numbers of serum specimens (Manaresi *et al.*, 2002b). High levels of sensitivity and specificity were found for the detection of B19 DNA. The LightCycler instrument was used in the present study.

Figure 1.11: The LightCycler instrument

As shown in figure 1.12, the LightCycler instrument consists of an upper unit with the heating coil and a lower unit, which contains the thermal chamber, fluorimeter, drive

units, electronic boards and power supply. During measurements, a stepper motor rotates the sample carousel to position the capillary tip, which contains the sample, precisely at the focal point of the fluorimeter optics.

Figure 1.12: Schematic of the LightCycler instrument (Source: operator's manual)

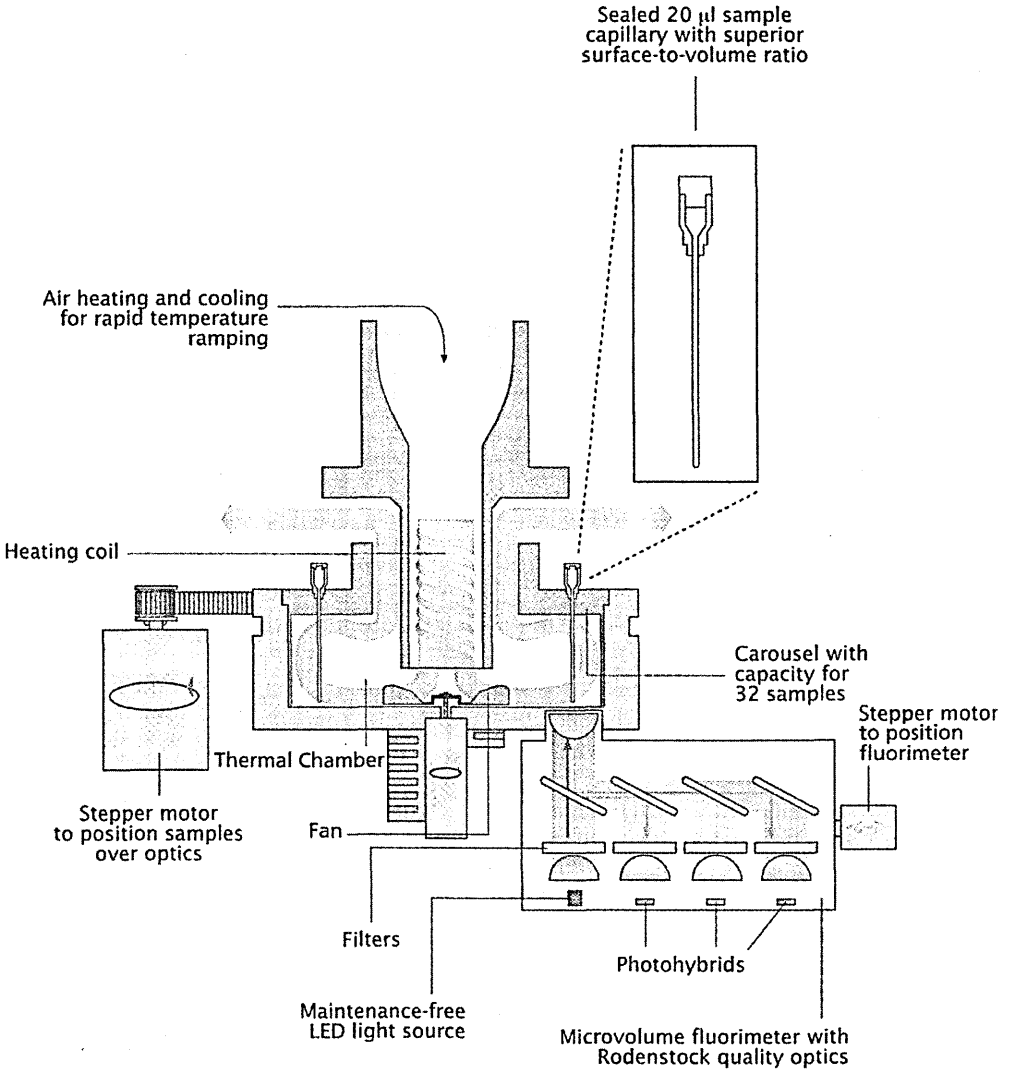

The kinetics of nucleic acid amplification by PCR has two phases: the exponential phase and the plateau phase. The former reflects the generation of PCR product molecules, which is directly proportional to input target molecules per PCR cycle.

During the plateau phase, there is little or no net increase in PCR product yield. Quantification of DNA is therefore possible during the exponential phase and can be one of two kinds: relative or absolute. The relative quantification is the determination of the target gene ratio in two samples. The advantage of this quantification is that no absolute concentration of target or reference is necessary. On the other hand, absolute quantification is the determination of the absolute amount of target molecules by using an internal or external standard (copy number, mass, etc.).

A standard curve is usully generated by using a well established external reference reagent such as the WHO B19 International Standard (IS) which allows consistent quantitation of B19 DNA over 7 orders of magnitude (Saldanha *et al.*, 2002). In order to quantify PCR product, the instrument has to acquire fluorescence once per cycle, thereby generating a fluorescence curve that increases in value with each cycle as the product accumulates. The most useful data can be found in the log-linear portion of the fluorescent curve and starts at the cycle number where fluorescence rises above background. The LightCycler software generates a best-fit line from this region of each curve called a crossing line. The crossing point (C_T) is then determined as the intersection between the crossing line and the log-linear region of the fluorescent curve. The crossing point values for a set of standards can be plotted against known $\log_{10}$ concentration to give a standard curve.

The PCR efficiency, which is a critical factor, can be calculated as shown in figure 1.13. An efficiency of 1.00 (100% doubling per cycle) is attained when the slope is -3.33 whereas PCR efficiency of 0.78 (78% doubling per cycle), which is the cut-off level, is obtained when the slope is -4.0. Any slope that is less than -3.33 would represent more than 100% efficiency, which is impossible and should therefore be disregarded.

Figure 1.13: Calculation of PCR efficiency

(Source: Qiagen seminar on strategies for quantification and lab results)

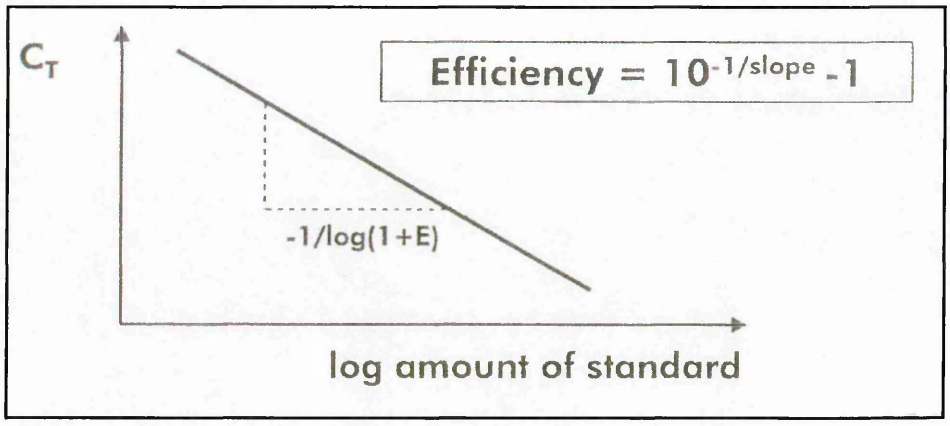

By comparing the C_T of an unknown sample with the standard curve, the LightCycler instrument generates a quantitative estimate of the starting concentration of the target DNA in that sample (figure 1.14).

Figure 1.14: Calculation of target concentration using the standard curve

(Source: Qiagen seminar on strategies for quantification and laboratory results)

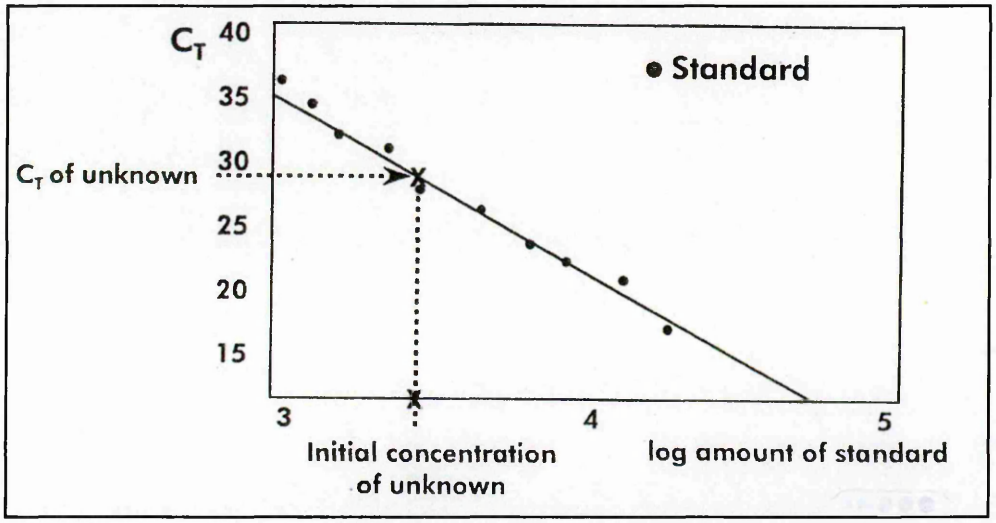

Comparison of compiled PCR and serological results showed that single serologic testing on a given clinical sample is highly inappropriate for the diagnosis of B19 infection (Cassinotti *et al.*, 1993a). A recent study showed that, although IgM ELISA was able to detect only 60% of infections, IgM antibodies were the unique diagnostic markers in 20.8% of infections and are thus fundamental for the diagnosis of recent and symptomatic infections where B19 DNA is no longer detectable (Gallinella *et al.*, 2003). PCR was able to detect 79.2% of documented infections and the presence of B19 DNA was the unique marker in as much as 32% of cases, making it fundamental for the detection of B19 acute infections, especially before onset of immune response. Dot-blot hybridisation was not sensitive enough to detect either all early acute infections or persistent infections in which IgM was not detectable. Hence, the most appropriate diagnosis should include determination of both B19 DNA by PCR and specific IgM by ELISA (Gallinella *et al.*, 2003).

I.1.6. Clinical features

I.1.6.1. Asymptomatic infection

Most individuals with B19-specific antibodies have no recollection of previous symptoms and thus asymptomatic infection is considered common. Studies have shown that 26%-31% of adults exposed to the virus, in a school outbreak or via household contact, were asymptomatic (Woolf *et al.*, 1989; Chorba *et al.*, 1986). In addition, differential rates of asymptomatic infection among black (68.8%) and white (20%) household members have been recorded but this is to be expected, as the characteristic rash of B19 infection is more difficult to detect on a dark skin (Chorba *et al.*, 1986). Although asymptomatic infection is common, a wide spectrum of clinical manifestations can result from B19 infection.

I.1.6.2. Dermatologic manifestations

B19 infection as been shown to cause a wide spectrum of dermatologic manifestations, including two specific B19-related dermatologic diseases: EI and papular purpuric "gloves-and-socks" syndrome (PPGSS), as well as other non-specific findings linked to parvovirus infection (Seishima *et al.*, 1999; Katta, 2002).

I.1.6.2.1. Erythema infectiosum (EI)

EI, also known as fifth disease, slapped cheek disease, academy rash or Sticker's disease, is the major manifestation of B19 infection. However, the distinct clinical features of EI were recognised long before the discovery of the aetiologic agent. The first description of this exanthematous rash illness of childhood was reported two centuries ago by a dermatologist, Robert Willan (Van Elsacker-Niele and Anderson, 1987). The first picture of a child with EI, called "rubeola sine catarrho" at the time, was shown in his dermatology book, written around 1800 (Figure 1.15). The rash was given the different names listed above, including fifth disease, as it was the fifth of the originally described childhood exanthematous diseases. It was thought that rubella virus could be associated with EI, but a study of a school outbreak revealed that a history of rubella vaccination did not affect the risk of developing EI (Lauer *et al.,* 1976). Moreover, no rubella virus could be recovered from the children's throat swabs.

The first reported EI in association with human parvovirus B19 was in 1983, during an outbreak in a London school, UK (Anderson *et al.*, 1983). Soon after, two studies from Japan confirmed the link between fifth disease and B19 infection (Nunoue *et al.*, 1985; Shiraishi *et al.*, 1985). In the first study, anti-B19 IgM antibodies were detected in 33 of 34 affected children (97%) but only in 21 of 141 healthy children (15%) while in the second study, B19-specific IgM was detected in all 19 patients tested.

Figure 1.15: First picture of a child with EI (Van Elsacker-Niele and Anderson, 1987)

The course of EI can be divided into three stages, the first occurring after an incubation period of four to fourteen days (Sabella and Goldfarb, 1999). This phase, often unrecognised, corresponds to a period of viraemia where the patient is contagious and can experience low fever, headache and gastrointestinal symptoms. The second stage of the illness, three to seven days later, is characterised by the distinctive "slapped cheek" appearance, a bright erythematous facial exanthem associated with surrounding relative pallor (figure 1.16). These clinical features vary depending on the age of the patient: in children, the classic rash described here is commonly present whereas in adults, it is more subtle and unusual.

Figure 1.16: Slapped cheek rash (courtesy of Dr B. Cohen)

The highest rate of fifth disease was found to be in the five to nine years-old age group (Kelly *et al.*, 1999). In adults, a higher incidence of associated arthralgia and arthritis was first recognised in 1966, and later confirmed in a second study (Ager *et al.*, 1966; Joseph, 1986). The third stage of EI occurs one to four days after the appearance of the facial rash and may last for one to three weeks, depending on exposure to sunlight, heat and stress (Anderson, 1987). This stage is characterised by a lacelike erythematous maculopapular exanthem on the trunk and/or the extremities. Patients presenting with such a rash are no longer contagious since it corresponds to the development of B19-specific IgM antibodies. Although the exanthem may recur or persist for several months, there are no long-term sequelae (Woolf *et al.*, 1989). In addition to the rash, generalised lymphadenopathy and splenomegaly was observed in a few patients (Plummer *et al.*, 1985). Lastly, the prevalence of the symptoms associated with EI can vary between outbreaks and individuals.

I.1.6.2.2. Papular purpuric "gloves-and-socks" syndrome (PPGSS)

PPGSS was first described in 1990 and associated with an acute infection by B19 in 1991 (Harms *et al.*, 1990; Bagot and Revuz, 1991). This distinctive painful rash takes its name from a symmetric erythema and oedema of the hands and feet, usually sharply demarcated at the wrists and ankles where the lesions progress gradually to purpura. The rash has mainly been described in young adults, although it has also been reported in children (Seabury Stone and Murph, 1993; Labbé *et al.*, 1994). Other body parts can occasionally be affected, including cheeks, elbows, knees, inner thighs and buttocks (Harms *et al.*, 1990; Nelson and Stone, 2000). Systemic symptoms in immunocompetent patients including fever, anorexia and arthralgias and lymphadenopathy have also been observed (Harms *et al.*, 1990; Bagot and Revuz, 1991). PPGSS usually resolves spontaneously within one to two weeks with no permanent sequelae whereas, in immunosuppressed patients, it may result in serious complications. For example, it has been reported that three HIV-positive patients who presented serological evidence of acute B19 and clinical signs of PPGSS, displayed persistent anaemia and prolonged skin lesions (Ghigliotti *et al.*, 2000). It is important to note that, unlike patients with EI, individuals suffering from PPGSS are considered contagious when the rash is present (Nelson and Stone, 2000).

I.1.6.2.3 Other dermatologic manifestations

Another clinical disease associated with B19 is a purpuric rash-like illness, often with other signs of vasculitis (Lefrère *et al.*, 1985b; Mortimer, 1985; Li Loong *et al.*, 1986). A case of a 27-year-old woman with a rash atypical for EI because of the presence of a haemorrhagic exanthem and an area of near-confluent pustules and pseudo-pustules

with a slightly purpuric base has been reported (Naides *et al.*, 1988). Various eruptions such as erythema nodosum may also appear in the viraemic phase of B19 infection (Borreda *et al.*, 1992).

I.1.6.3. Haematologic manifestations

I.1.6.3.1. Transient red blood cell aplasia or aplastic crisis (TAC)

TAC, which is the abrupt onset of severe anaemia with absent reticulocytes, can occur as a unique event in the life of patients with a variety of underlying haematologic abnormalities. The first link between TAC and B19 was made in 1981 when parvovirus B19 was detected in a child with sickle cell anaemia hospitalised for aplastic crisis (Pattison *et al.*, 1981). Further evidence, such as B19 viraemia, and a higher prevalence of B19-specific antibodies in TAC patients with sickle cell disease than in controls, supported this link (Pattison *et al.*, 1981; Serjeant *et al.*, 1981). Other studies have demonstrated B19 viremia and/or the presence of specific IgM in all nine children with sickle cell disease suffering from aplastic crisis (Anderson *et al.*, 1982b).

Since parvovirus B19 infects erythroid progenitor cells in the bone marrow and causes temporary cessation of red blood cell production, patients who have underlying haematologic abnormalities are prone to cessation of RBC production if they become infected. These patients consist of those suffering from decreased red cell production or increased destruction or loss. The former include α- and β-thalassemias (Chorba *et al.*, 1986; Lefrère *et al.*, 1986a; Lefrère *et al.*, 1986b; Lefrère and Decazes, 1986) and patients with iron deficiency (Lefrère and Bourgeois, 1986; Graeve and Elliott, 1991).

Infection can also cause TAC in individuals with increased red cell destruction or loss, such as in hereditary spherocytosis (Lefrère *et al.*, 1986a; Lefrère *et al.*, 1986c; Lefrère

and Decazes, 1986; Saarinen *et al.*, 1986; Baurmann *et al.*, 1992), sickle cell disease (Anderson *et al.*, 1982b; Chorba *et al.*, 1986; Lefrère *et al.*, 1986a; Lefrère and Decazes, 1986; Saarinen *et al.*, 1986), pyruvate kinase deficiency (Duncan *et al.*, 1983) and autoimmune haemolytic anaemia (Lefrère *et al.*, 1986a; Tomiyama *et al.*, 1988). The result of all these studies suggests that, in predisposed individuals, 60 to 70% of TAC cases are caused by B19 infection (Heegaard and Brown, 2002). Laboratory findings reveal reticulocytopenia (0 to 1% reticulocytes) and anaemia with haemoglobin concentrations falling dramatically (5g/dL) (Sabella and Goldfarb, 1999). Although recovery often follows the appearance of specific antibodies, severe disease with heart failure can be life threatening.

When hospitalisation is required, patients can be monitored and treated with red blood cell transfusions and clinical symptoms usually resolve within 3 to 6 days (Anderson, 1987). Unlike EI, these patients are often viraemic and therefore still contagious and need to be kept in respiratory isolation to prevent nosocomial transmission. Such transmissions have been documented where two outbreaks of EI among nursing staff were caused by two adolescent patients with sickle cell disease and aplastic crisis (Bell *et al.*, 1989).

Parvovirus-induced red blood cell aplasia has also been reported in a child with no underlying haemolytic anaemia (Murray *et al.*, 1993). In a study of volunteers, all four infected subjects had a reticulocytopenia, neutropenia, thrombocytopenia, lymphopenia and a gradual fall in haemoglobin, suggesting that reticulocytopenia can occur in any B19 infection, but usually disappears before development of a rash (Anderson *et al.*, 1985a). In a patient without shortened red cell survival time, the haemoglobin level is not low enough to be symptomatic or to be considered low. Thus anaemia, the other marker of TAC, often fails to be noticed (Anderson, 1987). However, there is no

evidence to support the role of B19 infection in transient erythroblastopenia of childhood (TEC) (Bhambhani *et al.*, 1986, Skeppner *et al.*, 2002).

Lastly, it is important to note that parvovirus-induced TAC has previously been mistaken for myelodysplastic syndrome (MDS), which comprises a heterogeneous group of clonal stem cell disorders characterised by blood cytopenia and dysplastic traits in the bone marrow (Baurmann *et al.*, 1992; Hasle *et al.*, 1994). It was therefore recommended that parvovirus B19 be considered in the differential diagnosis of MDS in both children and adult patients.

I.1.6.3.2. Bone marrow failure

Due to a bone marrow insufficiency triggered by B19 infection, immunocompromised patients are unable to mount a neutralising antibody response. This results in persistent B19 infection that may cause pure red blood cell aplasia (PRCA) and chronic anaemia. PRCA can be characterised as anaemia with the almost complete absence of RBC precursors in the bone marrow, but essentially normal granulopoiesis and megakaryopoisis (Fisch *et al.*, 2000).

Persistent B19 infection and resulting PRCA and chronic anaemia have been documented in five immunodeficient populations: congenital immunodeficiency, lymphoproliferative disorders, transplant patients, those with acquired immunodeficiency syndrome (AIDS) and those with haemophagocytic syndrome.

I.1.6.3.2.1. Congenital immunodeficiency

Several studies have reported the occurrence of PRCA in B19 infected individuals with congenital immunodeficiency, including combined immunodeficiency with immunoglobulins (Nezelof's syndrome) (Kurtzman *et al.*, 1987; 1989a; Gahr *et al.*, 1991). In such cases, the B19 infection resulted in severe bone marrow failure, with

erythroid hypoplasia and the presence of giant pronormoblasts. Studies on a patient with a 10-year history of PRCA showed a variety of symptoms starting with intermittent fever, back and abdominal pain and fatigue at an early age and progressing to anaemia which was finally corrected by immunoglobulin therapy (Kurtzman *et al.*, 1989a). Depressed serum antibody levels, low natural killer cell count and a high ratio of helper/suppressor T cells suggested underlying immunodeficiency. The notable feature of this case was that the patient's older brother had developed PRCA simultaneously but died later of sepsis and hepatic cirrhosis due to transfusion haemosiderosis. The post-mortem detection of B19 DNA in fixed spleen tissue confirmed chronic B19 infection in the sibling.

I.1.6.3.2.2. Lymphoproliferative disorders

Patients suffering lymphoproliferative disorders are mostly children with acute lymphoblastic leukaemia who are receiving chemotherapy. The latter is known to impair the immune system and thus persistent B19 infections with bone marrow failure have been described. Several case reports have linked B19 infection in children with malignancies with severe chronic anemia, bone marrow failure and severe prolonged cytopenia (Kurtzman *et al.*, 1988; Azzi *et al.*, 1989; Yoto *et al.*, 1993; Broliden *et al.*, 1998). Administration of immunoglobulin, as well as interruption of chemotherapy to reduce the level of immunosuppression may result in resolution of the B19-induced anaemia.

I.1.6.3.2.3. Transplant patients

Transplant recipients have to undergo immunosuppressive treatments, which make them susceptible to persistent B19 infection. B19 infection following kidney transplants can

result in a range of diseases from PRAC (Corral *et al.*, 1993; Uemura *et al.*, 1995; Holman *et al.*, 1997; Mathias, 1997), severe symptomatic anemia characterised by intranuclear inclusions in bone marrow and requiring transfusions (Pamidi *et al.*, 2000), and chronic anemia (Mathias, 1997). Such chronic B19 infection seems to be more common and severe in recipients of transplants that require more intensive immunosuppression, including liver and cardiac transplants (Thio and Janner, 1996; Anderson and Young, 1997; Wicki *et al.*, 1997). The presence of B19 DNA in a cardiac transplant recipient who presented with severe anaemia was demonstrated by PCR on the serum and a bone marrow aspirate revealed giant pronormoblasts, both findings implying an acute B19 infection (Thio and Janner, 1996). B19 was shown to be the causative agent for severe transfusion dependent anaemia in a lung transplant patient (Kariyawasam *et al.*, 2000) and severe anaemia with reticulocytopenia in two solid organ transplant recipients (one heart and one lung) (Wicki *et al.*, 1997).

Severe anaemia and PRCA have been reported in several cases following allogeneic bone marrow transplant (BMT) (Weiland *et al.*, 1989; Niitsu *et al.*, 1990). In the case of a patient who had suffered acute myeloid leukaemia and developed unexplained pancytopenia nine months after BMT, a bone marrow biopsy revealed a total absence of erythropoiesis and some enlarged cells with inclusions. A few weeks later, the patient developed a non-cardiogenic pulmonary oedema and died of an intracerebral haemorrhage. Post-mortem examination of the sera taken in the course of this illness revealed a prolonged B19 infection but the source of infection could not be determined (Weiland *et al.*, 1989). Similarly, a patient who had suffered acute promyelocytic leukaemia and developed PRCA one month after BMT was thought to have contracted parvovirus B19 from the platelet transfusion (Niitsu *et al.*, 1990).

However, an investigation of serum samples from 201 allogeneic bone marrow recipients, found 3 cases (~1.5%) of acute B19 infection during the second year following BMT, suggesting that B19 is not a frequent cause of anaemia, leukopenia or thrombocytopenia shortly after transplantation (Söderlund *et al.*, 1997a). Interestingly, the infections diagnosed during recovery may present either as primary or secondary immune responses, depending on the immune history of the donor but regardless of the serological status of the recipient before BMT. These findings have been confirmed by a study of 51 BMT recipients who did not develop B19 infection, at least until hospital discharge (Azzi *et al.*, 1993; Söderlund *et al.*, 1997a). It is possible that isolation measures and intravenous immunoglobulin treatment of these patients may have helped to prevent B19 infection.

I.1.6.3.2.4. AIDS

Due to the effect of the human immunodeficiency virus (HIV) on the cellular branch of the immune system, seropositive subjects have an impaired antibody production that can result in persistent infection. Persistent SPV infection and severe anaemia have been observed in monkeys with concurrent acute infection with simian immunodeficiency virus (SIV) (O'Sullivan *et al.*, 1996). This can also be applied to human parvovirus B19, since it was shown to persist in some AIDS patients who have developed PRCA (Frickhofen *et al.*, 1990) or chronic anaemia (Chernak *et al.*, 1995). Giant pronormoblasts in bone marrow suggested the diagnosis and B19 DNA was amplified intermittently over several months. One study found an unusual pattern in B19 infection in AIDS patients: the bone marrow was hypercellular and erythroid precursors increased with abundant intranuclear inclusions (Crook *et al.*, 2000). However, according to the authors, these findings are consistent with the hypothesis that failure to produce

effective B19-specific IgG neutralising antibodies may lead to persistent infection through viral tolerance. Although PRCA can be improved by immunglobulin therapy, some patients may develop EI symptoms, consistent with their immune complexes origin (Brown and Young, 1996). Moreover, a highly active antiretroviral therapy (HAART) that includes the use of protease inhibitors was found to play an effective role in clearing B19 virus leading to a complete remission of B19-associated PRCA, possibly due to an increase in cellular immunity due to HAART (Mylonakis *et al.*, 1999; Taguchi *et al.*, 2001). In a reported HIV positive case, HAART was shown to have restored the humoral immunity since the clinical course of primary B19 infection in this patient resembled that in an immunocompetent individual (Clarke and Lee, 2003). The prevalence of B19-associated anaemia has been investigated in two small-scale studies (10 and 50 individuals, respectively) and neither acute nor persistent B19 viraemia in any HIV-1 patients was reported (Goedert *et al.*, 1997; Anderson *et al.* 1985a). The rate of B19 infection in a larger cohort study of HIV-seropositive homosexuals was similar to that in the general population (0.5%) (Abkowitz *et al.*, 1993). Nevertheless, 4 of 24 (17%) transfusion-dependent HIV patients presented with B19 viraemia.

I.1.6.3.2.5. Virus-associated haemophagocytic syndrome (VAHS)

VAHS is characterised by histiocytic hyperplasia, prominent haemophagocytosis and cytopenia, as well as a systemic viral illness (Risdall *et al.*, 1979). Although VAHS is usually benign and self-limited, some patients present an underlying immunosuppression. Several studies have reported cases of malignant histiocytosis with PRCA as an unusual complication (Hanada *et al.*, 1986; Reiner and Spivak, 1988).

Parvovirus-associated VAHS have been observed in many cases in both adults and children (Uike *et al.*, 1993; Tsuda *et al.*, 1994; Shirono and Tsuda, 1995; Hoang *et al.*, 1998; Sadahira *et al.*, 1998). Although these studies suggest that B19 is not a rare cause of this condition, further research is needed to determine the role of B19.

I.1.6.3.3. Thrombocytopenia and neutropenia

A fall in white cell count was first noted in healthy volunteers infected with B19 (Anderson *et al.*, 1985a). Acute B19 infection and TAC are often associated with changes in the other blood lineages, resulting in neutropenia (Saunders *et al.*, 1986; Doran and Teall, 1988) and thrombocytopenia (Saunders *et al.*, 1986; Inoue *et al.*, 1991). The latter has shown to develop into idiopathic thrombocytopenic purpura (ITP) (Inoue *et al.*, 1991). The involvement of parvovirus B19 has been suspected in ITP since B19 DNA and/or IgM antibodies against B19, both markers of an acute infection, were detected in this population of patients (Foreman *et al.*, 1988; Lefrère *et al.*, 1989; van Elsacker-Niele *et al.*, 1996; Wehmeier *et al.*, 2000). B19-associated ITP were found in only 5% (Lefrère *et al.*, 1989), 1.7% (van Elsacker-Niele *et al.*, 1996) and 12% (Wehmeier *et al.*, 2000) of the investigated patients presenting ITP. The fact that the latter figure is higher than in the other two studies might be explained by the relatively small number of individuals included in the investigation. Parvovirus infection was suspected as the cause of chronic neutropenia of childhood in a study where B19 DNA by PCR was demonstrated in the bone marrow of 15 of 19 patients (79%), of whom only 6 had serological evidence of B19 infection (McClain *et al.*, 1993). In contrast, a later study detected B19 DNA in the bone marrow of only 1 of 56 (~2%) children and young adults with chronic neutropenia, suggesting no evidence of the involvement of the human parvovirus (Hartman *et al.*, 1994).

I.1.6.3.4. Vasculitis syndromes

Human parvovirus B19 has been associated with several systemic and local necrotising vasculitis syndromes, including polyarteritis nodosa (Corman and Dolson, 1992), Wegener's granulomatosis (Finkel *et al.*, 1994), Henoch-Schönlein purpura (Lefrère *et al.*, 1986d) and severe digital arterial occlusive disease (Dingli *et al.*, 2000). Although serological data, DNA detection by PCR and *in situ* hybridisation have suggested a link with B19, it may be that the virus is not directly responsible for the development of these diseases, but rather can aggravate the underlying disease (Bültmann *et al.*, 2003). Moreover, circulating immune complexes may worsen any preexisting vascular disorder. However, other studies have suggested B19 as the aetiologically responsible agent as immunoglobulin therapy led to rapid improvement of the systemic vasculitis manifestations in patients studied (Finkel *et al.*, 1994). Vascular events have also been reported in association with B19 infection and cerebral manifestations in sickle cell disease patients (Wierenga *et al.*, 2001).

I.1.6.4. Rheumatologic manifestations

Another common complication of B19 infection is joint involvement. However, compared with other infectious agents associated with arthritis, such as *Campylobacter* and *Chlamydia*, the prevalence of parvovirus B19 in adult patients with arthritis of less than 3 months' duration is low (<3%) (Söderlin *et al.*, 2003). Although rheumatologic manifestations only occur in 8% of infected children, they are more frequent in adults (60%) and especially in women (Török, 1992; Freitas *et al.*, 2002). While women usually develop an acute arthropathy with rash and flu-like illness, men rarely present joint symptoms (Woolf *et al.*, 1989). The most common presentation in adults was acute symmetric polyarthritis, usually starting 1 to 6 days after the eruption of the rash

(Scroggie *et al.*, 2000). The symptoms affect mainly the small joints of the hand followed by wrists, ankles, knees and elbows. Although the symptoms of arthropathy resolve within a few weeks in most cases, some patients (~20%) have been reported with chronic arthropathy for months to years (White *et al.*, 1985; Reid *et al.*, 1985; Woolf *et al.*, 1989). Parvovirus B19 arthropathy mainly affecting the wrists, elbows, shoulders and neck has been described (Luzzi *et al.*, 1985). Although the symptoms persisted for 8 months, the joints became normal to examination 2 months after onset. During this period, a rise in rheumatoid factor to high titre occurred and was noticed for the first time, suggesting that B19 might be responsible for the presence of rheumatoid factor.

B19 infections have also been linked to chronic arthropathy with an unusual involvement of some joints in the spine (Guillaume *et al.*, 2002) and to the development of a rash, stiffness and swelling of hands and arms (Sasaki *et al.*, 1995) in immunocompetent patients. The reappearance years later of fever, joint pain and a transient rash on hands and arms in some cases suggests that B19 may persist in bone marrow, where it may be reactivated. Several studies have reported viral arthritis and symptoms such as joint swelling, particularly of the hands, as well as pain and stiffness associated with lethargy and morning stiffness as common occurences in patients diagnosed with B19 infection (rash, EI, IgM seroprevalence) (Woolf *et al.*, 1989; Naides *et al.*, 1990; Cassinotti *et al.*, 1995). The presence of rheumatoid factor and B19 infection in arthritis patients is unclear: some studies have indicated an association (Jobanputra *et al.*, 1995, Luzzi *et al.*, 1985; Sasaki *et al.*, 1995) while others have failed to find a link between the presence of rheumatoid factor and B19 infection (Naides *et al.*, 1990).

Further studies have been reported on long-term follow-up of B19 infections with reference to chronic arthritis. In a study of 54 patients with recent B19 infections who had arthralgia, 72% presented with a skin rash, 64% with fever, 61% had arthritis (Speyer *et al.*, 1998). After a mean follow up of five years, arthralgia and malaise were still present in 40% of individuals but none of the patients reported persistence of joint swelling or restricted motion. In a survey involving patients with recent inflammatory polyarthritis, there was serologic evidence of recent B19 infection in just 4 of 147 patients (2.7%), only one of whom did not satisfy criteria for rheumatoid arthritis (RA) (Harrison *et al.*, 1998). Although these various findings tend to suggest that B19 does not typically cause chronic arthritis, other data are contradictory (Murai *et al.*, 1999). This report followed 67 patients suffering from acute inflammatory polyarthritis for up to six years. B19-specific IgM and B19 DNA were detected in 12 of them (~18%). All B19 cases but one were originally negative for the rheumatoid factor but, two to four months after the onset of infection, four patients became positive. Although B19 DNA could no longer be detected in serum samples of these four individuals, it was still present in bone marrow and synovial tissue long after the initial infection. The persistence of B19 in synovium of patients with chronic arthritis has been investigated despite the fact that the findings do not always agree. B19 DNA was detected in synovium of 15 of 90 patients (17%) with unexplained arthritis, whereas only 1 of 73 (1.37%) cases was positive when the synovial fluid was tested (Cassinotti *et al.*, 1998). Viral DNA has also been found in the synovial tissue of ~42% (5 of 12) of patients with undifferentiated monoarthriritis and in 75% (3 of 4) of those with oligoarthritis, suggesting that these two conditions might eventually evolve to fulfil the criteria for RA (Stahl *et al.*, 2000a), and has been demonstrated in synovium of 75% of RA patients and

in 17% of patients with osteoarthritis (OA) (Saal *et al.*, 1992). These findings indicated a highly disease-related persistence of parvovirus B19 in the RA synovium.

In contrast, an examination of serum and tissue from patients with RA and OA, found B19 DNA in synovium of 10 of 26 patients (~38%) with RA and 9 of 26 (~35%) with OA, but the data were not considered strong enough to support the involvement of B19 in RA pathogenesis (Kerr *et al.*, 1995b). A similar conclusion was drawn from a study including 37 children with juvenile chronic arthritis (JCA) and 27 young healthy adults undergoing joint surgery for trauma as controls (Söderlund *et al.*, 1997b). Although B19 DNA could not be detected in any synovial fluid, bone marrow or serum samples, it was found in the synovial membrane of 8 of 29 patients (28%) with JCA and in 13 of 27 controls (48%). Finally, the presence of B19 DNA was reported more frequently in the synovial membrane of patients with haemophilic arthritis (31%) in comparison to control individuals with athrosis or joint trauma (5%) (Zakrzewska *et al.*, 2001).

All these studies confirmed that B19 DNA might persist in synovium of both healthy immunocompetent individuals and patients with arthritis of unknown origin, whereas it rarely does in synovial fluid. Moreover, tissue was confirmed to be better than synovial fluid for detecting B19 persistence (Söderlund *et al.*, 1997b; Cassinotti *et al.*, 1998). Parvovirus was also found to persist in the bone marrow of asymptomatic individuals and patients with suspected B19 infection (Cassinotti *et al.*, 1997).

The involvement of B19 infection in JCA or juvenile rheumatoid arthritis (JRA) has also been studied by several groups (Nocton *et al.*, 1993; Kishore *et al.*, 1998) who have reported a link between B19 infection and JCA/JRA in 40% to 100% of patients. In contrast, in another study, B19 DNA was infrequently detected in patients with early RA (2 in 61 i.e. 3.3%) but not detected at all in patients with advanced RA (Nikkari *et al.*, 1995). Therefore, although these findings suggest that B19 does not play a

significant role in the aetiopathogenesis of RA, it may cause, in a few cases, a disease that is indistinguishable from RA. The presence of B19 DNA in bone marrow aspirates from four chronic arthropathy patients months to years following acute B19 infection, and in three patients with acute, but nonchronic, joint symptoms suggest that B19 arthropathy is associated with persistence of B19 virus (Foto *et al.*, 1993).

However, it can be argued that the presence of B19 DNA in bone marrow and/or synovium of a symptomatic patient does not prove that the disease is caused by B19 and that in order to demonstrate the role of parvovirus in the pathogenesis of RA, metabolic products such as viral mRNA and proteins, as well as a B19-specific immune response or inflammation should be demonstrated (Ishii *et al.*, 1999; Söderlund-Venermo *et al.*, 2002). One of the strongest indications of a link between B19 and RA was described by Takahashi and coworkers, who detected B19 DNA in the synovial tissues of 30 of 39 patients with RA (77%), OA (15%) and traumatic joint disorders (16%) (Takahashi *et al.*, 1998). Most importantly, a recent study of the link between B19 and RA demonstrated, by *in vivo* experiments, the presence of B19 as well as the expression of VP1 in follicular dendritic cells, macrophages, T cells and B cells in RA synovium from patients with RA. These findings suggested that the virus was replicating and infectious and that B19 might be involved in the initiation and perpetuation of RA synovitis leading to joint lesions.

The last aspect investigated was the role the HLA type in acute and persistent arthritis. Some studies have shown the association of HLA-DR4 with acute and persistent arthritis (Klouda *et al.*, 1986; Gendi *et al.*, 1996) but no link between HLA-DR1 and persistent arthropathy (Woolf *et al.*, 1989).

The conclusion from all these studies is that there is no significant evidence to conclude that B19 persistence alone is enough to cause chronic arthritis, RA or OA (Ytterberg, 1999; Moore, 2000; Lefrère *et al.*, 1985a; Stierle *et al.*, 1987). Further research might give an answer to this controversial question of the role of B19 in chronic arthritis and in RA in particular. Historical records reveal that RA is a relatively new disease in Europe, only appearing after the return of explorers from the new world at the end of the 15th century (Altschuler, 1999). In contrast, the disease existed in North America for many thousands of years. EI, which is known to be caused by parvovirus B19, was also first described in the old world in 18th century (Van Elsacker-Niele and Anderson, 1987). Thus, B19 may have been introduced into Europe around the 16th century about the same time as the appearance of RA (Altschuler, 1999).

Parvovirus B19 has also been suspected of being involved in the autoimmune connective tissue disease called systemic lupus erythematosus (SLE), which is characterised by auto-reactive cells and autoantibodies that can potentially affect all organ systems, including the heart, lungs, skin, kidneys and central nervous system (Severin *et al.*, 2003). Several infectious agents, such as retroviruses (Herrmann *et al.*, 1996), EBV (James *et al.*, 1997), and CMV (Rider *et al.*, 1997) have also been suspected of triggering the onset of SLE. However, the similarities between B19 infection and SLE are striking, making it sometimes difficult to differentiate between them (Negro *et al.*, 2001; Trapani *et al.*, 1999; Moore *et al.*, 1999; Nesher *et al.*, 1995). Other reports have demonstrated a link between B19 infection and SLE (Fawaz-Estrup, 1996) and connective tissue disease (Crowson *et al.*, 2000). Studies on SLE patients demonstrated that B19 DNA was detected more commonly in sera from SLE patients without specific-B19 antibodies than in those with antibodies, suggesting that B19 infection in SLE patients might be due to a lack of anti-B19 antibodies, either because

of the immunocompromised state of the host, or the use of immunosuppressive drugs (Hsu and Tsay, 2001). In contrast, a Swedish study concluded that while the possibility that B19 might be a trigger of SLE in a minor proportion of SLE patients, in the general population, B19 is unlikely to be the aetiologic agent in SLE (Bengtsson *et al.*, 2000). In conclusion, although these findings seem to indicate that parvovirus B19 may be involved in pathogenesis or expression of SLE, there are no clear causative associations to date (Severin *et al.*, 2003). No link between B19 and another autoimmune disease, dermatomyositis, which is characterised by inflammatory myopathy, has been demonstrated, either by the detection of B19 DNA in muscle biopsies or the expression of VP1 and VP2 capsid proteins by immunohistochemistry (Chevrel *et al.*, 2003).

To conclude, it is important to consider the diagnosis of coincidental parvovirus B19 in patients with pre-existing rheumatic diseases where there are unusual features, e.g. Behçet's disease, which is characterised by arthralgia, mouth, nasal and genital ulcers, conjunctivitis and facial swelling (Longhurst *et al.*, 2001).

I.1.6.5. B19 infection during pregnancy and hydrops fetalis

The classical definition of hydrops fetalis is "the presence of excessive fluid accumulation in at least two fetal serous cavities" (Forouzan, 1997). An example of one of these cavities is the amniotic sac. Hydrops fetalis is the final stage of a highly morbid condition, caused by many different fetal, placental, and maternal diseases. Although the condition was described more than 300 years ago, only recent advances have allowed the differentiation of the various aetiologies involved. Hydrops fetalis can be classified either as immune or nonimmune (White, 1999). The former results from a rhesus incompatibility between the mother and fetus that result in maternal antibodies against the fetal red blood cell antigens crossing through the placenta and causing

severe fetal anaemia. On the other hand, nonimmune hydrops can have many different causes. One of them can be haematological disorders causing fetal anaemia. A number of infections including syphilis, toxoplasmosis, coxsackievirus, herpes simplex virus (HSV), respiratory syncytial virus (RSV), rubella and CMV have also been associated with this condition (Forouzan, 1997).

Numerous studies have demonstrated a convincing causal link between intrauterine fetal infection by parvovirus B19 and nonimmune hydrops fetalis. One of the first publications reported a case of intrauterine B19 infection associated with hydrops fetalis during an outbreak of EI (Brown *et al.*, 1984). Postmortem examination revealed generalised subcutaneous oedema with serous effusions in the pleural, pericardial and peritoneal cavities. Shortly after, a case of intrauterine fetal death (IUFD) at term with serological evidence of recent B19 infection was reported (Knott *et al.*, 1984). A study in Germany looked at 2,279 pregnant women between 1985 and 1988 and found 54% with only anti-B19 IgG antibodies and 5% with both IgG and IgM antibodies, indicating an acute infection (Enders and Biber, 1990). Of these acute infections, 32% (36 of 114) were from women in the first, 54% (62 of 114) in the second and 14% (16 of 114) in the third trimester. The rate of hydrops fetalis was 8.7% while the rate of fetal death was 7.8%. Seroprevalence of anti-B19 IgG antibodies amongst pregnant women was 30% in Singapore (Wong *et al.*, 2000) whereas it was 64% in Melbourne, Australia (Karunajeewa *et al.*, 2001). The seroprevalence of anti-B19 IgG and IgM antibodies was investigated in pregnant women in Kuwait and found to be 53.3% and 2.2%, respectively (Makhseed *et al.*, 1999). Moreover, the rate of fetal loss was 15.4% in women with acute infection, all of which occurred in the first two trimesters. This rate was significantly higher than other studies (Enders and Biber, 1990; Miller *et al.*, 1998) possibly because of the difference in the size of the cohorts studied. Studies have

confirmed that fetal loss, with or without nonimmune hydrops, was confined to B19 infection in the first 20 weeks of gestation (Miller *et al.*, 1998; Nunoue *et al.*, 2002).

A prospective study of women experiencing third-trimester IUFD showed that 7.5% had detectable B19 DNA in freshly frozen placental tissue, suggesting that B19 PCR should be included in the routine investigation of IUFD, like it is with hydrops fetalis (Skjöldebrand-Sparre *et al.*, 2000). In a similar study during a nonepidemic period in Sweden, B19 was detected in 3% of placental tissues from first-trimester fetal losses but in 12% from second-trimester (Nyman *et al.*, 2002). None of the placental tissues from full-term normal pregnancies were DNA positive. Another Swedish survey confirmed that the presence of B19 DNA in cases of late second-trimester fetal death is common (15%) and that most cases are non-hydropic (Tolfvenstam *et al.*, 2001b). The authors reached the same conclusion for third-trimester fetal losses, which contradicts other findings (Nyman *et al.*, 2002) which suggest that the reduced rate of fetal loss during the third trimester seems to be due to the ability of the fetus to mount an immune response to the virus (Brown, 1989).

There are conflicting reports on the link between B19 infection and late intrauterine death in non-hydropic fetuses (Tolfvenstam *et al.*, 2001b; Sebire, 2001; Crowley *et al.*, 2001). Overall, B19 is not considered as a notable cause of late intrauterine death in non-hydropic fetuses as PCR detection of B19 DNA in placenta may be due to such specimens containing maternal blood, which may still be viraemic, even after resolution of B19 infection rather than fetal infection. Thus conventional techniques, including serological testing of maternal serum and immunohistochemical staining of fetal tissues are necessary to confirm diagnosis of B19 in IUFD. ISH and PCR of fetal tissues (including heart, lung, brain and thymus) have been used to confirm B19 infection in cases of IUFD (Salimans *et al.*, 1989b; Lowen and Weinstein, 1997). Studies on

hydropic fetuses have described numerous features including viral intranuclear inclusions in bone marrow and blood cells (Burton, 1986), erythroid precursor cells from most fetal tissues tested, including lung, liver, heart, kidney, thymus, spleen, pancreas, intestine, diaphragm, brain and rib and bone marrow (Morey *et al.*, 1992), lesions in the central nervous system and in the liver (Garcia *et al.*, 1998), multinucleated giant cells of macrophage/microglia lineage as well as many small calcifications around the vessels, especially in the cerebral white matter (Isumi *et al.*, 1999). Finally, histologic examination of hydropic fetal tissues sometimes have shown changes in all organs, particularly the liver, where many hepatocyte nuclei showed degeneration, and signs of apoptosis with peripheral condensation of chromatin in many erythroid cells, despite the absence of intranuclear inclusions (Anand *et al.*, 1987).

Thus, it is important to screen and identify all pregnant women who may have been exposed to B19 infection (Kelly *et al.*, 1999). In Great Britain, recent guidelines on management of parvovirus B19 and other rash illnesses in pregnancy have been compiled by the former Public Health Laboratory Services (PHLS), now known as the Health Protection Agency (HPA) (Morgan-Capner *et al.*, 2002). These recommendations include screening all pregnant women with a non-vesicular rash illness simultaneously for rubella and parvovirus B19 infection and all pregnant women who have had significant contact with a person suffering from a non-vesicular illness for asymptomatic parvovirus B19 infection, a significant contact being defined as "being in the same room for over 15 minutes, or face-to-face contact" (Morgan-Capner *et al.*, 2002). As for women with proven parvovirus B19 infection in the first 20 weeks of pregnancy, they "should be followed by regular ultrasound scanning, and referred to regional units of fetal medicine if hydrops fetalis is detected" (Morgan-Capner *et al.*, 2002). Different management of B19 infection in pregnancy can lead to different

outcomes in cases of hydropsis. Two options are available: either diagnostic cordocentesis and intrauterine transfusion or management of the case expectantly, although the latter option presents the highest risk of fetal death (Xu *et al.*, 2003). In some cases, spontaneous resolution of hydropsis occurs without the need of transfusion (Petrikovsky *et al.*, 1996). A useful marker in B19 infections is maternal serum alpha-fetoprotein (MsAFP) levels which have been shown to be elevated in several women who subsequently aborted B19-infected fetuses (Anderson and Hurwitz, 1988; Carrington *et al.*, 1987). Monitoring of this marker can also be useful for detecting abnormalities at least four weeks before detection by ultrasound. Such abnormalities include placentomegaly, myocarditis, and generalised subcutaneous oedema greater than 5mm and ascites, pleural and pericardia effusion (Suchet *et al.*, 2000). For those fetuses that make a spontaneous recovery, as well as for those, less fortunate, who develop hydrops fetalis, no signs of any structural fetal anomaly have been observed, either antenatally, at birth or post-mortem nor any serological evidence of persistent infection after maternofetal B19 infection (Suchet *et al.*, 2000; Miller *et al.*, 1998; Dembinski *et al.*, 2003).

In addition to the risks for the fetus, B19 infection can also affect the pregnant woman, who might experience complications. The first factor that comes to mind is psychological, since the irregular fetal heart rate pattern and the condition of the fetus in general can often lead to stress for the mother-to-be. Other complications include maternal anaemia, pregnancy-induced hypertension, antepartum hemorrhage but also malpresentation of the fetus at the time of birth, difficult vaginal delivery, leading to a higher caesarean delivery rate in those women and prematurity (Forouzan, 1997). However, no link has been demonstrated between B19 infection of the fetus (with no signs of maternal B19 infection and hydropsis fetalis) and premature birth (Koga *et al.*,

2001), but this conclusion is only based on a small scale study and further investigations are necessary using an appropriate control cohort.

I.1.6.6. Involvement of other organs

I.1.6.6.1. Liver

When there is no evidence of the involvement of the five major hepatitis viruses (A, B, C, D and E), the nature of the agent that causes acute fulminant liver failure (AFLF) has been unclear and controversial. Cases of hepatitis of unknown aetiology are often associated with aplasia (Pol *et al.*, 1993; Oriol *et al.*, 1994; Cattral *et al.*, 1994), which is itself commonly caused by parvovirus B19 infection. Studies have shown that aplastic anaemia is a common complication among children undergoing transplantation for AFLF (Cattral *et al.*, 1994) and have identified B19 DNA in native livers of several patients with cryptogenic FLF and undergoing such transplantation who did not have associated aplastic anaemia (Langnas *et al.* 1995; Sokal *et al.*, 1998). In addition, several groups have reported acute viral hepatitis of unknown origin associated with B19 infection, suggesting that testing for B19 infection in non-A, non-B, non-C hepatitis is as relevant as testing for EBV and CMV (Yoto *et al.*, 1996a; Naides *et al.*, 1996; Hillingsø *et al.*, 1998). However, detecting viral DNA in the liver tissue of patients with fulminant hepatitis is not sufficient to demonstrate active viral infection. Using a specific and sensitive immune adherence PCR (IA-PCR) assay in which B19 viral particles were captured by monoclonal antibodies on solid phase before PCR amplification, the presence of full virions was thus demonstrated in 83% of livers from patients with non-A to E AFLF associated with aplasia and in 75% without aplasia, compared to 17% from patients with AFLF of known aetiology and 18% of controls with chronic or neoplastic liver disease (Karetnyi *et al.*, 1999). Moreover, mRNA for

B19 structural proteins was detected in the tissues of IA-PCR positive livers, suggesting replication of the virus and providing evidence for B19 involvement in liver damage. B19 DNA has also been detected frequently in adults with severe liver damage. However, B19 DNA has also been detected in livers from anti-B19 IgG positive patients without hepatic disease suggesting that B19 DNA might persist in the liver but further research is needed to confirm this hypothesis (Eis-Hübinger *et al.*, 2001).

Other studies have reported hepatitis in a patient with B19 infection who also developed myositis and life-threatening interstitial lung disease (ILD) (Bousvaros *et al.*, 1998) and a renal transplant recipient who developed fibrosing cholestatic hepatitis (FCH), possibly related to a persistent B19 infection (Shan *et al.*, 2001). Following immunosuppressive therapy, a persistent and increased viral replication would indeed further aggravate an aplastic anaemia and a hepatic failure secondary to FCH. Parvovirus B19 DNA was detected in liver tissue and B19 particles accumulated in the cytoplasm of enlarged hepatocytes. In contrast, no evidence has been reported to link B19 to "cryptogenic" chronic hepatitis (Arista *et al.*, 2003).

I.1.6.6.2. Lungs

Reports of lung disease associated with B19 infection in humans are few. B19-specific IgM antibodies have been detected in 21 young children with prolonged obstructive respiratory diseases, including bronchitis, bronchiolitis, laryngitis and acute asthmatic attacks in those known to be suffering from bronchial asthma (Wiesrbitzky *et al.*, 1991), while a possible association with B19 in an immunodepressed patient with pneumonia has been described (Zerbini *et al.*, 1992). ILD was reported in a patient who showed a prolonged and severe illness but no clinical or laboratory evidence of underlying immunodeficiency but with confirmed serological and PCR data on B19 infection at the

time of onset of illness (Bousvaros *et al.*, 1998). In this case, the systemic persistence of B19 in the blood and lungs and the simultaneous development of ILD are unlikely to be coincidental. It is thus possible that the lung damage was indirectly caused by B19 infection, perhaps through the host immune response. In addition to ILD, it has been proposed that B19 is associated with acute chest syndrome (ACS), a major source of mortality among sickle cell disease (Lowenthal *et al.*, 1996; Wierenga *et al.*, 2001). This condition is characterised by the presence of pleuritic chest pain, fever, rales on lung auscultation and pulmonary infiltrates on chest X-ray. However, further research is necessary to establish an etiologic role of B19 in ACS.

I.1.6.6.3. Heart

Among the numerous complications following B19 infection are acute myocarditis and congenital heart disease (Saint-Martin *et al.*, 1990; Borreda *et al.*, 1992; Tsuda *et al.*, 1994; Heegaard *et al.*, 1998; Enders *et al.*, 1998). In these cases, B19 structural proteins were detected by immunocytochemistry on myocardial tissue sections, or B19 DNA was detected in the myocardial cells, or specific IgM antibodies were present, indicating an acute B19 infection. These cases include the first, and as yet only, case of myopericarditis due to parvovirus 6 months after acute B19 infection (Chia and Jackson, 1996). Studies have shown that B19 might be another cause of heart failure and should thus be considered in similar cases (Malm *et al.*, 1993) and may also be involved in congenital heart disease (Wang *et al.*, 2000).

I.1.6.6.4. Kidneys

Very little is known about the renal involvement caused by B19 infection. Several studies have investigated the link between B19 and focal and segmental glomerulosclerosis (FSGS) (Markenson *et al.*, 1978; Tanawattanacharoen *et al.*, 2000)

and glomerulonephritis with proteinuria following aplastic crisis caused by parvovirus B19 in patients with homozygous sickle cell disease (Wierenga *et al.*, 1995). However, in one of the studies on FSGS patients, although B19 DNA could be detected in these patients, ISH studies failed to detect B19 DNA in any of the kidney tissue samples, implying the lack of ongoing, high-level viral replication. These findings indicated that kidneys might be a frequent reservoir of latent parvovirus B19 DNA but did not establish a definitive role for that DNA. However, certain individuals with FSGS might have active, perhaps transient, infection. B19 infection has also been associated with EI and/or arthropathy with transient urinary abnormalities and (Takeda *et al.*, 2001), EI associated with nephritic syndrome (Ohtomo *et al.*, 2003) and nephritic syndrome with renal impairment and (one with transient acute renal failure) in patients with sickle cell disease (Wierenga *et al.*, 2001). Finally, persistent infection linked to renal involvement resulting in glomerulopathy was demonstrated in immunosuppressed patients, including renal transplant recipients (Moudgil *et al.*, 1997). Although the acute or persistent B19 infection preceding renal involvement tends to point to a possible causal link, the precise mechanism of pathogenesis is still unclear because of the failure to demonstrate viral antigen in the kidney using immunohistochemical techniques.

I.1.6.6.5. Central nervous system

Encephalitis meningitis and acute cerebellar ataxia are rare complications of EI in children (Balfour *et al.*, 1970; Okumura and Ichikawa, 1993; Shimizu *et al.*, 1999). There have been reports of direct invasion of B19 into the central nervous system (CNS) in a case of aseptic meningitis, in which B19 DNA, IgM and IgG antibodies were detectable in cerebrospinal fluid (CSF) (Okumura and Ichikawa, 1993). Moreover, B19 DNA was detected in the CSF of 7 of 162 patients (4.3%) with

meningoencephalitis, suggesting that B19 infection should be included in the differential diagnosis of this condition during the neonatal period, childhood and adolescence (Barah *et al.*, 2001) and in a paediatric case presenting with unexplained neurological illness (Yoto *et al.*, 1994). In contrast, B19 DNA could only be detected in the serum and not in the CSF of a 2-year-old boy with acute cerebellar ataxia (Shimizu *et al.*, 1999) suggesting that the mechanism for acute cerebellar ataxia might not involve direct viral invasion but could be caused by a transient vascular reaction in the cerebellum during B19 infection.

Parvovirus B19 infection of the fetus has already been shown to be associated with lesions in the central nervous system (Garcia *et al.*, 1998). In a retrospective study of aplastic crises in Jamaican patients with sickle cell disease, ten patients had cerebrovascular complications in temporal association with B19 infection and presented with haemiplegia, seizures and encephalitis, which might be related to B19-specific immune complexes (Wierenga *et al.*, 2001). Adult cases of B19-associated CNS infections are also few. There have been reports of B19 infection (persisting for up to nine months) in the blood and in CSF of an immunocompetent patient following an acute infection with meningitis (Cassinotti *et al.*, 1993b), in the CSF of a patient with malignant lymphoma who developed encephalitis and later died (Heegaard *et al.*, 1995) and in an immunocompetent patient who developed encephalitis complicated by prolonged status epilepticus (Skaff and Labiner, 2001). The possibility that a different B19 genotype may be associated with encephalopathy requires further confirmation (Umene and Nunoue, 1995).

B19 has also been shown to be the causative agent in a patient with neuralgic amyotrophy (Pellas *et al.*, 1993) and to result in a more severe meningoencephalitis in a patient with a cocomitant mumps infection (Yazawa et al., 2002). Finally, a study of

autistic children did not support a link between infantile autism and B19 (Anlar *et al.*, 1994). Tables 1.4, 1.5 and 1.6 show a summary of the clinical manifestations following B19 infection, those thought to be linked to B19 infection and those unlikely to be caused by B19.

Table 1.4: Major diseases following B19 infection

Clinical manifestation	References
EI	Lauer *et al.*, 1976; Anderson *et al.*, 1983; Nunoue *et al.*, 1985; Shiraishi *et al.*, 1985; Anderson, 1987; Woolf *et al.*, 1989; Brown and Young, 1996; Sabella and Goldfarb, 1999; Kelly *et al.*, 1999
Hydrops fetalis	Brown *et al.*, 1984; Knott *et al.*, 1984; Burton, 1986; Amand *et al.*, 1987; Salimans *et al.*, 1989b, Enders and Biber, 1990; Morey *et al.*, 1992; Lowen and Weinstein, 1997; Garcia *et al.*, 1998; Miller *et al.*, 1998; Makhseed *et al.*, 1999; Isumi *et al.*, 1999; Skjöldebrand-Sparre *et al.*, 2000; Nyman *et al.*, 2002; Wong *et al.*, 2000; Karunajeewa *et al.*, 2001; Tolfvenstam *et al.*, 2001c; Sebire, 2001; Crowley *et al.*, 2001; Nunoue *et al.*, 2002
Arthropathy	Ager *et al.*, 1966; Joseph, 1986; Török, 1992; Freitas *et al.*, 2002; Woolf *et al.*, 1989; Scroggie *et al.*, 2000; Luzzi *et al.*, 1985
Thrombocytopenia	Saunders *et al.*, 1986; Inoue *et al.*, 1991
Neutropenia	Saunders *et al.*, 1986; Doran and Teall, 1988
TAC	Pattison, 1981; Serjeant *et al.*, 1981; Anderson *et al*, 1982a; Duncan *et al.*, 1983; Chorba *et al.*, 1986; Lefrère *et al.*, 1986a; Lefrère *et al.*, 1986b; Lefrère *et al.*, 1986c; Lefrère and Decazes, 1986; Lefrère and Bourgeois, 1986; Saarinen *et al.*, 1986; Anderson, 1987; Bell *et al.*, 1989; Graeve and Elliott, 1991; Tomiyama *et al.*, 1988; Baurmann *et al.*, 1992; Heegaard and Brown, 2002
PRCA	Kurtzman *et al.*, 1987; Kurtzman *et al.*, 1988; Kurtzman *et al.*, 1989a; Azzi *et al.*, 1989; Gahr *et al.*, 1991; Yoto *et al.*, 1993; Corral *et al.*, 1993; Uemura *et al.*, 1995; Holman *et al.*, 1997; Mathias, 1997; Broliden *et al.*, 1998; Fisch *et al.*, 2000; Pamidi *et al.*, 2000;
Purpuric rash-like illness	Lefrère *et al.*, 1985b; Mortimer, 1985; Li Loong *et al.*, 1986; Naides *et al.*, 1988; Weiland *et al.*, 1989; Niitsu *et al.*, 1990; Harms *et al.*, 1990; Bagot and Revuz, 1991; Borreda *et al.*, 1992; Seabury Stone and Murph, 1993; Labbé *et al.*, 1994; Nelson and Stone, 2000; Ghigliotti *et al.*, 2000; Nelson *et al.*, 2000

Table 1.5: Clinical manifestations possibly linked with B19 infection

Clinical manifestation	References
Chronic arthropathy RA JCA and JRA VAHS ITP Vasculitis syndromes Hepatitis Acute myocarditis and CHD Manifestations in the central nervous system	White *et al.*, 1985; Reid *et al.*, 1985; Woolf *et al.*, 1989; Sasaki *et al.*, 1995; Speyer *et al.*, 1998; Murai *et al.*, 1999; Guillaume *et al.*, 2002 Lefrère *et al.*, 1985a; Stierle *et al.*, 1987; Saal *et al.*, 1992; Kerr *et al.*, 1995b; Nikkari *et al.*, 1995; Cassinotti *et al.*, 1998; Takahashi *et al.*, 1998; Ytterberg, 1999; Stahl *et al.*, 2000a; Moore, 2000; Nocton *et al.*, 1993; Söderlund *et al.*, 1997b; Kishore *et al.*, 1998 Uike *et al.*, 1993; Tsuda *et al.*, 1994; Shirono and Tsuda, 1995; Hoang *et al.*, 1998; Sadahira *et al.*, 1998 Foreman *et al.*, 1988; Lefrère *et al.*, 1989; Inoue *et al.*, 1991; van Elsacker-Niele *et al.*, 1996; Wehmeier *et al.*, 2000 Lefrère *et al.*, 1986d; Corman and Dolson, 1992; Finkel *et al.*, 1994; Dingli *et al.*, 2000; Wierenga *et al.*, 2001; Bültmann *et al.*, 2003 Yoto *et al.*, 1996a; Naides *et al.*, 1996; Hillingsø *et al.*, 1998; Bousvaros *et al.*, 1998; Karetnyi *et al.*, 1999; Eis-Hübinger *et al.*, 2001; Shan *et al.*, 2001; Arista *et al.*, 2003 Saint-Martin *et al.*, 1990; Borreda *et al.*, 1992; Tsuda *et al.*, 1994; Heegaard *et al.*, 1998; Enders *et al.*, 1998; Wang *et al.*, 2000 Balfour *et al.*, 1970; Cassinotti *et al.*, 1993b; Okumura and Ichikawa, 1993; Pellas *et al.*, 1993; Yoto *et al.*, 1994; Heegard *et al.*, 1995; Umene and Nunoue, 1995; Shimizu *et al.*, 1999; Wierenga *et al.*, 2001; Skaff and Labiner, 2001; Barah *et al.*, 2001

Table 1.6: Clinical manifestations unlikely to be linked with B19 infection

Clinical manifestation	References
TEC	Bhambhani *et al.*, 1986; Skeppner *et al.*, 2002
SLE	Nesher *et al.*, 1995; Trapani *et al.*, 1999; Moore *et al.*, 1999; Bengtsson *et al.*, 2000; Negro *et al.*, 2001; Severin *et al.*, 2003
ILD	Bousvaros *et al.*, 1998
ACS	Lowenthal *et al.*, 1996; Wierenga *et al.*, 2001
FSGS and other renal manifestations	Markenson *et al.*, 1978; Moudgil *et al.*, 1997; Tanawattanacharoen *et al.*, 2000; Takeda *et al.*, 2001; Wierenga *et al.*, 2001; Ohtomo *et al.*, 2003
Infantile autism	Anlar *et al.*, 1994

I.1.6.7. Pathogenesis

The clinical outcome of human parvovirus B19 infection involves three major pathogenic components: the cytopathic effect of the virus on susceptible and dividing cells, the humoral immune response and the result of antibody deficiency (Cherry, 1999). Although each potential pathogenic system will be discussed separately, the pathogenesis of B19 virus is complex and often involves a combination of these mechanisms.

The onset of viraemia occurs six days after infection and is associated with infection of erythrocytes in the bone marrow after attachment to these cells through the receptor (Brown *et al.*, 1993). The local replication is one of the first pathogenic mechanisms in several conditions, including EI, TAC, bone marrow failure, congenital red cell aplasia, vasculitis and hepatitis (Kerr, 2000). The reticulocytopenia observed in most patients is caused by the cytopathogenic effect of the virus on erythroid progenitors. Although this temporary phenomenon goes unnoticed in otherwise healthy children and adults, it can lead to TAC in those with underlying haemolytic disorders, or to PRCA in those unable to mount an immune response to the virus. Additionally, the massive destruction of the erythroid lineage cells through apoptosis leads to severe anaemia and results in heart failure of the infected fetus, and eventually to hydrops fetalis (Cherry, 1999; Yaegashi, 2000). However, in order to understand the potential risks involved in transplacental infection, it is important to establish which cell types in the developing fetus are susceptible to viral attack. Reports have shown the presence of viral non-structural gene products in the liver, lung and, to a smaller extent, other tissues (e.g. spleen) in the infected fetus (Cotmore *et al.,* 1986). These findings are suggestive of an active viral replication in at least one cell type in these tissues. Fetal liver contains islands of haematopoitic tissue, which are likely to contain susceptible cells. B19 can thus

presumably bind to the cell surface and penetrate liver cells not only in the fetus but also in the adult.

Similarly, replication in the lung tissue is not unexpected, since it is highly probable that B19 is transmitted as an infection of the respiratory tract (Anderson *et al.*, 1985a) and that it therefore replicates in at least one cell type present therein. It is likely that B19 can bind to other glycosphingolipids located in liver, kidney and bowel tissues, but not in lung (Cooling *et al.*, 1995). In comparison with the adult tissue, many more cell types are undergoing cell division in the fetus. Therefore, although B19 is mainly haematotropic in adults, it might have a more extensive tissue tropism in the fetus, thereby causing more damage to the fetal tissues and organs (Cotmore *et al.*, 1986). The destruction of erythrocytes can also lead to excess production of red blood cells by the fetus which tries to compensate for the loss, leading to hepato-splenomegaly (Garcia *et al.*, 1998). The direct infection of hepatocytes has been implicated in cases with severe liver disease (Morey *et al.*, 1992). Such severe necrosis may lead to decreased production of albumin with lowered plasma oncotic pressure (Suchet *et al.*, 2000). This, associated with severe anaemia, can produce oedema and thereby contribute to high cardiac output failure. In third-trimester fetuses, it seems that cardiac decompensation is the main determining factor affecting the survival of the fetus. However, the majority of reported fetal deaths appears to be in the second trimester, as the fetus is at greatest risk of hydrops because of the rapid increase in fetal red cell mass at that time of gestation. Since *in situ* hybridisation located B19 gene in the nucleus of cardiac cells of CHD sufferers, it might influence gene expression and thereby affect the development of the heart, which could result in CHD (Wang *et al.*, 2000). The cytopathic effect might involve the cytotoxicity of NS-1 protein (Ozawa *et al.*, 1988a) as well as its ability to upregulate cytokine production. Using a transgenic mouse model for nonimmune

hydrops fetalis induced by the NS-1 gene of B19, it has been demonstrated that the nonstructural protein plays a crucial role in the cytotoxocity and the outcome of intrauterine B19 infection (Chisaka *et al.*, 2002).

Previously, the involvement of NS-1 protein in apoptosis had been controversial. The initiation of cell death was observed to occur 24 hours after the induction of NS-1, suggesting that the nonstructural protein might mediate the apoptosis of the erythroid cell lines used in this study (Yaegashi, 2000). Apoptosis was characterised by cell rounding, chromatin condensation and DNA fragmentation. However, other studies could not find any correlation between the presence of anti-NS-1 antibodies in pregnant women and the occurrence of fetal complications (Searle *et al.*, 1998). As for upregulation of cytokine production, NS-1 protein has been shown to induce activation of IL-6 gene expression, which supports the possible relationship between B19 infection and polyclonal activation of B-cells in RA (Moffatt *et al.*, 1996). In addition, *in vitro* infectivity experiments, have shown that susceptible cell lines (tonsillar cells and macrophages) became infected when cocultured with RA synovial cells, but not OA synovium (Takahashi *et al.*, 1998). Coculture generated not only the expression of VP1, but also an enhanced production of IL-6 and TNF-α that was significantly inhibited by the induction of neutralising antibodies for B19. Therefore, it appears that B19-positive T cells and macrophages might infiltrate into the synovium and recruit circulating immunocytes. Synovial T cells and macrophages, continuously activated by B19, secrete inflammatory cytokines, such as TNF-α and IL-6, to stimulate a variety of synovial cells via the autocrine and paracrine network of cytokines. This leads to an excessive production of cytokines and proteolytic enzymes resulting in persistent inflammation and tissue destruction, including cartilage, joints and bone erosion (Ishii *et al.*, 1999).

Additionally, both TNF-α and NS1 have been involved in apoptosis of erythroid cells leading to reticulocytopenia (Moffatt *et al.*, 1998; Sol *et al.*, 1999). An increase in TNF-α has been described in an adult patient presenting with VAHS and myocarditis, as well as an increase in macrophage-colony stimulating factor (M-CSF) and granulocyte-colony stimulating factor (G-CSF) (Tsuda *et al.*, 1994). This patient had neutrophilia rather than the expected neutropenia and it was proposed that B19 might induce the production of M-CSF, which could in turn activate monocytes and macrophages to proliferate into abnormal haemophagocytes and to produce G-CSF and TNF-α (Tsuda *et al.*, 1994). Due to the disrupted release of G-CSF, mobilisation of neutrophils might have overcome the cell destruction.

Several mechanisms have been proposed regarding the implication of B19 in the pathogenesis of liver damage and hepatitis. Mutations identified in the NS1 gene might generate variant B19 virus with hepatotoxic NS1 that would result in apoptosis of hepatocytes (Naides *et al.*, 1996). Alternatively, B19 might have a direct effect on hepatocytes and the action of various cytokines (including IFN-γ) might result in liver dysfunction via immunological mediation (Yoto *et al.*, 1996a; Yoto *et al.*, 1996b).

The usual manifestations of primary B19 infection are EI in children and arthralgia in adults, both starting about 17 days after infection when the viraemia has cleared (Anderson *et al.*, 1985b). In patients with B19-associated arthritis, low serum complement levels and circulating immune complexes are found (White et al., 1985). Moreover, a study in Spain, involving 43 patients diagnosed with B19 infection resulting in various clinical outcomes, revealed that 81.6% of cases had detectable circulating immune complexes (García-Tapia *et al.*, 1995). Taken together, these findings tend to confirm that immune-mediated pathogenesis, in the form of deposition

of immune complexes, is involved. Such a mechanism was also found in mink affected with Aleutian disease as anti-B19 IgA-B19 antigen complexes deposited in renal glomeruli (Portis and Coe, 1979). In humans, the occasional renal involvement in B19 infection was discussed previously. Although it has been suggested that B19 could bind to and penetrate some kidney cells, it is more plausible that the renal lesions observed in some studies might be caused by an immune complex-mediated phenomenon which is closely related to B19 infection in the host (Cooling *et al.*, 1995; Takeda *et al.*, 2001). Such immune complex deposits were indeed recently found in the renal biopsy of an 8-year-old child who developed nephritic syndrome during the course of EI due to parvovirus B19 (Ohtomo *et al.*, 2003).

Serum antinuclear antibodies (ANA) have been described in several patients with acute polyarthritis caused by B19 (Cobeta-García and Rodilla, 2000). Three months later, the clinical symptoms had completely resolved, anti-B19 IgG antibodies were positive and IgM antibodies and ANA were undetectable. Whether these ANA play a role in the pathogenesis is still unclear. Several patients infected with B19 and suffering from chronic symmetric polyarthritis resembling RA have also been shown to produce autoantibodies (Lunardi *et al.*, 1998). Patients had symptoms and IgM antibodies to B19 for 4 months to 2 years. Cross-reactivity of these anti-B19 antibodies with a variety of antigens including keratin, collagen type II, single-stranded DNA and cardiolipin have been demonstrated. These findings were later confirmed by a study showing the production of anti-cardiolipin as well as anti-neutrophil cytoplasmic antibodies in patients with EI and polyarthralgia, polyarthritis and mild fever (Chou *et al.*, 2000) suggestive of molecular mimicry or epitope spreading, and a link of B19 to the induction of an autoimmune response that could perhaps lead to the development of some SLE cases. However, it is still not clear why antibodies would cross-react with

such a wide range of autoantigens (Ytterberg, 1999). Other studies have confirmed that a number of mechanisms might be involved in the induction of autoimmune disease by B19, including the molecular mimicry mentioned above and the induction of enhanced cytokine production via the NS1 protein (Lehmann *et al.*, 2002).

One of the mechanisms that could trigger the production of anti-phospholipid (aPL) antibodies, found in paediatric and adult patients with rheumatic disease, might be the phospholipase A2-like activity associated with the carboxy-terminal domain of the VP1 unique region (Zádori *et al.*, 2001; Lehmann *et al.*, 2002; Dorsch *et al.*, 2002). The latter mechanism has been supported by the fact that aPL antibodies are frequently found in serum of children with juvenile idiopathic arthritis previously infected by B19 and presenting a persistent infection (von Landenberg *et al.*, 2003). Moreover, adult patients with aPL antibodies also appear to have a high incidence of persistent B19 infection, indicating that parvovirus might be directly implicated in the development of autoimmune responses via aPL.

The implication of NS1 in cytotoxicity was recently proposed in the case of a patient with mixed connective tissue disease and arthralgia (Kerr and Behan, 2002). Although the patient was weakly positive for ANA, she did not develop any other autoantibodies and parvovirus B19 DNA was detected in the skeletal muscle. The NS1 gene had a high mutation rate (3.52%) compared to the wild type (<1%). All ten mutations were silent except one immediately downstream of the NTP binding site. Such a mutation might facilitate persistence of the virus by modifying cytotoxicity (Kerr and Behan, 2002). In contrast, the viral coding regions of B19 DNA found in the synovial tissue of both persistently and recently infected patients were in an apparently continuous, intact DNA molecule (Hokynar *et al.*, 2000). Thus, these findings suggest that persistence of B19 virus does not seem to be due to exceptional mutations or particular variants. Although

NS1 protein might be involved in cytotoxicity, no correlation was found between the presence of NS1-specific antibodies and the development of acute or chronic arthropathy (Mitchell *et al.*, 2001).

An altered immune function, such as the B-cell defects observed in immunocompromised patients, can also play a role in the pathogenesis of B19 virus. Such patients are indeed unable to produce effective neutralising antibodies, resulting in persistence of B19 in the host (Frickhofen and Young, 1989; Broliden *et al.*, 1998).
As far as the vascular events are concerned, strokes are known to occur in sickle cell disease patients (Wierenga *et al.*, 2001). They are commonly associated with blockage of major vessels, which is unexpected in such a condition characterised by occlusion of small vessels. A simultaneous B19-induced aplastic crisis would result in lowered haemoglobin levels, thereby reducing oxygen delivery to areas already rendered vulnerable by pre-existing vascular disease. However, this is only hypothetical and the pathogenesis of B19 in such vascular complications is still unclear.

In conclusion, the importance of each mechanism of pathogenesis in the clinical outcome varies depending on the virus/host interaction and thus on the host's immune status. More research is still needed to characterise further the role of B19 in this wide clinical outcome.

I.1.7. Treatment, vaccine and animal models

I.1.7.1. Treatment

The two main ways used to treat symptomatic B19 infection are RBCs transfusions and intravenous immunglobulin (IVIG).

I.1.7.1.1. Transfusions

Regular transfusions of erythrocytes were reported for a 12-month-old girl with severe combined immunodeficiency (Gahr *et al.*, 1991). These transfusions were usually necessary every 2 months and resulted in short periods with normal reticulocyte counts. However, a full and stable recovery of erythropoiesis was never achieved in this case and she died at the age of 4 before bone marrow transplantation could be done. Successful intrauterine treatment of two cases of fetal hydrops caused by B19 has been reported (Gloning *et al.*, 1990). Signs of hydrops disappeared after intrauterine transfusions and the infants were born healthy and developed normally. It is first recommended to perform fetal blood sampling to test for blood grouping, anaemia, viral infections, toxoplasmosis, bleeding disorders, severe combined immunodeficiencies and also for a rapid karyotyping in some conditions. In case of fetal anaemia, intrauterine intravascular transfusion can be used as therapy. The role of intrauterine transfusion for fetal hydrops arising from maternal parvovirus B19 infection has been investigated by following the progress of 38 hydropic fetuses in England and Wales between 1992 and 1994 (Fairley *et al.*, 1995). At the first abnormal scan, 12 of 38 received intrauterine transfusions and 3 (25%) died, whereas the other 26 fetuses did not receive any transfusion and 13 (50%) died. Even when taking into account the severity of the hydrops and gestational age, there was a significantly higher risk of fetal loss for those who had not received intrauterine transfusion, thereby emphasising the benefits of such treatment for some fetuses. Intrauterine transfusion can be performed at the first signs of hydrops fetalis. This therapeutic intervention, however, should be restricted only to specialised centres and only be considered in intact pregnancies. An informed consent of the parents should be mandatory. Moreover, it seems that an active treatment consisting of a combination of pre- and postnatal transfusions and IVIG can be

beneficial to correct severe hydrops fetalis and subsequent congenital anaemia (Heegaard *et al.*, 2000).

I.1.7.1.2. Intravenous immunoglobulins (IVIG)

Although functional T lymphocytes are required for recognition and final clearance of parvovirus, the very dramatic correction of anaemia with IVIG therapy is itself convincing evidence that antibody is the principal defence in human parvovirus disease (Kurtzman *et al.*, 1989b). A course of commercial Ig preparations is indicated in patients with anemia and parvoviraemia and also for those with documented persistent B19 infection. A drastic decline in viral concentrations in the blood within hours of administration is observed, followed by prompt reticulocytosis and return to normal or near-normal levels (Frickhofen *et al.*, 1990). Intravenous treatment with Ig, at a dose of 0.4g/kg body weight over 5 days, resulted in marked improvement in several patients suffering from chronic undifferentiated non- and oligoarthritis (Stahl *et al.*, 2000b).

Currently, HIV-positive patients are treated with the same dose as previously mentioned (Frickhofen *et al.*, 1990). Patients should be monitored for evidence of relapse, by observation of the reticulocyte counts, and assays for B19 viraemia when indicated (Brown, 2000). This applies especially if zidovudine treatment complicates the interpretation of reticulocyte counts (Frickhofen *et al.*, 1990). Relapses may occur early in patients with more advanced disease. Most patients with CD4 counts lower or equal to 80 cells/mm^3 suffer from relapse within 6 months, necessitating retreatment with IVIG, whereas patients with CD4 counts greater than 300 cells/mm^3 do not require routine maintenance therapy (Koduri *et al.*, 1999). If a relapse occurs less than 6 months after the initial treatment, an empiric maintenance treatment with a single-day infusion of 0.94 g/kg IgG every 4 weeks should be applied (Frickhofen *et al.*, 1990). Persistent erythroid aplasia caused by B19 in patients with other forms of immunodeficiency, such

as common variable immunodeficiency, can be treated with low-dose (50mg/kg for 6 days) Ig (Chuhjo *et al.*, 1999). Transplant recipients presenting PRCA or severe anaemia usually respond well to a high-dose treatment (Holman *et al.*, 1997; Moudgil *et al.*, 1997; Mathias, 1997; Marchand *et al.*, 1999; Pamidi *et al.*, 2000). In addition, reduction in immunosuppression may also be helpful as an approach to treat this infection in such patients (Pamidi *et al.*, 2000). A course of IVIG, along with isolation measures, also seems to contribute in preventing B19 infection in bone marrow transplant recipients (Azzi *et al.*, 1993). Additionally, high-dose IVIG has been used to treat patients with acute or chronic ITP, autoimmune neutropenia and autoimmune haemolytic anaemia (Berkman *et al.*, 1988).

However, the mechanism of action of high-dose Ig therapy is unclear and has been the subject of speculation. Many effects of IVIG on the function of the immune system have been proposed, including blockade of Fc receptors (Fehr *et al.*, 1982), decreased Fc-receptor-mediated phagocytosis (Kimberly *et al.*, 1984), enhancement of suppressor T-cell function (Delfraissy *et al.*, 1985), depression of natural killer cells activity (Engelhard *et al.*, 1986) and lowering of autoantibody titres through idiotypic/anti-idiotypic interactions (Sultan *et al.*, 1984). McGuire and colleagues have supported the latter therapeutic mechanism since they found that both the $F(ab')_2$ fragment of IgG and the whole intravenous gamma globulin preparation, but not an Fc fragment of IgG, were capable of neutralising the cytotoxic action of the patient's IgG fraction (McGuire *et al.*, 1987).

I.1.7.2. Vaccine

Treatment by blood transfusion, Ig or intrauterine transfusion is efficient in controlling human parvovirus B19 infection. However, prevention being better than treatment,

research has been undertaken to develop a safe and effective vaccine. Vaccines against a number of animal parvoviruses, such as PPV (Mengeling *et al.*, 1979; Pye *et al.*, 1990), CPV (Eugster, 1980) and FPV (Davis *et al.*, 1970; King and Gutekunst, 1970) have already been developed using live attenuated or killed viruses. As far as parvovirus B19 is concerned, development of a vaccine for B19 has been hampered by the limited availability of viral antigen. Firstly, it is complicated to identify a viraemic patient, since viraemia usually resolves before clinical symptoms of B19 virus infection appear. Secondly, when a viraemic individual has been identified, it is difficult to obtain sufficient quantities of virus. Cell culture production of B19 virus would be an alternative but has not yet been possible with the currently available cell lines. However, even if sufficient quantities of live virus could be obtained, there are safety issues associated to its use in a vaccine, such as the possibility of contamination with other viruses.

Finally, extensive investment in research is needed to either attenuate or inactivate such live viruses (Collett and Young, 1994). These limitations, however, have been overcome with the development of genetically engineered expression systems for the production of B19 parvovirus antigens. These expression systems allow for the efficient production of unlimited quantities of safe, non-infectious B19 virus antigen and thus offer an opportunity for the development of a B19 parvovirus vaccine. Bacterial expression was used by various groups, who inserted into *Escherichia coli* some plasmids with portions of the viral capsid protein sequences fused to other proteins such as β-galactosidase or protein A (Sisk and Berman, 1987; Rayment *et al.*, 1990; Morinet *et al.*, 1989; Rosenfeld *et al.*, 1992). Although large amounts of recombinant protein were produced in bacteria, they lacked the native conformation of B19 virion.

The first eukaryotic expression system to produce complete native B19 capsids was a mammalian cell line engineered from Chinese hamster ovary cells and designated 3-11-5 (Kajigaya *et al.*, 1989). The particles produced were composed of both VP1 and VP2 capsid proteins in a ratio similar to that observed in genuine virions (~4% and ~96%, respectively). The other eukaryotic system used as a source of native B19 capsid proteins (either VP2 alone or both VP1 and VP2) was the baculovirus/insect cell expression system (Brown CS *et al.*, 1991; Kajigaya *et al.*, 1991). It has been shown that in order to elicit a neutralising antibody response in rabbits, recombinant empty capsids had to contain VP1 since recombinant capsids consisting of VP2 only fail to elicit a neutralising immune response in animals (Kajigaya *et al.*, 1991). Moreover, an evaluation of the immune response elicited by recombinant B19 parvovirus capsids of various structural protein compositions (4%, 25%, 35% or 41% VP1 protein) found that recombinant capsids of a protein composition similar to that of naturally occurring B19 virions (4% VP1 capsids) were a relatively poor vaccine immunogen for the elicitation of virus neutralisating antibodies (Bansal *et al.*, 1993). However, given that human convalescent sera usually have strong virus neutralising activity, there might be slight differences of a structural and conformational nature between the natural and recombinant capsids that may be immunologically important. Additionally, there may be differences in the presentation to the immune system of a replicating virus and a nonreplicating particle. Another conclusion from this study was that the effective immune response was proportional to the quantity of VP1 contained in the empty capsid immunogen, although only up to a certain point (Bansal *et al.*, 1993). Capsids consisting of more than 25% VP1 did not appear to have a significantly improved ability to elicit neutralising antibody production. All formulations in Freud's adjuvant trigged significant levels of anti-B19 antibodies 4 weeks post inoculation in guinea pigs. Empty

capsids containing various VP1 concentrations were then tested with or without aluminium hydroxide. Vigorous neutralising response was induced at low doses when formulated with the latter adjuvant whereas a similar activity in the absence of adjuvant was elicited by 100 fold higher doses. These data suggest that recombinant VP1-enriched empty capsids could be a good candidate for a B19 vaccine. Furtherore, recombinant empty capsids were also able to stimulate human T helper lymphocytes, which are essential for B-cell maturation and antibody class switching (Franssila *et al.*, 2001). The immunogenicity of a more recent candidate recombinant B19 vaccine (MEDI-491; MedImmune), composed of ~25% VP1 and ~75% VP2 capsid proteins, was successfully evaluated in a randomized, double-blind, phase I clinical trial (Ballou *et al.*, 2003). All volunteers (n=24) developed neutralising antibody titres that peaked after the third immunisation and was sustained for one year.

The last approach to vaccine development has been via synthetic peptide immunogens containing neutralising epitopes. Protective immunity has already been observed in BALB/c mice after vaccination with a synthetic peptide derived from CPV capsid proteins (Rimmelzwaan *et al.*, 1990). As for parvovirus B19, this method is realistic providing a number of linear epitopes on the capsid proteins have been defined and showed involvement in virus neutralisation. The use of NS1 as a vaccine target is not recommended as no epitope was universally recognised by the different groups reviewed previously (Tolfvenstam *et al.*, 2000). Additionally, and as discussed previously, anti-NS antibodies are unlikely to induce a neutralising response (Von Poblotzki *et al.*, 1995b).

The first and so far only report of the use of synthetic peptides demonstrated that several of them, containing about 20 amino acids of the unique region of VP1, elicited neutralising antisera in rabbits (Saikawa *et al.*, 1993). Although those results are

encouraging, a lot more research will be required for the development of a useful synthetic peptide vaccine candidate containing a mixture of several neutralising epitopes. Major concerns about such a peptide are its presentation to the B-cell epitope and its capability to induce T helper cell activity (Collett and Young, 1994). Moreover, synthetic peptide-based vaccines are usually poor immunogens and consequently provide incomplete protection. The prospects for the development of a human parvovirus B19 vaccine are fairly good and a hopeful candidate appears to be based on recombinant empty capsids.

While it has proven difficult to develop vaccines against parvoviruses, it was ironical to discover that parvoviruses could be used as vectors for the presentation of foreign epitopes to the immune system (Miyamura *et al.*, 1994). Similarly, hepatitis B virus (HBV) core antigen has already proven to be a good presentation system for peptides of the foot-and-mouth disease virus (Clarke *et al.*, 1987), epitopes from the envelope protein of HIV-1 (Stahl and Murray, 1989) and for rhinovirus peptides (Francis *et al.*, 1990). Synthesis of virus-like particles (VLPs) mimicking authentic virions but lacking the genetic material has been used with autonomous parvoviruses to generate a collection of VLPs (Casal, 1999). Sedlik and coworkers have constructed a PPV VP2 chimera containing the poliovirus C3:T epitope that was able to induce a strong peptide-specific proliferative response *in vivo* (Sedlik *et al.*, 1995). The very good T CD4+ response obtained against the inserted T-cell epitope was later characterised as being of Th1 phenotype (Lo-Man *et al.*, 1998). Hybrid VLPs prepared by self-assembly of the modified PPV VP2 capsid protein carrying a CD8+ T cell epitope from lymphocytic choriomeningitis virus, was shown to induce vigorous CD8+ and CD4+ cell responses without adjuvant (Sedlik *et al.*, 1997). These VLPs were nonreplicative and the protective responses elicited were long-lived. Further research showed that these vectors

could initiate both humoral and cellular responses when delivered intranasally, whereas no immune response was observed when mice were orally immunised (Sedlik *et al.*, 1999). Interestingly, three sites suitable for the insertion of B- and T-cell epitopes were defined on the VP2 capsid protein: epitopes placed at the N-terminus of VP2 induce cellular immune response, both through T_H cells and cytotoxic cells, epitopes on loop 2 of VP2, located on the surface of the capsid, can elicit strong humoral immune response against the inserted epitope and some sites around the 5-fold axis, the region situated on the "neck" of the caspid, can present epitopes able to trigger a humoral response (Rueda *et al.*, 2000). Therefore, the possibility of combining different types of epitopes on different positions of a single particle to stimulate different branches of the immune system could pave the way to the production of more potent vaccines in a simple and cheap way. In addition, the heat resistance of human parvovirus B19 could become an advantage for vaccination programs in the warmer countries of the developing world (Miyamura *et al.*, 1994).

I.1.7.3. Animal models for B19 infection

Animal models for human parvovirus B19 can be used for two types of studies: pathogenesis of infection and virus inactivation.

Despite the fact that human parvovirus B19 is still the only officially accepted member of the Erythrovirus genus, several candidate viruses have been proposed for inclusion in this relatively new genus. Remarkable similarities have indeed been noticed between the simian and B19 parvoviruses, such as their predilection to infect bone marrow cells *in vitro* (Gallinella *et al.*, 1995b) and their capacity to cause severe anaemia in infected subjects, respectively cynomolgus monkeys and humans (O'Sullivan *et al.*, 1994; 1997). Two other outbreaks of anaemia were later reported to be caused by two distinct but similar SPV, namely pig-tailed macaque and rhesus parvoviruses, in the

corresponding hosts (Green *et al.*, 2000). All three SPV, which are highly tropic for erythroid progenitor cells, are currently being studied as animal models for the pathogenesis of B19 infection (Brown and Young, 1997). Another candidate erythrovirus was isolated from Korean Manchurian chipmunks (Yoo *et al.*, 1999). Its nucleotide and amino acid sequences showed significant homology to B19 and SPV, suggesting it might also be a potentially useful animal model for B19 infection. Additionally, a recent investigation aiming at understanding the role of B19 NS1 protein in non-immune hydrops fetalis led to the establishment of NS1-transgenic mice lines that can provide an animal model for the study of this condition (Chisaka *et al.*, 2002).

Due to the lack of a suitable infectivity assay for human parvovirus B19 to date, animal models have been widely used in virus inactivation studies, including MVM (House *et al.*, 1990), CPV (Hart *et al.*, 1994; Borovec *et al.*, 1998; Roberts and Hart, 2000), BPV (Brauniger *et al.*, 2000; Roberts and Hart, 2000) and PPV (Blümel *et al.*, 2002a). However, as will be discussed further in chapter V, the relevance of these models is debatable. A recent study by Blümel and colleagues has indeed showed that thermal resistance of B19 markedly differs from that of animal parvoviruses (Blümel *et al.*, 2002b).

I.2. Contamination of blood and blood products

I.2.1. Prevalence of human parvovirus B19

I.2.1.1. Blood donations and plasma pools

Two factors can influence the incidence of B19 in blood donations: the sensitivity of the detection method used and the epidemiology of the virus (Siegl and Cassinotti, 1998). The latter refers to the particularity of B19 infections to occur in late winter and spring (Anderson and Török, 1989) and in 4-year cycles, with 2 epidemic years followed by 2

endemic years (Kelly *et al.*, 2000). Therefore, taking into account both factors, the incidence of B19 virus in blood donations can vary greatly.

The first reported incidence of B19 in British donations in a non-epidemic situation was 11 instances being found in approximately 500,000 blood donations by CIE, which corresponds to about 1 in 45,000 (Mortimer *et al.*, 1983). Subsequently, although the primary aim of their study was to identify a B19 positive donation that could be used as a source of antigen for diagnostic purposes, Cohen and colleagues estimated the incidence of B19 viraemia in blood donors as 1 in 24,000 donations (Cohen *et al.*, 1990). The single donation showed a positive reaction for B19 antigen by CIE and was later confirmed by IEM. Although the positive donation was reported immediately to the North London Blood Transfusion Centre, where the sample was donated, it had already been incorporated in a plasma pool of 28 donations. This pool was then made available for further research. Neither CIE nor radio-immuno assay (RIA) could detect B19 antigen whereas the dot-blot hybridisation assay was positive for B19 DNA. Since the dilution effect would not explain those results, the presence of B19 antibodies from other donations of the pool might have blocked the antigen reactivity. Direct EM confirmed the presence of aggregates of B19 particles coated by antibodies, while direct EM on the single donation had not shown any antibody coating of the virus particles nor aggregation. Therefore, it seemed that the presence of antibodies did not interfere with DNA detection (Cohen *et al.*, 1990).

The importance of the sensitivity of the detection method used and B19 infection epidemiology was shown in a number of studies detailed below. While Japanese samples tested by ID and in a non-epidemic period showed an incidence of 1 in 35,000, that figure increased to 1:4,000 under an epidemic situation, when measured with the same method (Tsujimura *et al.*, 1995). Moreover, when using the more sensitive PCR

detection method during a minor epidemic of EI, the incidence of B19 viraemia in healthy blood donors was 1:167 (0.6%), which was considerably higher than in previous surveys (Yoto *et al.*, 1995). Still in Japan, Sato and coworkers first used double immunodiffusion (DID) to find 1 in about 14,000 donations positive for B19 in 1992, which was a prevalent year for EI (Sato *et al.*, 1995). The following year, which was not epidemic for EI, 1 in 90,000 donations was contaminated with B19. Nevertheless, when both DID and RHA were used for screening from April to July 1995 -again not prevalent for EI in Japan-, no positive donation was detected by DID, whereas RHA identified 27 positives among 45,735 tested (~1 in 1,700). However, only 7 of those were confirmed positive by PCR, thereby bringing the figure to 1 in 6,500 and underlining the weak specificity of the RHA screening method. Another study using PCR to detect B19 DNA in blood units in a non-epidemic year found approximately 1 positive in 3,300 (McOmish *et al.*, 1993). The most recent study reported the results of the implementation of PCR screening of plasma pool samples for B19 DNA at the "laboratoire francais du fractionement et des biotechnologies" in France (Aubin *et al.*, 2000). This was the most extensive of such studies reported to date since it was done over a 2-year period. During this time, the frequency of parvovirus B19 viraemic donations was 1 in 5,950, which correlated with previously published data. Moreover, the previously described seasonal and annual B19 epidemics were observed in this report as during the peak of the French epidemic in April 1997, B19 incidence in blood donors was as high as 1 in 1,420. B19 DNA levels in positive pools ranged from 10^2 to 10^{11} copies/ml. Table 1.7 summarises the data available to date.

Table 1.7: Incidence of parvovirus B19 viraemic sera

Situation	Incidence	Method of detection	Country	Reference
Non-epidemic	1:45,000	CIE	UK	Mortimer *et al.*, 1983
Non-epidemic	1:24,000	CIE	UK	Cohen *et al.*, 1990
Non-epidemic Epidemic	1:35,000 1: 4,000	ID	Japan	Tsujimura *et al.*, 1995
Epidemic	1:167	PCR	Japan	Yoto *et al.*, 1995
Epidemic Non-epidemic Non-epidemic	1:14,000 1:90,000 1:6,500	DID DID PCR	Japan	Sato *et al.*, 1995
Non-epidemic	1:3,300	PCR	UK	McOmish *et al.*, 1993
Non-epidemic Epidemic	1:5,950 1:1,420	PCR	France	Aubin *et al.*, 2000

These PCR-based data have raised the concern that B19 might frequently contaminate blood products, which are generated from pools of 3,000 to 10,000 plasma units. It appeared essential to screen blood products for B19 DNA and to investigate the effect of the virus removal/inactivation used.

I.2.1.2. Plasma products

I.2.1.2.1. Coagulation factors

The first group to test the hypothesis that parvovirus B19 was spread by blood products was Mortimer and colleagues as early as 1983 (Mortimer *et al.*, 1983). He demonstrated that young American haemophiliacs receiving factor VIII and IX concentrates showed a

higher prevalence of anti-B19 (97%) than in either blood donors or age-matched controls (20%). However, as far as individual blood donations were concerned, Mortimer did not show any significant increase in anti-B19 antibodies prevalence (36%) in a group of multiply transfused patients, compared to the untransfused control group.

A few years later, the prevalence of anti-B19 IgG in non-heat-treated factor VIII concentrates was found to be 89% (47 of 53), compared with 39% (53 of 135) of their age-matched controls (Williams *et al.*, 1990). On the other hand, treatment with single donor units of plasma or plasma fraction (cryoprecipitate) was not associated with an increase in the prevalence of anti-B19 IgG. Moreover, two of 12 boys (17%) who had received the NHS 8Y factor VIII concentrate were positive for IgG, compared to 11 of 36 (31%) of controls. Williams and colleagues emphasised the fact that those promising results were preliminary, and rightly so, since Yee and his team showed transmission of B19 by this product a few years later (Williams *et al.*, 1990; Yee *et al.*, 1995; Yee *et al.*, 1996).

B19 DNA was detected in clotting factor concentrates by dot-blot hybridisation, Southern blot hybridisation and by nested PCR (Zakrzewska *et al.*, 1992). Once again, the different sensitivities of these detection methods influenced the prevalence of the virus in the batches tested. Only two concentrates were shown to contain B19 DNA by either dot blot or Southern blot hybridisation, whereas seven samples out of 25 tested were reported to contain viral DNA after nested PCR amplification. Similarly, only one of these concentrates (steam-heated) contained sufficient B19 DNA to be detectable by all the assays used. Overall, B19 DNA was detected in 2 of 3 untreated concentrates and in 4 of 20 treated concentrates.

A Norwegian study investigated the prevalence of B19 antibodies among haemophiliacs with different types and severities of coagulation factor defects (Rollag *et al.*, 1991).

The results showed that the prevalence in the different groups varied from 52% to 88%, depending on type and severity of the defect, whereas 49% of household contacts had B19 antibodies. The highest prevalence was found among persons with severe haemophilia A and B, but with an even higher prevalence among individuals with haemophilia B than A. The latter finding could be explained by the fact that factor IX concentrates, used to treat haemophilia B, were extracted from a larger plasma pool (250 donors) than that used for production of factor VIII concentrates (6 donors), which is given to patients suffering from haemophilia A. The fact that the prevalence of B19 antibodies is higher among those with severe haemophilia reflects the increased factor concentrate requirement and therefore the increased risk of receiving a B19 infected concentrate. Although the factor concentrates themselves were not tested for B19 DNA, an indirect correlation was made between the use of coagulation factor concentrates to treat haemophilia and the high prevalence of B19 antibodies among the patients receiving those blood products, as was already suggested by Mortimer and colleagues (Rollag *et al.*, 1991; Mortimer *et al.*, 1983). This correlation was also proposed in another study, although there was no significant difference between Dutch patients with haemophilia A, B or von Willebrand's disease (Mauser-Bunschoten *et al.*, 1998). This report showed that, in children of 0-10 years, 42 of 55 (76%) of the haemophilia patients and 11 of 48 (23%) of the controls were positive for anti-B19 IgG, as well as a striking 100% of children with severe haemophilia A who were treated on a prophylactic basis with clotting factor concentrates. These data emphasized once more the high risk of B19 transmission through plasma-derived clotting products.

In addition, while 20% of clotting factor batches tested in France (both factor VIII and IX concentrates) contained B19 DNA (Lefrère *et al.*, 1994), as much as 100% (7 of 7) of factor VIII batches tested in Great Britain were also positive (Saldanha and Minor,

1996). Two German groups also tested batches of factor VIII and reported 47 of 70 (67%) (Eis-Hübinger *et al.*, 1996) and 15 of 19 (79%) positive for B19 DNA by PCR (Willkommen *et al.*, 1999).

I.2.1.2.2. Albumin

The first study to investigate contamination of albumin with human parvovirus B19 tested 29 commercial batches, of either 4% or 20% albumin solution, produced from European plasma by two different manufacturers (Lefrère *et al.*, 1995). No B19 DNA was found in albumin concentrates, which are routinely heated by pasteurisation at 60°C for 10 hours to inactivate blood-borne viruses. Although B19 is thermostable and non-enveloped, it was suggested that the ethanol fractionation process might have inactivated or eliminated B19. Saldanha and Minor, on the other hand, detected B19 DNA in 3 of 12 albumin batches (25%) (Saldanha and Minor, 1996). The limit of detection of B19 DNA had been improved from 400-4000 genome equivalents/ml (Lefrère *et al.*, 1995) to 115 genome equivalents/ml (Saldanha and Minor, 1996), which might explain in part the disparity of the results in those two studies.

Furthermore, while Willkommen and coworkers detected 3 of 44 albumin batches (7%) positive for B19 DNA (Willkommen *et al.*, 1999), they found it remarkable that some of their German colleagues reported the presence of B19 DNA in 5 of 30 (17%) lots of recombinant factor VIII from two manufacturers, to which human albumin was added as a stabiliser during the preparation and purification procedures (Eis-Hübinger *et al.*, 1996). Although albumin was also subjected to pasteurisation at 60°C for 10 hours, Eis-Hübinger *et al.* suggested that the differences in the manufacturing process for albumin, such as ethanol fractionation, purification by chromatography or filtration, could

contribute to the divergence seen between their results and Lefrère and colleagues' (Eis-Hübinger *et al.*, 1996; Lefrère *et al.*, 1995).

I.2.1.2.3. Immunoglobulins

Besides albumin and factor VIII batches, Saldanha and Minor investigated both intravenous (IV) and intramuscular (IM) immunoglobulin (IG) batches, finding B19 DNA in 3 of 15 IVIG samples and 3 of 4 IMIG samples (Saldanha and Minor, 1996). Those IMIG samples found positive for B19 DNA were from two different manufacturers who did not use any specific viral inactivation technique and one batch even presented with a B19 DNA titre that was the same as in the start pool. Regarding the start pools tested in the same study, the majority (65 of 75: ~87%) was found to contain B19 DNA.

In conclusion, the contamination risk depends on several factors that could facilitate the presence of human parvovirus B19 in blood and blood derivatives. Firstly, the number of potentially infected blood donors is significant as, by the age of 60 years old, 60% of the general population would have been infected by the parvovirus. Secondly, the vast majority of infected adults are clinically asymptomatic, making diagnosis at the time of donation difficult. The rash, when present, develops after the viraemic phase. Thirdly, the incubation period during primary infection usually results in very high viraemia of 10^{11}-10^{13} virus particles/ml (Frickhofen and Young, 1989). Fourthly, although the virus is normally cleared in 5 to10 days, some infected individuals present a long-lasting but low level viraemia (10^2 to 10^4 virus particles/ml), although they have developed an IgG response and are thus immunocompetent (Faden *et al.*, 1992; Cassinotti *et al.*, 1993; Kerr *et al.*, 1995; Sasaki *et al.*, 1995). Additionally, human parvovirus B19 might stay

latent in the bone marrow (Sasaki *et al.*, 1995; Cassinotti *et al.*, 1997). Last but not least, it is still unclear whether the presence of anti-B19 IgG in other donations within a pool is sufficient to neutralise infectious virus particles and to prevent susceptible recipients of blood and blood products from developing viraemia and possibly B19 infection. However, despite the incidence of parvovirus B19 in blood and blood products detailed previously, the actual transmission of clinical infection is rare in the recipients because the viruses might not be infectious or could have been destroyed by viral inactivation steps during the manufacturing process. Moreover, anti-B19 antibodies from other blood donations in large plasma pools might be sufficient to neutralize B19 virus particles present in a single donation and prevent the infection. The few cases of infectious virus transmission by blood and blood products over the years are detailed in the following paragraph.

I.2.2. Evidences of infectious virus transmission by blood and blood products

I.2.2.1. Blood donations

The first report of transmission of infectious B19 by a single-donor transfusion was in a young woman suffering from β-thalassemia (Zanella *et al.*, 1995). This patient developed a symptomatic B19 infection involving transitory heart failure as well as transient red cell aplasia. B19 DNA was detected in blood samples taken from both the patient and one of the donors of the blood transfused, whose child had EI one week before donation. Additionally, the presence of anti-B19 IgM in the patient's serum indicated an acute infection and could also implicate the RBC transfusion in B19 transmission. Such an unusual case of transfusion-related B19 infection, as well as B19 incidence mentioned previously illustrate the fact that its transmission through blood

donations is a rare event in a non-epidemic situation, whereas it can become a significant risk during an epidemic period. As Aubin *et al.* emphasised, "during peak epidemic periods, manufacturing pools of several thousands of donations could contain as many as ten viraemic donations" (Aubin *et al.*, 2000). Moreover, since a blood donation from an individual at the peak of viraemia can contain up to 10^{13} virus particles/ml, even this single positive donation will contaminate a large plasma pool. Even contamination to a smaller plasma pool can occur and was reported in a pool containing 28 donations (Cohen *et al.*, 1990). The contaminated plasma pool had not been given to patients nor used for fractionation and was withheld from processing on time. Unfortunately, this is not always the case and the health of blood products recipients can sometimes be put at risk, as demonstrated by the following cases of infectious B19 transmission.

I.2.2.2. Plasma products

I.2.2.2.1. Clotting factors

B19 infection was reported following a first dose of factor VIII into a previously untreated patient who developed viraemia and a B19-specific IgM response ten days after receiving the concentrate, without any other possible source of infection such as a proceeding or concurrent illness in a close contact (Mortimer *et al.*, 1983). This was the first direct evidence that factor concentrates can transmit B19 infection. Subsequently, evidence for B19 transmission by unheated commercial factor VIII was given in two patients who had been infrequently exposed to concentrates (Williams *et al.*, 1990). The presence of anti-B19 IgM demonstrated an acute infection, even though asymptomatic. Although both boys had received the same batch of factor VIII 3 to 4 weeks before testing, evidence of B19 contamination in this batch could not be found since all tests

performed were negative (RIA, EM and dot blot hybridisation). On one hand, the techniques used at the time might not have been sensitive enough to detect the virus as PCR would nowadays, while on the other hand, it seems more likely that the patients were infected through their treatment rather than by the natural route.

The introduction of a solvent/detergent (S/D) treatment was confirmed not to be efficient on human parvovirus B19 as was indicated by the first case of hypoplastic anaemia in a young haemophiliac who had been transfused for the first time with a S/D treated factor VIII concentrate (Morfini *et al.*, 1992). The patient showed all the signs of a B19 primary infection, with high level of IgM detected just after the treatment, as well as anaemia and extreme fatigue after 10 days. IgG were found in the second serum sample drawn 3 weeks after anaemia and the patient recovered well within a week. The second case of S/D treated clotting factor involved in B19 transmission was that of a female haemophilia B carrier, who acquired a symptomatic B19 infection via S/D-treated factor IX concentrates (Yee *et al.*, 1996). Blood samples from the patient were positive for B19 DNA by primary and nested PCR ($\geq 10^7$ genomes/ml). These cases emphasise the vulnerability of such patients and might become a significant problem if parvovirus infection following treatment was to occur during pregnancy.

In Britain, although heat-treated factor VIII concentrate 8Y was previously thought to be comparatively safe (Williams *et al.*, 1990), B19 infection of an immunocompetent adult who had received this product was suggested (Yee *et al.*, 1995). Despite the fact that the patient's serum sample was negative for anti-B19 antibodies immediately before the first treatment, both IgM and IgG became detectable by RIA at the time of admission for sepsis, myelosuppression and hepatic dysfunction. Moreover, the batch of factor VIII concentrate received by the patient was found to be positive for B19 DNA by nested PCR. It is important to note that even infrequent users of clotting factor

concentrates are still at high risk of contracting a transfusion-associated B19 infection. As for factor IX concentrates, there had been a previous report of three patients presumed to have contracted symptomatic B19 infection via such products (Lyon *et al*, 1989). The patients had only limited exposure to blood products and two had received only the National Health Service heat-treated factor IX concentrate. Despite the fact that none of these patients gave a history of contact with a person with a rash before the development of their own rash and that anti-B19 antibodies were negative in an earlier stored serum, both anti-B19 IgM and IgG were detected after the onset of the rash. B19 DNA was amplified by PCR in one particular batch of factor IX concentrate used to treat these patients, which suggested that parvovirus B19 might be transmitted by heat-treated factor VIII and IX.

Although recombinant factor VIII concentrates had been regarded as safe concerning blood borne viruses, seroconversion for B19 in 5 of 16 susceptible patients receiving this product was reported (Aygören-Pürsün *et al.*, 1997). Despite the fact that the results were ambiguous in 3 of the cases, concerns remained for the other two patients regarding the possible transmission of the virus via recombinant factor VIII. Additionally, and as mentioned previously, parvovirus B19 DNA had already been amplified by nested PCR in recombinant factor VIII preparations where human albumin was used as a stabiliser during the manufacturing process (Eis-Hübinger *et al.*, 1996). In Aygören-Pürsün and colleagues' study, albumin was also present as excipient in the recombinant product and could thus be suspected to be the cause of seroconversion (Aygören-Pürsün *et al.*, 1997). Nevertheless, the natural infection of the patients within the community cannot be ruled out.

I.2.2.2.2. Immunoglobulin

While evaluating the possible genetic changes related to chronic parvovirus B19 infection, Erdman and coworkers found an abrupt change in B19 sequences in samples collected in a 5-year-old patient after administration of different lots of IVIG (Erdman *et al.*, 1997). Possible explanations for this sequence change included a specimen cross-contamination in the laboratory, the genetic evolution or immune selection of B19 variants and a reinfection by natural exposure or from B19 contaminated IVIG. After investigation, given the timing of the appearance of this new B19 strain just after administration of IVIG and the fact that IVIG had been shown to frequently contain B19 DNA (Saldanha and Minor, 1996), transmission of infectious parvovirus B19 by contaminated IVIG seemed to be the most likely event to have occurred. Although B19 antibodies present in IVIG would normally neutralize both the patient's virus and any virus potentially present in the preparation, it is possible that the immune complexes formed by specific antibodies and the virus particles enable infection of cells bearing the Fc receptor, such as monocytes and macrophages (Erdman *et al.*, 1997; Morey *et al.*, 1992). Infection of those cells would be non-productive, short-term and clinically asymptomatic, which was the case for the young patient studied by Erdman and colleagues. However, some reservations about the possibility of B19 transmission from IVIG in this particular case were raised a few years later (Hayakawa *et al.*, 2002) as no correlation was indeed shown between the B19 genotype in the patient's serum sample and the IVIG administered to the patient in Saldanha and Minor's paper (Saldanha and Minor, 1996). Therefore, Hayakawa and coworkers claimed to have presented "the first report to clearly show parvovirus B19 transmission from IVIG" (Hayakawa *et al.*, 2002). Only a few days after administration of IVIG later, found to be contaminated by B19, a patient's serum sample had become positive for B19 IgM antibody and for B19

DNA by PCR. In this case, the patient suffered from fulminant hepatitis likely to have been caused by B19 infection following pre-existing coxsackie B4 infection. However, the implication of IVIG in transmitting B19 infection had not been clearly established and further evidence would be needed to establish the cause of infection in this particular case.

I.2.2.2.3. Fibrin sealant

Another blood derivative implicated in infectious B19 transmission is fibrin sealant, which consists of fibrinogen and thrombin mixed with factor XIII and calcium. It is used as a haemostatic agent. Despite dry-heat viral inactivation on both fibrinogen and thrombin components, three cases of symptomatic B19 infection due to the use of the same batch of fibrin sealant during surgery were reported (Hino *et al.*, 2000). The batch in question was found positive for B19 DNA by PCR. In addition, the possibility of transmission by medical staff members was excluded after they were all confirmed negative for B19 IgM. Following these cases, a careful follow-up of patients treated with fibrin sealant was advised and the need for recombinant products was emphasised.

The frequency of B19 infection transmission by fibrin sealant during surgery was estimated in a group of 85 patients who underwent thoracic surgery and needed fibrin sealant to stop air leak or haemorrhage (Kawamura *et al.*, 2002). In 6 of 29 patients (20.7%) whose blood samples were negative for anti-B19 IgG before surgery, samples obtained 12 to 48 weeks after surgery were positive for both anti-B19 IgG and B19 DNA by PCR. Batches of fibrin sealant used in 2 of those 6 patients also tested positive for B19 DNA. It was therefore suggested that these post-chest surgery infections were transmitted by B19 contaminated fibrin sealant.

The various reports of significantly elevated prevalence of anti-B19 antibodies in haemophiliacs, as well as in other patients receiving frequent treatment with plasma products derived from such pools, gave further evidence that the virus is very robust. It is able to withstand the treatment and purification steps of these plasma products and still be present -and sometimes infectious- in the final product.

I.2.3. "Inefficiency" of viral inactivation methods used in current processes

According to Burnouf, who reviewed virus inactivation treatments, "one problem in establishing these techniques is to ensure a high level of virus inactivation while preserving the biological activity of the coagulation factors" (Burnouf, 1992). It is essential to design effective inactivation methods that will avoid the alteration of the three-dimensional structure of therapeutic proteins. Moreover, it seems that plasma protein purification technologies, based on high-resolution chromatographic extractions, already play a role in viral safety. The manufacture of coagulation factor concentrates involves a combination of centrifugation, precipitation, chromatography, ultrafiltration and freeze-drying steps. All of these steps could, in theory, contribute to inactivate or remove viruses. In practice, at least one, but often two, validated viral inactivation/ removal techniques have to be included in blood products preparation.

PCR was used to detect B19 DNA in seven of seven factor VIII samples tested, which had been treated with either S/D plus monoclonal antibody purification, dry heat (80°C for 72 hours) or solvent-detergent followed by ion-exchange chromatography (Saldanha and Minor, 1996). Although Saldanha and Minor emphasised that further work on many more samples is required, Their results suggest that none of these viral inactivation methods are sufficient to destroy B19 viral DNA. As mentioned previously, the same

study showed that some IVIG batches were positive for B19 DNA. IVIG usually undergoes various viral inactivation steps. For instance, the manufacturers can use S/D treatment, pasteurisation (60°C for 10 hours), low pH step (pH 4.25) or treatment with protease at pH 6.5. All fifteen pools from one of the manufacturers who used pH 4.25 presented high levels of B19 DNA but the six IVIG batches derived from those were negative for B19 DNA, suggesting that such low pH could destroy the virus (Saldanha and Minor, 1996). However, B19 DNA was found in IVIG from the manufacturer who used a S/D step. The possible transmission of B19 virus by S/D treated factor VIII concentrate had been suggested in a young haemophiliac who developed hypoplastic anaemia after first infusion with the former product (Morfini *et al.*, 1992). It is well known that this inactivation technique destroys only lipid-enveloped viruses and that B19 virus can thus withstand such a virucidal method. Subsequently, Koenigbauer and coworkers published the case report of a patient who was infused with several units of solvent (tri(n-butyl)phosphate)-detergent (Triton X-100) treated plasma later found to have high levels of parvovirus B19 DNA (Koenigbauer *et al.*, 2000). The patient was positive for both IgG and IgM, which reflected an acute B19 infection. This particular case shows once more the inefficiency of S/D treatment to inactivate B19 virus.

In order to supplement S/D treatment with a technique that might be more effective on non-lipid-enveloped viruses, heating treatments, including dry-heating and pasteurisation, were investigated. Four of 20 treated clotting concentrates tested for B19 DNA were positive (Zakrzewska *et al.*, 1992). Only a small number of chloroform treated and dry-heated products were included in the study and, although none was found to contain B19 DNA, the number tested was too small to be representative of the effectiveness of these treatments. Similarly, B19 DNA was not detectable in the seven pasteurised concentrates tested in this study. Although the pasteurisation technique is

suggested to reduce the risk of B19 infection, it doesn't eliminate it (Lyon *et al.*, 1989; Azzi *et al.*, 1992). Even if the study by Mauser-Bunschoten *et al.* did not detect B19 virus particles directly, it showed a significant difference in prevalence of B19 IgG between haemophiliacs and healthy individuals but, interestingly, did not observe any change between the patients treated with S/D or with pasteurised products (Mauser-Bunschoten *et al.*, 1998). Furthermore, despite the fact that factor VIII 8Y was treated for 72 hours at 80°C (final product), this clotting factor concentrate still transmitted parvovirus B19 infection to an immunocompetent adult (Yee *et al.*, 1995). This product was previously thought to be associated with a lower incidence of B19 transmission (Lyon *et al.*, 1989). More recent data showed that blood products either vapour-treated (60°C for 10 hours followed by 80°C for 1 hour) or dry-heat treated (80°C for 72 hours), transmitted B19 infection, although asymptomatic, in two young recipients (Blümel *et al.*, 2002a). The use of dry heating at sterilising temperature (100°C for 10 to 30 minutes) was also recommended with minimal loss for factor VIII and IX concentrates (Rubinstein and Rubinstein, 1989; Rubinstein, 1990). Following this suggestion, an Italian manufacturer chose to add a terminal inactivation step based on heating at 100°C for 30 minutes in lyophilised clotting factor concentrates (Santagostino *et al.*, 1994). Nevertheless, an acute B19 infection developed in four patients out of the ten who were anti-B19 IgG negative before receiving the treated factor VIII or IX concentrates. This report was criticised by Prowse, who thought that the data should have been interpreted with regard to an age-matched healthy control group or an untransfused haemophilic group (Prowse, 1994). Most previously untreated haemophiliacs would be under the age of ten, which is an age group that would be expected to show a higher rate of B19 viraemia. The other comment on the study by Santagostino and colleagues came from Guillaume, who proposed to extend the terminal viral inactivation step at 100°C to 45 or

even 60 minutes in blood products in order to eliminate parvovirus B19 (Guillaume, 1994). However, it was argued that this final inactivation step might increase the risk of a reduced yield and the possibility of a higher frequency of inhibitors (Thomas, 1994). To this reservation, Lusher and coworkers replied that the same arguments were given in the early 1980s when the introduction of dry heat and pasteurisation treatments to clotting factors production was discussed, but neither of these events took place and a large number of infections by HIV and HCV were spared thanks to these inactivation techniques (Lusher *et al.*, 1994). To end this argument, Thomas seemed resilient to "acknowledge that absolute safety is a mirage", statement to which both Lusher *et al.* and Colvin reacted strongly as "no one should abandon the goal of achieving absolute safety" (Thomas, 1994; Colvin, 1994; Lusher *et al.*, 1994).

Other processes used to supplement S/D treatment included purification by anion exchange chromatography, as well as nanofiltration (pore size 0.2μm). The reduction of B19 DNA in factor VIII manufactured in such a way was investigated by spot hybridisation and Southern blotting (Schwarz *et al.*, 1991). It was thought that physic-chemical interaction occurred between B19 virus and the anion exchange material of the column since there was a reduction of at least $\log_{10}$ 2 of the total amount of B19 virus used to spike the start product. Additionally, DNA hybridisation could not detect any viral DNA after the filtration step, which showed that residual virus particles, seen as aggregates by EM, were cleared in this final step. Although these results were interesting, they were not obtained with the most sensitive nucleic acid detection method (PCR) and they still do not indicate whether B19 virus found after anion exchange chromatography represents infectious or inactivated virus.

Nanofiltration of factors IX and XI concentrates also showed promising results on the elimination of bovine parvovirus (BPV; 20-25nm) (Burnouf-Radosevich *et al.*, 1994).

The 15N filter (pore size 0.15μm) used was able to remove more than $\log_{10}$ 6.3 of BPV while virus aggregates were also eliminated by more than $\log_{10}$ 5.8 when passed through a 35N filter (pore size 0.35μm). Although BPV is a small non-enveloped virus resistant to S/D treatment and has been used as a model for parvovirus B19, further studies using human parvovirus B19 virus itself are still required to evaluate the efficiency of nanofiltration. Furthermore, this method cannot be applied to higher molecular weight plasma proteins, such as factor VIII molecule or von Willebrand factor concentrates.

Tables 1.8 and 1.9 summarise the characteristics of established viral removal and inactivation procedures regarding protein integrity and efficacy to inactivate parvovirus B19.

Table 1.8: Characteristics of well-recognized viral removal procedures

Treatment	Properties	Points to Consider
Precipitation	Purifies protein Can be effective against both enveloped and non-enveloped viruses including parvovirus B19	• Usually modest virus removal • Difficult to model
Chromatography	Purifies protein Can be effective against both enveloped and non-enveloped viruses including parvovirus B19	• Virus removal highly dependent of choice of resin, protein solution, and buffers • May be highly variable from one virus to another • Resin must be sanitized between lots
Nanofiltration	Effective against enveloped viruses Can be effective against non-enveloped viruses including parvovirus B19 Non-denaturing to proteins High recovery of "smaller" proteins such as coagulation factor IX	• Degree of virus removal depends on the pore size of filter used • Elimination of small viruses may not be total • Some filter defects may not be detected by integrity testing

Table 1.9: Characteristics of well-recognized viral inactivation procedures

Treatment	Properties	Points to Consider
Pasteurisation	Inactivates enveloped and some non-enveloped viruses including HAV Relatively simple equipment	• Protein stabilizers may also protect viruses • Does not inactivate parvovirus B19
Terminal Dry Heat	Inactivates enveloped and some non-enveloped viruses including HAV Treatment applied on the final product	• Does not inactivate Parvovirus B19 • Requires strict control of moisture content
Steam or vapour Heat	Inactivates enveloped and some non-enveloped viruses	• Does not inactivate Parvovirus B19 • Relatively complex to put in place
S/D	Very efficient against enveloped viruses Non-denaturing to proteins High process recovery Relatively simple equipment	• Non-enveloped viruses unaffected • Not generally affected by buffers used • S/D reagents must be removed
Acid pH	Effective against enveloped viruses Relatively simple equipment	• Limited efficacy against non-enveloped viruses • Use largely restricted to IgG • At pH 4, effective virus kill requires elevated temperatures
Methylene blue	Efficiency depends on nucleic acid content (greater for double stranded than single stranded) Good efficiency for enveloped viruses but variable efficiency for non-enveloped viruses	• Loss of functional activity of coagulation proteins (more severely affected are factor VIII and fibrinogen) • Can be applied to single unit system

The main conclusion that can be drawn from such data is the difficulty to evaluate the efficiency of established viral removal/inactivation methods to reduce the risk associated with infectious parvovirus B19. The first reason for this is that the actual

infectivity of the virus is not reflected by the B19 DNA titre, which highlights the lack of a reproducible and sensitive infectivity assay. Although the cell line KU812Ep6 has been used to detect infection by mRNA amplification (reverse-transcriptase-PCR: RT-PCR) or immunofluorescence staining (Blümel *et al.*, 2002b; Boschetti *et al.*, 2004), the UT-7/Epo-S1 cell line was found to be more susceptible to parvovirus B19 infection (Chaput and Saldanha, unpublished data). The second reason resides in the fact that the animal models available, including BPV, PPV, CPV and MMV are not representative of the behaviour of human parvovirus B19. For instance, recent studies have clearly shown that animal models have different susceptibility to pasteurisation and low pH treatment (Blümel *et al.*, 2002b; Boschetti *et al.*, 2004). Human parvovirus was shown to be inactivated by more than $\log_{10}$ 4 after 10 minutes at 60°C in albumin solutions, whereas PPV was resistant to pasteurisation treatment (Blümel *et al.*, 2002b). Similarly, when exposed to pH 4.0 for 2 hours, parvovirus was inactivated by more than $\log_{10}$ 5 whereas MMV was resistant for over 9 hours. These new data revealed not only that animal parvoviruses should not be used as models for B19, but also that human parvovirus B19 might be much more susceptible to inactivation treatments than previously suspected.

I.2.4. What solutions for safer, B19-free plasma?

A number of solutions can be applied to improve the safety of plasma pools regarding parvovirus B19 at the time of donation, during the manufacturing process or with the increasing use of recombinant clotting factor concentrates.

I.2.4.1. At the first stage of blood donation

Donors could be selected on the basis of being anti-B19 IgG positive, since they are likely to represent a resolved infection. However, reinfection can occur in those who

have a low level of anti-B19 IgG, resulting in a second IgM response (Anderson and Young, 1997).

One of the key solutions, which is already applied routinely by some manufacturers, is the screening of blood donors by nucleic acid testing (NAT) for B19 DNA to limit the number of B19 transmissions (McOmish *et al.*, 1993). The potential benefit of NAT for parvovirus B19 was discussed at a workshop on the implementation of NAT to screen donors of blood and plasma (Tabor *et al.*, 2000). At the time, it was considered to be an "in-process control" rather that a donor screening test. As of June 2000 in the United States, NAT screening for HCV RNA and HIV RNA in minipools was implemented efficiently, without compromising the availability of the blood supply (Busch and Dodd, 2000). However, in the context of the debate over minipool versus individual-donation NAT, the main concern was that the shorter window-period and yield of individual-donation NAT compared to minipool NAT for HIV and HCV would be very small and very expensive. The political and regulatory bodies in developed countries decided to apply minipool NAT but might introduce further safety, including individual-donation NAT and NAT for additional agents, such as West Nile virus in Canada and parvovirus B19 in Europe. However, such a decision should be an international consensus since "blood policies, like the viruses we are trying to avoid, ramify globally" (Busch and Dodd, 2000) although realistically, there is a huge gap between rich countries and developing countries, where both the high viral prevalence and the minimal, sometimes the absence of screening leads to hundreds of thousands of infections a year being transmitted through blood.

One disadvantage of donor-screening procedures is the lack of specificity in the deferral criteria, leading to a large number of safe donors being deferred (Kleinman, 2001). Additionally, the main limitation of NAT remains the fact that the presence of B19 in

concentrates does not necessarily indicate that the product is infectious (Luban, 1994). Therefore, *in vitro* infectivity studies are still needed, as well as a clear correlation between viral sequences as detected by PCR and infectivity of the virus.

I.2.4.2. During the manufacturing process

Another way to improve safety is the introduction in the manufacturing procedure of a new virucidal method effective on non-lipid enveloped viruses, such as psoralen treatment, iodine, UVC light irradiation, gamma-irradiation and *SuperFluids*™.

In the absence of ultraviolet (UV) light, psoralens reversibly intercalate into helical regions of DNA and RNA. When illumination with UVA occurs, they react with pyrimidine bases to form covalent mono-adducts and cross-links with the nucleic acids (Corash, 2003). Consequently, both nucleated cells (T cells, leukocytes) and pathogens are unable to replicate. Psoralen S-59 (Cerus Corporation, Concord, CA, USA) for use on platelet concentrates is now being introduced into clinical practice in Europe since it has received final CE Mark approval. However, when RBCs are processed through the system, they constitute a difficult environment for pathogen inactivation because of the light absorbance by haemoglobin and the viscosity of packed RBCs (Corash, 2003). A compound that does not require light activation, called S-303 (Cerus Corporation, Concord, CA, USA), is thus utilised and is activated by a pH shift created by the introduction of erythrocytes into the system. Phase III clinical trials on S-303-treated RBC are underway to evaluate their safety and efficacy in the treatment of acute and chronic anaemia. Another compound used for pathogen reduction in RBC concentrates is PEN 110 (INACTINE™; VI Technologies, Watertown, MA, USA). It is a highly water-soluble cation capable of diffusing through cell membranes and covalently interacts with nucleophilic centres of nucleic acids, essentially with N7 of guanine

residues (Lazo *et al.*, 2002). N7 guanine alkylation can cause opening of the imidazole ring, base loss and strand breakage, resulting in disruption of transcription and replication of the pathogen genome (Lazo *et al.*, 2002; Purmal *et al.*, 2002). The removal of PEN 110 to a non-toxic level is then performed using an automated cell-washing process.

A different chemical treatment is that of iodine, a strong oxidizing agent with powerful microbicidal properties. When it is bound to polymers or dextran chromatographic medium such as Sephadex®, there is a slow, controlled release of iodine into the protein solution, with virus inactivation occurring over a longer time course (hours) (Miekka *et al.*, 1998). In the case of the chromatographic medium, protein is passed through a bed of iodine-Sephadex® followed immediately by a bed of Sephadex® used to trap and remove free iodine. The factors that might affect the iodine inactivation system are iodine concentration, age of iodine-Sephadex®, temperature, contact and incubation times and composition of protein solution being treated. All these factors need to be defined and controlled. Liquid iodine has also been found to inactivate several enveloped and non-enveloped viruses in an antithrombin III concentrate (Highsmith *et al.*, 1995).

Several physical treatments can also be applied, such as UVC light (254nm), which targets nucleic acid, thereby inactivating a wide range of viruses, irrespectively to the presence of a lipid envelope. Both albumin and IVIG solutions had to be treated with 5,000 Joules/m^2 UVC before non-enveloped and heat and/or acid resistant viruses (polio 2, vaccinia and T4 phage) were effectively inactivated (Hart *et al.*, 1993). A recent study also showed that UVC can be used at doses that preserve protein activity but still inactivate MVM, parvovirus B19, the encephalomyocarditis virus, which is a model for

HAV, and bovine herpes virus type 1, a model for enveloped viruses such as HBV (Caillet-Fauquet *et al.*, 2004).

Gamma irradiation has been used extensively for the treatment of a variety of materials ranging from sterilizing medical devices (Doue, 2001) to reducing bacterial and viral contamination in animal sera (House *et al.*, 1990). Such irradiation readily penetrates protein solutions and has the potential to inactivate pathogens during the manufacture of bulk intermediates and in final products (Miekka *et al.*, 2003). It can act either by direct rupture of covalent bonds in target molecules including proteins and nucleic acids, or indirectly by producing reactive free radicals and other active, radiolytic products, which in turn can react with proteins and nucleic acids.

Lastly, the novel system of *SuperFluids*™ (Aphios Corporation, Woburn, MA, USA) has the ability to reduce the viral load of both enveloped and non-enveloped viruses. They are normally gases which, when compressed to a particular pressure and heated to a specific temperature, enter the supercritical fluid region and show enhanced solvation, penetration and expansion properties (Dr T Castor, personal communication). Treatment of viruses with these fluids results in inflation of the particles due to penetration of the *SuperFluids*™. Subsequent decompression causes their expansion within the virus particles resulting in rupturing of the particles at their weakest point. This technology does not damage proteins and enzymes since it is purely physical and does not involve the use of chemicals, heat or irradiation. The other advantages are the fact that they are readily separated, with no toxic residues and that the system can be easily scaled up to production levels with continuous flow operations. However, this technique cannot be used on blood donations that still contain red blood cells because these fluids would damage them.

I.2.4.3. Replacement therapy

The last point to consider is an alternative choice of replacement therapy, namely recombinant clotting factor concentrates. The first-generation recombinant factor VIII, formulated in albumin, was licensed in the early 1990s (Mannucci, 2002). Although they showed excellent efficiency and triggered no more inhibitors than plasma-derived factors do, the safety of the albumin used as a stabiliser was questioned, as discussed previously (Eis-Hübinger *et al.*, 1996; Aygören-Pürsün *et al.*, 1997). Second-generation recombinant factor VIII, in which no human albumin is added but includes a S/D step, is licensed in both the US and Europe (Mannucci, 2002). Additionally, clinical trials are underway for third-generation recombinant factor VIII, which are manufactured with no human or animal protein. Such formulated and manufactured recombinant factor IX is already available. However, those products cost 2 to 3 times more than blood products and few haemophiliacs can be prescribed this safer alternative. Moreover, the production capacity for recombinant factors is still limited, leading to a risk of shortage.

I.3 Aims of the thesis

In the present study, several continuous cell lines were evaluated for susceptibility to B19 infection with a view to developing a sensitive *in vitro* infectivity assay. As B19 does not produce any cytopathic effect in susceptible cell cultures, replication can be demonstrated by IFA detection of viral proteins, (particularly NS1, which is not present in the B19 inoculum), an increase in viral DNA or in the detection of B19 mRNA. Quantification by IFA is difficult due to the poor susceptibility of the cell lines used for B19 replication and the sensitivity of the technique. Similarly, accurate quantification by DNA amplification is complicated by the fact that it is difficult to ensure that all input viruses are thoroughly removed before analysis of progeny virus, especially at the

lower dilutions. The best method is thus detection of mRNA. In B19 replication, spliced mRNAs are transcribed off the B19 template and these are easily amplified by reverse transcriptase PCR (RT-PCR). They have a distinct size compared with amplicons that may possibly be amplified from the DNA template.

In addition to using B19-specific primers for RT-PCR, primers specific for the housekeeping gene β-actin were included in the amplification reaction. Housekeeping genes are expressed at a constant level in different tissues, stages of development and experimental treatment. The level of actin in samples for a particular assay was used to normalise the B19 mRNA results.

The initial work on the evaluation of cell lines for B19 infectivity assays was done with the KU812 and UT-7/EPO cell lines, which were easily available. Later in this study, the KU812Ep6 cell line, which was reported to be a better line for B19 infection, was obtained and some preliminary work was done with this cell line. However, due to restrictions on the use of the KU812Ep6 cell line, the clonally selected cell line, UT-7/EPO-S1, was obtained and evaluated.

Several parameters, such as the optimal time to infect the cell lines, the passage number, the conditions for culture and inoculation were investigated. In addition, the effects of cell synchronisation on susceptibility to B19 infection were studied. Cell synchronisation has been reported to enhance the susceptibility of the human megakaryocytoblastoid cell line UT-7 to B19 infection (Shimomura *et al.*, 1993). This was possibly due to the requirement of a product of the S phase of cell division for B19 replication. It has also been reported that B19 requires rapidly dividing cells for propagation (Anderson, 1987b). Finally, the effects of hypoxia on the susceptibility of the cell lines to B19 infection were studied. In contrast to standard cell culture conditions, characterized by 20% oxygen concentration, cells in the human body are

exposed to much lower oxygen concentrations, ranging from 16% in the pulmonary alveoli to less than 6% in most other organs of the body (Semenza, 2001). Moreover, oxygen concentration may even drop to extremely low concentrations, close to anoxia, in the presence of altered vascularization as observed at pathological sites such as tumors. Several studies have shown that severe hypoxia (1% oxygen) increased the number of erythroid BFU-E generated from CD34+ cells, as well as their maintenance in a liquid culture system (Cipolleschi *et al.*, 1997; Sun *et al.*, 2000). On the other hand, hypoxia inhibited the expression of CD36, a marker of erythroid CFU-E and maturing erythroid precursors (Cipolleschi *et al.*, 1997). The role of EPO levels in the differentiation and amplification of the CFU-E pool under hypoxia was found to be crucial in mouse model (Mide *et al.*, 2001). EPO, which is a hypoxia-inducible cytokine, might indeed act as a "survival factor" at the CFU-E level and/or increase the flow of cells from BFU-E to CFU-E. The enhancement of B19 replication in cells grown in low oxygen conditions could thus be due to the proliferation and maintenance of the virus target cells. In addition, this phenomenon could be explained by an increase in the expression of viral receptors on cells grown in hypoxia. Such conditions have recently been found to induce high expression of CXC-chemokine receptor 4 (CXCR4), one of the primary HIV-1 co-receptors *in vivo,* in different cell types: monocytes, monocyte-derived macrophages, tumor-associated macrophages, endothelial cells and cancer cells (Schioppa *et al.*, 2003).

In addition to quantification of B19 DNA, the present study describes optimization of a procedure to semi-quantitate B19 mRNA in B19-infected cell cultures.

The second part of the present study used the optimised B19 infectivity and quantitative B19 DNA assays to evaluate the efficacy of five methods for the inactivation or removal

of pathogens from blood products. Two chemical methods (psoralin and Inactin treatments) and two physical methods (pressure cycling and dry heating) for pathogen inactivation were studied. In addition, a pathogen removal method, nanofiltration, was included in this study.

Chapter II: Materials and methods

II.1. Materials

II.1.1. Agarose gel electrophoresis

- 50 x Tris-acetate-ethylenediamine tetraacetic acid (EDTA) (TAE) stock. Made at NIBSC: 2M Tris-acetate, 50mM EDTA. Working solution is 1 x TAE.
- Ethidium bromide tablets (EtBr) (BIO-RAD, 161-0430).
- Ethidium bromide-agarose gel: a 2% agarose gel was prepared by adding 100ml of 1x TAE buffer to 2g of agarose powder (Agargel H/M, CLP, #5410.500), which was then heated in a microwave oven for a couple of minutes to dissolve the agarose. The gel solution was stirred, left to cool down to just above body temperature. EtBr was then added at a final concentration of 1µg/ml (100µl of 1mg/ml stock). The agarose solution was poured into the gel apparatus and the combs were put in place.
- 6x blue/orange loading dye (Promega, G190A)
- The PCR markers (Promega, G3161A) contained lambda phage EcoR1fragmements 1000, 750, 500, 300, 150 and 50 base pairs in length. For gel analysis, the DNA ladder was prepared by adding 5µl of PCR markers to 2µl of blue/orange dye.
- The gel was placed into the gel tank of the electrophoresis apparatus (Horizon™ 11.14, BRL) and the combs removed carefully to avoid tearing the wells. The power was supplied through GenePower Supply GPS 200/400 (Pharmacia) and the gel was run for approximately 1 hour at 90V (110mA).

II.1.2. Nucleic acid extraction

All buffers for extraction, RT-PCR and PCR were prepared in a dedicated "clean" room. All sample dilutions and extraction of nucleic acids were done in a level 2+ laboratory in a class II cabinet.

- DNA extraction: QIAamp DNA blood mini kit (50 extractions) (Qiagen, 51304)

Buffer OL1 from QIAamp DNA mini kit: 30µl of β-mercaptoethanol (β-ME; Sigma-Aldrich, M6250) was added per 1ml of lysis buffer OL1, supplied in the Qiagen kit. Due to its toxicity, β-ME must be dispensed in a fume cabinet and appropriate protective clothing must be worn. OL1 buffer is then stable for 1 month at room temperature.

- mRNA extraction: Oligotex direct mRNA micro kit (Qiagen, 72012)
  - Buffer OCL (lysis buffer) made in-house for mRNA extraction:

10mM Tris.Cl pH 7.5 (made up from Trizma®Hydrocloride (Sigma, T-9285) 1M and Trizma®Base (Sigma, T-8524))

140mM NaCl (5M solution, Sigma, S5150)

5mM KCl (sigma, P5405)

1% IGEPAL CA-630 (Sigma, I3021)

Buffer OCL was stored at 4°C for one month and kept on ice during the extraction.

  - Buffer OCD (dilution buffer) was made fresh before each extraction:

1M lithium chloride (LiCl) (8M solution, Sigma, L7026)

20mM Tris.Cl pH 7.5

2mM Ethylenediamine-tetracetic acid (EDTA) (Sigma, E7889)

1% Sodium dodecyl sulfate solution (SDS; Sigma-Aldrich, L4522)

II.1.3. Nucleic acid amplification

II.1.3.1. DNA amplification

The kit used for DNA amplification was the LightCycler Faststart DNA Master SYBER Green kit (Roche, 3003230). The LightCycler glass capillaries were also supplied by Roche (1909339).

The primers (desalted) were first obtained from GIBCO BRL Life Technologies (UK), renamed (from October 2001) Invitrogen Life Technologies (UK). They were reconstituted in RNAase-free water to obtain a working solution at 25pmol/µl. However, the absorbance at 260nm of all the primers was also measured and the concentrations calculated using the following equation:

Concentration (nmole/ml) = A_{260} x weight per OD (given by the manufacturer on the data sheet) x dilution factor

The sequence of the forward primer, B19F, was:

5' GGC AGC ATG TGT TAA AGT GGA 3'. The annealing temperature of this primer in 50mM Na^+ was 55.8°C and it was located at positions 1538-1558 on the B19 genome. The sequence of the reverse primer, B19R, was:

5' CTC CAG GCA CAG CTA CAC TTC 3'. The annealing temperature of the reverse primer in 50mM Na^+ was 57.7°C and it was located at positions 1840-1820 on the B19 genome. This primer pair amplified a 302 base pair region of the NS1 gene.

II.1.3.2. mRNA amplification

The kit used for RNA amplification was the one step RT-PCR kit (100 reactions) (Qiagen, 210212).

The primers (desalted) used for mRNA amplification were first obtained from GIBCO BRL Life Technologies (UK), renamed (from October 2001) Invitrogen Life Technologies (UK). The relative positions of the primers on the B19 genome are shown on figure 2.1 and the primers sequences and the sizes of the specific amplification products are listed in table 2.1. The splicing donor and acceptor sites indicated on figure 2.1 were first described by Ozawa and coworkers, and then revised by St Amand and colleagues (Ozawa *et al.*, 1987; St Amand *et al.*, 1991). Map location of the primers was calculated from B19-Au accession number M13178 (Shade *et al.*, 1986). Details of the actin primer pair are showed in table 2.2. The primer concentration was calculated after measurement of their absorbance at 260nm.

Figure 2.1: Location of B19 primers on the genomic and transcription maps of B19

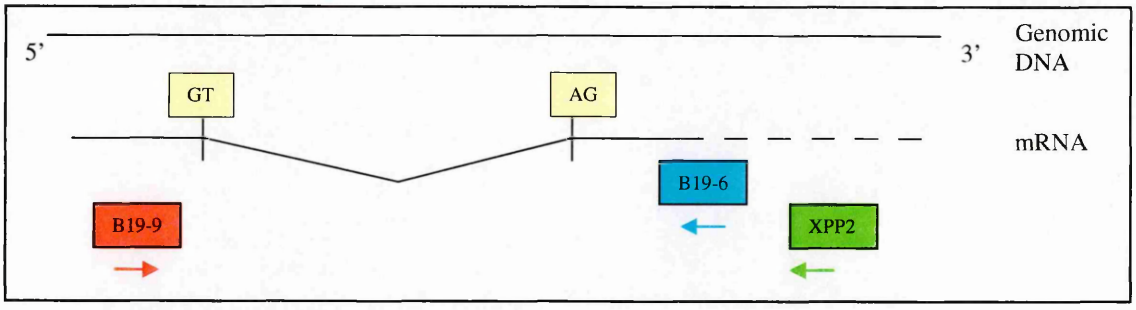

GT: splicing donor site (406)

AG: splicing acceptor site (1910; 1925; 1952; 2030)

Table 2.1: B19 primer pairs used in this study

Primer pair	Sequence (5'→3')	Map location	Primer Tm, (°C)	Expected products size (bp)	Regions amplified
Forward: B19-9	GTT TTT TGT GAG CTA ACT AAC A	384-405	49.3	155; 275; 1779	NS1
Reverse: B19-6	CAA AGG TGT GTA GAA GGC TT	2163-2144	52.6		
Forward: B19-9	GTT TTT TGT GAG CTA ACT AAC A	384-405	49.3	185; 305; 1810	NS1
Reverse: XPP2	ACC GTC CCA CAC ATA ATC AAC	2194-2214	55.1		

Table 2.2: Actin primer pair used in this study

Primer pair	Sequence (5'→3')	Map location	Primer Tm, (°C)	Expected products size (bp)
Forward: Actin 3	GAT GAC CCA GAT CAT GTT TG	427-446	51.1	621
Reverse: Actin 4	GGA GCA ATG ATC TTG ATC TTC	1068-1048	51.1	

II.1.4. Purification of amplified products from agarose gels for sequencing

Tris-EDTA (TE) buffer: 10mM tris, pH 8, 1mM EDTA. It was used to wash the spin column.

II.1.5. FACS analysis

- The wash buffer contained PBS (made at NIBSC) with 2% foetal calf serum (FCS) (GIBCO Invitrogen cell culture, 16000) and 0.05% w/v sodium azide (Sigma, S8032)
- The fixative buffer was 2% saline formaldehyde solution (formaldehyde solution from VWRInternational, 284216N)
- Mouse IgG negative control RPE (Serotec, MCA928PE)
- Mouse anti-human CD34 Class II-RPE (Serotec, MCA1578PE)

II.1.6. Primary cells

II.1.6.1. CD34+ cells

Cells expressing CD34 are normally present at a frequency of 0.05-0.2% in peripheral blood whereas the peripheral blood from patients whose stem cells have been mobilised contains up to 1% of CD34+ cells (Dr M. Watts, personal communication; Watts and Linch, 1997). Thus, Dr M. Watts (Department of Haematology, University College Hospital, London, UK) kindly provided mobilised peripheral blood (on a weekly basis), from which CD34+ cells were selected.

II.1.6.2. Aperesis cells

Samples of apheresis cells, or mobilised PBMC, were kindly given weekly by Dr M. Watts (Department of Haematology, University College Hospital, London, UK).

II.1.7. Continuous human erythroid cell lines

The human cell lines used in this study are shown in table 2.3.

Table 2.3: Human cell lines used in this study

Cell line	Origin	Reference	Growth medium	Source
KU812	Patient with chronic myeloid leukemia	Nakazawa *et al.*, 1989	RPMI 1640 +10% FCS + 1% glutamine + 1% pen/ strep	Dr Nakazawa, Niigata University, Japan
KU812Ep6	Erythropoeitin-dependent subline of KU812	Miyagawa *et al.*, 1999	RPMI 1640 +10% FCS +6 IU/ml EPO + 1% glutamine + 1% pen/ strep + 1% fungizone	Ube Research laboratory, Fujirebo, Japan
UT-7/EPO	Erythropoeitin-dependent subline of UT-7, a human leukaemia cell line	Komatsu *et al.*, 1993	IMDM +10% FCS + 2 IU/ml EPO + 1% pen/ strep + 1% fungizone	Dr.Komatsu, Jichi Medical School, Tochigi, Japan
UT-7/EPO-S1	Erythropoeitin-dependent subline of UT-7/EPO	Morita *et al.*, 2001	Iscoves modified DMEM + Glutamax-1 +10% FCS + 2 IU/ml EPO + 1% gentamycin + 1% fungizone	Dr Morita, Tohoku University, Japan

All the cell lines grew as suspension cultures, either as single cells or in aggregates. All cell lines were grown at 37°C in a 5% CO_2 atmosphere, either in 75mm^3 flasks (Falcon) or in 24-well or 96-well plates (Falcon). The stock cell cultures were split every 3-5 days at a split ratio of 1:3 to 1:5. The cell suspension was centrifuged at 715g for 10

minutes to pellet the cells. The pellet was then resuspended in a small volume of growth medium (usually 1-5ml), diluted 1:10 in trypan blue solution and the live cells (unstained) counted in a haemacytometer (Sigma).

UT-7/EPO-S1 cell aggregates, which can be seen on figures 2.2 and 2.3, had already been shown to be more susceptible to B19 infection than single cells (Dr Morita, personal communication). Thus before splitting, the cells were left for 30 minutes to settle at the bottom of the flask and most of the medium was carefully removed, leaving behind the cell aggregates. The latter were then resuspended in a small volume of growth medium, and the cell aggregates dispersed by pipetting before further processing.

Hypoxia studies on UT-7/EPO-S1 cells were performed in the laboratories of the Canadian Blood Services (Ottawa, Canada), which had a dedicated incubator required for tissue culture in a controlled low oxygen atmosphere, using regulated oxygen and nitrogen supplies.

Figure 2.2: UT-7/EPO-S1 cell aggregates under the light microscope (x20)

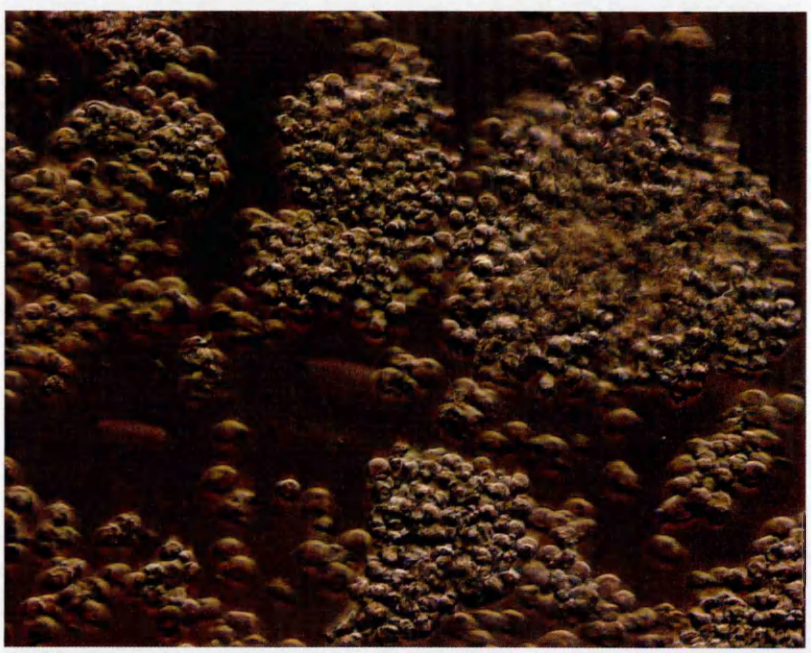

Figure 2.3: UT-7/EPO-S1 cell aggregate under the light microscope (x40)

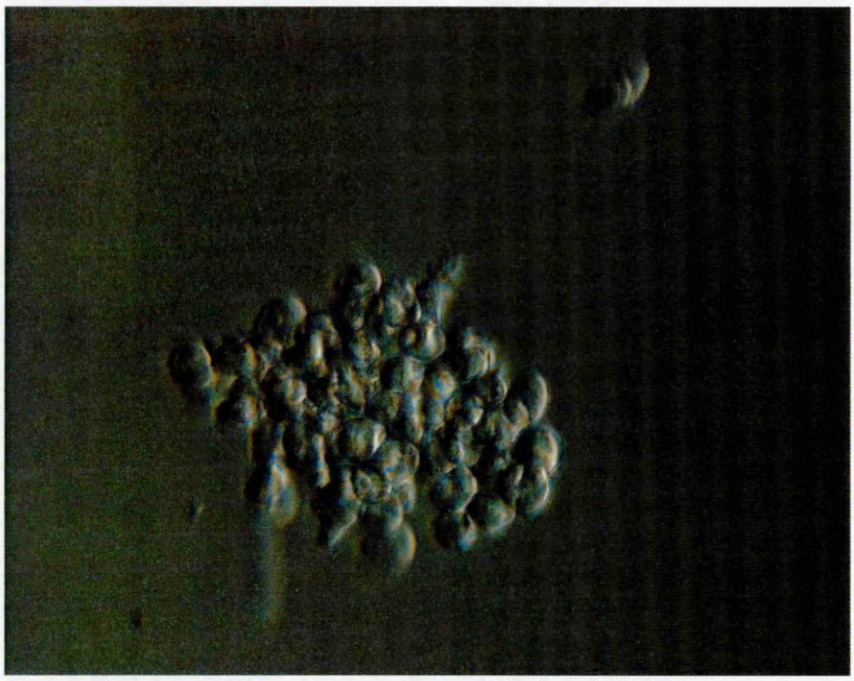

II.1.8. Cell culture reagents

- RPMI 1640 with L-glutamine and sodium biocarbonate (Sigma, R8758-500ml)
- Iscove's Modified Dulbecco's Medium (IMDM) (GIBCO BRL (Life Technologies Ltd, 21980-024)
- IDMEM with Glutamax-I (GIBCO BRL Life Technologies Ltd, 31980-022)
- TC100 insect culture medium (for SF9 cells) with L-glutamine and sodium biocarbonate (Sigma, T3160)
- GIBCO Invitrogen cell culture, 16000
- Erythropoeitin (EPREX, 1000IU/0.5ml) (Janssen-Cilag Ltd, 140165)
- Penicillin and streptomycin (Pen/strep) (Sigma, P0781)
- Fungizone (250µg/ml; 20ml) (VWR International, 700/0030/08)
- Trypan blue 0.4% solution (Sigma, T8154)
- Inverted light microscope (Olympus Tokyo)

- Fluorescence microscope (Zeiss, Axiovert 10)
- Collagen I from rat-tail (Sigma, C7661-5MG), at a working solution of 50µg/ml made in a solution of 0.02N acetic acid (0.57ml of glacial acetic acid (Fisons, A10400/PB17) in 500ml sterile glass distilled water).
- Fibronectin-like protein polymer genetically engineered (Sigma, F5022). The stock solution (1mg/ml) was diluted 1:10 in PBS-A (prepared in-house) to obtain a working solution at 100µg/ml.
- The stock solution of hydroxyurea was prepared as follows:

A 1M solution of hydroxyurea was prepared by adding 0.7605g of hydroxyurea (Sigma, H8627) into 10ml of sterile water. The solution was then filtered with a 25mm diameter filter, 0.2µm pore size (Whatman). The working solution of hydroxyurea was made by 1:100 dilution (10mM) of 1mM hydroxyurea in sterile, distilled water

- Culture of CD34+ cells: IMDM, 20% FCS, 20ng/ml human stem cell factor (SCF) (Sigma, S7901), 2u/ml EPO, 1ng/ml human IL-3 (Sigma, I1646), 1% fungizone and 1% penicillin/streptomycin
- Culture of BFU-E: 80ml FOX's complete medium (StemCell Technologies, Methocult™ H4230), 20ml IMDM, 30ng/ml IL-3, 2U/ml EPO, 25ng/ml G-CSF, 10ng/ml SCF and 25ng/ml GM-CSF.
- 5M NaCl: 290.2g NaCl (BDH AnalaR®, 102414J) were dissolved in 1 litre double-distilled water and dispensed into 100ml aliquots.
- Preparation of phosphate buffers:
    - 0.2M phosphate buffers: a stock solution of 0.2M NaH_2PO_4 was prepared by dissolving 24g of sodium phosphate monobasic (NaH_2PO_4) (Sigma, S5011) in 1 litre double distilled water. The stock solution was aliquoted in 100ml volumes and autoclaved.

- A stock solution of 0.2M of Na_2HPO_4 was prepared by dissolving 28.4g of sodium phosphate diphasic (Na_2HPO_4) in 1 litre double distilled water, aliquoted in 100ml volumes and autoclaved.

- The required pH was obtained by mixing the two buffer components as in the following proportions:

Table 2.4: Phosphate buffers composition

Phophate buffer (0.2M)	pH 5.7	pH 6.0	pH 6.5	pH 6.7
Volume of NaH_2PO_4 (ml)	93.5	87.7	68.5	56.5
Volume of Na_2HPO_4 (ml)	6.5	12.3	31.5	43.5

- Physiological phosphate buffers

In order to obtain 10mM physiological phosphate buffers (to keep the cells viable), 5 ml of 0.2M buffers shown above were mixed to 2.9ml of 5M NaCl (Sigma, S5150) and 92.1ml of sterile water to give a buffer containing 0.85% NaCl. The pH of the buffers was checked with a pH meter (3520 pHMeter, Jenway).

- Preparation of acetate buffers:

  - 0.2M acetate buffers: a stock solution of 0.2M sodium acetate was prepared by dissolving 16.4g sodium acetate ($C_2H_3O_2Na$) (Sigma, S2889) in 1 litre double distilled water. The stock solution was aliquoted in 100ml volumes and autoclaved.

  - The required pH was obtained by mixing the stock buffer solution with glacial acetic acid (Fisons, A10400/PB17) as in the following proportions:

Table 2.5: Acetate buffers composition

Acetate buffer (0.2M)	pH 5.6	pH 5.2	pH 4.8	pH 4.4	pH 4.0
Volume of glacial acetic acid (ml)	4.8	10.5	20	30.5	41
Volume of Na acetate (ml)	45.2	39.5	30	19.5	9

- Physiological acetate buffers:

In order to obtain a10mM physiological acetate buffers, (to keep the cells viable), 5 ml of 0.2M buffers shown above were mixed to 2.9ml of 5M NaCl and 92.1ml of sterile water to give a buffer containing 0.85% NaCl. The pH of the buffers was checked with a pH meter (3520 pHMeter, Jenway).

- Sterilization of stock and working cell culture reagents by autoclaving. All buffers and solutions were autoclaved (121°C for 15 minutes) before use.

II.1.9. Immunofluorescent reagents

PBS/0.05% Tween 20 (Sigma, P1379)

Evans blue/ PBS/Tween: 1 drop of Evans blue in 5ml of PBS/Tween

Polyvinyl alcohol mounting medium with DABCO (Sigma, 10981)

II.1.10. Antibodies

- Mouse monoclonal antibody against VP1 and VP2 proteins (Novocastra Laboratories Ltd, UK, R92F6)
- Mouse monoclonal antibody against VP1 and VP2 proteins (kindly given by Dr Miyagawa, Fujirebo, Japan)

- Mouse monoclonal antibody against VP1 and VP2 proteins (kindly supplied by Dr. J. Blumel, Paul Erhlich Institut, Germany)
- Rabbit polyclonal antibody against NS1 protein (kindly supplied by Dr. S. Doyle, National University of Ireland, Republic of Ireland)
- Anti-mouse IgG (whole molecule)–FITC antibody produced in goat (affinity isolated antibody buffered aqueous solution; Sigma, F2012)
- Monoclonal anti-rabbit immunoglobulins–FITC antibody produced in mouse (clone RG-16 purified immunoglobulin buffered aqueous solution; Sigma, F4890)
- Alexa Fluor® 488 signal amplification kit for mouse antibodies was obtained from Cambridge BioScience (catalogue number A-11054)

II.1.11. MACS

- MACS direct CD34 progenitor cell isolation kit (Miltenyi Biotech, 467-02)
- 50 Pre-Separation Filters (Miltenyi Biotech, 130-041-407)
- MiniMACS Starting Kit (Miltenyi Biotech, 130-090-312)
- Wash buffer: PBS-4salts/ 2mM EDTA/ 0.5% BSA. Keep cold.

II.1.12. Sequencing

GenElute™ Minus EtBr spin column (56501; Sigma-Aldrich, UK) was used to eliminate ethidium bromide from stained DNA. The PCR reaction to amplified the extracted DNA was run on the robocycler PCR machine called RoboCycler® gradient 96 (Stratagene). Sequencing itself was done using the ABI kit and the ABI 310 sequence analyzer (ABI, UK).

II.1.13. Human parvovirus B19 removal/inactivation studies

II.1.13.1. Virus removal by nanofiltration using Planova® filters: Asahi Kasei Pharma

Planova® filters are available as single-use, self-contained modules in four mean pore sizes of 15 nm, 19 nm, 35 nm, and 72 nm, which correspond to Planova® 15N, 20N, 35N, and 75N, respectively (figure 2.4).

Figure 2.4: Photograph of 15N and 35N Planova® filters

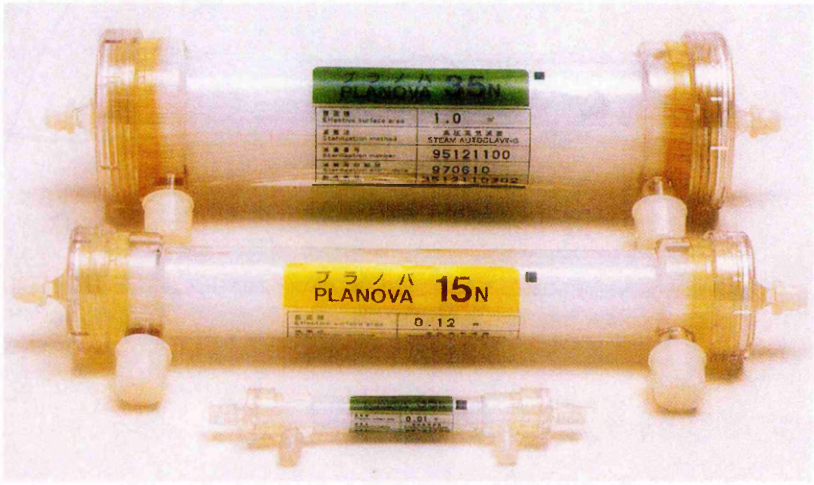

In the present study, the first three types of filters were used. A range of surface areas for each mean pore size allows simple scale-up from validation studies to process scale. Planova® filters were subject to two separate integrity tests by the manufacturer to confirm pore size distribution (Planova® New Pressure Hold Test) and the absence of membrane defects (leakage test).

Planova® filters utilise a hollow-fibre microporous membrane constructed of naturally hydrophilic cellulose with a narrow pore distribution. The Planova® membrane is actually a tortuous, three-dimensional structure of interconnected "voids" and "capillaries" (figure 2.5). Higher protein recoveries are possible due to the hydrophilic

properties of the membrane which lower the probability that product protein will be adsorbed to the surface of the membrane.

Figure 2.5: Capillary-void structure in a Planova® 15N (x 50,000)

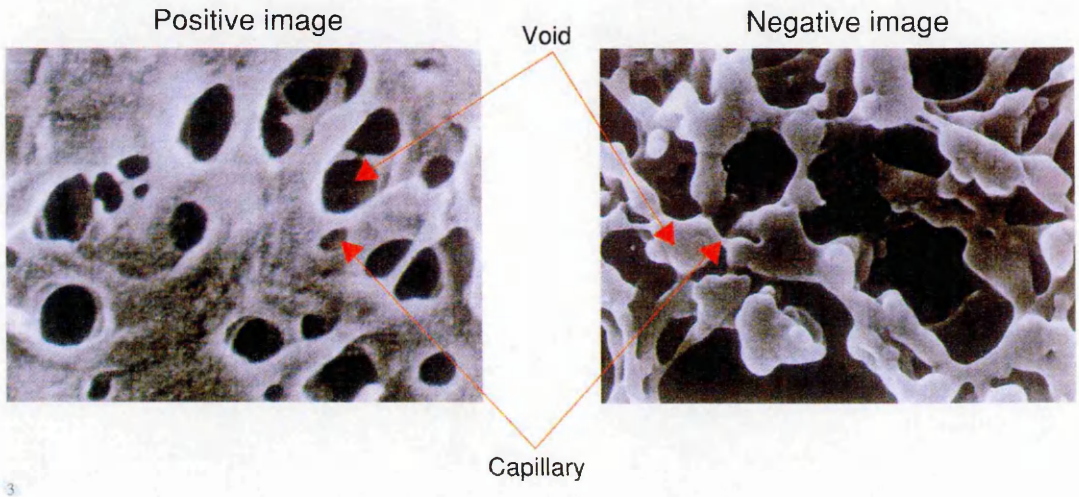

Human albumin was chosen as a model protein of plasma-derived product to test this virus removal technique. Reconstituted 25% albumin was obtained from department of Immunobiology at NIBSC.

II.1.13.2. Virus inactivation by SuperFluids™: Aphios Inc., USA

Aphios Corporation (Woburn, MA, USA) was granted a US Patent (No: 5,877,005) in March 1999, "Viral inactivation method using near-critical, supercritical or critical fluids" for pathogen inactivation. As shown on figure 2.6, *SuperFluids*™ are normally gases which, when compressed to a particular pressure (critical pressure P_c) and heated to a specific temperature (critical temperature T_c), enter the supercritical fluid region and show enhanced solvation, penetration and expansion properties.

Figure 2.6: *SuperFluids*™ zones

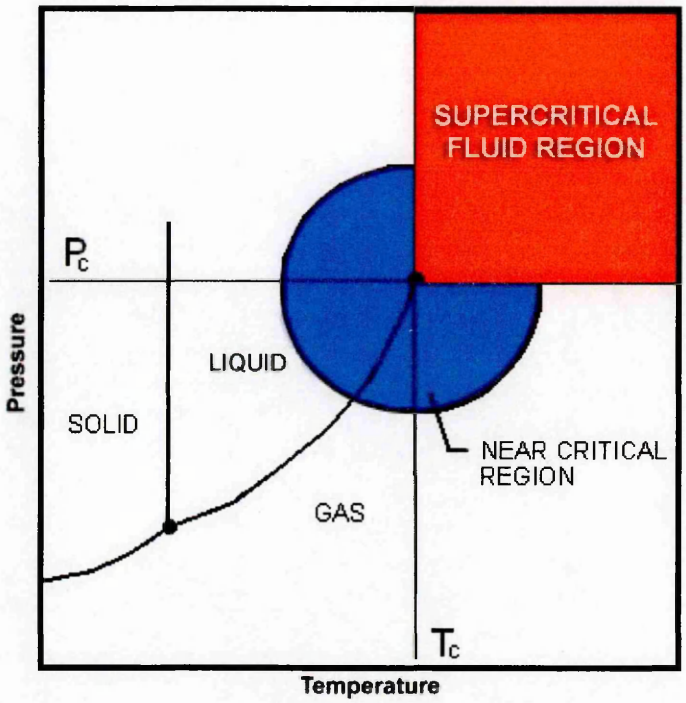

Three supercritical fluids were used in the present study, namely Freon-22, Freon-23 and N_2O/CO_2.

The laminar flow *SuperFluids*™ inactivation unit is composed of an isobaric chamber, *SuperFluids*™ and sample inputs, a decompression chamber and a collection system. Additionally, several isobaric chambers can be used in the system when a multistage laminar flow *SuperFluids*™ inactivation is set up that can further increase the reduction in viral load. The inactivation protocol consists of four steps: addition of *SuperFluids*™ to the product to be treated, adjustment of the operating pressure and temperature, mixing in order to reach a specific contact time between the *SuperFluids*™ and the virion, typically from 10 seconds to 1 minute. This step results in inflation of the particles due to penetration of the *SuperFluids*™. Finally, decompression of the system causes expansion of the *SuperFluids*™ within the virus particles resulting in rupturing of the particles at their weakest point.

II.1.13.3. Virus inactivation by the INACTINE™ system: Vitex, USA

The INACTINE™ System, which was developed by VI technologies or Vitex, features small molecules that, due to their size and stability in blood, are able to penetrate through the protective walls of resistant pathogens. These molecules, which can be synthesized in abundant quantities, are activated only when they bind to their target, the DNA or RNA of the pathogen. The loss of DNA or RNA replication is a fatal event for viruses or bacteria whereas the red blood cells do not need DNA or RNA to function. By purifying the red cells during the automated washing process to remove the INACTINE™ PEN110 (the Psoralen treatment compound) to trace levels, the INACTINE™-treated RBCs concentrates appear very safe.

II.1.13.4. Virus inactivation by S-59: the Helinx® technology; Cerus Corporation, USA

Cerus Corporation (CA, USA), has developed a family of novel small molecules which target and crosslink nucleic acids. These Helinx® compounds penetrate cellular and nuclear membranes and intercalate into the helical regions of DNA and RNA. The Cerus technology, the INTERCEPT Blood System, includes the INTERCEPT platelet system, the INTERCEPT plasma system and the INTERCEPT red blood cell system. They were developed in collaboration with Baxter Healthcare, for use in blood centres, and include a sterile disposable set pre-filled with Helinx® inactivation compounds.

When plasma and platelet concentrates are treated, the psoralen compound amotosalen hydrochloride (HCl) S-59 is used. Crosslinking of nucleic acids can be achieved in four steps, the first one being targeting, which involves the penetration of the psoralen compound amotosalen into cells, viruses, bacteria and other pathogens. The second step is the docking of the psoralen compound between the paired A, C, G and T bases of the

DNA ladder. The third step starts when, under illumination with 3.0 J/cm^2 ultraviolet A (UVA) light (a first photon), amotosalen reacts with the pyrimidine bases C or T, resulting in the formation of a link with the DNA. Finally, additional illumination can form a crosslink with both strands of DNA. This reaction can occur with the genomic material of DNA- and RNA-based viruses, in genomes that are either single or double stranded. Pathogens, as well as potentially harmful white blood cells with crosslinked DNA, can no longer replicate and cause infection or destructive transfusion reactions. Nevertheless, platelets, plasma and red cells do not contain nuclear DNA or RNA that can be targeted by this molecule and therefore retain their biological utility after Helinx® inactivation treatment (Wollowitz, 2001).

II.2. Methods

II.2.1.Virus quantification

Three B19 virus isolates were used for this study: two from Germany, isolates JS and JB, and one from the USA, named isolate LP. These isolates were quantitated using the established LightCycler quantitative assay. Dilutions of the WHO B19 International Standard (IS) were run in parallel in order to construct a standard curve for the quantitation.

Isolate JS (titre 1x10^{12} IU/ml) was used throughout this study for the establishment of all the assays and will be referred to as "B19 stock virus". In addition, this isolate was used to spike the samples that were treated for viral inactivation and removal. The DNA and infectivity titres of the three isolates were compared using the optimised mRNA assay. Isolate LP (titre 5x10^{13} IU/ml) was used as a positive control in infectivity assays to evaluate the efficacy of the viral inactivation studies (chapter IV).

EM and IEM by negative staining were done on B19 stock virus by Mr B. Megson and Ms H. Appleton (HPA). IEM used 50µl of JS isolate and 50µl of antibody, contained in serum Pickem (Cossart *et al.*, 1975). Normal EM was done with the isolate only (50µl).

II.2.2. Detection of virus infectivity by indirect immnunofluorescent assay (IFA)

II.2.2.1. Preparation of microscope slides

The Shandon Cytospin® 2 (Life Sciences International) was used to spin cell suspensions and simultaneously sediment the cells onto a microscope slide. The result was a monolayer of cells concentrated in a small-defined zone (6mm circle). The cell suspension was placed into a disposable cytofunnel, which had been attached to a cytoblock, with the slide and blotter. Up to 12 samples could be run during one spin, which lasted for 5 minutes at 45g. The disadvantage of this method was that only one sample could be spun on one microscope slide, which meant that many slides had to be processed. The slides used in this method were Apes slides which were made in-house by the histology laboratory at NIBSC by coating glass slides with 3-amino propyltriethoxysilane (Sigma). When the monolayer was dry, the cells were fixed in cold acetone for 10 minutes.

Alternatively, cells were spun for 5 minutes at 145g and the supernatant discarded. The pellets were resuspended in 50µl of PBS-A and 10µl of cell suspension was first place on the slide and left to air dry. The slides used were multispot microscope slides polytetrafluoroethylene (PTFE) coated from Hendley-Essex. The slide was observed under light microscope to ensure that an even layer of cells was obtained and the cell density adjusted accordingly. Once dry, the cells were fixed in cold acetone for 10 minutes.

II.2.2.2. Protocol

If the slide used did not already contain defined spots, as in the coated multispot microscope slides (Hendley-Essex), a circle was drawn around the fixed cells with a PAP pen (Cambridge BioScience) in order to define the area where the antibodies would be placed and to retain the reagents on the glass slide.

The slides were washed in PBS/Tween 20 (0.05%) and air dried in a class 1 cabinet. A mouse monoclonal anti-VP1/VP2 antibody (R92F6; Novocastra Laboratories Ltd, UK) was diluted 1:80 and a negative serum diluted 1:100 in PBS/Tween. 100 to 150µl of antibody or negative serum was added to the cells, which were then incubated for 30 minutes at 37°C (5% CO_2).

The slides were washed twice in PBS/Tween for 10 minutes each time. In the meantime, a goat anti-mouse FITC conjugate was diluted 1:100 in Evans blue/ PBS/Tween. Evans blue was used to avoid high background staining. The edges of the slides were carefully dried after the washes and 100µl of the conjugate was added to the cells, which were incubated for 30 minutes at 37°C (5% CO_2).

The slides were then washed twice again in PBS/Tween for 10 minutes each time, and once with distilled water. They were air dried inside the cabinet and mounted with Dabco using a cover slip. The slides were then ready to be viewed under the fluorescence microscope (oil immersion objective) or could be stored at -20°C for a few months.

II.2.2.3. Positive controls: baculovirus expressing B19 capsid antigens

Since baculovirus is an insect virus, either SF9 or SF21 insect cell lines could be used for culturing the recombinant viruses. Both cell lines were cultured at 28°C in TC100 medium with 10% fetal calf serum (FCS) and 1% fungizone in 75cm^3 flasks as a cell

monolayer. When the cells were confluent, the medium was discarded and the cells scraped off with a sterile cell scraper. The cells were resuspended into 60ml of fresh medium and 5ml of this cell suspension was dispensed into six $25cm^3$ flasks, labeled VP1, VP2 and negative control. The cells were left undisturbed for 6 hours at 28°C to allow the cells to attach to the flask and form a monolayer. Two types of inoculi were available: baculovirus expressing parvovirus VP1 or VP2 proteins (kindly provided by Dr J.Clewley and Dr B.Cohen, HPA; Hicks *et al.,* 1996). 100µl of each neat inoculum was added to the corresponding flask whereas nothing was added into the negative control flask. The flasks were incubated at 28°C for 3 days. The cells were then scraped off, harvested and centrifuged at 168g for 5 minutes. The cell pellets were resuspended in 1ml of TC100 medium. Microscope slides were prepared in one of the two ways described previously and the cells fixed in cold acetone for 10 minutes. Once dry, the slides were either treated immediately for immunofluorescence or stored at -20°C for later use.

II.2.3. Primary cells

II.2.3.1. CD34+ cells

II.2.3.1.1. Isolation of CD34+ cells from PBMC

The positive selection of CD34+ cells was performed using a direct CD34 progenitor cell isolation kit, using the MiniMACS (MAgnetic Cell Sorting) kit from Miltenyi Biotech GmbH (Germany). This technology is based on the use of MACS MicroBeads, MACS Columns and MACS Separators. The MicroBeads are superparamagnetic particles that are coupled to highly specific monoclonal antibodies, anti-CD34 in the present experiment. They are used to magnetically label the target cell population: CD34+ haematopoietic progenitor cells. As the MicroBeads are extremely small (50nm),

the use of a high-gradient magnetic field is required to retain the labeled cells. By using a MACS Column with a coated matrix placed in a permanent magnet, the MACS Separator, the magnetic force is sufficient to retain the target cells labeled with a minimum of MicroBeads. All the unlabeled cells are washed out thoroughly by rinsing the column with buffer, without affecting the labeled or unlabeled cell fractions. The labeled fraction can be collected by removing the column from the magnet. The entire procedure can be done in less than 30 minutes.

Approximately 4 to 5 ml of peripheral blood were kindly provided weekly by Dr M. Watts (Department of Haematology at University College Hospital, London, UK). The patients whose blood samples and apheresis cells were tested by BFU-E assay were assigned a number in order to respect their anonymity.

The first step consisted of harvesting mononuclear cells from PBMC by density gradient centrifugation over Ficoll Paque® (Pharmacia Biotech). The latter was added to the blood sample (10% of blood volume), mixed gently and centrifuged for 10 minutes at 168g. The supernatant, which was the platelet-rich plasma (PRP), was removed and stored at -20°C for later antibody testing. The peripheral blood was diluted a first time 1:1 (volume: volume) with RPMI and 10% FCS and the collection tube rinsed with this buffer. A second 1:1 (volume: volume) dilution of blood into Ficoll-Paque® was done at an angle so that the blood remained on top of the Ficoll-Paque®. The sample was centrifuged for 20 minutes at 543g. In the meantime, the MACS Column was prepared by placing a 30μm pre-separation filter on top of the reservoir, situated on the upper part of the column in order to remove cell clumps.

Three collection tubes (labeled 'Wash', 'Waste' and 'CD34+') were prepared and the wash tube was placed under the column. The azide in the MACS column was washed off with 1ml of cold wash buffer, through the pre-separation filter, which had to be lifted

to release the buffer. When the centrifugation of peripheral blood and Ficoll-Paque® was complete, the different cell types had migrated, leading to the formation of layers. The bottom layer contained erythrocytes, which had been aggregated by the Ficoll and, therefore, sedimented completely through the Ficoll-Paque®. The layer immediately above the red blood cells contained mostly granulocytes whereas the lymphocytes, platelets and monocytes, because of their lower density, were found in the interface between the remaining plasma and the Ficoll-Paque®. The lymphocytes were collected with care, transferred to a new tube and the cell clumps were broken by gentle pipetting. The cells were washed with wash buffer to remove any remaining Ficoll-Paque® and spun at 1050g for 5 to 7 minutes. Most of the supernatant was discarded and the cell pellet resuspended by gently flicking the tube. To these cells was added 100µl of magnetic beads to which CD34 specific antibodies were directly coupled. These beads were provided with the direct CD34 progenitor cell isolation kit (Miltenyi Biotech GmbH). The cells and the magnetic particles were left at 4°C for 30 minutes, with a gentle mix after 15 minutes.

The cells were then washed with wash buffer and centrifuged at 905g for 5 minutes. The supernatant was discarded and the cell pellet resuspended in 0.5ml of wash buffer. The waste tube was placed under the MACS column and the cell suspension added in the filter. Additional wash buffer was used to wash potential remaining cells from the tube and was added to the filter. The MACS column was rinsed with 3 to 4 volumes of wash buffer, thereby allowing all the unlabeled cells to be washed out thoroughly, without affecting the labeled or unlabeled cell fractions. The MACS column was then removed from the magnet and placed onto the CD34+ collection tube. Between 0.5ml and 1ml of wash buffer was added to the column and the CD34+ cells were forced out of the column by using a plunger. The expected cell count of the isolated CD34+ cells was

between 10^5 and 10^6 cells/ml. The cells were cultured at 37°C (5% CO_2) in CD34+ cell culture medium.

II.2.3.1.2. FACS analysis of isolated CD34+ cells

The cells were labeled with Phycoerythrin-(PE) conjugated anti-CD4 antibody, acquired using the FACS (Fluorescence Activated Cell Sorter) machine and the data were analysed using the Cellquest program.

CD34+ cells isolated from peripheral blood and apheresis cells were centrifuged for 5 minutes at 580g. The cell pellet was resuspended in 1 ml of buffer, which was kept at 4°C. The cells were spun again and most of the supernatant discarded, keeping ~100µl of liquid in the tube. To the cells was added 20µl (2mg/ml stock solution) of mouse anti-human CD34 IgG1 antibody PE-conjugated. In addition, a negative control was used with matching mouse IgG1-PE to assess for non-specific staining. Both samples were mixed and left for 1 hour at 4°C. A first wash was done using 1ml of wash buffer and the cells were centrifuged for 2 to 3 minutes at 6110g. The supernatant was discarded and the wash step repeated. Finally, 1ml of FACS fixative buffer was added to the apheresis cells.

The FACS machine (Becton Dickinson) was operated by Dr R. Stebbings (Department of Immunobiology, NIBSC).

II.2.3.1.3. Infection of CD34+ cells

Approximately four days after isolation from peripheral blood, CD34+ cells in culture (CD34+ cell culture medium supplemented with 1ng/ml of IL-3) were harvested and placed in a 1.5ml sterile Eppendorf tube. The cells were centrifuged for 5 minutes at 580g and the supernatant was removed.

For infection, cell pellets containing approximately 10^5 cells/ml, were resuspended in 30µl of neat B19 stock virus ($1x10^{12}$ IU/ml) or 1:10 dilution ($1x10^{12}$ IU/ml) whereas 30µl of IMDM was used for the negative control. The cell suspensions were mixed thoroughly by vortexing and placed at +4°C for 2 hours, with occasional mixing. At the end of the incubation period, 3ml of freshly prepared IMDM was added to each sample. Each sample was plated out in a 6-well plate (0.5ml cell suspension/well). After 3 to 4 days incubation at 37°C (5% CO_2), the cells were harvested and slides were prepared for indirect IFA in one of the two ways described previously (see section II.2.2.1).

II.2.3.2. Apheresis cells

II.2.3.2.1. Determination of anti-B19 IgG status of apheresis cell donors by EIA

The anti-B19 IgG status of some of the apheresis cells donors were kindly tested by Dr B. Cohen (HPA, London, UK), using serum samples from the donors where available. The kit used was the parvovirus B19 IgG sandwich enzyme immunoassay (3rd generation) by Biotrin (Dublin, Ireland). In this protocol, 100µl of diluted patient serum (1:10 dilution in sample diluent provided with the kit), 100µl of negative control (ready-to-use) and 100µl of positive control (ready-to-use) were added to the wells of a coated microwell plate. The plate was incubated for 1 hour at room temperature. During this step, specific parvovirus B19 IgG antibodies present in serum bound to the microtitre wells coated with a purified parvovirus B19 recombinant VP2 protein. Following a wash step with wash solution, peroxidase-labelled rabbit anti-human IgG was added (100µl), which bound to the human parvovirus B19 IgG if present. The samples were incubated for 30 minutes at room temperature. After a wash step, the whole complex was then detected by addition of substrate (100µl), which turned blue in the presence of

peroxidase. The plates were left at room temperature for a further 10 minutes and stop solution was added to the samples, leading to a stable yellow end product. Absorbance at 450nm was read for the controls and each sample tested.

II.2.3.2.2. Determination of anti-B19 IgG status of apheresis cells donors by IFA

This test was performed with the help of Dr B. Cohen (HPA, London, UK). Positive and negative controls, as well as serum samples from patients who had donated apheresis cells, were applied onto the slides and incubated. Following washes, a rabbit anti-human FITC conjugate antibody (1:40 dilution) was added onto the slides. Two washes with PBS/Tween were followed by one wash with distilled water. Once dried, the slides were mounted and observed using the water immersion objective of a fluorescent microscope.

II.2.3.2.3. BFU-E reduction assay

After a cell count, the hospital staff advised on the volume of sample containing 10^3 cells. Twice this volume (2 x 10^3 cells) was transferred into eight sterile 1.5ml Eppendorf tube and spun at 2,300g for 30 seconds at room temperature. Seven of these tubes were used for infection with parvovirus B19 while the eighth one was the uninfected negative control. The pellet in the latter was resuspended by vortexing. In the other samples, the supernatant (medium) was removed but saved. The pellet was resuspended in 30µl of B19 stock virus ($1x10^{12}$ IU/ml), which had been serially diluted 1:3 and vortexed. Both infected samples and negative control were left for minimum 2 hours at +4°C. The medium previously saved was then added to the corresponding infected sample and vortexed. Each sample (infected and control) was added to a 2.5ml aliquot of Fox's medium, mixed thoroughly by vortexing and plated out in a 24-well

plate (0.5ml in each well). The plate was incubated for 10 to 11 days at 37°C in a 5% CO_2 incubator without moving it. The red colonies formed in the negative control were counted with the naked eye (between 50 and 100 red colonies/well on average) and a cell count was also done in the infected wells if red colonies were visible.

The percentage BFU-E reduction was calculated using the formulae:

$$\text{Percentage reduction} = (A-B)/A \times 100$$

A being the total number of red colonies in the five control wells and B being the total number of red colonies in the five wells inoculated with virus.

II.2.4. Nucleic acid extractions

II.2.4.1. Nucleic acid extraction using QIAamp DNA blood mini kit (Qiagen)

The QIAamp DNA blood mini kit (Qiagen) is designed to purify genomic, mitochondrial, bacterial and viral nucleic acids from blood and related body fluids. Nucleic acids bind specifically to the QIAamp silica-gel membrane while contaminants pass through the spin columns. Wash buffers are then used to remove impurities, such as PCR inhibitors, and pure, ready-to-use nucleic acids are eluted in water.

Before starting the extraction procedure, and according to the manufacturer's recommendations, the carrier was redissolved in water to obtain a 1µg/µl solution, 1µl of which was added to 200µl the lysis buffer, labelled AL, resulting in a concentration of carrier of 1µg/reaction. Two hundred micorlitres of sample was gently mixed with 20µl of proteinase K (20mg/ml) in a 1.5ml Eppendorf tube. Two hundred and one microlitres of AL+carrier was then added to the tubes, which were mixed, spun briefly

and incubated at 56°C for 10 minutes. A brief spin preceded the addition of 250µl of ethanol (99% purity). The tubes were once more mixed, spun briefly and left at room temperature for 10 minutes. The samples were then loaded onto the columns provided and spun at 11,450g for 1 minute. The collection tubes were changed and the columns washed once with 500µl of AW1 and spun at 11,450g for 1 minute. The collection tubes were changed and the columns washed with 500µl of AW2 and spun at 11,450g for 1 minute. Once more, the collection tubes were replaced and the columns were spun at 17,530g for a further 3 minutes. The silica columns were then transferred to siliconised tubes (whose lids had been cut off) and left to stand for a couple of minutes to allow any residual ethanol to evaporate. To elute the nucleic acids, 60µl of water was added to the centre of the columns, which were left at room temperature for 1 minute then centrifuged at 11,450g for 3 minutes. The eluted nucleic acids were transferred to 0.5mL siliconised tubes for immediate amplification and quantification by the LightCycler system (Roche Molecular Biochemicals). Alternatively, nucleic acids were stored at -70°C.

II.2.4.2. Oligotex direct mRNA kit (Qiagen) for extraction of poly A^+ RNA from whole cells

The Oligotex direct mRNA kit (Qiagen) allows isolation of pure poly A^+ mRNA directly from cultured cells. Rigorous denaturing lysis conditions applied to the homogenised cells can generate an immediate RNAse-free environment for the extraction of intact mRNA. Moreover, the Oligotex resin used is composed of polystyrene-latex particles of uniform size (1.1µm diameter) and spherical shape. These particles form a stable suspension, thereby providing a large surface area for fast and efficient hybridisation with polyadenylic acids. After washing, mRNA is eluted in a

small volume of elution buffer (OEB) and can be used immediately for RT-PCR amplification.

Prior to extraction, the Oligotex suspension was heated for 10 to 15 minutes at 37°C, mixed by vortexing and then left at room temperature while buffer OEB was placed in a water bath at 70°C. Approximately $2x10^7$ cells (grown in suspension) were initially pelleted by centrifugation at 402g for 5 minutes in 1.5 ml RNAase-free Eppendorf tubes. The cells were disrupted by addition of lysis buffer OL1 (with β-ME) at room temperature. To achieve this, the cell pellet was loosened by flicking the tube and adding 600µl of OL1 (for $1x10^6$ to $1x10^7$ cells). The sample was vortexed for a few seconds or pipetted up and down. In order to homogenise the sample, the lysate was passed 5 to 10 times through a 20-gauge needle (0.9mm diameter) fitted to an RNAase-free syringe. At this stage, the lysate was either stored at -70°C (for several months) for later use or used immediately. To process frozen cell lysates, samples were thawed for 10 minutes ($\leq 2x10^7$ cells) in a 37°C water bath to redissolve the salts. Dilution buffer (ODB), supplied in the kit, was then added to the homogenised cells (1.2ml) and the samples were mixed thoroughly by pipetting. The samples were spun for 3 minutes at 15,115g and the supernatant transferred to a new RNAase-free tube. Thirty-five microlitres of Oligotex suspension was added to each sample, mixed by vortexing and left at room temperature for 10 minutes. The Oligotex-mRNA complex was pelleted at 15,115g for 5 minutes. The supernatants were carefully removed and discarded. The pellets were resuspended by adding 100µl of lysis buffer (OL1), followed by vortexing. Four hundred microlitres of ODB was added to the samples which were then incubated at 70°C for 3 minutes followed by incubation at room temperature for a further 10 minutes. This step slightly enriched for poly A^+ mRNA by decreasing the amount of rRNA. The samples were spun at 15,115g for 5 minutes and the supernatant removed

carefully. The pellets were resuspended with 350µl of wash buffer 1 (OW1) by vortexing. The samples were then transferred to spin columns provided in the kit and centrifuged for 1 minute at 15,115g. The collection tubes containing the flow-through were discarded and replaced. The columns were washed twice with 350µl of wash buffer 2 (OW2) as described above. The spin columns were then transferred to 1.5ml RNAase-free tubes and 30µl of preheated (at 70°C) elution buffer OEB added to the columns. The buffer was pipetted up and down three to four times to resuspend the resin and the columns spun for 1 minute at 15,115g. The eluted mRNA was carefully transferred to new RNAase-free centrifuge tubes, and either placed on ice for immediate use or stored at -70°C for later amplification.

II.2.4.3. Oligotex direct mRNA kit (Qiagen) for extraction of poly A^+ RNA from cell cytoplasm

The same Oligotex direct mRNA kit (Qiagen) was used to extract mRNA from cell cytoplasm. However, the lysis buffer (OCL) and dilution buffer (OCD) were prepared in-house according to the manufacturer's instructions (section I.1.2). Prior to extraction, the Oligotex suspension was heated in a 37°C water bath for 10 to 15 minutes, mixed by vortexing and then left at room temperature while buffer OEB was incubated in a second water bath heated to 70°C. The cells grown in suspension were harvested two days post-infection, placed in RNAase-free centrifuge tubes and spun for 5 minutes at 402g. The cell pellets were loosened by flicking the tubes and 0.2ml of chilled OCL buffer was added, followed by incubation on ice for 7 minutes. The tubes were then spun for 2 minutes at 755g at 4°C in a pre-chilled centrifuge to pellet the nuclei (the nuclear pellets were white and much smaller than the cell pellets). The supernatants, containing the cytoplasmic fraction, were transferred to an RNAase-free centrifuge tube.

Two hundred microlitres of OCD and 20µl of Oligotex suspension were added to the supernatant and mixed thoroughly. After 3 minutes incubation at 70°C, the samples were placed at room temperature for a further 10 minutes. The samples were spun for 5 minutes at 15,115g at room temperature. The supernatants were carefully removed and discarded. The pellets were then resuspended in 350µl of wash buffer OW1 by gently pipetting. Both spin column, supplied in the Oligotex kit, and batch format protocols were tested.

In the batch format, instead of collecting the Oligotex resin in a spin column, the polysyrene-latex particles were pelleted by centrifugation for 2 minutes at 15,115g. The supernatants were removed and the pellets resuspended in 350µl of OW2. The samples were spun again for 2 minutes at 15,115g and the OW2 wash and centrifugation repeated using a new tube. The pellet was then resuspended in 30µl of OEB prewarmed at 70°C. All samples were incubated in a water bath at 70°C while adding the buffer. Samples were left at this temperature for a couple of minutes, followed by centrifugation at 15,115g for 2 minutes. The supernatants containing the eluted mRNA were carefully transferred to new RNAase-free tubes, which were then either placed on ice for immediate use or stored at -70°C for later use.

In the spin column format, the cytoplasmic fraction was transferred to a spin column (supplied with the kit) and processed as above except that the wash buffers and supernatants flowed through the column into collection tubes. The collection tubes were changed at the end of each centrifugation step.

II.2.4.4. Nuclisens™ (Organon Teknika) extraction of total nucleic acids

The Nuclisens™ kit (Organon Teknika) allowed extraction of total (viral and cellular) nucleic acids. The silica supplied in the kit was resuspended by vortexing. Fifty microlitres of silica were added to 0.9ml of kit lysis buffer which itself lysed samples, stabilised nucleic acids and enhanced selective nucleic acid adsorption to the silica particles. Two hundred microlitres of sample were added to a tube containing lysis buffer and silica, and was mixed thoroughly. The samples were then left at room temperature for 10 minutes and vortexed every minute to ensure the nucleic acids bound to the silica. The samples were spun for 30 seconds at 15,115g. After removal of the supernatant, 1ml of wash buffer was added to each sample, followed by vortexing. The samples were spun for 30 seconds at 15,115g, the supernatants removed and the washing step repeated once. The silica pellets were resuspended in 1ml of 70% ethanol, the suspensions were transferred to clean 1.5ml Eppendorf tubes and spun for 30 seconds at 15,115g. After removing the supernatants, 1ml of ethanol was added as before and the samples vortexed and spun. The supernatants were discarded. The samples were washed with 1ml of acetone, vortexed, spun and the acetone discarded. The silica pellets were dried at 56°C for 30 minutes and 50µl of pre-warmed elution buffer was added to each sample. The samples were vortexed until resuspended and incubated for 30 minutes at 70°C in order to completely redissolve the nucleic acids. During this incubation step, samples were vortexed every 10 minutes to resuspend the silica. The samples were finally spun for 5 minutes at 15,115g and the supernatant containing total nucleic acids (~35µl) was carefully removed and transferred to clean RNAase-free tubes (0.5ml) which were either stored at -70°C for later use or placed on ice for immediate use.

II.2.4.5. QIAamp DNA mini kit (Qiagen) for extraction of total nucleic acids

QIAamp DNA mini kits (Qiagen) contained Proteinase K, which had been shown to be the optimal enzyme for use with the lysis buffer. Two hundred microlitres of samples were added to 1.5 ml microcentrifuge tubes which already contained 20µl of Proteinase K. Then 200µl of lysis buffer (AL) were added to each sample, mixed thoroughly by vortexing and incubated for 10 minutes at room temperature, followed by 10 minutes at 56°C. The centrifuge tubes were briefly centrifuged to remove drops from the inside of the lids. Two hundred microlitres of absolute ethanol were added to the samples, which were mixed by vortexing and briefly centrifuged. The mixture was carefully applied onto the QIAamp Spin Columns provided in the kit (in 2ml collection tubes) without wetting the rim. The caps were closed and the spin columns were centrifuged at 6000g for 1 minute. The spin columns were placed in clean 2ml collection tubes and the tubes containing the filtrate were discarded. Five hundred microlitres of wash buffer 1 (AW1) were added onto the spin columns, which were centrifuged at 6000g for 1 minute. The spin columns were again placed in clean 2ml collection tubes and the tubes containing the filtrate were discarded. The spin columns were washed twice with 500µl of wash buffer 2 (AW2) and centrifuged at 6000g for 1 minute. The spin columns were placed in clean 2ml collection tubes and the tubes containing the filtrate were discarded. An additional centrifugation at full speed (20,000g) was done after the second wash for 3 minutes. The spin columns were placed in clean 2ml collection tubes and the tubes containing the filtrate were discarded. Two hundred microlitres of elution buffer (AE) were added to each spin column. After incubation at room temperature for 5 minutes, the spin columns were centrifuged at 6000g for 1 minute. The eluted total nucleic acids were stored at -20°C for later use.

II.2.5. DNA quantification by LightCycler system (Roche Molecular Biochemicals)

The DNA FastStart Master SYBR Green I kit (Roche Applied Science) includes $MgCl_2$ stock solution (25mM, vial 2) to adjust the $MgCl_2$ concentration, sterile PCR grade water to adjust the final volume and the LightCycler FastStart enzyme (vial 1a), which is mixed with the LightCycler FastStart reaction mix SYBR Green I (vial 1b). This mixture contains FastStart Taq DNA polymerase, reaction buffer, dNTP mix, SYBR Green I dye and 10mM $MgCl_2$. FastStart Taq DNA polymerase is a modified form of thermostable recombinant Taq DNA polymerase. The heat-labile blocking groups on some of the amino acid residues of the enzyme allow it to stay inactive at room temperature. Therefore, there is no elongation during the period where primers can bind non-specifically. The pre-incubation step at 95°C, for a maximum of 10 minutes removes the blocking groups and activates the modified enzyme.

During each phase of DNA synthesis, the SYBR Green I dye binds to the amplified nucleic acids and produces a fluorescent signal. As SYBR Green I dye binds non-specifically to the minor grooves of double-stranded DNA, both specific amplicons and primer dimers will contribute to the overall fluorescent signal. However, since the melting curve of primer dimers is usually lower than that of specifically amplified PCR product, an analysis of the melting curve enables collection of fluorescence data at a temperature at which the primer dimers are denatured and do not contribute to the fluorescent signal. Previous studies in the laboratory had shown that the melting temperature of the primer dimers was below 80°C while that of the amplified product was above this temperature. Therefore, in the B19 assay, fluorescence data were collected at 80°C to exclude signals from primer dimers. The ideal target length would be 100 to 150bp and the use of SYBR Green allows a flexible detection of different

targets and is less expensive than fluorogenic probes (i.e. dual-labelled probes, FRET probes and molecular beacons).

In addition to the DNA quantification provided by the LightCycler instrument (Roche Diagnostics), the PCR products from the optimisation experiments were analysed on a 2% agarose gel containing ethidium bromide. The DNA samples were prepared by adding 2 to 3.5µl of 6x loading dye to a 1.5ml Eppendorf tube without a lid. The glass capillaries were gently removed from the LightCycler carousel, uncapped and placed inverted in the prepared tubes. The capillaries were then spun twice in a microcentrifuge at 700g for a few seconds to remove the amplicons. The samples were analysed on a 2% agarose gel run at 100 volts for 40-50 minutes. The bands were visualised under the UV light and photographed either using a Polaroid camera or by the Autochemi™ photographic system (UVP).

II.2.6. mRNA amplification by OneStep RT-PCR

The OneStep RT-PCR kit (Qiagen) contains 10x OneStep RT-PCR buffer, deoxynucleotides mix (dNTPs), 5x Q buffer solution, RT-PCR enzyme mix and RNAase-free water. OneStep RT-PCR buffer is designed to enable both reverse transcription and specific amplification. The buffer contains a balanced combination of KCl and $(NH_4)_2SO_4$ which allows specific primer annealing over a wide range of annealing temperatures and Mg^{2+} concentrations. The Q solution, supplied with the kit, was used to improve suboptimal RT-PCR amplification caused by RNA and DNA templates that have a high degree of secondary structure or that are GC-rich. Q buffer has also been shown to prevent the amplification of non-specific RT-PCR products. The OneStep RT-PCR enzyme mix contains enzymes for both reverse transcription (Omniscript™ and Sensiscript™ reverse transcriptases) and PCR amplification

(HotStarTaq™ DNA polymerase). Omniscript™ reverse transcriptase is directed at RNA amounts greater than 50ng whereas Sensiscript™ reverse transcriptase is optimised for use with very small amounts of RNA (less than 50ng), thereby providing sensitive RT of any amount of RNA from 1pg to 2µg. During the RT-step, HotStarTaq™ DNA polymerase is completely inactive and does not interfere with the RT reaction. Once the latter is completed, reactions are heated to 95°C for 15 minutes to activate HotStarTaq™ DNA polymerase while inactivating the reverse transcriptases. This procedure eliminates extension from non-specifically annealed primers and primer-dimers in the first cycle, allowing specific PCR amplification.

II.2.7. Statistical Analysis

All statistical analyses were kindly done by Mr Alan Heath (Informatics Division, NIBSC, UK).

II.2.7.2. LightCycler Standard curve

In the first validation study investigating the limit of detection of the LightCycler PCR assay, no statistical analysis was performed. It was sufficient to look at the melting temperatures to determine the limit of detection.

The second validation study looked at the linearity and precision of the LightCycler standard curve. Results were available from 7 separate assays. For each assay the estimated concentration ($\log_{10}$ IU/ml) for the four samples tested were obtained by reading off the standard curve using the LightCycler software. The overall means of the estimates of $\log_{10}$ IU/ml were calculated, along with the standard deviation across the 7 estimates in each case. To interpret the standard deviation, assuming a normal distribution of repeat estimates, 95% of estimates would fall within the range mean +/- 2

x standard deviation. Therefore, from the results shown on table 3.6, at $\log_{10}$ 6 IU/ml, the expected range would be +/- $\log_{10}$ 0.066 representing very good precision and repeatability. At $\log_{10}$ 3 IU/ml the expected range would be +/- $\log_{10}$ 0.6.

II.2.7.2. DNA extraction and amplification

As for the study above, analysis was based on the overall mean and standard deviation of the estimates of $\log_{10}$ IU/ml. Interpretation is again based on the expected range of +/- 2 x standard deviation.

II.2.7.3. Determination of 95% and 50% detection limits of the optimised infectivity assay

The methods used for determining the detection limits use a statistical model based on the Poisson distribution. This assumes that the number of "detectable units" (copies or genome equivalents) in an individual samples follows the Poisson distribution with mean given by the average number of "detectable units" at that dilution. Under this model, the dilution equivalent to a mean of one copy per sample tested would result in 63% of tests being positive. The dilution equivalent to three copies per sample would result in 95% of tests being positive. This is defined as the 95% detection limit. The Poisson model can be fitted to the data in table 3.12, represented as a number of positive out of number tested at each dilution, using the commercial statistical software package SAS.

II.2.8. Sequencing of PCR products

II.2.8.1. Purification of amplified products from agarose gels for sequencing

Amplified products obtained with the primer combination B19-9 and XPP-2 were separated on 2% agarose gels and the bands visualised on a UV transilluminator. A gel slice containing the specific band was cut out using a sterile blade and placed in a siliconised 1.5ml Eppendorf tube. The gel slice was snap frozen in a mixture of ethanol and dry ice for 30 minutes. The material used to eliminate ethidium bromide from this stained DNA was the GenElute™ Minus EtBr spin column (56501; Sigma-Aldrich, UK). Before starting the DNA recovery, the spin column was washed by adding 100µl of TE buffer (made in-house), placed in a 1.5ml Eppendorf tube and centrifuged at 17,005g for 5 seconds. The microcentrifuge tube containing TE buffer was discarded and replaced by a new one. Since the spin column should not be left to dry, the frozen gel slice was transferred onto it quickly. The column was centrifuged at 17,005g for 10 minutes to extract the DNA (in buffer) from the gel slice. The eluted DNA was precipitated by the addition of 2 volumes of ethanol and 0.1 volume of 5M ammonium acetate (pH 5.3), followed by incubation at -20°C for 10 minutes. The DNA precipitate was collected by centrifuging at 17,005g for 5 minutes. The supernatant was discarded and DNA was then redissolved in 10µl of TE buffer.

II.2.8.2. Sequencing protocol

Gel purified RT-PCR products were run on a 2% agarose gel with 5µl DNA markers and the concentration of DNA in the amplified products estimated by a comparison of the fluorescence of the product and one of the marker bands in the appropriate size range.

Sequencing was done using the ABI kit (ABI, UK). Approximately 10ng amplified DNA was further amplified in a reaction containing 4µl of terminator mixture, 1.6pmol of primers B19-6 and B19-9 and RNAase-free water to make the final volume 10µl. The PCR reaction was run with the following conditions: 1 cycle at 96°C for 1 minute, followed by 25 cycles of 96°C for 30 seconds, 55°C for 20 seconds and 60°C for 20 seconds and lastly 1 cycle at 60°C for 3 minutes. The PCR products were then purified from unincorporated primers by ethanol precipitation. In a 0.5ml Eppendorf tube were placed 1µl of 3M NaOAc, pH 4.6 and 10µl of the sequencing reaction. After mixing thoroughly, 25µl of absolute ethanol (EtOH) was added to the tube, then mixed again and left at room temperature for 15 minutes. The reaction was centrifuged at 28,215g for 15 minutes to pellet the DNA. The supernatant was carefully removed and 300µl of 70% EtOH was used to resuspend the pellet by flicking the tube. After centrifugation at 28,215g for 5 minutes, the supernatant was removed and another 300µl of 70% EtOH was added to the DNA pellet. The latter was resuspended by flicking again and spun at the same speed for 5 minutes. The supernatant was removed very carefully and the sample centrifuged again to collect any residual EtOH, which was then discarded. The tube was left opened (covered with tissue paper) to dry at room temperature for 30 to 40 minutes. Some template suspension buffer (TE buffer, 15µl) was used to re-dissolve the DNA pellet. The sample was transferred to a thin wall PCR tube and heated to 95°C for 2 minutes and immediately placed onto ice. The sample was transferred to a labelled sequencing tube and loaded onto the ABI 310 sequence analyzer.

II.2.9. Human parvovirus B19 removal/inactivation studies

The optimised tissue culture assay using UT-7/EPO-S1 cells and RT-PCR assay described previously were used to test one method of virus removal by nanofiltration

(Asahi Kasei Pharma) and four virus inactivation techniques: dry heat treatment (BPL), super critical fluids (Aphios Inc.), INACTINE™ system (Vitex) and Helinx® technology (Cerus Corporation). Each of these companies was provided with a sample of B19 virus stock (isolate JS; $1x10^{12}$ IU/ml). This inoculum was used to spike the products before inactivation or removal. Samples from different stages of these methods were then sent back to NIBSC for infectivity and B19 DNA assays.

Chapter III: Results

III.1. Characterisation of the virus isolates used in this study

III.1.1. Electron microscopy on the virus stock (JS isolate)

Three B19 virus isolates were used for this study: two from Germany, isolates JS and JB, and one from the USA, isolate LP. These three isolates were identified before the discovery of the B19 genotypes 2 and 3. They are therefore very likely to be genotype 1 isolates, which is that found most commonly in North America and Western Europe. The isolates were quantitated using the established LightCycler quantitative assay.

Figure 3.1 below shows EM and IEM photos of the virus stock (isolate JS).

Figure 3.1: IEM and EM of Human Parvovirus B19

(A, B and C: IEM; D: EM)

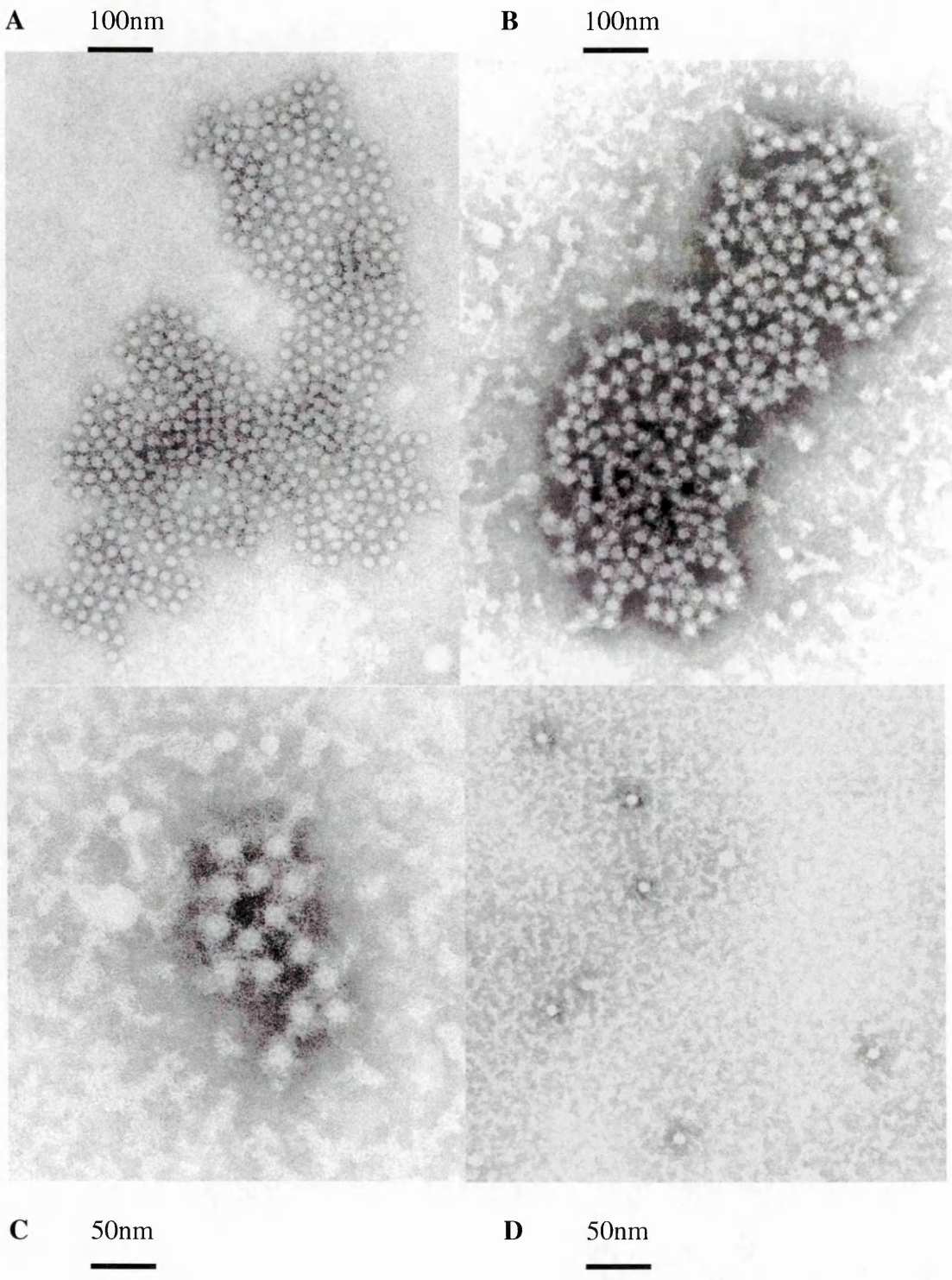

III.1.2. DNA Quantification of B19 samples

The DNA titres of the three isolates mentioned above were obtained by quantitative real-time LightCycler PCR as $1x10^{12}$ IU/ml, $3x10^{12}$ IU/ml and $5x10^{13}$ IU/ml for JS, JB and LP, respectively.

III.2. Detection of virus infectivity by IFA: controls

Insect cells SF9 were infected with baculovirus expressing either VP1 or VP2 recombinant protein as positive controls (figures 3.3 and 3.4) whereas some cells were mock infected to serve as negative control (figure 3.2). The mouse monoclonal anti-B19 VP1/VP2 antibody (Novocastra Laboratories Ltd) was used at a 1:80 dilution.

Figure 3.2: IFA in mock infected SF9 cells

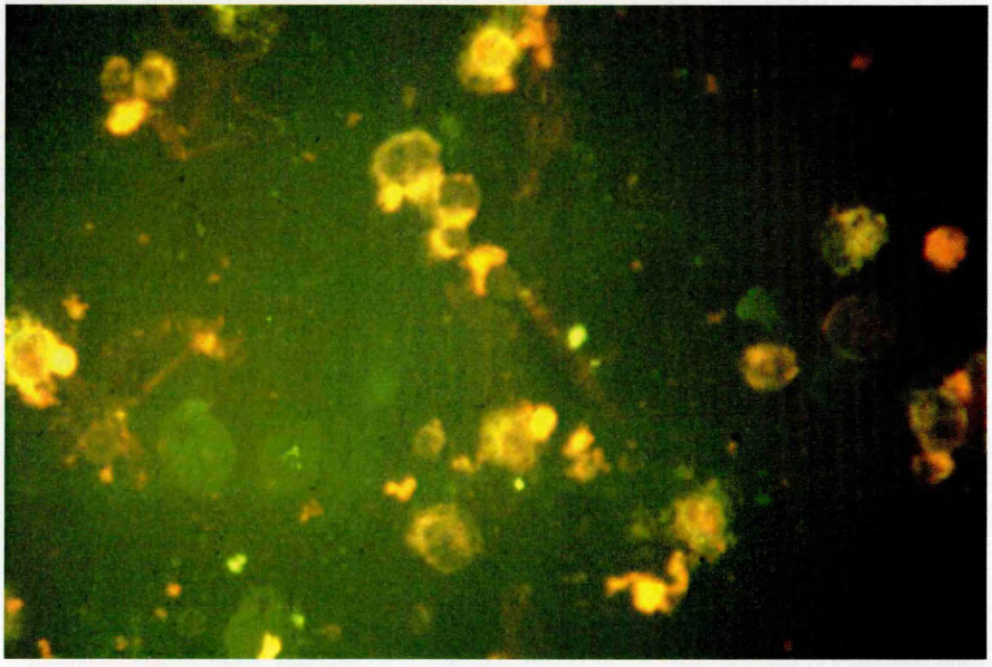

Figure 3.3: IFA in SF9 cells infected by baculovirus expressing VP1 recombinant protein

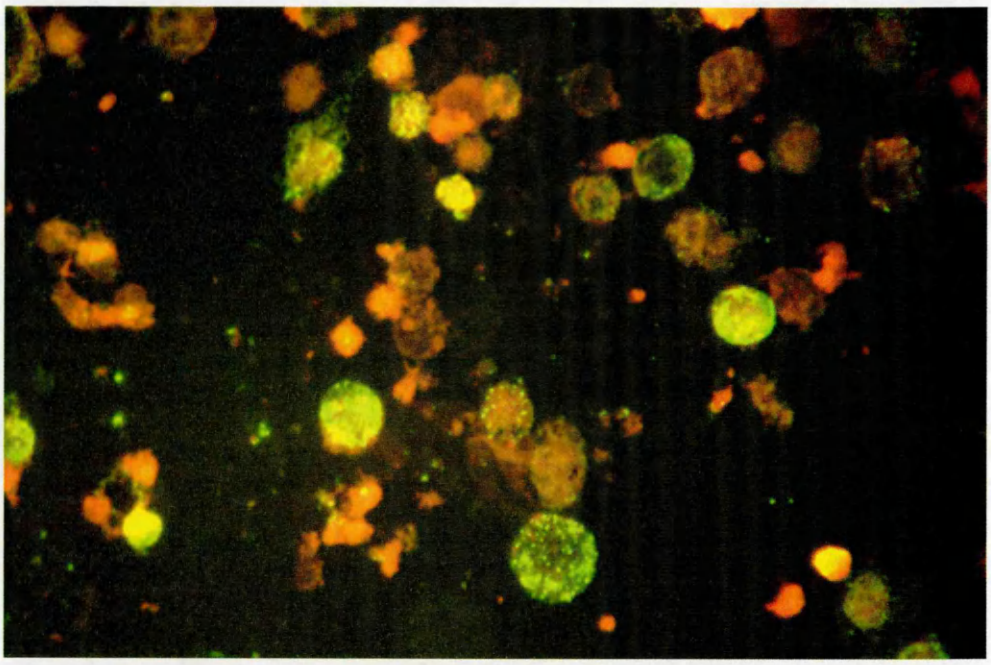

Figure 3.4: IFA in SF9 cells infected by baculovirus expressing VP2 recombinant protein

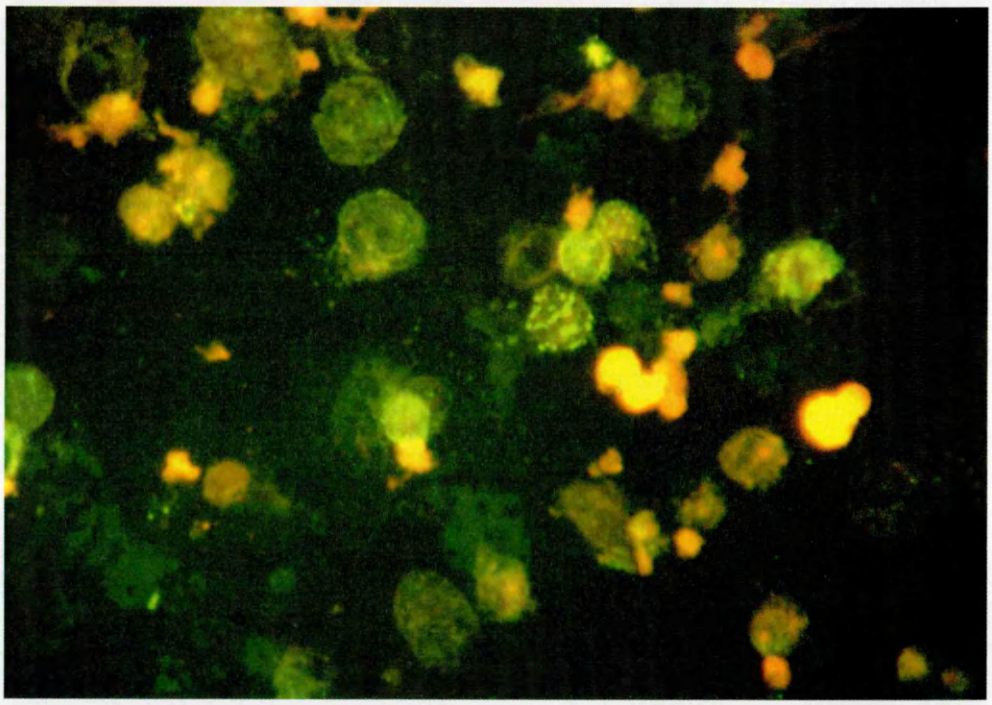

Infected SF9 cells were easily identified by the presence of green dots where the recombinant proteins were produced. Another type of fluorescence was seen, which was brighter and more diffuse in the cell.

III.3. Primary cells

III.3.1. CD34+ cells

III.3.1.1. FACS results

The aim of this experiment was to access the proportion of haematopoietic stem cells present in the CD34+ isolated samples. In addition to the negative control, three test runs were performed: CD34 test.001, CD34 test.002 and CD34 test.003. CD34 test.001 and test.003 were looking at isolated CD34+ cells from two different patients while CD34 test.002 was investigating apheresis cells from a patient who had not been included in the BFU-E studies. Two graphs were obtained with the Cellquest program after measurements by the cytometer. The first graph was a plot of cell granulosity (SSC-H) versus size (FSC-H) (figures 3.5, 3.8 and 3.11) while the second was a plot of CD34+ versus size (figures 3.6, 3.9 and 3.12). Additionally, and in order to visualise the fluorescence associated with CD34+ cells, a histogram of events versus CD34 fluorescence was plotted (figures 3.7, 3.10, 3.13).

- **CD34 test.001 (isolated CD34+ cells)**

Figure 3.5: Dot plot of the cell granulosity (SSC-H) versus cell size (FSC-H) for CD34

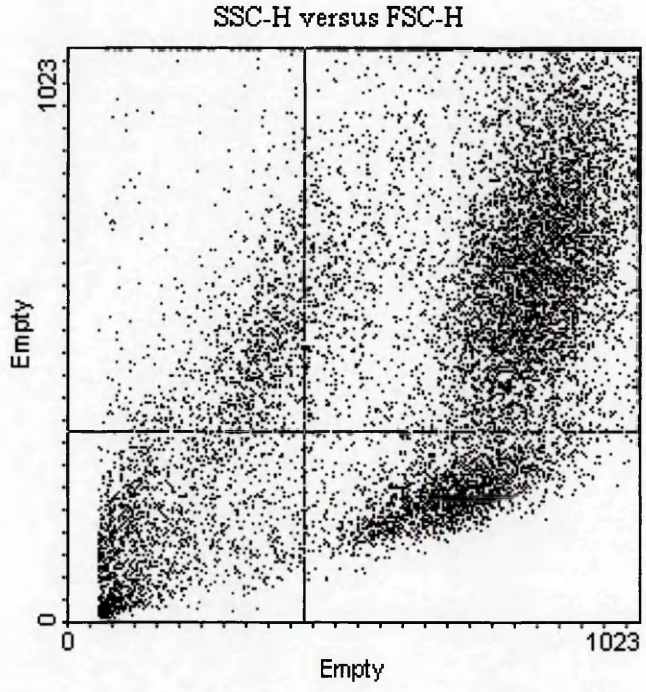

Figure 3.6: Dot plot of CD34+ versus cell size (FSC-H) for CD34 test.001

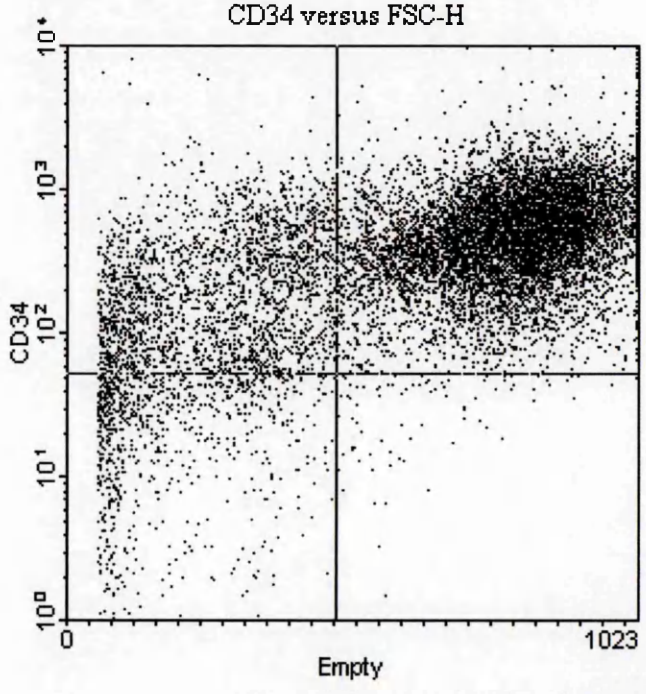

Figure 3.7: Histogram of events versus CD34 fluorescence for CD34 test.001

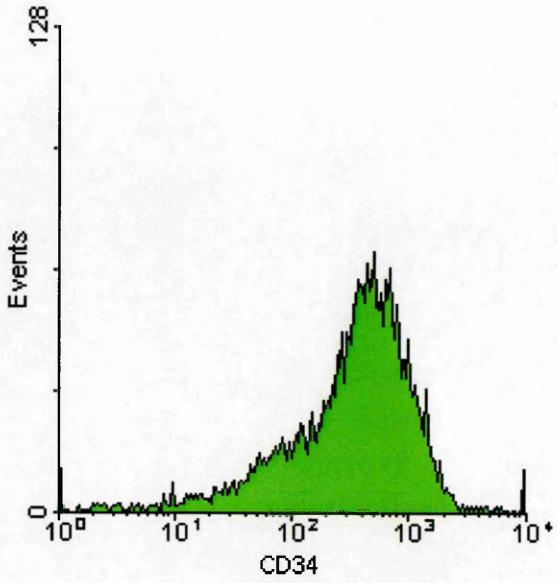

- **CD34 test.003**

Figure 3.8: Dot plot of the cell granulosity (SSC-H) versus cell size (FSC-H) for CD34 test.003

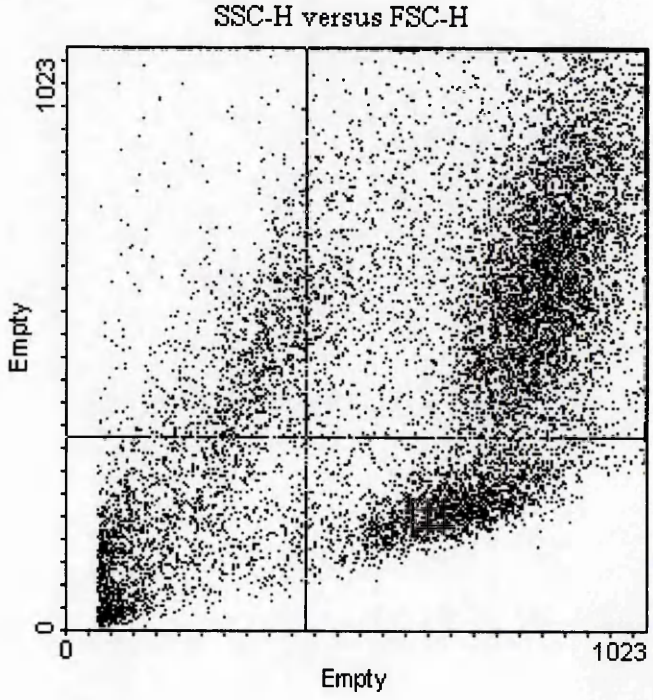

Figure 3.9: Dot plot of CD34+ versus cell size (FSC-H) for CD34 test.003

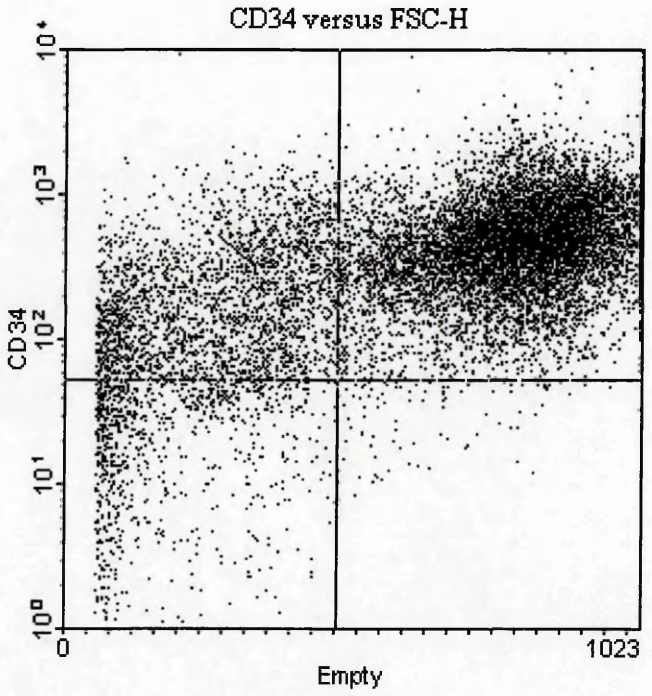

Figure 3.10: Histogram of events versus CD34 fluorescence for CD34 test.003

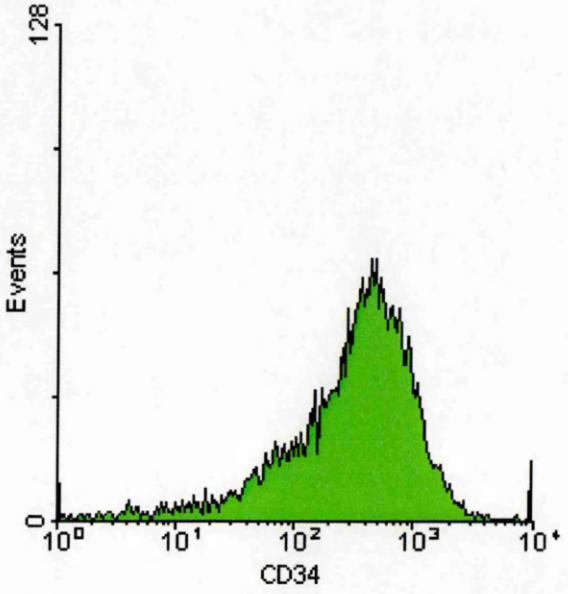

- **CD34 test.002 (apheresis cells)**

Figure 3.11: Dot plot of the cell granulosity (SSC-H) versus cell size (FSC-H) for CD34 test.002

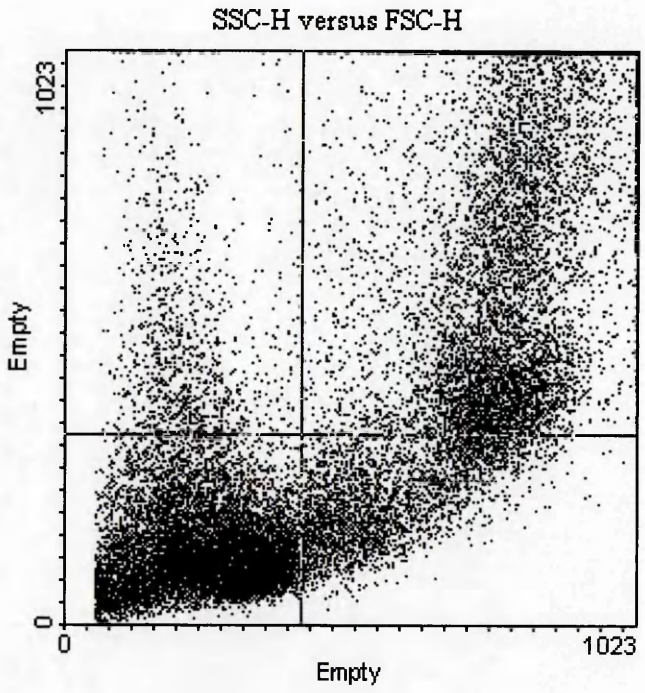

Figure 3.12: Dot plot of CD34+ versus cell size (FSC-H) for CD34 test.002

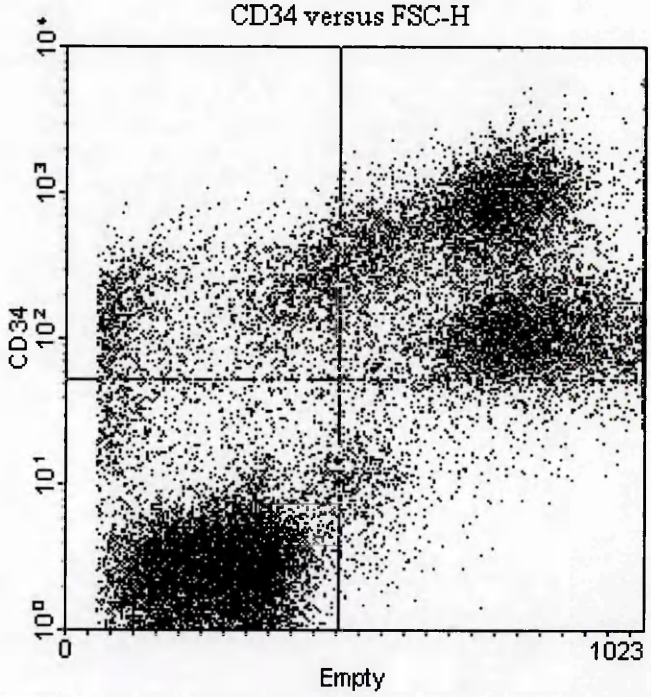

Figure 3.13: Histogram of events versus CD34 fluorescence for CD34 test.002

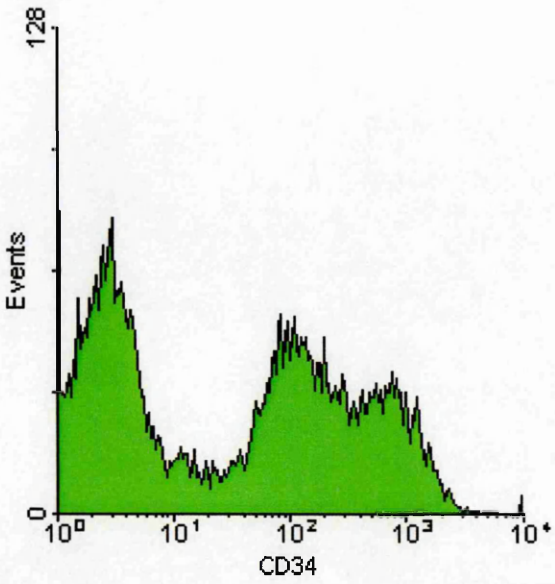

In figures 3.5 and 3.8 (experiments CD34 test-001 and CD34 test.003), CD34+ cells could be seen in the lower right-hand quadrant: 17.5% and 17.2%, respectively. On figures 3.6 and 3.9, these cells were in majority in the upper right-hand quadrant: 73.6% and 72.4%, respectively. However, it was clear that CD34+ cells were not the only cell population in the samples where the CD34+ cells had been isolated from mobilized peripheral blood. Figures 3.11, 3.12 and 3.13 (experiment CD34 test.002), which represented the cell populations in the apheresis sample, showed, as expected, that the CD34+ cell density was not as high as that of the CD34+ isolated sample. The proportion of CD34+ labelled cells was indeed only 37% (figure 3.13).

III.3.1.2. Detection of infectious parvovirus B19 particles in CD34+ cells by IFA

B19 infected CD34+ isolated cells were stained by IFA to investigate the presence of B19-specific fluorescence. The initial experiments using cells from patients 9, 13, 15 and 19 failed due to poor cell growth or bacterial contamination prior to IFA. Therefore, in subsequent experiments, 1% penicillin/streptomycin and 1% fungizone were added to the medium before and after B19 infection CD34+ cells. Those CD34+ cells isolated from the peripheral blood of a patient whose cells were not tested in the BFU-E reduction assay were inoculated with 1:10 dilution of B19 stock virus ($1x10^{11}$ IU/ml) 5 days after CD34+ isolation. Microscope slides were prepared (using the method of the drops on slide) on day 3 and 4 post-infection and IFA was performed using a mouse monoclonal anti-VP1/VP2 antibody (R92F6; Novocastra Laboratories Ltd, UK) followed by a goat anti-mouse FITC conjugate (Sigma). Observation under the fluorescence microscope revealed no evidence of positive staining. This suggested either the absence of infected CD34+ cells or the absence of viral replication in those cells or again a poor sensitivity of the IFA.

The final experiment attempted to detect infectious parvovirus B19 particles in CD34+ cells by IFA using cells isolated from two further patients who were not included in the BFU-E study. The volume of cell suspension used for culture after isolation was reduced to 200µl of $2x10^5$ cells/ml suspension in each well of a 96-well plate (flat bottom with low evaporation lid, Falcon). After 4 days at 37°C, the cells were settled at the bottom of the wells and the medium was removed carefully and discarded. Only 20µl of 1:10 dilution of B19 stock virus ($1x10^{11}$ IU/ml) were added to two wells while 20µl of negative serum were added to two negative control wells. Then the infection proceeded as detailed previously and slides were made 4 days post-infection. Three

types of antibodies were used in this IFA: human monoclonal antibody anti-NS1, 1:50 and 1:100 dilutions (kindly provided by Dr S. Modrow, Germany), mouse monoclonal antibody anti-VP1/VP2, 1:80 dilution (R92F6, from Novocastra, UK) and rabbit polyclonal antibody anti-NS1, 1:100 dilution (kindly provided by Dr S. Doyle, Ireland). No fluorescence was detected with any of the antibodies tested.

Slides of infected SF9 cells were also tested with the above corresponding monoclonal antibodies, with the exception of the rabbit polyclonal antibody anti-NS-1. The presence of contaminating anti-insect cell antibodies in the latter prevented it from being used in our insect expression systems such as baculovirus expressing recombinant VP1, VP2 and NS1 proteins. When stained with anti-VP1/VP2 antibodies, SF9 cells infected with baculovirus expressing VP1 protein presented bright fluorescence whereas those cells infected with baculovirus expressing VP2 protein showed a weaker signal. As far as SF9 cells inoculated with baculovirus expressing NS1 protein were concerned, no positive staining could be observed. This could have been due to a lack of sensitivity and/or specificity of the anti-NS-1 antibodies.

These experiments suggested that infectious virus particles could not be detected in CD34+ cells isolated from different patients using indirect IFA with different B19 antibodies.

III.3.1.3. Detection of infectious parvovirus B19 particles in CD34+ cells by detection of mRNA transcripts

Attempts were made to demonstrate the replication of B19 in inoculated CD34+ cells by detection of B19 specific transcripts. Cells expressing CD34 were isolated from the peripheral blood of patients 31 and 32 (not tested by BFU-E reduction assay), with final concentrations of $8.6x10^5$ cells/ml and $9x10^5$ cells/ml, respectively. After 4 days at 37°C

(5% CO_2) in CD34+ medium, the cell count was $1x10^7$ cells/ml and $1.5x10^5$ cells/ml for patients 31 and 32, respectively. CD34+ cells were then harvested and inoculated with 100µl of either negative serum or a 1:10 dilution of B19 stock virus ($1x10^{11}$ IU/ml). The cells were plated out in 4 wells of a 96-well plate using 200µl of medium/well for patient 31 and 2 wells of a 96-well plate for patient 32. Cells from patient 31 were harvested on days 1, 2, 3 and 4 post-infection while cells from patient 32 were harvested on days 5 and 6 post-infection. Total nucleic acids were isolated using the Nuclisens™ extraction method that will be described later (see section II.2.4.4).

Two reverse transcription (RT)-PCR reactions were prepared with either actin-specific primers (actin-3 and actin-4) or B19-specific primers (B19-6 and B19-9) (see section II.1.3.2). The total volume for each RT-PCR reaction was 50µl, including 5µl mRNA template added last. Each reaction contained 10µl of RT-PCR buffer, 2µl of 10mM dNTP mix, 1.2µl of 25pmol/µl forward and reverse primers, 2µl of RT-PCR enzyme mix and finally 28.6µl of RNAase-free water to make up the reaction volume to 50µl. The RT-PCR conditions were as follows: 1 cycle at 50°C for 30 minutes, 1 cycle at 94°C for 15 minutes, 43 cycles of 94°C for 45 seconds, 55°C for 45 seconds and 72°C for 2 minutes and finally 1 cycle at 72°C for 5 minutes. A 2% agarose gel was run with the RT-PCR products and visualised under UV light.

The results are shown in figures 3.14 and 3.15. The internal control, actin (~635bp), was present in all samples tested (figure 3.14), confirming that the cellular nucleic acids had been extracted from all samples. Considering the brightness of the actin bands, 2µl of template would have been sufficient for the amplification of mRNA transcripts. The expected sizes for B19-specific mRNA transcripts amplified with B19-6 and B19-9 primers were 155bp, 275bp and 1779bp. All three bands could be detected in all CD34+ samples inoculated with the virus from day 1 to day 6 post-infection (figure 3.15). The

smear seen in these samples could be due to the absence of Q buffer in the RT-PCR reaction, which would have prevented unspecific amplification. The large product seen in lane 11 (figure 3.15; day 6, negative serum) might have been due to a contamination from the neighbouring wells during loading of the samples. As far as CD34+ cells from patient 31 were concerned, the intensity of the amplification seemed to be greatest on days 1 and 2 post-infection. These time points were not tested for cells from patient 32, which showed the greatest intensity of amplification on day 6 post-infection.

By detecting B19-specific mRNA transcripts, this experiment demonstrated that CD34+ cells isolated from mobilised peripheral blood were able to support the replication of human parvovirus B19, from day 1 to at least day 6 post-infection.

Figure 3.14: Agarose gel with RT-PCR products amplified with actin-specific primers

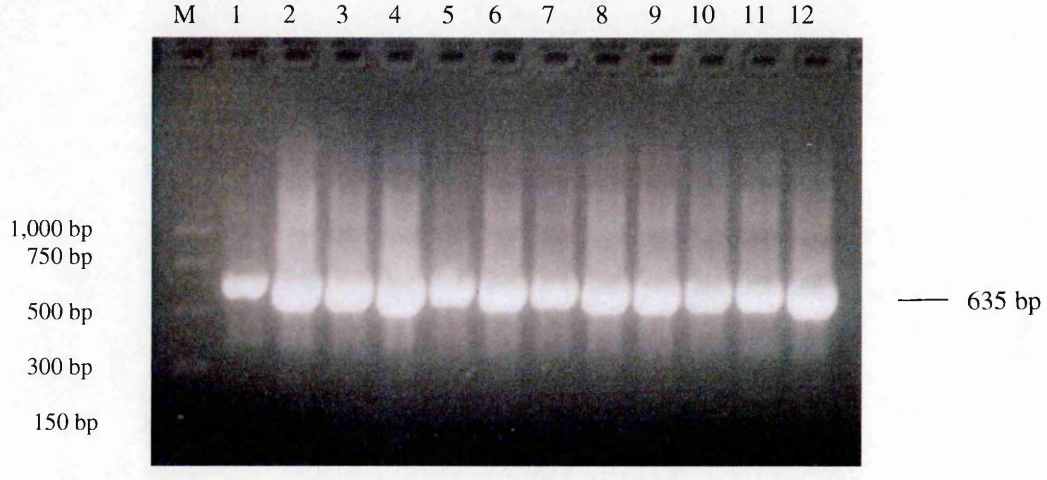

Lane	Sample	Lane	Sample
M.	PCR markers		
1.	Day 1, negative serum (patient 31)	8.	Day 4, $2x10^{11}$ IU/ml (patient 31)
2.	Day 1, $2x10^{11}$ IU/ml (patient 31)	9.	Day 5, negative serum (patient 32)
3.	Day 2, negative serum (patient 31)	10.	Day 5, $2x10^{11}$ IU/ml (patient 32)
4.	Day 2, $2x10^{11}$ IU/ml (patient 31)	11.	Day 6, negative serum (patient 32)
6.	Day 3, $2x10^{11}$ IU/ml (patient 31)	12.	Day 6, $2x10^{11}$ IU/ml (patient 32)
7.	Day 4, negative serum (patient 31)	13.	RNAase-free water

Figure 3.15: Agarose gel with RT-PCR products amplified with B19-specific primers

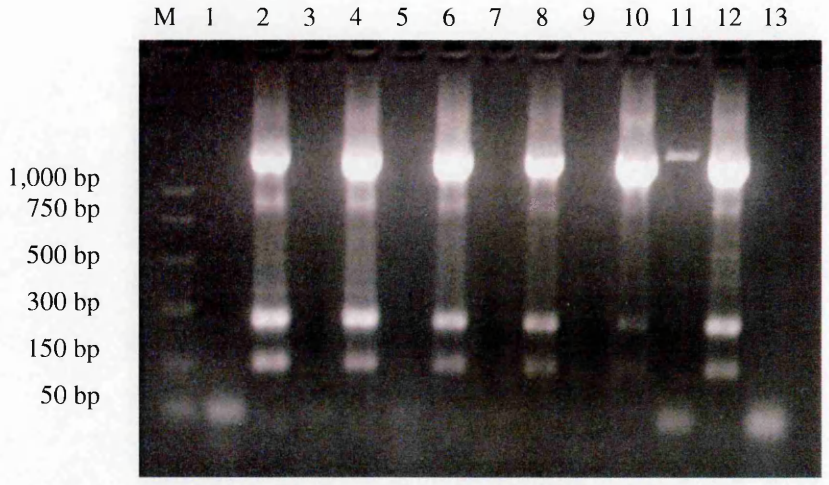

Lane	Sample
M.	PCR markers
1.	Day 1, negative serum (patient 31)
2.	Day 1, $2x10^{11}$ IU/ml (patient 31)
3.	Day 2, negative serum (patient 31)
4.	Day 2, $2x10^{11}$ IU/ml (patient 31)
6.	Day 3, $2x10^{11}$ IU/ml (patient 31)
7.	Day 4, negative serum (patient 31)
8.	Day 4, $2x10^{11}$ IU/ml (patient 31)
9.	Day 5, negative serum (patient 32)
10.	Day 5, $2x10^{11}$ IU/ml (patient 32)
11.	Day 6, negative serum (patient 32)
12.	Day 6, $2x10^{11}$ IU/ml (patient 32)
13.	RNAase-free water

III.3.2. BFU-E reduction assay

III.3.2.1. Anti-B19 IgG status of apheresis cells donors

SF9 insect cells were used in this IFA and were infected with baculovirus expressing either VP1 or VP2 recombinant proteins and fixed on microscope slides as positive controls. Some uninfected SF9 cells were also included in the test as negative controls. The IgG status of some of the apheresis donors was tested using IEA and IFA and the results are shown in table 3.1 below.

Table 3.1: Anti-B19 IgG status of some apheresis cells donors

Patient nb	Anti-B19 IgG (T/CO)	IFA VP1	IFA VP2
1	+ (7.8)	+	+
9	- (0.1)	-	-
13	+ (2.2)	-	-
14	+ (4.4)	+ (low)	-
15	- (0.0)	-	-
16	+ (5.2)	+ (low)	-
17	+ (9.3)	+ (strong)	+
18	+ (1.7)	-	-
19	- (0.1)	-	-
20	- (0.1)	-	-
24	+	N/A	N/A
25	+	N/A	N/A
26	+	N/A	N/A
27	+	N/A	N/A
29	-	N/A	N/A

Ten of fifteen patients tested for anti-B19 IgG antibodies were found positive using IEA. Of these ten, six were also tested by IFA and only the one with the highest cutoff value of 9.3 showed strong fluorescence with VP2 protein and some fluorescence with VP1 protein. Patient 1 had a cutoff value of 7.8 and the IFA was positive for both capsid proteins. On the other hand, the two patients with the lowest cutoff values of 2.2 and 1.7 (patients 13 and 18, respectively) didn't show any fluorescence with either VP1

or VP2 proteins. The last two patients with intermediate cutoff values of 4.4 and 5.2 (patients 14 and 16, respectively) displayed weak fluorescence with the VP1 protein only and none with VP2 in the IFA.

III.3.2.2. BFU-E reduction assay results

An example of the red colonies formed from BFU-E after plating the cells on Fox's medium is shown in figure 3.16.

Figure 3.16: Red colonies in a negative control of BFU-E reduction assay

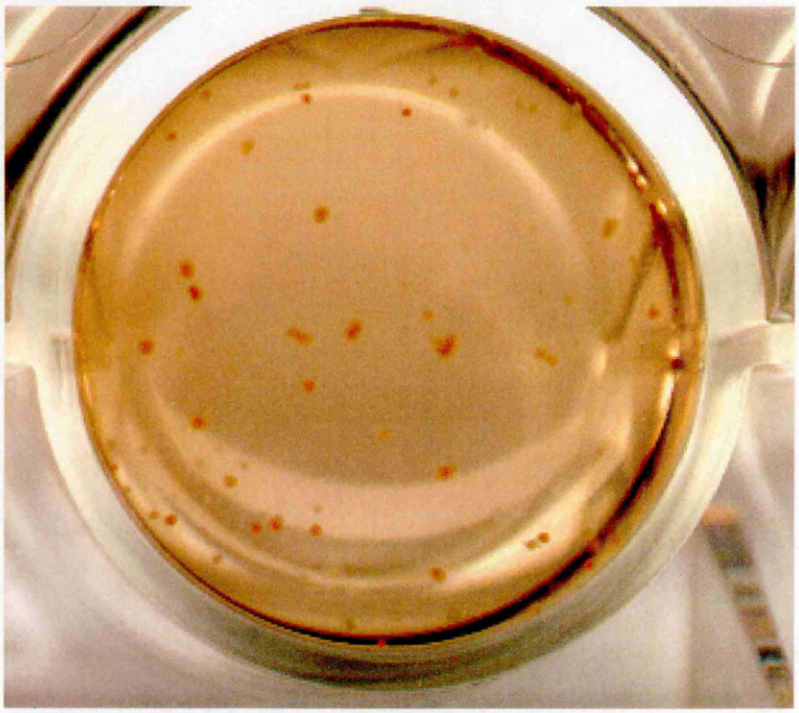

The red colonies were counted in each well and the percentage BFU-E reduction calculated for each dilution. The raw data of the BFU-E reduction assay of all the patients who donated apheresis cells are shown in appendix 1. The results indicated a significant discrepancy between the different patients who donated apheresis cells. To confirm this observation, the virus dilution containing $2x10^7$ IU/ml was looked at more

closely. When this virus dilution was added to apheresis cells collected from donors 15 and 30, no reduction in the formation of red colonies was noted (0% reduction). There were two hypotheses for this result: the first one was that there were not enough B19 infectious particles in the sample to interfere with the differentiation of haemapoitic progenitors into erythrocytes, and the second one was that the apheresis cells from these patients were not fully permissive to B19 infection.

When inoculated onto apheresis cells of patients 1, 18, 27 and 29, the same virus dilution ($2x10^7$ IU/ml) induced a percentage BFU-E reduction lower than 10% i.e. 7.14, 9.35, 3.57 and 5.74%, respectively. This observation ruled out the first hypothesis proposed above since the same virus dilution resulted in reduction of red colony formation in different patients. Therefore, cells collected from patients 1, 18, 27 and 29 seemed to be more permissive than those from patients 15 and 30. Even more permissive to B19 infection were all the cell samples in which $2x10^7$ IU/ml gave rise to a red colony formation reduction from 11.46% (patient 24) to 63.49% (patient 21). These apheresis cells were collected from patients 14 (19.16%), 23 (23.51%), 25 (25.46%), 19 (31.01%), 20 (31.87%), 26 (32.42%), 28 (39.29%), 17 (54.88%), 22 (57.75%) and 13 (57.8%). The major discrepancies noted between patients seemed to be due to a difference in cell susceptibility to B19 infection.

III.3.2.3. Detection of infectious parvovirus B19 in cells from BFU-E colonies by indirect IFA

The aim of the experiments in this section was to assess the susceptibility to B19 infection of apheresis cells differentiated into erythrocytes.

In the first experiment, patient 7 was specifically chosen because of the apparent lack of susceptibility to B19 infection suggested by the BFU-E reduction assay results (Appendix 1). When inoculated with $1x10^{10}$ IU/ml of B19 stock virus, the apheresis

cells from patient 7 only showed 3.4% BFU-E reduction, whereas the same virus dilution tested in 18 other samples induced on average 79% BFU-E reduction. Results from patient 8 at that virus dilution was slightly lower than average at 66.83% (Appendix 1). The red colonies formed in the negative control of BFU-E assays of patients 7 and 8 were thus picked by aspiration using a sterile glass Pasteur pipette and placed in 1ml of fresh IMDM medium (Appendix 1). The cell counts were $2.1x10^6$ cell/ml and $2.3x10^6$ cells/ml, for patients 7 and 8, respectively. The cells were centrifuged for 10 minutes at 145g and the supernatant discarded. The differentiated cells were inoculated with either 100µl of medium or 100µl neat B19 stock virus ($1x10^{12}$ IU/ml) and incubated at 4°C for 2 hours with occasional mixing. Fresh medium was then added to the samples to obtain a final concentration of $5x10^5$ cells/ml and this cell suspension was plated out in a 96-well plate using $1x10^5$ cells/well (i.e. 200µl/well). The plate was placed at 37°C (5% CO_2) and the cells harvested on the day of infection, as well as on days 1, 2, 3, 4 and 7 post-infection. Microscope slides were prepared and IFA was performed using mouse monoclonal antibody anti-VP1/VP2, 1:80 dilution (R92F6, Novocastra).

As expected, neither of the samples (patients 7 and 8) inoculated with B19 stock virus ($1x10^{12}$ IU/ml) presented fluorescence on the day of infection since the virus had not had time to replicate. Cells from patient 7 harvested on day 3 post-infection presented only a few positive cells (~5%; not shown) whereas on day 4, the proportion of infected cells was slightly greater (~10%; figure 3.17). The fluorescence was brighter than on the previous day and mainly diffuse, although fluorescent spots could be seen on a few cells, as shown on figure 3.17. On day 7 post-infection, the type of fluorescence remained the same but it was detected in a higher proportion of the cells (~20%), as can be seen on figure 3.18.

Figure 3.17: IFA in differentiated cells from patient 7 infected with parvovirus B19, day 4 post-infection

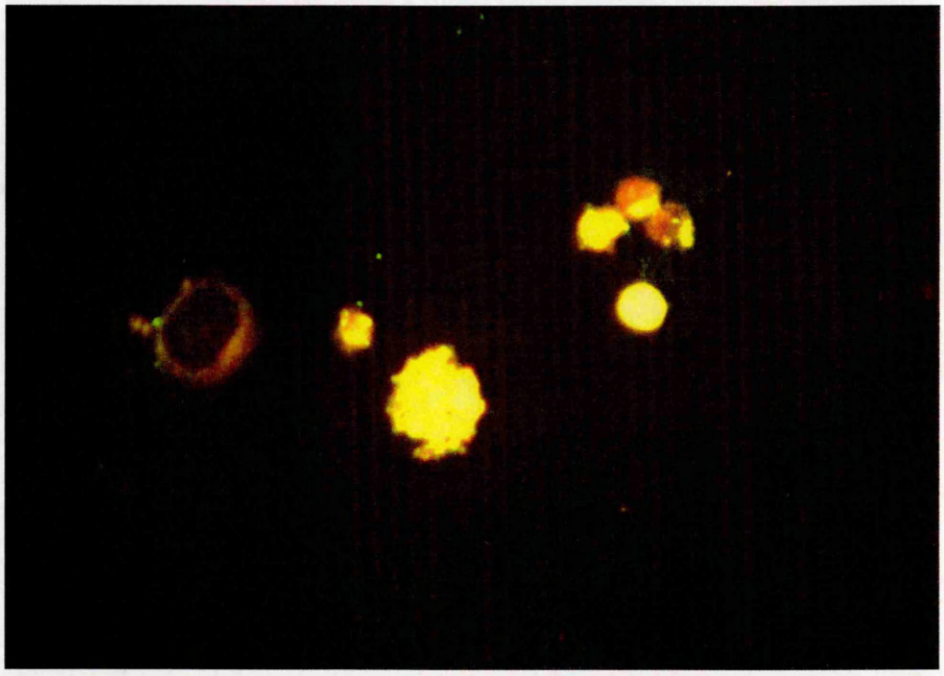

Figure 3.18: IFA in differentiated cells from patient 7 infected with parvovirus B19, day 7 post-infection

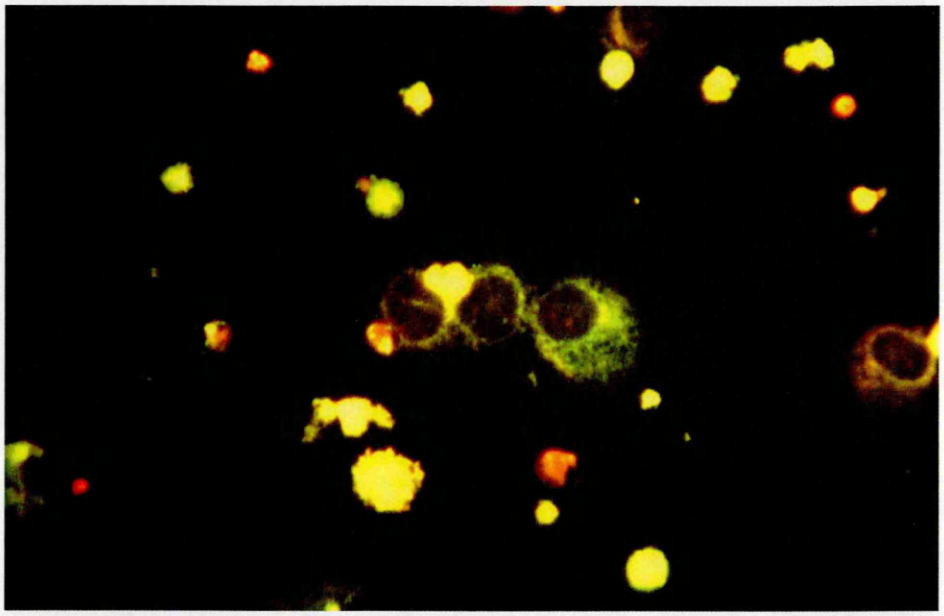

As for patient 8, very few cells presented positive staining on days 3 and 4 post-infection (not shown). Of those infected, the majority showed diffuse fluorescence in the whole cells rather than spots. On day 7 post-infection, a larger proportion of cells were infected (~25%) and showed fluorescence for VP1/VP2 proteins (not shown). When compared to each other on day 7 post-infection, cells from patient 8 seemed to be slightly more susceptible to B19 infection than cells from patient 7 since there were more positive cells in the former. The type of fluorescence seemed to be overall more diffuse in cells from patient 8 compared to those from patient 7 where some infected cells showed fluorescent spots. This phenomenon might have been explained by the fact that infection in cells from patient 8 was more significant, with possibly a higher viral replication rate than in cells from patient 7. Results from a previous BFU-E reduction assay (Appendix 1) had indeed suggested that cells from patient 7 were less susceptible to B19 infection than those from patient 8 when inoculated with $1x10^{10}$ IU/ml. However, when inoculated with $1x10^{12}$ IU/ml, 100% reduction had been induced in both these patients. Therefore, if more cells had been available, this IFA experiment would have been repeated using a lower virus titre for inoculation in order to assess better the susceptibility to B19 infection of erythrocytes differentiated from those apheresis cells.

In order to compare these results with those of another patient, a second time-course experiment was performed using cells from patient 6. The cell count was $3.3x10^6$ cells/ml and cell harvest was done every day from day 2 to day 10 post-infection. In this experiment, the microscope slides were prepared using the cytospin method. The IFA results of this experiment showed that no positive staining could be detected in cells until day 3 post-infection. Figure 3.19 shows the negative control on that day. In the

sample inoculated with B19 stock virus, only a few cells (~1%) showed fluorescent dots representing VP1/VP2 proteins, as shown on figure 3.20.

Figure 3.19: IFA in uninfected differentiated cells from patient 6, day 3 post-

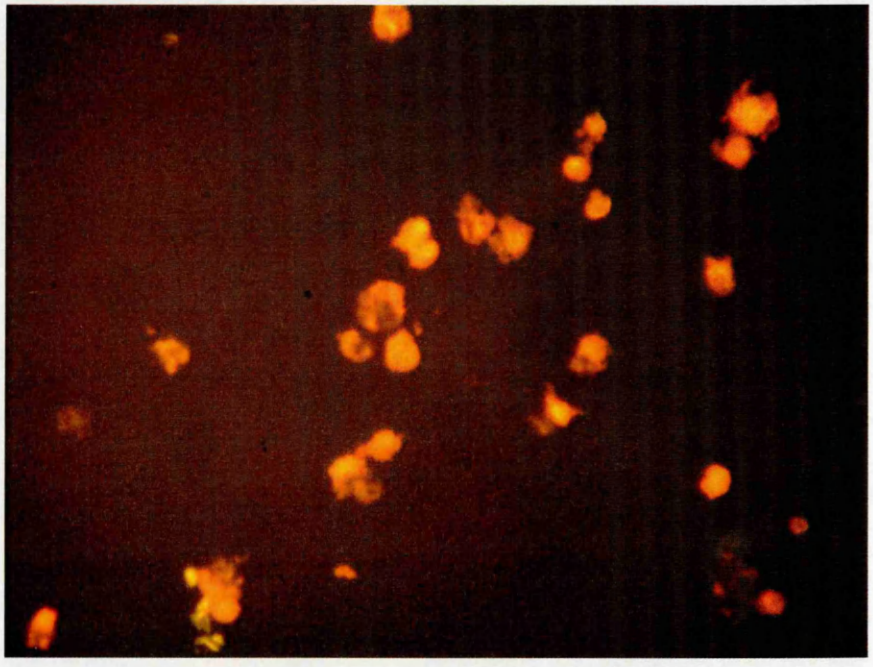

Figure 3.20: IFA in infected differentiated cells from patient 6, day 3 post-infection

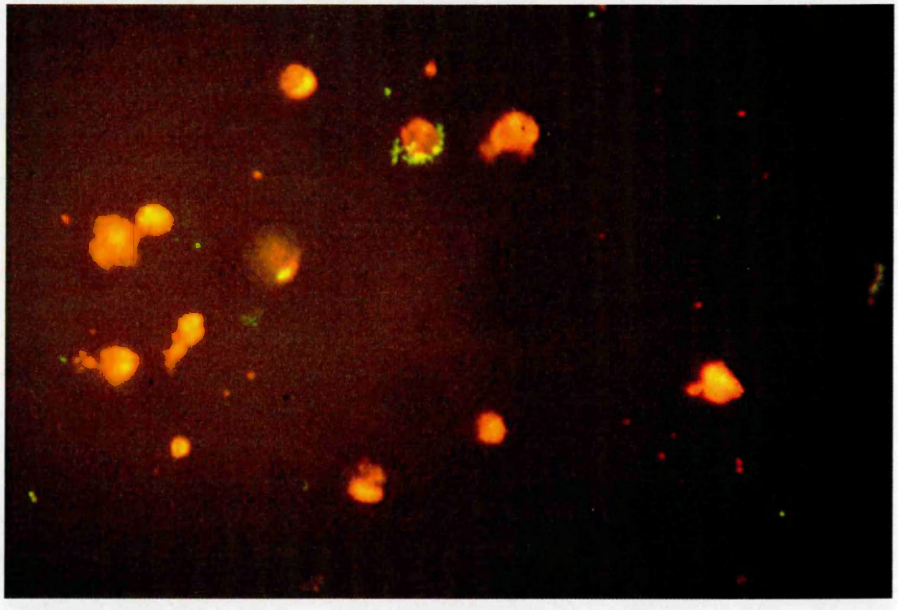

Lastly, a third time-course experiment investigated the cells from two more patients: 3 and 4. The protocol above was followed and the cell counts of picked red colonies were $2.5x10^6$cell/ml and $9.5x10^5$ cells/ml for patients 3 and 4, respectively. The IFA results showed that few cells were actually fixed on the microscope slides and that no positive staining was present in the differentiated cells from either patient on any day (not shown). The absence of fluorescence might have been due to either the lack of susceptibility of those particular primary cells or to the fact that the cells might have been dying of a different cause before they were harvested. This second hypothesis might explain why there were so few cells on the slides.

III.4. Continuous human erythroid cell lines

III.4.1. Growth curves

As human parvovirus B19 is known to infect cells in S phase (Kishore and Kapoor, 2000), it was crucial to determine the growth pattern of the cells and thereby decide on the optimum time for viral inoculation.

III.4.1.1. KU812Ep6 cell line

For the KU812Ep6 cell line, the growth curves of cells at both early (n+19) and late passage (n+81) were compared. For each cell passage, cell suspension concentrations (prepared using fresh medium) of $1x10^5$, $5x10^4$ and $1x10^4$ cells/ml were tested. In addition to providing an indication on the best time to infect the cells, this experiment allowed the determination of the best starting concentration when splitting the cells. Each cell suspensions was seeded into two 24-well plates using 1ml of cell suspension per well. The plates were incubated at 37°C (5% CO_2). Every day and for 8 days, 100µl

of trypan blue was added to 4 wells of each cell suspension dilution and the live cells (unstained) counted using a haemacytometer.

The cell counts and growth curves for KU812Ep6 cells are shown in appendix 2, tables A2.1 to A2.6 and in figures 3.21 and 3.22.

Figure 3.21: KU812Ep6 growth curves (n+19)

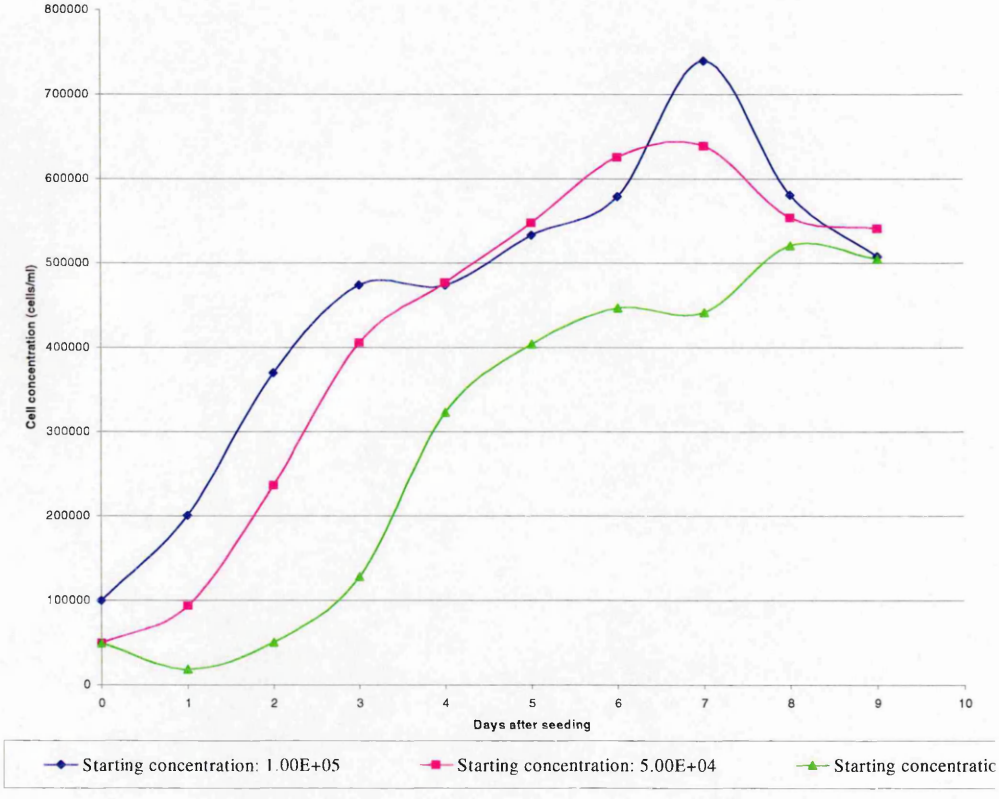

Figure 3.22: KU812Ep6 growth curves (n+81)

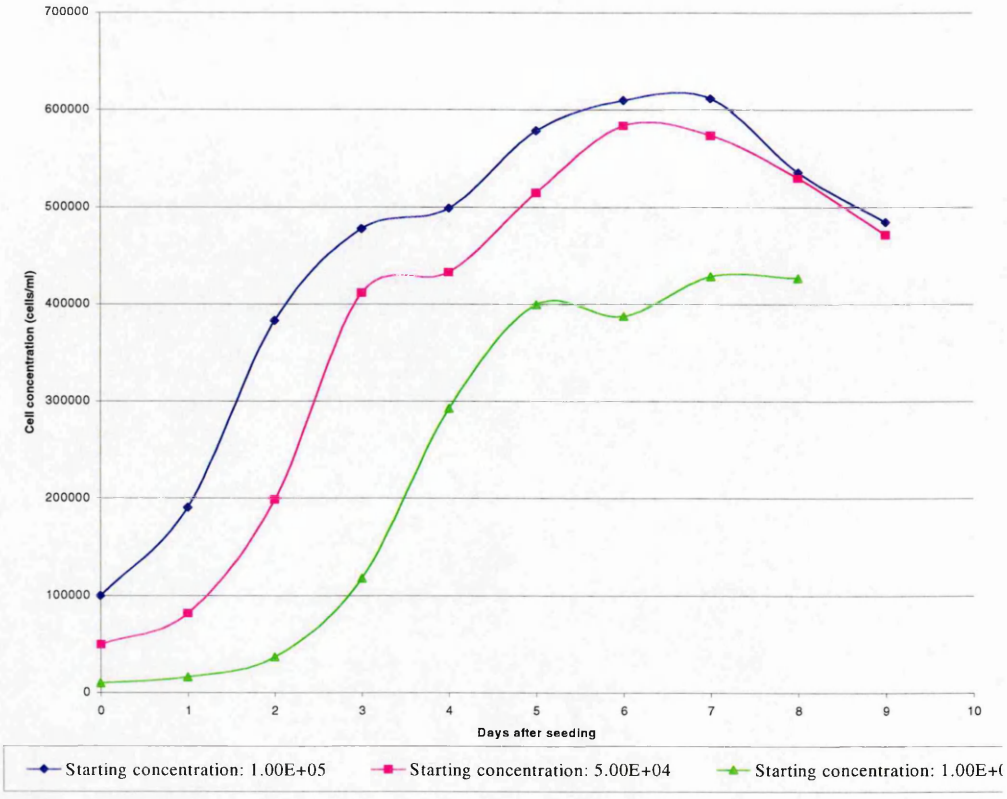

The results suggested that these cells should be used at a starting concentration of $1x10^5$ cells/ml and should be harvested 5 days after passaging them to optimise the yield of dividing cells, which have been reported to be the most permissible for parvovirus B19. The study showed that an earlier passage (n+19) led to higher cell concentrations than a later cell passage (n+81) suggesting that the former might be more suitable regarding a higher cell yield.

III.4.1.2. UT-7/EPO cell line

The protocol described above for KU812Ep6 cells was followed for UT-7/EPO cells at passages n+19 and n+80 and for UT-7/EPO-S1 cells at passage n+14, using cell suspensions at starting concentrations of $1x10^5$, $5x10^4$ and $1x10^4$ cells/ml.

The cell count results are displayed in appendix 2, tables A2.7 to A2.12 and the growth curves are shown in figures 3.23 and 3.24.

When UT-7/EPO cells were used at passage n+80 (tables A2.10 to A2.12, figure 3.24), they showed an earlier exponential phase than that of the lower passage n+19 (tables A2.7 to A2.9, figure 3.23). Additionally, the growth of ealier passage cells (n+19) showed a plateau phase (figure 3.23) whereas the growth curves of cells at a later passage (n+80) were decreasing quickly after reaching the peak, revealing rapid cell death (figure 3.24). The use of such late passage (n+80) was therefore not recommended. These data suggested that UT-7/EPO cells should be passaged at the starting concentration of $1x10^5$ cells/ml and virus inoculation should be done 3 days after splitting them.

Figure 3.23: UT-7/EPO growth curves (n+19)

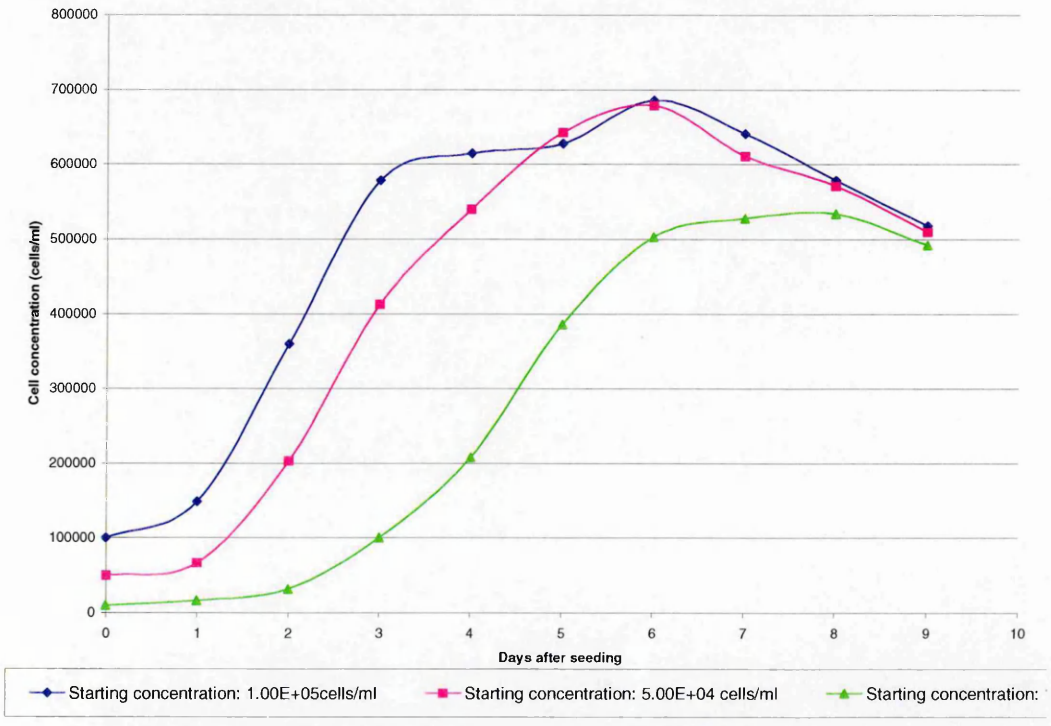

Figure 3.24: UT-7/EPO growth curves (n+80)

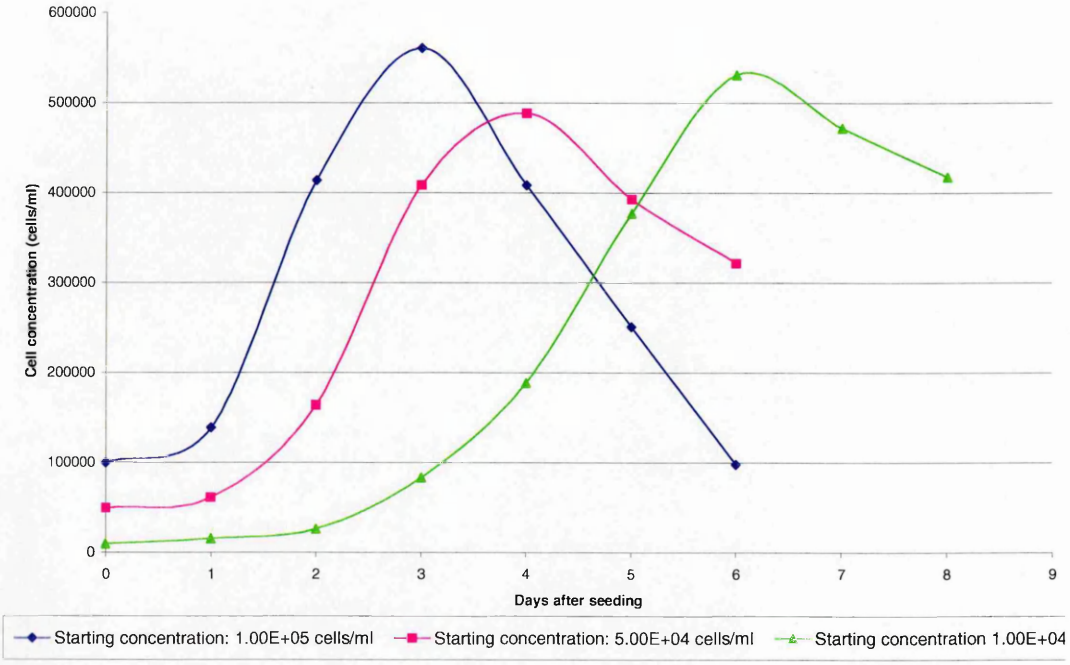

III.4.1.3. UT-7/EPO-S1 cell line

The same protocol as described for KU812Ep6 cells (see section III.4.1.1) was followed but the results of the cell counts for UT-7/EPO-S1 cell line with a starting cell concentration of $1x10^4$ cells/ml were too low to be significant and thus the results are not shown. Tables A2.13 and A2.14 in appendix 2 and figure 3.25 show the cell counts for the starting cell concentrations of $1x10^5$ and $1x10^4$ cells/ml. The growth curve using $1x10^4$cells/ml (green) did not show the typical shape, i.e. exponential growth, plateau and decrease. The cells were still multiplying 9 days after seeding. It was therefore decided that UT-7/EPO-S1 cells would be split to obtain the starting concentration of $1x10^5$ cells/ml in all experiments using this cell line, and that the cells should be used for virus inoculation 5 days after passaging them.

Figure 3.25: UT-7/EPO-S1 growth curves (n+14)

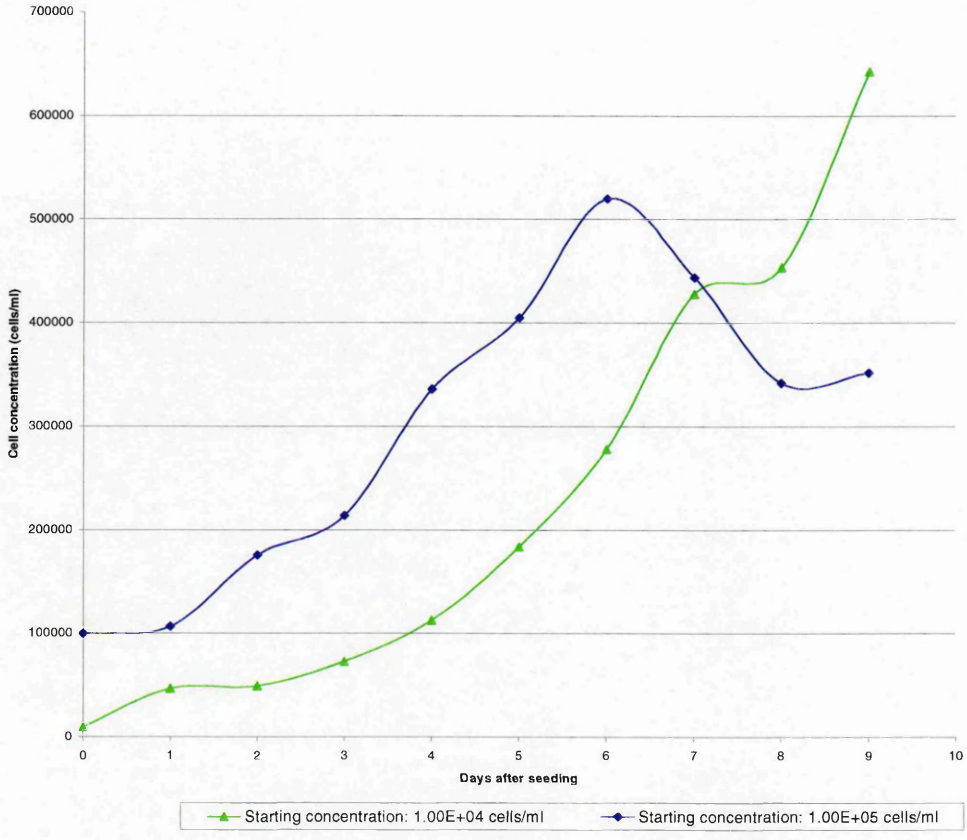

III.4.2. Cell attachment study

The aim of this experiment was to evaluate whether any of the suspension cell lines could form a monolayer on suitably treated plates in order to establish a plaque assay for B19, which would be more user friendly. Accordingly, the bottom of a 96-well plate was treated with either collagen or fibronectin, known to promote cell attachment, in order to determine whether KU812, KU812Ep6 and UT-7/EPO cells would adhere to the wells.

To coat each well of a 96-well plate (0.32 cm^2) with 2.5µg of Collagen I, 50µl of a working solution of Collagen I (rat-tail, Becton-Dickinson), containing 50µg/ml was added (5µg/cm^2). The plate was left at room temperature for 1 hour, the Collagen I

solution discarded from the wells and replaced with 200µl of PBS-A. The plate was left to stand for 30 seconds and the buffer discarded. The plate was air-dried and used immediately. Alternatively, the coated plate could be stored at 4°C for up to a week.

A second plate was coated with fibronectin-like engineered protein polymer (Sigma). In order to coat each well of a 96-well plate (0.32cm^2) with 3.2µg of fibronectin-like engineered protein polymer, 32µl of the working solution (100µg/ml) was added to each well (10µg/cm^2). The plate was left for 5 minutes at room temperature, fibronectin-like engineered protein polymer was discarded and the coated plate was immediately rinsed twice with PBS-A and air-dried. The coated plate could either be used immediately or stored at room temperature for up to 4 months. An example of part of the 96-well plate is shown below in table 3.2. Columns 1, 3 and 5 of the plate were coated (+ sign) with either Collagen I or fibronectin-like engineered protein polymer as described above, whereas columns 2, 4 and 6 were not coated (- sign). The latter served as negative controls.

Table 3.2: Plate for cell attachment experiment

	1	2	3	4	5	6
A	+	-	+	-	+	-
B	+	-	+	-	+	-
C	+	-	+	-	+	-
D	+	-	+	-	+	-
E	+	-	+	-	+	-
F	+	-	+	-	+	-

Rows A and B were used for UT-7/EPO cell line (duplicate), rows C and D for KU812 cell line (duplicate), and rows E and F for KU812Ep6 cell line (duplicate). A cell concentration of $1x10^5$ cells/ml was used in columns 1 and 2, $5x10^5$ cells/ml in columns 3 and 4 and $1x10^6$ cells/ml in columns 5 and 6. 200µl of cell suspension in fresh medium was added to the corresponding well in the two coated plates, which were then placed in an incubator (37°C, 5% CO_2).

After 4 hours, the cells were disturbed by shaking gently and observed under a light microscope for any sign of adherence to the coated plate. Only a few cells in each well, coated or non-coated, seemed attached to the plate. All three cell lines tested presented the same results. The plates were replaced in the incubator. After 24 hours, the medium was removed by inverting the plates and the cells observed under the light microscope. When the cell concentration was high i.e. $1x10^6$ cells/ml, some cells situated at the periphery of the wells stayed attached whereas the rest of the cells in suspension were removed when the medium was removed. This observation was made in both coated and non-coated wells, suggesting that neither treatment with Collagen I nor with fibronectin-like engineered protein polymer was responsible for this phenomenon. As far as lower cell concentrations were concerned, the cells were removed with the medium, thereby confirming that no attachment took place. Once more, all cell lines tested showed the same results.

In conclusion, this experiment suggested that KU812, KU812Ep6 and UT-7/EPO suspension cells could adhere to neither Collagen I nor fibronectin-like engineered protein polymer-coated plates. The development of a plaque assay for human parvovirus B19 using one of the above suspension cell lines was therefore ruled out, and an infectivity assay detecting viral mRNA transcripts was developed using those cells.

III.4.3. Detection of B19 proteins by indirect IFA in continuous cell lines

III.4.3.1. Comparison of KU812, KU812Ep6 and UT-7/EPO cell lines

Three cell lines: KU812, KU812Ep6 and UT-7/EPO ($2x10^5$ cells), were inoculated with either 30µl of neat B19 stock virus ($1x10^{12}$ IU/ml) or 30µl of negative serum. The cells were incubated at 4°C for 2 hours, with occasional mixing by flicking the tubes in order to keep the cells in suspension. Fresh medium (1ml) was added to each sample, which was then seeded into a 24-well plate (0.5ml per well). The plate was incubated at 37°C (5% CO_2) and the cells were harvested 5 days post-infection. Microscope slides were prepared using the cytospin method (200µl of cell suspension).

Two different primary antibodies were tested in this indirect IFA: mouse monoclonal anti-VP1 and VP2 proteins (1:80 dilution; Novocastra), mouse monoclonal anti-VP1 and VP2 proteins (1:50, 1:80, 1:100, 1:500, 1:1,000 dilutions; kindly provided by Ube Research laboratory, Fujirebo, Japan). A negative serum (1:100 dilution) was also included as a control.

As expected, no fluorescence was seen in any cell line when the negative serum was used as primary antibody with B19 inoculated cells. Similarly, no staining was detected in cells inoculated with negative serum (negative controls). With the Novocastra monoclonal antibody, positive staining was observed equally in cell lines KU812 and KU812Ep6 (~10%) whereas less fluorescence was seen in cell line UT-7/EPO (~5%). However, the proportion of positive cells was much higher when the monoclonal antibody from Ube Research laboratory, Fujirebo (Japan) was used as the primary antibody (>30%). Overall, the cell line UT-7/EPO also presented slightly less fluorescence than the other two cell lines. Although all three cell lines showed positive staining when the highest dilution (1:1,000 dilution) of the antibody from Ube Research laboratory, Fujirebo (Japan) was used, the highest proportion of infected cells and the

brightest fluorescence were displayed in the KU812Ep6 cell line. Photos of each cell line stained with the Japanese antibody (1:80 dilution) are shown on figures 3.26 to 3.28.

Figure 3.26: IFA in UT-7/EPO cells inoculated with human parvovirus B19, 5 days post-infection

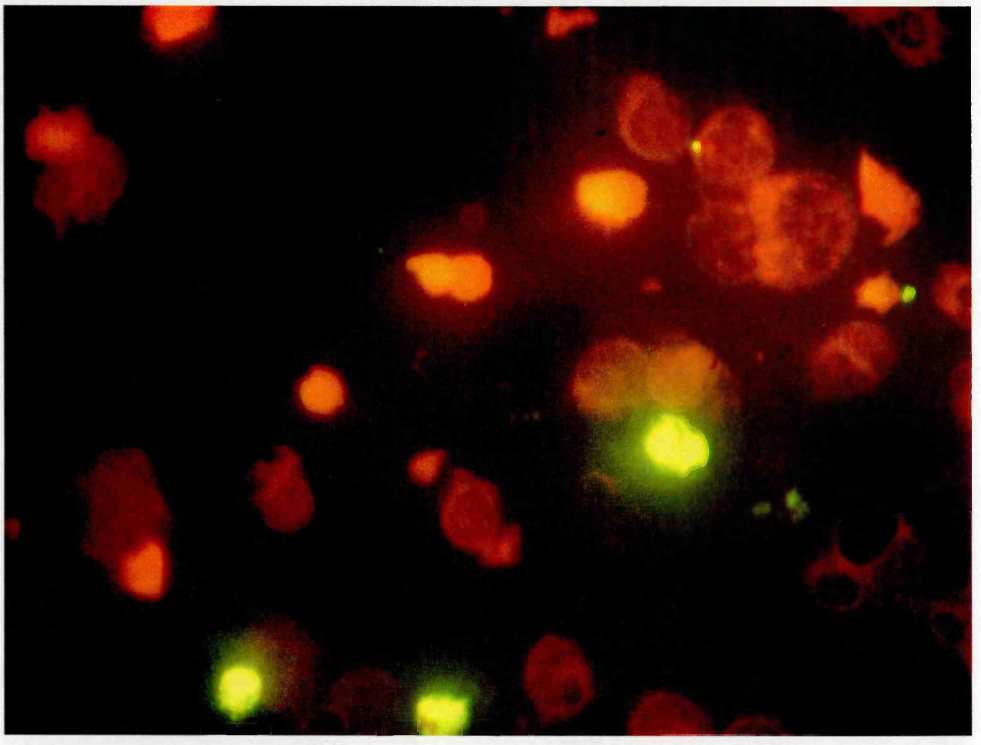

Figure 3.27: IFA in KU812 cells inoculated with human parvovirus B19, 5 days post-infection

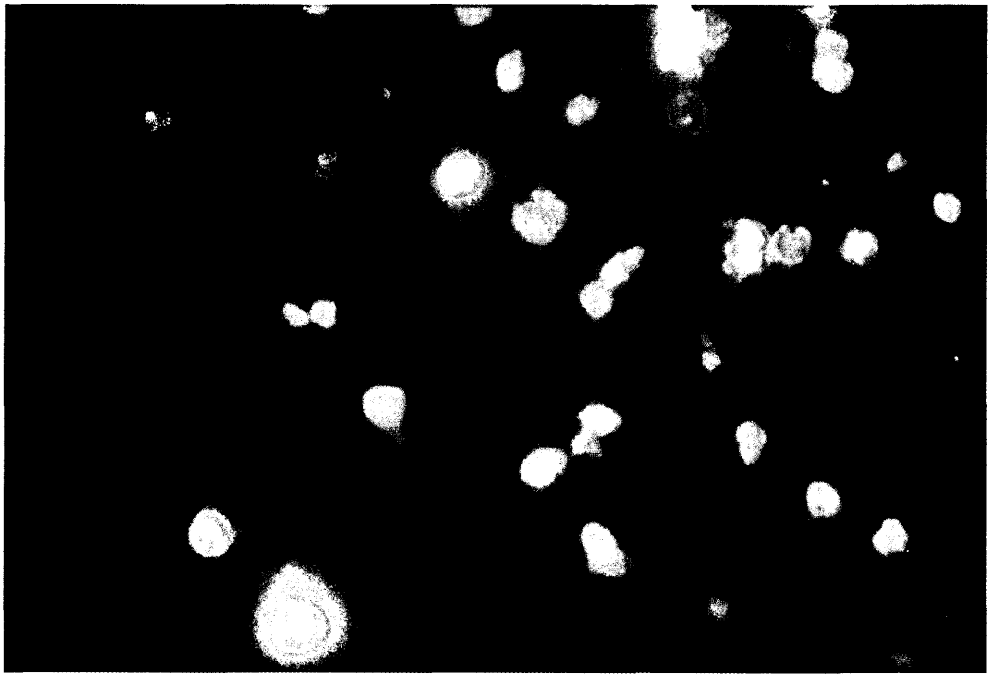

Figure 3.28: IFA in KU812Ep6 cells inoculated with human parvovirus B19, 5 days post-infection

III.4.3.2. KU812Ep6 cell line

Comparison of UT-7/EPO, KU812, KU812Ep6 cell lines in the previous experiment suggested that the KU812Ep6 cell line might be the most permissive one for human parvovirus B19 infection. This cell line was therefore investigated further. Infection of KU812Ep6 cells (passage n+72; $2x10^6$ cells) was done with either 300µl of a 1:10 dilution of the B19 stock virus ($1x10^{11}$ IU/ml) or 300µl of negative serum. Cells were left at 4°C for 2 hours, with occasional mixing to resuspend the cells, and washed twice with PBS-A. Fresh medium (1ml) was added to both positive and negative samples, which were then seeded into a 24-well plate. The plate was incubated at 37°C (5% CO_2) and the cells were harvested 5 days post-infection. Microscope slides were prepared using the cytospin method (200µl of cell suspension).

IFA was performed using either rabbit polyclonal anti-NS1 protein (1:100 dilution; from Dr S. Doyle, National University of Ireland, Republic of Ireland) or a commercial mouse monoclonal antibody anti-VP1/VP2 (1:50, 1:100, 1:1,000, 1:10,000 dilutions; Novocastra) with the Alexa Fluor® 488 signal amplification kit (Cambridge BioScience, UK). The latter system includes the Alexa Fluor 488 rabbit anti-mouse IgG (1:100 dilution), followed by enhancement with the Alexa Fluor goat anti-rabbit IgG (1:100 dilution). These conjugates are claimed to be significantly brighter and more photostable than fluorescein-labelled probes. Alexa Fluor goat anti-rabbit IgG conjugate only was used as the secondary antibody for cells stained with rabbit polyclonal anti-NS1 protein.

As expected, the cells which had been inoculated with negative serum did not show evidence of positive staining with either antibody used. KU812Ep6 cells inoculated with B19 and stained using mouse monoclonal anti-VP1/VP2 proteins presented

positive staining in only a couple of cells in each slide in the form of fluorescent spots, as seen on figure 3.29.

Figure 3.29: IFA in KU812Ep6 cells inoculated with human parvovirus B19, 5 days post-infection (stained with mouse monoclonal anti-VP1/VP2)

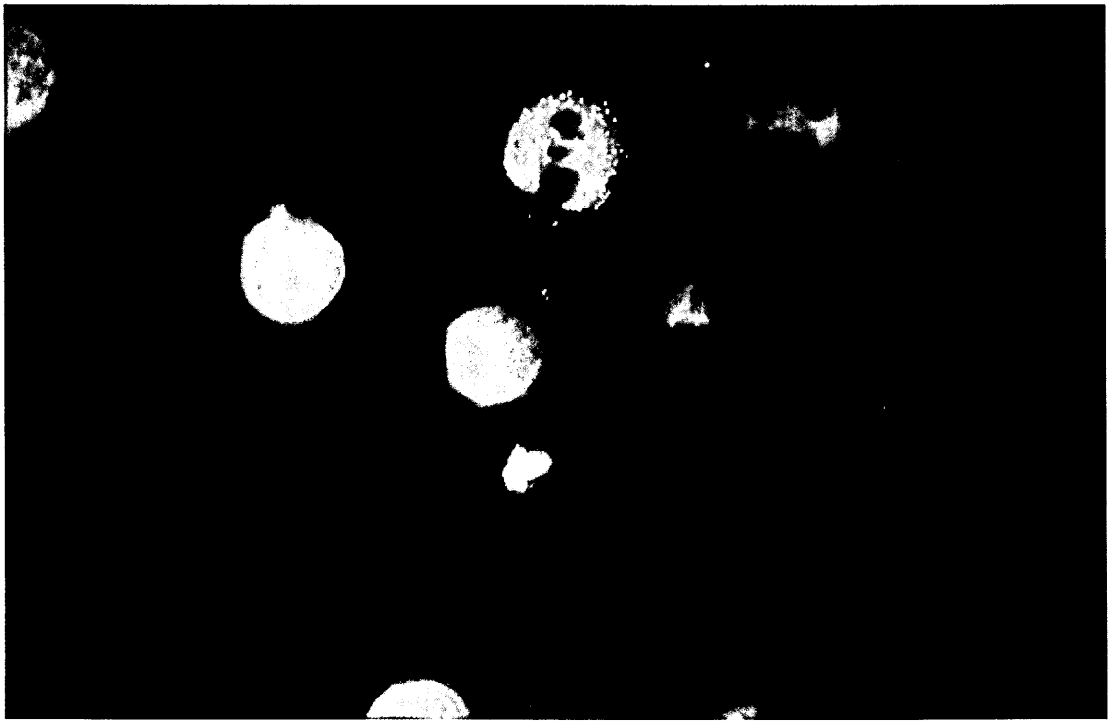

When the cells inoculated with the virus were stained with rabbit polyclonal anti-NS1 protein, some fluorescence was detected in a small proportion of the cells (~1%; not shown).

III.4.3.3. UT-7/EPO-S1 cell line

The IFA method kindly provided by Dr. J. Blümel (Paul Erhlich Institut, Germany) was tested on the UT-7/EPO-S1 cells. This protocol differed slightly from the one described previously in the method of infection, as well as in the use of a different mouse monoclonal antibody anti-VP1/VP2.

Cell aggregates were harvested, pelleted by centrifugation at 580g for 1 minute, and 7 samples were prepared with $2x10^5$ cells/sample. The cell pellet was resuspended in 200µl of medium without FCS (IMDM with 2U/ml EPO, 1% penicillin/streptomycin and 1% fungizone). Serial dilutions of the B19 stock virus were also prepared in medium without FCS, with concentrations ranging from $1x10^{11}$ to $1x10^6$ IU/ml. 100µl of either a virus dilution or medium without FCS (negative control) was added to the corresponding cell sample. The cells were then placed in a 37°C water bath for 2 hours. One millilitre of complete medium (IMDM with 10% FCS, 2U/ml EPO, 1% penicillin/streptomycin and 1% fungizone) was added to each sample, without washing. The cell suspensions were seeded in a 24-well plate and incubated at 37°C (5% CO_2). The cells were harvested 4 days post-infection and centrifuged at 715g for 1 minute. The medium was discarded (poured out rather than pipetted out) and the cell pellet washed with 1ml of PBS-A. The samples were centrifuged again (715g for 1 minute) and most of the supernatant discarded, leaving about 50µl. A volume of 8µl of this cell suspension was placed onto each spot of a multi spot slide (12 spots; Dunn, UK), air dried and fixed in cold acetone/methanol (1:1, volume:volume) for 10 minutes.

One slide was stained with the commercial mouse monoclonal antibody anti-VP1/VP2 (Novocastra, 1:100 dilution) while the other was incubated with a mouse monoclonal antibody (kindly provided by Dr J. Blümel) directed the VP1/VP2 proteins (1:100 dilution), followed by the goat anti-mouse FITC-conjugated secondary antibody (F0257, Sigma).

As expected, all cells inoculated with negative serum (negative controls) did not show any fluorescence. When the commercial mouse monoclonal (Novocastra) was used to stain UT-7/EPO-S1 cells, specific fluorescence, although very faint, was detected in a small proportion (~1%) of cells inoculated with dilutions of the B19 stock virus

containing $2x10^{11}$ and $2x10^{10}$ IU/ml. On the other hand, when the antibody provided by Dr Blümel was used, positive staining was bright and a few infected cells (~2-5%) could still be seen in cells inoculated with $2x10^{9}$ IU/ml of B19 virus. The differences in staining between the two antibodies can be seen in figures 3.30 and 3.31.

Figure 3.30: IFA in UT-7/EPO-S1 cells inoculated with human parvovirus B19 ($2x10^{10}$ IU/ml), 4 days post-infection

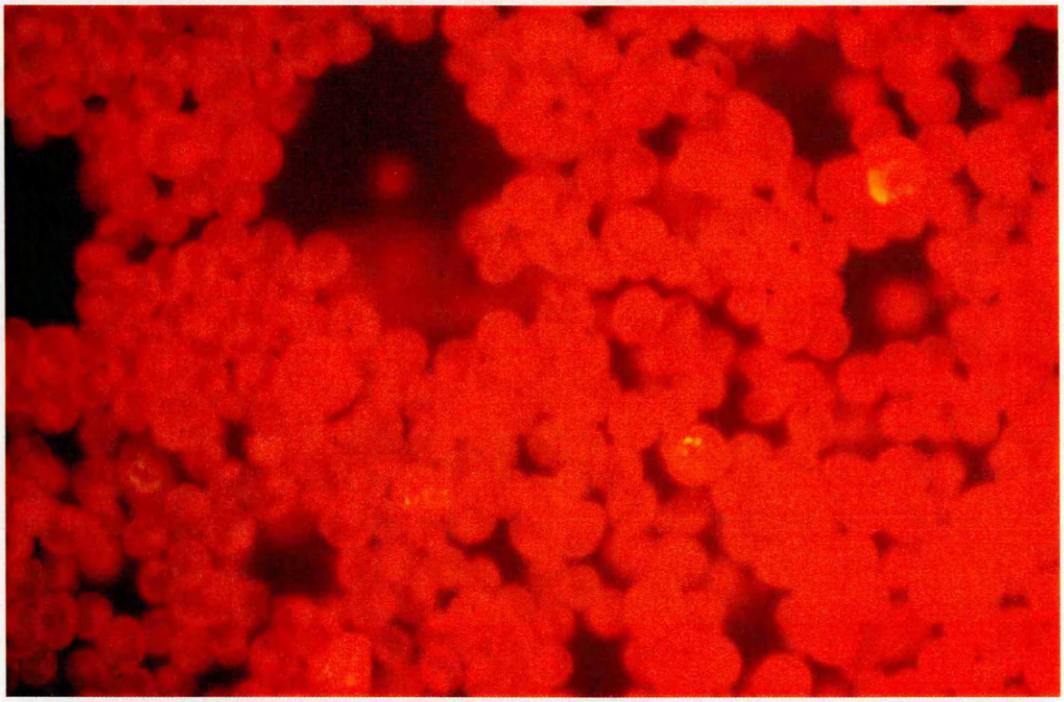

Figure 3.31: IFA in UT-7/EPO-S1 cells inoculated with human parvovirus B19 ($2x10^{10}$ IU/ml), 4 days post-infection

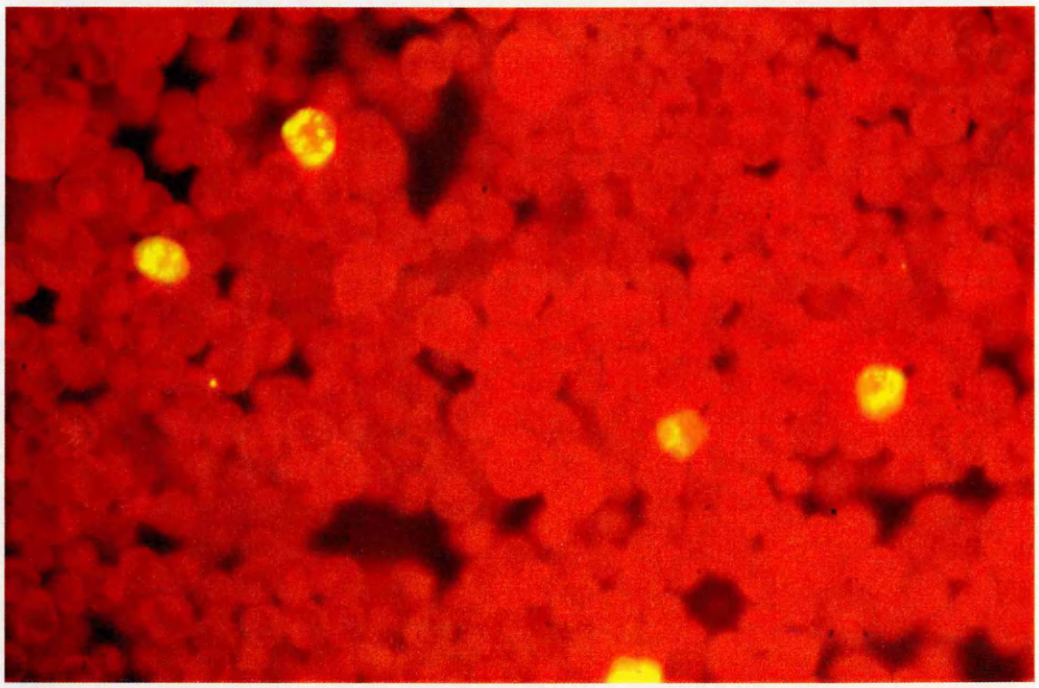

The major difference between the infection method used in the present research project and Dr Blümel's protocol was the use of a larger inoculum volume in the latter method, thereby increasing the multiplicity of infection. This experiment suggested that the mouse monoclonal antibody provided by Dr Blümel was $\log_{10}$ 1 more sensitive at detecting fluorescence in infected UT-7/EPO-S1 cells than the commercially available antibody (Novocastra). However, the virus titre at which the cells had to be inoculated with was still very high ($2x10^9$ IU/ml).

Consequently, an infectivity assay using nucleic acid amplification (RT-PCR) to detect viral mRNA transcripts seemed a much more sensitive and specific alternative to IFA.

III.4.4. B19 infectivity assay for the detection of B19-specific mRNAs in continuous cell lines

In the B19 infectivity assay developed in the present study, the number of infectious units/ml can be calculated by taking the product of the reciprocal of the highest dilution giving a positive signal in the mRNA assay and a factor to allow for the volume of inoculum. Since the volume of virus used to infect the cells was 30µl, the factor was x33.3 or $\log_{10}$ 1.5.

III.4.4.1. KU812 cell line

This experiment was aimed at determining whether KU812 cells were able to support parvovirus B19 replication and thereby to assess its possible use in the B19 infectivity assay. This was done by detecting viral mRNA transcripts using nucleic acid amplification (RT-PCR). As it was the first attempt at infecting these cells with B19, a high titre of virus was used and a time-course experiment was done for the isolation of mRNA from KU812 cells.

Two samples, each containing 10^6 cells, were prepared and centrifuged at 580g for 5 minutes. One sample (negative control) was inoculated with 100µl of negative serum while the other sample was resuspended in 100µl of B19 stock virus diluted 1:10 in PBS-A ($1x10^{11}$ IU/ml). The cells were left at 4°C for 2 hours and washed twice with 200µl of PBS-A. The cell pellets were then resuspended in 5ml of fresh medium and seeded into 5 wells of a 24-well plate. The plate was incubated at 37°C. One negative control and one sample inoculated with the virus were harvested on day 1, 2, 3, 4 and 5 post-infection. The isolation of total nucleic acids was carried out following Nuclisens™ extraction protocol.

Two different amplification assays were done, one with actin-specific primers (actin-3 and actin-4; 25pmol/µl) and the second with B19-specific primers (B19-6 and B19-9; 25pmol/µl). The RT-PCR conditions were 1 cycle at 50°C for 30 minutes, 1 cycle at 94°C for 15 minutes, 43 cycles of 94°C for 45 seconds, 55°C for 45 seconds and 72°C for 2 minutes and finally 1 cycle at 72°C for 5 minutes.

Figures 3.32 shows a photo of the agarose gel run with mRNA products amplified using actin- (A) and B19-specific (B) primers.

Although actin transcripts (figure 3.32, panel A) were present in all samples, the concentration of actin (as judged by the brightness of the band) progressively decreased from day 4 post-infection. When B19-specific primers were used (figure 3.32, panel B), all samples that had been inoculated with B19 virus (samples 2, 4, 6, 8 and 10) showed both B19-specific bands. The very faint bands seen in the negative samples 1 and 3 were due to a contamination from the neighbouring well when loading sample 2. The other negative samples did not show any amplification (samples 5, 7 and 9). This experiment showed that, when inoculated with high titre parvovirus B19, KU812 cells did allow the replication of the virus, at least from days 1 to 5 post-infection.

Figure 3.32: Analysis of mRNA products in KU812 cells

(A) Amplified with actin-specific primers

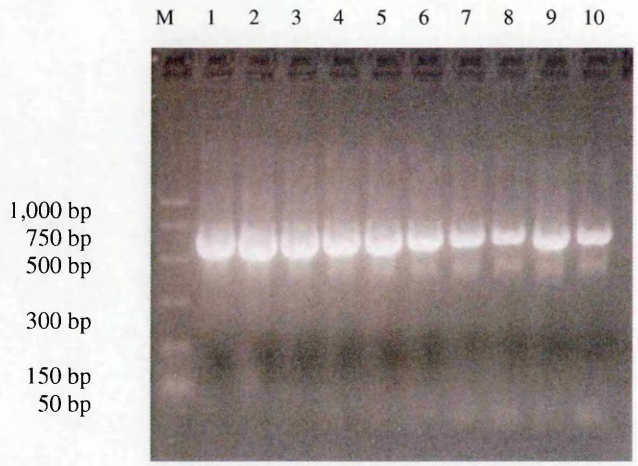

(B) Amplified with B19-6 and B19-9 primers

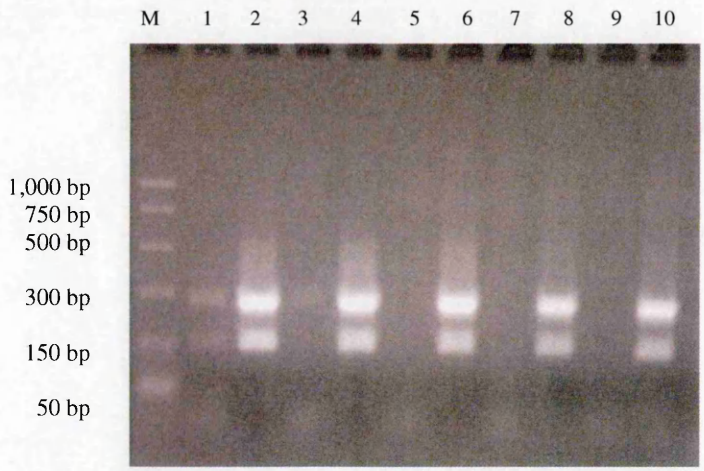

Lane	Samples
M	PCR markers
1.	day 1 post-infection, negative serum
2.	day 1 post-infection, $2x10^{11}$ IU/ml inoculum
3.	day 2 post-infection, negative serum
4.	day 2 post-infection, $2x10^{11}$ IU/ml inoculum
5.	day 3 post-infection, negative serum
6.	day 3 post-infection, $2x10^{11}$ IU/ml inoculum
7.	day 4 post-infection, negative serum
8.	day 4 post-infection, $2x10^{11}$ IU/ml inoculum
9.	day 5 post-infection, negative serum
10.	day 5 post-infection, $2x10^{11}$ IU/ml inoculum

III.4.4.2. KU812Ep6 cell line

A number of parameters regarding infection of cell cultures with parvovirus B19 were investigated in order to determine the optimum conditions for the use of KU812Ep6 cells in an infectivity assay. These parameters were concentration of erythropoietin (EPO) in the culture medium, passage number of cells for infection, pH of phosphate buffer used as the virus diluent and temperature of incubation of the infected cells.

III.4.4.2.1. Concentration of erythropoietin (EPO)

The aim of this study was to grow KU812Ep6 cells in medium containing increasing concentrations of EPO in order to determine the optimum culture conditions for this cell line with respect to susceptibility to B19 infection.

The cells were passaged and placed at 37°C in 5 tissue culture flasks ($25mm^3$; Falcon) containing medium supplemented with 2, 4, 6, 8 and 10U/ml of EPO. Four days later, the cells were harvested and counted. Six samples with 10^6 cells were prepared and centrifuged at 580g for 5 minutes. Serial 1:3 dilutions of the B19 stock virus were made in PBS-A to contain $1x10^{8.5}$, $1x10^8$, $1x10^{7.5}$, $1x10^7$ and $1x10^{6.5}$ IU/ml. Five cell samples were resuspended in these virus dilutions (30µl) whereas the negative control was resuspended in negative serum (30µl).

After 2 hours at 4°C, the cells were washed twice with 200µl PBS-A and the supernatant discarded. Each sample was resuspended in 5ml fresh medium containing the corresponding EPO concentration of 2, 4, 6, 8 or 10U/ml and was seeded in 5 wells of a 24-well plate. The latter was then incubated at 37°C (5% CO_2).

The cells were harvested two days post-infection and mRNA was isolated from whole cells using the Oligotex direct mRNA kit (Qiagen). Extracted mRNA was used as template in a multiplex RT-PCR assay using actin-specific primers (actin-3 and actin-4;

2.5pmol/μl) and B19-specific primers (B19-6 and B19-9; 25pmol/μl). The amplification conditions were 1 cycle at 50°C for 30 minutes, 1 cycle at 94°C for 15 minutes, 43 cycles of 94°C for 45 seconds, 55°C for 45 seconds and 72°C for 2 minutes and finally 1 cycle at 72°C for 5 minutes.

The results are shown in figure 3.33. As expected, none of the negative controls (samples 6, 12, 19, 25 and 31) showed amplification of B19-specific transcripts while all samples from which mRNA had been isolated showed amplification of the actin-specific transcript.

When KU812Ep6 cells were cultured with EPO concentrations of 2, 4, 8 and 10U/ml, the last sample in which B19-mRNA transcripts could be amplified was that inoculated with a dilution of the B19 stock virus containing $1x10^8$ IU/ml. When the cells were grown with 6U/ml of EPO, the last sample in which B19-mRNA transcripts could be amplified was that inoculated with a dilution of the stock virus containing $1x10^7$ IU/ml (sample 17). Therefore, this experiment showed that the sensitivity of the infectivity assay was optimum when KU812Ep6 cells were cultured in medium containing 6U/ml of EPO (which was also the concentration used by the laboratory which originally described this cell line).

Figure 3.33: Analysis of mRNA products in KU812Ep6 cells with increasing EPO concentrations

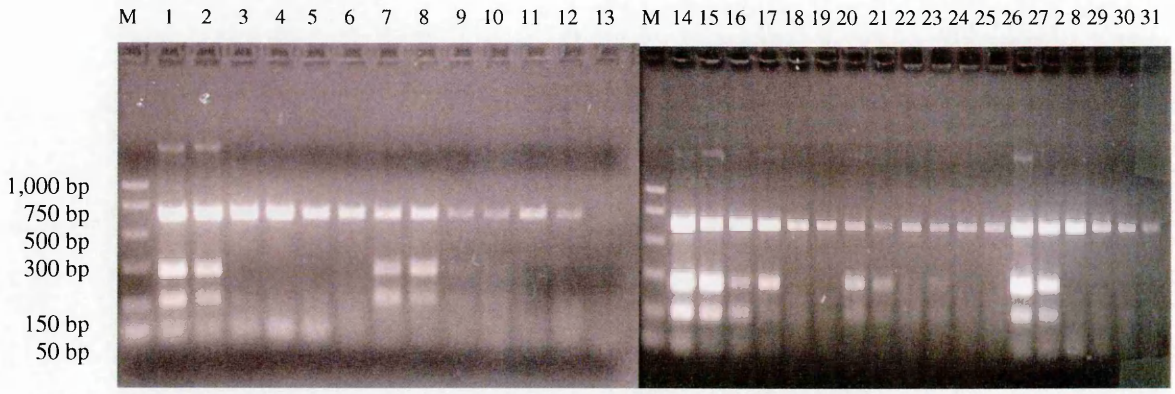

Lane M. PCR markers

Lanes 1 to 6: 2U/ml EPO

1. $1x10^{8.5}$ IU/ml inoculum
2. $1x10^{8}$ IU/ml inoculum
3. $1x10^{7.5}$ IU/ml inoculum
4. $1x10^{7}$ IU/ml inoculum
5. $1x10^{6.5}$ IU/ml inoculum
6. Negative serum

7 to 12: 4U/ml EPO

7. $1x10^{8.5}$ IU/ml inoculum
8. $1x10^{8}$ IU/ml inoculum
9. $1x10^{7.5}$ IU/ml inoculum
10. $1x10^{7}$ IU/ml inoculum
11. $1x10^{7}$ IU/ml inoculum
12. Negative serum
13. RNAase-free water

14 to 19: 6U/ml EPO

14. $1x10^{8.5}$ IU/ml inoculum
15. $1x10^{8}$ IU/ml inoculum
16. $1x10^{7.5}$ IU/ml inoculum
17. $1x10^{7}$ IU/ml inoculum
18. $1x10^{6.5}$ IU/ml inoculum
19. Negative serum

20 to 25: 8U/ml EPO

20. $1x10^{8.5}$ IU/ml inoculum
21. $1x10^{8}$ IU/ml inoculum
22. $1x10^{7.5}$ IU/ml inoculum
23. $1x10^{7}$ IU/ml inoculum
24. $1x10^{6.5}$ IU/ml inoculum
25. Negative serum

26 to 31: 10U/ml EPO

26. $1x10^{8.5}$ IU/ml inoculum
27. $1x10^{8}$ IU/ml inoculum
28. $1x10^{7.5}$IU/ml inoculum
29. $1x10^{7}$ IU/ml inoculum
30. $1x10^{6.5}$ IU/ml inoculum
31. Negative serum

III.4.4.2.2. Cell passage number

Since previous experiments (not shown) had suggested that KU812Ep6 cells at a higher passage number might be more susceptible to B19 infection than cells at a lower passage, it was considered important to compare different passage number in terms of infectivity assay results.

KU812Ep6 cells at passages n+8, n+29, n+81 and n+93 were counted and 5 samples containing $4x10^5$ cells each were pelleted by centrifugation (715g for 5 minutes) for each passage tested. The cells were washed once with 500µl of phosphate buffer pH5.7 and centrifuged at 715g for 5 minutes. The cell pellets were resuspended in 30µl of dilutions of the B19 stock virus (made in phosphate buffer pH5.7) containing $1x10^8$, $1x10^7$, $1x10^6$ and $1x10^5$ IU/ml. The negative control was resuspended in buffer only. All samples were left at 4°C for 2 hours and washed twice with PBS-A. To each sample, 1ml of fresh medium was added and the cells seeded in a 24-well plate. After two days in a 37°C (5% CO_2) incubator, the cells were harvested and the mRNA isolated from cell cytoplasm using the Oligotex direct mRNA kit.

Extracted mRNA was used as template in a multiplex RT-PCR assay using actin-specific primers (actin-3 and actin-4; 2.5pmol/µl) and B19-specific primers (B19-6 and B19-9; 25pmol/µl). The amplification conditions were: 1 cycle at 50°C for 30 minutes, 1 cycle at 95°C for 15 minutes, 43 cycles of 94°C for 45 seconds, 54°C for 40 seconds and 72°C for 50 seconds and finally 1 cycle at 72°C for 5 minutes.

The results are shown on figure 3.34.

Figure 3.34: Analysis of mRNA products in KU812Ep6 cells at various passages

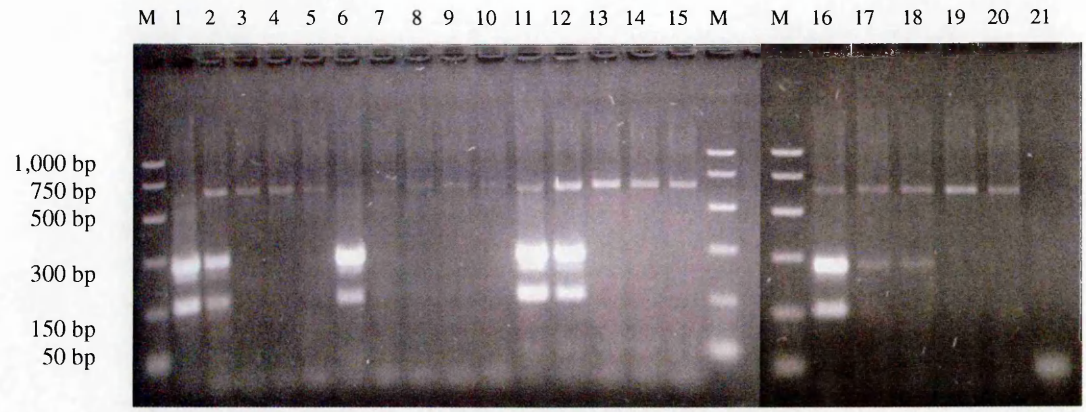

Lane M. PCR markers

Lanes 1 to 5: passage n+8

1. $1x10^8$ IU/ml inoculum
2. $1x10^7$ IU/ml inoculum
3. $1x10^6$ IU/ml inoculum
4. $1x10^5$ IU/ml inoculum
5. Negative serum

Lanes 6 to 10: passage n+29

6. $1x10^8$ IU/ml inoculum
7. $1x10^7$ IU/ml inoculum
8. $1x10^6$ IU/ml inoculum
9. $1x10^5$ IU/ml inoculum
10. Negative serum

Lanes 11 to 15: passage n+81

11. $1x10^8$ IU/ml inoculum
12. $1x10^7$ IU/ml inoculum
13. $1x10^6$ IU/ml inoculum
14. $1x10^5$ IU/ml inoculum
15. Negative serum

Lanes 16 to 20: passage n+93

16. $1x10^8$ IU/ml inoculum
17. $1x10^7$ IU/ml inoculum
18. $1x10^6$ IU/ml inoculum
19. $1x10^5$ IU/ml inoculum
20. Negative serum
21. RNAase-free water

In KU812Ep6 cells at passage n+29, the only sample in which B19-mRNA transcripts could be amplified was that inoculated with a dilution of the stock virus containing $1x10^8$ IU/ml (sample 6). When cells at passages n+8 and n+81 were used, the last sample in which B19-mRNA transcripts were detected was that inoculated with $1x10^7$ IU/ml of virus stock (samples 2 and 12). In the case of cells at passage n+93, the 275bp band specific for B19 was very faint and the only one detected in samples 17 and 18, inoculated with dilutions of the stock virus containing $1x10^7$ and $1x10^6$ IU/ml respectively. In conclusion, this study suggested that KU812Ep6 cells from a higher the

passage number were more susceptible to B19 infection than cells from a lower passage number.

III.4.4.2.3. pH of diluent buffer

Since it has been reported that a low pH is preferable in a B19 haemagglutination assay (Sato *et al.*, 1995) to allow better adsorption of the virus onto the cells, low pH phosphate buffers were investigated for use as a diluent for the virus serial dilutions used in the infectivity assay. Phosphate buffers (10mM) at pH 5.7, 6.0, 6.5 and 6.7, containing 0.85% NaCl, were investigated.

Sixteen samples (three inoculated with B19 and one negative control for each of the four pHs) were prepared with 10^6 KU812Ep6 cells (passage n+42) per sample. The cells were washed once with 0.5ml of phosphate buffer and centrifuged (580g for 5 minutes). The cell pellets were resuspended in 30µl of the respective phosphate buffer containing $1x10^9$, $1x10^8$ and $1x10^7$ IU/ml of B19 virus stock. The negative control was resuspended in the corresponding buffer only. The samples were incubated at 4°C for 2 hours and washed twice with 200µl of PBS-A to restore the pH to 7.2. The cell pellets were resuspended in 5ml of fresh medium and seeded into 5 wells of a 24-well plate and incubated at 37°C for 2 days, after which the cells were harvested. Isolation of mRNA from whole cells was done using the Oligotex direct mRNA kit (Qiagen). Extracted mRNA was used as template in multiplex RT-PCR using actin-specific primers (actin-3 and actin-4; 2.5pmol/µl) and B19-specific primers (B19-6 and B19-9; 25pmol/µl). The amplification conditions were 1 cycle at 50°C for 30 minutes, 1 cycle at 94°C for 15 minutes, 43 cycles of 94°C for 45 seconds, 55°C for 45 seconds and 72°C for 2 minutes and finally 1 cycle at 72°C for 5 minutes.

The results are shown on figure 3.35.

Figure 3.35: Analysis of mRNA products in KU812Ep6 cells with various pHs of diluent buffer

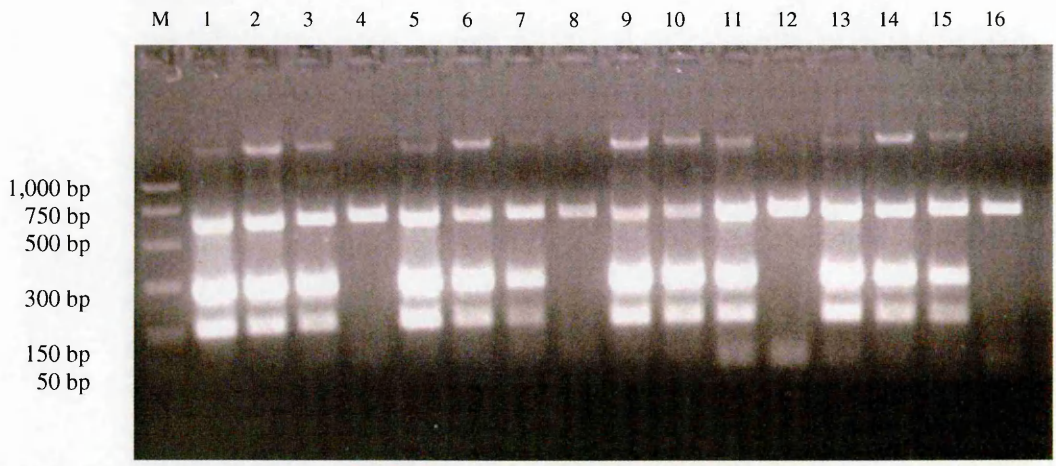

Lane M. PCR markers

Lanes 1 to 4: Phosphate buffer pH 5.7

1. $1x10^9$ IU/ml inoculum
2. $1x10^8$ IU/ml inoculum
3. $1x10^7$ IU/ml inoculum
4. Negative serum

5 to 8: Phosphate buffer pH 6.0

5. $1x10^9$ IU/ml inoculum
6. $1x10^8$ IU/ml inoculum
7. $1x10^7$ IU/ml inoculum
8. Negative serum

9 to 12: Phosphate buffer pH 6.5

9. $1x10^9$ IU/ml inoculum
10. $1x10^8$ IU/ml inoculum
11. $1x10^7$ IU/ml inoculum
12. Negative serum

13 to 16: Phosphate buffer pH 6.7

13. $1x10^9$ IU/ml inoculum
14. $1x10^8$ IU/ml inoculum
15. $1x10^7$ IU/ml inoculum
16. Negative serum
17. RNAase-free water

The bright actin band in all samples suggested that the cells did not loss significant viability as the pH decreased. The results showed that all pHs tested allowed detection of $1x10^{6.5}$ B19 infectious units/ml. Moreover, at pH 5.7, the B19-specific bands were the brightest. Therefore it appeared that phosphate buffer pH 5.7 could be used as diluent in the B19 infectivity assay.

In addition to phosphate buffer pH 5.7, 10mM acetate buffer (with 0.85% NaCl) at lower pHs (pH 5.6, 5.2, 4.8, 4.4 and 4.0) were tested the second study for comparison purposes. Twenty-five samples (three inoculated with B19 and one negative control for each of the five pHs) were prepared with 10^6 KU812Ep6 cells (n+47) per sample. The protocol described in the previous experiment was followed using dilutions of the B19 stock virus, made in the appropriate buffer, containing $1x10^8$, $1x10^7$ and $1x10^6$ IU/ml. Isolation and amplification of mRNA were performed in the same way as in the first study. The results are shown in figure 3.36.

There was a clear decrease in the brightness of the actin band as the pH decreased, suggesting that the cells were not viable at a very low pH. When acetate buffer at pH 5.6 and 5.2 were used as diluent of B19 stock virus, the last sample in which B19-specific mRNA transcripts were detected was that inoculated with a dilution of the B19 stock virus containing $1x10^7$ IU/ml (samples 3 and 7). When acetate buffers at pH 4.8 and 4.4 were used, the infectivity assay was able to detect $\log_{10}$ 1 less infectious virus particles per ml than at pH 5.6 and 5.2. There was no amplification of B19-specific transcripts when acetate buffer pH 4.0 was used However, the use of phosphate buffer at pH 5.7 led the detection of $1x10^{7.5}$ infectious units/ml, suggesting that it was the most efficient buffer to use for optimum B19 infection of KU812Ep6 cells. This buffer was therefore chosen as the virus diluent in the infectivity assay with KU812Ep6 cells.

Figure 3.36: Analysis of mRNA products in KU812Ep6 cells with various pHs of diluent buffer

(A)

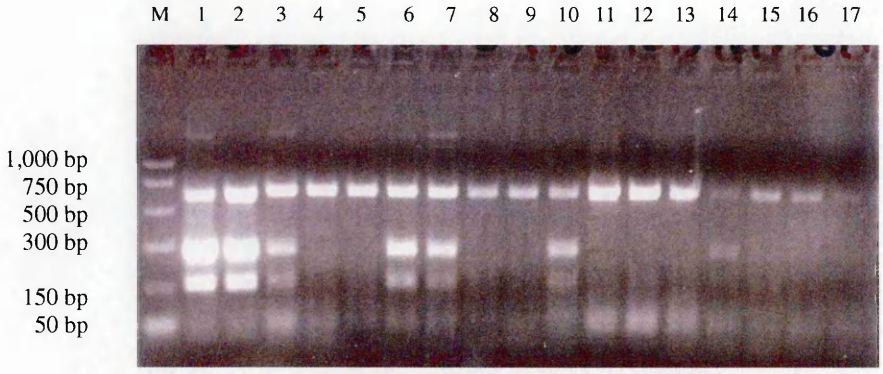

(B)

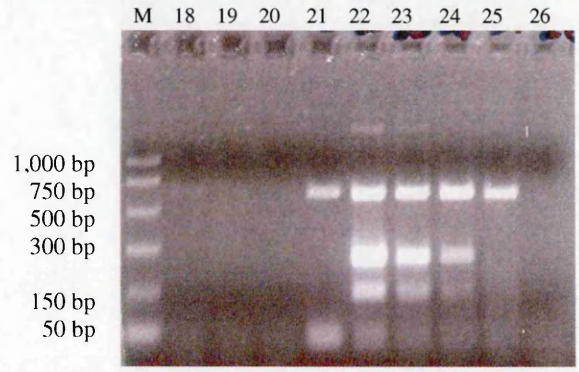

Lane M PCR markers

(A) Lanes 1 to 5: acetate buffer pH 5.6

1. $1x10^8$ IU/ml inoculum
2. $1x10^8$ IU/ml inoculum (duplicate)
3. $1x10^7$ IU/ml inoculum
4. $1x10^6$ IU/ml inoculum
5. Negative serum

Lanes 6 to 9: acetate buffer pH 5.2

6. $1x10^8$ IU/ml inoculum
7. $1x10^7$ IU/ml inoculum
8. $1x10^6$ IU/ml inoculum
9. Negative serum

Lanes 10 to 13: acetate buffer pH 4.8

10. $1x10^8$ IU/ml inoculum
11. $1x10^7$ IU/ml inoculum
12. $1x10^6$ IU/ml inoculum
13. Negative serum

Lanes 14 to 17: acetate buffer pH 4.4

14. $1x10^8$ IU/ml inoculum
15. $1x10^7$ IU/ml inoculum
16. $1x10^6$ IU/ml inoculum
17. Negative serum

(B) Lanes 18 to 21: acetate buffer pH 4.0

18. $1x10^8$ IU/ml inoculum
19. $1x10^7$ IU/ml inoculum
20. $1x10^6$ IU/ml inoculum
21. Negative serum

Lanes 22 to 25: phosphate buffer pH 5.7

22. $1x10^8$ IU/ml inoculum
23. $1x10^7$ IU/ml inoculum
24. $1x10^6$ IU/ml inoculum
25. Negative serum
26. RNAase-free water

III.4.4.2.4. Incubation temperature

The incubation period, during which cells and viruses were in contact, lasted for 2 hours and was done at 4°C. However, in order to ensure that this incubation temperature was optimal for B19 infection of KU812Ep6 cells, the results of the infectivity assay were compared to incubation at 37°C and room temperature. Eighteen samples of KU812Ep6 cells (passage n+39; $8x10^5$ cells/sample) were prepared and inoculated in triplicate with either negative serum or dilutions of the B19 stock virus containing $1x10^{10}$, $1x10^9$, $1x10^8$, $1x10^7$ and $1x10^6$ IU/ml, prepared in PBS-A. One set of samples was placed in a 37°C water bath, another at 4°C and the last set left at room temperature for 2 hours. The cells were washed twice with PBS-A and 4ml of fresh medium added to each sample. The cells were seeded in a 24-well plate (1ml per well), incubated at 37°C for 2 days, after which they were harvested. Isolation of mRNA from whole cells was done using the Oligotex direct mRNA kit. Extracted mRNA was used as template in multiplex RT-PCR using actin-specific primers (actin-3 and actin-4; 2.5pmol/µl) and B19-specific primers (B19-6 and B19-9; 25pmol/µl). The amplification conditions were 1 cycle at 50°C for 30 minutes, 1 cycle at 94°C for 15 minutes, 43 cycles of 94°C for 45 seconds, 55°C for 45 seconds and 72°C for 2 minutes and finally 1 cycle at 72°C for 5 minutes. The RT-PCR products were run on agarose gels, which are shown on figure 3.37.

Figure 3.37: Analysis of mRNA products in KU812Ep6 cells using various incubation temperatures

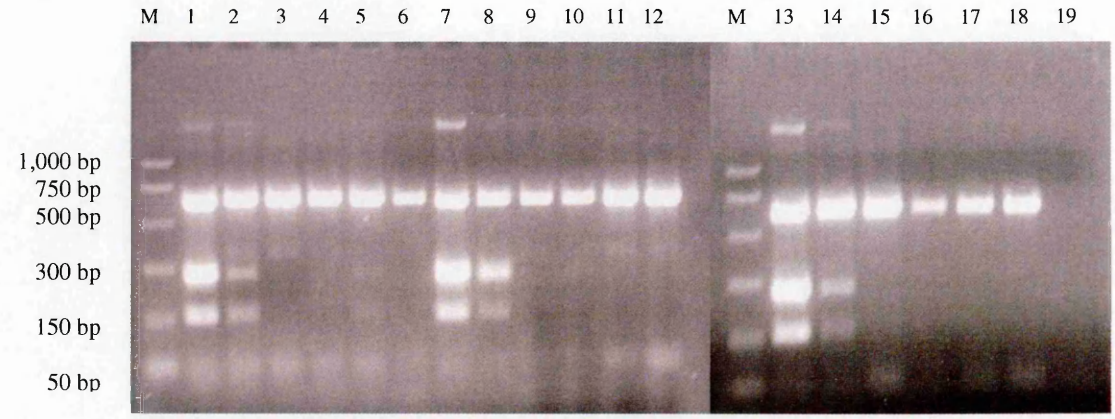

Lane M. PCR markers

Lanes 1 to 6: incubation at 37°C

1. $1x10^{10}$ IU/ml inoculum
2. $1x10^{9}$ IU/ml inoculum
3. $1x10^{8}$ IU/ml inoculum
4. $1x10^{7}$ IU/ml inoculum
5. $1x10^{6}$ IU/ml inoculum
6. Negative serum

Lanes 7 to 12: incubation at room temperature

7. $1x10^{10}$ IU/ml inoculum
8. $1x10^{9}$ IU/ml inoculum
9. $1x10^{8}$ IU/ml inoculum
10. $1x10^{7}$ IU/ml inoculum
11. $1x10^{6}$ IU/ml inoculum
12. Negative serum

Lanes 13 to 18: incubation at 4°C

13. $1x10^{10}$ IU/ml inoculum
14. $1x10^{9}$ IU/ml inoculum
15. $1x10^{8}$ IU/ml inoculum
16. $1x10^{7}$ IU/ml inoculum
17. $1x10^{6}$ IU/ml inoculum
18. Negative serum
19. RNAase-free water

As expected, a bright actin band was present in all samples where mRNA was extracted. When the cells and virus were incubated at 37°C, the last sample in which B19-specific mRNA transcripts were detected was the one inoculated with a dilution of the stock virus containing $1x10^{9}$ IU/ml (sample 2). Although very faint bands of the size of the B19-specific mRNA transcripts were seen in sample 5 inoculated with a dilution of the stock virus containing $1x10^{6}$ IU/ml, no specific bands were detected in samples 3 and 4, inoculated with $1x10^{8}$ and $1x10^{7}$ IU/ml, respectively. Therefore, this result might have

been due to the Poisson distribution and might not have been significant. The same infectivity assay results were obtained when the incubation period was done at 37°C, room temperature and 4°C. At these temperatures, the assay could detect $1x10^9$ IU/ml. The conclusion of this experiment was that the incubation temperature did not seem to be a significant parameter that could influence the susceptibility of KU812Ep6 cells to B19 infection. Therefore, 4°C was used as the incubation temperature for the optimised infectivity assay.

Overall, the experiments described in this section suggested that KU812Ep6 cells of a higher rather than lower passage number grown in medium supplemented with 6U/ml of EPO were optimum for the B19 infectivity assay. In addition, phosphate buffer, pH 5.7, was shown to be a good diluent for B19 virus in the infectivity assay and the study indicated that the incubation temperature of cells with virus was not a significant parameter in the inoculation step of the assay.

III.4.4.3. UT-7/EPO cell line

The optimal conditions for B19 infection of the UT-7/EPO cell line were also investigated. Three different virus diluents, namely phosphate buffer pH 5.7, acetate buffer pH 5.6 and PBS-A, were compared in this infectivity assay using UT-7/EPO cells. Twelve samples, including three inoculated with three dilutions of B19 stock virus and one negative control for each of the three buffers tested, were prepared with UT-7/EPO cells (passage n+46; $4x10^5$ cells/sample). The cells were washed once with phosphate buffer pH 5.7, acetate buffer pH 5.6 or PBS-A. Three different virus dilution series were prepared using each of the three buffers as diluent, and the cell pellets were resuspended in 30µl of virus dilution, containing $1x10^8$, $1x10^6$ or $1x10^4$ IU/ml, or with

the corresponding buffer alone. The samples were incubated at 37°C for 2 hours, after which UT-7/EPO cells were washed twice with 0.5ml of PBS-A. The cell pellets were resuspended in 2ml of freshly made medium and seeded in 2 wells of a 24-well plate. After 2 days incubation at 37°C (5% CO_2), the cells were harvested and the mRNA extracted from cell cytoplasm using the Oligotex direct mRNA kit (Qiagen). As the RT-PCR step could not be done immediately following mRNA isolation, the extracted mRNA samples were stored at -70°C. Two different pairs of primers were used for the amplification step: multiplex RT-PCR using B19-6 and B19-9 (25pmol/µl) with actin-3 and actin-4 primers (2.5pmol/µl), and single RT-PCR using the B19 primer pair XPP2 and B19-9 (25pmol/µl). The amplification conditions were 1 cycle at 50°C for 30 minutes, 1 cycle at 95°C for 15 minutes, 43 cycles of 95°C for 45 seconds, 57°C for 40 seconds and 72°C for 40 seconds and finally 1 cycle at 72°C for 10 minutes.

Figure 3.38 and 3.39 show the results of RT-PCR amplification using B19-6 and B19-9 (multiplex) and XPP2 and B19-9, respectively.

It is important to note, on figure 3.38, that most actin bands were very faint, except for samples 10, 11 and 12. The cell loss observed was probably not due to low pH since the actin bands were also faint when PBS-A was used. Moreover, previous experiments with KU812Ep6 cells suggested that cell loss only occurred at and below pH 4.4. This low level of isolated mRNA could have explained the lack of amplification of the B19-specific transcripts when B19-6 and B19-9 primers were used. Only sample 10, which had been inoculated with a dilution of the stock virus containing $1x10^6$ IU/ml (diluted in phosphate buffer pH 5.7), showed amplification of B19-specific transcripts.

Figure 3.38: Analysis of mRNA products in UT-7/EPO cells amplified with B19-6 and B19-9 primers

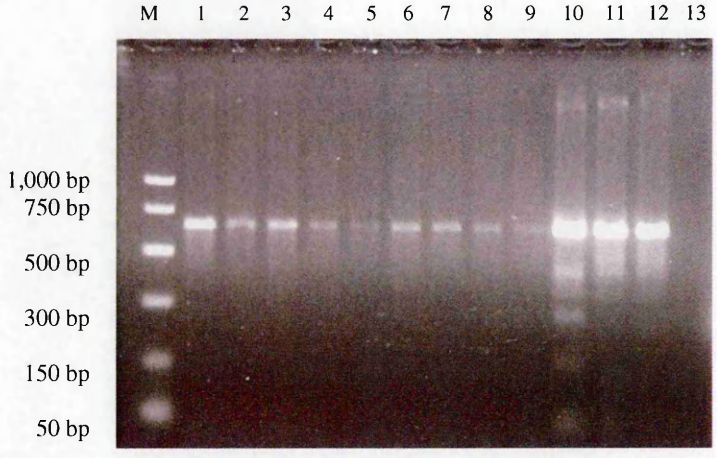

Lane M. PCR markers

Lanes 1 to 4: PBS-A

1. $1x10^8$ IU/ml inoculum
2. $1x10^6$ IU/ml inoculum
3. $1x10^4$ IU/ml inoculum
4. PBS-A

Lanes 5 to 8: acetate buffer pH 5.6

5. $1x10^8$ IU/ml inoculum
6. $1x10^6$ IU/ml inoculum
7. $1x10^4$ IU/ml inoculum
8. Acetate buffer pH 5.6

Lanes 9 to 12: phosphate buffer pH 5.7

9. $1x10^8$ IU/ml inoculum
10. $1x10^6$ IU/ml inoculum
11. $1x10^4$ IU/ml inoculum
12. Phosphate buffer pH 5.7
13. RNAase-free water

Figure 3.39: Analysis of mRNA products in UT-7/EPO cells amplified with XPP2 and B19-9 primers

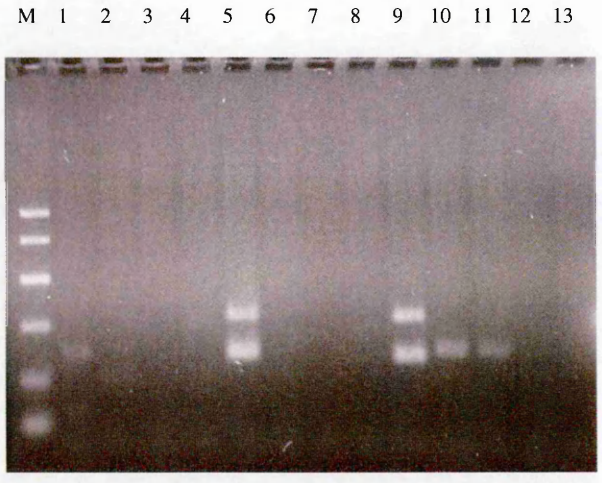

Lane M. PCR markers

Lanes 1 to 4: PBS-A

1. $1x10^8$ IU/ml inoculum
2. $1x10^6$ IU/ml inoculum
3. $1x10^4$ IU/ml inoculum
4. PBS-A

Lanes 5 to 8: acetate buffer pH 5.6

5. $1x10^8$ IU/ml inoculum
6. $1x10^6$ IU/ml inoculum
7. $1x10^4$ IU/ml inoculum
8. Acetate buffer pH 5.6

Lanes 9 to 12: phosphate buffer pH 5.7

9. $1x10^8$ IU/ml inoculum
10. $1x10^6$ IU/ml inoculum
11. $1x10^4$ IU/ml inoculum
12. Phosphate buffer pH 5.7
13. RNAase-free water

Amplification with primers XPP2 and B19-9 primers gave faint bands specific to B19 (figure 3.39). Amplification was seen in samples 1 and 5, which had been inoculated with a dilution of the stock virus containing $1x10^8$ IU/ml diluted in PBS-A and acetate buffer pH 5.6, respectively. When phosphate buffer pH 5.7 was used as diluent, amplification of B19-specific transcripts occurred in all three samples inoculated with the virus (samples 9, 10 and 11). In these conditions, the infectivity assay was able to detect $1x10^4$ IU/ml of B19. The difference in results between the different buffers tested

might have been due to the fact that more mRNA was present in samples 10, 11 and 12 than in the other samples. However, phosphate buffer pH 5.7 was still confirmed to be the most suitable buffer to use as virus diluent in infectivity assays using UT-7/EPO cells.

III.4.4.4. Comparison of the susceptibility of the KU812, KU812Ep6 and UT-7/EPO cell lines to infection with B19

III.4.4.4.1. B19 infectivity assays using the KU812Ep6, KU812 and UT-7/EPO cell lines

Since all three cell lines had been shown to support B19 replication, this experiment was aimed at determining which one was the most suitable for establishing a sensitive, B19 infectivity assay by inoculating the cells with serial, half-log_{10} dilutions (1:3 dilutions) of the B19 stock virus. Seven samples, containing $2x10^5$ cells per sample, were prepared for each of the cell line, KU812Ep6 (passage n+54), KU812 (passage n+68) and UT-7/EPO (passage n+53), and centrifuged at 580g for 5 minutes. Serial dilutions of virus in phosphate buffer pH 5.7, containing $1x10^8$, $1x10^{7.5}$, $1x10^7$, $1x10^{6.5}$, $1x10^6$ and $1x10^{5.5}$ IU/ml were prepared. For each cell line, six of the cell pellets were resuspended in 30µl of the corresponding virus dilution while the remaining cell pellet was inoculated with phosphate buffer pH 5.7 only. After 2 hours incubation at 4°C, the cells were washed twice with PBS-A and seeded in 1ml of the corresponding medium. The 24-well plate was placed at 37°C. Two days later, isolation of mRNA from whole cells was done using the Oligotex direct mRNA kit (Qiagen). Extracted mRNAs were used as templates in a multiplex RT-PCR assay with actin primers and the B19-specific primer pair B19-6 and B19-9. The amplification conditions were1 cycle at 50°C for 30

minutes, 1 cycle at 94°C for 15 minutes, 43 cycles of 94°C for 45 seconds, 55°C for 45 seconds and 72°C for 2 minutes and finally 1 cycle at 72°C for 5 minutes.

Figure 3.40 shows that B19-specific mRNA transcripts were present in all samples inoculated with the virus. All three cell lines displayed similar results, although KU812 cell line seemed slightly better than the other two cell lines because both bands of 155bp and 275bp were present in all samples inoculated with parvovirus B19.

Since KU812Ep6 cells were derived from KU812 cell line, these two cell lines were compared in the following experiment using higher virus dilutions.

Figure 3.40: Analysis of mRNA products in various cell lines amplified with B19-6 and B19-9

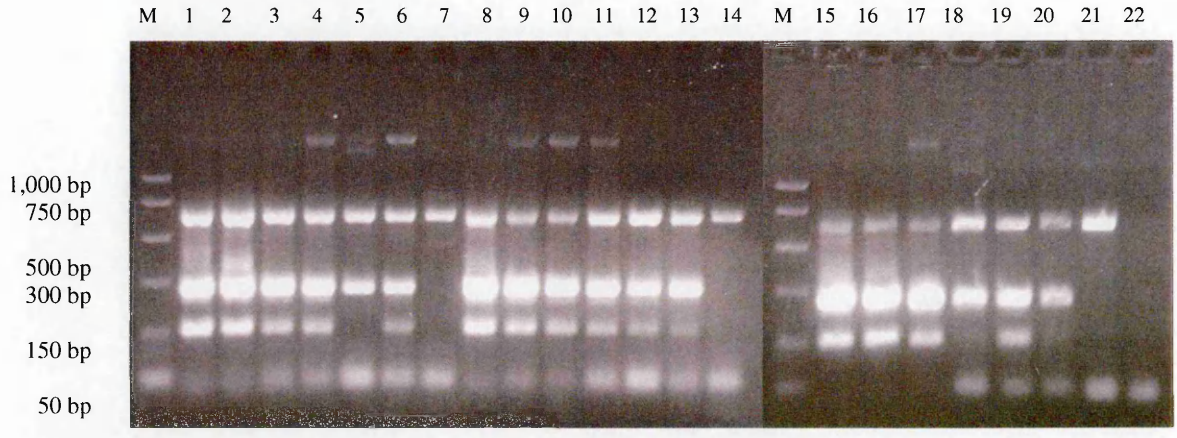

Lane M. PCR markers

Lanes 1 to 7: KU812Ep6 cells

1. $1x10^{8}$ IU/ml inoculum
2. $1x10^{7.5}$ IU/ml inoculum
3. $1x10^{7}$ IU/ml inoculum
4. $1x10^{6.5}$ IU/ml inoculum
5. $1x10^{6}$ IU/ml inoculum
6. $1x10^{5.5}$ IU/ml inoculum
7. Phosphate buffer pH 5.7

Lanes 8 to 14: KU812 cells

8. $1x10^{8}$ IU/ml inoculum
9. $1x10^{7.5}$ IU/ml inoculum
10. $1x10^{7}$ IU/ml inoculum
11. $1x10^{6.5}$ IU/ml inoculum
12. $1x10^{6}$ IU/ml inoculum
13. $1x10^{5.5}$ IU/ml inoculum
14. Phosphate buffer pH 5.7

Lanes 15 to 21: UT-7/EPO cell

15. $1x10^{8}$ IU/ml inoculum
16. $1x10^{7.5}$ IU/ml inoculum
17. $1x10^{7}$ IU/ml inoculum
18. $1x10^{6.5}$ IU/ml inoculum
19. $1x10^{6}$ IU/ml inoculum
20. $1x10^{5.5}$ IU/ml inoculum
21. Phosphate buffer pH 5.7
22. RNAase-free water

III.4.4.4.2. B19 infectivity assay using KU812 and KU812Ep6 cell lines

This experiment was done in order to investigate the relative sensitivities of the KU812 (passage n+70) and KU812Ep6 (passage n+56) cell lines to infection with B19. The protocol described above was followed using lower virus dilutions (in phosphate buffer pH 5.7) for inoculation of the cells. Cells were thus inoculated with dilutions of the B19 stock virus containing $1x10^7$, $1x10^6$, $1x10^5$, $1x10^4$, $1x10^3$, $1x10^2$, $1x10^1$ and $1x10^0$ IU/ml. A negative control with buffer only was also included for both cell lines. Isolation of mRNA from whole cells was done using the Oligotex direct mRNA kit (Qiagen). Extracted mRNAs were used as templates in a multiplex RT-PCR assay with actin primers and the B19 primer pair B19-6 and B19-9. The amplification conditions were the same as in the previous experiment (section III.4.4.4.1).

The results of nucleic acids amplification are shown on figure 3.41.

The housekeeping gene actin was present in samples 1 to 18, suggesting that mRNA had been extracted in all samples tested. Although there seemed to have been some non-specific bands in some samples using KU812Ep6 cells (samples 2, 3 and 4), the last sample that showed amplification of B19-specific transcripts was sample 5, which had been inoculated with a dilution of the stock virus containing $1x10^3$ IU/ml. However, only the 275bp band was detected in samples 1, 3 and 5, while no B19 transcripts were amplified in sample 4 (inoculated with $1x10^4$ IU/ml). This could have been due to the Poisson distribution. In comparison, when cells KU812 were used in the infectivity assay, the last sample that showed amplification of B19-specific transcripts was sample 11, inoculated with $1x10^6$ IU/ml. Therefore, in this particular study, B19 infectivity assay was able to detect $\log_{10}$ 3 more infectious virus units per ml with KU812Ep6 cells than with the parent cell line KU812. This was in contrast to the previous experiment,

which had found KU812 to be more permissive for B19 infection than KU812Ep6 or UT-7/EPO cell lines. However, since lower virus titres were used to infect the cells in the present experiment, the variation in sensitivity between the cell lines might have been due to the Poisson distribution of virus at limiting dilutions.

Figure 3.41: Analysis of mRNA products in KU812 and KU812Ep6 cell lines amplified with B19-6 and B19-9

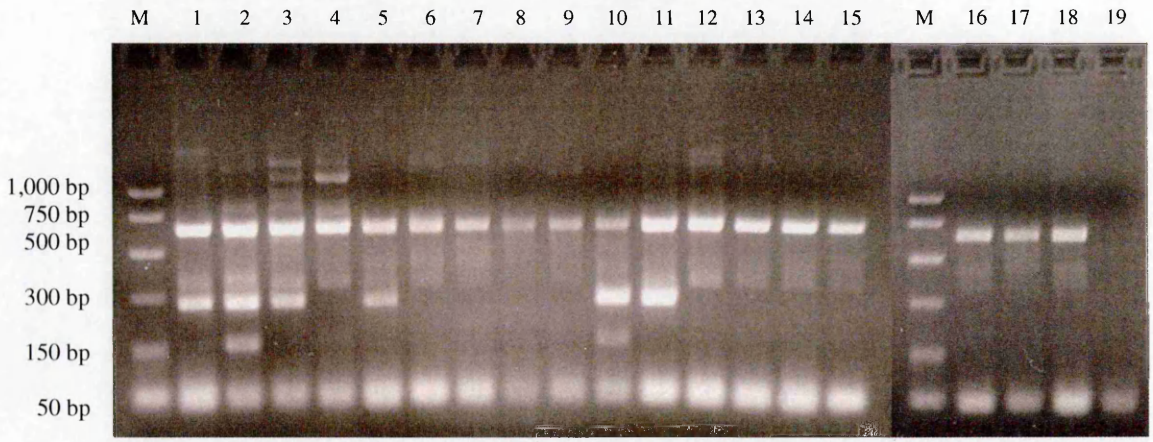

Lane M. PCR markers

Lanes 1 to 9: KU812Ep6 cells

1. $1x10^7$ IU/ml inoculum
2. $1x10^6$ IU/ml inoculum
3. $1x10^5$ IU/ml inoculum
4. $1x10^4$ IU/ml inoculum
5. $1x10^3$ IU/ml inoculum
6. $1x10^2$ IU/ml inoculum
7. $1x10^1$ IU/ml inoculum
8. $1x10^0$ IU/ml inoculum
9. Phosphate buffer pH 5.7

Lanes 10 to 18: KU812 cell

10. $1x10^7$ IU/ml inoculum
11. $1x10^6$ IU/ml inoculum
12. $1x10^5$ IU/ml inoculum
13. $1x10^4$ IU/ml inoculum
14. $1x10^3$ IU/ml inoculum
15. $1x10^2$ IU/ml inoculum
16. $1x10^1$ IU/ml inoculum
17. $1x10^0$ IU/ml inoculum
18. Phosphate buffer pH 5.7
19. RNAase-free water

III.4.4.4.3. Cell synchronisation

The aim of this experiment was to determine whether cells synchronised in S phase were more susceptible to B19 infection. Three cell lines: KU812 (passage n+73), KU812Ep6 (passage n+59) and UT-7/EPO (passage n+58) were treated with hydroxyurea, which is a drug that inhibits ribonucleotide reductase and arrests the cell cycle at the G1/S boundary or in the S phase, depending upon the hydroxyurea concentration, the time of exposure and the type of cells.

For each cell line, 10^6 cells were counted and pelleted by centrifugation at 580g for 5 minutes. The cells were resuspended in 10ml of the appropriate cell culture medium containing 1mM hydroxyurea (without antibiotics or fungizone), placed in a $25mm^3$ flask and incubated at 37°C (5% CO_2) for 36 to 40 hours. The cell suspensions were centrifuged for 5 minutes at 670g and washed twice in 5ml of the appropriate cell culture medium without FCS, prewarmed at 37°C. A cell count was performed after the second wash in order to establish the volume of cell suspension to be used for infection ($2x10^5$ cells/sample). Six samples, including five inoculated with serial dilutions of the B19 stock virus and one inoculated with phosphate buffer at pH 5.7, were prepared for each cell line. Serial dilutions of the virus stock containing $1x10^7$, $1x10^6$, $1x10^5$, $1x10^4$ and $1x10^3$ IU/ml were prepared in phosphate buffer pH 5.7. The cell pellets were resuspended in 30µl of the appropriate virus dilution or 30µl of buffer only (negative control). After 2 hours incubation at 4°C, the cells were washed twice with 200µl of PBS-A, resuspended in 1ml of the appropriate fresh cell culture medium and seeded into a 24-well plate. The latter was incubated at 37°C for 2 days (5% CO_2). The cells were harvested two days post-infection and poly A^+ RNA was extracted from whole cells using the Oligotex direct mRNA kit (Qiagen). Isolated mRNA was used as template in a multiplex RT-PCR assay using actin-specific primers (actin-3 and actin-4; 2.5pmol/µl)

and B19-specific primers (B19-9 and B19-6; 25pmol/µl). The amplification conditions were 1 cycle at 50°C for 30 minutes, 1 cycle at 94°C for 15 minutes, 43 cycles of 94°C for 45 seconds, 55°C for 45 seconds and 72°C for 2 minutes and finally 1 cycle at 72°C for 10 minutes.

The results are shown on figure 3.42. Actin-specific transcripts were present in all samples except sample 14, which had been lost during mRNA extraction. As expected, all three negative controls (samples 6, 12 and 19) did not show any B19-specific bands. Both B19-specific transcripts were still detected in KU812Ep6 cells inoculated with $1x10^4$ IU/ml (sample 4). However, no amplification of B19-specific transcripts was detected in sample 3, which could be due to the Poisson distribution at limiting dilutions.

In KU812 cells, although no amplification was detected in sample 7, faint B19-specific bands could be seen in sample 8, where cells had been inoculated with $1x10^6$ IU/ml.

In UT-7/EPO cells, the total lack of amplification of B19-specific mRNA transcripts suggested that the cells did not support B19 replication. However, B19-specific transcripts had previously been detected in those cells using the same infectivity assay. The second hypothesis was that the treatment with hydroxyurea might not have had the expected effect on the cells and possibly have interfered with cell growth of susceptibility to B19 infection. However, the parent cell line UT-7 had previously been reported to support the replication of B19 following treatment with hydroxyurea (Shimomura *et al.*, 1993). Lastly, the fact that the actin-specific band was faint in all UT-7/EPO samples suggested that less mRNA was isolated from these cells compared with other cell lines. Thus, this experiment suggested that the best infectivity results after cell synchronisation were obtained with KU812Ep6 cell line.

Figure 3.42: Analysis of mRNA products in various cell lines treated with hydroxyurea and amplified with B19-6 and B19-9

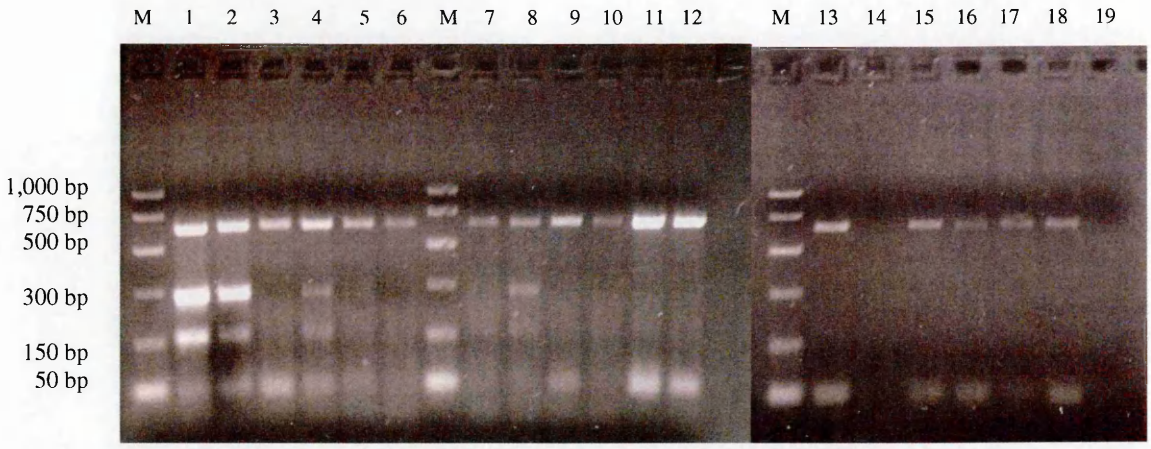

Lane M. PCR markers

Lanes 1 to 6: KU812Ep6 cells	**Lanes 7 to 12: KU812 cells**
1. $1x10^7$ IU/ml inoculum	7. $1x10^7$ IU/ml inoculum
2. $1x10^6$ IU/ml inoculum	8. $1x10^6$ IU/ml inoculum
3. $1x10^5$ IU/ml inoculum	9. $1x10^5$ IU/ml inoculum
4. $1x10^4$ IU/ml inoculum	10. $1x10^4$ IU/ml inoculum
5. $1x10^3$ IU/ml inoculum	11. $1x10^3$ IU/ml inoculum
6. Phosphate buffer pH 5.7	12. Phosphate buffer pH 5.7

Lanes 13 to 19: UT-7/EPO cell

13. $1x10^7$ IU/ml inoculum
14. $1x10^6$ IU/ml inoculum (sample lost during extraction)
15. $1x10^5$ IU/ml inoculum
16. $1x10^4$ IU/ml inoculum
17. $1x10^3$ IU/ml inoculum
18. Phosphate buffer pH 5.7
19. RNAase-free water

When compared to non-synchronised cells, the results of the infectivity assay were similar for the KU812 cell line whereas the detection of B19 transcripts was $\log_{10}$ 1 higher with non-synchronised KU812Ep6 cells than with synchronised cells. As far as the UT-7/EPO cell line was concerned, the highest dilution detected was $1x10^{5.5}$ IU/ml

of the B19 stock virus when the cells were not synchronised whereas no amplification was detected after cell synchronisation.

Overall, it seemed that cell synchronisation did not significantly improve the permissibility of the cells to parvovirus B19 infection. In conclusion, the data obtained in this study comparing the three cell lines suggested that non synchronised KU812Ep6 cells were the best candidate for use in a B19 infectivity assay, in terms of permissiveness to B19 infection as well as in being able to support virus replication. However, due to confidentiality issues with the group from which the cells had been obtained, work was discontinued on this cell line. A new cell line, UT-7/EPO-S1, which had been reported to be more susceptible to B19 replication than the parental cell line, UT-7/EPO (Morita *et al.*, 2001), was obtained for evaluation in the B19 infectivity assay.

III.4.5. Optimisation of B19 infectivity assay using UT-7/EPO-S1 cells

The newly obtained cell line UT-7/EPO-S1 was investigated to determine whether it was able to support B19 replication and to assess its susceptibility to the virus compared to other cell lines previously studied. UT-7/EPO-S1 cells (passage n+4) were pelleted and washed once with phosphate buffer pH 5.7. Approximately $2x10^5$ cells were inoculated with either 30µl of buffer (negative control) or serial dilutions of the stock B19 virus, diluted in phosphate buffer pH 5.7, containing $1x10^9$, $1x10^8$, $1x10^7$, $1x10^6$, $1x10^5$, $1x10^4$ and $1x10^3$ IU/ml. After 2 hours incubation at 4°C, the cells were washed twice with 500µl of PBS-A. The cells were resuspended in 1ml of fresh medium and seeded in a 24-well plate placed at 37°C (5% CO_2). Two days post-infection, the cells were harvested and the mRNA isolated from the cell cytoplasm using the Oligotex direct mRNA kit (Qiagen). Nucleic acids amplification was done using the B19-specific

primers XPP2 and B19-9. The amplification conditions, which were used for all experiments using UT-7/EPO-S1 cells, were 1 cycle at 50°C for 30 minutes, 1 cycle at 95°C for 15 minutes, 43 cycles of 95°C for 45 seconds, 50°C for 40 seconds and 72°C for 40 seconds and finally 1 cycle at 72°C for 10 minutes.

Amplification of the housekeeping gene actin (not shown) confirmed successful isolation of mRNA from all cell samples. Figure 3.43 shows the amplified RT-PCR products on the agarose gel.

Figure 3.43: Analysis of mRNA products in UT-7/EPO-S1 cells amplified with XPP2 and B19-9

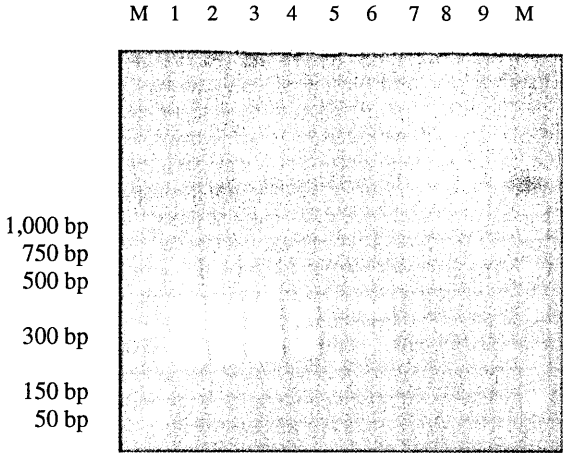

M PCR markers

1. $1x10^9$ IU/ml inoculum
2. $1x10^8$ IU/ml inoculum
3. $1x10^7$ IU/ml inoculum
4. $1x10^6$ IU/ml inoculum
5. $1x10^5$ IU/ml inoculum
6. $1x10^4$ IU/ml inoculum
7. $1x10^3$ IU/ml inoculum
8. Phosphate buffer pH 5.7
9. RNAase-free water

The results indicated that the infectivity assay using UT-7/EPO-S1 cells was able to detect B19-specific mRNA transcripts in cells inoculated with $1x10^4$ IU/ml (sample 6). The absence of B19 transcripts amplification in sample 5, which had been inoculated

with $1x10^5$ IU/ml of virus, might have been due to the Poisson distribution. Therefore, this preliminary study indicated that this new cell line was able to support B19 replication and also appeared to be slightly more susceptible to B19 infection, i.e. more permissive, than the parent cell line, UT-7/EPO. A comparison of the infectivity results with the UT-7/EPO-S1 cells with results previously obtained with KU812Ep6 cells suggested that the UT-7/EPO-S1 cell line would be a very good candidate cell line for the B19 infectivity assay. The following sections describe the optimisation of the assay using this new cell line.

III.4.5.1. Virus diluent buffer

In order to establish that phosphate buffer pH 5.7 was the optimum buffer for inoculation of the UT-7/EPO-S1 cell line as it was for the other cell lines studied, a further experiment was done to compare the sensitivity of this cell line to virus diluted in phosphate buffer pH 5.7 and cell culture medium without FCS. Cells (passage n+5) were prepared as above and inoculated with serial dilutions of the stock B19 virus, prepared in either phosphate buffer pH 5.7, or cell culture medium without FCS, containing $1x10^7$, $1x10^6$ and $1x10^5$ IU/ml. mRNA isolated from the cell cytoplasm using the Oligotex direct mRNA kit. Nucleic acids amplification was done using the B19-specific primers XPP2 and B19-9 and the conditions were as previously described (section III.4.5).

Figure 3.44 shows amplification of the nucleic acid extracted from UT-7/EPO-S1 cells.

Figure 3.44: Analysis of mRNA products in UT-7/EPO-S1 cells amplified with XPP2 and B19-9

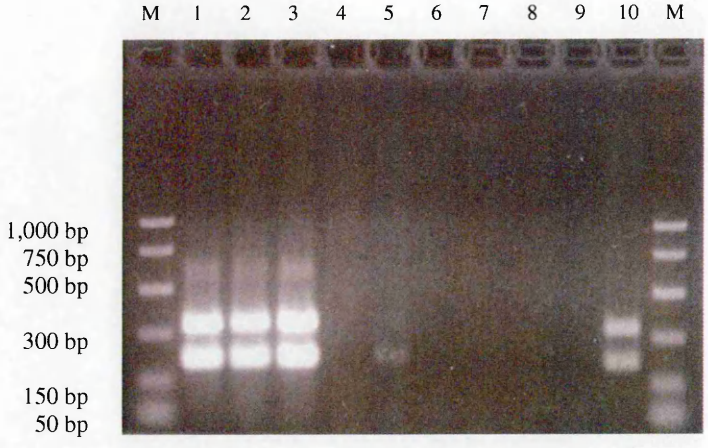

Lane M. PCR markers

Lanes 1 to 4: phosphate buffer pH 5.7

1. $1x10^7$ IU/ml inoculum
2. $1x10^6$ IU/ml inoculum
3. $1x10^5$ IU/ml inoculum
4. Phosphate buffer pH 5.7

Lanes 5 to 8: medium without FCS

5. $1x10^7$ IU/ml inoculum
6. $1x10^6$ IU/ml inoculum
7. $1x10^5$ IU/ml inoculum
8. Medium without FCS

Lanes 9 and 10: controls

9. RNAase-free water
10. RT-PCR positive control: $2x10^7$ IU/ml inoculum

Amplification of the housekeeping gene actin (non-shown) confirmed successful isolation of mRNA from all cell samples. The results shown on figure 3.44 indicated that, when phosphate buffer pH 5.7, was used as the virus diluent, the assay was able to detect at least $1x10^5$ IU/ml of virus (sample 3). The RT-PCR B19-specific bands were still very bright in the sample from cell inoculated with the highest dilution of virus, suggesting that an even higher dilution might be detected. In contrast, only a very faint band was seen in sample 5, which had been inoculated with a dilution of the stock virus containing $1x10^7$ IU/ml diluted in medium without FCS. This study clearly confirmed that B19 infection at low pH increased the cells susceptibility to the virus and phosphate

buffer pH 5.7 was therefore chosen as the virus diluent buffer for the B19 infectivity assay with UT-7/EPO-S1 cells.

III.4.5.2. Cell passage number

The two experiments in this section investigated the influence of the cell passage number on the susceptibility of UT-7/EPO-S1 cells to infection with B19. The first experiment studied cells, at passage n+5 and n+45, inoculated with serial dilutions of the B19 stock virus, diluted in phosphate buffer pH 5.7, containing $1x10^{6.5}$, $1x10^{6}$, $1x10^{5.5}$, $1x10^{5}$, $1x10^{4.5}$ and $1x10^{4}$ IU/ml. mRNA was isolated from the cell cytoplasm using the Oligotex direct mRNA kit (Qiagen) and amplified in a multiplex assay with actin-specific primers (actin-3 and actin-4; 5pmol/µl) and B19-specific primers (XPP2 and B19-9; 25pmol/µl). The amplification conditions were as previously described (section III.4.5).

The results comparing passage number n+5 and n+45 are shown on figure 3.45. The presence of a bright actin band in all samples confirmed that mRNA had been extracted successfully. The results showed that there was a $\log_{10}$ 1 difference between the results obtained with UT-7/EPO-S1 n+5 and n+45. The assay was able to detect $1x10^{6}$ IU/ml when passage n+5 was used (sample 2) whereas $1x10^{5}$ IU/ml were detected with passage n+45 (sample 11). This first experiment thus suggested that a late, rather than early, cell passage might improve the results of the B19 infectivity assay.

Figure 3.45: Analysis of mRNA products in UT-7/EPO-S1 cells (passages n+5 and n+45) amplified with XPP2 and B19-9

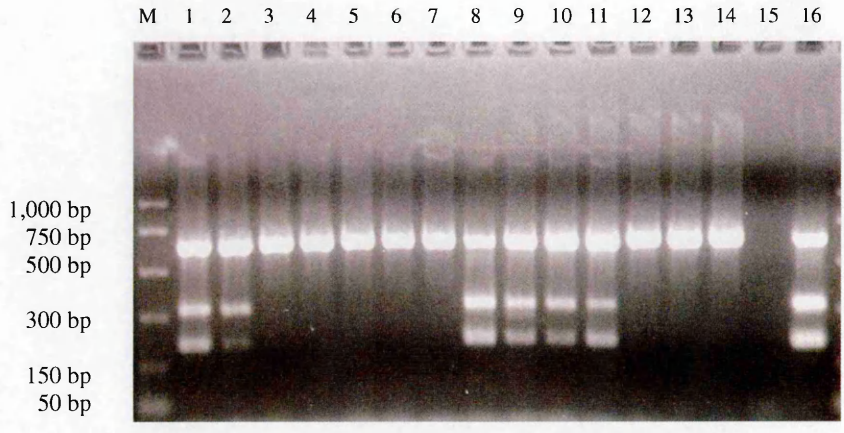

Lane M. PCR markers

Lanes 1 to 7: cell passage n+5	**Lanes 8 to 14: passage number n+45**
1. $1x10^{6.5}$ IU/ml inoculum	8. $1x10^{6.5}$ IU/ml inoculum
2. $1x10^{6}$ IU/ml inoculum	9. $1x10^{6}$ IU/ml inoculum
3. $1x10^{5.5}$ IU/ml inoculum	10. $1x10^{5.5}$ IU/ml inoculum
4. $1x10^{5}$ IU/ml inoculum	11. $1x10^{5}$ IU/ml inoculum
5. $1x10^{4.5}$ IU/ml inoculum	12. $1x10^{4.5}$ IU/ml inoculum
6. $1x10^{4}$ IU/ml inoculum	13. $1x10^{4}$ IU/ml inoculum
7. Phosphate buffer pH 5.7	14. Phosphate buffer pH 5.7

Lanes 15 and 16: controls

15. RNAase-free water

16. RT-PCR positive control: $1x10^{7}$ IU/ml inoculum

The above experiment was repeated using cells at passage number n+14 and n+53. The cells were inoculated with dilutions of the B19 stock virus, diluted in phosphate buffer pH 5.7, containing $1x10^{7}$, $1x10^{6.5}$, $1x10^{6}$, $1x10^{5.5}$, $1x10^{5}$, $1x10^{4.5}$ and $1x10^{4}$ IU/ml. The results are shown on figure 3.46.

Figure 3.46: Analysis of mRNA products in UT-7/EPO-S1 cells (passages n+14 and n+53) amplified with XPP2 and B19-9

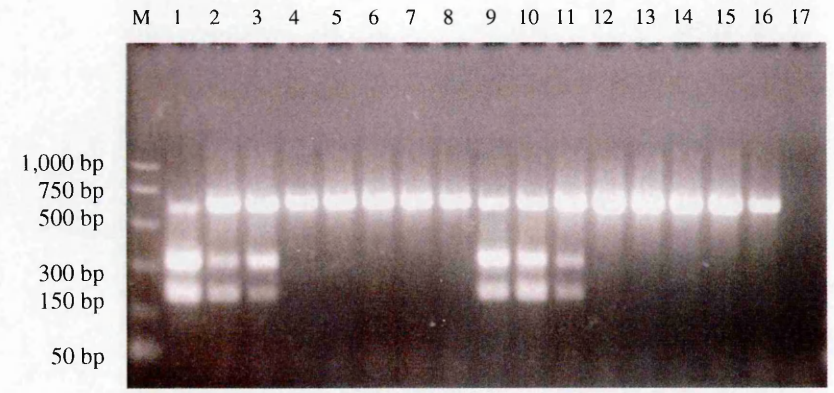

Lane M. PCR markers

Lanes 1 to 8: cell passage n+14	**Lanes 9 to 16: passage number n+53**
1. $1x10^{7}$ IU/ml inoculum	9. $1x10^{7}$ IU/ml inoculum
2. $1x10^{6.5}$ IU/ml inoculum	10. $1x10^{6.5}$ IU/ml inoculum
3. $1x10^{6}$ IU/ml inoculum	11. $1x10^{6}$ IU/ml inoculum
4. $1x10^{5.5}$ IU/ml inoculum	12. $1x10^{5.5}$ IU/ml inoculum
5. $1x10^{5}$ IU/ml inoculum	13. $1x10^{5}$ IU/ml inoculum
6. $1x10^{4.5}$ IU/ml inoculum	14. $1x10^{4.5}$ IU/ml inoculum
7. $1x10^{4}$ IU/ml inoculum	15. $1x10^{4}$ IU/ml inoculum
8. Phosphate buffer pH 5.7	16. Phosphate buffer pH 5.7
	17. RNAase-free water

The amplification of the housekeeping gene, actin, suggested that the extraction of mRNA had been successful. Figure 3.46 also showed that the use of both cell passages n+14 and n+53 allowed the detection of $1x10^{6}$ IU/ml of virus (samples 3 and 11). When compared to the first experiment in this series, the data were similar to those obtained with cell passage n+5.

Therefore, the $\log_{10}$ 1 difference between passages n+5, n+14, n+53 and n+45 might have been insignificant and was probably due to detection variation from one experiment to another. It appeared that UT-7/EPO-S1 passage number did not have a significant impact on the outcome of the B19 infectivity assay.

III.4.5.3. Hypoxia studies

III.4.5.3.1. Growth curves

The cell line UT-7/EPO-S1 at passage n+16 was used at a starting concentration of $1x10^5$ cells/ml. Two 24-well plates were incubated at 37°C, one in a normal 20% oxygen atmosphere while the second was in an incubator with 3% oxygen. Every day and for 7 days, 100µl of trypan blue was added to 4 wells of each cell suspension dilution. The live cells (unstained) were counted using a haemacytometer in order to construct a growth curve. Table A2.15 in appendix 2 shows the cell concentrations calculated from the cell counts done everyday for 10 days and figure 3.47 is a plot of these values.

Figure 3.47: Growth curves of UT-7/EPO-S1 cell line (n+17) in a 20% and 3% oxygen atmosphere

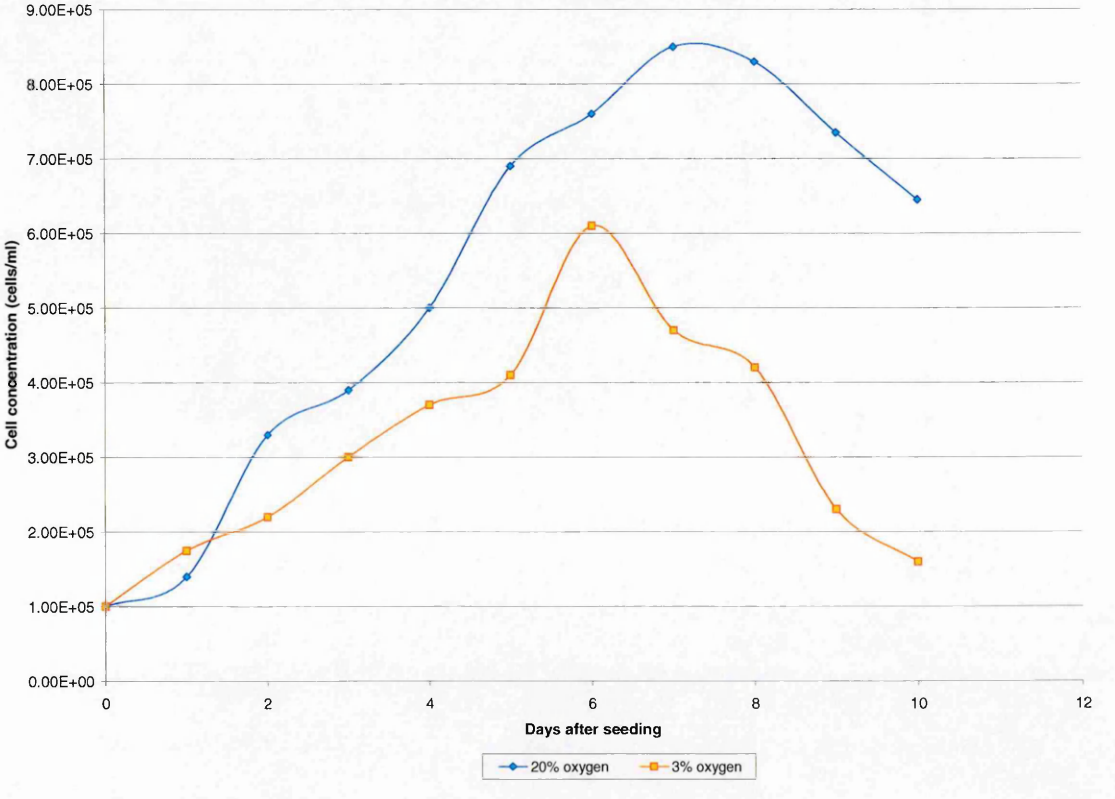

As expected, the cells grown in 3% oxygen showed a slower growth than those cultured in normal atmospheric conditions. However, the optimum time for cell harvest to provide the highest number of dividing cells for the B19 infectivity assay was 5 days after cell passage for both set of conditions.

III.4.5.3.2. Hypoxia conditions

The effect of hypoxia on the susceptibility of UT-7/EPO-S1 cells to B19 infection was investigated. Table 3.3 below shows the oxygen concentration at which the cells were incubated before infection with B19, as well as after B19 infection. Samples marked "A" were incubated in 20% oxygen both before and after inoculation with parvovirus while samples "B" were grown in 20% oxygen before infection and in 3% oxygen post-infection. Finally, samples labelled "C" were grown in a 3% oxygen atmosphere and were incubated in the same hypoxic conditions post-infection.

Table 3.3: Conditions and samples names for hypoxia study

Pre-infection oxygen	Post-infection oxygen	Time of harvesting	Name of samples
20%	20%	24 hours	A24-1 to 10
20%	20%	48 hours	A48-1 to 10
20%	20%	72 hours	A72-1 to 10
20%	3%	24 hours	B24-1 to 10
20%	3%	48 hours	B48-1 to 10
20%	3%	72 hours	B72-1 to 10
3%	3%	24 hours	C24-1 to 10
3%	3%	48 hours	C48-1 to 10
3%	3%	72 hours	C72-1 to 10

Ten samples for each harvest time i.e. 24, 48 and 72 hours (30 samples for A, 30 samples for B and 30 samples for C) were prepared with UT-7/EPO-S1 cells ($2x10^5$ cells per sample; passage n+17). Thirty microlitres of serial dilution of the B19 stock virus, prepared in phosphate buffer pH 5.7 and containing $1x10^8$, $1x10^{7.5}$, $1x10^7$, $1x10^{6.5}$, $1x10^6$, $1x10^{5.5}$, $1x10^5$, $1x10^{4.5}$ and $1x10^4$ IU/ml were used to inoculate the cells. One negative sample for A, B and C was inoculated with 30µl of buffer only. All samples were incubated at 4°C for 2 hours, washed twice with PBS-A and resuspended in 1ml of fresh medium. The cell suspensions were seeded in 24-well plates and cultured for 24 hours, 48 hours or 72 hours at 37°C (5% CO_2) with either 20% or 3% oxygen (table 2.3). Once harvested, the mRNA was extracted from cell cytoplasm using the Oligotex direct mRNA kit (Qiagen). Multiplex RT-PCR was performed using

primers specific for the housekeeping gene (actin-3 and actin-4; 5pmol/µl) and for parvovirus B19 (XPP2 and B19-9; 25pmol/µl). The amplification conditions were as previously described (section III.4.5).

The results of the hypoxia experiment are shown in table 3.4.

Table 3.4: Hypoxia experiment results

Pre- infection oxygen	Post- infection oxygen	Time of harvesting (hours)	Log_{10} infectious particles/ ml
20%	20%	24	<limit of detection
20%	20%	48	7
20%	20%	72	7
20%	3%	24	<limit of detection
20%	3%	48	7
20%	3%	72	7
3%	3%	24	<limit of detection
3%	3%	48	8
3%	3%	72	8

III.4.6. Quantification of B19 DNA by LightCycler system

III.4.6.1. $MgCl_2$ titration

The effects of $MgCl_2$ concentration on the efficiency of the PCR assay was investigated by testing increasing amounts of $MgCl_2$ from 1 to 5mM. The total reaction volume was 20µl, including 2µl of SYBR Green master mix, B19F and B19R primers at a final concentration of 0.5µM, $MgCl_2$ at a concentration optimum for the amplification of B19

DNA and nuclease-free water to give a final volume of 20µl. The PCR mix was loaded into glass capillaries, followed by the addition of 5µl of DNA template. The DNA samples used for this study were the B19 IS (99/800) and 1:10 and 1:100 of this standard. The B19 IS has an established concentration of 10^6 IU/ml. From the collaborative study used to establish this standard, 1IU is approximately equivalent to 0.6–0.8 genome equivalents (Saldanha *et al.*, 2002). The four steps of PCR amplification were 1 cycle at 95°C for 10 minutes (pre-incubation), 40 cycles of 20 seconds at 95°C, 30 seconds at 65°C (amplification) and 5 seconds at 80°C (fluorescent data collection), 1 cycle at 65°C for 15 seconds (melting), and a final cycle at 40°C for 30 seconds (cooling). The $MgCl_2$ concentration was titrated by testing increasing concentrations of 1, 2, 3, 4 and 5mM (0, 0.8, 1.6, 2.4 and 3.2µl, respectively) in order to optimise the DNA amplification reaction.

The results are shown on figure 3.48 and the concentrations of 1mM and 2mM $MgCl_2$ proved inadequate for an efficient DNA amplification. $MgCl_2$ concentrations from 3 to 5mM seemed to be optimum for this assay since the bands on the agarose gel were much neater and brighter than the lower concentrations.

Figure 3.48: Analysis of DNA products amplified by LightCycler for $MgCl_2$ titration

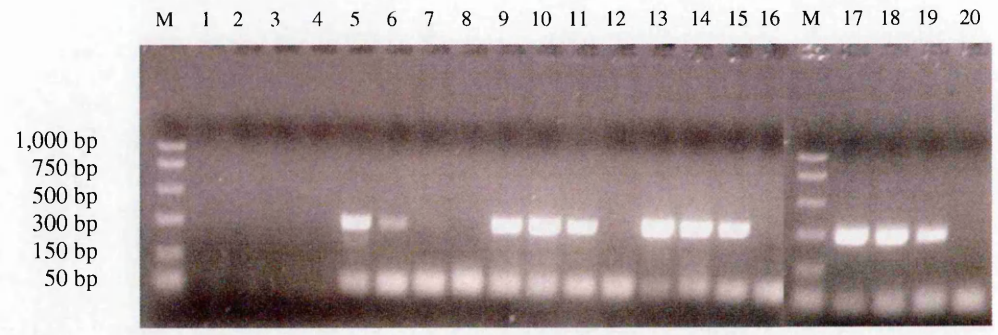

Lane M. PCR markers

Lanes 1 to 4: 1mM $MgCl_2$

1. B19 IS 10^6 IU/ml
2. B19 IS 10^5 IU/ml
3. B19 IS 10^4 IU/ml
4. Carrier tRNA (control)

Lanes 5 to 8: 2mM $MgCl_2$

5. B19 IS 10^6 IU/ml
6. B19 IS 10^5 IU/ml
7. B19 IS 10^4 IU/ml
8. Carrier tRNA (control)

Lanes 9 to 12: 3mM $MgCl_2$

9. B19 IS 10^6 IU/ml
10. B19 IS 10^5 IU/ml
11. B19 IS 10^4 IU/ml
12. Carrier tRNA (control)

Lanes 13 to 16: 4mM $MgCl_2$

13. B19 IS 10^6 IU/ml
14. B19 IS 10^5 IU/ml
15. B19 IS 10^4 IU/ml
16. Carrier tRNA (control)

Lanes 17 to 20: 5mM $MgCl_2$

17. B19 IS 10^6 IU/ml
18. B19 IS 10^5 IU/ml
19. B19 IS 10^4 IU/ml
20. Carrier tRNA (control)

III.4.6.2. Validation studies

The validation studies used the optimised conditions of nucleic acid extraction and DNA quantification. Therefore, QIAamp DNA blood mini kit (Qiagen) was used to extract total nucleic acid, which was in turn quantified by real-time PCR on the LightCycler instrument (Roche). The PCR kit used for this amplification was FastStart DNA Master SYBR Green I kit (Roche). The total reaction volume was 20µl, including

2µl of SYBR Green master mix, 0.5µl of each primers (B19F and B19R) at the working concentration of 20pmol/µl (10pmol per reaction), $MgCl_2$ at the optimum concentration of 5mM (3.2µl), 8.8µl of nuclease-free water and 5µl of template. The conditions for amplification were 1 cycle at 95°C for 10 minutes, 40 cycles of 20 seconds at 95°C, 30 seconds at 65°C and 5 seconds at 80°C, 1 cycle at 65°C for 15 seconds, and a final cycle at 40°C for 30 seconds.

III.4.6.2.1. B19 DNA Standard curve

Two studies were performed to establish the validity of the B19 standard curve. Firstly, in order to determine the limit of quantitation of the assay, serial dilutions of the B19 IS DNA were prepared as follows: neat (10^6 IU/ml), 1:10 dilution (10^5 IU/ml), 1:10^2 dilution (10^4 IU/ml), 1:10^3 dilution (10^3 IU/ml), 1:10^4 dilution (10^2 IU/ml), 1:10^5 dilution (10 IU/ml) and 1:10^6 dilution (1 IU/ml). Two negative controls were added to each of the four runs, namely RNAase-free water and B19 negative plasma. The B19 IS DNA samples and the B19 negative plasma samples used in this first study had been extracted on different days. The PCR kit used was the FastStart DNA Master SYBR Green I (Roche Diagnostics) and the primers were B19F and B19R. A standard curve was then constructed using the LightCycler software. All PCR products were visualised on a 2% agarose gel.

In all four runs, although the LightCycler computer program calculated a value for the "B19 DNA concentration" below 1x10^3 IU/ml, this value corresponded to a fluorescence generated by the formation of primer dimers and was therefore not specific for B19. In order to confirm this, both melting peaks (figures 3.49, 3.50 and 3.51) and agarose gels (figure 3.52) were examined. Taking into account all four runs, the melting temperature of the IS DNA samples ranging from 10^6 to 10^3 IU/ml was between 84.4

and 85°C (figure 3.49, from run 2). As shown on figure 3.50, the 1:10^4 dilution of the IS ($1x10^2$ IU/ml) in run 2 presented two melting peaks: a large one at a melting temperature of 79.94°C and a smaller one at a melting temperature of 84.57°C. Although the latter temperature was within the range specific for B19 DNA, the fluorescence measured was mainly generated by primer dimers. The latter have a melting temperature between 79.9 and 80.5°C. Primer dimers could also be seen on the agarose gels for this particular sample (50bp band), while a faint band specific for B19 was still visible in 3 of 4 runs. This sample was therefore considered below the limit of quantitation. Even higher dilutions of the standard (10 and 1IU/ml), as well as the negative controls (water and negative plasma), also showed two melting peaks but the smaller one was not specific for B19 DNA since the melting temperature was lower than 84°C. In conclusion, all calculated values lower than $1x10^3$ IU/ml were considered negative for B19 DNA.

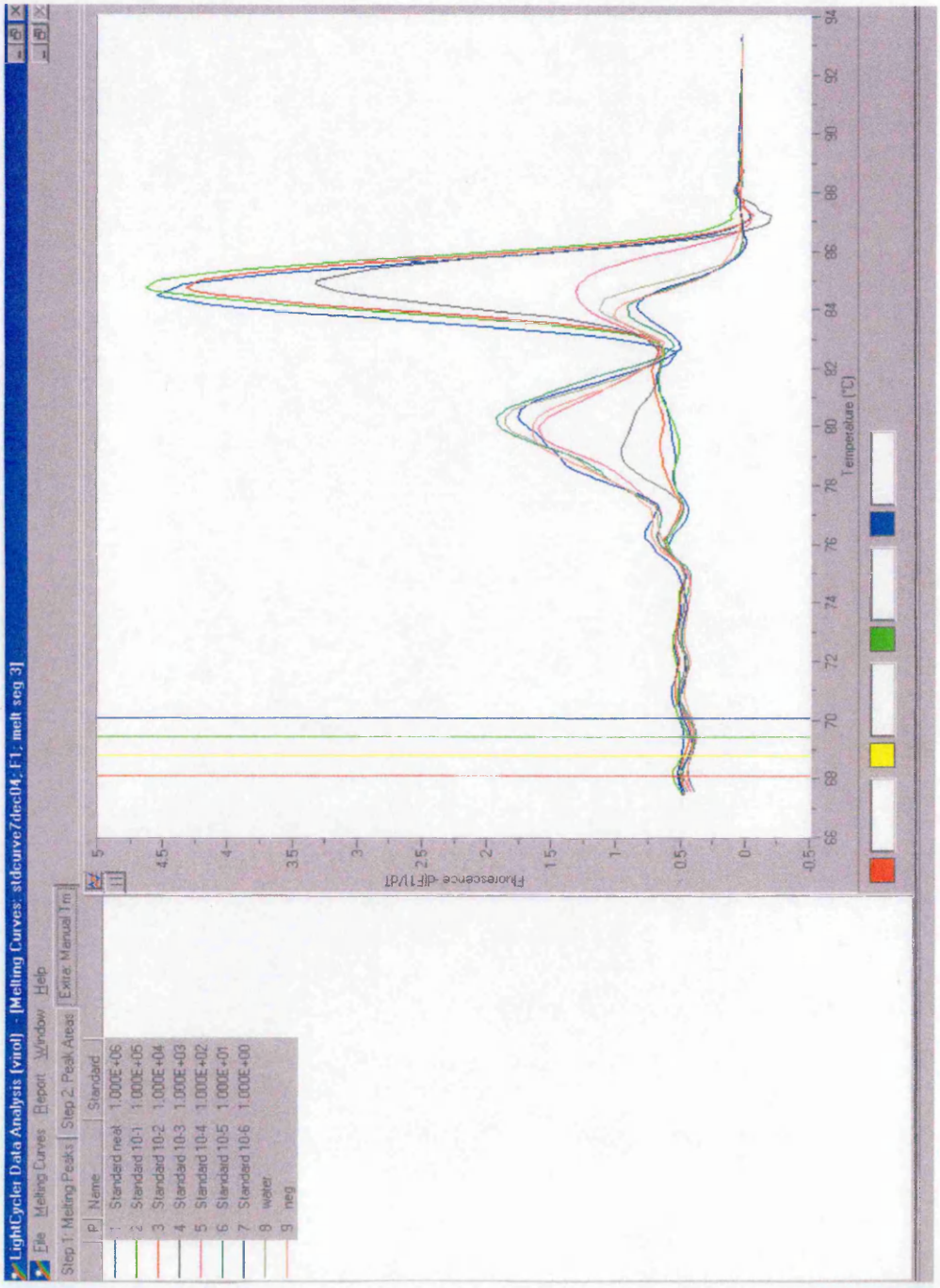

Figure 3.49: Melting peaks of the standard curve samples

Figure 3.50: Melting peaks of the 1:10^4 dilution of the International Standard ($1x10^2$ IU/ml)

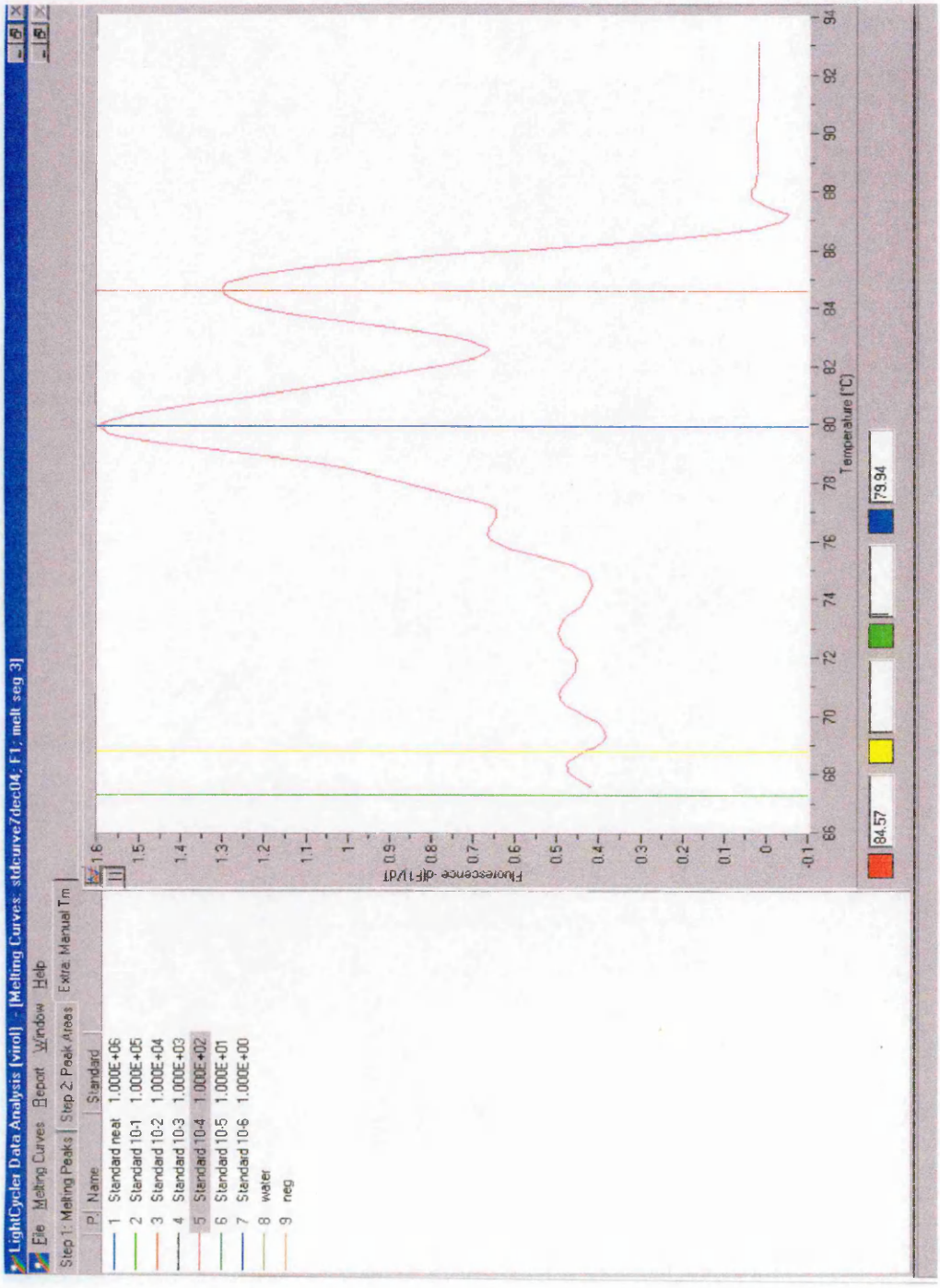

Figure 3.51: Melting peaks of the negative plasma sample

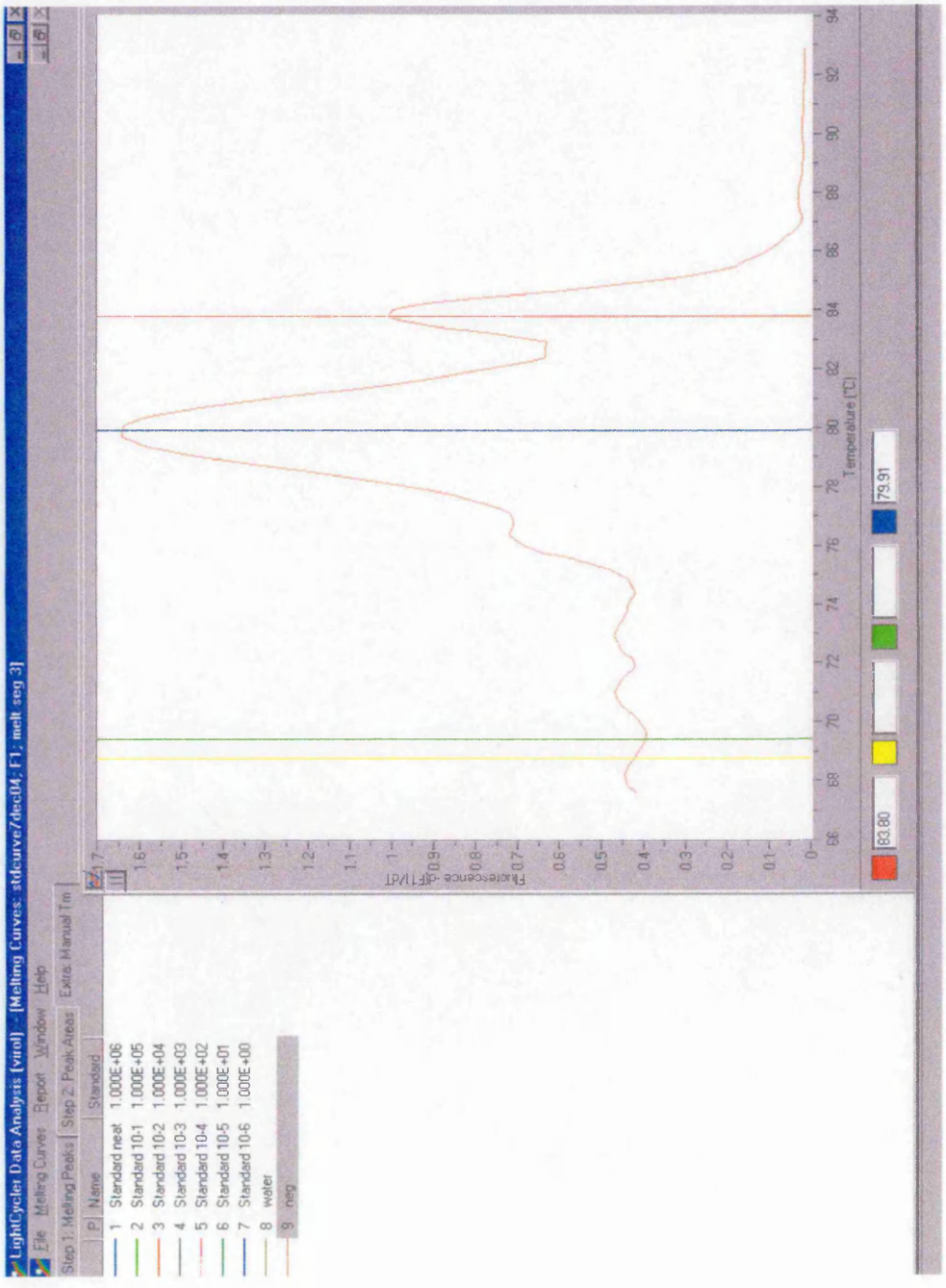

Figure 3.52: Analysis of PCR products for the 1st validation study

(A)

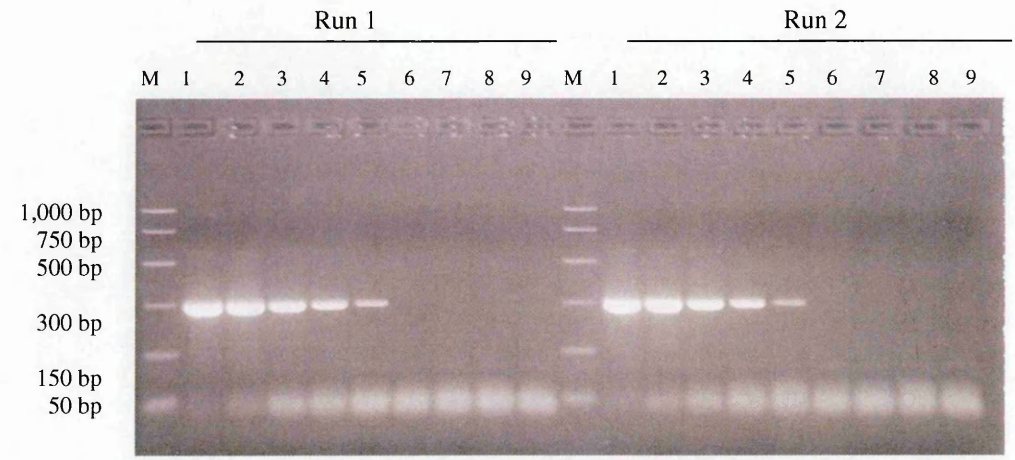

(B)

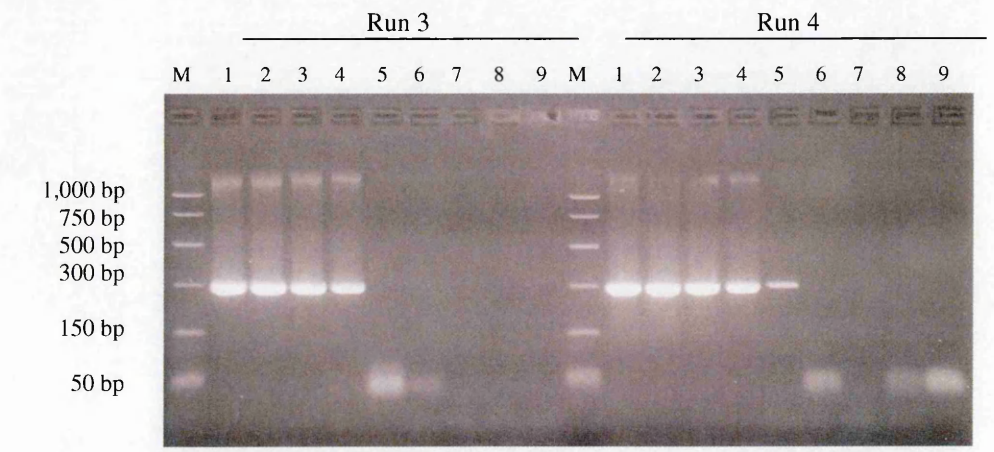

Lane M. PCR markers

Lanes 1 to 7: B19 IS DNA

1. B19 IS neat (10^6 IU/ml)
2. B19 IS 10^{-1} (10^5 IU/ml)
3. B19 IS 10^{-2} (10^4 IU/ml)
4. B19 IS 10^{-3} (10^3 IU/ml)
5. B19 IS 10^{-4} (10^2 IU/ml)
6. B19 IS 10^{-5} (10 IU/ml)
7. B19 IS 10^{-6} (1 IU/ml)

Lanes 8 and 9: Controls

8. PCR negative control: RNAase-free water
9. B19 negative plasma

In a second validation study, standard curves set up in 7 different amplification runs were statistically analysed in order to evaluate the linearity of the standard curve. The virus concentrations ranged was from 10^6 to 10^3 IU/ml. The results of the expected values and the calculated values obtained for 7 standard curves from 7 different assays are shown in table 3.5 ($\log_{10}$ values). Statistical analysis was kindly done by A. Heath (Department of Informatics, NIBSC; see section II.2.7.1) and the results are shown in table 3.6.

Table 3.5: Validation results for B19 standard curve

Study number	Std 1 ($\log_{10}$ 6) $\log_{10}$ DNA concentration (IU/ml)	Std 2 ($\log_{10}$ 5) $\log_{10}$ DNA concentration (IU/ml)	Std 3 ($\log_{10}$ 4) $\log_{10}$ DNA concentration (IU/ml)	Std 4 ($\log_{10}$ 3) $\log_{10}$ DNA concentration (IU/ml)
1	6.029	5.073	3.764	3.132
2	6.029	5.073	3.764	3.132
3	6.059	4.929	3.962	3.048
4	6.016	4.966	4.016	2.726
5	6.029	4.941	4.029	2.307
6	6.024	4.951	4.024	2.709
7	5.951	5.022	4.100	2.925

Table 3.6: B19 standard curve statistics

Log_{10} DNA concentration (IU/ml)	Mean estimate	Standard deviation
6	6.020	0.033
5	4.994	0.062
4	3.951	0.134
3	2.854	0.298

This study examined the linearity of the standard curve over the range $\log_{10} 6$ to $\log_{10} 3$ IU/ml and the reproducibility of the curve. The mean estimates were very close to the expected concentrations at $\log_{10} 6$- $\log_{10} 4$, but were poor at $\log_{10} 3$ (Std 4), indicating a good linearity over most of the range. The standard deviations also showed excellent reproducibility at $\log_{10} 6$, but the reproducibility decreased as the concentrations got lower. Although the limit of detection might be 10^2 IU/ml, the first validation study suggested to chose $\log_{10} 3$ IU/ml as the lower limit of quantitation for this assay.

Overall, it was decided that the standard curve should include the following dilutions of the B19 IS DNA: neat (10^6 IU/ml), 1:10 dilution (10^5 IU/ml), 1:10^2 dilution (10^4 IU/ml), 1:10^3 dilution (10^3 IU/ml), as well as a negative sample (RNAase-free water). An example of such a curve is shown on figure 3.53, with the calculated efficiency and slope. According to the manufacturers' instructions, curves with a slope less than –3.33 were considered satisfactory.

Figure 3.53: Example of a standard curve established with the B19 IS generated on the LightCycler

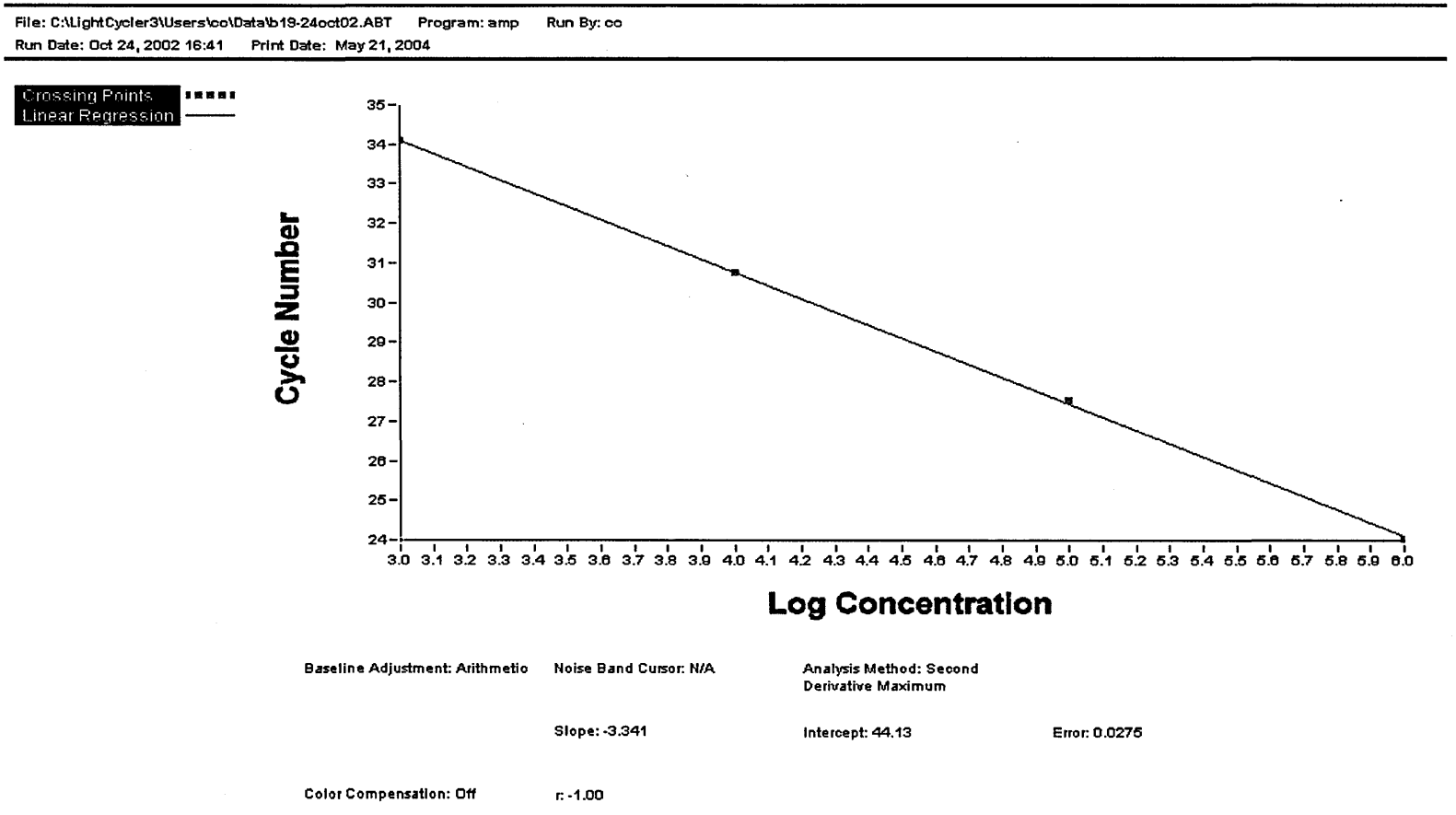

III.4.6.2.2. Study 1: validation of DNA extraction and amplification on the LightCycler

In order to study the reproducibility of the quantitative PCR assay, the first validation study included six DNA extractions done in 6 separate runs. The samples included one positive control (B19 IS neat), three negative controls (one anti-B19 antibody negative plasma, one anti-B19 antibody negative serum, one water control) and a test sample, which was a 1:10 dilution of the IS in water (10^5 IU/ml). The positive and negative controls for each run were first amplified by LightCycler PCR in order to check that there were no false positive/negative results. The test samples from each extraction run were amplified by LightCycler PCR in two separate LightCycler PCR runs on different days (days 1 and 2) with an expected B19 DNA titre of 10^5 IU/ml. B19 DNA titres were calculated using a standard curve obtained from serial dilutions of one B19 IS extracted in the first run and the results are shown in table 3.7.

Table 3.7: Results of validation study 1

DNA extraction run number	Log_{10} DNA concentration (IU/ml) day 1	Log_{10} DNA concentration (IU/ml) day 2
1	4.770	4.841
2	4.231	4.504
3	4.934	4.985
4	4.397	4.244
5	5.695	5.542
6	4.710	4.784

Statistical analysis, kindly performed by Alan Heath (Informatics Department, NIBSC) was based on the $\log_{10}$ titres. It was noted that the titres for extraction run 5 were considerably higher than for the other samples (about $\log_{10}$ 1). The overall mean of the $\log_{10}$ titres was $\log_{10}$ 4.804 IU/ml, again slightly lower than the anticipated $\log_{10}$ 5 IU/ml. This represents a geometric mean of 6.368×10^4 IU/ml.

The variability between extractions was assessed by calculating the mean $\log_{10}$ titre from the two repeat runs for each sample, and then calculating the standard deviation of the means across samples, which was 0.472. Therefore 95% of results from repeated extractions should fall approximately within +/- $\log_{10}$ 0.94 IU/ml. This figure was relatively high, and had been influenced by the high results for sample 5 noted above. However, it is possible that there may have been a dilution error with run 5. A 1:10 dilution is a required step. If this had been omitted, it may have accounted for the results for run 5, being 10-fold higher than for the other samples. The analysis was thus repeated omitting run 5. The overall mean of the $\log_{10}$ titre was $\log_{10}$ 4.641 IU/ml. This represented a geometric mean of 4.37×10^4 IU/ml. The standard deviation across samples was 0.282. Therefore 95% of results from repeated extractions should fall approximately within +/- $\log_{10}$ 0.56 IU/ml. This figure represents the overall expected variability in the test, including the extraction step, based on two replicate LightCycler runs.

III.4.6.2.3. Study 2: Validation of B19 LightCycler PCR

The second study included six repeat nucleic acid amplifications on different days of a sample from a single extraction in order to study the variability in the amplification step of the assay. B19 DNA was extracted from the IS (sample 1) and diluted in RNAase-free water 1:10 to make a stock B19 DNA solution containing 10^5 IU/ml for testing.

This test sample for the validation study was amplified by LightCycler PCR on 6 different days and the B19 DNA titre of the test sample (expected concentration 10^5 IU/ml) was calculated against a standard curve obtained from serial dilutions of the B19 IS, which was extracted in parallel with the test sample.

The overall mean of the six $\log_{10}$ titres was $\log_{10}$ 4.915 IU/ml, slightly lower than the anticipated $\log_{10}$ 5.0 IU/ml. This represents a geometric mean of 8.214×10^4 IU/ml. The standard deviation of the $\log_{10}$ titres was 0.092 i.e. 95% of individual results from repeat testing of this sample would be expected to fall within approximately two standard deviations of the mean i.e. +/- $\log_{10}$ 0.18 IU/ml. This gives a measure of the expected variability from the LightCycler PCR, independent of the extraction process.

III.4.6.3. Quantification of B19 samples used in this study

Three high titre B19 samples were used in this study; samples JS (B19 stock virus) and JB, which were obtained from Germany and sample LP, which was from the USA. B19 DNA was extracted from these samples in parallel with the B19 IS (10^6 IU/ml). Ten-fold serial dilutions from 10^{-1} to 10^{-8} of the samples were prepared in DNAse-free water. Ten-fold serial dilutions from 10^{-1} to 10^{-5} of the IS were also prepared. All samples were amplified in duplicate by real-time PCR on the LightCycler instrument. A standard curve was constructed from the dilutions of the IS and B19 DNA was quantified in the B19 samples by reading the results off this curve.

III.4.7. Optimisation of mRNA isolation

III.4.7.1. Time course experiments

The studies described in the following section were all aimed at finding the optimum time to harvest infected cells for maximum yield of B19 mRNA. The cell line used in

the first experiment was KU812Ep6 and infection was done using 100µl of either negative serum as the negative control or a 1:10 dilution of the B19 stock virus ($1x10^{11}$ IU/ml). Each well of a 24-well plate was seeded with $1.8x10^5$ cells. One well of both infected and uninfected cells was harvested on day 2, 3, 4, 5, 6, 7, 8, 9, 10, 12, 13, 14, 15, 16 and 21 post infection (15 samples). Fresh medium (1ml) was added to all remaining wells on day 14 since considerable evaporation of medium had occurred by this time. A cell count was done after each harvest in order to note any major difference in the cell number, which might have influenced the outcome of the mRNA extraction step. The harvested cells were centrifuged and frozen at -70°C until extracted all together. The mRNA isolation method used was the Nuclisens™ extraction of total nucleic acids. The RT-PCR step was performed separately for B19 (primers B19-6 and B19-9; 25pmol/µl) and actin genes (primers actin-3 and actin-4; 25pmol/µl). The RT-PCR conditions were similar for amplification using B19- and actin-specific primers: 1 cycle at 50°C for 30 minutes, 1 cycle at 94°C for 15 min, 43 cycles at 94°C for 45 seconds, 55°C for 45 seconds and at 72°C for 2 minutes and lastly, 1 cycle at 72°C for 5 minutes. The products were analysed on 2% agarose gels.

Table 3.8 shows the cell count performed after each harvest for both KU812Ep6 cells infected with a 1:10 dilution of the B19 stock virus ($1x10^{11}$ IU/ml) and uninfected cells. The cell counts suggested that there was no major difference over time for infected cells and negative controls. The number of surviving cells was lower after 21 and 16 days in culture for infected and uninfected cells, respectively. This phenomenon was expected because of natural cell death, even after addition of fresh medium on day 14 post-infection. When infected and uninfected cells were compared, there seemed to be fewer cells in the infected samples compared with the negative controls. This was also to be

expected since B19 virus would lyse and thus kill a proportion of the cells in the infected samples.

Table 3.8: Cell counts of infected and uninfected KU812Ep6 cells over time post-infection

Day post infection	Infected sample (cells/ml)	Negative sample (cells/ml)
0	1.8×10^5	1.8×10^5
3	3.4×10^5	5.3×10^5
4	5.2×10^5	6.7×10^5
5	7.3×10^5	7.8×10^5
6	6.6×10^5	7.5×10^5
7	4.1×10^5	7.6×10^5
8	4.3×10^5	8.4×10^5
9	2.4×10^5	7.3×10^5
10	2.8×10^5	8.5×10^5
12	2.7×10^5	3.9×10^5
13	4.7×10^5	5.2×10^5
14	4.3×10^5	6.3×10^5
15	4.4×10^5	7.9×10^5
16	4.5×10^5	4.7×10^5
21	1.8×10^5	4.8×10^5

mRNA was extracted from infected and uninfected cells and amplified, in separate assays, with actin primers and with B19-specific primers (primers B19-6 and B19-9), as shown on figure 3.54 (panels A and B, respectively).

Figure 3.54: Analysis of mRNA products extracted from KU812Ep6 cells

(A) Amplified with actin-specific primers

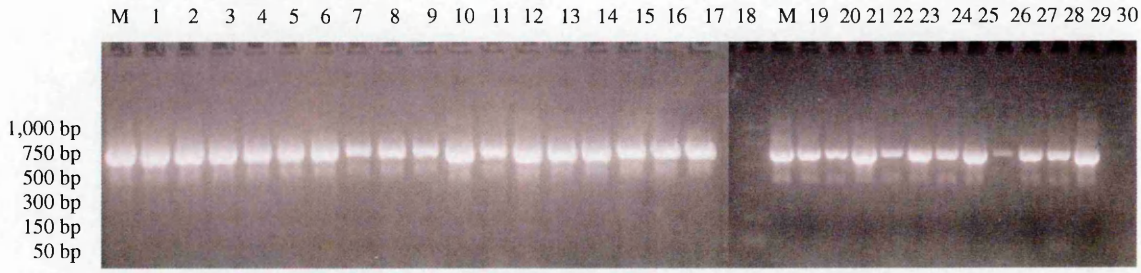

(B) Amplified with B19-specific primers

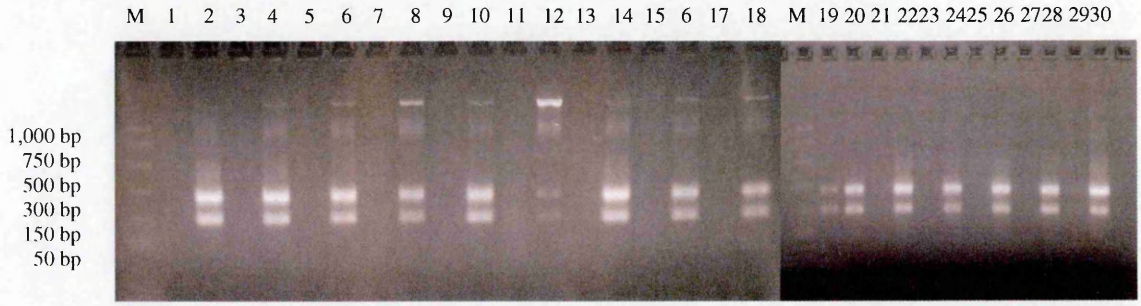

Lane M. PCR markers

1. Day 2, negative serum
2. Day 2, $1x10^{11}$ IU/ml inoculum
3. Day 3, negative serum
4. Day 3, $1x10^{11}$ IU/ml
5. Day 4, negative serum
6. Day 4, $1x10^{11}$ IU/ml inoculum
7. Day 5, negative serum
8. Day 5, $1x10^{11}$ IU/ml inoculum
9. Day 6, negative serum
10. Day 6, $1x10^{11}$ IU/ml inoculum
11. Day 7, negative serum
12. Day 7, $1x10^{11}$ IU/ml inoculum
13. Day 8, negative serum
14. Day 8, $1x10^{11}$ IU/ml inoculum
15. Day 9, negative serum
16. Day 9, $1x10^{11}$ IU/ml inoculum
17. Day 10, negative serum
18. Day 10, $1x10^{11}$ IU/ml inoculum
19. Day 12, negative serum
20. Day 12, $1x10^{11}$ IU/ml inoculum
21. Day 13, negative serum
22. Day 13, $1x10^{11}$ IU/ml inoculum
23. Day 14, negative serum
24. Day 14, $1x10^{11}$ IU/ml inoculum
25. Day 15, negative serum
26. Day 15, $1x10^{11}$ IU/ml inoculum
27. Day 16, negative serum
28. Day 16, $1x10^{11}$ IU/ml inoculum
29. Day 21, negative serum
30. Day 21, $1x10^{11}$ IU/ml inoculum

From the agarose gel analysis, the internal control was amplified and the band was bright in all extracted samples. This suggests that the mRNA isolation was successful and that the products amplified with B19-specific primers could be compared. The two RT-PCR products of 155bp and 275bp, which are characteristic of B19 mRNA transcripts with this primer pair, were present in all samples infected with parvovirus B19. These two bands were very bright over time, except on days 5, 6 and 7, when fainter bands were detected. The largest RT-PCR product (1,779bp), which could not always be detected, was also present in most infected samples up to day 10 post-infection. The negative control on day 12 post-infection (lane 19) showed specific B19 bands, which are most probably due to a contamination from the neighbouring well (infected sample, day 12, lane 20). In conclusion, this experiment indicated that cell harvesting could be done as early as 2 days post-infection and that B19 mRNA transcripts were still produced 21 days post-infection.

In order to investigate the time course of B19 infection in other cell lines, the second and third experiments used UT-7/EPO and KU812 cells, respectively. Since the first experiment showed that the cells begin to die after about 2 weeks in culture, studies 2 and 3 only investigated the presence of mRNA transcripts until 10 days post-infection. Moreover, unlike experiment 1, the cells were harvested from day 1 post-infection. The protocols for infection (inoculation with a 1:10 dilution of the B19 stock virus ($1x10^{11}$ IU/ml) or mock-infected with negative serum), harvest, cell count, mRNA extraction, RT-PCR and analysis on agarose gels were similar to those described for the first experiment. Tables 3.9 and 3.10 show the cell counts after each harvest of UT-7/EPO and KU812 cells, respectively cells. Extracted mRNA was amplified in separate assays,

with actin primers and B19-specific primers (B19-6 and B19-9), as displayed on figures 3.55 and 3.56, panels A and B, for UT-7/EPO and KU812 cells, respectively.

Table 3.9: Cell counts of infected and uninfected UT-7/EPO cells over time post-infection

Day post infection	Infected sample (cells/ml)	Negative sample (cells/ml)
0	2×10^5	2×10^5
1	1.8×10^5	2.8×10^5
2	3.5×10^5	4.9×10^5
3	3.1×10^5	4.7×10^5
4	3.5×10^5	5.5×10^5
5	4.6×10^5	7×10^5
6	4.4×10^5	8.7×10^5
7	4.2×10^5	1.2×10^5
8	6×10^5	1.4×10^5
9	5.1×10^5	3.7×10^5
10	6.8×10^5	1.9×10^6

No major difference in the cell count was noted either between infected and uninfected samples or over time. The RT-PCR step with actin primers showed that all samples were extracted successfully since a bright band on the agarose gel was seen in all samples.

Figure 3.55: Analysis of mRNA products extracted from UT-7/EPO cells

(A) Amplified with actin-specific primers

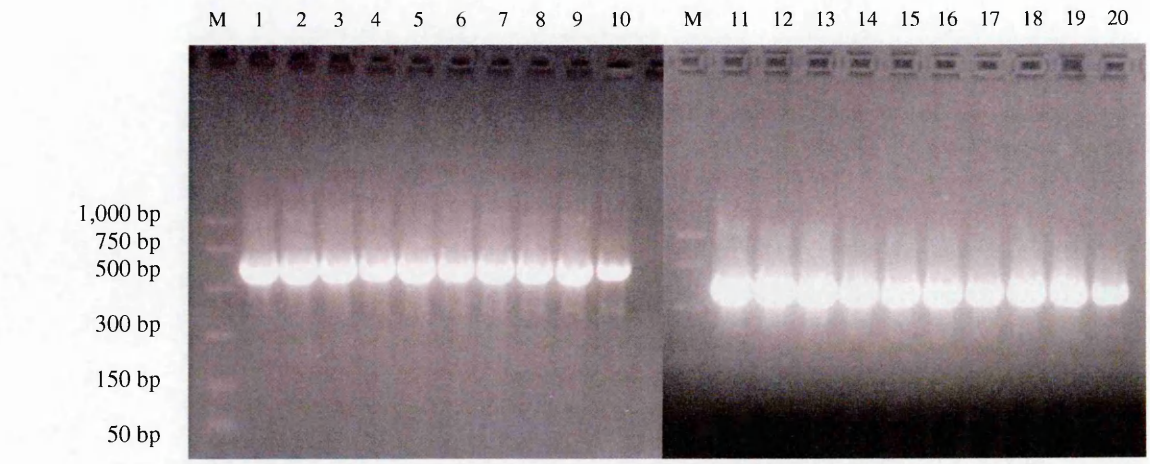

(B) Amplified with B19-specific primers

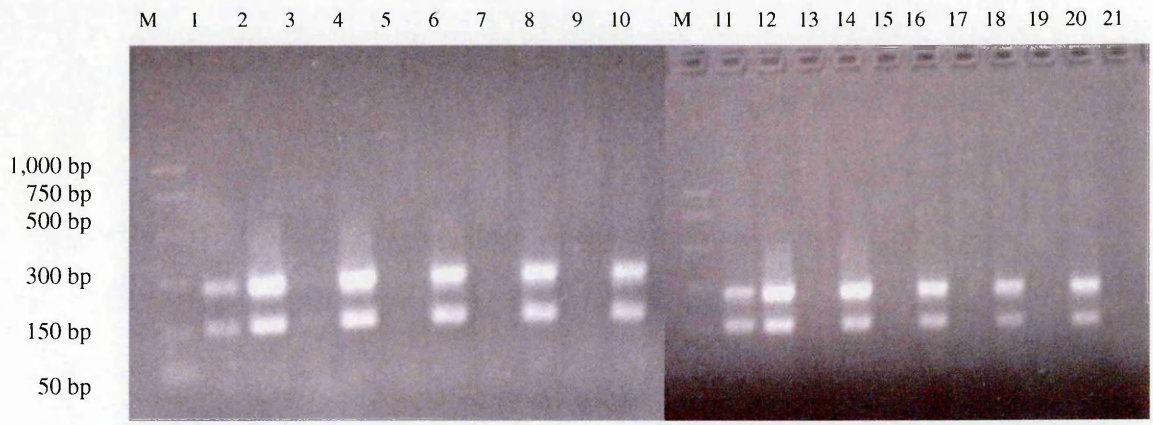

Lane M. PCR markers

1. Day 1, negative serum
2. Day 1, $1x10^{11}$ IU/ml inoculum
3. Day 2, negative serum
4. Day 2, $1x10^{11}$ IU/ml inoculum
5. Day 3, negative serum
6. Day 3, $1x10^{11}$ IU/ml inoculum
7. Day 4, negative serum
8. Day 4, $1x10^{11}$ IU/ml inoculum
9. Day 5, negative serum
10. Day 5, $1x10^{11}$ IU/ml inoculum
11. Day 6, negative serum
12. Day 6, $1x10^{11}$ IU/ml inoculum
13. Day 7, negative serum
14. Day 7, $1x10^{11}$ IU/ml inoculum
15. Day 8, negative serum
16. Day 8, $1x10^{11}$ IU/ml inoculum
17. Day 9, negative serum
18. Day 9, $1x10^{11}$ IU/ml inoculum
19. Day 10, negative serum
20. Day 10, $1x10^{11}$ IU/ml inoculum
21. RNAase-free water

As far as amplification with B19-specific primers was concerned, two negative samples (day 1, lane 1 and day 6, lane 11) showed two faint bands characteristic of RT-PCR products. This was due to overloading from the neighbouring wells. These B19-specific bands were present in all infected samples from days 1 to 10, with the brightest bands on days 1 and 2 post-infection. When compared with the results obtained with the KU812Ep6 cell line in the first experiment, the largest RT-PCR product (1,779bp) was not present on the gel. The fainter bands observed 7 days post-infection with KU812Ep6 cells were not seen with UT-7/EPO cells. There was no other variation between the two cell lines.

Table 3.10: Cell counts of infected and uninfected KU812 cells over time post-infection

Day post infection	Infected sample (cells/ml)	Negative sample (cells/ml)
0	2×10^5	2×10^5
1	2.9×10^5	2.5×10^5
2	2.9×10^5	4.2×10^5
3	3.2×10^5	2.7×10^5
4	1.9×10^5	3.5×10^5
5	2.3×10^5	3.2×10^5
6	2.2×10^5	3.8×10^5
7	2.7×10^5	3.3×10^5
8	2.6×10^5	4.3×10^5
9	2×10^5	2.3×10^5
10	3×10^5	4.1×10^6

Figure 3.56: Analysis of mRNA products extracted from KU812 cells

(A) Amplified with actin-specific primers

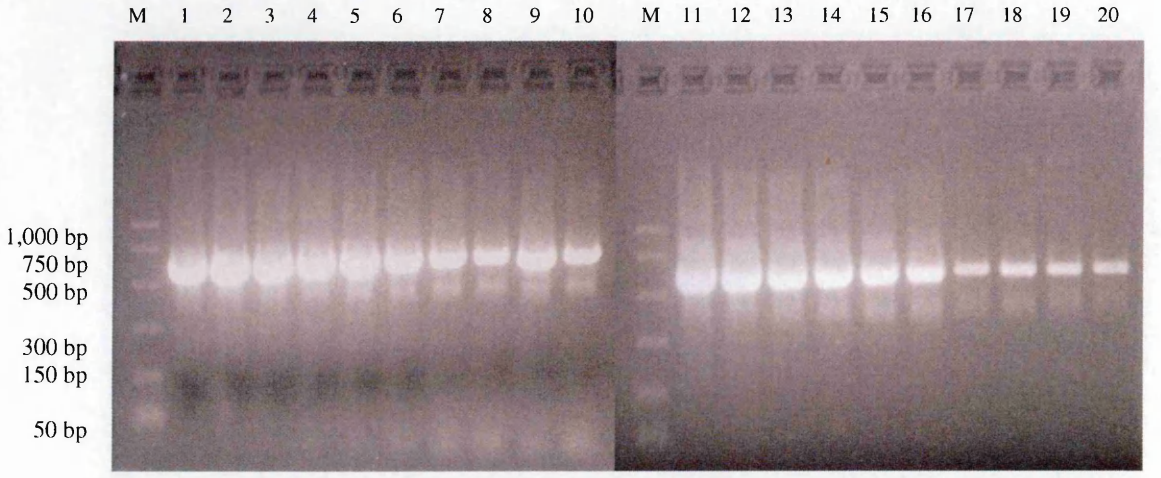

(B) Amplified with B19-specific primers

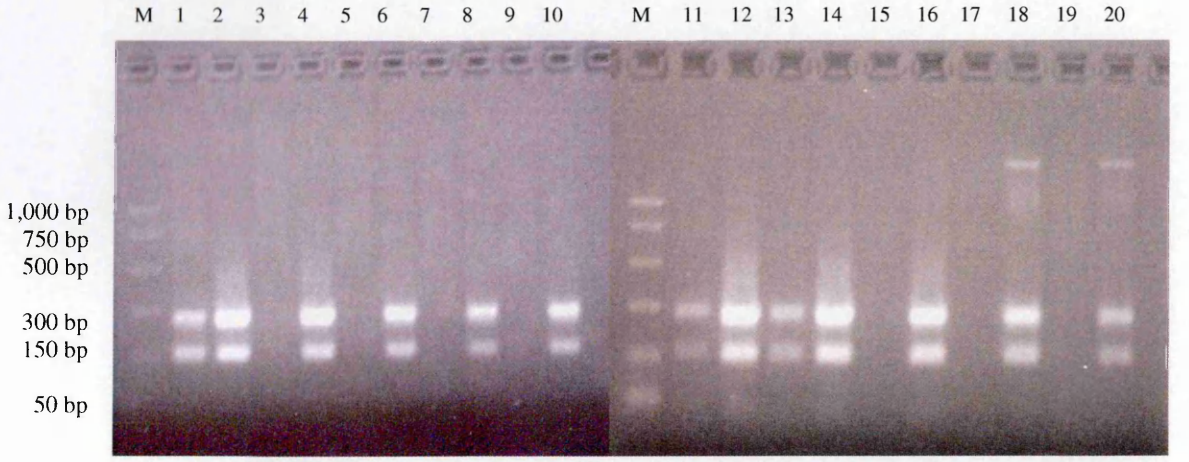

Lane M. PCR markers

1. Day 1, negative serum
2. Day 1, $1x10^{11}$ IU/ml inoculum
3. Day 2, negative serum
4. Day 2, $1x10^{11}$ IU/ml inoculum
5. Day 3, negative serum
6. Day 3, $1x10^{11}$ IU/ml inoculum
7. Day 4, negative serum
8. Day 4, $1x10^{11}$ IU/ml inoculum
9. Day 5, negative serum
10. Day 5, $1x10^{11}$ IU/ml inoculum
11. Day 6, negative serum
12. Day 6, $1x10^{11}$ IU/ml inoculum
13. Day 7, negative serum
14. Day 7, $1x10^{11}$ IU/ml inoculum
15. Day 8, negative serum
16. Day 8, $1x10^{11}$ IU/ml inoculum
17. Day 9, negative serum
18. Day 9, $1x10^{11}$ IU/ml inoculum
19. Day 10, negative serum
20. Day 10, $1x10^{11}$ IU/ml inoculum

As observed with the other two cell lines tested in the first and second experiments (KU812Ep6 and UT-7/EPO, respectively), the two B19-specific RT-PCR products of 155bp and 275bp were detected from days 1 to 10 post-infection in KU812 cells. Although the actin band was present in all samples extracted, it was weaker in lanes 17 to 20 (days 9 and 10), which suggested that a lower amount of mRNA was extracted. This could explain why the B19-specific bands from samples harvested on these days were weaker than the other samples in the studies. The other explanation for this phenomenon is that the non-specific amplification observed in these studies, may have reduced amplification of the B19 specific products. A number of uninfected samples (days 1, 6 and 7; lanes 1, 11 and 13, respectively) seemed to show faint B19-specific bands. This was most probably due to a contamination from the neighbouring wells during loading. Extra care during sample loading was therefore taken in subsequent experiments.

The fourth and last experiment in this series investigated the time course of the suspension cell line UT-7/EPO-S1 (passage n+22) focusing on days 2, 3 and 4 post-infection which had been shown in the previous experiments to be the optimum times for B19 mRNA expression. In addition to investigating the best time for cell harvest, this experiment used lower dilutions of the inoculum to study sensitivity. Infection was done with dilutions (in phosphate buffer pH 5.7) of the B19 stock virus containing $1x10^7$ IU/ml, $1x10^6$ IU/ml, $1x10^5$ IU/ml and $1x10^4$ IU/ml and the diluent as the negative sample. Unlike experiments 1 to 3, extraction was performed on freshly harvested cells using the Oligotex direct mRNA extraction method from cell cytoplasm, which was shown to be the best method for mRNA extraction (see section II.2.4.3). Since the cell count did not seem to differ between cell lines, infected and uninfected samples or over

time, these parameters were not investigated with the UT-7/EPO-S1 cell line. was performed using. The multiplex RT-PCR amplification conditions, using B19 primers (XPP-2 and B19-9; 25pmol/µl) and actin primers (2.5pmol/µl), were 1 cycle at 50°C for 30 minutes, 1 cycle at 95°C for 15 min, 43 cycles at 95°C for 45 seconds, 57°C for 40 seconds and at 72°C for 40 seconds and lastly, 1 cycle at 72°C for 10 minutes. The amplified products were analysed on a 2% agarose gel, which is shown below on figure 3.57.

Figure 3.57: Analysis of mRNA products extracted from UT-7/EPO-S1 cells amplified with XPP2 and B19-9

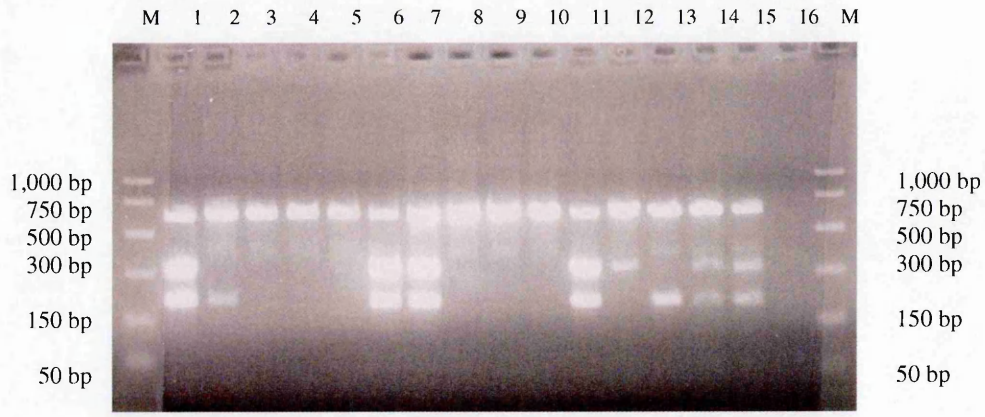

Lane M. PCR markers

1. Day 2, 1x10^7 IU/ml inoculum
2. Day 2, 1x10^6 IU/ml inoculum
3. Day 2, 1x10^5 IU/ml inoculum
4. Day 2, 1x10^4 IU/ml inoculum
5. Day 2, phosphate buffer pH 5.7
6. Day 3, 1x10^7 IU/ml inoculum
7. Day 3, 1x10^6 IU/ml inoculum
8. Day 3, 1x10^5 IU/ml inoculum
9. Day 3, 1x10^4 IU/ml inoculum
10. Day 3, phosphate buffer pH 5.7
11. Day 4, 1x10^7 IU/ml inoculum
12. Day 4, 1x10^6 IU/ml inoculum
13. Day 4, 1x10^5 IU/ml inoculum
14. Day 4, 1x10^4 IU/ml inoculu
15. Day 4, phosphate buffer pH 5.7
16. RNAase-free water

The first conclusion from the above experiment was that samples from day 4 post-infection are not reliable since the negative control (lane 16) shows clear, B19-specific bands. This could be due to a contamination problem during mRNA extraction or, less likely, multiplex RT-PCR. The end point for harvest and mRNA extraction on days 2 and 3 post-infection was $1x10^6$ IU/ml. Although the 262bp band was not visible 2 days post-infection and the 125bp band was fainter than that seen 3 days post-infection, the end point remained the same.

Overall, since it was useful to reduce the overall time of infectivity assay without loss of sensitivity, cell harvest was done 2 days post-infection. Since there did not seem to be any difference between the cell lines tested, KU812, KU812Ep6, UT-7/EPO and UT-7/EPO-S1, day 2 post-infection was established for cell harvest, mRNA extraction and multiplex RT-PCR assays.

III.4.7.2. Comparison of different extraction protocols

The first study, which aimed at finding the most efficient mRNA extraction protocol, compared three different nucleic acid isolation methods. These include total nucleic acid extraction by the QIAamp DNA mini kit (Qiagen) and the Nuclisens™ kit (Organon Teknika), and mRNA isolation from whole cells using the Oligotex direct mRNA mini kit (Qiagen). KU812 cell line was infected with 1:10 ($1x10^{11}$ IU/ml) and 1:100 ($1x10^{10}$ IU/ml) dilutions of the B19 stock virus (in phosphate buffer pH 5.7). Negative serum was used as a negative control in each extraction tested. Cells were harvested three days post-infection and the protocols described previously were followed. Separate RT-PCR assays were done using the following conditions: 1 cycle at 50°C for 30 minutes, 1 cycle at 94°C for 15 min, 43 cycles at 94°C for 45 seconds, 55°C for 45 seconds and at 72°C for 2 minutes and lastly, 1 cycle at 72°C for 5 minutes. Amplifications of actin (actin-3

and actin-4; 25pmol/µl) and B19 genes (B19-6 and B19-9; 25pmol/µl) were done separately and the results are shown on figure 3.58, panels A and B, respectively.

All samples showed bright bands for the actin internal controls, suggesting successful extractions. Although all three extractions showed similar brightness of the RT-PCR products bands, the methods isolating total nucleic acids presented smears on the gels, even in the negative samples (lanes 1 and 7). This suggested a lack of specificity of these extraction methods. Therefore, as expected, the most specific method for the isolation of mRNA was Oligotex direct mRNA extraction from whole frozen cells.

Figure 3.58: Analysis of mRNA products extracted from KU812 cells

(A) Amplified with actin-specific primers

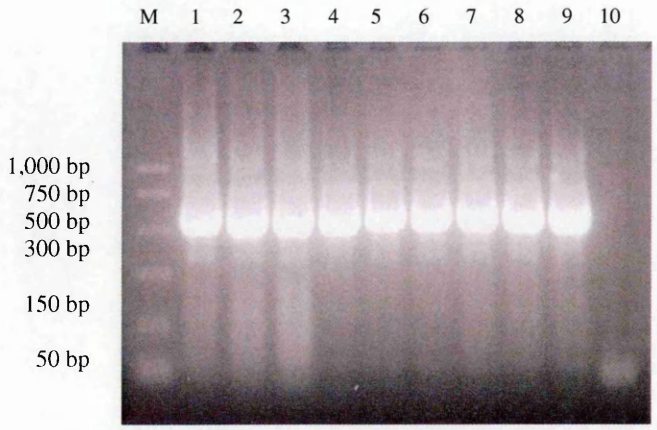

(B) Amplified with B19-specific primers

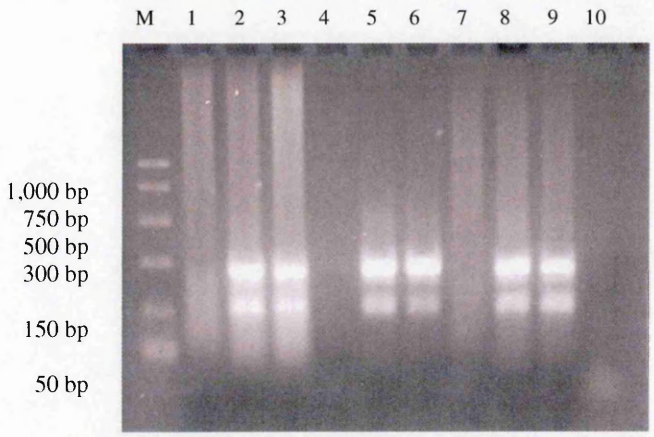

Lane M: PCR markers

Lanes 1 to 3: Extraction with QIAamp DNA mini kit

1. Negative serum
2. $1x10^{11}$ IU/ml inoculum
3. $1x10^{10}$ IU/ml inoculum

Lanes 4 to 6: Extraction with Oligotex direct mRNA mini kit from whole frozen cells

4. Negative serum
5. $1x10^{11}$ IU/ml inoculum
6. $1x10^{10}$ IU/ml inoculum

Lanes 7 to 9: Extraction with Nuclisens™ kit

7. Negative serum
8. B19 $1x10^{11}$ IU/ml inoculum
9. B19 $1x10^{10}$ IU/ml inoculum
10. RNAase-free water

The second study compared extraction of mRNA from whole frozen cells with those from whole fresh cell and cell cytoplasm, using the Oligotex direct mRNA protocol. Serial dilutions of the B19 stock virus were prepared in phosphate buffer pH 5.7 and used to infect KU812Ep6 cells (n+58): 30 µl of dilutions of virus containing $1x10^7$ IU/ml, $1x10^6$ IU/ml, $1x10^5$ IU/ml, $1x10^4$ IU/ml and phosphate buffer pH 5.7 as the negative control. Cells were harvested 2 days post-infection and mRNA extracted as described previously. Nucleic acid amplification by multiplex RT-PCR was performed with actin (2.5pmol/µl) and B19 specific primers (B19-6 and B19-9; 25pmol/µl) and the amplification conditions were as previously described in the first experiment in this section. Evaluation of the efficiency of the different extraction methods tested was done by comparing amplified products on a 2% agarose gel, as shown on figure 3.59.

The agarose gels showed that, as far as efficiency was concerned, the extraction method using fresh whole cells allowed the detection of mRNA transcripts in cells inoculated by 10^6 IU/ml. The other two methods, namely Oligotex direct mRNA extraction from whole frozen cells and from cell cytoplasm were only able to detect mRNA transcripts in cells inoculated by 10^7 IU/ml. However, as far as the specificity of the extraction methods was concerned, extractions using whole cells (fresh and frozen) showed a number of non-specific bands, suggesting that Oligotex direct mRNA extraction from cell cytoplasm was a "cleaner" and more specific isolation method. Additionally, the latter method was less time consuming and more user-friendly than the other two methods of mRNA isolation. Moreover, the $\log_{10}$ 1 difference in the end point between those methods could most probably be improved by optimising the RT-PCR conditions. Therefore, Oligotex direct mRNA extraction from cell cytoplasm (Qiagen) was the method chosen for further research on the infectivity assay for human parvovirus B19.

Figure 3.59: Analysis of mRNA products extracted from KU812Ep6 cells amplified by multiplex RT-PCR

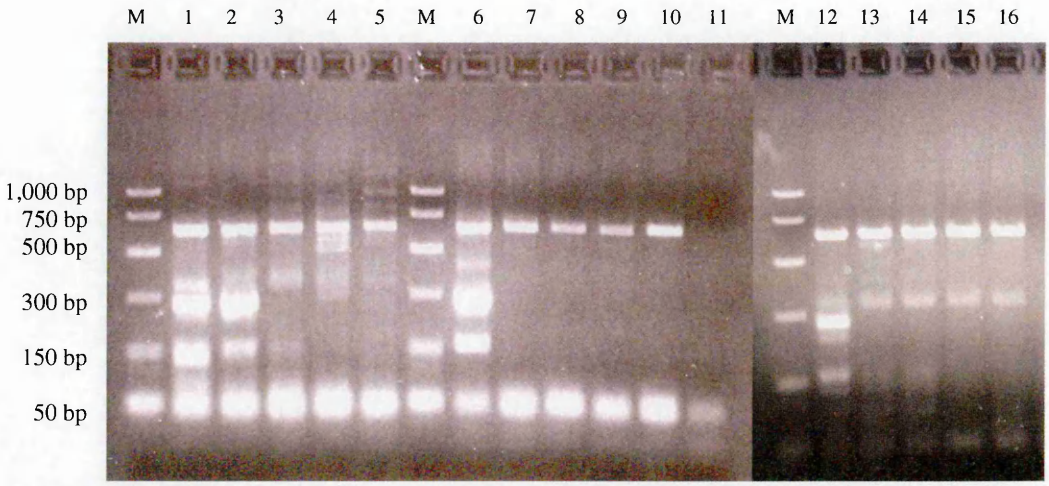

Lane M. PCR markers

Lanes 1 to 5: Oligotex direct mRNA extraction from fresh whole cells

1. $1x10^7$ IU/ml inoculum
2. $1x10^6$ IU/ml inoculum
3. $1x10^5$ IU/ml inoculum
4. $1x10^4$ IU/ml inoculum
5. Phosphate buffer pH 5.7

Lanes 6 to 10: Oligotex direct mRNA extraction from cell cytoplasm

6. $1x10^7$ IU/ml inoculum
7. $1x10^6$ IU/ml inoculum
8. $1x10^5$ IU/ml inoculum
9. $1x10^4$ IU/ml inoculum
10. Phosphate buffer pH 5.7
11. RNAase-free water

Lanes 12 to 16: Oligotex direct mRNA extraction from whole frozen cells

12. $1x10^7$ IU/ml inoculum
13. $1x10^6$ IU/ml inoculum
14. $1x10^5$ IU/ml inoculum
15. $1x10^4$ IU/ml inoculum
16. Phosphate buffer pH 5.7

The third study was a comparison of the batch format with the vacuum manifold format for the Oligotex direct mRNA extraction (Qiagen) from cell cytoplasm (see section II.2.4.3). UT-7/EPO-S1 cells (passage n+41) were used for this experiment. Serial dilutions of the B19 stock virus were prepared in phosphate buffer pH 5.7 and cells were infected with 30 µl of the diluted virus range: $1x10^7$ IU/ml, $1x10^6$ IU/ml, $1x10^5$

IU/ml, $1x10^4$ IU/ml and phosphate buffer pH 5.7 as the negative sample. Duplicate cell samples were infected for each extraction protocol, giving a total of 20 samples. Cells were harvested 2 days post-infection and mRNA extracted as described. In the vacuum manifold format, the columns were placed on the manifold (supplied by Qiagen), the buffers added and a vacuum applied to the columns. For the elution step, the spin columns were placed in RNAase-free centrifuge tubes for collection of the mRNA. Since UT-7/EPO-S1 cells were used, the B19-specific primers (XPP2 and B19-9) and the multiplex amplification conditions (1 cycle at 50°C for 30 minutes, 1 cycle at 95°C for 15 min, 43 cycles at 95°C for 45 seconds, 50°C for 40 seconds and at 72°C for 40 seconds and 1 cycle at 72°C for 10 minutes) differed from the previous two experiments. Comparison of the two formats tested was done by analysing the RT-PCR products on a 2% agarose gel, as shown on figure 3.60.

A clear difference of $\log_{10}$ 1 was observed between the batch format (end point $\log_{10}$ 8.5 inf.u./ml) and the vacuum manifold format (end point $\log_{10}$ 7.5 inf.u./ml). Although the vacuum manifold format provided a quicker alternative to the classical spin columns since less handling was required, the batch format was much gentler for the nucleic acids and the yield was higher. The latter was thus chosen as the best method of mRNA extraction using Oligotex direct isolation from cell cytoplasm (Qiagen).

Figure 3.60: Analysis of mRNA products extracted from UT-7/EPO-S1 cells amplified by multiplex RT-PCR

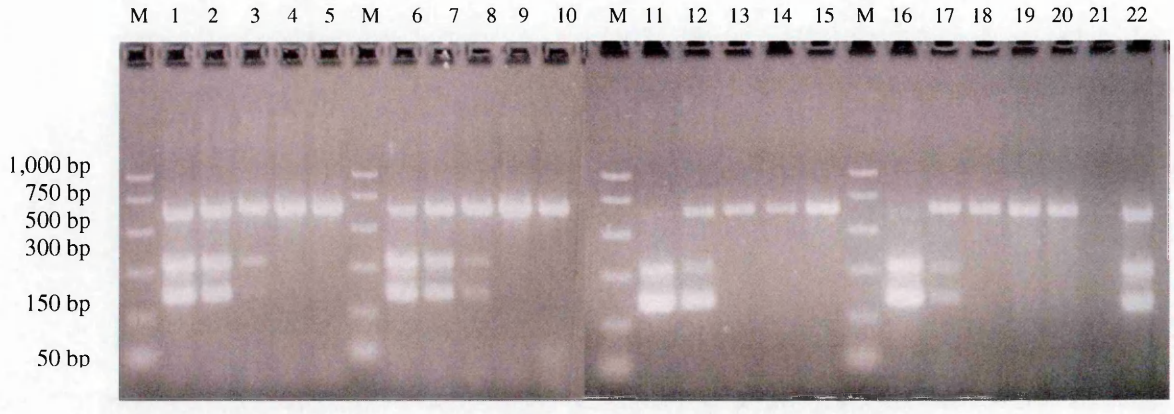

Lane M PCR marker

Lanes 1 to 10: extraction with batch format

1 and 6. $1x10^7$ IU/ml inoculum

2 and 7. $1x10^6$ IU/ml inoculum

3 and 8. $1x10^5$ IU/ml inoculum

4 and 9. $1x10^4$ IU/ml inoculum

5 and 10. Phosphate buffer pH 5.7

21. RNAase-free water

22. Positive control

Lanes 11 to 20: extraction with vacuum manifold format

11 and 16. $1x10^7$ IU/ml inoculum

12 and 17. $1x10^6$ IU/ml inoculum

3 and 18. $1x10^5$ IU/ml inoculum

14 and 19. $1x10^4$ IU/ml inoculum

15 and 20. Phosphate buffer pH 5.7

III.4.8. Optimisation of RT-PCR

III.4.8.1. Primer combinations

Two combinations of forward and reverse primers were tested using mRNA extracted from cells inoculated with serial dilutions of B19 or mock-infected with PBS-A in order to evaluate the sensitivity and specificity of each primer pair.

The first combination of primers, B19-6 and B19-9, was tested using B19 mRNA from cells infected with dilutions of the B19 stock virus containing $1x10^9$ IU/ml, $1x10^8$ IU/ml, $1x10^7$ IU/ml or phosphate buffer pH 5.7 as negative control. The mRNAs used had previously been extracted from KU812Ep6 cells (10^6 cells/sample) using the Oligotex direct mRNA method with fresh, whole cells. The total volume for each RT-

PCR reaction was 25µl, including 5µl mRNA template. Each reaction contained 5µl each of RT-PCR buffer and Q buffer, 1µl of 10mM dNTP mix, 0.6µl of 25pmol/µl forward and reverse primers, 1µl of RT-PCR enzyme mix and finally 6.8µl of RNAase-free water to make up the reaction volume to 25µl. The RT-PCR conditions included 1 cycle at 50°C for 30 minutes, 1 cycle at 95°C for 15 minutes, 43 cycles of 95°C for 50 seconds, 55°C for 40 seconds and 72°C for 45 seconds and finally 1 cycle at 72°C for 10 minutes. The RT-PCR products were analysed on a 2% agarose gel and the results are shown on figure 3.61

This combination of B19-6 and B19-9 primers resulted in two specific RT-PCR products (275bp and 155bp) in all three samples inoculated with parvovirus B19 (lanes 1 to 3 on figure 3.61). No non-specific band could be seen in the negative controls: sample inoculated with phosphate buffer only and RT-PCR negative control (RNAase-free water), lanes 4 and 5 respectively.

Figure 3.61: Analysis of mRNA products extracted from KU812Ep6 cells amplified with B19-6 and B19-9 primer combination

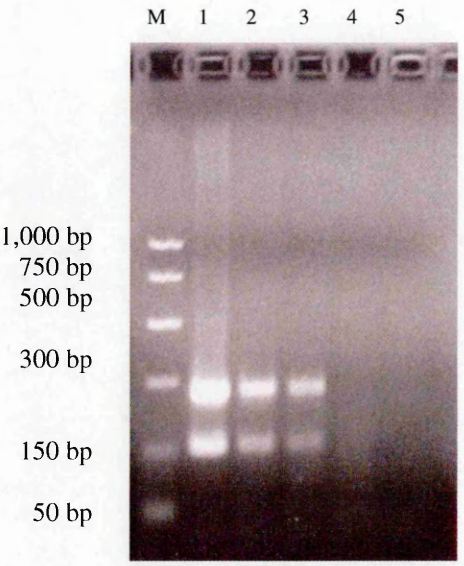

M: PCR markers
1. $1x10^9$ IU/ml inoculum
2. $1x10^8$ IU/ml inoculum
3. $1x10^7$ IU/ml inoculum
4. Phosphate buffer pH 5.7
5. RNAase-free water

The second experiment was aimed at assessing the sensitivity of the primer combination XPP2 and B19-9 compared with that of the B19-6 and B19-9 primer pair. Several mRNA samples, which the B19-6/ B19-9 primer pair had not been able to amplify previously (results not shown), were processed again with both sets of primers. The mRNAs had previously been extracted from synchronised KU812 cells ($2x10^5$ cells/sample) using the Oligotex direct mRNA method with fresh, whole cells infected with serial dilutions of the B19 stock virus containing $1x10^7$ IU/ml, $1x10^6$ IU/ml, $1x10^5$ IU/ml, $1x10^4$ IU/ml or phosphate buffer pH 5.7 as the negative control. The RT-PCR conditions were the same as above but the annealing temperature was raised to 57°C to

minimise amplification of non-specific products. The RT-PCR products were analysed on a 2% agarose gel, which is shown on figure 3.62.

Figure 3.62: Analysis of mRNA products extracted from KU812 cells amplified with XPP2 and B19-9 primer combination

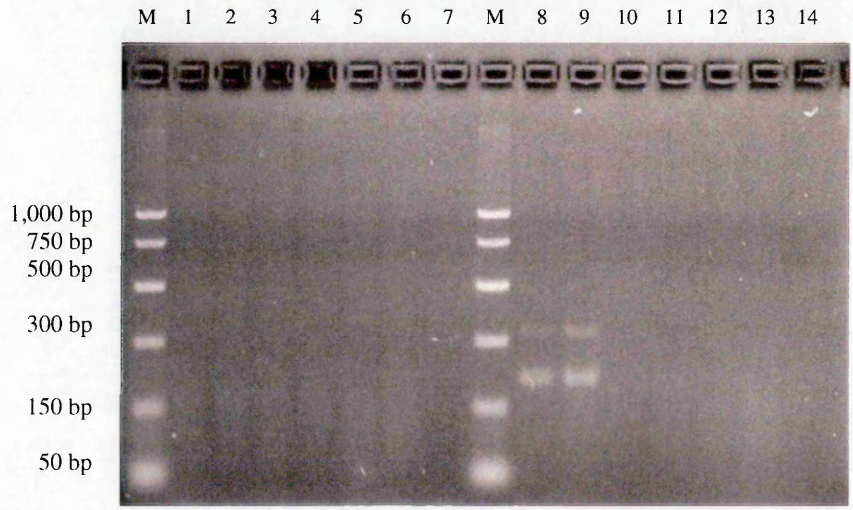

Lane M: PCR markers

Lanes 1 to 7: primer pair B19-6 and B19-9

1. $1x10^7$ IU/ml inoculum
2. $1x10^6$ IU/ml inoculum
3. $1x10^5$ IU/m inoculum
4. $1x10^4$ IU/ml inoculum
5. $1x10^3$ IU/ml inoculum
6. Phosphate buffer pH 5.7
7. RNAase-free water

Lanes 7 to 14: primer pair XPP2 and B19-9

7. $1x10^7$ IU/ml inoculum
8. $1x10^6$ IU/ml inoculum
9. $1x10^5$ IU/ml inoculum
10. $1x10^4$ IU/ml inoculum
11. $1x10^3$ IU/ml inoculum
12. Phosphate buffer pH 5.7
13. RNAase-free water

As in the previous attempt (not shown), amplification with primers B19-6 and B19-9 was unsuccessful since no bands were seen (lanes 1–5). Possible explanations could be failure at the infection step or at the mRNA extraction stage, or again low sensitivity of the RT-PCR step. The second possibility was ruled out because the initial attempt to amplify the mRNA samples with these primers was done in a multiplex format and

actin bands, although faint, were seen in all samples (results not shown). The infection step was successful since the samples inoculated with $1x10^7$ and $1x10^6$ IU/ml showed B19-specific mRNA transcripts (although faint) amplified by XPP2 and B19-9 primers (lanes 8 and 9). Therefore, it appeared that primers XPP2 and B19-9 gave more sensitive RT-PCR results than primers B19-6 and B19-9. The primer pair XPP2 and B19-9 was thus chosen to amplify mRNA in all further B19 infectivity assays.

III.4.8.2. Multiplex RT-PCR

The optimisation of the multiplex RT-PCR step was achieved by evaluating several parameters, namely the use of Q buffer, the concentration of actin primers and the annealing temperature of the PCR step.

III.4.8.2.1. Q buffer

The use of Q buffer to increase the sensitivity and specificity of the RT-PCR assay was investigated. Two sets of RT-PCR mix were prepared, one containing Q buffer (5µl per reaction) and one without Q buffer, and used for the amplification of B19 mRNA using the multiplex RT-PCR assay with the B19 primer pair XPP2 and B19-9. The samples used consisted of mRNA which had previously been extracted from KU812Ep6 cells inoculated with serial dilutions of the B19 stock virus containing $1x10^7$ IU/ml, $1x10^6$ IU/ml, $1x10^5$ IU/ml, $1x10^4$ IU/ml and phosphate buffer pH 5.7 as the negative control ($2x10^5$ cells/sample). mRNA was extracted from whole, frozen cells using the Oligotex direct mRNA protocol described previously (see section II.2.4.2) and the amplification conditions were as described in section III.4.8.1. Analysed samples are shown on figure 3.63.

Figure 3.63: Analysis of mRNA products extracted from KU812Ep6 cells amplified by multiplex RT-PCR with and without Q buffer

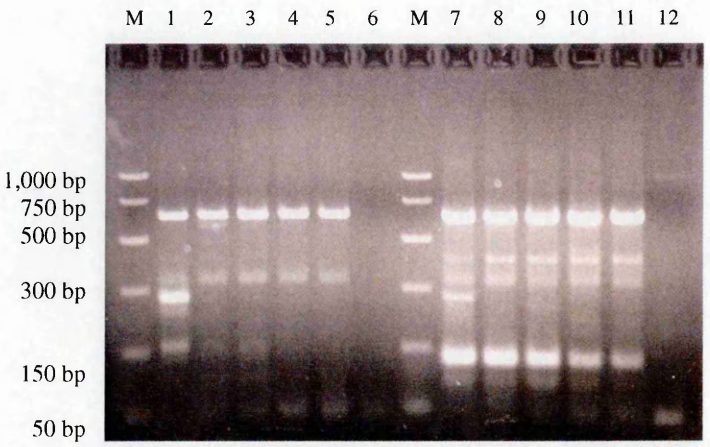

Lane M: PCR marker

Lanes 1 to 6: with Q buffer

1. $1x10^7$ IU/ml inoculum
2. $1x10^6$ IU/ml inoculum
3. $1x10^5$ IU/ml inoculum
4. $1x10^4$ IU/ml inoculum
5. Phosphate buffer pH 5.7
6. RNAase-free water

Lanes 6 to 11: without Q buffer

7. $1x10^7$ IU/ml inoculum
8. $1x10^6$ IU/ml inoculum
9. $1x10^5$ IU/ml inoculum
10. B19 International Standard, $2x10^4$ IU/ml
11. Phosphate buffer pH 5.7
12. RNAase-free water

The actin-specific band was detected in all samples containing mRNA. When Q buffer was present in the RT-PCR mix, a faint non-specific band above the larger band specific for B19 (305bp) was seen in all samples, even the mock-infected sample (lane 5). In addition, some more non-specific faint bands were seen above and below the B19-specific 185bp band. However, when Q solution was not used in the amplification reaction, a large number of bright non-specific bands were detected in all samples, suggesting a lack of specificity of the amplification reaction in the absence of Q buffer. Therefore, Q buffer was considered essential for the nucleic acid amplification reaction.

III.4.8.2.2. Concentration of actin primers

When the RT-PCR assay was performed separately for actin- and B19-specific primers, the concentration of B19 primers as well as actin-3 and actin-4 stock solutions was 25pmol/µl. Although 5µl of template was added per B19-specific reaction, only 2µl of mRNA was needed for actin amplification. Since the volume of each actin primer per reaction was 0.6µl, the final primer concentration per reaction was 0.6pmol/µl (15pmol/reaction). However, since this concentration may have been sub-optimal in a multiplex assay (the concentrations of actin primers could decrease the amplification of B19 specific products by interference), four experiments were performed with various actin primer concentrations and a constant B19 primer concentration of 25pmol/µl.

In the first experiment, the actin primer working solutions were diluted 1:3, 1:4 and 1:5, resulting in respective concentrations of 8.33pmol/µl, 6.25pmol/µl and 5pmol/µl. The mRNAs used in this experiment had previously been extracted from KU812Ep6 cells infected with dilutions of the B19 stock virus containing $1x10^{12}$ IU/ml and $1x10^{9}$ IU/ml as well as cells mock infected with negative plasma. The mRNAs were extracted from fresh, whole cells using the Oligotex direct mRNA protocol. The total volume for each multiplex reaction was 25µl, including 5µl mRNA template added last. Each reaction contained 5µl of RT-PCR buffer and Q buffer, 1µl of 10mM dNTP mix and RT-PCR enzyme mix, 0.6µl of each primer (actin-3, actin-4, B19-6, B19-9) and finally 5.6µl of RNAase-free water. The conditions for amplification were as described previously in section III.4.8.1. The products were analysed on a 2% agarose gel, which is shown on figure 3.64.

Figure 3.64: Analysis of mRNA products extracted from KU812Ep6 cells amplified by multiplex RT-PCR using various actin primers concentrations

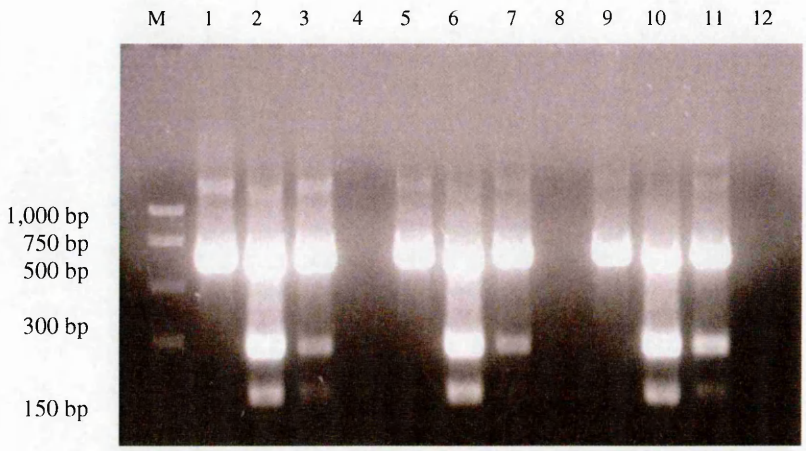

Lane M: PCR markers

Lanes 1 to 4: actin primers at 1:3 dilution (8.33pmol/µl)

1. Negative serum
2. $1x10^{12}$ IU/ml inoculum
3. $1x10^{9}$ IU/ml inoculum
4. RNAase-free water

Lanes 5 to 8: actin primers at 1:4 dilution (6.25pmol/µl)

5. Negative serum
6. $1x10^{12}$ IU/ml inoculum
7. $1x10^{9}$ IU/ml inoculum
8. RNAase-free water

Lanes 9 to 12: actin primers at 1:5 dilution (5pmol/µl)

9. Negative serum
10. $1x10^{12}$ IU/ml inoculum
11. $1x10^{9}$ IU/ml inoculum
12. RNAase-free water

This experiment demonstrated that all three primer dilutions were suitable for amplification of the actin gene. The fact that the lower band was not present in sample 7 (inoculated with $1x10^{9}$ IU/ml) suggested that the 1:4 actin primers dilution was inhibiting the amplification of this B19 transcript. The lower bands in samples 3 and 11 (inoculated with $1x10^{9}$ IU/ml) with dilutions 1:3 and 1:5, respectively, were also very

faint. Therefore, the lower concentration of actin primers was considered to be necessary to prevent loss of amplification with the B19 primers.

The second experiment in this series compared actin primer working solutions concentrations of 12.5pmol/µl (1:2 dilution), 5pmol/µl (1:5 dilution) and 2.5pmol/µl (1:10 dilution) using the B19-specific primers pair XPP2 and B19-9, which were, by then, found to be more specific than the B19-6 and B19-9 combination. In addition, in order to evaluate the sensitivity of the assay, mRNA from cells infected with lower concentrations of parvovirus B19 (compared with the first experiment) were used. Thus, the mRNA samples used had previously been extracted from cells infected with dilutions of the B19 stock virus containing $1x10^7$ IU/ml, $1x10^6$ IU/ml and $1x10^5$ IU/ml and cells mock infected with PBS pH 5.7. The mRNA samples were extracted from UT-7/EPO-S1 cell cytoplasm using the Oligotex direct mRNA protocol. The multiplex RT-PCR conditions were similar to that of the previous experiments but the annealing step was slightly modified by increasing the temperature from 55°C to 57°C and the elongation step was reduced from 2 minutes to 40 seconds. The products were analysed on 2% agarose gels, as shown on figure 3.65.

As expected, the more diluted the actin primers, the fainter the actin-specific bands on the agarose gel. The two B19-specific bands were visible in samples inoculated with $1x10^7$ IU/ml and $1x10^6$ IU/ml. These bands were very faint with the 1:2 and 1:5 dilutions of actin primers whereas they were brighter when 1:10 dilution was used. However, in this case, the actin band was very faint (lanes 11 to 14 on figure 3.65). This suggests that the 1:10 dilution (2.5pmol/µl) was not sufficient to amplify the housekeeping gene transcript in these samples. A lower dilution of actin-3 and actin-4 primers was therefore tested in a further experiment.

Figure 3.65: Analysis of mRNA products extracted from UT-7/EPO-S1 cells amplified by multiplex RT-PCR using various actin primers concentrations

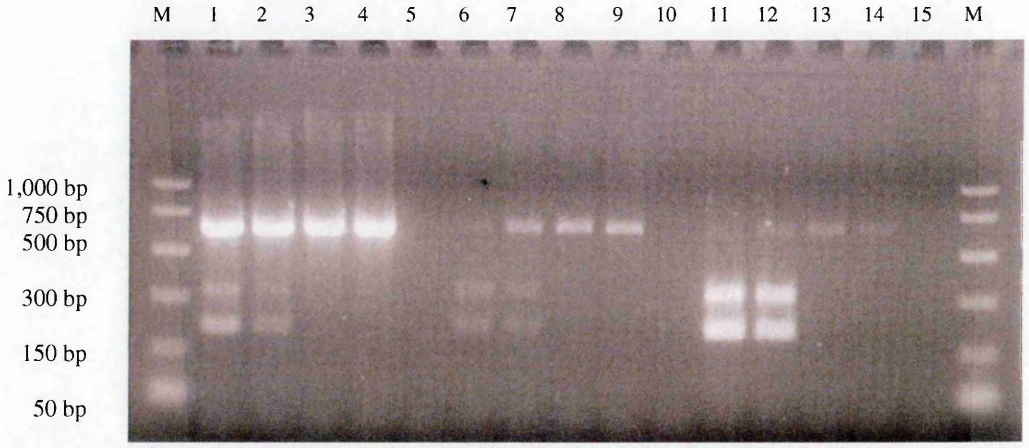

Lane M: PCR markers

Lanes 1 to 5: actin primers at 1:2 dilution (12.5pmol/µl)

1. $1x10^7$ IU/ml inoculum
2. $1x10^6$ IU/ml inoculum
3. $1x10^5$ IU/ml inoculum
4. Phosphate buffer pH 5.7
5. RNAase-free water

Lanes 6 to 10: actin primers at 1:5 dilution (5pmol/µl)

6. $1x10^7$ IU/ml inoculum
7. $1x10^6$ IU/ml inoculum
8. $1x10^5$ IU/ml inoculum
9. Phosphate buffer pH 5.7
10. RNAase-free water

Lanes 11 to 15: actin primers at 1:10 dilution (2.5pmol/µl)

11. $1x10^7$ IU/ml inoculum
12. $1x10^6$ IU/ml inoculum
13. $1x10^5$ IU/ml inoculum
14. Phosphate buffer pH 5.7
15. RNAase-free water

The third experiment investigated actin primer concentrations between 1:5 and 1:10 dilutions, namely 1:6 (4.16pmol/µl) and 1:8 (3.125pmol/µl). The nucleic acids samples used had previously been extracted from UT-7/EPO-S1 cells (passage n+22) using the Oligotex direct mRNA protocol from cell cytoplasm. The cells were infected with 1:10 dilutions of the B19 stock virus containing from $1x10^7$ IU/ml to $1x10^4$ IU/ml and a

negative control (phosphate buffer pH 5.7). The RT-PCR conditions were similar to those described in the previous experiment. Two separate amplifications were run in parallel, namely with B19-specific primers only (B19-9 and XPP2) and multiplex RT-PCR including both the same B19-specific primers and actin-specific primers at the dilutions tested in this experiment (1:6 and 1:8). The amplified products were analysed on 2% agarose gels shown on figure 3.66 (panel A and B, respectively).

When B19-specific primers alone were used in the RT-PCR step (panel A, figure 3.66), the end point was sample 3, cells inoculated with $1x10^5$ IU/ml. Although the B19-specific bands were also detected by multiplex amplification in sample 3, they were very faint and the 305bp band could not be seen when amplified with actin primers diluted 1:6. In addition, the actin bands were not well defined and very faint with either dilution tested and a number of non-specific bands were present on panel B, figure 3.66. Therefore, the concentration of actin-specific primers seemed to be too low for consistent detection in the multiplex assay. The actin primer concentration of 1:5 dilution, which had previously been tested, was therefore investigated once again in the fourth and final experiment.

Figure 3.66: Analysis of mRNA products extracted from UT-7/EPO-S1 cells

(A) Amplified with B19-specific primers (B19-9 and XPP2)

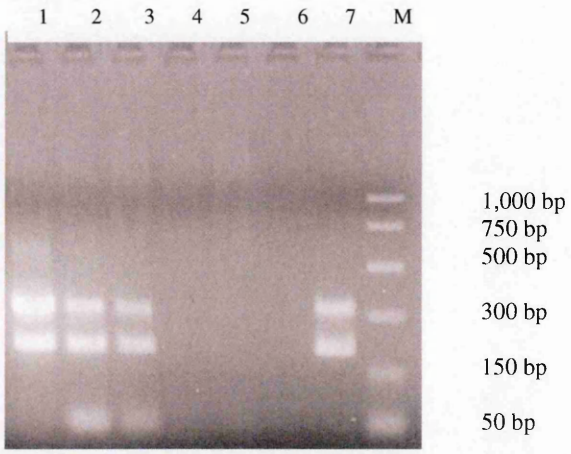

(B) Amplified by multiplex RT-PCR with various actin primers concentrations

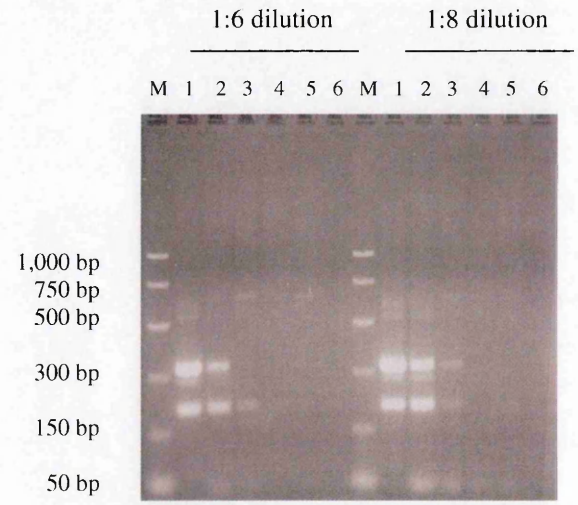

M PCR markers

1. $1x10^7$ IU/ml inoculum
2. $1x10^6$ IU/ml inoculum
3. $1x10^5$ IU/ml inoculum
4. $1x10^4$ IU/ml
5. Phosphate buffer pH 5.7
6. RNAase-free water (negative control)
7. RT-PCR positive control ($1x10^6$ IU/ml)

The last experiment aiming at determining the optimal actin primers concentration for multiplex RT-PCR investigated the 1:5 dilution (5pmol/µl) again, using mRNA samples from different inoculation and extraction experiments in order to evaluate the reproducibility of the assay. The RNA samples were extracted from UT-7/EPO-S1 cells (passage n+22) using the Oligotex direct mRNA protocol from cell cytoplasm. The cells had been inoculated in duplicate with dilutions of the B19 stock virus containing $1x10^7$ IU/ml, $1x10^6$ IU/ml and $1x10^5$ IU/ml and from cells mock infected with phosphate buffer pH 5.7. Samples were amplified in a multiplex RT-PCR assay with the B19-specific primers (B19-9 and XPP2) at a concentration of 25pmol/µl and actin primers (actin-3 and actin-4) diluted 1:5 (5pmol/µl). The RT-PCR conditions were similar to those described for the two previous experiments and again two separate amplifications were run in parallel, one with B19-specific primers only (B19-9 and XPP2) and the other with both B19-specific primers and actin-specific primers at the 1:5 dilution in a multiplex format. The amplified products obtained were analysed on 2% agarose gels, as shown on figure 3.67, panels A and B, respectively.

When the RT-PCR step was first performed using B19-specific primers only, the two mRNA transcripts were amplified in only one out of two samples inoculated with $1x10^6$ IU/ml (panel A, sample 3). On the other hand, when the multiplex RT-PCR (using 5pmol/µl of actin primers) was performed, both samples inoculated with $1x10^6$ IU/ml showed B19-specific bands, although only a faint 305bp band was seen in sample 3, panel B. The B19-specific bands in samples 1 and 2 were much brighter with actin primers (panel B) than without (panel A). In addition, the actin gene transcript was clearly amplified in all samples with extracted mRNA. Therefore, a concentration of 5pmol/µl for actin-specific primers and 25pmol/µl for B19-specific primers seemed to

be the best combination for the optimal amplification of both B19 and actin transcripts by multiplex RT-PCR.

Figure 3.67: Analysis of mRNA products extracted from UT-7/EPO-S1 cells

(A) Amplified with B19-specific primers (B19-9 and XPP2)

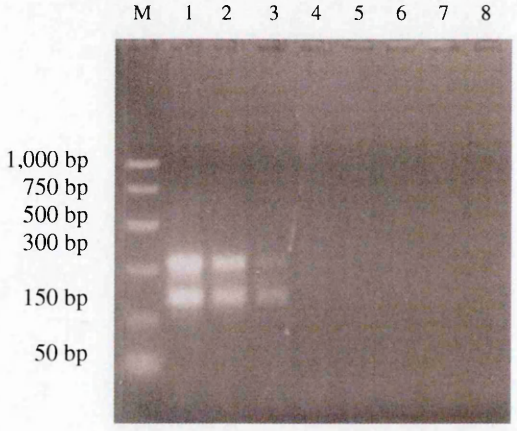

(B) Amplified by multiplex RT-PCR (1:5 dilution of actin primers)

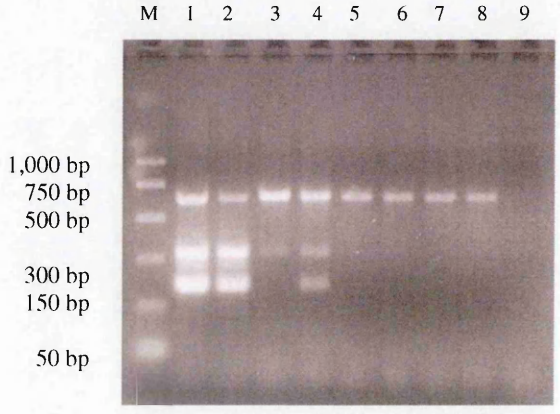

M PCR markers
1. $1x10^7$ IU/ml inoculum
2. $1x10^7$ IU/ml inoculum
3. $1x10^6$ IU/ml inoculum
4. $1x10^6$ IU/ml inoculum
5. $1x10^5$ IU/ml inoculum
6. $1x10^5$ IU/ml inoculum
7. Phosphate buffer pH 5.7
8. Phosphate buffer pH 5.7
9. RNAase-free water

III.4.8.2.3. Annealing temperature

In addition to determining the optimal actin primer concentration as 5pmol/µl, the data obtained by testing different primer combinations showed that the most specific primer pair was XPP2 and B19-9. When used on their own, the annealing temperature chosen for this set of primers was 57°C. However, since the present experiment aimed at optimising the annealing temperature for the multiplex RT-PCR, it was lowered in order to increase the sensitivity of the assay. Therefore, the temperatures tested were 48°C, 50°C, 52°C and 55°C, using mRNA samples extracted from UT-7/EPO-S1 cells which had been infected with serial dilutions of the three different B19 isolates, namely JS (B19 stock virus), JB and LP and extracted from cell cytoplasm using the Oligotex direct mRNA protocol. The 1:10 viral dilutions ranged from 10^{-4} to 10^{-8} and one sample inoculated with phosphate buffer pH 5.7 was also included as the negative control. The RT-PCR negative and positive controls were RNAase-free water and mRNA previously extracted from UT-7/EPO-S1 cells inoculated with $1x10^{7}$IU/ml of B19 virus stock, respectively. Multiplex RT-PCR using actin-specific primers (actin-3 and actin-4 at 5pmol/µl) and B19-specific primers (XPP2 and B19-9 at 25pmol/µl) was set up with the following conditions: 1 cycle at 50°C for 30 minutes, 1 cycle at 95°C for 15 minutes, 43 cycles of 95°C for 45 seconds, 55°C/ 52°C/ 50°C/ 48°C for 45 seconds and 72°C for 40 seconds and finally 1 cycle at 72°C for 10 minutes. The products of each of the four mRNA amplifications at 55°C, 52°C, 50°C and 48°C were analysed on 2% agarose gels and are shown on figure 3.68, panels A, B, C and D, respectively.

Figure 3.68: Analysis of mRNA products extracted from UT-7/EPO-S1 cells amplified by multiplex RT-PCR

(A) Annealing temperature: 55°C

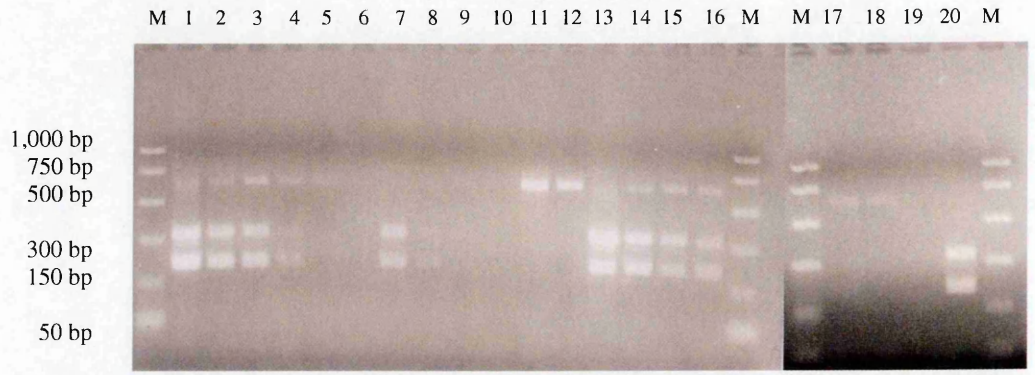

(B) Annealing temperature: 52°C

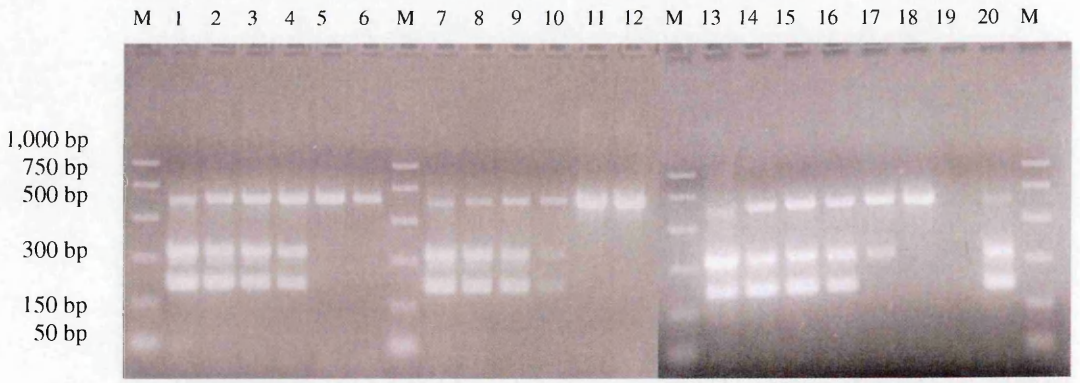

(C) Annealing temperature: 50°C

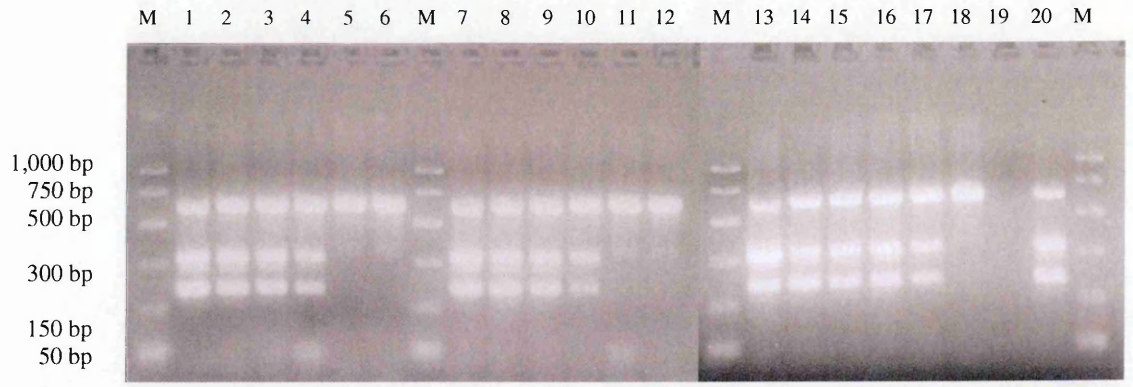

(D) Annealing temperature: 48°C

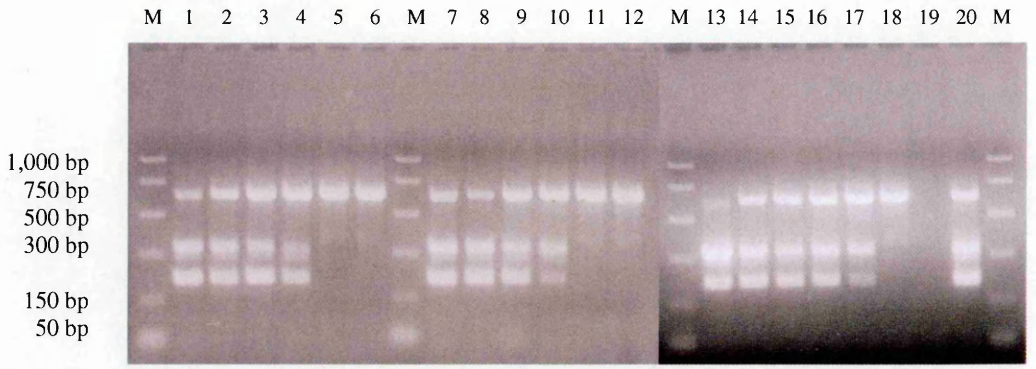

Lane M. PCR marker

Lanes 1 to 6: JS virus	**Lanes 7 to 12: JB virus virus**	**Lanes 13 to 18: LP**
1. $1x10^8$ IU/ml	7. $3x10^8$ IU/ml	13. $5x10^9$ IU/ml
2. $1x10^7$ IU/ml	8. $3x10^7$ IU/ml	14. $5x10^8$ IU/ml
3. $1x10^6$ IU/ml	9. $3x10^6$ IU/ml	15. $5x10^7$ IU/ml
4. $1x10^5$ IU/ml	10. $3x10^5$ IU/ml	16. $5x10^6$ IU/ml
5. $1x10^4$ IU/ml	11. $3x10^4$ IU/ml	17. $5x10^5$ IU/ml
6. Phosphate buffer, pH5.7	12. Phosphate buffer, pH5.7	18. Phosphate buffer, pH5.7

19. RNAase-free water (RT-PCR negative control)

20. $2x10^7$ IU/ml (RT-PCR positive control)

The end points for all three inoculi at each annealing temperature tested are shown in table 3.11. For the B19-specific mRNA transcripts, figure 3.68, panels A to D and table 3.11 all showed that a lower annealing temperature such as 50°C or 48°C resulted in a higher sensitivity of the amplification reaction. The optimisation of the multiplex RT-PCR was a balance between amplification of B19-specific mRNA transcripts and the housekeeping gene transcripts, to ensure that the amplification of the one did not interfere with that of the other. Thus, the second parameter that was investigated was the amplification of the actin gene when using decreasing temperatures. At 55°C, many of the samples containing mRNA did not show any actin-specific band and, in the samples

that did show a band, it was very faint. However, when the annealing temperature was lowered to 52°C, 50°C and 48°C, all samples showed the actin band, although it was still faint in some samples at 52°C and 48°C.

In conclusion, taking all parameters into account, it appeared that an annealing temperature of 50°C would provide the best amplification, in terms of sensitivity, of the housekeeping gene (actin) and parvovirus B19 transcripts using the primer pair XPP2 and B19-9.

Table 3.11: Results of annealing temperature optimisation

B19 isolate	RT-PCR annealing temperature (°C)	Log_{10} DNA titre (IU/ml)	End point dilution	Log_{10} infectious units (inf.u./ml)
JS	55	12.0	5.0	8.5
	52	12.0	5.0	8.5
	50	12.0	5.0	8.5
	48	12.0	5.0	8.5
JB	55	12.5	7.0	7.0
	52	12.5	5.0	9.0
	50	12.5	5.0	9.0
	48	12.5	5.0	9.0
LP	55	13.7	6.0	9.2
	52	13.7	5.0	10.2
	50	13.7	5.0	10.2
	48	13.7	5.0	10.2

III.4.9. Optimised human parvovirus B19 infectivity assay

III.4.9.1. Infectivity assay conditions

The infectivity assay was optimised at several levels, including tissue culture, virus inoculation and incubation, and mRNA extraction and amplification. Detection of B19 replication was indeed found to be more sensitive than IFA.

The non-synchronised UT-7/EPO-S1 cell line, at passages between n+14 and n+53, was chosen after extensive tissue culture studies. The growth curves for this cell line showed that the optimum time for virus inoculation, which was when the cells were multiplying the most, was 5 days after splitting them at a concentration of $1x10^5$ cells/ml.

After being washed with phosphate buffer pH 5.7, $2x10^5$ cells were inoculated with 30µl of B19 virus diluted in phosphate buffer pH 5.7. An incubation of 2 hours at 4°C was followed by the addition of 1ml of fresh medium (Iscoves modified DMEM, with Glutamax-1, 10% FCS, 2 IU/ml EPO, 1% gentamycin, 1% fungizone). The cells were incubated at 37°C (5% CO_2) and the optimum time for harvesting was 2 days post-inoculation.

The best method for the extraction of mRNA was found to be from cell cytoplasm using the Oligotex direct mRNA kit (Qiagen). Isolated mRNA was amplified by multiplex RT-PCR using the optimum primer combination: B19-9 (forward) and XPP-2 (reverse). OneStep RT-PCR kit (Qiagen) was used and each reaction contained 5µl of 10x OneStep RT-PCR buffer, 5µl of 5x Q buffer solution, 1µl of dNTPs, actin primers (Actin-3 and Actin-4) at a concentration of 3pmol per reaction (0.6µl of 5pmol/µl stock) and B19 primers (B19-9 and XPP-2) at a concentration of 15pmol per reaction (0.6µl of 15pmol/µl stock), 1µl of RT-PCR enzyme mix and 5.6µl of RNAase-free water. Template (5µl) was added to complete the volume of a full reaction to 25µl reaction mix. The amplification conditions were 1 cycle at 50°C for 30 minutes, 1 cycle at 95°C

for 15 minutes, 43 cycles of 95°C for 45 seconds, 50°C (optimum annealing temperature) for 40 seconds and 72°C for 40 seconds and finally 1 cycle at 72°C for 10 minutes.

III.4.9.2. Validations studies

The aim of these studies was to determine the limit of detection of the optimised B19 infectivity assay.

The optimised protocols for inoculation of cells, extraction of mRNA and RT-PCR as determined in the initial experiments were used for this study. Briefly, the UT-7/EPO-S1 cell line was used at passages between n+48 and n+52 and six assays with duplicate sample dilutions of the stock virus were performed. Serial dilutions of the B19 stock virus, ranging from $10^{-5.0}$ to $10^{-8.0}$, were prepared in phosphate buffer pH 5.7 and cells were inoculated with 30µl of diluted virus containing $1x10^{7}$ IU/ml, $1x10^{6.5}$ IU/ml, $1x10^{6}$ IU/ml, $1x10^{5.5}$ IU/ml, $1x10^{5}$ IU/ml, $1x10^{4.5}$ IU/ml, $1x10^{4}$ IU/ml and phosphate buffer pH 5.7 as the negative sample. The infectivity assay conditions detailed previously (section III.4.9.1) were applied for these validation studies.

Table 3.12 summaries the detection (+) or absence (-) of B19 specific transcripts for each study.

Table 3.12: Record of B19 specific transcripts presence (+) or absence (-) in the validation studies of the optimised infectivity assay

Log_{10} DNA concentration of inoculum (IU/ml)	7.0	6.5	6.0	5.5	5.0	4.5	4.0	Negative control
Log_{10} dilution of inoculum	-5.0	-5.5	-6.0	-6.5	-7.0	-7.5	-8.0	Negative control
Study number								
1	+	+	+	-	+	+	-	-
1	+	+	+	+	+	-	-	-
2	+	+	+	+	+	-	-	-
2	+	+	+	-	-	-	-	-
3	+	+	+	-	-	-	-	-
3	+	+	+	-	-	-	-	-
4	+	+	+	-	+	-	-	-
4	+	+	+	-	-	-	-	-
5	+	+	+	+	+	-	-	-
5	+	+	+	+	+	-	-	-
6	+	+	+	-	-	-	-	-
6	+	+	+	+	-	-	-	-

Statistical analysis kindly done by A. Heath (Department of Informatics, NIBSC) showed that the 95% detection limit for this assay was log_{10} -6.03 dilution (range -5.82 to -6.24), or log_{10} 5.97 IU/ml (log_{10} 7.53 inf.u./ml) and the 50% detection limit was log_{10} -6.67 dilution (range -6.46 to -6.87) or log_{10} 5.35 IU/ml (log_{10} 8.15 inf.u./ml). The calculated DNA concentration to infectious unit ratios for this study are shown in the table 3.13 The calculated mean ratio for the DNA concentration to infectious units was $10^{3.91}$:1.

Table 3.13 Infectivity results and DNA concentration to infectious unit ratio for the optimised infectivity assay

Study number	Log_{10} DNA concentration (IU/ml)	Log_{10} infectious units/ml	DNA concentration: infectious unit ratio
1	12.0	9.0	$10^{3.0}$:1
1	12.0	8.5	$10^{3.5}$:1
2	12.0	8.5	$10^{3.5}$:1
2	12.0	7.5	$10^{4.5}$:1
3	12.0	7.5	$10^{4.5}$:1
3	12.0	7.5	$10^{4.5}$:1
4	12.0	8.5	$10^{3.5}$:1
4	12.0	7.5	$10^{4.5}$:1
5	12.0	8.5	$10^{3.5}$:1
5	12.0	8.5	$10^{3.5}$:1
6	12.0	7.5	$10^{4.5}$:1
6	12.0	8.0	$10^{4.0}$:1

III.4.10. Sequencing of PCR products

The two mRNA transcripts amplified with B19-9 (position 384-405) and XPP-2 (position 2194-2214), which are shown below, were sequenced. As far as the longer transcript was concerned (upper band), only the reverse sequence was obtained, which was enough to identify its size and position on the reference genomic DNA (M13178).

Forward primer B19-9: GTT TTT TGT GAG CTA ACT AAC A

Reverse primer XPP2: ACC GTC CCA CAC ATA ATC AAC

Longer transcript (305bp on gel) sequenced with the reverse primer XPP-2:

5'CCCACTAACATTCACGAAANTGGTCTGCCAAAGGTGTGTAGAAGGCTTCT
TCCCACGATGCAGCTACAACTTCGGAGGAAACTGGGCTTCCGACAAATGAT
TCTCCTGAACTGGTCCCGGGGATGGGCGTACTAGAGCGCGGGGTTTCAGTG
TTCCAGGCGCCTGGGGTGATGAGGTTAAAAAAGCTGCTTTCACTGAGTTCTT
CAGAGCTTTCACCACCACTGCTGCTGATACTGGTGTCTGTGACAATTGGGGT
GGTTTGGAGGTCTGGGTGGAGGGCATCTGTTAGTTAGCTCACAAAAAACAG
3'

Shorter transcript (185bp on agarose gel) sequenced with the reverse primer XPP-2:

5'CCCACTAACATTCACGAAACTGGTCTGCCAAAGGTGTGTAGAAGGCTTCT
TCCCACGATGCAGCTACAACTTCGGAGGAAACTGGGCTTCCGACAAATGAT
TCTCCTGAACTGGTCCCGGGGATGGGCGTACTAGAGCGCGGGGTTTCAGTG
TTCCAGGCGCCTGTTAGTTAGCTCACAAAAAACAGGCGC 3'

Shorter transcript (185bp on agarose gel) sequenced with the forward primer B19-9:

5'GNCGCNCGGNACACTGTANCCCCGCGCTCTAGTACGCCCATCCCCGGGAC
CAGTTCAGGAGTAATCATTTGTCGGAAGCCCAGTTTCCTCCGAAGTTGTAGC
TGCATCGTGGGAAGAAGCCTTCTACACACCTTTGGCAGACCAGTTTCGTGAA
CTGTTAGTTGGGGTTGATTATGTGTGGGACGGTA 3'

When compared to B19 genomic DNA (M13178), the longer transcript (upper band) corresponds to positions: 384-406 and 1910-2193, with an actual transcript size of 305 bp.

When compared to B19 genomic DNA (M13178), the shorter transcript (lower band) corresponds to positions: 384-406 and 2030-2193, with an actual size of 185 bp.

In accordance with previous reports (Ozawa *et al.*, 1987; St Amand *et al.*, 1991), this study confirmed the presence of one splicing donor site (GT) and two acceptor sites (AG) at position 407-408, 1908-1909 and 2028-2029, respectively. A more recent study observed a slice donor site at nt 441 always coupled with the acceptor site at position 2030 (Brunstein *et al.*, 2000), a splicing pattern that was not found in the present study.

III.5. Human parvovirus B19 removal/inactivation studies

The results of the DNA assay and infectivity assay for all five virus removal/inactivation techniques are given below. The B19 DNA titre was determined from the standard curve using the B19 International Standard and the number of infectious units/ml for each sample was calculated from the end-point dilution of the infectivity assay as described previously.

III.5.1. Virus removal by nanofiltration using Planova® filters: Asahi Kasei Pharma

The filtration experiments were performed at NIBSC by Dr S. Satoh (Asahi Kasei Pharma Coropration, Japan) and Mr T. Sato (Asahi Kasei Deutchland, Germany). Reconstituted 25% human albumin was diluted 1:50 in saline to obtain a 0.5% albumin solution (600ml). The latter was prefiltered through a 35N Planova® filter (0.5 bar) in order to remove aggregates of protein, which might have been generated by the

lyophilisation process. Control samples A1 and A2 (0.5ml) were taken from the 0.5% albumin prefiltration feed while samples B1 and B2 (0.5ml) were from the prefiltration filtrate. The second step included the preparation of the spiked solution by mixing 550ml of the prefiltered albumin with 1000µl of stock virus ($1x10^{12}$ IU/ml). Spiked albumin was then filtered through a 35N Planova® filter (0.5 bar).

Controls C1 and C2 (0.5ml) were duplicate samples of the parvovirus B19 spiked albumin (feed solution) while samples D1 and D2 (0.5ml) were taken after filtration with the 35N Planova® filter. The melting curve of sample C1 at 1:10,000 dilution on figure 3.69 showed only the B19-specific peak at the melting temperature of 84.8°C. This temperature was within the melting temperature range determined previously for validation purposes (84.4°C to 85°C).

Figure 3.69: Melting curve of spiked albumin (sample C1 diluted 1:10,000)

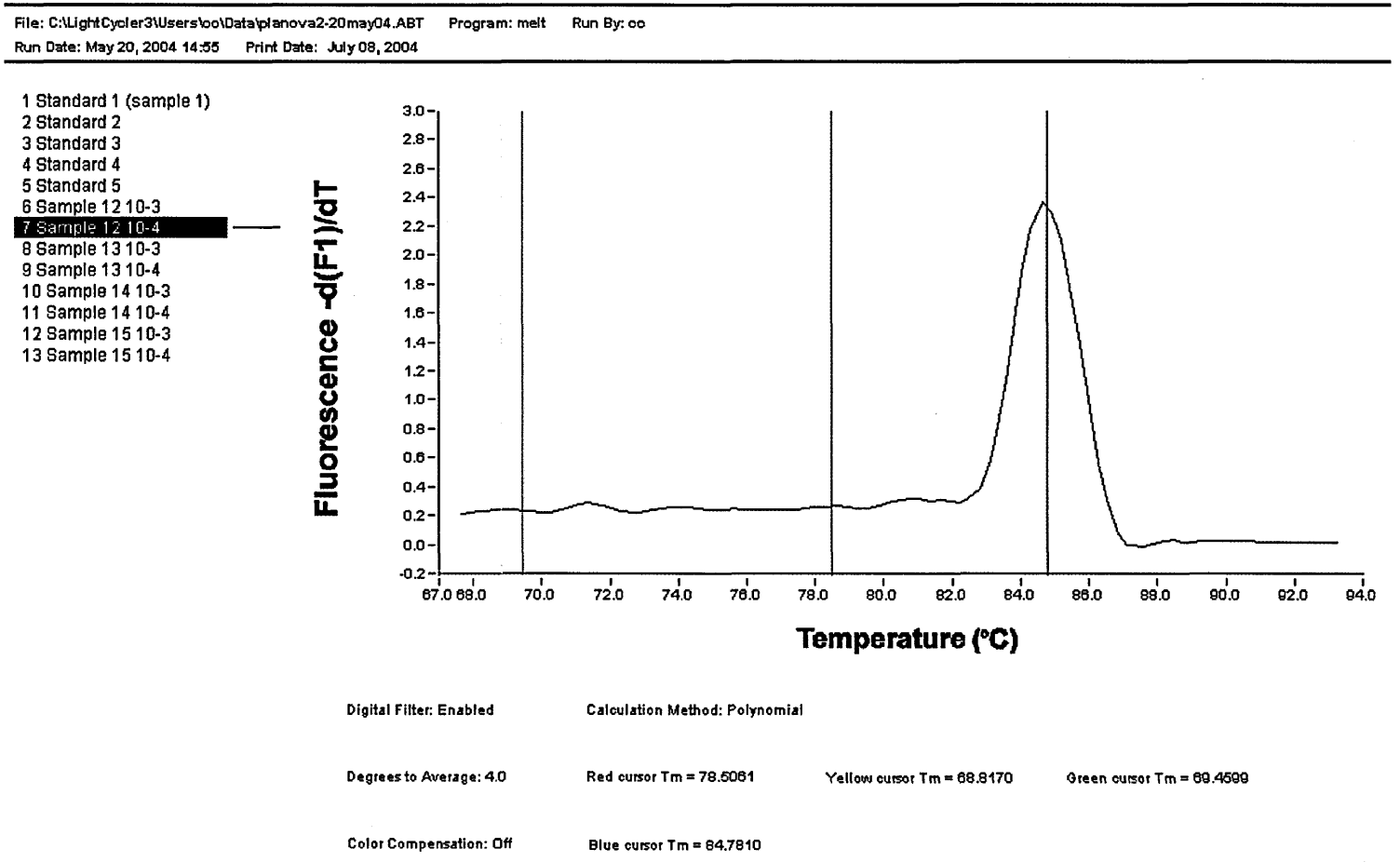

Two pore sizes of Planova® filters were tested in this experiment, namely 15N and 20N. Three different runs were performed for each filter size, using a new filter for each run (60ml of feed for each run). The filtrations were run under a dead-end mode (figure 3.70), under constant pressure (0.5 bar) and at room temperature in a Class 1 Microbiological Safety cabinet.

Figure 3.70: Dead-end and constant pressure Planova® filtration procedure

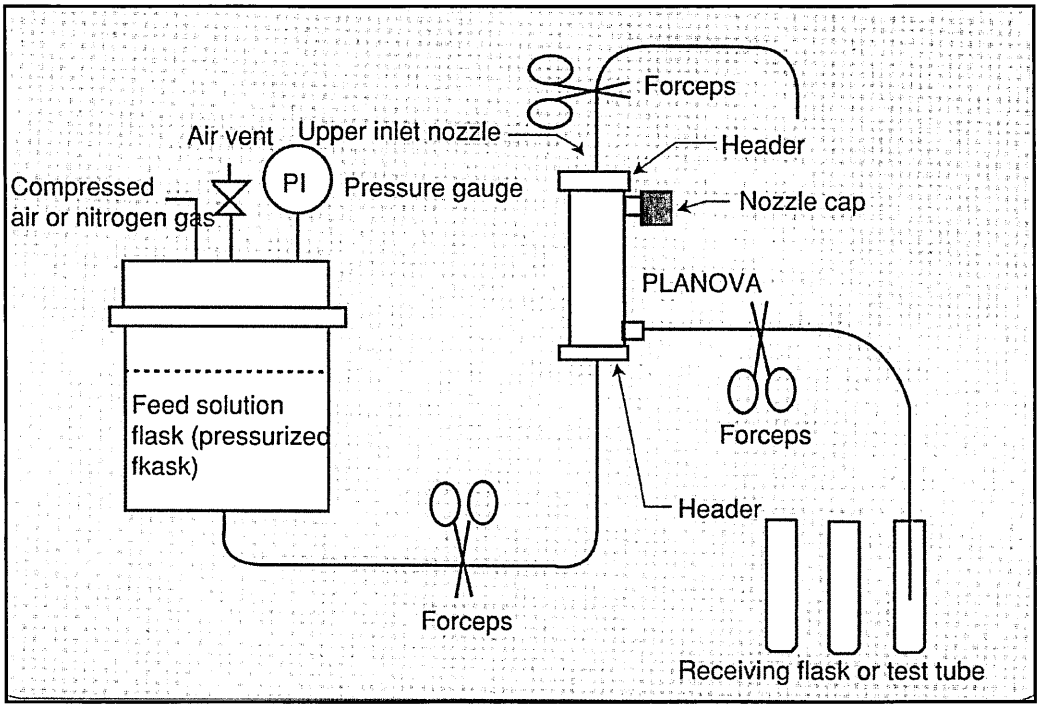

Eluate fractions of ~0.7ml were collected for each filtration. These collection samples were numbered 1 to 43 for the first 15N Planova® filter, 44 to 86 for the first 20N Planova® filter, 87 to 129 for the second 15N Planova® filter, 130 to 172 for the second 20N Planova® filter, 173 to 215 for the third 15N Planova® filter and lastly 216 to 258 for the third 20N Planova® filter. The fractions were stored at -70°C.

Parvovirus B19 DNA of every other collection sample was extracted, together with a sample of the B19 IS 99/800, and several negative controls (B19-antibody negative plasma provided by Dr J. Saldanha, B19-antibody negative serum given by Dr B. Cohen and duplicate RNAse-free water controls). The extracted DNA was then amplified by LightCycler PCR. Ten-fold dilutions (ranging in concentration from 10^6 to 10^3 IU/ml) of the DNA extracted from the B19 IS were amplified in parallel and the results used to plot a standard curve. The concentrations of the samples were read off the standard curve. Fluorescence was generated by both the amplicon and the primer dimers, as shown by the samples melting curves. Observation of the latter showed that, in samples whose concentration was less than $1x10^3$ IU/ml, the fluorescent signal was due to the generation of primer dimers. Such samples were thus considered to be negative. In order to test all the samples (and to include dilutions of the B19 international standard for generation of a standard curve in each run), it was necessary to perform a total of twelve runs on the LightCycler.

Table 3.14 records the different LightCycler runs with the controls and nanofiltration collection samples tested in each run. All three negative controls (negative plasma, negative serum and RNAase-free water) were found negative in all the LightCycler runs.

Table 3.14: LightCycler runs and negative controls results for nanofiltration

Run	Controls and collection samples tested
1	A1, A2, B1, B2, C1, C2, D1, D2, 1 to 13
2	15 to 41
3	43 to 68
4	68 to 86
5	87 to 107
6	109 to 130
7	132 to 154
8	156 to 173
9	175 to 177
10	179 to 215
11	216 to 244
12	246 to 258

The following tables (3.15 to 3.21) compile the $\log_{10}$ of B19 DNA concentrations, as well as the gel electrophoresis result for the experimental controls and the collection samples for each filter tested. Photos of all the agarose gels can be viewed in appendix 3.

Table 3.15: Experimental controls for nanofiltration

Control sample	Log_{10} DNA concentration (IU/ml)	Agarose gel result
A1	3.30	+ (faint)
A2	<limit of quantitation	+ (faint)
B1	3.30	+ (faint)
B2	3.00	+
C1	10.69	+
C2	10.77	+
D1	9.60	+
D2	9.77	+

Table 3.16: Results for the first 15N Planova® filter

Collection sample	Log_{10} DNA concentration (IU/ml)	Agarose gel result
1	3.69	+
3	4.60	+
5	4.60	+
7	4.60	+
9	4.69	+
11	4.77	+
13	4.84	+
15	4.30	+
17	4.30	+
19	4.30	+
21	4.00	+
23	4.00	+
25	4.00	+
27	4.30	+
29	4.47	+
31	4.00	+
33	4.00	+
35	4.00	+
37	4.00	+
39	4.00	+
41	4.30	+
43	4.30	+

Table 3.17: Results for the first 20N Planova® filter

Collection sample	Log_{10} DNA concentration (IU/ml)	Agarose gel result
44	4.00	+
46	4.00	+
48	4.30	+
50	4.30	+
52	4.00	+
54	4.30	+
56	4.47	+
58	4.30	+
60	4.30	+
62	4.30	+
64	4.00	+
66	4.30	+
68	4.47	+
70	4.30	+
72	4.60	+
74	3.84	+
76	3.84	+
78	3.30	+
80	3.84	+
82	3.69	+
84	3.69	+
86	3.30	+

Table 3.18: Results for the second 15N Planova® filter

Collection sample	Log_{10} DNA concentration (IU/ml)	Agarose gel result
87	3.00	+
89	4.00	+
91	4.00	+
93	4.00	+
95	4.00	+
97	3.77	+
99	3.84	+
101	3.47	+
103	4.00	+
105	3.77	+
107	3.69	+
109	3.84	+
111	3.69	+
113	3.77	+
115	3.69	+
117	3.69	+
119	3.84	+
121	3.69	+
123	4.00	+
125	4.00	+
127	3.47	+
129	3.30	+

Table 3.19: Results for the second 20N Planova® filter

Collection sample	Log_{10} DNA concentration (IU/ml)	Agarose gel result
130	<limit of quantitation	+ (faint)
132	3.00	+
134	3.60	+
136	4.00	+
138	3.47	+
140	3.60	+
142	3.60	+
144	3.69	+
146	3.69	+
148	3.60	+
150	4.00	+
152	3.90	+
154	4.00	+
156	3.60	+
158	3.60	+
160	3.30	+
162	3.60	+
164	3.47	+
166	3.00	+
168	3.47	+
170	3.00	+
172	3.30	+

Table 3.20: Results for the third 15N Planova® filter

Collection sample	Log_{10} DNA concentration (IU/ml)	Agarose gel result
173	<limit of quantitation	+ (faint)
175	3.30	+
177	3.00	+
179	3.30	+
181	3.60	+
183	3.00	+
185	3.30	+
187	3.30	+
189	3.30	+
191	3.00	+
193	3.47	+
195	3.47	+
197	3.00	+
199	3.30	+
201	3.00	+
203	3.47	+
205	3.30	+
207	3.30	+
209	3.17	+
211	3.60	+
213	3.60	+
215	3.69	+

Table 3.21: Results for the third 20N Planova® filter (N/D: Not Done)

Collection sample	Log_{10} DNA concentration (IU/ml)	Agarose gel result
216	<limit of quantitation	N/D
218	<limit of quantitation	N/D
220	3.00	N/D
222	<limit of quantitation	N/D
224	3.30	N/D
226	<limit of quantitation	N/D
228	3.00	N/D
230	<limit of quantitation	N/D
232	3.00	N/D
234	3.30	N/D
236	<limit of quantitation	N/D
238	<limit of quantitation	N/D
240	<limit of quantitation	N/D
242	<limit of quantitation	N/D
244	3.30	N/D
246	3.00	+
248	3.30	+
250	3.47	+
252	3.00	+
254	3.30	+
256	3.39	+
258	<limit of quantitation	+

A summary of the six experiments with 15N and 20N filters is shown in table 3.22, where the average log_{10} reduction was calculated.

The statistics were done by Mr A. Heath (Department of Informatics, NIBSC). The overall log_{10} reduction mean for the 15N and 20N filters were 5.88 and 6.26, respectively, and the standard deviations were 0.44 and 0.51, respectively. Given the variability in the data, the difference in log_{10} reduction was found not significant ($p=0.38$) between the two filter sizes, using a t-test. Therefore, both 15N and 20N filters can efficiently be used for parvovirus B19 nanofiltration.

Table 3.22: Results summary

Experiment number	Filter size	Pre-filtration log_{10} DNA concentration (IU/ml)	Post-filtration log_{10} DNA concentration (IU/ml)	Log_{10} reduction
1	15	9.68	4.27	5.41
2	15	9.68	3.75	5.93
3	15	9.68	3.39	6.29
4	20	9.68	3.89	5.79
5	20	9.68	3.49	6.19
6	20	9.68	2.87	6.81

III.5.2. Virus inactivation by dry-heat treatment at 80°C on the freeze-dried 8Y product: Bioproducts Laboratory, UK

High titre B19 virus stock ($1x10^{12}$ IU/ml) was used by Dr P. Roberts at BPL for the inactivation experiment by dry heating. The spiking step, for both controls and test samples, was performed at a ratio of 1 in 100 before freeze-drying and dry-heating. Three controls were prepared; the spiked product control, the spiked medium control and the unspiked 8Y product. The first control contained the product: BPL's intermediate purity factor VIII (8Y), which had been spiked with B19. The second control consisted of medium (MEM with FCS), which had also been spiked with human parvovirus B19. Finally, the last control was unspiked factor VIII (8Y). Duplicates were prepared for each of the control samples. Three additional samples were product spiked with B19 and subjected to freeze-drying using the standard cycle for this product. The freeze-dried products were either left unheated, as was the case for spiked test sample 1, or subjected to dry-heat treatment for various times: spiked test sample 2 was heated to

80°C for 24 hours while spiked sample 3 was incubated at 80°C for 72 hours. The parvovirus B19 DNA titres and the infectivity were determined in all six samples. Table 3.23 shows the results of the B19 DNA concentrations obtained by LightCycler PCR and the number of infectious units per ml obtained by the infectivity assay.

Table 3.23: Results of virus inactivation by dry-heat treatment at 80°C on freeze-dried factor VIII (8Y), including controls

Sample	Log_{10} DNA concentration (IU/ml)	Log_{10} infectious units/ ml
Spiked product control	10.60	5.0
Spiked medium control	10.60	7.0
Unspiked 8Y product	4.46	<limit of detection
Spiked test sample 1 (unheated)	10.17	6.0
Spiked test sample 2 (heated at 80°C for 24 hours)	9.43	3.5
Spiked test sample 3 (heated at 80°C for 72 hours)	9.49	<limit of detection

A contamination of the 8Y unspiked product was detected as the B19 DNA titre was found to be 10^4 IU/ml. However, no infectious units could be detected, suggesting that either the infectivity assay was not sensitive enough to detect such low infectivity or the virus present was not infectious. The dry-heat treatment at 80°C for 24 hours reduced infectivity by log_{10} 2.2 while a longer treatment of 72 hours resulted in a reduction of infectivity to such a level that it became undetectable by the assay. Dry-heating

treatment at 80°C for 72 hours thus seemed to be an effective inactivation method for human parvovirus B19.

III.5.3. Virus inactivation by *SuperFluids*™: Aphios Inc., USA

For each of the six experiments showed in table 3.24, 0.5ml of B19 virus stock ($1x10^{12}$ IU/ml) was diluted in 12.25ml of normal human plasma (supplied by NIBSC) and 12.25ml of MEM media (Gibco). All experiments were done at Aphios Inc and three supercritical fluids (Freon-22, Freon-23 and N_2O/CO_2) were used at either 25°C or 50°C.

Table 3.24: Experimental Conditions for virus inactivation by *SuperFluids*™

Experiment number	*SuperFluids*™	Pressure (bars)	Temperature (°C)	Flow rate (ml/min)	No. of Stages
NIBSC-01	Freon-22	206	50	4	2
NIBSC-02	Freon-22	206	25	4	1
NIBSC-03	Freon-23	206	50	4	1
NIBSC-04	Freon-23	206	25	4	1
NIBSC-05	N_2O/CO_2[a]	206/137[b]	50	4	2
NIBSC-06	N_2O/CO_2[a]	206/137[b]	25	4	2

[a] N_2O/CO_2 : N_2O with trace quantities of CO_2

[b] 206 bars in first chamber and 137 bars in the second chamber

Five or six samples were produced in each of the six experiments. A 2.5ml aliquot of the feed was taken at the start of the treatment and stored at 4°C during the run (named

"before") and a second 2.5ml sample was placed at the same temperature as the *SuperFluids*™ system for the same duration as a control (named "time and temperature"). The remaining 20ml of 1:50 diluted B19 was used as feed for the run.

Once the system (isobaric chamber, connecting lines, valves and gauges) was pressurised with the supercritical fluid, the sample was pumped through the isobaric chamber at the rate of 4 ml/min. Sample #1 was collected at this stage and was considered representative of the product stream. The supercritical fluid was then pumped through the system at a lower flow rate (1ml/min), in order to displace any sample remaining in the system, at which stage sample #2 was collected. Finally, the system was depressurised to atmospheric pressure (1.01bars) and sample #3 was collected. Samples #2 and #3 are considered representative of waste streams.

The results of these experiments are shown in tables 3.25 to 3.30.

Table 3.25: Results for experiment NIBSC-01

Sample	Log_{10} DNA concentration (IU/ml)	Log_{10} infectious units/ ml
"Before"	11.00	5.0
CFI-treated #1	10.69	3.0
CFI-treated #2	11.47	3.5
CFI-treated #2	10.77	3.0
CFI-treated #3	11.69	<limit of detection
"Time and temperature"	11.69	5.0

Table 3.26: Results for experiment NIBSC-02

Sample	Log_{10} DNA concentration (IU/ml)	Log_{10} infectious units/ ml
"Before"	11.47	5.0
CFI-treated #1	11.30	5.0
CFI-treated #1	11.30	4.5
CFI-treated #2	10.69	5.5
CFI-treated #3	10.90	5.0
"Time and temperature"	10.88	4.0

Table 3.27: Results for experiment NIBSC-03

Sample	Log_{10} DNA concentration (IU/ml)	Log_{10} infectious units/ ml
"Before"	11.30	4.0
CFI-treated #2	11.95	3.5
CFI-treated #3 (3ml)	11.84	4.0
CFI-treated #3 (3.7ml)	11.23	4.5
"Time and temperature"	11.23	4.5

Table 3.28: Results for experiment NIBSC-04

Sample	Log_{10} DNA concentration (IU/ml)	Log_{10} infectious units/ ml
"Before"	10.47	4.5
CFI-treated #1	10.47	6.0
CFI-treated #1	10.30	5.5
CFI-treated #2	10.47	4.5
CFI-treated #3	10.00	6.5
"Time and temperature"	10.47	6.0

Table 3.29: Results for experiment NIBSC-05

Sample	Log_{10} DNA concentration (IU/ml)	Log_{10} infectious units/ ml
"Before"	10	4.0
CFI-treated #1	10	<limit of detection
CFI-treated #1	10	<limit of detection
CFI-treated #2	10.47	4.5
CFI-treated #3	10.47	5.0
"Time and temperature"	10.69	4.5

Table 3.30: Results for experiment NIBSC-06

Sample	Log_{10} DNA concentration (IU/ml)	Log_{10} infectious units/ ml
"Before"	10.30	5.5
CFI-treated #1	10.30	4.5
CFI-treated #1	10.30	5.0
CFI-treated #2	10.30	6.5
CFI-treated #2	9.90	6.0
"Time and temperature"	10.30	5.0

The B19 DNA titre remained relatively unchanged for all the samples in these experiments. In NIBSC-01, with SuperFluids™ Freon-22 at 206 bars and 50°C in a two-stage laminar flow CFI unit, no infectivity was detected in "CFI-treated #3" sample (infectivity assay repeated twice). This experiment showed that the treatment resulted in at least a log_{10} 4 reduction in infectivity. On the other hand, there was no significant reduction in the infectivity of the treated samples compared with the controls was observed in experiments NIBSC-02, 03, 04 and 06. In experiment NIBSC-05 using a

mixture of N_2O and CO_2 at 206 bars at 50°C and a two-stage laminar flow CFI unit, more than $\log_{10}$ 5 of parvovirus B19 spiked into plasma were inactivated.

III.5.4. Virus inactivation by the INACTINE™ system: Vitex, USA

Some B19 virus stock ($1x10^{12}$ IU/ml) was sent to VI Technologies, where it was diluted 1:20 in negative serum and where all inactivation experiments were performed. As preliminary experiments, these studies were performed on AS1 RBCs storage solution only, which was spiked 10% v/v with the 1:20 virus dilution.

The inactivation experiments were done in duplicate and samples was labelled A and B. Samples labelled TS3, TS6, TS18 and TS22 were treated for 3, 6, 18 and 22 hours, respectively. Samples labelled PC0 and PC22 were controls, which were spiked samples incubated for 0 and 22 hours, but not treated with INACTINE™. Three additional controls were included in the experiments; the spiked dilution of human parvovirus B19 (1:20) used for spiking and two cytotoxicity controls. Cytotoxicity control 1 (CC1) contained AS1, PEN 110 and the medium used to quench the PEN110 (STS/MOPS). Instead of removing PEN 110 to a non-toxic level by cell washing, the PEN 110 reaction was chemically quenched, which is common practice for virus inactivation studies (Lazo *et al.*, 2002). Cytotoxicity control 2 (CC2) consisted of the RBC resuspension medium AS1.

In order to evaluate the potential cytotoxic effect of AS1 medium, PEN 110 and STS/MOPS medium, both cytotoxicity controls were incubated with UT-7/EPO-S1 cells following the same protocol as the infectivity assay. CC1 and CC2 were diluted into pH 5.7 phosphate buffer and a negative control inoculated with pH 5.7 phosphate buffer only was included in the experiment. Two time points were investigated: 2 hours after incubation of the cells and controls at 4°C and 2 days post-inoculation. At each

time point, the cells were examined under the light microscope for cytopathic effects and the live cells were counted.

The microscopic examination of the UT-7/EPO-S1 cells after 2 hours and 2 days post-inoculation did not detect any cytopathic effect as compared to the negative controls which were inoculated with pH 5.7 phosphate buffer only. The cell counts are shown in tables 3.31 (CC1) and 3.32 (CC2). There was no significant difference between the cell counts of the negative controls and those of the cytotoxicity controls CC1 and CC2, which suggested that AS1 medium, STS/MOPS medium, STS/MOPS medium and PEN 110 did not have any cytotoxic effect on UT-7/EPO-S1 cells.

Table 3.31: Cell counts with cytotoxicity control 1 (CC1)

Sample	Cell count after 2 hours incubation at 4°C (cells/ml)	Cell count 2 days post-inoculation at 37°C (cells/ml)
CC1 neat	2.95×10^5	4.97×10^5
CC1 1:10	3.65×10^5	4.27×10^5
CC1 1:100	2.52×10^5	4.35×10^5
CC1 1:1,000	2.47×10^5	4.32×10^5
CC1 1:10,000	2.1×10^5	4.8×10^5
Negative control	2.22×10^5	3.9×10^5

Table 3.32: Cell counts with cytotoxicity control 2 (CC2)

Sample	Cell count after 2 hours incubation at 4°C (cells/ml)	Cell count 2 days post-inoculation at 37°C (cells/ml)
CC1 neat	2.07×10^5	4.25×10^5
CC1 1:10	1.82×10^5	3.65×10^5
CC1 1:100	2.22×10^5	4.01×10^5
CC1 1:1,000	2.1×10^5	4.15×10^5
CC1 1:10,000	2×10^5	4.2×10^5
Negative control	2.62×10^5	4.8×10^5

Samples were tested by the B19 infectivity assay after determination of the B19 DNA concentration and the results are shown in table 3.33.

Table 3.33: Results of virus inactivation by INACTINE™ treatment, including controls

Sample	Log_{10} DNA concentration (IU/ml)	Log_{10} infectious units/ ml
TS3A	7.30	<limit of detection
TS6A	6.47	<limit of detection
TS18A	4.47	<limit of detection
TS22A	3.60	<limit of detection
PC0A	10	5.5
PC22A	10	5
TS3B	5	<limit of detection
TS6B	4	<limit of detection
TS18B	<limit of quantitation	<limit of detection
TS22B	<limit of quantitation	<limit of detection
PC0B	7.47	3.0
PC22B	7.69	1.5
B19 1:20	11.60	7.0

In experiment A, the results for the non-treated spiked controls (PC0A and PC22A) showed high DNA titres of $\log_{10}$ 10 and comparable $\log_{10}$ infectivity titres of 5.5 and 5, respectively. The DNA titre $\log_{10}$ reduction between PC0A and TS3A, the first sample taken out, was $\log_{10}$ 3, which was quite significant after only 3 hours of treatment. Then the B19 DNA titre in samples decreased by $\log_{10}$ 1 at each time point, except between 6 and 18 hours, where the DNA titre decreased by $\log_{10}$ 2. Infectivity at the different time point samples was not detectable, even at the first time point after 3 hours of treatment. In experiment B, a $\log_{10}$ 2 reduction was observed in the DNA titre from time 0 to time 3 hours followed by a further $\log_{10}$ 1 reduction after another 3 hours treatment. No B19 DNA could be detected in the following two time points after 18 and 22 hours. As in experiment A, the infectivity of these time point samples was not detectable, suggesting a decrease in infectivity when compared to PC0B sample.

III.5.5. Virus inactivation by S-59: the Helinx® technology: Cerus Corporation, USA

High titre B19 virus JS isolate ($1x10^{12}$ IU/ml) was used for the spiking experiments, where it was diluted at 1:10 into PBS, with a final volume of 10ml. A 6 mL aliquot was treated with 150µM Amotosalen HCl (S-59) and 3.0 Joules/cm^2 (J/cm^2) UVA illumination. A 1ml aliquot of the untreated 1:10 sample, which was also a control for the shipping and multiple freeze/ thaws was sent back to NIBSC for analysis, along with a 3ml aliquot of the treated sample. Aliquots of the same samples were also kept at Cerus Corporation to assay in an EliSpot assay.

Parvovirus B19 DNA titres were measured by LightCycler real-time PCR, using B19 international standard as a reference. In addition, serial dilutions of the samples were

used to infect UT-7/EPO-S1 cells, from which RNA was extracted after 2 days. The presence of B19-specific mRNA transcripts was detected by RT-PCR amplification. Table 3.34 shows the results obtained at NIBSC for the B19 DNA quantification and the infectivity assay.

Table 3.34: Results of photochemical inactivation with S-59

Sample	Log_{10} DNA concentration (IU/ml)	Log_{10} infectious units/ ml
Untreated	10.95	7.5
Treated 3J	9.30	3.0

The results showed that the log_{10} DNA concentration for the untreated and 3J treated samples were 8.45 and 3.3, respectively. The infectivity titre for the treated sample was log_{10} 2.8 while that of the untreated sample was log_{10} 6.8, suggesting a log_{10} 4 reduction.

Chapter IV: General discussion

Up to now, model viruses, such as canine (CPV), porcine (PPV) and murine (MVM) parvoviruses, have been used to study the efficacy of inactivation procedures for human parvovirus B19 because of the lack of a reproducible infectivity assay for the latter. Although CPV and B19 have similar properties, notably antigenic, there is no cross-reactivity of antibodies to CPV with B19, indicating different surface structures (Chapman and Rossmann, 1993; Agbandje *et al.*, 1994). These differences were confirmed by recent studies at the Paul Erlich Institute, Germany. The first study, which investigated the efficacy of viral inactivation by pasteurisation using both PPV and B19, revealed that heat resistance of B19 markedly differs from heat resistance of animal parvoviruses (Blümel, 2004). B19 was inactivated after 10 minutes at 60°C by at least $\log_{10}$ 4 whereas porcine parvovirus was resistant at 60°C. The second study looked at low pH treatment to inactivate MMV and B19 and found that the virus clearance for the latter was greater than $\log_{10}$ 5 after 2 hours at pH 4, whereas MMV was resistant over 9 hours (Boschetti *et al.*, 2004). These data show that parvovirus B19 was much more vulnerable toward low pH conditions than MMV. These new findings highlight the fact that animal parvoviruses are not suitable models to evaluate B19 inactivation since they seem to behave differently.

The present study was designed to develop a robust and reproducible infectivity assay for parvovirus B19. This assay was then used to evaluate several novel pathogen inactivation and removal methods. In addition, a reproducible quantitative DNA assay was developed using the WHO International Standard for B19 DNA.

Several approaches were investigated to determine parvovirus B19 infectivity. The initial attempts used mobilized stem cells (CD34+) from peripheral blood in a variety of formats: IFA staining of inoculated cells, detection of mRNA transcripts specific for parvovirus B19 in inoculated cells and a BFU-E reduction assay for B19. The FACS

results for the CD34+ cell preparations showed that CD34+ cell isolation from mobilised peripheral blood was not completely efficient since these cells were not the sole cell population in the samples. However, since the majority of the cells isolated were actually bearing CD34, this result might not have interfered with the outcome of the IFA. It was not possible to demonstrate viral replication in any of the samples of CD34+ cells inoculated with B19 virus with the antibodies tested i.e. mouse monoclonal antibody anti-VP1/VP2, human monoclonal antibody anti-NS1 or rabbit polyclonal antibody. However, it was possible to amplify B19 specific mRNA transcripts from B19 inoculated cells isolated from the peripheral blood of one of the patients. This result suggested that viral replication was occurring in these haematopoitic stem cell progenitors, but at a level that was not detectable by immunofluorescence. In contrast, when CD34+ cells were plated in Fox's medium to obtain BFU-E colonies, cells from the resulting colonies were susceptible to B19 infection and this could be demonstrated by IFA using anti VP1/VP2 monoclonal antibody. However, this result was not consistent, and positive results were only obtained with cells from a few patients. Only a minority of the cells was infected and specific fluorescence, in contrast to detection of mRNA, could only be detected 3-7 days post infection.

Since cells from different patients were used in the IFA and RT-PCR detection of mRNA transcripts, this might account for the difference in results. Such variability had already been observed in data from the BFU-E reduction assay, which used apheresis cells collected from different patients every week. It would have been better to have tested CD34+ cells isolated from the same patient by IFA and mRNA transcript amplification but this was not possible due to the limited number of cells obtained from any one patient. Another explanation could be that these CD34+ cells might only support viral transcription but not translation into proteins, which could account for the

detection of B19 specific mRNA transcripts by PCR but not detection of viral proteins by IFA.

The results of the BFU-E reduction assays were dependent on the source of the cells. One factor that could have influenced the results of the BFU-E reduction assay was the anti-B19 IgG status of the donors and this was tested in some of the samples, where serum was available. Theoretically, CD34+ cells from patients who were anti-B19 IgG positive could contain sufficient antibody which could neutralise all or part of the B19 inoculum resulting in a decrease in the BFU-E reduction percentage compared with cells from B19 antibody negative patients. In practice, the data showed that this was not the case and the figures for donors 17 and 19 were examined more closely. These two patients were chosen because the former presented the strongest IFA results and the highest cut off value (9.3) for anti-B19 IgG whereas the latter showed no positive staining by IFA and a clear negative result in EI. When inoculated with the same virus dilution, $2x10^7$ IU/ml, the percentage BFU-E reduction for patient 17 (IgG positive) was 54.88% whereas that for patient 19 (IgG negative) was 31.01%. These results do not support the theory that cells from B19 antibody positive patients lead to a decrease in the BFU-E percentage reduction result. Alternatively, the anti-B19 IgG present in the serum of patients might not have been neutralising antibodies or that the apheresis samples used in this study were free from antibodies.

In addition to the discrepancy of results seen for B19 infection in primary cells from different patients, other important issues were the availability of these cells and their accessibility. Since one of the aims of this thesis was to develop an infectivity assay that could be used widely in research and diagnostic laboratories, it was crucial for the cells used to be readily available and accessible. This was not the case for either the apheresis cells or the mobilised peripheral blood from which CD34+ cells could be isolated.

Therefore, B19 susceptible continuous cell lines, which subsequently became available, were used for the establishment of a B19 infectivity assay.

When continuous cell lines were investigated, either no immunofluorescence could be detected, such as in TF-1 cells, or a very small proportion of cells showed infectivity: only ~1% of UT-7/EPO-S1 cells, ~5% of UT-7/EPO cells and ~10% of KU812 and KU812Ep6 cells displayed fluorescence when inoculated with high titre parvovirus B19 ($\geq 10^9$ IU/ml) and stained with mouse monoclonal antibody anti-VP1/VP2 (Novocastra). The brightest fluorescence was found in KU812Ep6 cells. The semi-permissiveness of the cells might account for the lack of sensitivity of the IFA. Alternatively, incomplete replication, such as production of replicative intermediates and transcription without translation resulting in a non-productive infection or cell death by apoptosis as has been observed in previous studies may also explain these results (Leruez *et al*, 1994; Gallinella *et al*, 2000; Morita *et al*, 2001). In addition to the other drawbacks, the need for very high titre inoculum resulted in the use of this assay being abandoned for a more sensitive and reliable assay, which was the detection of mRNA transcripts by nucleic acid amplification.

Although there have been several reports in the literature of continuous cell lines, usually of erythroid lineage, supporting the replication of parvovirus B19 (Shimomura *et al.*, 1992; Munshi *et al.*, 1993; Takahashi *et al.*, 1993; Kumatsu *et al.* 1993; Nakazawa *et al.*, 1989; Miyagawa *et al.*, 1999), the ability of these cells to support replication of B19 has been poor compared with other virus-cell culture systems (such as polio virus replication in Vero cells (Montagnon *et al.*, 1983).

Early on in this study, a comparison of various continuous cell lines, namely KU812, KU812Ep6 and UT-7/EPO, showed that the most suitable cells for the B19 infectivity

assay were KU812Ep6. However, due to a strict confidentiality agreement with the Japanese laboratory providing those cells, they could not be used to determine the efficacy of virus removal/ inactivation techniques by private companies. In the meantime, a clonal cell line, called UT-7/EPO-S1, was reported to be superior to its parental line (UT-7/EPO) at supporting the replication of B19 (Morita *et al.*, 2001). The UT-7/EPO-S1 cells were thus tested in the B19 infectivity assay and appeared to be stable and reliable, giving consistent results at various passages (tested up to passage n+53). Optimisation of the infectivity assay, which depended on the detection of B19 mRNA transcripts, was done, including the number of cells to be inoculated with the virus ($2x10^5$ cells), mRNA extraction method (from cell cytoplasm) and time of extraction post-infection (2 days). The evaluation of the optimal method of nucleic acid extraction for this particular assay involved the comparison of extraction of total nucleic acids (Nuclisens™; Organon Teknika) with extraction of poly A^+ RNA from whole cells (Oligotex direct mRNA kit; Qiagen) or from cell cytoplasm (Oligotex direct mRNA kit; Qiagen). The best method was found to be poly A^+ RNA from cell cytoplasm. This result was to be expected since it would result in a better yield of mRNA than the extraction of total nucleic acid and since the spliced transcripts would be found in the cell cytoplasm. The splicing event occurs in the nucleus, where the transcript is capped at the 5' end, has the introns removed and is polyadenylated at the 3' end. The mRNA is then transported through nuclear pores to the cytoplasm, where it is available to be translated. In conclusion, after establishing that the Oligotex direct mRNA extraction from cell cytoplasm (Qiagen) was the most suitable and specific method for the isolation of mRNA, the batch format was also confirmed to be the most efficient way to provide optimum yield. Replicate infectivity assays of a stock of B19 indicated that the 95% detection limit of this assay was $\log_{10}$ -6.03 dilution (range -5.82

to 6.24), equivalent to $\log_{10}$ 5.97 IU/ml and the 50% detection limit was $\log_{10}$ -6.67 (range -6.46 to -6.87), equivalent to $\log_{10}$ 5.35 IU/ml. This validation study showed good reproducibility of the infectivity assay, which was much better than that of the BFU-E reduction assay. This assay was used for the evaluation of the inactivation protocols investigated. The B19 isolate JS, which had high DNA and infectivity titres, was used in these studies. High DNA titre inoculi were essential since the ratio of DNA concentration to infectious units was high (10^4:1 to10^5:1). This phenomenon was mainly due to the semi-permissive nature of the cell line UT-7/EPO-S1 used in the infectivity assay, although the presence of a high proportion of defective, non-infectious particles cannot be ruled out.

Multiplex RT-PCR conditions were also optimised by looking at different primer combinations, actin primers concentration and annealing temperature. Parvovirus B19-specific primers B19-9 and XPP-2 were chosen in the presence of Q buffer for greater specificity. The optimum concentration of actin-specific primers was found to be 5pmol/µl and the annealing temperature was set at 50°C for best results.

A final parameter examined in this study was the influence of hypoxia on the susceptibility of cells to B19 infection following the results of a published study which indicated that cells grown in hypoxic conditions had increased susceptibility to B19 infection (Caillet-Fauquet *et al.*, 2004a). Three sets of conditions were investigated: normal oxygen concentration (20%) before and after inoculation with JS isolate, normal oxygen concentration (20%) before but hypoxia (3%) post-inoculation and lastly hypoxia (3%) before and after inoculation. Extraction of mRNA was performed 24, 48 and 72 hours post-inoculation. No B19 replication could be detected in the first time point (24 hours). However, in those UT-7/EPO-S1 cells cultured in normal conditions (20%) before and after inoculation, as well as those first cultured with 20% oxygen then

3%, the number of infectious particles detected was 10^7 inf.u./ml after 48 and 72 hours. When the cells were incubated in hypoxia (3%) before and after inoculation with B19, the number of infectious particles detected was 10^8 inf.u./ml after 48 and 72 hours. Hypoxic conditions only after the addition of the virus did not seem to change the number of infectious units detected whereas hypoxia before and after infection seem to improve the results of the infectivity assay slightly ($\log_{10}$ 1). Even if this variation was not due to the assay variability but to the actual hypoxic conditions, it was not significant enough to justify the use of special equipment that might not be accessible to all laboratories. Although both the cell lines used in the present study (UT-7/EPO-S1) and that of Caillet-Fauquet and colleagues (KU812F) were from the erythroid lineage (Caillet-Fauquet *et al.*, 2004a), they could have reacted differently to hypoxic conditions, which might explain why their observations could not be reproduced in the system presented here. It would be interesting to test incubation of the cells in even more severe hypoxic conditions (1%) since it might increase the number of erythroid bursts generated from full-term CD34+ (Cipolleschi *et al.*, 1997) and was also claimed to increase viral capsid protein synthesis, virus replication and virus production in primary erythroid cells (Pillet *et al.*, 2004).

The establishment of the infectivity assay also allowed the study of parvovirus transcription since it was based on the detection of mRNA transcripts. According to a research study by Ozawa *et al.*, there is a splicing donor site (GT) at positions 407 and 408 (on the genome of M13784) and acceptor sites (AG) at positions 1908 and 1909, as well as at positions 2028 and 2029 (Ozawa *et al.*, 1987). The primers used for RT-PCR amplification, named B19-9 and XPP-2, were situated at position 384-405 and 2194-2214, respectively. Therefore, two products were expected of 305bp and 185bp.

Sequencing of these two transcripts was therefore performed to confirm the nature and positions of the spliced products specific to parvovirus B19. When compared to B19 genomic DNA (M13178), the longer transcript (upper band) corresponded to positions 384-406 and 1910-2193 while the shorter transcript (lower band) corresponded to positions 384-406 and 2030-2193. The transcripts sizes were therefore confirmed to be 305 bp and 185 bp, respectively. These results were thus in complete agreement with those of Ozawa *et al.* since they recognised the splicing donor site and the two splicing acceptor sites described in their transcription map (Ozawa *et al.*, 1987). Nevertheless, the novelty about the present study was that this transcription pattern was observed in the continuous cell line UT-7/EPO-S1, whereas human erythroid bone marrow cells obtained from patients with sickle cell disease had been used by Ozawa and colleagues. This observation thus confirmed that, although semi-permissive to B19 infection, this cell line was a good substitute to primary cells, which were less readily available.

A reproducible, quantitative B19 DNA NAT assay was successfully established. Dilutions of the WHO B19 International Standard were used for quantitation. This reagent was calibrated in arbitrary units, International Units (IU), which were closely related to the number of genomic copies. Thus, 1IU of this reference reagent corresponded to approximately 0.6-0.8 copies, depending on the assay method used (Saldanha *et al.*, 2002). Since it is very difficult to accurately quantitate the number of copies of viral genome in a sample, this titre represents the nearest approximation to the concentration of the virus.

SYBR green was used to detect the amplicons in this assay. However, despite attempts to reduce the background due to primer dimer formation by taking the fluorescence reading at a high temperature where the primer dimers would be expected to be

dissociated, it was clear that some fluorescence due to primer dimers was still obtained. This resulted in a "titre" which was read off the standard curve. However, examination of such samples by ethidium bromide agarose gel electrophoresis showed that these samples were negative as the specific B19 amplicon band was not observed. Therefore, sample with titres at or below $1x10^3$IU/ml were considered negative and this was taken as the lower limit of quantitation of the assay. It is now possible to overcome such problems with the use of fluorescently labeled, specific probes to detect amplicons. Such probes will only hybridise to the target amplicons and any primer dimers or non-specifically amplified DNA will not give a signal. Probes exist in a variety of formats, such as TaqMan, hybridization, Scorpion probes and Molecular Beacons. Programs exist for the optimum selection and design of primers and probes (Strategene). The majority of recent quantitative assays use some form of fluorescently-labelled probe to detect specific amplicons and this would now be the chosen method for any quantitative assay. However, at the time that this work was initiated, quantitative assays using probe technology were relatively rare and expensive. Therefore, an assay based on SYBR green detection was developed for the quantitation of B19 DNA.

The established quantitative assay was very reproducible with a standard deviation of the $\log_{10}$ titres for replicate assays done on different days of 0.092 i.e. 95% of individual results from repeat testing of this sample would be expected to fall within approximately two standard deviations of the mean i.e. +/- $\log_{10}$ 0.18IU/ml. The assay was used to titrate three B19 virus isolates which were used in the study as inoculi (JS, LP and JB). In addition, the titres of samples from the inactivation/removal studies were obtained with this assay.

Although the reliability of the infectivity assay was verified by statistical analysis, the clearance figures obtained with these methods are preliminary and approximate and it was not possible (due to time constraints and difficulty in repeating the inactivation protocols several times) to obtain more accurate figures for the inactivation. Nevertheless, the results of this study are sufficient to indicate the success or otherwise of these protocols.

According to the WHO guidelines on viral inactivation and removal procedures intended to assure the viral safety of human blood plasma products, "a robust, effective, reliable process step will be able to remove or inactivate substantial amounts of virus, typically $\log_{10}$ 4 or more, be easy to model convincingly and be relatively insensitive to changes in process conditions" (WHO Expert committee on Biological standardization, 2001). Moreover, if the $\log_{10}$ reduction is equal to or less than 1, it is considered insignificant.

The present study investigated five methods of virus removal/inactivation, in collaboration with various private companies. The techniques of inactivation were the well established dry-heat treatment at 80°C (BPL, UK) and the novel methods of super critical fluids (Aphios Inc., USA), INACTINE™ (Vitex, USA) and Helinx® (Cerus Corporation, USA). The last two methods of inactivation are similar in that both coumpounds used (INACTINE™ and S-59) are able to cross viral membranes and bind to and crosslink nucleic acids (DNA and RNA), thereby preventing replication. High titre human parvovirus B19 (B19 stock virus: isolate JS) was sent to the companies for spiking experiments and samples taken before, during and after the inactivation step were tested.

Viral removal procedures, which include chromatography and nanofiltration, should be distinguished from viral inactivation methods. In the case of viral removal, nucleic acid amplification is enough to evaluate the efficacy of the procedure. The latter is assessed by the viral clearance, which compares the viral load of the spiked material before removal step and at the end of the procedure. Removal depends on the protein composition and the separation conditions used, for instance the constant pressure applied during dead-end nanofiltration. The latter procedure, being non-invasive, has been the preferred virus removal technique because it can preserve both the structure and function of the plasma proteins. The efficacy of this method for the removal of B19 has been hampered by the lack of a suitable *in vitro* infectivity assay. Instead, model parvoviruses such as BPV (Burnouf-Radosevich *et al.*, 1994; Omar and Kempf, 2002), PPV (Troccoli *et al.*, 1998) and MVM (Omar and Kempf, 2002) have been used to test this system. These animal parvoviruses have a diameter between 15 and 20nm, whereas the B19 virus particles measure between 22 and 24nm in diameter (Cossart *et al.*, 1975). Thus the removal procedure evaluated in the present study was the nanofiltration using 15N and 20N Planova® filters, in collaboration with Asahi Kasei Pharma, Japan. These Planova® filters have already been shown to remove more than $\log_{10}$ 6.2 of CPV in IVIG with Planova® 15N and more than $\log_{10}$ 4.3 of PPV in factor VIII with Planova® 20N. Therefore, since nanofiltration is dependent on filter pore size, this clearance of animal parvoviruses suggests that human parvovirus B19 might also be removed by such a technique. The spiked product used in this study was 0.5% albumin solution. It was worth noting that the unspiked albumin solution was found to contain a small amount of B19 DNA (~$1x10^3$ IU/ml in samples A, the prefiltration feed and B, the prefiltration eluate). Since the presence of parvovirus B19 DNA in albumin batches has been reported previously (Saldanha and Minor, 1996), in the present study, the albumin

solution, which was of intermediate quality, might also have been contaminated with a low level of B19. As far as the nanofiltration efficiency was concerned, a good virus clearance was observed since the $\log_{10}$ reduction was between 5.41 and 6.81, when looking at 15 and 20N filters, respectively. Although at first glance, it seemed that B19 removal using 20N Planova® filter might be slightly better or almost the same compared to nanofiltration through a 15N filter, statistical analysis demonstrated that there was no significant difference between the two filters.

One of the advantages of Planova® filters, apart from its virus clearance properties, is the good product recovery rates (>95%) with the Planova® 35N filter for proteins up to molecular weight (MW) of about 800,000 (e.g., Factor VIII and IgG), with the Planova® 20N filter for proteins up to MW about 350,000 (e.g., Factor VIII and IgG), and with the Planova® 15N filter for proteins up to MW about 160,000 (e.g., Factor IX and IgG). The latter filter can thus allow the passage of the albumin protein used in the present study. However, the counterpart of this is the loss of larger proteins, as well as the difficult filtration of complex solutions, including whole plasma. The main limitations of nanofiltration remain the pore size of the filters and the relatively low flow rates.

Only one other study had already investigated the removal of parvovirus B19 from haemoglobin solutions by nanofiltration using a BMM-35 filter (mean pore size 35nm) followed by a BMM-15 filter (Abe *et al.*, 2000b). Although the median PCR titre was not changed after the BMM-35 filtration step, the second filter with smaller pore size resulted in more than $\log_{10}$ 6 reduction. Therefore, there was a correlation between the results obtained by Abe and colleagues and those presented here. Omar and Kempf used a different kind of membrane filter, from Pall Corporation, to determine whether antibody-coated viruses become large enough to be retained by nanofiltration with filters having apparent pore size larger than the free virions (Omar and Kempf, 2002).

Their theory was that, if the plasma pool would accidentally become contaminated with B19 from an infected donation, the antibodies present in other donations would bind to the virus particles, which thereby might lose all or part of their infectivity. These immune complexes would have an increased diameter, which should facilitate their removal by nanofiltration. These authors showed that BPV and MVM bound to antibodies were efficiently eliminated by filtration through Pall 20nm filters. However, according to their method, and since the filters pore sizes are larger than the diameter of the free virions, the latter, which are the potentially harmful viruses, would not be removed from the product. Therefore, this technique seems inappropriate to use in the manufacturing process of therapeutic products.

The use of filters with smaller pore sizes, such as Planova® 20N and 15N filters, thus appears the most suitable option for the effective elimination of human parvovirus B19 from albumin solution by nanofiltration.

A production process should include two complementary steps of virus inactivation/removal. The advantages of two methods acting through different mechanisms, frequently an inactivation step by a chemical treatment followed by a robust physical removal step, is the large spectrum of viruses susceptible.

As mentioned in chapter I, several cases of parvovirus B19 transmission by dry heat-treated coagulation factor concentrates have been reported (Yee *et al.*, 1995; Santagostino *et al.*, 1997; Blümel *et al.*, 2002b). Therefore, the efficacy of dry-heating treatment to inactivate human parvovirus B19 needed to be investigated further. In the present study, the average DNA concentrations of the spiked product and medium controls were 10^{10} IU/ml whereas the B19 infectivity titres were $\log_{10}$ 5.6 and $\log_{10}$ 7.6,

respectively. The $\log_{10}$ 2 difference between the product control and the medium control suggest that there might be some effect of the product on the infectivity assay itself. However, since the dry-heat treated spiked samples were compared with the unheated spiked sample, this effect of the product on the assay would not have altered the outcome of the inactivation experiment. Although the DNA titre of factor VIII 8Y (unspiked product) was 10^4 IU/ml, indicating a contamination of the product, no infectious units could be detected since the assay was not sensitive enough to detect such low infectivity. When human parvovirus B19 was studied, the dry-heat treatment at 80°C for 24 hours reduced infectivity by $\log_{10}$ 2.2 whereas a longer treatment of 72 hours allowed reduction of infectivity to such a level that it became undetectable in the infectivity assay. Dry-heating treatment at 80°C for 72 hours thus seemed to be an effective inactivation method for human parvovirus B19. However, even after such dry-heat treatment, product 8Y was reported to have transmitted B19 infection to an immunocompetent individual (Yee *et al.*, 1995). This implies that there must have been a massive challenge in that particular batch, possibly during an epidemic year.

Although the experimental conditions used here differed from the ones used to study CPV and BPV, the data obtained suggested that this inactivation method might be more effective on human parvovirus B19 than on model animal parvoviruses (Roberts and Hart, 2000). This would be in agreement with the study of human albumin pasteurisation, where human parvovirus B19 was inactivated much faster than the animal model PPV (Blümel *et al.*, 2002b). When the dry heat treatment studied here is compared to pasteurisation, it seems that the latter would be more rapid at inactivating B19. However, the data presented is preliminary and further studies should be performed, mainly to evaluate the efficacy of the dry heat procedure at several time points between 24 and 72 hours. This would allow the study of inactivation kinetics and

the determination of the best exposure time for a product such as BPL's intermediate purity factor VIII (8Y). As briefly mentioned above, the other important point that should be investigated is the influence of residual moisture in the lyophilised product. This matter was not taken into consideration in the present study because of its preliminary nature. However, a report investigating the thermal resistance of BPV showed that reducing the residual moisture from 2% to less than 1% resulted in the exposure time at 100°C being prolonged by 2.5 times in order to achieve the same level of inactivation (Brauniger *et al.*, 2000). Whether inactivation of human parvovirus B19 would also be susceptible to the amount of residual moisture in the lyophilised product tested remains to be determined. Both pasteurisation and dry heat treatments have been investigated using these viruses. As far as the former is concerned, although CPV was inactivated within 30 seconds at 60°C in the presence of 0.1M sodium hydroxide (NaOH), the model virus was shown to remain unaffected by heat treatment alone, at 60°C for 16 minutes (Borovec *et al.*, 1998). At a similar temperature, BPV also showed thermal resistance (Brauniger *et al.*, 2000). A recent study compared inactivation of B19 with that of PPV during pasteurisation of human serum albumin (Blümel *et al.*, 2002b). The model virus was resistant to treatment at 60°C whereas B19 was inactivated by $\log_{10}$ 4 or more after 10 minutes. This report highlighted that thermal resistance of B19 markedly differs from that of animal parvoviruses. Therefore, inactivation protocol efficiency data obtained with such animal models might not reflect the behaviour of human parvovirus B19. When the efficacy of dry heat treatment for the inactivation of CPV was evaluated, the animal virus presented no residual infectivity after 48 hours at 80°C or 10 hours at 90°C (Hart *et al.*, 1994). An even higher heat resistance was found for BPV at 100°C (Brauniger *et al.*, 2000). When the inactivation of both CPV and BPV by dry heating was compared in two high purity factor VIII concentrates, BPV was also

more resistant to heat treatment than CPV (Roberts and Hart, 2000). The inactivation after 72 hours at 80°C was indeed $\log_{10}$ 1.3 and 3.1, respectively in the first product, whereas it was $\log_{10}$ 0.2 and 1.3, respectively in the second product. This experiment thus suggested that dry-heat resistance depended not only on the virus itself, but also on the specific product tested. In contrast, Blümel and coworkers found that inactivation of B19 was independent of the albumin product tested (5, 20 and 25% albumin from three manufacturers) and of the specific virus source used for the inactivation (Blümel *et al.*, 2002b). This divergence of opinion about the influence of the product tested might be due to the fact that the products investigated were different: factor VIII concentrate in one case and human serum albumin in the other. Additionally, the viruses used to test the efficacy of the inactivation procedure were also different: animal parvoviruses (CPV and BPV) on one side and human parvovirus B19 on the other. Since these viruses have been shown to behave differently to heat treatment (Blümel *et al.*, 2002b), their thermal resistance might be influenced by different factors such as virus type or product being tested. The other possible explanation for the difference in resistance reported between the products could be differences in the available residual water rather than the products per se.

A couple of other research groups have studied the effects of pasteurisation on B19 erythrovirus by determining the decrease of viral DNA replication (Southern Blotting) and viral protein production (enzyme immunoassay) (Schwarz *et al.*, 1992b) or by infecting the erythroid cell line KU812Ep6, expressing the viral infectivity by its TCID50 ml (Miyagawa *et al.*, 1999). In the first study, plasma was spiked with B19 and treated at 60°C (Schwarz *et al.*, 1992b). Southern blot analysis showed no viral DNA after 20 minutes or more and no viral protein production could be detected in samples treated for 12 minutes or more. However, it was not possible to determine whether the

heat treatment completely inactivated parvovirus B19. The second study showed that B19 infectivity declined from 10^4 TCID50ml to less than 10 TCID50ml, which was the lower limit of detection, after 3 hours at 60°C or 30 minutes at 70°C, while it only decreased to $10^{2.5}$ TCID50ml in samples treated for 8 hours at 50°C (Miyagawa *et al.*, 1999).

The third method tested used *SuperFluids™* at various temperatures and pressure. In NIBSC-01, with SuperFluids™ Freon-22 at 206 bars and 50°C in a two-stage laminar flow CFI unit, there was approximately a $\log_{10}$ 2 clearance in infectivity titre of samples #1 and #2 compared with the untreated sample, but this may not be significant given the variability of the infectivity assay. In contrast, no infectivity was detected in "CFI-treated #3" sample (infectivity assay repeated twice). The "time and temperature" control sample had a similar infectious titre to the untreated sample indicating that the loss of infectivity was due to the treatment rather than incubation of the sample at an elevated temperature. This experiment showed that the treatment resulted in at least a $\log_{10}$ 4 reduction in infectivity. On the other hand, there was no significant reduction in the infectivity of the treated samples compared with the controls observed in experiments NIBSC-02, 03, 04 and 06.

In the NIBSC-05 experiment, more than $\log_{10}$ 5 of parvovirus B19 spiked into plasma were inactivated. The SuperFluid™ was a mixture of N_2O and CO_2 at 50°C and a two-stage laminar flow CFI unit was used (206 and 137 bars). The inactivation was more effective when N_2O/CO_2 was used compared with Freon-22 and Freon-23. In addition, higher levels of inactivation were obtained by SuperFluids™ at 50°C compared with 25°C. The absolute effect of temperature by itself was negligible and accounted for in time and temperature controls. It should be noted that at 25°C, the N_2O/CO_2 mixture is

sub-critical whereas the mixture is supercritical at 50°C (the critical temperatures of N_2O and CO_2 are respectively 36.41°C and 31.1°C). At 50°C, the N_2O/CO_2 mixture was supercritical since its pressure (206 bars) exceeded the critical pressures (respectively, 72.7 and 73.8 bars) of both N_2O and CO_2. It appears necessary that these fluids (N_2O/CO_2) must be supercritical, which can be achieved at pressures in excess of 74 bars and 37°C, in order to achieve high levels of B19 inactivation. In addition, the residence time was remarkably short (less than one minute). Finally, the use of additional isobaric chambers can improve the level of inactivation as seen in the experiment NIBSC-05 where two chambers were used. Thus, these preliminary studies showed that the *SuperFluids™* method using N_2O/CO_2 at 206 bars and 50°C in a two-stage laminar flow CFI unit seemed to be the most efficient one to inactivate human parvovirus B19.

The main advantage that *SuperFluids*™ have over currently available virus inactivation techniques is their ability to reduce the viral load of both enveloped and non-enveloped viruses. For instance, the viral load of enveloped viruses, such as Sindbis virus, can be reduced more than $\log_{10}$ 6 (Dr T Castor, personal communication). Similarly, non-enveloped virus loads, like adenovirus or poliovirus, can be decreased by $\log_{10}$ 5 and 4, respectively. Additionally, the integrity and therapeutic activity of plasma products treated with *SuperFluids*™ are preserved. However, this technique cannot be used on blood donations that still contain red blood cells because these fluids would damage them. The other advantages of this technique are the fact that they are readily separated, with no toxic residues and that the system can be easily scaled up to production levels with continuous flow operations.

The effect of the INACTINE™ treatment on human parvovirus B19, using PEN110, was also investigated. For experiment A, the results for the non-treated spiked controls (PC0A and PC22A) showed high DNA titres of $\log_{10}$ 10 and comparable $\log_{10}$ infectivity titres of 5.5 and 5, respectively. During the treatment, samples were taken at various time points: 3, 6, 18 and 22 hours. The B19 DNA titre in these samples decreased by $\log_{10}$ 1 at each time point, except between 6 and 18 hours, where the DNA titre decreased by $\log_{10}$ 2. This can be easily explained by the fact that the time interval was higher between the two samples: 12 hours compared to 3 and 4 hours between the other time points. On average, B19 DNA titres would thus drop by $\log_{10}$ 1 every 3 to 6 hours. Moreover, the DNA titre $\log_{10}$ reduction between PC0A and TS3A, the first sample taken out, was $\log_{10}$ 3, which was quite significant after only 3 hours of treatment. Infectivity at the different time point samples was not detectable, even at the first time point after 3 hours of treatment with compound A, when the DNA titre was $\log_{10}$ 7.3. Therefore, treatment with compound A seems to be very efficient at inactivating human parvovirus B19, even after a short incubation of 3 hours. In experiment B, the untreated spiked controls showed a B19 DNA titre of 10^7 IU/ml, whereas the infectivity titres were $\log_{10}$ 3.47 and 2.19 infectious units per ml, after 0 and 22 hours (PC0B and PC22B), respectively. A $\log_{10}$ 2 reduction was observed in the DNA titre from time 0 to time 3 hours followed by a further $\log_{10}$ 1 reduction after another 3 hours treatment. No B19 DNA could be detected in the following two time points after 18 and 22 hours. Similarly to experiment A, the infectivity of these time point samples was not detectable, suggesting a decrease in infectivity when compared to PC0B sample.

Although phase I clinical evaluation had shown that the PEN 110 process was able to inactivate both enveloped and non-enveloped viruses and that treated RBCCs were

therapeutically useful (AuBuchon *et al.*, 2002), phase III trials had to be suspended in PRT RBCs transfused repetitively because of the appearance of antibodies to treated cells (neoantibodies) (Vitex press release, 17th November 2003). The (photo)chemical treatments can indeed potentially interact with other targets than their intended ones (i.e. nucleic acid) and thereby yield an immunogen that could cause a response to treated cells or, by cross-reactivity, to untreated cells (AuBuchon, 2004). Nevertheless, the efficacy of this technique to inactivate other pathogens had already been proven in red blood cells with protozoan parasites (Zavizion *et al.*, 2004), WNV (Mather *et al.,* 2003), duck HBV (DHBV) as a model of HBV (Aytay *et al.*, 2004) and HIV (Ohagen *et al.*, 2002). In addition, toxicology studies have found that the trace amount of residual PEN110 in the purified blood component is well below the level that could present a risk of reproductive toxicity to the patient (Chapman *et al.*, 2003). Although the DNA titre of the treated sample was not significantly lower than one of the untreated samples (greater than $\log_{10} 2$), the number of infectious units, as determined by the infectivity assay, was reduced significantly by $\log_{10} 5.15$.

Finally, the Baxter INTERCEPT method (treatment with amotosalen S-59 and UVA), also known as the Helinx® technology, has been demonstrated to inactivate a variety of blood-borne pathogens, including viruses such as HIV, HBV, HCV (Sawyer *et al.*, 2003), West Nile virus and SARS coronavirus (Dupuis and Sampson-Johannes, 2003; Sawyer *et al.*, 2004) and murine CMV (Lin, 2001; Jordan *et al.*, 2004). Bacteria (both gram negative and positive) and protozoa such as *Plasmodium falciparum* (Dupuis *et al.*, 2003) or *Trypanosoma cruzi* (Van Voorhis et *al.*, 2003) have also been shown to be inactivated by amotosalen HCL (S-59) and ultraviolet light. However, apart from one abstract recently submitted to the American Association of Blood Banks (AABB)

meeting (Hanson *et al.*, 2004), there is no report to date on the efficacy of this method on human parvovirus B19. The present collaborative study with Cerus Corporation investigated the efficacy of this photochemical treatment on the inactivation of B19. The results showed that the $\log_{10}$ DNA concentration for the untreated and 3J treated samples were 8.45 and 3.3, respectively. The infectivity titre for the untreated sample was $\log_{10}$ 6.8 whereas that of the treated sample was $\log_{10}$ 2.8, resulting in a $\log_{10}$ 4 reduction. Aliquots of the same untreated and treated 3J samples were also tested by scientists at Cerus using an ELISpot assay (Dr. Kent Dupuis, personnel communication). The virus reduction was comparable in both the ELISpot and the infectivity assay developed in the present study. However, the latter seems to be more sensitive than the ELISpot assay since it was able to detect more infectious particles in both the untreated and 3J treated materials. The $\log_{10}$ reduction was also more than $\log_{10}$ 1 greater in the optimised infectivity assay compared with the ELISpot assay.

Unpublished data concerning B19 inactivation were obtained at Cerus and were kindly communicated by Dr. K Dupuis and Dr. L Sawyer (CA, USA). The restriction linked to inactivation of non-enveloped viruses such as B19 lies in the time necessary for amotosalen S-59 to penetrate the virus capsid. The influence of a pre-incubation period with S-59 prior to UVA illumination was thus investigated. The viable virus titres in both untreated and treated infected platelet concentrates were evaluated by infection of CD34+ cells and detection of their progeny by ELISpot assay. Data have shown that the longer the pre-incubation period with amotosalen, the higher the mean $\log_{10}$ reduction (Hanson *et al.*, 2004). When the sample was pre-incubated for less than 5 minutes, the mean $\log_{10}$ reduction was only 2.0 whereas it increased to 4.4 after 45 minutes and to 5.8 after 90 minutes pre-incubation with S-59. In comparison with the present study, which did not include a pre-incubation period with S-59 prior to illumination with

UVA, the $\log_{10}$ reduction was only slightly lower than a sample pre-incubated for 90 minutes ($\log_{10}$ 5.8) and almost equivalent to a 60 minutes pre-incubation period ($\log_{10}$ 5.3). However, it was difficult to conclude on this comparison since the methods used to determine viral infectivity were different: infection of CD34+ cells and ELISpot assay in one case (Hanson *et al.* 2004) and infection of UT-7/EPO-S1 cells and RT-PCR assay in the present experiment. In the latter, the sample was not deliberately pre-incubated but the time between the addition of S-59 and UVA treatment was around 10-15 minutes. At the time this study was done, the pre-illumination data mentioned above (Hanson *et al.*, 2004) had not been obtained. Due to the divergence of results, further work should be undertaken to investigate the exact role of a pre-exposure to S-59 and whether it is a necessary step in the inactivation of B19.

Platelets constitute an essential component of the coagulation process and may be required by patients with bleeding disorders or those undergoing surgery, cancer chemotherapy, transplantation. Some of the concerns in introducing a viral inactivation step in the manufacture of any product with medicinal properties are the safety aspect as well as the retention of the functional characteristics of the treated product. In the case of platelet concentrates, both these aspects have been investigated regarding the implementation of the Helinx® technology in their preparation. Preclinical safety studies of treated platelets concentrates showed no specific target organ toxicity, reproductive toxicity or carcinogenicity was observed (Ciaravino, 2001; Ciaravi *et al.*, 2001). Moreover, the quality of platelet concentrates prepared from pooled buffy coats and treated by INTERCEPT (S-59 and UVA) was found compatible with that of untreated platelets for up to 7 days of storage (van Rhenen *et al.*, 2000). In addition, a recent study reported only minor *in vitro* effects on the quality of treated platelets (Jansen *et al.*, 2004).

Taking into account that the inactivation rate by this method is related to genome size, another limiting factor in the inactivation of B19 is the small size of its genome. Large genomes such as those in leukocytes are indeed much more susceptible to inactivation than are viruses, such as hepatitis B virus (HBV), which can be inactivated by more than $\log_{10}$ 5 (Wollowitz, 2001). Inactivation of parvovirus B19 (by $\log_{10}$ 5.15 and 4) therefore seemed comparable to that of HBV, which has, however, a smaller genome than B19 (3.2 kb and 5.5 kb, respectively).

Although the INTERCEPT system appeared to be an efficient method for the inactivation of human parvovirus B19, the data obtained in the present experiment are preliminary and further research should be carried out to determine the optimum conditions that could be applied to blood-bank use.

The results of all the inactivation and removal protocols tested in the present study are summarized in table 4.1.

Table 4.1: Summary of virus inactivation/ removal data

PRT	$\mathbf{Log_{10}}$ reduction	Treated product
Nanofiltration	>5 for 15N filter >6 for 20N filter	0.5% albumin
Dry heat	>2 after 24 hours Not detected after 72 hours	Factor VIII
Super critical fluids	>5	Human plasma
PEN 110 (INACTINE™)	Not detected	RBCs storage solution
Psoralen S-59	>5	PBS

Overall, chemical methods have the advantage that they can be used on cells which do not have a nucleus (RBCs and platelets). However, the chemical introduced into the product can potentially be toxic, mitotic or/and carcinogenic and all traces of it need to be removed, adding another step to the inactivation process. Cell washing is usually used to remove the chemical at the completion of the red cell treatment. Moreover, recent press releases from Cerus (Cerus press release, 4th September 2003) and Vitex (Vitex press release, 23rd November 2004) have exposed the issue of autoantibodies production by some patients in their phase III clinical trials for S-303-treated RBCs and INACTINE™-treated RBCs, respectively. Cerus announced that they halted their trials when two patients who were enrolled indeed showed an antibody response but no clinical adverse events after transfusion with the S-303 treated RBCs. Similarly, Vitex announced that it was temporarily suspending enrolment in the ongoing Phase III surgical study for the INACTINE™ pathogen inactivation system for red blood cells. This decision was also made following identification of an immune response to treated RBCs in one patient. Although no clinical consequences of the immune response were apparent, potential modifications to the INACTINE™ treatment process which may result in red cells with reduced immunogenicity have already been identified and the revised process could potentially be ready for clinical trials in the second half of 2005. I would personally be interested in following the progress of these future trials to find out whether this improved chemical inactivation method can reduce the risk of autoantibodies being produced.

On the other hand, physical methods of inactivation have the distinct advantage that no chemical is introduced in the treated product, thereby abolishing any risk for toxicity. However, theses processes cannot be used to treat cells (RBCs and platelets), which

would be destroyed by such treatment. The fact that physical methods can only be used on plasma products is indeed a limiting factor.

In conclusion, this work will enable a better evaluation and characterisation of established pathogen removal /inactivation techniques using B19 rather than a model virus which may have different properties. The selection of the viral inactivation and removal methods to be employed depends on the size and labile nature of the protein being prepared, the method(s) of purification the manufacturer wishes to use, and the nature and titre of viruses which are of concern. Each method of inactivation and removal has special characteristics which need to be taken into account. Whether one or more methods of inactivation and removal are used, in addition to viral safety, the maintenance of protein structure and function is equally important and must be evaluated thoroughly.

Because of its preliminary functions, the present study did not include testing of the final product to show whether the removal/inactivation procedure had affected its biological and medicinal properties. Further investigations should therefore evaluate the product tested before and after the removal/inactivation step. This test seems less relevant for a virus removal step by nanofiltration since the protein chosen to be spiked should be much smaller than the filter pore size.

As far as the established infectivity assay is concerned, its uses are various. As mentioned above, further viral inactivation studies should be performed using this assay to evaluate the efficacy of the technique. In addition, considering the greater incidence and the possible impact of human parvovirus variants on blood products safety, this infectivity assay could be utilised to determine whether such variants might be potentially infectious. It might also be of interest to compare the behaviour of

parvovirus variants with that of B19 as far as viral inactivation is concerned. Although they might be unlikely to differ from B19 when novel inactivation methods are involved, such as INACTINE™, Helinx®, and Superfluids™, they might show different properties when physical inactivation such as dry-heat is applied.

References

Aalberse RC, van der Gaag R and van Leeuwen J. 1983. Serologic aspects of IgG4 antibodies: prolonged immunisation results in an IgG4-restricted response. J Immunol. 130(2): 722-726.

Abe H, Yamada-Ohnishi Y, Hirayama J, Owada T, Ikeda H and Ikebuchi K. 2000a. Elimination of both cell-free and cell-associated HIV infectivity in plasma by a filtration/methylene blue photoinactivation system. Transfusion 40(9): 1081-7.

Abe H, Sugawara H, Hirayama J, Ihara H, Kato T, Ikeda H and Ikebuchi K. 2000b. Removal of parvovirus B19 from hemoglobin solution by nanofiltration. Artif Cells Blood Substit Immobil Biotechnol. 28(5): 375-83.

Abe H and Wagner SJ. 1995. Analysis of viral DNA, protein and envelope damage after methylene blue, phthalocyanine derivative or merocyanine 540 photosensitization. Phototochem Photobiol 61: 402-409.

Aberham C, Pendl C, Gross P, Zerlauth G and Gessner M. 2001. A quantitative, internally controlled real-time PCR assay for the detection of parvovirus B19 DNA. J Virol Methods 92: 183-191.

Abkowitz JL, Brown KE, Wood RW, Cohen BJ, Kovach NL and Young NS. 1993. Human parvovirus B19 (HPV B19) is not a rare cause of anemia in HIV-seropositive individuals. Clin res 41(2): 393A.

Abraham M, Rudraraju R, Kannangai R, George K, Cherian T, Daniel D, Ramalingam S and Sridharan G. 2002. A pilot study on the seroprevalence of parvovirus B19 infection. Indian J Med Res. 115:139-43.

Adcock WL, MacGregor A, Davies JR, Hattarki M, Anderson DA, Goss NH. 1998. Chromatographic removal and heat inactivation of hepatitis A virus during manufacture of human albumin. Biotechnol Appl Biochem 28(1): 85-94.

Agbandje M, McKenna R, Rossmann MG, Kajigaya S and Young NS. 1991. Preliminary X-ray crystallographic investigation of human parvovirus B19. Virology 184: 170-174.

Agbandje M, McKenna R, Rossmann MG, Strassheim ML and Parrish CR. 1993. Structure determination of feline panleukopenia virus empty particles. Proteins: structure, function and genetics 16: 155-171.

Agbandje M, Kajigaya S, McKenna R, Young NS and Rossmann MG. 1994. The structure of human parvovirus B19 at 8 Å resolution. Virology 203: 106-115.

Ager EA, Chin TDY and Poland JD. 1966. Epidemic erythema infectiosum. N Engl J Med 275(24): 1326-1331.

Alexandersen S, Bloom ME and Wolfinbarger J. 1988. Evidence of restricted viral replication in adult mink infected with Aleutian disease of mink parvovirus. J Virol 62(5): 1495-1507.

Altschuler EL. 1999. Parvovirus B19 and the pathogenesis of rheumatoid arthritis: a case for historical reasoning. Lancet 354: 1026-1027.

Anand A, Gray ES, Brown T, Clewley JP and Cohen BJ. 1987. Human parvovirus B19 infection in pregnancy and hydrops fetalis. N Engl J Med 316(4): 183-186.

Anderson LJ, Tsou C, Parker RA, Chorba TL, Wulff H, Tattersall P and Mortimer PP. 1986. Detection of antibodies and antigens of human parvovirus B19 by enzyme-linked immunosorbent assay. J Clin Microbiol 24(4): 522-526.

Anderson LJ. 1987. Role of parvovirus B19 in human disease. Pediatr Infect Dis J 6(8): 711-718.

Anderson LJ, Gillespie SM, Török TJ, Hurwitz ES, Tsou CJ and Gary GW. 1990. Risk of infection following exposure to human parvovirus B19. Behring Inst Mitt 85: 60-63.

Anderson LJ and Hurwitz ES. 1988. Human parvovirus B19 and pregnancy. Clinics in Perinatology 15(2): 273-287.

Anderson LJ and Török TJ. 1989. Human parvovirus B19. N Engl J Med 321(8): 536-538.

Anderson LJ and Young NS (eds). 1997, Human Parvovirus B19. Monographs in Virology. Basel, Karger, vol 20.

Anderson MJ, Davis LR, Jones SE and Pattison JR. 1982a. The development and use of an antibody capture radioimmunoassay for specific IgM to a human parvovirus-like agent. J Hyg Camb 88: 309-324.

Anderson MJ, Davis LR, Hodgson J, Jones SE, Murtaza L, Pattison JR, Stroud CE and White JM. 1982b. Occurrence of infection with a parvovirus-like agent in children with sickle cell anaemia during a two-year period. J Clin Pathol 35: 744-749.

Anderson MJ, Jones SE, Fisher-Hoch SP, Lewis E, Hall SM, Bartlett CLR, Cohen BJ, Mortimer PP and Pereira MS. 1983. Human parvovirus, the cause of erythema infectiosum (fifth disease)? Lancet I: 1378.

Anderson MJ, Higgins PG, Davis LR, Willam JS, Jones SE, Kidd IM, Pattison JR and Tyrrell DAJ. 1985a. Experimental parvoviral infection in humans. J Infect Dis 152(2): 257-265.

Anderson MJ, Jones SE and Minson AC. 1985b. Diagnosis of human parvovirus infection by dot-blot hybridisation using cloned viral DNA. J Med Virol 15: 163-172.

Anderson MJ. 1987. Human parvovirus infections. J Virol Methods 17(1-2): 175-81.

Anderson S, Momoeda M, Kawase M, Kajigaya S and Young NS. 1995. Peptides derived from the unique region of B19 parvovirus minor capsid protein elicit neutralizing antibodies in rabbits. Virology 206: 626-632.

Anlar B, Öktem F and Török T. 1994. Human parvovirus B19 antibodies in infantile autism. J Child Neurol 9(1): 104-105.

Arista S, De Grazia S, Di Marco V, Di Stefano R and Craxì A. 2003. Parvovirus B19 and "cryptogenic" chronic hepatitis. J Hepatol 38(3): 375-376.

Arrighi S, Pacenti L and Borri MG. 1993. Factor VIII:c concentrate virus inactivated: progress in purification by using classic chromatographic methods. Vox Sang 64(1):13-8.

Astell CR, Thomson M, Merchlinsky M and Ward DC. 1983. The complete DNA saequence of minute virus of mice, an autonomous parvovirus. Nucleic Acids Res. 11: 999-1018.

Astell CR, Luo WL, Brunstein J and St Amand J. 1997. Parvoviruses and molecular features. In Monographs in Virology, Basel, Karger. Anderson LJ and Yougs (eds): Human parvovirus B19 vol 20, pp 16-41.

Aubin JT, Defer C, Vidaud M, Maniez Montreuil M and Flan B. 2000. Large-scale screening for human parvovirus B19 DNA by PCR: application to the quality control for fractionation. Vox Sang 78: 7-12.

AuBuchon JP, Pickard CA, Herschel LH, Roger JC, Tracy JE, Purmal A, Chapman J, Ackerman S and Beach KJ. 2002. Production of pathogen-inactivated RBC concentrates using PEN110 chemistry: a Phase I clinical study. Transfusion 42(2):146-152.

AuBuchon JP. 2004. Pathogen reduction technologies: what are the concerns? Vox Sang 87 Suppl 2: 84-89.

Avanzi GC, Brizzi MF, Giannotti J, Ciarletta A, Yang YC, Pegoraro L and Clark SC. 1990. M-07e human leukemic factor-dependent cell line provides a rapid and sensitive bioassay for the human cytokines GM-CSF and IL-3.J Cell Physiol. 145(3):458-64.

Aytay S, Ohagen A, Busch MP, Alford B, Chapman JR and Lazo A. 2004. Development of a sensitive PCR inhibition method to demonstrate HBV nucleic acid inactivation. Transfusion 44(4): 476.

Aznar JA, Molina R and Montoro JM. 1999. Factor VIII/von Willebrand factor complex in methylene blue-treated fresh plasma. Transfusion 39(7): 748-50.

Azzi A, Macchia PA, Favre C, Nardi M, Zakrzewska K and Bartolomei Corsi B. 1989. Aplastic crisis caused by B19 virus in a child during induction therapy for acute lymphoblastic leukaemia. Haematologica 74: 191-194.

Azzi A, Zakrzewska K, Gentilomi G, Musiani M and Zerbini M. 1990. Detection of B19 parvovirus infections by a dot-blot hybridisation assay using a digoxigenin-labelled probe. J Virol Methods 27: 125-134.

Azzi A, Ciappi S, Zakvrzewska K, Morfini M, Mariani G and Mannucci PM. 1992. Human parvovirus B19 infection in hemophiliacs first infused with two high-purity, virally attenuated factor VIII concentrates. Am J Hematol. 39(3): 228-30.

Azzi A, Fanci R, Ciappi S, Zakrzewska K and Bosi A. 1993. Human parvovirus B19 infection in bone marrow transplantation patients. Am J Hematol 44: 207-209.

Azzi A, Manaresi E, Zakrzewska K, DeSantis R, Musiani M, Zerbini M. Antibody response to B19 parvovirus VP1 and VP2 linear epitopes in patients with haemophilic arthritis. 2004. J Med Virol. 72(4): 679-82.

Bagot M and Revuz J. 1991. Papular-purpuric "gloves and socks" syndrome: primary infection with parvovirus B19? J Am Acad Dermatol 25: 341.

Balfour HH, Schiff GM and Bloom JE. 1970. Encephalitis associated with erythema infectiosum. J Pediatr 77(1): 133-135.

Ballou WR, Reed JL, Noble W, Young NS and Koenig S. 2003. Safety and immunogenicity of a recombinant parvovirus B19 vaccine formulated with MF59C.1. J Infect Dis 187: 675-8.

Bansal GP, Hatfiled JA, Dunn FE, Kramer AA, Brady F, Riggin CH, Collett MS, Yoshimoto K, Kajigaya S and Young NS. 1993. Candidate recombinant vaccine for human B19 parvovirus. J Infect Dis. 167: 1034-44.

Barah F, Vallely PJ, Chiswick ML, Cleator GM and Kerr JR. 2001. Association of human parvovirus B19 infection with acute meningoencephalitis. Lancet 358: 729-730.

Barrett PN, Meyer H, Wachtel I, Eibl J and Dorner F. 1997. Inactivation of hepatitis A virus in plasma products by vapor heating. Transfusion 37(2): 215-20.

Bartolomei Corsi O, Azzi A, Morfini M, Fanci R and Rossi Ferrini P. 1988. Human parvovirus infection in haemophiliacs first infused with treated clotting factor concentrates. J Med Virol 25(2): 165-70.

Baurmann H, Schwarz TF, Oertel J, Serke S, Roggendorf M and Huhn D. 1992. Acute parvovirus infection mimicking myelodysplastic syndrome of the bone marrow. Ann Hematol 64: 43-45.

Beard C, St Amand J and Astell CR. 1989. Transient expression of B19 parvovirus gene products in COS-7 cells transfected with B19-SV40 hybrid vectors. Virology 172(2): 659-64.

Bell LM, Naides SJ, Stoffman P, Hodinka RL and Plotkin SA. 1989. Human parvovirus B19 infection among hospital staff members after contact with infected patients. N Engl J Med 321(8): 485-491.

Bengtsson A, Widell A, Elmståhl S and Sturfelt G. 2000. No serological indications that systemic lupus erythematosus is linked with exposure to human parvovirus B19. Ann Rheum Dis 59: 64-66.

Berkman SA, Lee ML and Gale RP. 1988. Clinical uses of intravenous immunoglobulins. Sem Hematol 25(2): 140-158.

Berns KI. 1996. *Parvoviridae*: the viruses and their replication. Pages 2173-2197 in Fields Virology, Third edition, edited by Fields BN, Knipe DM, Howley PM *et al.*, Lippincott-Raven Publishers, Philadelphia.

Berns KI and Alder S. 1972. Separation of two types of adeno-associated virus particles containing complementary polynucleotide chains. J Virol 9(2): 394-396.

Bhambhani K, Inoue S, Sarnaik SA and Merline J. 1986. Transient erythroblastopenia of childhood not associated with human parvovirus infection. Lancet I: 509.

Blümel J, Schmidt I, Willkommen H, and Löwer J. 2002a. Inactivation of parvovirus B19 during pasteurization of human serum albumin. Transfusion 42(8): 1011.

Blümel J, Schmidt I, Effenberger W, Seitz H, Willkommen H, Herrmann Brackmann H, Löwer J, and Eis-Hübinger A-M. 2002b. Parvovirus B19 transmission by heat-treated clotting factor concentrates. Transfusion 42(11): 1473.

Blümel J. 2004. Cell culture-based assay of parvovirus B19 and the relevance of animal model viruses. Dev Biol (Basel) 118:107-112.

Blundell MC, Beard C and Astell CR. 1987. *In vitro* identification of a B19 parvovirus promoter. Virology 157(2): 534-538.

Blundell MC and Astell CR. 1989. A GC-box motif upstream of the B19 parvovirus unique promoter is important for in vitro transcription. J Virol 63(11): 4814-4823.

Bonsi L, Grossi A, Strippoli P, Tumietto F, Tonelli R, Vannucchi AM, Ronchi A, Ottolenghi S, Visconti G, Avanzi GC, Pegoraro L and Bagnara GP. 1997. An erythroid and megakaryocytic common precursor cell line (B1647) expressing both c-mpl and erythropoietin receptor (Epo-R) proliferates and modifies globin chain synthesis in response to megakaryocyte growth and development factor (MGDF) but not to erythropoietin (Epo). Br J Haematol 98(3): 549-59.

Borovec S, Broumis C, Adcock W, Fang R and Uren E. 1998. Inactivation Kinetics of Model and Relevant Blood-borne Viruses by Treatment with Sodium Hydroxide and Heat. Biologicals 26(3): 237-244.

Borreda D, Palomera S, Gilbert B, Lienhardt A and de Lumley L. 1992. A propos de vingt-quatre observations d'infections à parvovirus human B19 chez l'enfant. Ann Pédiatr (Paris) 39(9): 543-549.

Bos OJ, Sunye DG, Nieuweboer CE, van Engelenburg FA, Schuitemaker H and Over J. 1998. Virus validation of pH 4-treated human immunoglobulin products produced by the Cohn fractionation process. Biologicals 26(4): 267-76.

Boschetti N, Niederhauser I, Kempf C, Stuhler A, Lower J and Blumel J. 2004. Different susceptibility of B19 virus and mice minute virus to low pH treatment. Transfusion 44(7): 1079-1086.

Bourguignon GJ, Tattersall PJ and Ward DC. 1976. DNA of minute virus of mice: self-priming, nonpermuted, single-stranded genome with a 5'-terminal hairpin duplex. J Virol 20(1): 290-306.

Bousvaros A, Sundel R, Thorne GM, McIntosh K, Cohen M, Erdman DD, Perez-Atayde A, Finkel TH and Colin AA. 1998. Parvovirus B19-associated interstitial lung disease, hepatitis, and myositis. Pediatr Pulmon 26: 365-369.

Brauniger S, Peters J, Borchers U, Kao M. 2000. Further studies on thermal resistance of bovine parvovirus against moist and dry heat. Int J Hyg Environ Health 203(1): 71-5.

Broliden K, Tolfvenstam T, Ohlsson S and Henter J-I. 1998. Persistent B19 infection in pediatric malignancies. Med and Pediatr Oncol 31: 66-72.

Brown CS, Salimans MMM, Noteborn MHM and Weiland HT. 1990a. Antigenic parovirus B19 coat proteins VP1 and VP2 produced in large quantities in a baculovirus expression system. Virus Research 15: 197-212.

Brown CS, van Bussel MJAWM, Wassenaar ALM, van Elsacker-Niele A-MW, Weiland HT and Salimans MMM. 1990b. An immunofluorescence assay for the detection of parvovirus B19 IgG and IgM antibodies based on recombinant viral antigen. J Virol Methods. 29: 53-62.

Brown CS, Van Lent JWM, Vlak JM and Spaan WJM. 1991. Assembly of empty capsids by using baculovirus recombinants expressing human parvovirus B19 structural proteins. J Virol 65(5): 2702-2706.

Brown CS, Jensen T, Meloen RH, Puijk W, Sugamura Z, Sato H and Spaan WJM. 1992. Localization of an immunodominant domain on baculovirus-produced parvovirus B19 capsids: correlation to a major surface region on the native virus particle. J Virol. 66(12): 6989-96.

Brown KE. 1989. What threat is human parvovirus B19 to the fetus? Br J Obstet Gynaecol 96: 764-767.

Brown KE, Mori J, Cohen BJ and Field AM. 1991. In vitro propagation of parvovirus B19 in primary foetal liver culture. J Gen Virol 72 (Pt 3): 741-5.

Brown KE, Anderson SM and Young NS. 1993. Erythrocyte P antigen: cellular receptor for B19 parvovirus. Science 262: 114-117.

Brown KE, Hibbs JR, Gallinella G, Anderson SM. Lehman ED, Mc-Carthy P and Young NS. 1994. Resistance to parvovirus B19 infection due to lack of virus receptor (erythrocyte P antigen). N Engl J Med 330: 1192.

Brown KE. 2000. Haematological consequences of parvovirus B19 infection. Baillière's Clinical Haematology. 13(2): 245-259.

Brown KE and Young NS. 1995. Parvovirus B19 infection and hematopoiesis. Blood Rev 9: 176-182.

Brown KE and Young NS. 1996. Parvoviruses and bone marrow failure. Stem Cells 14: 151-163.

Brown KE and Young NS. 1997. The simian parvoviruses. Rev in Med Virol 7(4): 211-218.

Brown T, Anand A, Ritchie LD, Clewley JP and Reid TMS. 1984. Intrauterine parvovirus infection associated with hydrops fetalis. Lancet ii: 1033-1034.

Brunstein J, Söderlund-Venermo M and Hedman K. 2000. Identification of a novel RNA splicing pattern as a basis of restricted cell tropism of erythrovirus B19. Virology 274: 284-291.

Bruu A-L and Nordbø SA. 1995. Evaluation of five commercial tests for detection of immunoglobulin M antibodies to human parvovirus B19. J Clin Microbiol 33(5): 1363-1365.

Bültmann BD, Klingel K, Sotlar K, Bock CT and Kandolf R. 2003. Parvovirus B19: a pathogen responsible for more than hematologic disorders. Virchows Arch 442: 8-17.

Burnouf T. 1993. Chromatographic removal of viruses from plasma derivatives. Dev Biol Stand 81: 199-209.

Burnouf-Radosevich M, Appourchaux P, Huart JJ, Burnouf T. 1994. Nanofiltration, a new specific virus elimination method applied to high-purity factor IX and factor XI concentrates. Vox Sang. 67(2):132-8.

Burton PA. 1986. Intranuclear inclusions in marrow of hydropic fetus due to parvovirus infection. Lancet ii: 1155.

Caillet-Fauquet P, Draps ML, Di Giambattista M, de Launoit Y, Laub R. Hypoxia enables B19 erythrovirus to yield abundant infectious progeny in a pluripotent erythroid cell line. 2004a. J Virol Methods 121(2): 145-153.

Caillet-Fauquet P, DiGiambattista M, Draps ML, Sandras F, Branel T, de Launoit Y and Laub R. 2004b. Continuous-flow UVC irradiation: a new, effective, protein activity-preserving system for inactivating bacteria and viruses including erthrovirus B19. J Virol Methods 118(2): 131-139.

Cameron R, Davies J, Adcock W, MacGregor A, Barford JP, Cossart Y and Harbour C. 1997. The removal of model viruses, poliovirus type 1 and canine parvovirus, during the purification of human albumin using ion-exchange chromatographic procedures. Biologicals 25(4): 391-401.

Carrington D, Gilmore DH, Whittle MJ, Aitken D, Gibson AAM, Patrick WJA, Brown T, Caul EO, Field AM, Clewley JP and Cohen BJ. 1987. Maternal serum α-fetoprotein-a marker of fetal aplastic crisis during intrauterine human parvovirus infection. Lancet I: 433-435.

Cartter ML, Farley TA, Rosengren S, Quinn DL, Gillespie SM, Gary GW and Hadler JL. 1991. Occupational risk factors for infection with parvovirus B19 among pregnant women. J Infect Dis 163: 282-285.

Casal JI. 1999. Use of parvovirus-like particles for vaccination and induction of multiple immune responses. Biotechnol Appl Biochem 29: 141-150.

Cassinotti P, Weitz M and Siegl G. 1993a. Human parvovirus B19 infections: routine diagnosis by a new nested polymerase chain reaction assay. J Med Virol 40: 228-234.

Cassinotti P, Schultze D, Schlageter P, Chevili S and Siegl G. 1993b. Persistent human parvovirus B19 infection following an acute infection with meningitis in an immunocompetent patient. Eur J Clin Microbiol Infect Dis 12: 701-704.

Cassinotti P, Bas S, Siegl G and Vischer TL. 1995. Association between human parvovirus B19 infection and arthritis. Ann Rheum Dis 54: 498-500.

Cassinotti P, Burtonboy G, Fopp M and Siegl G. 1997. Persistence of human parvovirus B19 DNA in bone marrow. J Med Virol 53: 229-232.

Cassinotti P, Siegl G, Michel BA and Brühlmann P. 1998. Presence and significance of human parvovirus B19 DNA in synovial membranes and bone marrow from patients with arthritis of unknown origin. J Med Virol 56: 199-204.

Cattral MS, Langnas AN, Markin RS, Antonson DL, Heffron TG, Fox IJ, Sorrell MF and Shaw BW. 1994. Aplastic anemia after liver transplantation for fulminant liver failure. Hepatology 20: 813-818.

Cerus press release. 4th September 2003. Baxter And Cerus Halt Red Blood Cell Clinical Trials For Investigational Pathogen Inactivation System. http://www.cerus.com

Chandra S, Cavanaugh JE, Lin CM, Pierre-Jerome C, Yerram N, Weeks R, Flanigan E and Feldman F. 1999. Virus reduction in the preparation of intravenous immune globulin: in vitro experiments. Transfusion 39(3): 249-57.

Chapman JR, Moore K and Butterworth BE. 2003. Pathogen inactivation of RBCs: PEN110 reproductive toxicology studies. Transfusion 43(10): 1386.

Chapman MS and Rossmann MG. 1993. Structure, sequence, and function correlations among parvoviruses. Virology 194: 491-508.

Chernak E, Dubin G, Henry D, Naides SJ, Hodinka RL, MacGregor RR and Friedman HM. 1995. Infection due to parvovirus B19 in patients infected with human immunodeficiency virus. Clin Infect Dis 20: 170-173.

Cherry JD. 1999. Parvovirus infections in children and adults. Advances in Pediatrics 46: 245-269.

Chevrel G, Borsotti JP and Miossec P. 2003. Lack of evidence for a direct involvement of muscle infection by parvovirus B19 in the pathogenesis of inflammatory myopathies: a follow-up study. Rheumatol 42: 349-352.

Chia JKS and Jackson B. 1996. Myopericarditis due to parvovirus B19 in an adult. Clin Infect Dis 23: 201-202.

Chipman PR, Agbandje-McKenna M, Kajigaya S, Brown KE, Young NS, Baker TS and Rossmann MG. 1996. Cryo-electron microscopy studies of empty capsids of human parvovirus B19 complexed with its cellular receptor. Proc Natl Acad Sci USA. 93: 7502-7506.

Chisaka H, Morita E, Murata K, Ishii N, Yaegashi N, Okamura K and Sugamura K. 2002. A transgenic mouse model for non-immne hydrops fetalis induced by the NS1 gene of human parvovirus B19. J Gen Virol 83: 273-281.

Chorba T, Coccia P, Holman RC, Tattersall P, Anderson LJ, Sudman J, Young NS, Kurczynski E, Saarinen UM, Moir R, Lawrence DN, Jason JM and Evatt B. 1986. The role of parvovirus B19 in aplastic crisis and erythema infectiosum (fifth disease). J Infect Dis 154(3): 383-393.

Chou T-NK, Hsu T-C, Chen R-M, Lin L-I and Tsay GJ. 2000. Parvovirus B19 infection associated with the production of anti-neutrophil cytoplasmic antibody (ANCA) and anticardiolipin antibody (aCL). Lupus 9: 551-554.

Chuhjo T, Nakao S and Matsuda T. 1999. Successful treatment of persistent erythroid aplasia caused by parvovirus B19 infection in a patient with common variable immunodeficiency with low-dose immunoglobulin. Am J Hematol 60: 222-224.

Ciaravi V, McCullough T and Dayan AD. 2001. Pharmacokinetic and toxicology assessment of INTERCEPT (S-59 and UVA treated) platelets. Hum Exp Toxicol 20(10): 533-50.

Ciaravino V. 2001. Preclinical safety of a nucleic acid-targeted Helinx compound: a clinical perspective. Semin Hematol 38(4 Suppl 11): 12-9.

Cipolleschi MG, D'Ippolito G, Bernabei PA, Caporale R, Nannini R, Mariani M, Fabbiani M, Rossi-Ferrini P, Olivotto M and Dello Sbarba P. 1997. Severe hypoxia enhances the formation of erythroid bursts from human cord blood cells and the maintenance of BFU-E in vitro. Exp Hematol 25(11): 1187-1194.

Clarke BE, Newton SE, Carroll AR, Francis MJ, Appleyard G, Syred AD, Highfield PE, Rowlands DJ and Brown F. 1987. Improved immunogenicity of a peptide epitope after fusion to hepatitis B core protein. Nature 330: 381-384.

Clarke J and Lee JD. 2003. Primary human parvovirus B19 infection in an HIV infected patient on highly active antiretroviral therapy. Sex Transm Infect 79: 336.

Clemens KE and Pintel D. 1987. Minute virus of mice (MVM) mRNAs predominantly polyadenylate at a single site. Virology 160(2): 511-4.

Clewley JP. 1984. Biochemical characterization of the human parvovirus. J Gen Virol 65: 241-245.

Clewley JP. 1985. Detection of human parvovirus using a molecular cloned probe. J Med Virol 15: 173-181.

Clewley JP. 1989. Polymerase chain reaction assay of parvovirus B19 DNA in clinical specimens. J Clin Microbiol 27(12): 2647-2651.

Cobeta-García JC and Rodilla F. 2000. Antinuclear antibodies and parvovirus B19 arthritis. Clin Exp Rheumatol 18(4): 537.

Cohen BJ, Mortimer PP and Pereira MS. 1983. Diagnostic assays with monoclonal antibodies for the human serum parvovirus-like virus (SPLV). J Hyg Cam 91: 113-130.

Cohen BJ, Field AM, Gudnadottir S, Beard S and Barbara JAJ. 1990. Blood donor screening for parvovirus B19. J of Virol Methods 30: 233-238.

Cohen BJ, Field AM, Mori J, Brown KE, Clewley JP, St Amand J, Astell CR. 1995a. Morphology and antigenicity of recombinant B19 parvovirus capsids expressed in transfected COS-7 cells. J Gen Virol 76: 1233-1237.

Cohen BJ, Millar A and Schwind P. 1995b. Screening blood donations for parvovirus B19. The Lancet 346:1631.

Cohen BJ. 1997. Detection of parvovirus B19-specific IgM by antibody capture radioimmunoassay. J Virol Methods 66: 1-4.

Collett MS and Young NS, 1994. Prospects for a human B19 parvovirus vaccine. Reviews in Medical Virology 4: 91-103.

Colombo, M., Mannucci PM, Carnelli V, Savidge GF, Gazengel C and Schimpf K. 1985. Transmission of non-A, non-B hepatitis by heat-treated factor VIII concentrate. Lancet 2: 1-4.

Colvin BT. 1994. Viral contamination of blood products-letter to the editor. The Lancet 344(8919): 405.

Cooling LLW, Koerner TAW and Naides SJ. 1995. Multiple glycosphingolipids determine the tissue tropism of parvovirus B19. J Infect Dis 172: 1198-1205.

Corash L. 2003. Pathogen reduction technology: methods, status of clinical trials, and future prospects. Curr Hematol Rep 2(6): 495-502.

Corcoran A, Mahon BP and Doyle S. 2004. B cell memory is directed toward conformational epitopes of parvovirus B19 capsid proteins and the unique region of VP1. J Infect Dis 189(10): 1873-80.

Cordell RL. 2001. The risk of infectious diseases among child care providers. JAMWA 56: 109-112.

Corman LC and Dolson DJ. 1992. Polyarteritis nodosa and parvovirus B19 infection. Lancet 339: 491.

Corral DA, Darras FS, Jensen CWB, Hakala TR, Naides SJ, Krause JR, Starzl TE and Jordan ML. 1993. Parvovirus B19 infection causing pure red cell aplasia in a recipient of pediatric donor kidneys. Transplantation 55(2): 427-430.

Cossart YE, Field AM, Cant B and Widdows D. 1975. Parvovirus-like particles in human sera. Lancet I: 72-73.

Cotmore SF, Sturzenbecker LJ and Tattersall P. 1983. The autonomous parvovirus MVM encodes two nonstructural proteins in addition to its capsid polypeptides. Virology 129(2): 333-43.

Cotmore SF, McKie VC, Anderson LJ, Astell CR and Tattersall P. 1986. Identification of the major structural and nonstructural proteins encoded by human parvovirus B19 and mapping of their genes by prokaryotic expression of isolated genomic fragments. J Virol 60(2): 548-557.

Cotmore SF, Nuesch JP and Tattersall P. 1992. In vitro excision and replication of 5' telomeres of minute virus of mice DNA from cloned palindromic concatemer junctions. Virology 190(1): 365-377.

Cotmore SF, Nüesch JP and Tattersall P. 1993. Asymmetric resolution of a parvovirus palindrome *in vitro*. J Virol 67(3): 1579-1589.

Cotmore SF and Tattersall P. 1984. Characterization and molecular cloning of a human parvovirus genome. Science 226: 1161-1165.

Courcoucé AM, Ferchal F, Morinet F, Pérol Y, Drouet J, Muller A and Soulier JP. 1984a. Parvovirus (SPLV) et antigène Aurillac; étude de 18 observations. Rev Fran Transf Immuno-hématol 27(1): 5-19.

Couroucé AM, Ferchal F, Morinet F, Muller A, Drouet J, Soulier JP and Perol Y. 1984b. Human parvovirus infections in France. Lancet i: 160-161.

Crook TW, Barton Rogers B, McFarland RD, Kroft SH, Muretto P, Hernandez JA, Latimer MJ and McKenna RW. 2000. Unusual bone marrow manifestations of parvovirus B19 infection in immunocompromised patients. Hum Pathol 31(2): 161-168.

Crowley B, Kokai G and Cohen BJ. 2001. Correspondence: human parvovirus B19 and fetal death. Lancet 358: 1180-1181.

Crowson AN, Magro CM and Dawood MR. 2000. A causal role for parvovirus B19 infection in adult dermatomyositis and other autoimmune syndromes. J Cutan Pathol 27: 505-515.

Cubie HA, Grzybowski J, da Silva C, Duncan L, Brown T and Smith NM. 1995. Synthetic oligonucleotide cocktails as probes for detection of human parvovirus B19. J Virol Methods 53: 91-102.

Cunningham DA, Pattison JR and Craig RK. 1988. Detection of parvovirus DNA in human serum using biotinylated RNA hybridisation probes. J Virol Methods 19: 279-288.

Davis EV, Gregory GG and Beckenhauer WH. 1970. Infectious feline panleukopenia (development report of a tissue culture origin formalin-inactivated vaccine). Vet Med Small Anim Clin 1970 65: 237-242.

De Filippi F, Castelli R, Cicardi M, Soffredini R, Rumi MG, Silini E, Mannucci PM and Colombo M. 1998. Transmission of hepatitis G virus in patients with angioedema treated with steam-heated plasma concentrates of C1 inhibitor. Transfusion 38: 307-11.

Deiss V, Tratschin J-D, Weitz M and Siegl G. 1990. Cloning of the human parvovirus B19 genome and structural analysis of its palindromic termini. Virology 175: 247-254.

Delfraissy JF, Tchernia G, Laurian Y, Wallon C, Galanaud P and Dormont J. 1985. Suppressor cell function after intravenous gammaglobulin treatment in adult chronic idiopathic thrombocytopenic purpura. Br J Haematol 60: 315-322.

Dembinski J, Eis-Hübinger AM, Maar J, Schild R and Bartmann P. 2003. Long term follow up of serostatus after maternofetal parvovirus B19 infection. Arch Dis Child 88: 219-221.

Dieck D, Schild RL, Hansmann M and Eis-Hübinger AM. 1999. Prenatal diagnosis of congenital parvovirus B19 infection: value of serological and PCR techniques in maternal and fetal serum. Prenat Diagn 19: 1119-1123.

Dingli D, Pfizenmaier DH, Arromdee E, Wennberg P, Spittell PC, Chang-Miller A and Clarke BL. 2000. Severe digital arterial occlusive disease and acute parovivrus B19 infection. Lancet 356: 312-314.

Doerig C, Beard P and Hirt B. 1987. A transcriptional promoter of the human parvovirus B19 active in vitro and in vivo. Virology 157(2): 539-42.

Doerig C, Hirt B, Antonietti JP and Beard P. 1990. Nonstructural protein of parvoviruses B19 and minute virus of mice controls transcription. J Virol 64(1): 387-96.

Doran HM and Teall AJ. 1988. Neutropenia accompanying erythroid aplasia in human parvovirus infection. Br J Haematol 69: 287-288

Dorsch S, Kaufmann B, Schaible U, Prohaska E, Wolf H and Modrow S. 2001. The VP1-unique region of parvovirus B19: amino acid variability and antigenic stability. J Gen Virol. 82: 191-199.

Dorsch S, Liebisch G, Kaufmann B, von Landenberg P, Hoffmann JH, Drobnik W and Modrow S. 2002. The VP1 unique region of parvovirus B19 and its constituent phospholipase A2-like activity. J Virol 76(4): 2014-2018.

Doue B. 2001. Radiation doses and dose distribution during industrial sterilisation by gamma rays and accelerated electrom beams. Medical Device Part 1: 32-35.

Dowell SF, Török TJ, Thorp JA, Hedrick J, Erdman DD, Zaki SR, Hinkle CJ, Bayer WL and Anderson LJ. 1995. Parvovirus B19 infection in hospital workers: community or hospital acquisition? J Infect Dis 172: 1076-1079.

Doyle S, Kerr S, O'Keeffe G, O'Carroll D, Daly P and Kilty C. 2000. Detection of parvovirus B19 IgM by antibody capture enzyme immunoassay: receiver operating characteristic analysis. J Virol Methods 90: 143-152.

Duncan JR, Potter CG, Cappellini MD, Kurtz JB, Anderson MJ and Weatherall DJ. 1983. Aplastic crisis due to parvovirus infection in pyruvate kinase deficiency. Lancet ii: 14-16.

Dupuis K, Bernard K, Janes S, Grellier P, Labaid M, Van Voorhis W, Barrett L, Benach J, Monsalve G, Gil-Gil H and Sawyer L. 2003. Helinx®technology inactivates pathogens of emerging importance in red blood cell concentrates. Abstract presented at the American Society of Hematology (ASH), December 6-9.

Dupuis K and Sampson-Johannes A. 2003. The Causative Agent of SARS in Platelet and Red Cell Concentrates is Inactivated by Helinx® Technology. Abstract presented at the American Society of Hematology (ASH), December 6-9.

Eis-Hübinger AM, Sasowski U, Brackmann HH, Kaiser R, Matz B and Schneweis KE. 1996. Parvovirus B19 DNA is frequently present in recombinant coagulation factor VIII products- letter to the Editor. Thrombosis and Haemostasis 76(6): 1118-22.

Eis-Hübinger AM, Reber U, Abdul-Nour T, Glatzel U, Lauschke H and Pütz U. 2001. Evidence for persistence of parvovirus B19 DNA in livers of adults. J Med Virol 65: 395-401.

Enders G, Dötsch J, Bauer J, Nützenadel W, Hengel H, Haffner D, Schalasta G, Searle K and Brown KE. 1998. Life-threatening parvovirus B19-associated myocarditis and cardiac transplantation as possible therapy: two case reports. Clin Infect Dis 26: 355-358.

Enders G and Biber M. 1990. Parvovirus B19 infection in pregnancy. Behring Inst Mitt 85: 74-78.

Engelhard D, Waner JL, Kapoor N and Good RA. 1986. Effect of intravenous immune globulin on natural killer cell activity: possible association with autoimmune neutropenia and idiopathic thrombocytopenia. J Pediatr 108: 77-81.

Erdman DD, Usher MJ, Tsou C, Caul EO, Gary GW, Kajigaya S, Young NS and Anderson LJ. 1991. Human parvovirus B19 specific IgG, IgA, and IgM antibodies and DNA in serum specimens from persons with erythema infectiosum. J Med Virol 35: 110-115.

Erdman DD, Durignon EL, Wang Q-Y and Anderson LJ. 1996. Genetic diversity of human parvovirus B19: sequence analysis of the VP1/VP2 gene from multiple isolates. J Gen Virol. 77: 2767-2774.

Erdman DD, Anderson BC, Török TJ, Finkel TH and Anderson LJ. 1997. Possible transmission of parvovirus B19 from intravenous immune globulin. J Med Virol 53: 233-236.

Erickson-Miller CL, Pelus LM and Lord KA. 2000. Signaling induced by erythropoietin and stem cell factor in UT-7/Epo cells: transient versus sustained proliferation. Stem Cells 18(5): 366-73.

Estep TN, Bechtel MK, Miller TJ and Bagdasarian A. 1988. Virus inactivation in hemoglobin solutions by heat. Biomater Artif Cells Artif Organs 16(1-3):129-34.

Eugster AK. 1980. Studies on canine parvovirus infections: development of an inactivated vaccine. Am J Vet Res 41(12): 2020-2024.

Evans JPM, Rossiter MA, Kumaran TO, Marsh GW and Mortimer PP. 1984. Human parvovirus aplasia: case due to cross infection in a ward. Br Med J 288: 681.

Fairley C, Smoleniec JS, Caul OE and Miller E. 1995. Observational study of effect of intrauterine transfusions on outcome of fetal hydrops after parvovirus B19 infection. Lancet 346: 1335-1337.

Fan MM, Tamburic L, Shippam-Brett C, Zagrodney DB and Astell CR. 2001. The small 11-kDa protein from B19 parvovirus binds growth factor receptor-binding protein 2 in vitro in a Src homology 3 domain/ligand-dependent manner. Virology 291(2): 285-91.

Fawaz-Estrup F. 1996. Human parvovirus infection: rheumatic manifestations, angioedema, C1 esterase inhibitor, ANA positivity, and possible onset of systemic lupus erythematosus. J Rheum 23(7): 1180-1185.

Fehr J, Hofmann V and Kappeler U. 1982. Transient reversal of thrombocytopenia in idiopathic thrombocytopenic purpura by high-dose intravenous gamma globulin. N Engl J Med 306: 1254-1258.

Fini F, Gallinella G, Girotti S, Zerbini M and Musiani M. 1999. Development of a chemiluminescence competitive PCR for the detection and quantitation of parvovirus B19 DNA using a microplate luminometer. Clin Chem 45(9): 1391-1396.

Finkel TH, Török TJ, Ferguson PJ, Durigon EL, Zaki SR, Leung DYM, Harbeck RJ, Gelfand EW, Saulsbury FT, Hollister JR and Anderson LJ. 1994. Chronic parvovirus B19 infection and systemic necrotising vasculitis: opportunistic infection or aetiological agent? Lancet 343: 1255-1258.

Fisch P, Handgretinger R and Schaefer H-E. 2000. Pure red cell aplasia. Br J Haematol 111: 1010-1022.

Foreman NK, Oakhill A and Caul EO. 1988. Parvovirus-associated thrombocytopenic purpura. Lancet ii: 1426-1427.

Forouzan I. 1997. Hydrops fetalis: recent advances. Obstetr Gynecol Survey 52(2): 130-138.

Foto F, Saag KG, Scharosch LL, Howard EJ and Naides SJ. 1993. Parvovirus B19-specific DNA in bone marrow from B19 arthropathy patients: evidence for B19 virus persistence. J Infect Dis 167: 744-748.

Francis MJ, Hastings GZ, Brown AL, Grace KG, Rowlands DJ, Brown F and Clarke BE. 1990. Immunological properties of hepatitis B core antigen fusion proteins. Proc Natl Acad Sci USA 87: 2545-2549.

Franssila R, Söderlund M, Brown CS, Spaan WJM, Seppälä I and Hedman K. 1996. IgG subclass response to human parvovirus B19 infection. Clinical and Diagnostic Virology 6: 41-49.

Franssila R, Hokynar K and Hedman K. 2001. T helper cell-mediated in vitro responses of recently and remotely infected subjects to a candidate recombinant vaccine for human parvovirus B19. J Infect Dis 183: 805-809.

Freitas RB, Monteiro TAF, Silva Filho MG and Linhares AC. 2002. Association between human parvovirus B19 and arthropathy in Belém, Pará, north Brazil. Rev Inst Med Trop S Paulo 44(1): 17-22.

Frickhofen N, Abkowitz JL, Safford M, Berry JM, Antunez-de-Mayolo J, Astrow A, Cohen R, Halperin I, King L, Mintzer D, Cohen B and Young NS. 1990. Persistent B19 parvovirus infection in

patients infected with human immunodeficiency virus type1 (HIV-1): a treatable cause of anemia in AIDS. Ann Intern Med 113(12): 926-933.

Frickhofen N and Young NS. 1989. Persistent parvovirus B9 infections in humans. Microbial Pathogenesis 7: 319-327.

Frickhofen N and Young NS. 1990. Polymerase chain reaction for detection of parvovirus B19 in immunodeficient patients with anaemia. Behring Inst Mitt 85:46-54.

Fridell E, Cohen BJ and Wahren B. 1991. Evaluation of a synthetic-peptide enzyme-linked immunosorbent assay for immunoglobulin M to human parvovirus B19. J Clin Microbiol 29(7): 1376-1381.

Fukada K, Matumoto K, Takakura F, Yamaki M, Sato H, Okochi K and Maeda Y. 2000. Four putative subtypes of human parvovirus B19 based on amino acid polymorphism in the C-terminal region of non-structural protein. J Med Virol 62(1): 60-9.

Gahr M, Pekrun A and Eiffert H. 1991. Persistence of parvovirus B19-DNA in blood of a child with severe combined immunodeficiency associated with chronic pure red cell aplasia. Eur J Pediatr 150: 470-472.

Gallinella G, Venturoli S, Gentilomi G, Musiani M and Zerbini M. 1995a. Extent of sequence variability in a genomic region coding for capsid proteins of B19 parvovirus. Arch Virol 140(6): 1119-25.

Gallinella G, Anderson SM, Young NS and Brown KE. 1995b. Human parvovirus B19 can infect cynomolgus monkey marrow cells in tissue culture. J Virol 69(6): 3897-9.

Gallinella G, Zerbini M, Musiani M, Venturoli S, Gentilomi G and Manaresi E. 1997. Quantitation of parvovirus B19 DNA sequences by competitive PCR: differential hybridisation of the amplicons and immunoenzymatic detection on microplate. Mol and Cell Probes 11: 127-133.

Gallinella G, Manaresi E, Zuffi E, Venturoli S, Bonsi L, Bagnara GP, Musiani M and Zerbini M. 2000. Different patterns of restriction to B19 parvovirus replication in human blast cell lines. Virology 278(2): 361-7.

Gallinella G, Zuffi E, Gentilomi G, Manaresi E, Venturoli S, Bonvicini F, Cricca M, Zerbini M and Musiani M. 2003. Relevance of B19 markers in serum samples for a diagnosis of parvovirus B19-correlated diseases. J Med Virol 71: 135-139.

Gareus R, Gigler A, Hemauer A, Leruez-Ville M, Morinet F, Wolf H and Modrow S. 1998. Characterization of cis-acting and NS1 protein-responsive elements in the p6 promoter of parvovirus B19. J Virol 72(1): 609-16.

Garcia AGP, Pegado CS, Cubel RCN, Fonseca MEF, Sloboda I and Nascimento JP. 1998. Feto-placentary pathology in human parvovirus B19 infection. Rev Inst Med Trop S Paulo 40(3): 145-150.

García-Tapia AM, Fernandez-Gutiérrez del Alamo C, Girón JA, Mira J, de la Rubia F, Martínez-Rodríguez A, Martín-Reina MV, López-Caparros R, Cáliz R, Caballero MS and Bascuñana A. 1995. Spectrum of parvovirus B19 infection: analysis of an outbreak of 43 cases in Cadiz, Spain. Clin Infect Dis 21: 1424-1430.

Gendi NST, Gibson K and Wordsworth BP. 1996. Effect of HLA type and hypocomplementaemia on the expression of parvovirus arthritis: one year follow up of an outbreak. Ann Rheum Dis 55: 63-65.

Gentilomi G, Musiani M, Zerbini M, Gallinella G, Venturoli S and Manaresi E. 1997. Dot immunoperoxidase assay for detection of parvovirus B19 antigens in serum samples. J Clin Microbiol 35(6): 1575-1578.

Ghigliotti G, Mazzarello G, Nigro A, Fusco F, Del Bono V and De Marchi R. 2000. Papular-purpuric gloves and socks syndrome in HIV-positive patients. J Am Acad Dermatol 43: 916-917.

Gigler A, Dorsch S, Hemauer A, Williams C, Kim S, Young NSJ, Zolla-Pazner S, Wolf H, Gorny MK and Modrow S. 1999. Generation of neutralising human monoclonal antibodies against pavovirus B19 proteins. J of Virol 73(3): 1974-1979.

Gloning K-PH, Schramm TH, Brusis E, Schwarz T and Roggendorf M. 1990. Successful intrauterine treatment of fetal hydrops caused by parvovirus B19 infection. Behring Inst Mitt 85: 79-85.

Goedert JJ, Erdman DD, Konkle BA, Torok TJ, Lederman MM, Kleinert D, Mandalaki T, Kessler CM, Anderson LJ nad Luban NL. 1997. Parvovirus B19 quiescence during the course of human immunodeficiency virus infection in persons with hemophilia. Am J Hematol 56(4): 248-251.

Gorbalenya AE and Koonin EV. 1989. Viral proteins containing the purine NTP-binding sequence pattern. Nucleic Acids Res 17(21): 8413-40.

Gottschalck E, Alexandersen S, Cohn A, Poulsen LA, Bloom ME and Aasted B. 1991. Nucleotide sequence analysis of Aleutian mink disease parvovirus shows that multiple virus types are present in infected mink. J Virol 65(8): 4378-86.

Graeve JA and Elliott SC. 1991. Neurologic symptoms, iron deficiency anemia and parvovirus infection. J Pediatr 118: 830.

Green SW, Malkovska I, O'Sullivan MG and Brown KE. 2000. Rhesus and pig-tailed macaque parvoviruses: identification of two new members of the Erythrovirus genus in monkeys. Virology 269: 105-112.

Grilli R, Izquierdo MJ, Fariña MC, Kutzner H, Gadea I, Martin L and Requena L. 1999. Papular-purpuric "gloves and socks" syndrome: polymerase chain reaction demonstration of parvovirus B19 DNA in cutaneous lesions and sera. J Am Acad Dermatol 41(5): 793-796.

Gruber F, Falkner FG, Dorner F and Hämmerle T. 1998. Precise quantitation of human parvovirus B19 DNA in biological samples by PCR. Biologicals 26: 213-216.

Gruber F, Falkner FG, Dorner F and Hämmerle T. 2001. Quantitation of viral DNA by real-time PCR applying duplex amplification, internal standardization, and two-color fluorescence detection. Applied and Environmental Microbiology 67(6): 2837-2839.

Guillaume T. 1994. The Lancet 343:1101

Guillaume MP, Hermanus N and Peretz A. 2002. Unusual localisation of chronic arthropathy in lumbar facet joints after parvovirus B19 infection. Clin Rheumatol 21: 306-308.

Hanada T, Yamamura H, Isobe T, Nakazawa M, Abe T and Takita H. 1986. Pure red cell aplasia in association with malignant histiocytosis. Cancer 57: 2325-2328.

Hanson DF, Dupuis KW and Sawyer L. 2004. Inactivation of parvovirus B19 in platelets by Helinx® technology. Abstract submitted to the American Association of Blood Banks (AABB) meeting.

Harley A and Rotbart MD. 1990. Human parvovirus infections. Annu. Rev. Med. 41: 25-34.

Harms M, Feldmann R and Saurat J-H. Papular-purpuric "gloves and socks" syndrome. 1990. J Am Acad Dermatol 23: 850-854.

Harrison B, Silman A, Barrett E and Symmons D. 1998. Low frequency of recent parvovirus infection in a population-based cohort of patients with early inflammatory polyarthritis. Ann Rheum Dis 57: 375-377.

Hart H, Reid K and Hart W. 1993. Inactivation of viruses during ultraviolet light treatment of human intravenous immunoglobulin and albumin. Vox Sang 64: 82-8.

Hart HF, Hart WG, Crossley J, Perrie AM, Wood DJ, John A and McOmish F. 1994. Effect of terminal (dry) heat treatment on non-enveloped viruses in coagulation factor concentrates. Vox Sang 67(4): 345-50.

Hartman KR, Brown KE, Green SW and Young NS. 1994. Correspondence: Lack of evidence for parvovirus B19 viraemia in children with chronic neutropenia. Br J Haematol 84: 895-896.

Haseyama K, Kudoh T, Yoto Y, Suzuki N and Chiba S. 1998. Analysis of genetic diversity in the VP1 unique region gene of human parvovirus B19 using the mismatch detection method and direct nucleotide sequencing. J Med Virol 56(3): 205-209.

Hasle H, Kerndrup G, Brock Jacobsen B, Heegaard ED, Hornsleth A and Lillevang ST. 1994. Chronic parvorius infection mimicking myelodysplastic syndrome in a child with subclinical immunodeficiency. Am J Pediatr Hematol Oncol 16(4): 329-333.

Heegaard ED, Peterslund NA and Hornsleth A. 1995. Parvovirus B19 infection associated with encephalitis in a patient suffering from malignant lymphoma. Scand J Infect Dis 27(6): 631-633.

Heegaard ED, Eiskjær H, Baandrup U and Hornsleth A. 1998. Parvovirus B19 infection associated with myocarditis following adult cardiac transplantation. Scand J Infect Dis 30: 607-610.

Heegaard ED, Hasle H, Skibsted L, Bock J and Brown KE. 2000. Congenital anemia caused by parvovirus B19 infection. Pediat infect Dis J 19(2): 1216-1218.

Heegaard ED, Panum Jensen I and Christensen J. 2001. Novel PCR assay for differential detection and screening of erythrovirus B19 and erythrovirus V9. J Med Virol 65(2): 362-367.

Heegaard ED, Qvortrup K and Christensen J. 2002. Baculovirus expression of erythrovirus V9 capsids and screening by ELISA: serologic cross-reactivity with erythrovirus B19. J Med Virol 66(2): 246-252.

Heegaard ED and Brown KE. 2002. Human parvovirus B19. Clin Microbiol Rev 15(3): 485-505.

Heegaard ED and Taaning EB. 2002. Parvovirus B19 and parvovirus V9 are not associated with Henoch-SchÃ¶nlein purpura in children. Pediatr Infect Dis J 21(1): 31-34.

Heldebrant CM, Gomperts ED, Kasper CK, McDougal JS, Friedman AE, Hwang DS, Muchmore E, Jordan S, Miller R, Sergis-Davenport E and Lam W. 1985. Evaluation of two viral inactivation methods for the preparation of safer factor VII and factor IX concentrates. Transfusion 25: 510-515.

Hemauer A, Von Poblotski A, Gigler A, Cassinotti P, Siegl G, Wolf H and Modrow S. 1996. Sequence variability among different parvovirus B19 isolates. J Gen Virol. 77: 1781-1785.

Hemauer A, Gigler A, Gareus R, Reichle A, Wolf H and Modrow S. 1999. Infection of apheresis cells by parvovirus B19. J Gen Virol 80: 627-630.

Hemauer A, Gigler A, Searle K, Beckenlehner K, Raab U, Broliden K, Wolf H, Enders G and Modrow S. 2000. Seroprevalence of parvovirus B19 NS1-specific IgG in B19-infected and uninfected individuals and in infected pregnant women. J Med Virol 60: 48-55

Herrmann M, Hagenhofer M and Kalden JR. 1996. Retroviruses and systemic lupus erythematosus. Immunol Rev 152: 145-156.

Hicks KE, Beard S, Cohen BJ and Clewley JP. 1995. A simple and sensitive DNA hybridisation assay used for the routine diagnosis of human parvovirus B19 infection. J Clin Microbiol 33(9): 2473-2475.

Hicks KE, Cubel RC, Cohen BJ, Clewley JP. 1996. Sequence analysis of a parvovirus B19 isolate and baculovirus expression of the non-structural protein. Arch Virol 141(7): 1319-1327.

Hiemstra H, Tersmette M, Vos AH, Over J, van Berkel MP and de Bree H. 1991. Inactivation of human immunodeficiency virus by gamma radiation and its effect on plasma and coagulation factors. Transfusion 31: 32-39.

Highsmith F, Xue H, Chen X, Benade L, Owens J, Shanbrom and Drohan W. 1995. Iodine-mediated inactivation of lipid and nonlipid-enveloped viruses in human antithrombin III concentrate. Blood 86(2): 791-796.

Hilfenhaus J, Geiger H, Lemp J and Hung CL. 1987. A strategy for testing established human plasma protein manufacturing procedures for their ability to inactivate or eliminate human immunodeficiency virus. J Biol Stand 15(3): 251-263.

Hilgartner M, Aledort L, Andes A and Gill J (FEIBA Study Group). 1990. Efficacy and safety of vapor-heated anti-inhibitor coagulant complex in hemophilia patients. Transfusion 30(7):626-30.

Hillingsø JG, Jensen IP and Tom-Petersen L. 1998. Parvovirus B19 and acute hepatitis. Lancet 351: 955-956.

Hoang MP, Dawson B, Rogers ZR, Scheuermann RH and Barton Rogers B. 1998. Polymerase chain reaction amplification of archival material for Epstein-Barr virus, cytomegalovirus, human herpesvirus 6, and parvovirus B19 in children with bone marrow hemophagocytosis. Hum Pathol 29: 1074-1077.

Hokynar K, Brunstein J, Söderlund-Venermo M, Kiviluoto O, Partio EK, Konttinen Y and Hedman K. 2000. Integrity and full coding sequences of B19 virus DNA persisting in human synovial tissue. J Gen Virol 81: 1017-1025.

Hokynar K, Soderlund-Venermo M, Pesonen M, Ranki A, Kiviluoto O, Partio EK and Hedman K. 2002. A new parvovirus genotype persistent in human skin. Virology 302(2):224-228.

Hokynar K, Norja P, Laitinen H, Palomaki P, Garbarg-Chenon A, Ranki A, Hedman K and Soderlund-Venermo M. 2004. Detection and differentiation of human parvovirus variants by commercial quantitative real-time PCR tests. J Clin Microbiol 42(5): 2013-2019.

Holman AN, Grocke CD, Groff JA and Yang HC. 1997. Pure red cell aplasia due to parvovirus B19 infection in solid organ transplantation. Clin Transpl 11: 265-270.

Hoque M, Ishizu K, Matsumoto A, Han SI, Arisaka F, Takayama M, Suzuki K, Kato K, Kanda T, Watanabe H and Handa H. 1999. Nuclear transport of the major capsid protein is essential for adeno-associated virus capsid formation. J Virol 73(9): 7912-7915.

Hornsey VS, Krailadsiri P, MacDonald S, Seghatchian J, Williamson LM and Prowse CV. 2000. Coagulation factor content of cryoprecipitate prepared from methylene blue plus light virus-inactivated plasma. Br J Haematol 109(3): 665-70.

Horowitz B, Weibe ME, Lippin A and Stryker MH. 1985. Inactivation of viruses in labile blood derivatives. Disruption of lipid-enveloped viruses by tri (n-butyl) phosphate detergent combinations. Transfusion 25: 516-522.

House C, House JA and Yedloutschnig RJ. 1990. Inactivation of viral agents in bovine serum by gamma irradiation. Can J Microbiol 36: 737-740.

Hsu T-C and Tsay GJ. 2001. Human parovirus B19 infection in patients with systemic lupus erthematosus. Rhumatology 40: 152-157.

Inoue S, Kinra NK, Mukkamala SR and Gordon R. 1991. Parvovirus B19 infection: aplastic crisis, erythema infectiosum and idiopathic thrombocytopenic purpura. Pediat Infect Dis J 10(3): 251-252.

International Committee on Taxonomy of Viruses (ICTV). 2000. Virus taxonomy: classification and nomenclature of viruses. Seventh report of the International Committee on Taxonomy of Viruses. Springer-Verlag. Vienna, Austria.

International Committee on Taxonomy of Viruses (ICTV). 2005. Virus taxonomy: classification and nomenclature of viruses. Eighth report of the International Committee on Taxonomy of Viruses.

Ishii KK, Takahashi Y, Kaku M and Sasaki T. 1999. Role of human parvovirus B19 in the pathogenesis of rheumatoid arthritis. Jpn J Infect Dis 52: 201-207.

Iskander R, Das PK and Aalberse RC. 1981. IgG4 antibodies in Egyptian patients with schistosomiasis. Int Archs Allergy appl Immun 66: 200-207.

Isumi H, Nunoue T, Nishida A and Takashima S. 1999. Fetal brain infection with human parvovirus B19. Pediatr Neurol 21: 661-663.

James JA, Kaufman KM, Farris AD, Taylor-Albert E, Lehman TJA and Harley JB. 1997. An increased prevalence of Epstein-Barr virus infection in young patients suggests a possible etiology for systemic lupus erythematosus. J Clin Invest 100(12): 3019-3026.

Jansen GA, van Vliet HH, Vermeij H, Beckers EA, Leebeek FW, Sonneveld P and van Rhenen DJ. 2004. Functional characteristics of photochemically treated platelets. Transfusion 44(3): 313-319.

Jindal HK, Yong CB, Wilson GM, Tam P and Astell CR. 1994. Mutations in the NTP-binding motif of minute virus of mice (MVM) NS-1 protein uncouple ATPase and DNA helicase functions. J Biol Chem 269(5): 3283-3289.

Jobanputra P, Davidson F, Graham S, Yap LP, O'Neill H and Simmonds P. 1995. High frequency of parvovirus B19 in patients tested for rheumatoid factor. BMJ 311: 1542.

Jones LP, Erdman DD and Anderson LJ. 1999. Prevalence of antibodies to human parvovirus B19 nonstructural protein in persons with various clinical outcomes following B19 infection. J Infect Dis 180: 500-504.

Jongeneel CV, Sahli R, McMaster GK and Hirt B. 1986. A precise map of splice junctions in the mRNAs of minute virus of mice, an autonomous parvovirus. J Virol 59(3): 564-573.

Jordan JA. 2000. Comparison of a baculovirus-based VP2 enzyme immunoassay (EIA) to an *Escherichia coli*-based VP1 EIA for detection of human parvovirus B19 immunoglobulin M and immunoglobulin G in sera of pregnant women. J Clin Microbiol 38(4): 1472-1475.

Jordan CT, Saakadze N, Newman JL, Lezhava LJ, Maiers TT, Hillyer WM, Roback JD and Hillyer CD. 2004. Photochemical treatment of platelet concentrates with amotosalen hydrochloride and ultraviolet A light inactivates free and latent cytomegalovirus in a murine transfusion model. Transfusion 44(8): 1159-1165.

Jordan JA and Penchansky L. 1995. Diagnosis of human parvovirus B19-induced anemia: correlation of bone marrow morphology with molecular diagnosis using PCR and immunocytochemistry. Cell Vision 2(4): 279-282.

Joseph PR. 1986. Fifth disease: the frequency of joint involvement in adults. NY State J Med 86: 560-563.

Kajigaya S, Shimada T, Fujita S and Young NS. 1989. A genetically engineered cell line that produces empty capsids of B19 (human) parvovirus. Proc Natl Acad Sci USA 86: 7601-7605.

Kajigaya S, Fujii H, Field A, Anderson S, Rosenfeld S, Anderson LJ, Shimada T and Young NS. 1991. Self-assembled B19 parvovirus capsids, produced in a baculovirus system, are antigenically and immunogenically similar to native virions. Proc Natl Acad Sci USA 88: 4646-4650.

Kaplan AA. 2003. The use of apheresis in immune renal disorders. Ther Apher Dial 7(2): 165-172.

Karetnyi YV, Beck PR, Markin RS, Langnas AN and Naides SJ. 1999. Human parvovirus B19 infection in acute fulminant liver failure. Arch Virol 144: 1713-1724.

Kariyawasam HH, Gyi KM, Hodson ME and Cohen BJ. 2000. Anaemia in lung transplant patient caused by parvovirus B19. Thorax 55: 619-620.

Karunajeewa H, Siebert D, Hammond R, Garland S and Kelly H. 2001. Seroprevalence of varicella zoster virus, parvovirus B19 and *toxoplama gondii* in a Melbourne obstetric population: implications for management. Aust N Z J Obstet Gynaecol 41(1): 23-28.

Katta R. 2002. Parvovirus B19: a review. Dermatol Clin 20: 333-342.

Kaufmann B, Simpson AA and Rossmann MG. 2004. The structure of human parvovirus B19. Proc Natl Acad Sci U S A 101(32): 11628-11633.

Kawase M, Momoeda M, Young NS and Kajigaya S. 1995. Most of the VP1 unique region of B19 parvovirus is on the capsid surface. Virology 211: 359-366.

Kelleher JF, Luban NLC, Mortimer PP and Kamimura T. 1983. Human serum "parvovirus": a specific cause of aplastic crisis in children with hereditary spherocytosis. Clinical and laboratory observations 102(5): 720-722.

Kelly HA, Rae PB, Donnelly JK and Leydon JA. 1999. Fifth disease in a small rural community. What are the consequences? Austr Fam Physi 28(2): 139-144.

Kelly HA, Siebert D, Hammond R, Leydon J, Kiely P and Maskill W. 2000. The age-specific prevalence of human parvovirus immunity in Victoria, Australia compared with other parts of the world. Epidemiol Infect 124(3): 449-457.

Kerr JR, Curran MD, Moore JE, Erdman DD, Coyle PV, Nunoue T, Middleton D and Ferguson WP. 1995a. Genetic diversity in the non-structural gene of parvovirus B19 detected by single-

stranded conformational polymorphism assay (SSCP) and partial nucleotide sequencing. J Virol Methods 53: 213-222.

Kerr JR, Cartron JP, Curran MD, Moore JE, Elliott JRM and Mollan RAB. 1995b. A study of the role of parvovirus B19 in rheumatoid arthritis. Br J Rheumatol 34: 809-813.

Kerr JR. 2000. Pathogenesis of human parvovirus B19 in rheumatic disease. Ann Rheum Dis 59: 672-683.

Kerr JR and Behan WMH. 2002. High mutation rate in the NS1 gene of parvovirus B19 DNA amplified from skeletal muscle of a case of mixed connective tissue disease. Rheumatology 41: 833-834.

Kerr JR and Cunniffe VS. 2000. Antibodies to parvovirus B19 non-structural protein are associated with chronic but not acute arthritis following B19 infection. Rheumatology 39: 903-908.

Kerr S, O'Keeffe G, Kilty C and Doyle S. 1999. Undenaturated parvovirus B19 antigens are essential for the accurate detection of parvovirus B19 IgG. J Med Virol 57: 179-185.

Kimberly RP, Salmon JE, Bussel JB, Kuntz Crow M and Hilgartner MW. 1984. Modulation of mononuclear phagocyte function by intravenous γ-globulin. J Immunol 132(2): 745-750.

King DA and Gutekunst DE. 1970. A new mink enteritis vaccine for immunization against feline panleukopenia. Vet Med/Small Anim Clini 65: 377-383.

Kishore J, Misra R, Gupta D and Ayyagari A. 1998. Raised IgM antibodies to parvovirus B19 in juvenile rheumatois arthritis. Indian J Med Res 107: 15-18.

Kishore J and Kapoor A. 2000. Erythrovirus B19 infection in humans. Indian J Med Res 112: 149-164.

Kitamura T, Tange T, Terasawa T, Chiba S, Kuwaki T, Miyagawa K, Piao YF, Miyazono K, Urabe A and Takaku F. 1989. Establishment and characterization of a unique human cell line that proliferates dependently on GM-CSF, IL-3, or erythropoietin. J Cell Physiol 140(2): 323-334.

Kleim JP, Bailly E, Schneweis KE, Brackmann HH, Hammerstein U, Hanfland P, van Loo B and Oldenburg J. 1990. Acute HIV-1 infection in patients with hemophilia B treated with beta-propiolactone-UV-inactivated clotting factor. Thromb Haemost 64(2): 336-337.

Klenerman P, Tolfvenstam T, Price DA, Nixon DF, Broliden K and Oxenius A. 2002. T lymphocyte responses against human parvovirus B19: small virus, big response. Pathol Biol 50: 317-325.

Klouda PT, Corbin SA, Bradley BA, Cohen BJ and Woolf AD. 1986. HLA and acute arthritis following human parvovirus infection. Tissue Antigens 28: 318-319.

Knott PD, Welply GAC and Anderson MJ. 1984. Serologically proved intrauterine infection with parvovirus. Br Med J 289: 1660.

Koch WC and Adler SP. 1989. Human parvovirus B19 infections in women of childbearing age and within families. Pediatr Infect Dis J 8: 83-87.

Koch WC and Adler SP. 1990. Detection of human parvovirus B19 DNA by using the polymerase chain reaction. J Clin Microbiol 28(1): 65-69.

Koduri PR, Kumapley R, Valladares J and Teter C. 1999. Chronic pure red cell aplasia caused by parvovirus B19 in AIDS: use of intravenous immunoglobulin-a report of eight patients. Am J Hematol 61: 16-20.

Koenigbauer UF, Eastlung T and Day JW. 2000. Clinical illness due to parvovirus B19 infection after infusion of solvent/detergent-treated pooled plasma. Transfusion 40:1203-1206.

Koga M, Matsuoka T, Katayama K, Takeda K, Nakata M, Sase M, Kato H and Furukawa S. 2001. Human parvovirus B19 in cord blood of premature infants. Am J Perinat 18(5): 237-240.

Komatsu N, Nakauchi H, Miwa A, Ishihara T, Eguchi M, Moroi M, Okada M, Sato Y, Wada H, Yawata Y, Suda T and Miura Y. 1991. Establishment and characterization of a human leukemic cell line with megakaryocytic features: dependency on granulocyte-macrophage colony-stimulating factor, interleukin 3, or erythropoietin for growth and survival. Cancer Res 51(1): 341-348.

Komatsu N, Yamamoto M, Fujita H, Miwa A, Hatake K, Endo T, Okano H, Katsube T, Fukumaki Y, Sassa S and Miura Y. 1993. Establishment and characterisation of an erythropoietin-dependent subline, UT-7/EPO, derived from human leukaemia cell line, UT-7. Blood 82: 456-464.

Koziol DE, Kurtzman G, Ayub J, Young NS and Henderson DK. 1992. Nosocomial human parvovirus B19 infection: lack of transmission from a chronically infected patient to hospital staff. Infect Control Hosp Epidemiol 13: 343-348.

Krumbholz A, Wurm R, Scheck O, Birch-Hirschfeld E, Egerer R, Henke A, Wutzler P and Zell R. 2003.Detection of porcine teschoviruses and enteroviruses by LightCycler real-time PCR. J Virol Methods 113: 51-63.

Kurtzman GJ, Ozawa K, Cohen B, Hanson G, Oseas R and young NS. 1987. Chronic bone marrow failure due to persistent B19 infection. N Engl J Med 317(5): 287-294.

Kurtzman GJ, Cohen BJ, Meyers P, Amunullah A and Young NS. 1988. Persistent B19 parvovirus infection as a cause of severe chronic anaemia in children with acute lymphocytic leukaemia. Lancet ii: 1159-1162.

Kurtzman GJ, Cohen BJ, Field AM, Oseas R, Blease RM and Young NS. 1989a. Immune response to B19 parvovirus and an antibody defect in persistent viral infection. J Clin Invest. 84: 1114-1123.

Kurtzman GJ, Frickhofen N, Kimball J, Jenkins DW, Nienhuis AW and Young NS. 1989b. Pure red-cell aplasia of 10 years' duration due to persistent parvovirus B19 infection and its cure with immunoglobulin therapy. The New England Journal of Medicine. 321(8): 519-523.

Labbé L, Mortreux P, Leauté-Labreze C and Taïeb. 1994. Parvovirose cutanée: syndrome "gants et chaussettes". Ann Dermatol Venereol 121: 553-556.

Lambrecht B, Mohr H, Knűver-Hopf J, Schmitt H. 1991. Photoinactivation of viruses in human fresh plasma by phenothiazine dyes in combination with visible light. Vox Sang 60: 207-213.

Langeveld JPM, Ignacio Casal J, Vela C, Dalsgaard K, Smale SH, Puijk WC and Meloen RH. 1993. B-cell epitopes of canine parvovirus: distribution on the primary structure and exposure on the viral surface. J Virol. 67(2): 765-772.

Langnas AN, Markin RS, Cattral MS and Naides SJ. 1995. Parvovirus B19 as a possible causative agent of fulminant liver failure and associated aplastic anemia. Hepatology 22: 1661-1665.

Lauer BA, MacCormack JN and Wilfert C. 1976. Erythema infectiosum. An elementary school outbreak. Am J Dis Child 130: 252-254.

Laurian Y, Dussaix E, Parquet A, Chalvon-Demersay A, d'Oiron R and Tchernia G. 1994. Transmission of human parvovirus B19 by plasma derived factor VIII concentrates. Nouv Rev Fr Hematol 36(6): 449-453.

Lawrence JE. 1993. Affinity chromatography to remove viruses during preparation of plasma derivatives. Dev Biol Stand 81: 191-7.

Lazo A, Tassello J, Jayarama V, Ohagen A, Gibaja V, Kramer E, Marmorato A, Billia-Shaveet D, Purmal A, Brown F and Chapman J. 2002. Broad-spectrum virus reduction in red cell concentrates using INACTINE PEN110 chemistry. Vox Sang 83(4): 313-323.

Lefrère JJ, Meyer O, Menkes C-J, Beaulieu M-J and Couroucé A-M. 1985a. Human parvovirus and rheumatoid arthritis. Lancet I: 982

Lefrère JJ, Boutard P, Couroucé A-M, Lacaze T and Girot R. 1985b. Familial human parvovirus infections. Lancet ii: 333-334.

Lefrère JJ, Couroucé AM, Bertrand Y and Soulier JP. 1986a. Infections à parvovirus B19. Revue Française de Transfusion et Immuno-hématologie 29(3): 149-162.

Lefrère JJ, Couroucé AM, Girot R and Cornu P. 1986b. Human parvovirus and thalassaemia. J Infect 13: 45-49.

Lefrère JJ, Couroucé AM, Bertrand Y, Girot R and Soulier JP. 1986c. Human parvovirus and aplastic crisis in chronic haemolytic anemias: a study of 24 observations. Am J Hematol 23: 271-275.

Lefrère JJ, Couroucé A-M., Soulier JP, Cordier MP, Guesne Girault, Polonovski C and Bensman A. 1986d. Henoch-Schönlein purpura and human parvovirus infection. Pediatrics 78(1): 183-184.

Lefrère JJ, Couroucé AM and Kaplan C. 1989. Parvovirus and idiopathic thrombocytopenic purpura. Lancet I: 279.

Lefrère JJ, Mariotti M and Thauvin M. 1994. B19 parvovirus DNA in solvent/detergent-treated anti-haemophilia concentrates. Lancet 343(8891): 211-212.

Lefrère JJ, Mariotti M, De La Croix I, Lerable J, Thauvin M, Burnouf T and Folléa G. 1995. Albumin batches and B19 parvovirus DNA. Transfusion 35(5): 389-391.

Lefrère JJ and Bourgeois H. 1986. Human parvovirus associated with erythroblastopenia in iron deficiency anaemia. J Clin Pathol 39: 1277-1278.

Lefrère JJ and Decazes J-M. 1986. Aplastic crisis or erythroid hypoplasia. JAMA 256(22): 3096.

Legendre D and Rommelaere J. 1992. Terminal regions of the NS-1 protein of the parvovirus minute virus of mice are involved in cytotoxicity and promoter trans inhibition. J Virol 66(10): 5705-5713.

Legendre D and Rommelaere J. 1994. Targeting of promoters for trans activation by a carboxy-terminal domain of the NS-1 protein of the parvovirus minute virus of mice. J Virol 68(12): 7974-7985.

Lehmann HW, von Landenberg P and Modrow S. 2002. Parvovirus B19 infection and autoimmune disease. Autoimmun Rev 2(4): 218-223.

Leruez M, Pallier C, Vassias I, Elouet JF, Romeo P and Morinet F. 1994. Differential transcription, without replication, of non-structural and structural genes of human parvovirus B19 in the UT7/EPO cell as demonstrated by in situ hybridization. J Gen Virol 75: 1475-1478.

Leruez-Ville M, Vassias I, Pallier C, Cecille A, Hazan U and Morinet F. 1997. Establishment of a cell line expressing human parvovirus B19 non-structural protein from an inducible promoter. J Gen Virol 78: 215-219.

Li X and Rhode III SL. 1990. Mutation of lysine 405 to serine in the parvovirus H-1 NS1 abolishes its functions for viral DNA replication, late promoter *trans* activation, and cytotoxicity. J Virol 64(10): 4654-4660.

Li Loong TC, Coyle PV, Anderson MJ, Allen GE and Connolly JH. 1986. Human serum parovirus associated vasculitis. Postgrad Med J 62: 493-494.

Lin L. 2001. Inactivation of cytomegalovirus in platelet concentrates using Helinx® technology. Semin Hematol 38(4 suppl 11): 27-33.

Liu JM, Fujii H, Green SW, Komatsu N, Young NS and Shimada T. 1991a. Indiscriminate activity from the B19 parvovirus p6 promoter in nonpermissive cells. Virology 182(1): 361-364.

Liu JM, Green SW, Hao YS, McDonagh KT, Young NS and Shimada T. 1991b. Upstream sequences within the terminal hairpin positively regulate the P6 promoter of B19 parvovirus. Virology 185(1): 39-47.

Liu JM, Green SW, Shimada T and Young NS. 1992. A block in full-length transcript maturation in cells nonpermissive for B19 parvovirus. J Virol 66: 4686-4692.

Liu Q, Yong CB and Astell CR. 1994. In vitro resolution of the dimer bridge of the minute virus of mice (MVM) genome supports the modified rolling hairpin model for MVM replication. Virology 201(2): 251-262.

Lo-Man R, Rueda P, Sedlik C, Deriaud E, Casal I and Leclerc C. 1998. A recombinant virus-like particle system derived from parvovirus as an efficient antigen carrier to elicit a polarized Th1 immune response without adjuvant. Eur J Immunol 28: 1401-1407.

Lombardo E, Ramirez JC, Agbandje-McKenna M and Almendral JM. 2000. A beta-stranded motif drives capsid protein oligomers of the parvovirus minute virus of mice into the nucleus for viral assembly. J Virol 74(8): 3804-3814.

Lombardo E, Ramirez JC, Garcia J and Almendral JM. 2002. Complementary roles of multiple nuclear targeting signals in the capsid proteins of the parvovirus minute virus of mice during assembly and onset of infection. J Virol 76(14): 7049-7059.

Longhurst HJ, Letellier E, D'Cruz D and McCurdie I. 2001. Parvovirus arthropathy masquerading as the arthritis of Behçet's disease. Ann Rheum Dis 60(11): 1080.

Louie RE, Galloway CJ, Dumas ML, Wong MF and Mitra G. 1994. Inactivation of hepatitis C virus in low pH intravenous immunoglobulin. Biologicals 22(1):13-19.

Lowden E and Weinstein L. 1997. Unexpected second trimester pregnancy loss due to maternal parvovirus B19 infection. Southern Med J 90(7): 702-704.

Lowenthal EA, Wells A, Emanuel PD, Player R and Prchal JT. 1996. Sickle cell acute chest syndrome associated with parvovirus B19 infection: case series and review. Am J Hematol 51: 207-213.

Lui SL, Luk WK, Cheung CY, Chan TM, Lai KN and Peiris JSM. 2001. Nosocomial outbreak of parvovirus B19 infection in a renal transplant unit. Transplantation 71(1): 59-64.

Lunardi C, Tiso M, Borgato L, Nanni L, Millo R, De Sandre G, Bargellesi Severi A and Puccetti A. 1998. Chronic parvovirus B19 infection induces the production of anti-virus antibodies with autoantigen binding properties. Eur J Immunol 28: 936-948.

Luo W and Astell CR. 1993. A novel protein encoded by small RNAs of parvovirus B19. Virology 195: 448-455.

Lusby E, Fife KH and Berns KI. 1980. Nucleotide sequnce of the inverted terminal repetition in adeno-associated virus DNA. J Virol 34(2): 402-409.

Lusher J, Kessler C, Laurian Y and Pierce G. 1994. Viral contamination of blood products-letter to the editor. The Lancet 344.

Luzzi GA, Kurtz JB and Chapel H. 1985. Human parvovirus arthropathy and rheumatoid factor. Lancet 1(8439): 1218.

Macara IG. 2001. Transport into and out of the nucleus. Microbiol Mol Biol Rev 65(4): 570-594.

Makhseed M, Pacsa A, Abrar Ahmed M and Sultan Essa S. 1999. Pattern of parvovirus B19 infection during different trimesters of pregnancy in Kuwait. Infect Dis Obstet Gynecol 7: 287-292.

Malm C, Fridell E and Jansson K. 1993. Heart failure after parvovirus B19 infection. Lancet 341: 1408-1409.

Manaresi E, Gallinella G, Zerbini M, Venturoli S, Gentilomi G and Musiani M. 1999a. IgG immune response to B19 parvovirus VP1 and VP2 linear epitopes by immunoblot assay. J Med Virol 57: 174-178.

Manaresi E, Pasini P, Gallinella G, Gentilomi G, Venturoli S, Roda A, Zerbini M and Musiani M. 1999b. Chemiluminescence western blot assay for the detection of immunity against parvovirus B19 VP1 and VP2 linear epitopes using a videocamera based luminograph. J Virol Methods 81: 91-99.

Manaresi E, Zuffi E, Gallinella G, Gentilomi G, Zerbini M and Musiani M. 2001. Differential IgM response to conformational and linear epitopes of parvovirus B19 VP1 and VP2 structural proteins. J Med Virol. 64: 67-73.

Manaresi E, Gallinella G, Gentilomi G, Venturoli S, Zuffi E, Bonvincini F, Cricca M, Zerbini M and Musiani M. 2002a. Humoral immune response to parvovirus B19 and serological diagnosis of B19 infection. Clin Lab 48: 201-205.

Manaresi E, Gallinella G, Zuffi E, Bonvicini F, Zerbini M and Musiani M. 2002b. Diagnosis and quantitative evaluation of parvovirus B19 infections by real-time PCR in the clinical laboratory. J Med Virol 67: 275-281.

Mannucci PM., Schimpf K, Abe T, Aledort LM, Anderle K, Brettler DB, Hilgartner MW, Kernoff PB, Kunschak M, McMillan CW, *et al.* (International Investigator Group). 1992. Low risk of viral infection after administration of vapor-heated factor VIII concentrate. Transfusion 32: 134-138.

Marchand S, Tchernia G, Hiesse C, Tertian G, Cartron J, Kriaa F, Boubenider S, Goupy C, Lecointe D and Charpentier B. 1999. Human parvovirus B19 infection in organ transplant recipients. Clin Transplant 13: 17-24.

Markenson AL, Chandra M, Lewy JE and Miller DR. 1978. Sickle cell anemia, the nephrotic syndrome and hypoplastic crisis in a sibship. Am J Med 64: 719-723.

Mather T, Takeda T, Tassello J, Ohagen A, Serebryanik D, Kramer E, Brown F, Tesh R, Alford B, Chapman J and Lazo A. 2003. West Nile virus in blood: stability, distribution, and susceptibility to PEN110 inactivation. Transfusion 43(8): 1029-1037.

Mathias RS. 1997. Chronic anemia as a complication of parvovirus B19 infection in a pediatric kidney transplant patient. Pediatr Nephrol 11: 355-357.

Mauser-Bunschoten EP, Zaaijer HL, Van Drimmelen, de Vries S, Roosendaal G, van den Berg HM and Lelie PN. 1998. High prevalence of parvovirus B19 IgG antibodies among Dutch hemophilia patients. Vox Sang 74:225-227.

McClain K, Estrov Z, Chen H and Mahoney DH. 1993. Chronic neutropenia of childhood: frequent association with parvovirus infection and correlations with bone marrow culture studies. Br J Haematol 85: 57-62.

McGuire WA, Yang HH, Brumo E, Brandt J, Briddell R, Coates TD and Hoffman R. 1987. Treatment of antibody-mediated pure red-cell aplasia with high-dose intravenous gamma globulin. N Engl J Med 317(16): 1004-1007.

McOmish F, Yap PL, Jordan A, Hart H, Cohen BJ and Simmonds P. 1993. Detection of parvovirus B19 in donated blood: a model system for screening by polymerase chain reaction. J Clin Microbiol 31(2): 323-8.

Mengeling WL, Brown TT, Paul PS and Gutekunst DE. 1979. Efficacy of an inactivated virus vaccine for prevention of porcine parvovirus-induced reproductive failure. Am J Vet Res 40(2): 204-207.

Messori A, Morfini M, Blomback M, Cinotti S, Longo G, Schimpf K, Schumacher K, Novakova-Banet A, Delvos U and Kjellman H. 1992. Pharmacokinetics of two pasteurized factor VIII concentrates by different and multicenter assays of factor VIII activity. Thromb Res 65(6): 699-708.

Mide SM, Huygens P, Bozzini CE and Fernandez Pol JA. 2001. Effects of human recombinant erythropoietin on differentiation and distribution of erythroid progenitor cells on murine medullary and splenic erythropoiesis during hypoxia and post-hypoxia. In Vivo 15(2): 125-132.

Miekka SI, Busby TF, Reid B, Pollock R, Ralston A and Drohan WN. 1998. New methods for inactivation of lipid-enveloped and non-enveloped viruses. Haemophilia 4(4): 402.

Miekka SI, Forng RY, Rohwer RG, MacAuley C, Stafford RE, Flack SL, MacPhee M, Kent RS and Drohan WN. 2003. Inactivation of viral and prion pathogens by γ-irradiation under conditions that aintain the integrity of human albumin. Vox Sang 84: 36-44.

Miller E, Fairley CK, Cohen BJ and Seng C. 1998. Immediate and long term outcome of human parvovirus B19 infection in pregnancy. Br J Obstet Gynaecol 105: 174-178.

Mitchell LA, Leong R and Rosenke KA. 2001. Lymphocyte recognition of human parvovirus B19 non-structural (NS1) protein: associations with occurrence of acute and chronic arthropathy? J Med Microbiol 50: 627-635.

Miyagawa E, Yoshida T, Takahashi H, Yamaguchi K, Nagano T, Kiriyama Y, Okochi K, Sato H. 1999. Infection of the erythroid cell line, KU812Ep6 with human parvovirus B19 and its application to titration of B19 infectivity. J Virol Methods. 83(1-2): 45-54.

Miyamoto K, Ogami M, Takahashi Y, Mori T, Akimoto S, Terashita H and Terashita T. 2000. Outbreak of human parvovirus B19 in hospital workers. J Hosp Infect 45: 238-241.

Miyamura K, Kajigaya S, Momoeda M, Smith-Gill SJ and Young NS. 1994. Parvovirus particles as platforms for protein presentation. Proc Natl Acad Sci USA 91: 8507-8511.

Moffatt S, Tanaka N, Tada K, Nose M, Nakamura M, Muraoka O, Hirano T and Sugamura K. 1996. A cytotoxic non-structural protein, NS1, of human parvovirus B19 induces activation of interleukin-6 gene expression. J Virol 70(12): 8458-8491.

Moffatt S, Yaegashi N, Tada K, Tanaka N and Sugamura K. 1998. Human parovirus B19 nonstructural (NS1) protein induces apoptosis in erythroid lineage cells. J Virol 72(4): 3018-3028.

Mohr H, Knuver-Hopf J, Gravemann U, Redecker-Klein A and Muller TH. 2004. West Nile virus in plasma is highly sensitive to methylene blue-light treatment. Transfusion 44(6): 886-890.

Momoeda M, Wong S, Kawase M, Young NS and Kajigaya S. 1994a. A putative nucleoside triphosphate-binding domain in the nonstructural protein of B19 parvovirus is required for cytotoxicity. J Virol 68(12): 8443-8446.

Momoeda M, Kawase M, Jane SM, Miyamura K, Young NS and Kajigaya S. 1994b. The transcriptional regulator YY1 binds to the 5'-terminal region of B19 parvovirus and regulates P6 promoter activity. J Virol 68(11): 7159-7168.

Montagnon B, Vincent-Falquet JC and Fanget B. 1983. Thousand litre scale microcarrier culture of Vero cells for killed polio virus vaccine. Promising results. Dev Biol Stand 55: 37-42.

Morey AL, Keeling JW, Porter HJ and Fleming KA. 1992. Clinical and histopathological features of parvovirsu B19 infection in the human fetus. Br J Obstet Gynaecol 99: 566-574.

Morey AL, Ferguson DJ and Fleming KA. 1993. Ultrastructural features of fetal erythroid precursors infected with parvovirus B19 in vitro: evidence of cell death by apoptosis. J Pathol 169(2): 213-220.

Morfini M, Longo G, Rossi Ferrini P, Azzi A, Zakrewska C, Ciappi S and Kolumban P. 1992. Letter to the Editor: hypoplastic anemia in a hemophiliac first infused with solvent-detergent treated factor VIII concentrate: the role of human B19 parvovirus. Am J of Hematol 39:149-150.

Morgan WR and Ward DC. 1986. Three splicing patterns are used to excise the small intron common to all minute virus of mice RNAs. J Virol 60(3): 1170-1174.

Morgan-Capner P, Crowcroft NS, on behalf of the PHLS joint working party of the advisory committees of virology and vaccines and immunisation. 2002. Guidelines on the management of, and exposure to, rash illness in pregnancy (including consideration of relevant antibody screening programmes in pregnancy). Comm Dis Public Health 5(1): 59-71.

Morgenthaler JJ and Omar A. 1993. Partitioning and inactivation of viruses during isolation of albumin and immunoglobulins by cold ethanol fractionation. Dev Biol Stand 81: 185-190.

Mortimer PP, Luban NLC, Kelleher JF and Cohen BJ. 1983. Transmission of serum parvovirus-like virus by clotting-factor concentrates. The Lancet Aug, 27:482-484.

Mori J, Beattie P, Melton DW, Cohen BJ and Clewley JP. 1987. Structure and mapping of the DNA of human parvovirus B19. J Gen Virol 68: 2797-2806.

Morinet F, Tratschin J-D, Perol Y and Siegl G. 1986. Comparison of 17 isolates of the human parvovirus B19 by restriction enzyme analysis. Arch Virol 90: 165-172.

Morinet F, D'Auriol L, Tratschin JD and Galibert F. 1989. Expression of the human parvovirus B19 protein fused to protein A in *Escherichia coli*: recognition by IgM and IgG antibodies in human sera. J Gen Virol 70: 3091-3097.

Morinet F, Pallier C, Foulon-Sol N and Pillet S. 2000. Molecular biology of erythroviruses. In Parvoviruses: from molecular biology to pathology and therapeutic uses. Faisst S and Rommelaere J (eds). Basel, Karger. Pp 123-132, vol 4.

Morita E, Tada K, Chisaka H, Asao H, Sato H, Yaegashi N and Sugamura K. 2001. Human parvovirus B19 induces cell cycle arrest at G2 phase with accumulation of mitotic cyclins. J Virol 75(16): 7555-7563.

Moore TL, Bandlamudi R, Alam SM and Nesher G. 1999. Parvovirus infection mimicking systemic lupus erythematosus in a pediatric population. Sem Arthr Rheum 28(5): 314-318.

Moore TL. 2000. Parvovirus-associated arthritis. Curr Opin Rheumatol 12: 289-294.

Moudgil A, Shidban H, Nast CC, Bagga A, Aswad S, Graham SL, Mendez Ra and Jordan SC. 1997. Parvovirus B19 infection-related complications in renal transplant recipients. Transplantation 64(12): 1847-1850.

Muller D-E and Siegl G. 1983. Maturation of parvovirus LuIII in a subcellular system. II. Identification and characterization of nucleoprotein intermediates. J Gen Virol 64: 1055-1067.

Muller-Breitkreutz K and Mohr H. 1998. Hepatitis C and human immunodeficiency virus RNA degradation by methylene blue/light treatment of human plasma. J Med Virol 56(3): 239-45.

Mullis K, Faloona F, Scharf S, Saiki R, Horn G and Erlich H. 1986. Specific enzymatic amplification of DNA in vitro: the polymerase chain reaction. Cold Spring Harb Symp Quant Biol 51: 263-273.

Mullis KB and Faloona FA. 1987. Specific synthesis of DNA in vitro via a polymerase-catalyzed chain reaction. Methods Enzymol 155: 335-350.

Munshi NC, Zhou S, Woody MJ, Morgan DA and Srivastava A. 1993. Successful replication of parvovirus B19 in human megakaryocytic cell line MB-02. J Virol 67: 562-566.

Murai C, Munakata Y, Takahashi Y, Ishii T, Shibata S, Muryoi T, Funato T, Nakamura M, Sugamura K and Sasaki T. 1999. Rheumatoid arthritis after human parvovirus B19 infection. Ann Rheum Dis 58: 130-132.

Murray JC, Gresik MV, Leger F and McClain KL. 1993. B19 parvovirus-induced anemia in a normal child. Am J Pediat Hematol/Oncol 15(4): 420-423.

Musiani M, Azzi A, Zerbini M, Gibellini D, Venturoli S, Zakrzewska K, Re MC, Gentilomi G, Gallinella G and La Placa M. 1993. Nested polymerase chain reaction assay for the detection of B19 parvovirus DNA in human immunodeficiency virus patients. J Med Virol 40: 157-160.

Musiani M, Manaresi E, Gallinella G, Venturoli S, Zuffi E and Zerbini M. 2000. Immunoreactivity against linear epitopes of parvovirus B19 structural proteins. Immunodominance of the amino-terminal half of the unique region of VP1. J Med Virol 60: 347-352.

Mylonakis E, Dickinson BP, Mileno MD, Flanigan T, Schiffman F, Mega A and Rich JD. 1999. Persistent parvovirus B19 related anemia of seven years' duration in an HIV-infected patients:

complete remission associated with highly active antiretroviral therapy. Am J Hematol 60: 164-166.

Naides SJ, Piette W, Veach LA and Argenyi Z. 1988. Human parvovirus B19-induced vesiculopustular skin eruption. Am J Med 84: 968-972.

Naides SJ, Scharosch LL, Foto F and Howard EJ. 1990. Rheumatologic manifestations of human parvovirus B19 infection in adults. Arthr Rheum 33(9): 1297-1309.

Naides SJ, Karetnyi YV, Cooling LLW, Mark RS and Langnas AN. 1996. Human parvovirus B19 infection and hepatitis. Lancet Letter 347: 1563.

Naides SJ and Weiner CP. 1989. Antenatal diagnosis and palliative treatment of non-immune hydrops fetalis secondary to fetal parvovirus B19 infection. Prenatal Diagnosis 9: 105-114.

Nakazawa M, Mitjavila MT, Debili N, Casaderall N, Mayeux P, Rouyer-Fessard P, Dubart A, Romeo P, Beuzard Y, Kishi K, Breton-Gorius J and Vainchenker W. 1989. KU812: a pluripotent human cell line with spontaneous erythroid terminal maturation. Blood 7: 2003-2013.

Negro A, Regolisti G, Perazzoli F, Coghi P, Tumiati B and Rossi E. 2001. Human parvovirus B19 infection mimicking systemic lupus erythematosus in an adult patient. Ann Ital Med Int 16: 125-127.

Nelson JSB and Stone MS. 2000. Update on selected viral exanthems. Curr Opin Pediatr 12: 359-364.

Nesher G, Osborn TG and Moore TL. 1995. Parvovirus infection mimicking systemic lupus erythematosus. Sem Arthr Rheum 24(5): 297-303.

Nguyen QT, Sifer C, Schneider V, Bernaudin F, Auguste V and Garbarg-Chenon A. 1998. Detection of an erythrovirus sequence distinct from B19 in a child with acute anaemia. Lancet 352(9139): 1524.

Nguyen QT, Sifer C, Schneider V, Allaume X, Servant A, Bernaudin F, Auguste V and Garbarg-Chenon A. 1999. Novel human erythrovirus associated with transient aplastic anemia. J Clin Microbiol 37(8): 2483-2487.

Nguyen QT, Wong S, Heegaard ED and Brown KE. 2002. Identification and characterization of a second novel human erythrovirus variant, A6. Virology 301(2): 374-380.

Nicolis S, Ottolenghi S, Papayannopoulou T, Baiocchi M, Migliaccio G, Adamson J and Migliaccio AR. 1993. Dependence for the proliferative response to erythropoietin on an established erythroid differentiation program in a human hematopoietic cell line, UT-7. Exp Hematol 21(5): 665-670.

Niitsu H, Takatsu H, Miura I, Chubachi A, Ito T, Hirokawa M, Endo Y, Miura A, Fukuda M and Sasaki T. 1990. Pure red cell aplasia induced by B19 parvovirus during allogeneic bone marrow transplantation (in Japanese). Jpn J Clin Hematol 31(9): 1566-1571.

Nikkari S, Roivainen A, Hannonen P, Möttönen T, Luukkainen R, Yli-Jama T and Toivanen P. 1995. Persistence of parvovirus B19 in synovial fluid and bone marrow. Ann Rheum Dis 54: 597-600.

Nocton JJ, Miller LC, Tucker LB and Schaller JG. 1993. Human parvovirus B19-associated arthritis in children. J Pediatr 122: 186-190.

Nowak T, Niedrig M, Bernhardt D, Hilfenhaus J. 1993. Inactivation of HIV, HBV, HCV related viruses and other viruses in human plasma derivatives by pasteurisation. Dev Biol Stand 81:169-76.

Nunoue T, Okochi K, Mortimer PP and Cohen BJ. 1985. Human parvovirus (B19) and erythema infectiosum. J Pediatr 107: 38-40.

Nunoue T, Koike T, Koike R, Sanada M, Tsukada T, Mortimer PP and Cohen BJ. 1987. Infection with human parvovirus (B19), aplasia of the bone marrow and a rash in hereditary spherocytosis. J Infect 14(1): 67-70.

Nunoue T, Kusuhara K and Hara T. 2002. Human fetal infection with parvovirus B19: maternal infection time in gestation, viral persistence and fetal prognosis. Pediatr Infect Dis J 21(12): 1133-1136.

Nyman M, Tolfvenstam T, Petersson K, Krassny C, Skjöldebrand-Sparre L and Broliden K. 2002. Detection of human parvovirus B19 infection in first-trimester fetal loss. Obstet and Gynecol 99(5): 795-798.

O'Grady J, Losikoff A, Poiley J, Fickett D and Oliver C. 1996. Virus removal studies using nanofiltration membranes. Dev Biol Stand 88: 319-26.

Ohagen A, Gibaja V, Aytay S, Horrigan J, Lunderville D and Lazo A. 2002. Inactivation of HIV in blood. Trasfusion 42(10): 1308.

Ohtomo Y, Kawamura R, Kaneko K, Yamashiro Y, Kiyokawa N, Taguchi T, Mimori K and Fujimoto J. 2003. Nephrotic syndrome associated with human parvovirus B19 infection. Pediatr Nephrol 18: 280-282.

Okochi K, Mori R, Miyazaki M, Cohen BJ and Mortimer PP. 1984. Nakatani antigen and human parvovirus (B19) Lancet 1(8369): 160-161.

Okumura A and Ichikawa T. 1993. Aseptic meningitis caused by human parvovirus B19. Arch Dis Child 68: 784-785.

Okuno Y, Suzuki A, Ichiba S, Takahashi T, Nakamura K, Hitomi K, Sasaki R, Tada K and Imura H. 1990. Establishment of an erythroid cell line (JK-1) that spontaneously differentiates to red cells. Cancer 66(7):1544-1551.

Omar A, Kempf C, Immelmann A, Rentsch M and Morgenthaler JJ. 1996. Virus inactivation by pepsin treatment at pH 4 of IgG solutions: factors affecting the rate of virus inactivation. Transfusion 36: 866-872.

Omar A and Kempf C. 2002. Removal of neutralized model parvoviruses and enteroviruses in human IgG solutions by nanofiltration. Transfusion. 42(8):1005-10.

Oriol A, Ribera J-M, Hernández A, Soriano V, Millá F and Feliu E. 1994. Aplastic anemia after non-A, non-B, non-C hepatitis. Haematologica 79: 168-169.

O'Sullivan MG, Anderson DK, Fickes JD, Bain FT, Carlson CS, Green SW, Young NS and Brown KE. 1994. Identification of a novel simian parvovirus in cynomolgus monkeys with severe anemia. J Clin Invest 93: 1571-1576.

O'Sullivan MG, Anderson DK, Lund JE, Brown WP, Green SW, Young NS and Brown KE. 1996. Clinical and epidemiological features of simian parvovirus infection in cynomolgus macaques with severe anemia. Lab Anim Sci 46(3): 291-297.

O'Sullivan MG, Anderson DK, Goodrich JA, Tulli H, Green SW, Young NS and Brown KE. 1997. Experimental infection of cynomolgus monkeys with simian parvovirus. J Virol 71(6): 4517-4521.

Ozawa K, Kurtzman G and Young NS. 1986. Replication of B19 parvovirus in human bone marrow cell cultures. Science 233: 883-886.

Ozawa K, Ayub J, Kurtzman G, Shimada T and Young N. 1987a. Novel transcription map for the B19 (human) pathogenic parvovirus. J Virol 61(8): 2395-2406.

Ozawa K, Kurtzman G and Young N. 1987b. Productive infection by B19 parvovirus of human erythroid bone marrow cells in vitro. Blood 70(2): 384-391.

Ozawa K, Ayub J, Kajigaya S, Shimada T and Young N. 1988a. The gene encoding the nonstructural protein of B19 (human) parvovirus may be lethal in transfected cells. J Virol 62(8): 2884-2889.

Ozawa K, Ayub J and Young N. 1988b. Translational regulation of B19 parvovirus capsid protein production by multiple upstream AUG triplets. J Biol Chem 263(22): 10922-10926.

Ozawa K, Ayub J and Young N. 1988c. Functional mapping of the genome of the B19 (human) parvovirus by in vitro translation after negative hybrid selection. J Virol. 1988 Jul;62(7):2508-11.

Ozawa K and Young N. 1987. Characterization of capsid and noncapsid proteins of B19 parvovirus propagated in human erythroid bone marrow cell cultures. J Virol 61(8): 2627-2630.

Pallier C, Greco A, Le Junter J, Saib A, Vassias I, Morinet F. 1997. The 3' untranslated region of the B19 parvovirus capsid protein mRNAs inhibits its own mRNA translation in nonpermissive cells. J Virol 71(12): 9482-9489.

Palmer P, Pallier C, Leruez-ville M, Deplanche M and Morinet F. 1996. Antibody response to human parvovirus B19 in patients with primary infection by immunblot assay with recombinant proteins. Clinical and Diagnostic Laboratory Immunology 3(2): 236-238.

Pamidi S, Friedman K, Kampalath B, Eshoa C and Hariharan S. 2000. Human parvovirus B19 infection presenting as persistent anemia in renal transplant recipients. Transplantation 69(12): 2666-2669.

Pattison JR, Jones SE, Hodgson J, Davis LR, White JM, Stroud CE and Murtaza L. 1981. Parvovirus infections and hypoplastic crisis in sickle-cell anaemia. Lancet I: 665-664.

Pellas F, Olivares JP, Zandotti C and Delarque A. 1993. Neuralgic amyotrophy after parvovirus B19 infection. Lancet 342: 503-504.

Pereira RFA, de Paula WNS, de Cássia N Cubel R and Nascimento JP. 2001. Anti-VP1 and anti-VP2 antibodies detected by immunofluorescence assays in patients with acute human parvovirus B19 infection. Mem Inst Oswaldo Cruz 96(4): 507-513.

Petrikovsky BM, Baker D and Schneider E. 1996. Fetal hydrops secondary to human parvovirus infection in early pregnancy. Prenat Diagn 16: 342-344.

Pickering JW, Forghani B, Shell GR and Wu L. 1998. Comparative evaluation of three recombinant antigen-based enzyme immunoassays for detection of IgM and IgG antibodies to human parvovirus B19. Clin Diagn Virol 9(1): 57-63.

Pillay D, Patou G, Hurt S, Kibbler CC and Griffiths PD. 1992. Parvovirus B19 outbreak in a children's ward. Lancet 339: 107-109.

Pillet S, Annan Z, Fichelson S and Morinet F. 2003. Identification of a nonconventional motif necessary for the nuclear import of the human parvovirus B19 major capsid protein (VP2). Virology 306(1): 25-32.

Pillet S, Le Guyader N, Hofer T, NguyenKhac F, Koken M, Aubin JT, Fichelson S, Gassmann M, Morinet F. 2004. Hypoxia enhances human B19 erythrovirus gene expression in primary erythroid cells. Virology 327(1): 1-7.

Pintel D, Dadachanji D, Astell CR and Ward DC. 1983. The genome of minute virus of mice, an autonomous parvovirus, encodes two overlapping transcription units. Nucleic Acids Res 11(4): 1019-1038.

Plummer FA, Hammond GW, Forward K, Sekla L, Thompson LM, Jones SE, Kidd IM and Anderson MJ. 1985. An erythema infectiosum-like illness caused by human parvovirus infection. N Engl J Med 313(2): 74-79.

Pol S, Thiers V, Driss F, Devergie A, Berthelot P, Bréchot C and Gluckman E. 1993. Lack of evidence for a role of HCV in hepatitis-associated aplastic crisis. Br J Haematol 85: 808-810.

Ponnazhagan S, Woody MJ, Wang XS, Zhou SZ and Srivastava A. 1995. Transcriptional transactivation of parvovirus B19 promoters in nonpermissive human cells by adenovirus type 2. J Virol 69(12): 8096-8101.

Pont J, Puchhammer-Stöckl E, Chott A, Popow-Kraupp T, Kienzer H, Postner G and Honetz N. 1992. Recurrent granulocytic aplasia as clinical presentation of a persistent parvovirus B19 infection. Brit J Haematol 80: 160-165.

Porter HJ, Quantrill AM and Fleming KA. 1988. B19 parvovirus infection of myocardial cells. Lancet 1(8584): 535-536.

Portis JL and Coe JE. 1979. Deposition of IgA in renal glomeruli of mink affected with Aleutian disease. Am J Pathol 96: 227-236.

Prato C, Paper T and Morinet F. 1991. Use of M13 single-stranded DNA digoxigenin labelled probe for detection of human parvovirus B19 viraemia. J Virol Methods 43: 227-231.

Prince AM, Horowitz B, Brotman B, Huima T, Richardson L and van der Ende MC. 1984. Inactivation of hepatitis B and Hutchinson strain non-A, non-B viruses by exposure to Tween 80 and ether. Vox Sang 46: 36-43.

Prowse CV. 1994. Parvovirus B19 and blood products. The Lancet Apr, 30. 343:1101.

Pruss A, Kao M, Gohs U, Koscielny J, von Versen R and Pauli G. 2002. Effect of gamma irradiation on human cortical bone marrow transplants contaminated with enveloped and non-enveloped viruses. Biologicals 30: 125-133.

Purmal A, Valeri CR, Dzik W, Pivacek L, Ragno G, Lazo A and Chapman J. 2002. Process for the preparation of pathogen-inactivated RBC concentrates by using PEN110 chemistry: preclinical studies. Transfusion 42(2): 139-145.

Pye D, Bates J, Edwards SJ and Hollingworth J. 1990. Development of a vaccine preventing parvoviurs-induced reproductive failure in pigs. Aust Vet J 67: 179-182.

Raab U, Beckenlehner K, Lowin T, Niller HH, Doyle S and Modrow S. 2002. NS1 protein of parvovirus B19 interacts directly with DNA sequences of the p6 promoter and with the cellular transcription factors Sp1/Sp3. Virology 293(1): 86-93.

Rayment FB, Crosdale E, Morris DJ, Pattison JR, Talbot P and Clare JJ. 1990. The production of human parvovirus capsid proteins in Escherichia coli and their potential as diagnostic antigens. J Gen Virol 71: 2665-2672.

Reid DM, Reid TMS, Brown T, Rennie JAN and Eastmond CJ. 1985. Human parvovirus-associated arthritis: a clinical and laboratory description. Lancet I: 422-425.

Reid KG, Cuthbertson B, Jones AD and McIntosh RV. 1988. Potential contribution of mild pepsin treatment at pH4 to the viral safety of human immunoglobulin products. Vox Sang 55(2):75-80.

Reiner AP and Spivak JL. 1988. Hematophagic histiocytosis: a report of 23 patients and a review of the literature. Medicine 67(6): 369-388.

Rhode SL III and Paradiso PR. 1983. Parvovirus genome: nucleotide sequence of H-1 and mapping of its genes by hybrid-arrested translation. J Virol 45(1): 173-184.

Rider JR, Ollier WER, Lock RJ, Brookes ST and Pamphilon DH. 1997. Human cytomegalovirus infection and systemic lupus erythematosus. Clin Exp Rheum 15: 405-409.

Rimmelzwaan GF, Carlson J, UytdeHaag FGCM and Osterhaus ADME. 1990. A synthetic peptide derived from the amino acid sequence of canine parvovirus structural proteins which defines a B cell epitope and elicits antiviral antibody in BALB c mice. J Gen Virol 71: 2741-2745.

Risdall RJ, McKenna RW, Nesbit ME, Krivit W, Balfour HH, Simmons RL and Brunning RD. 1979. Virus-associated hemophagocytic syndrome. A benign histiocytic proliferation distinct from malignant histiocytosis. Cancer 44: 993-1002.

Roberts PL, Walker and Feldman. 1994. Removal and inactivation of enveloped and non-enveloped viruses during the purification of a high-purity factor IX by metal chelate affinity chromatography. Vox Sang 67(suppl 1): 69-71.

Roberts PL. 1996. Removal of parvovirus and hepatits A virus by metal chelate affinity chromatography during the preparation of Replenine®: a high-purity factor IX concentrate. Vox Snag 71: 129-130.

Roberts PL and Dunkerley C. 2003. Effect of manufacturing process parameters on virus inactivation by solvent-detergent treatment in a high-purity factor IX concentrate. Vox Sang 84: 170-175.

Roberts PL and Hart H. 2000. Comparison of the inactivation of canine and bovine parvovirus by freeze-drying and dry-heat treatment in tow high purity factor VIII concentrates. Biologicals 28(3): 185-188.

Roitt I, Brostoff J and Male D (eds). 1998, Immunology Fifth Edition. London, Mosby.

Rollag H, Patou G, Pattison JR, Degré M, Evenson SA, Fröland SS and Glomstein A. 1991. Prevalence of antibodeis against parvovirus B19 in Norwegians with congenital coagulation factor defects treated with plasma products from small donor pools. Scand J Infect Dis 23: 675-679.

Rosenfeld SJ, Yoshimoto K, Kajigaya S, Anderson S, Young NS, Field A, Warrener P, Bansal G and Collett MS. 1992. Unique region of the minor capsid protein of human parvovirus B19 is exposed on the virion surface. J Clin Invest. 89: 2023-2029.

Rouger P, Gane P and Salmon C. 1987. Tissue distribution of H, Lewis and P antigens as shown by a panel of 18 monoclonal antibodies. Rev Fr Transfus Immunohematol 30(5): 699-708.

Rubinstein AI and Rubinstein DB. 1989. Thermal inactivation by sequential dry-heat treatments at sterilizing temperatures (100 degrees C-boiling) of factor VIII and factor IX concentrates to produce sterile concentrates. Vox Sang 57(4): 272.

Rubinstein AI and Rubinstein DB. 1990. Letter to the editor: inability of solvent-detergent (S-D) treated factor VIII concentrate to inactivate parvoviruses and non-lipid enveloped non-A, non-B hepatitis virus in factor VIII concentrate: advantages to using sterilizing 100°C dry heat treatment. Am. J. Hematol. 35: 142.

Rueda P, Martinez-Torrecuadrada JL, Sarraseca J, Sedlik C, del Barrio M, Hurtado A, Leclerc C and Casal JI. 2000. Engineering parvovirus-like particles for the induction of B-cell, CD4+ and CTL responses. Vaccine 18: 325-332

Saal JG, Steidle M, Einsele H, Muller CA, Fritz P and Zacher J. 1992. Persistence of B19 parvovirus in synovial membranes of patients with rheumatoid arthritis. Rheumatol Int 12: 147-151.

Saarinen UM, Chorba TL, Tattersall P, Young NS, Anderson LJ, Palmer E and Coccia PF. 1986. Human parvovirus B19-induced epidemic acute red cell aplasia in patients with hereditary haemolytic anemia. Blood 67(5): 1411-1417.

Sabella C and Goldfarb J. 1999. Parvovirus B19 infections. American Family Physician 60(5): 1455-1460.

Sadahira Y, Yoshimoto S and Manabe T. 1998. Parvovirus B19-associated transient pure red cell aplasia lymphadenopathy: a case report. Pathol Inter 48: 829-833.

Saikawa T, Anderson S, Momoeda M, Kajigaya S and Young NS. 1993. Neutralizing linear epitopes of B19 parvovirus cluster in the VP1 unique and VP1-VP2 junction regions. J Virol. 67(6): 3004-3009.

Saint-Martin J, Choulot JJ, Bonnaud E and Morinet F. 1990. Myocarditis caused by parvovirus. J Pediatr 116(6): 1007-1008.

Saldanha J, Lelie N, Yu MW, Heath A and the B19 collaborative study group. 2002. Establishment of the first World Health Organization international standard for human parvovirus B19 DNA nucleic acid amplification techniques. Vox Sang 82: 24-31.

Saldanha J and Minor P. 1996. Detection of human parvovirus B19 DNA in plasma pools and blood products derived from these pools: implications for efficiency and consistency of removal of B19 DNA during manufacture. Br J Haematol 93: 714-719.

Salimans MMM, Holsappel S, van de Rijke FM, Jiwa NM, Raap AK and Weiland HT. 1989a. Rapid detection of human parvovirus B19 DNA by dot-hybridization and the polymerase chain reaction. J Virol Methods 23: 19-28.

Salimans MMM, van de Rijke FM, Raap AK, van Elsacker-Niele AMW. 1989b. Detection of parvovirus B19 DNA in fetal tissues by in situ hybridisation and polymerase chain reaction. J Clin Pathol 42: 525-530.

Salimans MMM. 1990. Detection of human parvovirus B19 DNA by dot-hybridization and the polymerase chain reaction: applications for diagnosis of infections. Behring Inst Mitt 85: 39-45.

Salimans MMM, van Bussel MJAWM, Brown CS and Spaan WJM. 1992. Recombinant parvovirus B19 capsids as a new substrate for detection of B19-specific IgG and IgM andtibodies by an enzyme-linked immunosorbent assay. J Virol Methods 39: 247-258.

Santagostino E, Mannucci PM, Gringeri A, Azzi A and Morfini M. 1994. Eliminating parvovirus B19 from blood products. The Lancet March, 26. 343: 798.

Santagostino E, Mannucci PM, Gringeri A, Azzi A, Morfini M, Musso R, Santoro R and Schiavoni M. 1997. Transmission of parvovirus B19 by coagulation factor concentrates exposed to 100 degrees C heat after lyophilization. Transfusion 37(5): 517-22.

Sasaki T, Murai C, Muryoi T, Takahashi Y, Munakata Y, Sugamura K and Abe K. 1995. Persistent infection of human parvovirus B19 in a normal subject. Lancet 346(8978): 851.

Sato H, Hirata J, Furukawa M, Kuroda N, Shiraki H, Maeda Y and Okochi K. 1991a. Identification of the region including the epitope for a monoclonal antibody which can neutralize human parvovirus B19. J Virol. 65(4): 1667-1672.

Sato H, Hirata J, Kuroda N, Shiraki H, Maeda Y and Okochi K. 1991b. Identification and mapping of neutralizing epitopes of human parvovirus B19 by using human antibodies. J Virol. 65(10): 5485-5490.

Sato H, Takakura F, Kojima E, Fukada K, Okochi K and Maeda Y. 1995. Screening of blood donors for human parvovirus B19. The Lancet 346: 1237-1238.

Sato K, Matsuda E, Kamisango K, Iwasaki H, Matsubara S and Matsunaga Y. 2000. Development of a hypersensitive detection method for human parvovirus B19 DNA. J Clin Microbiol 38(3): 1241-1243.

Saunders PWG, Reid MM and Cohen BJ. 1986. Human parvovirus induced cytopenias: a report of five cases. Br J Haematol 63: 407-410.

Sawyer L, Dupuis K, Samson-Johannes A, Corten L, Propst M, Hanson D, Bernard K and Alter H. 2003. Helinx® technology inactivates high titers of traditional and emerging viruses in platelet concentrates and plasma. Abstract presented at the National Hemophilia Foundation (NHF) conference (November 6-8).

Sawyer L, Dupuis K, Samson-Johannes A and Bernard K. 2004. Helinx® technology inactivates high titers of SARS-CoV, WNV and vaccinia in platelet concentrates. Abstract presented at the 13th international symposium on HIV & emerging infectious disesase (ISHEID) Toulon, France (June 3-5).

Schioppa T, Uranchimeg B, Saccani A, Biswas SK, Doni A, Rapisarda A, Bernasconi S, Saccani S, Nebuloni M, Vago L, Mantovani A, Melillo G and Sica A. 2003. Regulation of the Chemokine Receptor CXCR4 by Hypoxia. J Exp Med 198(9):1391-402.

Schlegel A, Immelmann A and Kempf C. 2001. Virus inactivation of plasma-derived proteins by pasteurization in the presence of guanidine hydrochloride. Transfusion 41(3):382-9.

Schwarz TF, Roggendorf M and Deinhardt. 1988. Human parvovirus B19: ELISA and immunoblot assays. J Virol Methods 20: 155-168

Schwarz TF, Nerlich A and Roggendorf M. 1990. Parvovirus B19 infection in pregnancy. Behring Inst Mitt 85: 69-73.

Schwarz TF, Modrow S, Hottenträger B, Höflacher B, Jäger G, Schartl W, Sumazaki R, Wolf H, Middeldorp J, Roggendorf M and Deinhardt F. 1991a. New oligopeptide immunoglobulin G test for human parvovirus B19 antibodies. J Clin Microbiol 29(3): 431-435.

Schwarz TF, Roggendorf M, Hottenträger B, Stolz W and Schwinn H. 1991b. Removal of parvovirus B19 from contaminated factor VIII during fractionation. J Med Virol 35: 28-31.

Schwarz TF, Serke S, Hottentrager B, von Brunn A, Baurmann H, Kirsch A, Stolz W, Huhn D, Deinhardt F and Roggendorf M. 1992a. Replication of parvovirus B19 in hematopoietic progenitor cells generated in vitro from normal human peripheral blood. J Virol 66(2):1273-6.

Schwarz TF, Serke S, Von Brunn A, Hottenträger B, Huhn D, Deinhardt F, Roggendorf M. 1992b. Heat stability of parvovirus B19: kinetics of inactivation. Zentralbl Bakteriol. 277(2): 219-23.

Scroggie DA, Carpenter MT, Cooper RI and Higgs JB. 2000. Parvovirus arthropathy outbreak in Southwestern United States. J Rheum 27(10): 2444-2448.

Seabury Stone M and Murph JR. Papular-purpuric gloves and socks syndrome: a characteristic viral exanthem. 1993. Pediatrics 92: 864-865.

Searle K, Schalasta G and Enders G. 1998. Development of antibodies to the nonstructural protein NS1 of parvovirus B19 during acute symptomatic and subclinical infection in pregnancy: implications for pathogenesis doubtful. J Med Virol 56: 192-198.

Sebire NJ. 2001. Correspondence: human parvovirus B19 and fetal death. Lancet 358: 1180.

Sedlik C, Sarraseca J, Rueda P, Leclerc C and Casal I. 1995. Immunogenicity of poliovirus B and T cell epitopes presented by hybrid porcine parvovirus particles. J Gen Virol 76: 2361-2368.

Sedlik C, Saron MF, Sarraseca J, Casal I and Leclerc C. 1997. Recombinant parvovirus-like particles as an antigen carrier: a novel nonreplicative exogenous antigen to elicit protective antiviral cytotoxic T cells. Proc Natl Acad Sci USA 94: 7503-7508.

Sedlik C, Dridi A, Deriaud E, Saron MF, Rueda P, Sarraseca J, Casal JI and Leclerc C. 1999. Intranasal delivery of recombinant parvovirus-like particles elicits cytotoxic T-cell and neutralizing antibody responses. J Virol 73(4): 2739-2744.

Seishima M, Kanoh H, Izumi T. 1999. The spectrum of cutaneous eruptions in 22 patients with isolated serological evidence of infection by parvovirus B19. Arch Dermatol 135: 1556-1557.

Semenza G.L. 2001. Hypoxia-inducible factor 1: oxygen homeostasis and disease pathophysiology. Trends Mol. Med. 7:345–350.

Serjeant GR, Mason M, Topley JM, Serjeant BE, Pattison JR, Jones SE and Mohamed R. 1981. Outbreak of aplastic crises in sickle cell anaemia associated with parvovirus-like agent. Lancet II: 595-597.

Servant A, Laperche S, Lallemand F, Marinho V, De Saint Maur G, Meritet JF and Garbarg-Chenon A. 2002. Genetic diversity within human erythroviruses: identification of three genotypes. J Virol 76(18): 9124-9134.

Severin MC, Levy Y and Shoenfeld. 2003. Systemic lupus erythematosus and parvovirus B19. Clin Rev Allergy Immunol 25: 41-46.

Shade RO, Blundell MC, Cotmore SF, Tattersall P and Astell CR. 1986. Nucleotide sequence and genome organization of human parvovirus B19 isolated from the serum of a child during aplastic crisis. J Virol 58(3): 921-936.

Shan Y-S, Lee P-C, Wang J-R, Tsai H, Sung C-M and Jin T-T. 2001. Fibrosing cholestatic hepatitis possibly related to persistent parvovirus B19 infection in a renal transplant recipient. Nephrol Dial Transplant 16: 2420-2422.

Shi Y, Seto E, Chang LS and Shenk T. 1991. Transcriptional repression by YY1, a human GLI-Krüppel-related protein, and relief of repression by adenovirus E1A protein. Cell 67(2): 377-388.

Shimizu Y, Ueno T, Komatsu H, Takada H and Nunoue T. 1999. Acute cerebellar ataxia with human parvovirus B19 infection. Arch Dis Chil 80: 72-73.

Shimomura S, Komatu N, Frickhofen N, Anderson S, Kajigaya S and Young NS. 1992. First continuous propagation of B19 parvovirus in a cell line. Blood 79: 18-24.

Shimomura S, Wong S, Brown KE, Komatsu N, Kajigaya S, Young NS. 1993. Early and Late Gene Expression in UT-7 Cells Infected with B19 Parvovirus. Virology 194: 149-156

Shiraishi H, Wong D, Purcell RH, Shirachi R, Kamasaka E and Numazaki Y. 1985. Antibody to human parvovirus in outbreak of erythema infectiosum in Japan. Lancet I: 982-983.

Shirono K and Tsuda T. 1995. Parvovirus B19-associated haemophagocytic syndrome in healthy adults. Br J Haematol 89: 923-926.

Shneerson JM, Mortimer PP and Vandervelde EM. 1980. Febrile illness due to a parvovirus. Br Med J 280: 1580.

Siegl G, Bates RC, Berns KI, Carter BJ, Kelly DC, Kurstak E and Tattersall P. 1985. Characteristics and taxonomy of *Parvoviridae*. Intervirology 23: 61-73.

Siegl G and Cassinotti P. 1998. Presence and significance of parvovirus B19 in blood and blood products. Biologicals 26:89-94.

Sisk WP and Berman ML. 1987. Expression of human parvovirus B19 structural protein in *E. coli* and detection of antiviral antibodies in human serum. Biotechnology 5: 1077-1080.

Skaff PT and Labiner DM. 2001. Status epilepticus due to human parvovirus B19 encephalitis in an immunocompetent adult. Neurology 57: 1336-1337.

Skeppner G, Kreuger A and Elinder G. 2002. Transient erythoblastopenia of childhood: prospective study of 10 patients with special reference of viral infections. J Pediatr Hematol/Oncol 24(4): 294-298.

Skjöldebrand-Sparre L, Tolfvenstam T, Papadogiannakis N, Wahren B, Broliden K and Nyman M. 2000. Parvovirus B19 infection: association with third-trimester intrauterine fetal death. Br J Obstet Gynaecol 107: 476-480.

Sloots T and Devine PL. 1996. Evaluation of four commercial enzyme immunoassays for detection of immunoglobulin M antibodies to human parvovirus B19. Eur J Clin Microbiol Infect Dis 15: 758-761.

Smith JW, Weinstein R and Hillyer KL for the AABB Hemapheresis Committee. 2003. Therapeutic apheresis: a summary of current indication categories endorsed by the AABB and the American Society for Apheresis. Transfusion 43: 820-822.

Snyder RO, Samulski RJ and Muzyczka N. 1990. In vitro resolution of covalently joined AAV chromosome ends. Cell 60(1): 105-113.

Söderlin MK, Kautiainen H, Puolakkainen M, Hedman K, Söderlund-Venermo M, Skogh T and Leirisalo-Repo M. 2003. Infections preceding early arthritis in southern Sweden: a prospective population-based study. J Rheumatol 30: 459-464.

Söderlund M, Brown KE, Meurman O and Hedman K. 1992. Prokaryotic expression of a VP1 polypeptide antigen for diagnosis by a human parvovirus B19 antibody enzyme immunoassay. J Clin Microbiol 30(2): 305-311.

Söderlund M, Brown CS, Spaan WJM, Hedman L and Hedman K. 1995a. Epitope type-specific IgG responses to capsid proteins VP1 and VP2 of human parvovirus B19. J Infect Dis 172: 1431-1436.

Söderlund M, Brown CS, Cohen BJ and Hedman K. 1995b. Accurate serodiagnosis of B19 parvovirus infections by measurment of IgG avidity. J Infect 171: 710-713.

Söderlund M, Ruutu P, Ruutu T, Asikainen K, Franssila R and Hedman K. 1997a. Primary and secondary infections by human parvovirus B19 following bone marrow transplantation: characterisation by PCR and B-cell molecular immunology. Scand J Infect Dis 29: 129-135.

Söderlund M, von Essen R, Haapasaari J, Kiistala U, Kiviluoto O and Hedman K. 1997b. Persistence of parvovirus B19 DNA in synovial membranes of young patients with and without chronic arthropathy. Lancet 349: 1063-1065.

Söderlund-Venermo M, Hokynar K, Nieminen J, Rautakorpi H and Hedman K. 2002. Persistence of human parvovirus B19 in human tissues. Pathol Biol 50: 307-316.

Sokal EM, Melchior M, Cornu C, Vandenbroucke A-T, Buts JP, Cohen BJ and Burtonboy G. 1998. Acute parvovirus B19 infection associated with fulminant hepatitis of favourable prognosis in young children. Lancet 352: 1739-1741.

Sol N, Le Junter J, Vassias I, Freyssinier JM, Thomas A, Prigent AF, Rudkin BB, Fichelson S and Morinet F. 1999. Possible interactions between the NS-1 protein and tumor necrosis factor alpha pathways in erythroid cell apoptosis induced by human parvovirus B19. J Virol 73(10): 8762-8770.

Solheim BG, Rollag H, Svennevig JL, Arafa O, Fosse E and Bergerud U. 2000. Viral safety of solvent/ detergent-treated plasma. Transfusion 40: 84-90.

Sosa CE, Mahony JB, Luinstra KE, Sternbach M and Chernesky MA. 1992. Replication and cytopathology of human parvovirus B19 in human umbilical cord blood erythroid progenitor cells. J Med Virol 36(2): 125-130.

Speyer I, Breedveld FC and Dijkmans BAC. 1998. Human parvovirus B19 infection is not followed by inflammatory joint disease during long term follow-up. A retrospective study of 54 patients. Clin Exp Rheumatol 16: 576-578.

Srivastava A, Bruno E, Briddell R, Cooper R, Srivastava C, van Besien K and Hoffman R. 1990. Parvovirus B19-induced perturbation of human megakaryocytopoiesis in vitro. Blood 76(10): 1997-2004.

Srivastava CH, Zhou S, Munshi NC and Srivastava A. 1992. Parvovirus B19 replication in human umbilical cord blood cells. Virology 189(2): 456-461.

Stahl H-D, Seidl B, Hubner B, Altrichter S, Pfeiffer R, Pustowoit B, Liebert UG, Hofmann J, von Salis-Soglio G and Emmrich F. 2000a. High incidence of parvovirus B19 DNA in synovial tissue of patients with undifferentiated mono- and oligoarthritis. Clin Rheum 19: 281-286.

Stahl H-D, Pfeiffer R and Emmrich F. 2000b. Intravenous treatment with immunoglobulins may improve chronic undifferentiated non- and oligoarthritis. Clin Exp Rheumatol 18: 515-517.

Stahl SJ and Murray K. 1989. Immunogenicity of peptide fusions to hepatits B virus core antigen. Proc Natl Acad Sci USA 86: 6283-6287.

St Amand J, Beard C, Humphries K and Astell CR. 1991. Analysis of splice junctions and in vitro and in vivo translation potential of the small, abundant B19 parvovirus RNAs. Virology 183(1): 133-142.

St Amand J and Astell CR. 1993. Identification and characterization of a family of 11-kDa proteins encoded by the human parvovirus B19. Virology 192(1): 121-131.

Stierle G, Brown KA, Rainsford SG, Smith CA, Hamerman D, Stierle HE and Dumonde DC. 1987. Parovirus associated antigen in the synovial membrane of patients with rheumatoid arthritis. Ann Rheum Dis 46: 219-223.

Study Group of the UK Haemophilia Centre Directors on Surveillance of Virus Transmission by Concentrates. 1988. Effect of dry-heating of coagulation factor concentrates at 80 degrees C for 72 hours on transmission of non-A, non-B hepatitis. Lancet 2(8615): 814-6.

Suchet I, Ens W and Suchet R. 2000. Parvovirus B19 infection in utero-a natural history and spectrum of sonographic manifestations in 7 cases. Can Assoc Radiol J 51(3): 198-204.

Sugawara H, Motokawa R, Abe H, Yamaguchi M, Yamada-Ohnishi Y, Hirayama J, Sakata H, Sato S, Kamo N, Ikebuchi K and Ikeda H. 2001. Inactivation of parvovirus B19 in coagulation concentrates by UVC radiation: assessmnent by in vitro infectivity assay using CFU-E derived from peripheral blodd CD34+ cells. Transfusion 41: 456-461.

Sultan Y, Maisonneuve P, Kazatchkine MD and Nydegger UE. 1984. Anti-idiotypic suppression of autoantibodies to factor VIII (antihaemophilic factor) by high-dose intravenous gammaglobulin. Lancet II: 765-768.

Summerford C, Bartlett JS and Samulski RJ. 1999. AlphaVbeta5 integrin: a co-receptor for adeno-associated virus type 2 infection. Nat Med 5(1): 78-82.

Summers J, Jones SE and Anderson MJ. 1983. Characterisation of the genome of the agent of erythrocyte aplasia permits its classification as a human parvovirus. J Gen Virol 64: 2527-2532.

Sun B, Bai CX, Feng K, Li L, Zhao P, Pei XT. 2000. Abstract [Effects of hypoxia on the proliferation and differentiation of CD34+ hematopoietic stem/progenitor cells and their response to cytokines]. Sheng Li Xue Bao 52(2):143-146.

Taguchi H, Takahashi T, Goto M, Nakamura T and Iwamoto A. 2001. Acute parvovirus B19 infection during anti-retroviral therapy. J Infect Chemother 7: 110-112.

Takahashi M, Ito M, Sakamoto F, Shimizu N, Furukawa T, Takahashi M and Matsunaga Y. 1995. Human parvovirus B19 infection: immunohistochemical and electron microscopic studies of skin lesions. J Cutan Pathol 22: 168-172.

Takahashi T, Ozawa K, Takahashi K. 1990. Susceptibility of human erythropoietic cells to B19 parvovirus in vitro increases with differentiation. Blood 75: 603-610.

Takahashi T, Ozawa K, Takahashi K, Okuno Y, Takahashi T, Muto Y, Takaku F and Asano S. 1993. DNA replication of parvovirus B19 in a human erythroid leukaemia cell line (JK-1) in vitro. Arch Virol 131: 201-208.

Takahashi Y, Murai C, Shibata S, Munakata Y, Ishii T, Ishii K, Saitoh T, Sawai T, Sugamura K and Sasaki T. 1998. Human parvovirus B19 as a causative agent for rheumatoid arthritis. Proc Natl Acad Sci USA. 95: 8227-8232.

Takeda S-I, Takaeda C, Takazakura E and Haratake J. 2001. Renal involvement induced by human parvovirus B19 infection. Nephron 89: 280-285.

Tanawattanacharoen S, Falk RJ, Jennette JC and Kopp JB. 2000. Parvovirus B19 DNA in kidney tissue of patients with focal segmental glomerulosclerosis. Am J Kid Dis 35(6): 1166-1174.

Thio K and Janner D. 1996. Aplastic anemia in a cardiac transplant recipient. Pediatr Infect Dis J 15: 1139.

Thomas DP. 1994. Viral contamination of blood products. The Lancet 343(8913): 1583-1584.

Tolfvenstam T, Rubén U and Broliden K. 1996. Evaluation of serological assays for the identification of parvovirus B19 immunoglobulin M. Clin Diagn Lab Immunol 3(2): 147-150.

Tolfvenstam T, Lundqvist A, Levi M, Wahren and Broliden. 2000. Mapping of B-cell epitopes on human parvovirus B19 non-structural and structural proteins. Vaccine 19: 758-763.

Tolfvenstam T, Oxenius A, Price DA, Shacklett BL, Spiegel HML, Hedman K, Norbeck O, Levi M, Kantzanou M, Nixon DF, Broliden K and Klenerman. 2001a. Direct ex vivo measurement of CD8+T-lymphocyte responses to human parvovirus B19. J Virol 75(1): 540-543.

Tolfvenstam T, Papadogiannakis N, Norbeck O, Patersson K and Broliden K. 2001b. Frequency of human parvovirus B19 infection in intrauterine fetal death. Lancet 357: 1494-1497.

Tomiyama J, Adachi Y, Hanada T and Matsunaga Y. 1988. Human parvovirus B19-induced aplastic crisis in autoimmune haemolytic anaemia. Br J Haematol 69: 288-289.

Török TJ. 1992. Parvovirus B19 and human disease. Adv Inter Med 37: 431-455.

Trapani S, Ermini M and Falcini F. 1999. Human parvovirus B19 infection: its relationship with systemic lupus erythematosus. Semin Arthr Rheum 28: 319-325.

Troccoli NM, McIver J, Losikoff A, Poiley J. 1998. Removal of viruses from human intravenous immune globulin by 35 nm nanofiltration. Biologicals 26(4):321-9.

Tsao J, Chapman MS, Agbandje M, Keller W, Smith K, Wu H, Luo M, Smith TJ, Rossmann MG, Compans RW and Parrish CR. 1991. The three-dimensional structure of canine parvovirus and its functional implications. Science 251: 1456-1464.

Tsuda H, Maeda Y, Nakagawa K, Nakayama M, Nishimura H, Ishihara A and Miyayama H. 1994. Parvovirus B19-associated haemophagocytic syndrome with prominent neutrophilia. Br J Haematol 86: 413-414.

Tsujimura M, Matsushita K, Shiraki H, Sato H, Okochi K and Maeda Y. 1995. Human parvovirus B19 infection in blood donors. Vox Sang 69(3): 206-212.

Uemura Y, Yang YH, Heldebrant CM, Takechi K and Yokoyama K. 1994. Inactivation and elimination of viruses during preparation of human intravenous immunoglobulin. Vox Sang 67(3): 246-54.

Uemura N, Ozawa K, Tani K, Nishikawa M, Inoue S, Nagao T, Uchida H, Matsunaga Y and Asano S. 1995. Pure red cell aplasia caused by parvovirus B19 infection in a renal transplant recipient. Eur J Haematol 54: 68-69.

Uike N, Miyamura T, Obama K, Takahira H, Sato H and Kozuru M. 1993. Parvovirus B19-associated haemophagocytosis in Evans syndrome: aplastic crisis accompanied by severe thrombocytopenia. Br J Haematol 84: 530-532.

Umene K and Nunoue T. 1990. The genome type of human parvovirus B19 strains isolated in Japan during 1981 differs from types detected in 1986 to 1987: a correlation between genome type and prevalence. J Gen Virol 71: 983-986.

Umene K and Nunoue T. 1993. Partial nucleotide sequencing and characterization of human parvovirus B19 genome DNAs from damaged human fetuses and from patients with leukaemia. J Med Virol 39: 333-339.

Umene K and Nunoue T. 1995. A new genome type of human parvovirus B19 present in sera of patients with encephalopathy. J Gen Virol 76: 2645-2651.

Valeur-Jensen JK, Pedersen CB, Westergaard T, Jensen IP, Lebech M, Andersen PK, Aaby P, Nørgaard Pedersen B and Melbye M. 1999. Risk factors for parvovirus B19 infection in pregnancy. JAMA 281(12): 1099-1105.

Van Elsacker-Niele A-MW, Weiland HT, Kroes ACM and Kappers-Klunne MC. 1996. Parvovirus B19 infection and idiopathic thrombocytopenia purpura. Ann Hematol 72: 141-144.

Van Elsacker-Niele A-M and Anderson MJ. 1987. First picture of erythema infectiosum? Lancet I: 229.

Van Rhenen DJ, Vermeij J, Mayaudon V, Hind C, Lin L and Corash L. 2000. Functional characteristics of S-59 photochemically treated platelet concentrates derived from buffy coats. Vox Sang 79(4): 206-214.

Van Voorhis WC, Barrett LK, Eastman RT, Alfonso R and Dupuis K. 2003. Trypanosoma cruzi inactivation in human platelet concentrates and plasma by a psoralen (amotosalen HCl) and long-wavelength UV. Antimicrob Agents Chemother 47(2): 475-479.

Vassias I, Hazan U, Michel Y, Sawa C, Handa H, Gouya L and Morinet F. 1998. Regulation of human B19 parvovirus promoter expression by hGABP (E4TF1) transcription factor. J Biol Chem 273(14): 8287-8293.

Venturoli S, Gallinella G, Manaresi E, Gentilomi G, Musiani M and Zerbini M. 1998. IgG response to the immunoreactive region of parvovirus B19 nonstructural protein by immunoblot assay with a recombinant antigen. J Infect Dis 178: 1826-1829.

Vihinen-Ranta M, Kakkola L, Kalela A, Vilja P and Vuento M. 1997. Characterization of a nuclear localization signal of canine parvovirus capsid proteins. Eur J Biochem 250(2): 389-394.

Vitex press release. 2003, 17th November. Vitex Halts Enrollment in Phase III Chronic Trial of the INACTINE™ Pathogen Reduction System for Red Blood Cells. http://www.vitechnologies.com

Vitex press release. 200, 23th November. Vitex Provides an Update on the Development Program for INACTINE™ Pathogen Inactivation System for Red Blood Cells. http://www.vitechnologies.com

Von Landenberg P, Lehmann HW, Knöll A, Dorsch S and Modrow S. 2003. Antiphospholipid antibodies in pediatric and adult patients with rheumatic disease are associated with parvovirus B19 infection. Arthr Rhem 48(7): 1939-1947.

Von Poblotzki A, Gigler A, Lang B, Wolf H and Modrow S. 1995a. Antibodies to parvovirus B19 NS-1 protein in infected individuals. J Gen Virol. 76: 519-527.

Von Poblotzki A, Hemauer A, Gigler A, Puchhammer-Stöckl, Heinz FX, Pont J, Laczika K, Wolf H and Modrow S. 1995b. Antibodies to the nonstructural protein of parvovirus B19 in persistently infected patients. J Infect Dis 172: 1356-9.

Von Poblotzki A, Gerdes C, Reischl U, Wolf H and Modrow S. 1996. Lymphoproliferative responses after infection with human parvovirus B19. J Virol 70(10): 7327-7330.

Wagner AD, Goronzy JJ, Matteson EL and Weyland CM. 1995. Systemic monocyte and T-cell activation in a patient with human parvovirus B19 infection. Mayo Clin Proc 70: 261-265.

Wang XS, Yoder MC, Zhou SZ and Srivastava A. 1995. Parvovirus B19 promoter at map unit 6 confers autonomous replication competence and erythroid specificity to adeno-associated virus 2 in primary human hematopoietic progenitor cells. Proc Natl Acad Sci USA 92(26): 12416-12420.

Wang X, Zhang G and Han M. 2000. The localization of parvovirus B19 in cardiac biopsy tissue of congenital heart disease. Chinese J Exp Clin Virol 14(2): 175-177.

Watts MJ and Linch DC. 1997. Peripheral blood stem cell transplantation. Vox Sang 73(3): 135-142.

Wehmeier A, Eis-Hübinger AM, Maas Enriquez M and Beckmann H. 2000. Parvovirus B19 in idiopathic thrombocytopenic purpura. Vox Sang 79: 118.

Weigel-Kelley KA, Yoder MC and Srivastava A. 2001. Recombinant human parvovirus B19 vectors: erythrocyte P antigen is necessary but no sufficient for successful transduction of human hematopoietic cells. J Virol 75(9): 4110-4116.

Weigel-Kelley KA, Yoder MC and Srivastava A. 2003. Alpha5beta1 integrin as a cellular coreceptor for human parvovirus B19: requirement of functional activation of beta1 integrin for viral entry. Blood 102(12): 3927-3933.

Weiland HT, Salimans MMM, Fibbe WE, Kluin PM and Cohen BJ. 1989. Prolonged parvovirus B19 infection with severe anaemia in a bone marrow transplant recipient. Br J Haematol 71: 300.

White DG, Woolf AD, Mortimer PP, Cohen BJ, Blake DR and Bacon PA. 1985. Human parvovirus arthropathy. Lancet I: 419-421.

White LE. 1999. Nonimmune hydrops fetalis. Neonat Net 18(6): 25-30.

WHO Expert committee on Biological standardization. 26 to 30 November 2001, Geneva. Guidelines on Viral Inactivation and Removal Procedures Intended to Assure the Viral Safety of Human Blood Plasma Products. Available on Internet web site: http://www.who.int/biologicals/Guidelines/WHOguidanceSEARO-SRL240403.pdf

Wicki J, Samii K, Cassinotti P, Voegeli J, Rochat T and Beris P. 1997. Parvovirus B19-induced red cell aplasia in solid-organ transplant recipients. Two case reports and review of the literature. Hematol Cell Ther 39: 199-204.

Wierenga KJJ, Pattison JR, Brink N, Griffiths M, Miller M, Shah DJ, Williams W, Serjeant BE and Serjeant GR. 1995. Glomerulonephritis after human parvovirus infection in homozygous sickle-cell disease. Lancet 346:475-476.

Wierenga KJJ, Serjeant BE and Serjeant GR. 2001. Cerebrovascular complications and parvovirus infection in homozygous sickle cell disease. J Pediatr 139: 438-442.

Wiersbitzky S, Schwarz TF, Bruns R, Ballke EH, Roggendorf M, Wiersbitzky H and Deinhardt. 1991. Acute obstructive respiratory diseases in infants and children associated with parvovirus B19 infection. Infection 19(4): 252.

Williams MD, Cohen BJ, Beddall AC, Pasi KJ, Mortimer PP and Hill FGH. 1990. Transmission of human parvovirus B19 by coagulation factor concentrates. Vox Sang 58: 177-181

Williamson LM, Llewelyn CA, Fisher NC, Allain JP, Bellamy MC, Baglin TP, Freeman J, Klinck JR, Ala FA, Smith N, Neuberger J and Wreghitt TG. 1999. A randomized trial of solvent-detergent-treated and standard fresh-fozen plasma in the coagulopathy of liver disease and liver transplantation. Transfusion 39: 1227-1234.

Williamson LM, Cardifan R and Prowse CV. 2003. Methylene blue-treated fresh-fozen plasma: what is its contribution to blood safety? Transfusion 43: 1322-1329.

Willkommen H, Schmidt I and Löwer J. 1999. Safety issues for plasma derivatives and benefit from NAT testing. Biologicals 27: 325-331.

Wilson GM, Jindal HK, Yeung DE, Chen W and Astell CR. 1991. Expression of minute virus of mice major nonstructural protein in insect cells: purification and identification of ATPase and helicase activities. Virology 185(1): 90-98.

Wollowitz S. 2001. Fundamentals of the psoralen-based Helinx technology for inactivation of infectious pathogens and leukocytes in platelets and plasma. Semin Hematol 38(4 Suppl 11): 4-11.

Wong S, Momoeda M, Field A, Kajigaya S and Young NS. 1994. Formation of empty B19 parvovirus capsids by the truncated minor capsid protein. J Virol 68(7): 4690-4694.

Wong A, Tan KH, Tee CS and Yeo GSH. 2000. Seroprevalence of cytomegalovirus, toxoplasma and parvovirus in pregnancy. Singapore Med J 41(4): 151-155.

Woolf AD, Campion GV, Chishick A, Wise S, Cohen BJ, Klouda PT, Caul O and Dieppe PA. 1989. Clinical manifestations of human parvovirus B19 in adults. Arch Intern Med 149: 1153-1156.

Xie Q, Bu W, Bhatia S, Hare J, Somasundaram T, Azzi A and Chapman MS. 2002. The atomic structure of adeno-associated virus (AAV-2), a vector for human gene therapy. Proc Natl Acad Sci USA 99(16): 10405-10410.

Xu J, Raff TC, Muallem NS and Neubert AGN. 2003. Hydrops fetalis secondary to parvovirus B19 infections. J Am Board Fam Pract 16: 63-68.

Yaegashi N, Shiraishi H, Takeshita T, Nakamura M, Yajima A and Sugamura K. 1989. Propagation of human parvovirus B19 in primary culture of erythroid lineage cells derived from fetal liver. J Virol 63(6): 2422-2426.

Yaegashi N. 2000. Pathogenesis of nonimmune hydrops fetalis cause by intrauterine B19 infection. Tohoku J Exp Med 190: 65-82.

Yazawa S, Kawasaki S, Fujimoto C and Ohi T. 2002. Case report of meningoencephalitis during a concomitant mumps and parvovirus B19 infection. Clin Neurol Neurosurg 104: 380-382.

Yee TT, Lee CA and Pasi KJ. 1995. Life-threatening human parvovirus B19 infection in immunocompetent haemophilia. The Lancet 345:794-95.

Yee TT, Cohen BJ, Pasi KJ and Lee CA. 1996. Transmission of symptomatic parvovirus B19 infection by clotting factor concentrate. Br J Haematol 93(2): 457-459.

Yokoyama T, Murai K, Murozuka T, Wakisaka A, Tanifuji M, Fujii N and Tomono T. 2004. Removal of small non-enveloped viruses by nanofiltration. Vox Sang 86(4): 225.

Yoo BC, Lee DH, Park SM, Park JW, Kim CY, Lee H-S, Seo JS, Park KJ and Ryu W-S. 1999. A novel parvovirus isolated from Manchurian chipmunks. Virology 253: 250-258.

Yoshimoto K, Rosenfeld S, Frickhofen N, Kennedy D, Hills R, Kajigaya S and Young NS. 1991. A second neutralizing epitope of B19 parvovirus implicates the spike region in the immune response. J Virol. 65(12): 7056-7060.

Yoto Y, Kudoh T, Suzuki N, Matsunaga Y and Chiba S. 1993. Retrospective study on the influence of human parvoviurs B19 infection among children with malignant diseases. Acta Haematol 90: 8-12.

Yoto Y, Kudoh T, Asanuma H, Numazaki K, Tsutsumi Y, Nakata S and Chiba S. 1994. Transient disturbance of consciousness and hepatic dysfunction associated with human parvovirus B19 infection.

Yoto Y, Kudoh T, Haseyama K, Suzuki N, Oda T, Katoh T, Takahashi T, Sekiguchi S and Chiba S. 1995. Incidence of human parvovirus B19 DNA detection in blood donors. Br J Haematol 91(4): 1017-1018.

Yoto Y, Kudoh T, Haseyama K, Suzuki N and Chiba S. 1996a. Human parovirus B19 infection associated with acute hepatitis. Lancet 347: 868-869.

Yoto Y, Kudoh T, Haseyama K, Suzuki N and Chiba S. 1996b. Human parovivrus B19 infection and hepatitis. Lancet Letter 347: 1563-1564.

Ytterberg SR. 1999. Viral arthritis. Curr Opin Rheumatol 11: 275-280.

Yu MW and Finlayson JS. 1984. Stabilization of human albumin by caprylate and acetyltryptophanate. Vox Sang 47(1):28-40.

Zádori Z, Szelei J, Lacoste M-C, Li Y, Gariépy S, Raymond P, Allaire M, Nabi IR and Tijssen P. 2001. A viral phospholipase A2 is required for parvovirus infectivity. Dev Cell 1: 291-302.

Zakrzewska K, Azzi A, Patou G, Morfini M, Rafanelli D and Pattison JR. 1992. Human parvovirus B19 in clotting factor concentrates: B19 DNA detection by the nested polymerase chain reaction. British Journal of Haematology 81: 407-412.

Zakrzewska K, Azzi A, De Biasi E, Radossi P, De Santis R, Davoli PG and Tagariello G. 2001. Persistence of parvovirus B19 DNA in synovium of patients with haemophilic arthritis. J Med Virol 65: 402-407.

Zavizion B, Pereira M, de Melo Jorge M, Serebryanik D, Mather TN, Chapman J, Miller NJ, Alford B, Bzik DJ and Purmal A. 2004. Inactivation of protozoan parasites in red blood cells using INACTINE PEN110 chemistry. Transfusion 44(5): 731.

Zerbini M, Musiani M, Venturoli S, Gallinella G, Gibellini D, Gentilomi G and La Placa M. 1992. Different syndromes associated with B19 parvovirus viraemia in paediatric patients: report of four cases. Eur J Pediatr 151: 815-817.

Zerbini M, Musiani M, Gibellini D, Gentilomi G, Venturoli S, Gallinella G and La Placa M. 1993. Evaluation of strand-specific RNA probes visualised by colorimetric and chemiluminescent reactions for the detection of B19 parvovirus DNA. J Virol Methods 45: 169-178.

Zerbini M, Cricca M, Gentilomi G, Venturoli S, Gallinella G and Musiani M. 2000. Tyramide signal amplification of biotinylated probe in dot-blot hybridisation assay for the detection of parvovirus B19 DNA in serum samples. Clinica Chemica Acta 302: 79-87.

Zerbini M, Gentilomi G, Cricca M, Manaresi E, Bonvicini F and Musiani M. 2001. A system to enhance the sensitivity of digoxigenin-labelled probe: detection of B19 DNA in serum samples. J Virol Methods 93: 137-144.

Zerbini M, Gallinella G, Cricca M , Bonvicini F and Musiani M. 2002. Diagnostic procedures in B19 infection. Pathol Biol 50: 332-338.

Zuffi E, Manaresi E, Gallinella G, Gentilomi G, Venturoli S, Zerbini M and Musiani M. 2001. Identification of an immunodominant peptide in the parvovirus B19 VP1 unique region able to elicit a long-lasting immune response in humans. Virla Immunology 14(2): 151-158.

Appendix 1: BFU-E reduction assay results

Table A1.1: BFU-E reduction assay results for patient 1 (a)

Inoculum (IU/ml)	Red colony count					Percentage BFU-E reduction **Patient 1a**
	Well 1	Well 2	Well 3	Well 4	Total	
Control	45	43	37	43	168	N/A
$1x10^{10}$	21	22	19	23	85	49.40
$1x10^{9.5}$	25	22	29	23	99	41.07
$1x10^{9}$	25	32	18	27	102	39.29
$1x10^{8.5}$	34	28	28	23	113	32.74
$1x10^{8}$	35	29	41	20	125	25.60
$1x10^{7.5}$	38	27	26	32	123	26.79
$1x10^{7}$	43	45	27	41	156	7.14

Table A1.2: BFU-E reduction assay results for patient 1 (b)

Inoculum (IU/ml)	Red colony count					Percentage BFU-E reduction **Patient 1b**
	Well 1	Well 2	Well 3	Well 4	Total	
Control	20	19	24	18	81	N/A
$1x10^{10.5}$	0	0	0	0	0	100.00
$1x10^{10}$	3	1	1	0	5	93.83
$1x10^{9.5}$	6	7	8	9	30	62.96
$1x10^{9}$	8	9	12	10	39	51.85
$1x10^{8.5}$	13	10	6	12	41	49.38
$1x10^{8}$	9	7	11	11	38	53.09

Table A1.3: BFU-E reduction assay results for patient 2

Inoculum (IU/ml)	Red colony count					Percentage BFU-E reduction **Patient 2**
	Well 1	Well 2	Well 3	Well 4	Total	
Control	124	110	112	118	464	N/A
$1x10^{10.5}$	33	16	30	26	105	77.37
$1x10^{10}$	36	21	33	39	129	72.20
$1x10^{9.5}$	60	46	46	61	213	54.09
$1x10^{9}$	66	50	53	70	239	48.49
$1x10^{8.5}$	80	77	61	65	283	39.01
$1x10^{8}$	62	78	76	65	281	39.44
$1x10^{7.5}$	98	92	92	102	384	17.24

Table A1.4: BFU-E reduction assay results for patient 3

Inoculum (IU/ml)	Red colony count					Percentage BFU-E reduction **Patient 3**
	Well 1	Well 2	Well 3	Well 4	Total	
Control	33	38	43	41	155	N/A
Control	42	41	37	39	159	N/A
Control mean	37.5	39.5	40	40	157	N/A
$1x10^{11}$	0	0	0	0	0	100.00
$1x10^{10.5}$	0	0	0	0	0	100.00
$1x10^{10}$	3	1	1	2	7	95.54
$1x10^{9.5}$	10	13	12	13	48	69.43
$1x10^{9}$	22	17	18	19	76	51.59
$1x10^{8.5}$	37	35	31	30	133	15.29

Table A1.5: BFU-E reduction assay results for patient 4

Inoculum (IU/ml)	Red colony count					Percentage BFU-E reduction **Patient 4**
	Well 1	Well 2	Well 3	Well 4	Total	
Control	34	25	23	29	28	N/A
Control	28	23	20	22	93	N/A
Control mean	31	24	21.5	25.5	102	N/A
$1x10^{11}$	0	0	0	0	0	100.00
$1x10^{10.5}$	0	0	0	0	0	100.00
$1x10^{10}$	2	1	2	1	6	94.12
$1x10^{9.5}$	3	3	4	2	12	88.24
$1x10^{9}$	14	19	15	25	73	28.43
$1x10^{8.5}$	27	25	20	26	98	3.92

Table A1.6: BFU-E reduction assay results for patient 5

Inoculum (IU/ml)	Red colony count					Percentage BFU-E reduction **Patient 5**
	Well 1	Well 2	Well 3	Well 4	Total	
Control	3	3	9	10	25	N/A
$1x10^{12}$	0	0	0	0	0	100.00
$1x10^{11.5}$	0	0	0	0	0	100.00
$1x10^{11}$	0	0	0	0	0	100.00
$1x10^{10.5}$	0	0	0	0	0	100.00
$1x10^{10}$	0	0	0	0	0	100.00
$1x10^{9.5}$	2	1	0	2	5	80.00

Table A1.7: BFU-E reduction assay results for patient 6

Inoculum (IU/ml)	Red colony count					Percentage BFU-E reduction **Patient 6**
	Well 1	Well 2	Well 3	Well 4	Total	
Control	84	79	105	92	360	N/A
$1x10^{12}$	0	0	0	0	0	100.00
$1x10^{11.5}$	0	0	0	0	0	100.00
$1x10^{11}$	0	0	0	0	0	100.00
$1x10^{10.5}$	0	2	0	3	5	98.61
$1x10^{10}$	34	39	31	40	144	60.00

Table A1.8: BFU-E reduction assay results for patient 7

Inoculum (IU/ml)	Red colony count					Percentage BFU-E reduction **Patient 7**
	Well 1	Well 2	Well 3	Well 4	Total	
Control	95	110	91	86	382	N/A
$1x10^{12}$	0	0	0	0	0	100.00
$1x10^{11.5}$	1	0	0	0	1	99.74
$1x10^{11}$	79	90	109	102	380	0.52
$1x10^{10.5}$	N/A	N/A	70	82	N/A	N/A
$1x10^{10}$	67	69	110	123	369	3.40

Table A1.9: BFU-E reduction assay results for patient 8

Inoculum (IU/ml)	Red colony count					Percentage BFU-E reduction **Patient 8**
	Well 1	Well 2	Well 3	Well 4	Total	
Control	103	112	97	107	419	N/A
$1x10^{12}$	0	0	0	0	0	100.00
$1x10^{11.5}$	0	0	0	0	0	100.00
$1x10^{11}$	0	0	0	1	1	99.76
$1x10^{10.5}$	11	9	6	11	37	91.17
$1x10^{10}$	46	29	36	28	139	66.83

Table A1.10: BFU-E reduction assay results for patient 9

Inoculum (IU/ml)	Red colony count					Percentage BFU-E reduction **Patient 9**
	Well 1	Well 2	Well 3	Well 4	Total	
Control	36	21	28	25	110	N/A
Control	28	16	26	21	91	N/A
Control mean	32	18.5	27	23	100.5	N/A
$1x10^{10}$	7	9	9	6	31	69.15
$1x10^{9.5}$	16	13	18	12	59	41.29
$1x10^{9}$	25	17	19	11	72	28.36
$1x10^{8.5}$	20	17	16	N/A	N/A	N/A
$1x10^{8}$	23	19	25	18	85	15.42
$1x10^{7.5}$	12	27	19	22	80	20.40

Table A1.11: BFU-E reduction assay results for patient 10 (a and b)

Inoculum (IU/ml) **Patient 10a**	Red colony count					Percentage BFU-E reduction **Patient 10a**
	Well 1	Well 2	Well 3	Well 4	Total	
Control	68	87	56	58	269	N/A
$1x10^{11}$	0	0	0	0	0	100.00
$1x10^{10.5}$	1	0	0	4	5	98.14
$1x10^{10}$	12	11	17	13	53	80.30
$1x10^{9.5}$	28	36	32	33	129	52.04
$1x10^{9}$	43	38	41	40	162	39.78
$1x10^{8.5}$	67	52	60	54	233	13.38
Inoculum (IU/ml) **Patient 10b**	Red colony count					Percentage BFU-E reduction **Patient 10b**
	Well 1	Well 2	Well 3	Well 4	Total	
Control	56	65	61	58	240	N/A
$1x10^{11}$	0	0	0	0	0	100.00
$1x10^{10.5}$	0	0	0	0	0	100.00
$1x10^{10}$	3	0	0	0	3	98.75
$1x10^{9.5}$	12	9	3	4	28	88.33
$1x10^{9}$	30	19	10	15	74	69.17
$1x10^{8.5}$	23	29	19	36	107	55.42

Table A1.12: BFU-E reduction assay results for patient 11

Inoculum (IU/ml)	Red colony count					Percentage BFU-E reduction **Patient 11**
	Well 1	Well 2	Well 3	Well 4	Total	
Control	3	6	7	6	22	N/A
$1x10^{11}$	0	0	0	0	0	100.00
$1x10^{10.5}$	0	0	0	0	0	100.00
$1x10^{10}$	0	0	0	0	0	100.00
$1x10^{9.5}$	0	0	0	0	0	100.00
$1x10^{9}$	1	0	0	0	1	95.45
$1x10^{8.5}$	7	6	5	7	25	0.00

Table A1.13: BFU-E reduction assay results for patient 12

Inoculum (IU/ml)	Red colony count					Percentage BFU-E reduction **Patient 12**
	Well 1	Well 2	Well 3	Well 4	Total	
Control	7	11	8	12	38	N/A
$1x10^{11}$	0	0	0	0	0	100.00
$1x10^{10.5}$	0	0	0	0	0	100.00
$1x10^{10}$	0	0	0	0	0	100.00
$1x10^{9.5}$	2	0	2	2	6	84.21
$1x10^{9}$	3	1	4	6	14	63.16
$1x10^{8.5}$	11	3	11	12	37	2.63

Table A1.14: BFU-E reduction assay results for patient 13

Inoculum (IU/ml)	Red colony count					Percentage BFU-E reduction **Patient 13**
	Well 1	Well 2	Well 3	Well 4	Total	
Control	90	96	92	94	372	N/A
$1x10^{9.5}$	4	5	7	5	21	94.35
$1x10^{9}$	12	16	17	11	56	84.95
$1x10^{8.5}$	18	21	31	13	83	77.69
$1x10^{8}$	25	36	33	23	117	68.55
$1x10^{7.5}$	27	38	35	39	139	62.63
$1x10^{7}$	50	37	38	32	157	57.80

Table A1.15: BFU-E reduction assay results for patient 14

Inoculum (IU/ml)	Red colony count					Percentage BFU-E reduction **Patient 14**
	Well 1	Well 2	Well 3	Well 4	Total	
Control	33	35	27	48	143	N/A
Control	53	35	31	25	144	N/A
Control mean	43	35	29	36.5	143.5	N/A
$1x10^{11.5}$	0	0	0	0	0	100.00
$1x10^{11}$	0	0	0	0	0	100.00
$1x10^{10.5}$	3	0	1	1	5	96.52
$1x10^{10}$	9	5	4	7	25	82.58
$1x10^{9.5}$	14	16	11	10	51	64.46
$1x10^{9}$	14	13	18	21	66	54.01
$1x10^{8.5}$	15	24	24	21	84	41.46
$1x10^{8}$	21	20	17	23	81	43.55
$1x10^{7.5}$	34	35	42	38	149	0.00
$1x10^{7}$	28	22	37	29	116	19.16
$1x10^{6.5}$	45	51	48	37	181	0.00
$1x10^{6}$	39	40	40	43	162	0.00

Table A1.16: BFU-E reduction assay results for patient 15

Inoculum (IU/ml)	Red colony count					Percentage BFU-E reduction **Patient 15**
	Well 1	Well 2	Well 3	Well 4	Total	
Control	27	34	36	35	132	N/A
Control	23	40	41	24	128	N/A
Control mean	25	37	38.5	29.5	130	N/A
$1x10^{9.5}$	6	6	3	8	23	82.31
$1x10^{9}$	15	21	18	18	72	44.62
$1x10^{8.5}$	25	15	24	15	79	39.23
$1x10^{8}$	26	17	20	22	85	34.62
$1x10^{7.5}$	39	28	31	18	116	10.77
$1x10^{7}$	34	37	46	19	136	0.00
$1x10^{6.5}$	26	43	24	17	110	15.38
$1x10^{6}$	49	36	24	48	157	0.00

Table A1.17: BFU-E reduction assay results for patient 16

Inoculum (IU/ml)	Red colony count					Percentage BFU-E reduction **Patient 16**
	Well 1	Well 2	Well 3	Well 4	Total	
Control	45	60	54	42	201	N/A
$1x10^{8.5}$	32	24	17	35	108	46.27
$1x10^{8}$	37	24	30	29	120	40.30
$1x10^{7.5}$	24	43	42	41	150	25.37
$1x10^{6.5}$	36	33	40	31	140	30.35
$1x10^{6}$	40	40	36	38	154	23.38

Table A1.18: BFU-E reduction assay results for patient 17

Inoculum (IU/ml)	Red colony count					Percentage BFU-E reduction **Patient 17**
	Well 1	Well 2	Well 3	Well 4	Total	
Control	112	123	118	108	461	N/A
$1x10^{7.5}$	63	77	66	93	299	35.14
$1x10^{7}$	53	43	48	64	208	54.88
$1x10^{6.5}$	73	66	95	71	305	33.84
$1x10^{6}$	92	89	74	72	327	29.07

Table A1.19: BFU-E reduction assay results for patient 18

Inoculum (IU/ml)	Red colony count					Percentage BFU-E reduction **Patient 18**
	Well 1	Well 2	Well 3	Well 4	Total	
Control	82	90	95	95	362	N/A
Control	67	69	71	73	280	N/A
Control mean	74.5	79.5	83	84	321	N/A
$1x10^{11.5}$	0	0	0	0	0	100.00
$1x10^{11}$	0	0	0	0	0	100.00
$1x10^{10.5}$	21	2	7	7	37	88.47
$1x10^{10}$	36	6	19	26	87	72.90
$1x10^{9.5}$	105	56	67	85	313	2.49
$1x10^{9}$	92	97	105	97	391	0.00
$1x10^{8.5}$	68	120	73	75	336	0.00
$1x10^{8}$	64	73	49	87	273	14.95
$1x10^{7.5}$	67	58	57	67	249	22.43
$1x10^{7}$	74	84	67	66	291	9.35
$1x10^{6.5}$	81	58	73	68	280	12.77
$1x10^{6}$	86	93	62	70	311	3.12

Table A1.20: BFU-E reduction assay results for patient 19

Inoculum (IU/ml)	Red colony count					Percentage BFU-E reduction **Patient 19**
	Well 1	Well 2	Well 3	Well 4	Total	
Control	36	27	35	31	129	N/A
$1x10^{8.5}$	28	23	30	18	99	23.26
$1x10^{8}$	28	25	33	27	113	12.40
$1x10^{7.5}$	23	10	19	38	90	30.23
$1x10^{7}$	23	25	19	22	89	31.01
$1x10^{6.5}$	24	23	23	39	109	15.50
$1x10^{6}$	31	24	29	15	99	23.26

Table A1.21: BFU-E reduction assay results for patient 20

Inoculum (IU/ml)	Red colony count					Percentage BFU-E reduction **Patient 20**
	Well 1	Well 2	Well 3	Well 4	Total	
Control	115	84	71	116	386	N/A
$1x10^{8.5}$	20	26	28	31	105	72.80
$1x10^{8}$	24	27	34	42	127	67.10
$1x10^{7.5}$	28	34	38	52	152	60.62
$1x10^{7}$	60	46	52	105	263	31.87
$1x10^{6.5}$	99	65	73	108	345	10.62
$1x10^{6}$	114	112	104	105	435	0.00

Table A1.22: BFU-E reduction assay results for patient 21

Inoculum (IU/ml)	Red colony count					Percentage BFU-E reduction **Patient 21**
	Well 1	Well 2	Well 3	Well 4	Total	
Control	18	21	20	33	92	N/A
Control	10	9	6	9	34	N/A
Control mean	14	15	13	21	63	N/A
$1x10^{7.5}$	1	3	5	10	19	69.84
$1x10^{7}$	7	2	4	10	23	63.49
$1x10^{6.5}$	16	5	4	17	42	33.33
$1x10^{6}$	7	10	12	19	48	23.81
$1x10^{5.5}$	27	13	17	12	69	0.00
$1x10^{5}$	30	18	23	15	86	0.00

Table A1.23: BFU-E reduction assay results for patient 22

Inoculum (IU/ml)	Red colony count					Percentage BFU-E reduction **Patient 22**
	Well 1	Well 2	Well 3	Well 4	Total	
Control	38	21	33	24	116	N/A
Control	22	19	33	23	97	N/A
Control mean	30	20	33	23.5	106.5	N/A
$1x10^{7.5}$	9	10	18	18	55	48.36
$1x10^{7}$	11	11	12	11	45	57.75
$1x10^{6.5}$	24	15	15	18	72	32.39
$1x10^{6}$	20	14	18	24	76	28.64
$1x10^{5.5}$	20	18	23	21	82	23.00
$1x10^{5}$	19	23	13	27	82	23.00

Table A1.24: BFU-E reduction assay results for patient 23

Inoculum (IU/ml)	Red colony count					Percentage BFU-E reduction **Patient 23**
	Well 1	Well 2	Well 3	Well 4	Total	
Control	47	40	28	20	135	N/A
Control	30	23	32	31	116	N/A
Control mean	38.5	31.5	30	25.5	125.5	N/A
$1x10^{7.5}$	39	14	24	21	98	21.91
$1x10^{7}$	21	20	27	28	96	23.51
$1x10^{6.5}$	28	31	20	39	118	5.98
$1x10^{6}$	34	29	31	35	129	0.00
$1x10^{5.5}$	29	21	28	35	113	9.96
$1x10^{5}$	32	31	31	28	122	2.79

Table A1.25: BFU-E reduction assay results for patient 24

Inoculum (IU/ml)	Red colony count					Percentage BFU-E reduction **Patient 24**
	Well 1	Well 2	Well 3	Well 4	Total	
Control	34	40	21	31	126	N/A
Control	29	41	36	21	127	N/A
Control mean	31.5	40.5	28.5	26	126.5	N/A
$1x10^{8}$	19	37	27	27	110	13.04
$1x10^{7.5}$	23	28	33	37	121	4.35
$1x10^{7}$	26	33	29	24	112	11.46
$1x10^{6.5}$	29	33	25	53	140	0.00
$1x10^{6}$	44	41	34	42	161	0.00
$1x10^{5.5}$	30	48	41	31	150	0.00

Table A1.26: BFU-E reduction assay results for patient 25

Inoculum (IU/ml)	Red colony count					Percentage BFU-E reduction **Patient 25**
	Well 1	Well 2	Well 3	Well 4	Total	
Control	85	46	51	38	220	N/A
Control	35	38	38	50	161	N/A
Control mean	60	42	44.5	44	190.5	N/A
$1x10^{8}$	33	35	35	36	27.03	27.03
$1x10^{7.5}$	35	33	27	40	29.13	29.13
$1x10^{7}$	39	23	31	49	25.46	25.46
$1x10^{6.5}$	37	29	28	55	21.78	21.78
$1x10^{6}$	38	35	23	29	34.38	34.38
$1x10^{5.5}$	53	40	39	31	14.44	14.44

Table A1.27: BFU-E reduction assay results for patient 26

Inoculum (IU/ml)	Red colony count					Percentage BFU-E reduction **Patient 26**
	Well 1	Well 2	Well 3	Well 4	Total	
Control	29	29	56	38	152	N/A
Control	32	36	45	28	141	N/A
Control mean	30.5	32.5	50.5	33	146.5	N/A
$1x10^{8}$	41	16	29	43	129	11.95
$1x10^{7.5}$	24	12	8	24	68	53.58
$1x10^{7}$	24	19	28	28	99	32.42
$1x10^{6.5}$	27	14	28	26	95	35.15
$1x10^{6}$	26	21	20	29	96	34.47
$1x10^{5.5}$	38	23	35	35	131	10.58

Table A1.28: BFU-E reduction assay results for patient 27

Inoculum (IU/ml)	Red colony count					Percentage BFU-E reduction **Patient 27**
	Well 1	Well 2	Well 3	Well 4	Total	
Control	13	7	10	6	36	N/A
Control	7	5	2	6	20	N/A
Control mean	10	6	6	6	28	N/A
$1x10^{10}$	3	1	0	1	5	82.14
$1x10^{9.5}$	4	1	1	3	9	67.86
$1x10^{9}$	3	3	1	2	9	67.86
$1x10^{8.5}$	5	1	2	7	15	46.43
$1x10^{8}$	5	7	7	2	21	25.00
$1x10^{7.5}$	4	3	5	8	20	28.57
$1x10^{7}$	7	4	5	11	27	3.57
$1x10^{6.5}$	3	6	0	3	12	57.14
$1x10^{6}$	7	7	4	7	25	10.71
$1x10^{5.5}$	5	3	9	4	21	25.00
$1x10^{5}$	4	5	4	4	17	39.29

Table A1.29: BFU-E reduction assay results for patient 28

Inoculum (IU/ml)	Red colony count					Percentage BFU-E reduction **Patient 28**
	Well 1	Well 2	Well 3	Well 4	Total	
Control	21	18	11	12	62	N/A
Control	15	24	20	23	82	N/A
Control mean	18	21	15.5	17.5	72	N/A
$1x10^{9}$	14	12	20	20	66	8.33
$1x10^{8.5}$	7	10	11	19	47	0.00
$1x10^{8}$	15	14	12	14	55	0.00
$1x10^{7.5}$	7	4	12	12	35	0.00
$1x10^{7}$	8	3	1	5	17	39.29
$1x10^{6.5}$	9	6	7	6	28	0.00
$1x10^{6}$	12	13	8	13	46	0.00
$1x10^{5.5}$	13	12	11	5	41	0.00
$1x10^{5}$	10	13	15	20	58	0.00

Table A1.30: BFU-E reduction assay results for patient 29

Inoculum (IU/ml)	Red colony count					Percentage BFU-E reduction **Patient 29**
	Well 1	Well 2	Well 3	Well 4	Total	
Control	88	65	110	65	328	N/A
Control	68	99	79	105	351	N/A
Control mean	78	82	94.5	85	339.5	N/A
$1x10^{10.5}$	4	4	8	11	27	92.05
$1x10^{10}$	28	35	36	33	132	61.12
$1x10^{9.5}$	43	43	34	45	165	51.40
$1x10^{9}$	54	64	52	62	232	31.66
$1x10^{8.5}$	72	61	57	67	257	24.30
$1x10^{8}$	44	61	46	71	222	34.61
$1x10^{7.5}$	77	84	85	63	309	8.98
$1x10^{7}$	87	84	62	87	320	5.74
$1x10^{6.5}$	75	85	82	81	323	4.86
$1x10^{6}$	81	99	89	70	339	0.15
$1x10^{5.5}$	93	85	84	94	356	0.00

Table A1.31: BFU-E reduction assay results for patient 30

Inoculum (IU/ml)	Red colony count					Percentage BFU-E reduction **Patient 30**
	Well 1	Well 2	Well 3	Well 4	Total	
Control	48	49	44	38	179	N/A
Control	30	34	28	27	119	N/A
Control mean	39	41.5	36	32.5	149	N/A
$1x10^{12}$	0	0	0	0	0	100.00
$1x10^{11.5}$	0	0	0	0	0	100.00
$1x10^{11}$	0	0	1	0	1	99.33
$1x10^{10.5}$	7	8	2	8	25	83.22
$1x10^{10}$	20	19	21	23	83	44.30
$1x10^{9.5}$	23	23	23	23	92	38.26
$1x10^{9}$	34	27	33	21	115	22.82
$1x10^{8.5}$	37	21	26	22	106	28.86
$1x10^{8}$	26	28	33	36	123	17.45
$1x10^{7.5}$	36	35	31	33	135	9.40
$1x10^{7}$	43	34	37	38	152	0.00
$1x10^{6.5}$	47	38	42	40	167	0.00
$1x10^{6}$	50	29	40	40	159	0.00
$1x10^{5.5}$	33	49	43	41	166	0.00
$1x10^{5}$	55	36	40	35	166	0.00

Appendix 2: Cell counts for continuous cell lines growth curves

Table A2.1: Cell count results for KU812Ep6 cell line at $1x10^5$ cells/ml starting concentration (n+19)

Day after seeding	0	1	2	3	4	5	6	7	8	9
Well 1	-	85	144	189	189	206	254	358	261	238
Well 2	-	82	153	191	191	226	229	266	220	207
Well 3	-	75	155	187	187	207	219	244	216	165
Well 4	-	79	140	192	192	214	225	316	220	201
Mean	-	80.25	148	189.75	189.75	213.25	231.75	296	232	203
Cell concentration (cells/ml)	$1.00x10^5$	$2.01x10^5$	$3.70x10^5$	$4.74x10^5$	$4.74x10^5$	$5.33x10^5$	$5.79x10^5$	$7.40x10^5$	$5.81x10^5$	$5.08x10^5$

Table A2.2: Cell count results for KU812Ep6 cell line at $5x10^4$ cells/ml starting concentration (n+19)

Day after seeding	0	1	2	3	4	5	6	7	8	9
Well 1	-	59	81	177	206	239	244	263	233	241
Well 2	-	29	92	154	203	228	242	261	246	214
Well 3	-	37	87	158	179	226	231	256	186	194
Well 4	-	25	119	161	175	183	285	242	241	220
Mean	-	37.5	94.75	162.5	190.75	219	250.5	255.5	222	216
Cell concentration (cells/ml)	$5.00x10^4$	$9.38x10^4$	$2.37x10^5$	$4.06x10^5$	$4.77x10^5$	$5.48x10^5$	$6.26x10^5$	$6.39x10^5$	$5.54x10^5$	$5.41x10^5$

Table A2.3: Cell count results for KU812Ep6 cell line at $1x10^4$ cells/ml starting concentration (n+19)

Day after seeding	0	1	2	3	4	5	6	7	8	9
Well 1	-	7	28	59	143	180	181	200	223	219
Well 2	-	5	15	43	135	146	180	151	214	196
Well 3	-	8	14	54	110	159	175	179	188	191
Well 4	-	10	24	49	143	174	178	170	188	171
Mean	-	7.5	20.25	51.25	129	162	179	177	208	202
Cell concentration (cells/ml)	$5.00x10^4$	$1.88x10^4$	$5.06x10^4$	$1.28x10^5$	$3.23x10^5$	$4.04x10^5$	$4.47x10^5$	$4.42x10^5$	$5.21Ex10^5$	$5.05x10^5$

Table A2.4: Cell count results for KU812Ep6 cell line at $1x10^5$ cells/ml starting concentration (n+81)

Day after seeding	0	1	2	3	4	5	6	7	8	9
Well 1	-	97	133	227	206	243	256	242	227	197
Well 2	-	52	159	156	184	202	243	243	209	197
Well 3	-	61	150	194	197	234	244	233	204	187
Well4	-	96	171	188	212	247	233	261	217	195
Mean	-	76.5	153.25	191.25	199.75	231.5	244	244.75	214.25	194
Cell concentration (cells/ml)	$1.00x10^5$	$1.91x10^5$	$3.83x10^5$	$4.78x10^5$	$4.99x10^5$	$5.79x10^5$	$6.10x10^5$	$6.12x10^5$	$5.36x10^5$	$4.85x10^5$

Table A2.5: Cell count results for KU812Ep6 cell line at $5x10^4$ cells/ml starting concentration (n+81)

Day after seeding	0	1	2	3	4	5	6	7	8	9
Well 1	-	28	75	172	169	235	246	229	208	185
Well 2	-	30	67	144	175	198	222	236	214	183
Well 3	-	41	95	173	173	201	217	204	214	198
Well 4	-	32	81	170	176	190	250	250	-	-
Mean	-	32.75	79.5	164.75	173.25	206	233.75	229.75	212	188.66
Cell concentration (cells/ml)	$1.00x10^5$	$8.19x10^4$	$1.99x10^5$	$4.12x10^5$	$4.33x10^5$	$5.15x10^5$	$5.84x10^5$	$5.74x10^5$	$5.30x10^5$	$4.72x10^5$

Table A2.6: Cell count results for KU812Ep6 cell line at $1x10^4$ cells/ml starting concentration (n+81)

Day after seeding	0	1	2	3	4	5	6	7	8
Well 1	-	3	19	48	130	160	153	161	169
Well 2	-	7	9	37	115	159	167	183	164
Well 3	-	11	13	49	106	161	145	171	179
Well 4	-	5	18	55	-	-	-	-	-
Mean	-	6.5	14.75	47.25	117	160	155	171.66	170.66
Cell concentration (cells/ml)	$1.00x10^4$	$1.63x10^4$	$3.69x10^4$	$1.18x10^5$	$2.93x10^5$	$4.00x10^5$	$3.88x10^5$	$4.29x10^5$	$4.27x10^5$

Table A2.7: Cell count results for UT-7/EPO cell line at $1x10^5$ cells/ml starting concentration (n+19)

Day after seeding	0	1	2	3	4	5	6	7	8	9
Well 1	-	61	172	258	240	278	283	263	229	209
Well 2	-	43	154	238	261	241	277	229	248	230
Well 3	-	72	123	200	236	226	274	235	238	194
Well4	-	63	127	230	247	259	263	298	212	195
Mean	-	60	144	232	246	251	274	256	232	207
Cell concentration (cells/ml)	$1.00x10^5$	$1.49x10^5$	$3.60x10^5$	$5.79x10^5$	$6.15x10^5$	$6.28x10^5$	$6.86x10^5$	$6.41x10^5$	$5.79x10^5$	$5.18x10^5$

Table A2.8: Cell count results for UT-7/EPO cell line at $5x10^4$ cells/ml starting concentration (n+19)

Day after seeding	0	1	2	3	4	5	6	7	8	9
Well 1	-	23	78	163	252	296	275	239	252	202
Well 2	-	23	85	186	220	203	285	233	225	236
Well 3	-	36	86	147	196	264	243	238	197	195
Well4	-	25	75	165	196	265	283	267	239	183
Mean	-	27	81	165	216	257	272	244	228	204
Cell concentration (cells/ml)	$5.00x10^4$	$6.69x10^4$	$2.03x10^5$	$4.13x10^5$	$5.40x10^5$	$6.43x10^5$	$6.79x10^5$	$6.11x10^5$	$5.71x10^5$	$5.10x10^5$

Table A2.9: Cell count results for UT-7/EPO cell line at $1x10^4$ cells/ml starting concentration (n+19)

Day after seeding	0	1	2	3	4	5	6	7	8	9
Well 1	-	9	12	40	101	160	214	216	199	218
Well 2	-	13	13	31	74	125	185	205	227	201
Well 3	-	3	10	44	75	178	205	212	215	174
Well4	-	1	16	46	79	134	204	223	195	194
Mean	-	7	13	40	83	154	201	211	214	197
Cell concentration (cells/ml)	$1.00x10^4$	$1.63x10^4$	$3.19x10^4$	$1.01x10^5$	$2.08x10^5$	$3.86x10^5$	$5.03x10^5$	$5.28x10^5$	$5.34x10^5$	$4.92x10^5$

Table A2.10: Cell count results for UT-7/EPO cell line at $1x10^5$ cells/ml starting concentration (n+80)

Day after seeding	0	1	2	3	4	5	6
Well 1	-	50	171	268	166	123	40
Well 2	-	56	211	217	176	88	43
Well 3	-	59	165	206	161	87	43
Well 4	-	58	116	207	152	103	31
Mean	-	55.75	165.75	224.5	163.75	100.25	39.25
Cell concentration (cells/ml)	$1.00x10^5$	$1.39x10^5$	$4.14x10^5$	$5.61x10^5$	$4.09x10^5$	$2.51x10^5$	$9.81x10^4$

Table A2.11: Cell count results for UT-7/EPO cell line at $5x10^4$ cells/ml starting concentration (n+80)

Day after seeding	0	1	2	3	4	5	6
Well 1	-	24	66	174	211	177	181
Well 2	-	31	67	159	205	151	125
Well 3	-	22	68	154	196	144	125
Well 4	-	21	62	168	171	156	84
Mean	-	24.5	65.75	163.75	195.75	157	128.75
cell concentration (cells/ml)	$5.00x10^4$	$6.13x10^4$	$1.64x10^5$	$4.09x10^5$	$4.89x10^5$	$3.93x10^5$	$3.22x10^5$

Table A2.12: Cell count results for UT-7/EPO cell line at $1x10^4$ cells/ml starting concentration (n+80)

Day after seeding	0	1	2	3	4	5	6	7	8
Well 1	-	2	11	23	69	171	232	190	156
Well 2	-	7	12	31	70	148	216	185	175
Well 3	-	5	11	34	81	138	199	181	170
Well 4	-	11	8	46	82	146	203	199	168
Mean	-	6.25	10.5	33.5	75.5	150.75	212.5	188.75	167.25
Cell concentration (cells/ml)	$1.00x10^4$	$1.56x10^4$	$2.63x10^4$	$8.38x10^4$	$1.89x10^5$	$3.77x10^5$	$5.31x10^5$	$4.72x10^5$	$4.18x10^5$

Table A2.13: Cell count results for UT-7/EPO-S1 cell line at $1x10^5$ cells/ml starting concentration

Day after seeding	0	1	2	3	4	5	6	7	8	9
Well 1	-	50	78	68	119	165	243	160	134	115
Well 2	-	32	66	86	127	127	207	152	131	106
Well 3	-	41	65	103	138	170	190	201	139	99
Well4	-	48	72	85	154	186	192	198	143	102
Mean	-	42.75	70.25	85.5	134.5	162	208	177.75	136.75	140.67
Cell concentration (cells/ml)	$1.00x10^5$	$1.07x10^5$	$1.76x10^5$	$2.14x10^5$	$3.36x10^5$	$4.05x10^5$	$5.20x10^5$	$4.44x10^5$	$3.42x10^5$	$3.52x10^5$

Table A2.14: Cell count results for UT-7/EPO-S1 cell line at $1x10^4$ cells/ml starting concentration

Day after seeding	0	1	2	3	4	5	6	7	8	9
Well 1	-	18	20	33	52	69	99	168	188	172
Well 2	-	12	20	26	57	82	115	166	182	214
Well 3	-	20	13	28	35	71	108	150	147	198
Well4	-	25	26	30	37	72	122	200	210	188
Mean	-	18.75	19.75	29.25	45.25	73.5	111	171	181.75	257.33
Cell concentration (cells/ml)	$1.00x10^4$	$4.69x10^4$	$4.94x10^4$	$7.31x10^4$	$1.13x10^5$	$1.84x10^5$	$2.78x10^5$	$4.28x10^5$	$4.54x10^5$	$6.43x10^5$

Table A2.15: Cell count results for UT-7/EPO-S1 cell line (n+17) in a 20% and 3% oxygen atmosphere

Days after seeding	Cell count at 20% oxygen (cells/ml)	Cell count at 3% oxygen (cells/ml)
0	1.00×10^5	1.00×10^5
1	1.40×10^5	1.75×10^5
2	3.30×10^5	2.20×10^5
3	3.90×10^5	3.00×10^5
4	5.00×10^5	3.70×10^5
5	6.90×10^5	4.10×10^5
6	7.60×10^5	6.10×10^5
7	8.50×10^5	4.70×10^5
8	8.30×10^5	4.20×10^5
9	7.35×10^5	2.30×10^5
10	6.45×10^5	1.60×10^5

Appendix 3: PCR data for viral removal study and RT-PCR data for viral inactivation studies

1. Planova study

Figure A3.1: LightCycler PCR products for Planova experimental controls and samples 1 to 13 (first 15N filter)

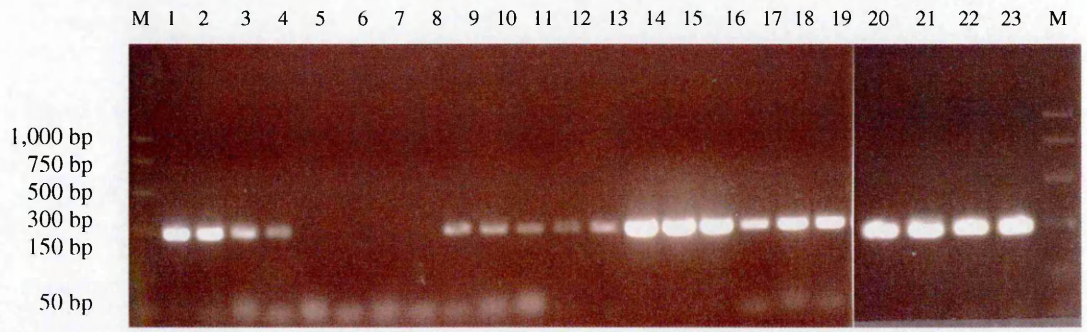

Lane M. PCR markers

Lanes 1 to 4: IS (99/686, positive control)

1. $1x10^{6.0}$ IU/ml
2. $1x10^{5.0}$ IU/ml
3. $1x10^{4.0}$ IU/ml
4. $1x10^{3.0}$ IU/ml

Lanes 9 to 16: Planova experimental controls

9. Sample A1 neat
10. Sample A2 neat
11. Sample B1 neat
12. Sample B2 neat
13. Sample C1 neat
14. Sample C2 neat
15. Sample D1 neat
16. Sample D2 neat

5. RNAase-free water (PCR negative control)

Lanes 6 to 8: Extraction negative controls

6. Negative plasma
7. Negative serum
8. RNAase-free water

Lanes 17 to 23: Planova samples

17. Sample 1 neat
18. Sample 3 neat
19. Sample 5 neat
20. Sample 7 neat
21. Sample 9 neat
22. Sample 11 neat
23. Sample 13 neat

Figure A3.2: LightCycler PCR products for Planova samples 17 to 41 (first 15N filter)

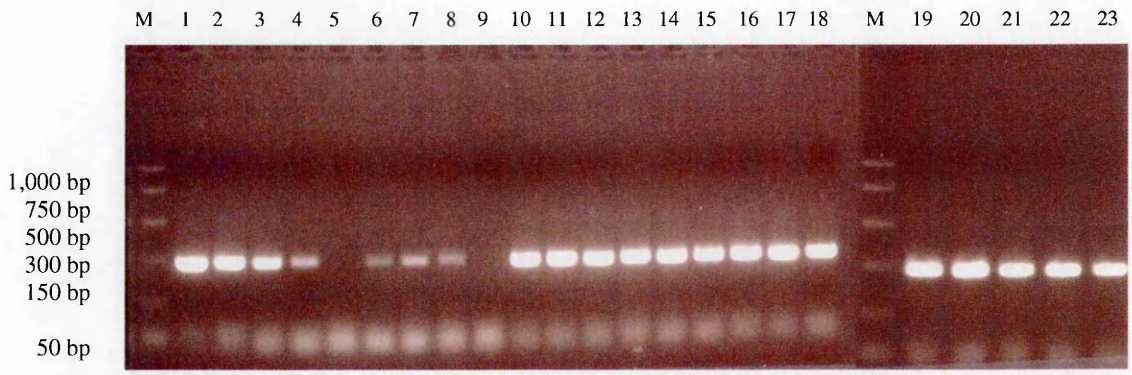

Lane M. PCR markers

Lanes 1 to 4: IS (99/686, positive control)

1. $1x10^{6.0}$ IU/ml
2. $1x10^{5.0}$ IU/ml
3. $1x10^{4.0}$ IU/ml
4. $1x10^{3.0}$ IU/ml

5. RNAase-free water (PCR negative control)

Lanes 6 to 9: Extraction negative controls

6. Negative plasma
7. Negative serum
8. RNAase-free water
9. RNAase-free water

Lanes 10 to 23: Planova samples

10. Sample 15 neat
11. Sample 17 neat
12. Sample 19 neat
13. Sample 21 neat
14. Sample 23 neat
15. Sample 25 neat
16. Sample 27 neat
17. Sample 29 neat
18. Sample 31 neat
19. Sample 33 neat
20. Sample 35 neat
21. Sample 37 neat
22. Sample 39 neat
23. Sample 41 neat

Figure A3.3: LightCycler PCR products for Planova samples 17 to 41 (first 15N filter)

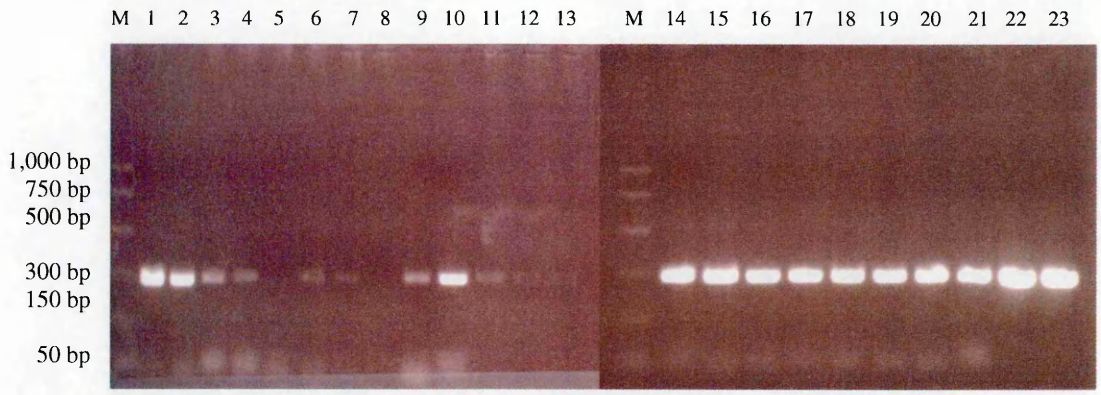

Lane M. PCR markers

Lanes 1 to 4: IS (99/686, positive control)

1. $1x10^{6.0}$ IU/ml
2. $1x10^{5.0}$ IU/ml
3. $1x10^{4.0}$ IU/ml
4. $1x10^{3.0}$ IU/ml

5. RNAase-free water (PCR negative control)

Lanes 6 to 9: Extraction negative controls

6. Negative plasma
7. Negative serum
8. RNAase-free water
9. RNAase-free water

Lanes 10 to 23: Planova samples

10. Sample 43 neat
11. Sample 44 neat
12. Sample 46 neat
13. Sample 48 neat
14. Sample 50 neat
15. Sample 52 neat
16. Sample 54 neat
17. Sample 56 neat
18. Sample 58 neat
19. Sample 60 neat
20. Sample 62 neat
21. Sample 64 neat
22. Sample 66 neat
23. Sample 68 neat

Figure A3.4: LightCycler PCR products for Planova samples 68 to 86 (second 15N filter)

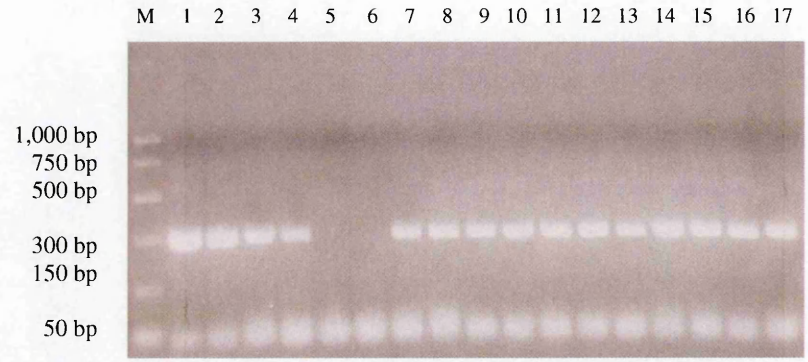

Lane M. PCR markers

Lanes 1 to 4: IS (99/800, positive control)

1. $1x10^{6.0}$ IU/ml
2. $1x10^{5.0}$ IU/ml
3. $1x10^{4.0}$ IU/ml
4. $1x10^{3.0}$ IU/ml

5. RNAase-free water (PCR negative control)

6. Negative plasma (extraction negative control)

7. Positive control ($2x10^{3}$ IU/ml)

Lanes 8 to 17: Planova samples

8. Sample 68 neat
9. Sample 70 neat
10. Sample 72 neat
11. Sample 74 neat
12. Sample 76 neat
13. Sample 78 neat
14. Sample 80 neat
15. Sample 82 neat
16. Sample 84 neat
17. Sample 86 neat

Figure A3.5: LightCycler PCR products for Planova samples 87 to 107 (first 20N filter)

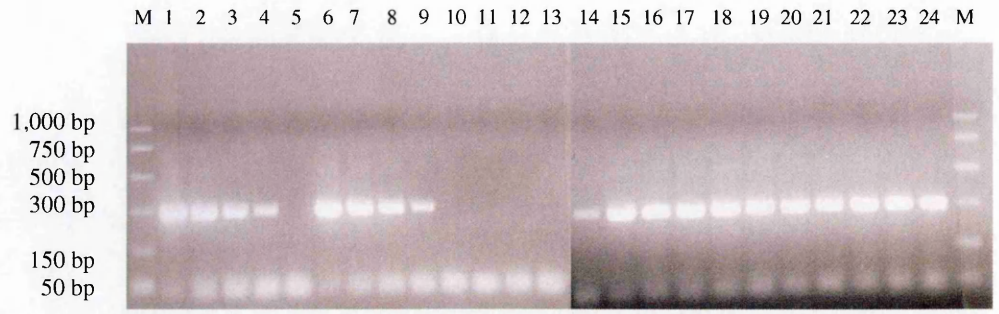

Lane M. PCR markers

Lanes 1 to 4: IS (99/800, positive control)

1. $1x10^{6.0}$ IU/ml
2. $1x10^{5.0}$ IU/ml
3. $1x10^{4.0}$ IU/ml
4. $1x10^{3.0}$ IU/ml

5. RNAase-free water (PCR negative control)

Lanes 6 to 9: IS (99/800, positive control)

6. $1x10^{6.0}$ IU/ml
7. $1x10^{5.0}$ IU/ml
8. $1x10^{4.0}$ IU/ml
9. $1x10^{3.0}$ IU/ml

Lanes 10 to 13: Extraction negative controls

10. Negative plasma
11. Negative serum
12. RNAase-free water
13. RNAase-free water

Lanes 14 to 24: Planova samples

14. Sample 87 neat
15. Sample 89 neat
16. Sample 91 neat
17. Sample 93 neat
18. Sample 95 neat
19. Sample 97 neat
20. Sample 99 neat
21. Sample 101 neat
22. Sample 103 neat
23. Sample 105 neat
24. Sample 107 neat

Figure A3.6: LightCycler PCR products for Planova samples 109 to 130 (first and second 20N filters)

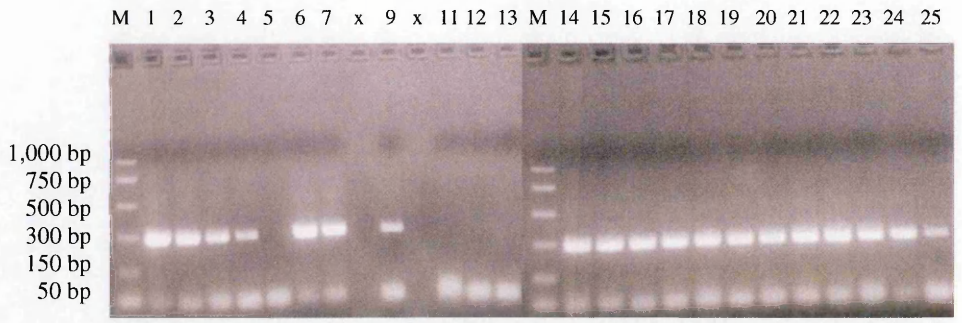

Lane M. PCR markers

Lanes 1 to 4: IS (99/800, positive control)

1x$10^{6.0}$ IU/ml

2. 1x$10^{5.0}$ IU/ml

3. 1x$10^{4.0}$ IU/ml

4. 1x$10^{3.0}$ IU/ml

5. RNAase-free water (PCR negative control)

Lanes 6 to 9: IS (99/800, positive control)

6. 1x$10^{6.0}$ IU/ml

7. 1x$10^{5.0}$ IU/ml

9. 1x$10^{3.0}$ IU/ml

Lanes 14 to 25: Planova samples

14. Sample 109 neat
15. Sample 111 neat
16. Sample 113 neat
17. Sample 115 neat
18. Sample 117 neat
19. Sample 119 neat

x: no sample

Lanes 11 to 13: Extraction negative controls1.

11. Negative serum
12. RNAase-free water
13. RNAase-free water

20. Sample 121 neat
21. Sample 123 neat
22. Sample 125 neat
23. Sample 127 neat
24. Sample 129 neat
25. Sample 130 neat (second 20N filter)

Figure A3.7: LightCycler PCR products for Planova samples 132 to 154 (second 20N filter)

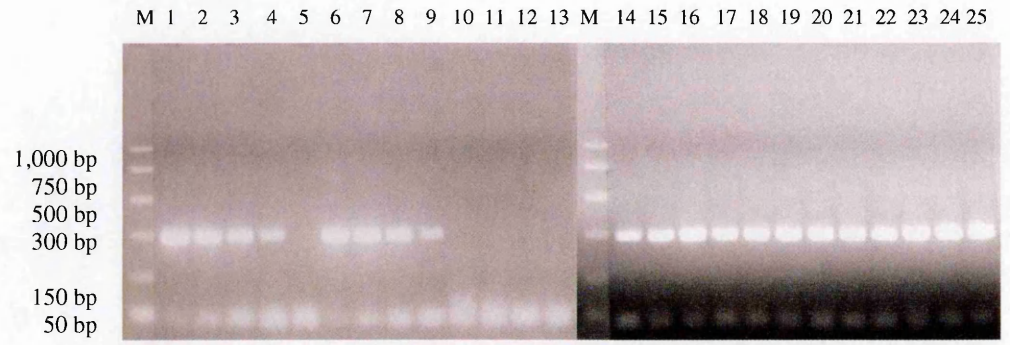

Lane M. PCR markers

Lanes 1 to 4: IS (99/800, positive control)

1. $1x10^{6.0}$ IU/ml
2. $1x10^{5.0}$ IU/ml
3. $1x10^{4.0}$ IU/ml
4. $1x10^{3.0}$ IU/ml

5. RNAase-free water (PCR negative control)

Lanes 6 to 9: IS (99/800, positive control)

6. $1x10^{6.0}$ IU/ml
7. $1x10^{5.0}$ IU/ml
8. $1x10^{4.0}$ IU/ml
9. $1x10^{3.0}$ IU/ml

Lanes 10 to 13: Extraction negative controls

10. Negative plasma
11. Negative serum
12. RNAase-free water
13. RNAase-free water

Lanes 14 to 25: Planova samples

14. Sample 132 neat
15. Sample 134 neat
16. Sample 136 neat
17. Sample 138 neat
18. Sample 140 neat
19. Sample 142 neat
20. Sample 144 neat
21. Sample 146 neat
22. Sample 148 neat
23. Sample 150 neat
24. Sample 152 neat
25. Sample 154 neat

Figure A3.8: LightCycler PCR products for Planova samples 156 to 173 (second 20N and third 15N filter)

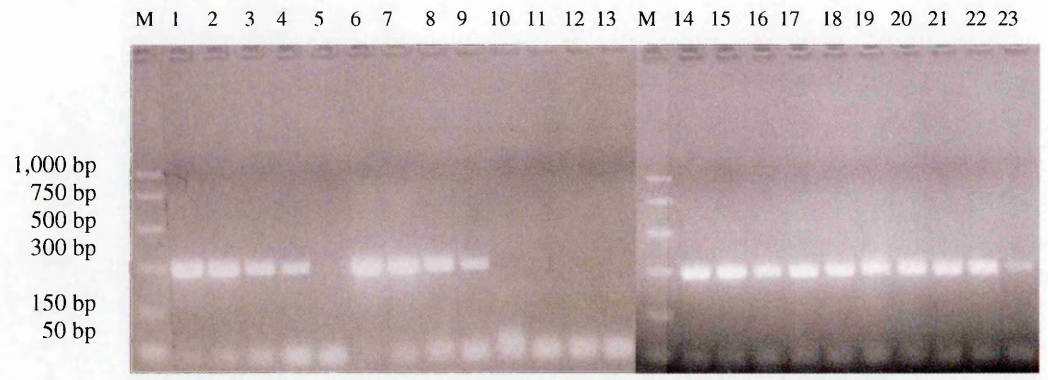

Lane M. PCR markers

Lanes 1 to 4: IS (99/800, positive control)

1. $1x10^{6.0}$ IU/ml
2. $1x10^{5.0}$ IU/ml
3. $1x10^{4.0}$ IU/ml
4. $1x10^{3.0}$ IU/ml

5. RNAase-free water (PCR negative control)

Lanes 6 to 9: IS (99/800, positive control)

6. $1x10^{6.0}$ IU/ml
7. $1x10^{5.0}$ IU/ml
8. $1x10^{4.0}$ IU/ml
9. $1x10^{3.0}$ IU/ml

Lanes 10 to 13: Extraction negative controls

10. Negative plasma
11. Negative serum
12. RNAase-free water
13. RNAase-free water

Lanes 14 to 25: Planova samples

14. Sample 156 neat
15. Sample 158 neat
16. Sample 160 neat
17. Sample 162 neat
18. Sample 164 neat
19. Sample 166 neat
20. Sample 168 neat
21. Sample 170 neat
22. Sample 172 neat
23. Sample 173 neat (third 15N filter)

Figure A3.9: LightCycler PCR products for Planova samples 175 and 177 (third 15N filter)

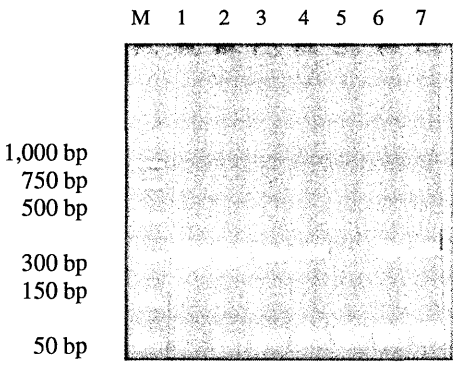

Lane M. PCR markers

Lanes 1 to 4: IS (99/800, positive control)

1. $1x10^{6.0}$ IU/ml
2. $1x10^{5.0}$ IU/ml
3. $1x10^{4.0}$ IU/ml
4. $1x10^{3.0}$ IU/ml

5. RNAase-free water (PCR negative control)

Lanes 6 and 7: Planova samples

6. Sample 175 neat
7. Sample 177 neat

Figure A3.10: LightCycler PCR products for Planova samples 179 to 215 (third 15N filter)

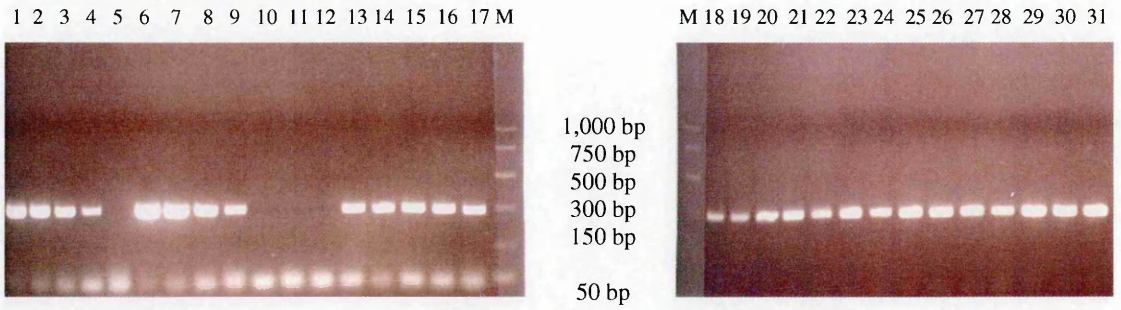

Lane M. PCR markers

Lanes 1 to 4: IS (99/800, positive control)

1. $1x10^{6.0}$ IU/ml
2. $1x10^{5.0}$ IU/ml
3. $1x10^{4.0}$ IU/ml
4. $1x10^{3.0}$ IU/ml

5. RNAase-free water (PCR negative control)

Lanes 6 to 9: IS (99/800, positive control)

6. $1x10^{6.0}$ IU/ml
7. $1x10^{5.0}$ IU/ml
8. $1x10^{4.0}$ IU/ml
9. $1x10^{3.0}$ IU/ml

Lanes 10 to 12: Extraction negative controls

10. Negative plasma
11. Negative serum
12. RNAase-free water

Lanes 13 to 31: Planova samples

13. Sample 179 neat
14. Sample 181 neat
15. Sample 183 neat
16. Sample 185 neat
17. Sample 187 neat
18. Sample 189 neat
19. Sample 191 neat
20. Sample 193 neat
21. Sample 195 neat
22. Sample 197 neat
23. Sample 199 neat
24. Sample 201 neat
25. Sample 203 neat
26. Sample 205 neat
27. Sample 207 neat
28. Sample 209 neat
29. Sample 211 neat
30. Sample 213 neat
31. Sample 215 neat

Figure A3.11: LightCycler PCR products for Planova samples 246 to 258 (third 20N filter)

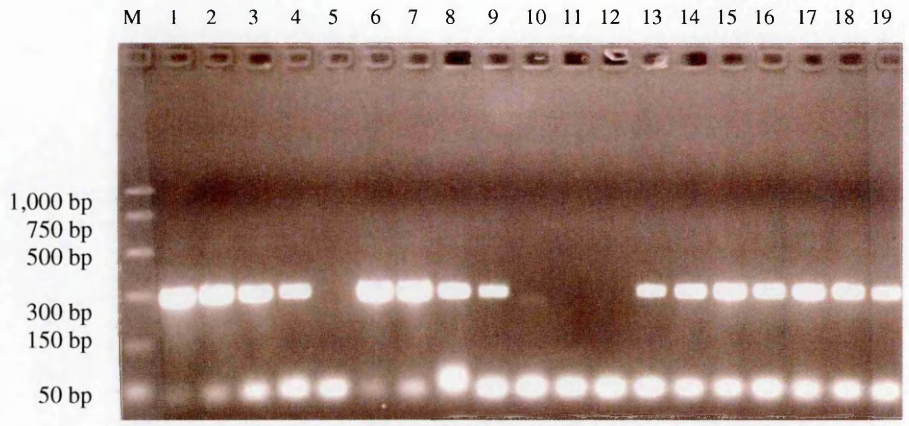

Lane M. PCR markers

Lanes 1 to 4: IS (99/800, positive control)

1. $1x10^{6.0}$ IU/ml
2. $1x10^{5.0}$ IU/ml
3. $1x10^{4.0}$ IU/ml
4. $1x10^{3.0}$ IU/ml

5. RNAase-free water (PCR negative control)

Lanes 6 to 9: IS (99/800, positive control)

6. $1x10^{6.0}$ IU/ml
7. $1x10^{5.0}$ IU/ml
8. $1x10^{4.0}$ IU/ml
9. $1x10^{3.0}$ IU/ml

Lanes 10 to 12: Extraction negative controls

10. Negative plasma
11. Negative serum
12. RNAase-free water

Lanes 13 to 19: Planova samples

13. Sample 246 neat
14. Sample 248 neat
15. Sample 250 neat
16. Sample 252 neat
17. Sample 254 neat
18. Sample 256 neat
19. Sample 258 neat

2. BPL study

Figure A3.12: Infectivity assay results for BPL spiked product control

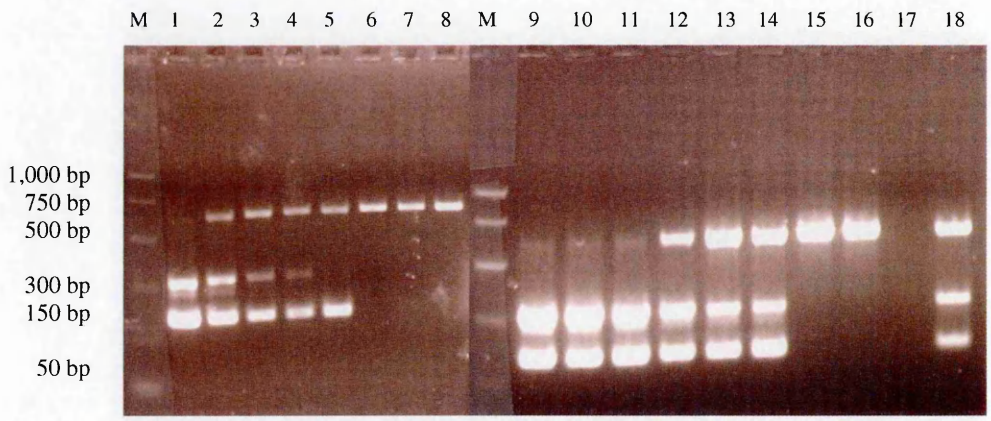

Lane M. PCR markers

Lanes 1 to 8: LP isolate (positive control)

1. $5x10^{8.0}$ IU/ml inoculum
2. $5x10^{7.5}$ IU/ml inoculum
3. $5x10^{7.0}$ IU/ml inoculum
4. $5x10^{6.5}$ IU/ml inoculum
5. $5x10^{6.0}$ IU/ml inoculum
6. $5x10^{5.5}$ IU/ml inoculum
7. $5x10^{5.0}$ IU/ml inoculum
8. Phosphate buffer pH 5.7

Lanes 9 to 16: BPL spiked product control

9. $4x10^{9.0}$ IU/ml inoculum
10. $4x10^{8.5}$ IU/ml inoculum
11. $4x10^{8.0}$ IU/ml inoculum
12. $4x10^{7.5}$ IU/ml inoculum
13. $4x10^{7.0}$ IU/ml inoculum
14. $4x10^{6.5}$ IU/ml inoculum
15. $4x10^{6.0}$ IU/ml inoculum
16. Phosphate buffer pH 5.7

Lanes 17 and 18: RT-PCR positive controls

16. $5x10^{7.0}$ IU/ml inoculum
17. RNAase-free water

Figure A3.13: Infectivity assay results for BPL spiked medium control and spiked test sample 1

Lane M. PCR markers

Lanes 1 to 8: LP isolate (positive control)

1. $5x10^{8.0}$ IU/ml inoculum
2. $5x10^{7.5}$ IU/ml inoculum
3. $5x10^{7.0}$ IU/ml inoculum
4. $5x10^{6.5}$ IU/ml inoculum
5. $5x10^{6.0}$ IU/ml inoculum
6. $5x10^{5.5}$ IU/ml inoculum
7. $5x10^{5.0}$ IU/ml inoculum
8. Phosphate buffer pH 5.7

Lanes 9 to 16: BPL spiked medium control

9. $4x10^{7.0}$ IU/ml inoculum
10. $4x10^{6.5}$ IU/ml inoculum
11. $4x10^{6.0}$ IU/ml inoculum
12. $4x10^{5.5}$ IU/ml inoculum
13. $4x10^{5.0}$ IU/ml inoculum
14. $4x10^{4.5}$ IU/ml inoculum
15. $4x10^{4.0}$ IU/ml inoculum
16. Phosphate buffer pH 5.7

Lanes 17 to 24: BPL spiked test sample 1

17. $1.5x10^{7.0}$ IU/ml inoculum
18. $1.5x10^{6.5}$ IU/ml inoculum
19. $1.5x10^{6.0}$ IU/ml inoculum
20. $1.5x10^{5.5}$ IU/ml inoculum
21. $1.5x10^{5.0}$ IU/ml inoculum
22. $1.5x10^{4.5}$ IU/ml inoculum
23. $1.5x10^{4.0}$ IU/ml inoculum

Lanes 25 and 26: RT-PCR positive controls

25. $5x10^{8.0}$ IU/ml inoculum
26. RNAase-free water

Figure A3.14: Infectivity assay results for BPL spiked test sample 2

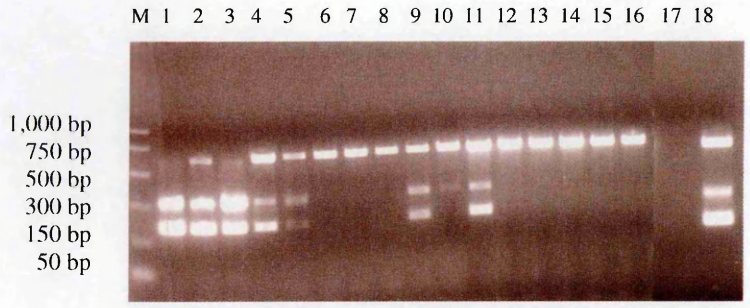

Lane M. PCR markers

Lanes 1 to 8: LP isolate (positive control)

1. $5x10^{8.0}$ IU/ml inoculum
2. $5x10^{7.5}$ IU/ml inoculum
3. $5x10^{7.0}$ IU/ml inoculum
4. $5x10^{6.5}$ IU/ml inoculum
5. $5x10^{6.0}$ IU/ml inoculum
6. $5x10^{5.5}$ IU/ml inoculum
7. $5x10^{5.0}$ IU/ml inoculum
8. Phosphate buffer pH 5.7

Lanes 9 to 16: BPL spiked test sample 2

9. $2.7x10^{8.0}$ IU/ml inoculum
10. $2.7x10^{7.5}$ IU/ml inoculum
11. $2.7x10^{7.0}$ IU/ml inoculum
12. $2.7x10^{6.5}$ IU/ml inoculum
13. $2.7x10^{6.0}$ IU/ml inoculum
14. $2.7x10^{5.5}$ IU/ml inoculum
15. $2.7x10^{5.0}$ IU/ml inoculum
16. Phosphate buffer pH 5.7

Lanes 17 and 18: RT-PCR positive controls

17. $5x10^{7.0}$ IU/ml inoculum
18. RNAase-free water

Figure A3.15: Infectivity assay results for BPL spiked test sample 3

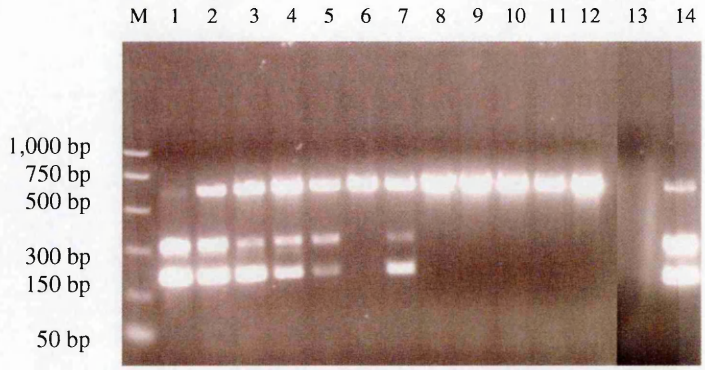

Lane M. PCR markers

Lanes 1 to 8: LP isolate (positive control)

1. $5x10^{8.0}$ IU/ml inoculum
2. $5x10^{7.5}$ IU/ml inoculum
3. $5x10^{7.0}$ IU/ml inoculum
4. $5x10^{6.5}$ IU/ml inoculum
5. $5x10^{6.0}$ IU/ml inoculum
6. $5x10^{5.5}$ IU/ml inoculum
7. $5x10^{5.0}$ IU/ml inoculum
8. Phosphate buffer pH 5.7

Lanes 9 to 12: BPL spiked test sample 3

9. $3.1x10^{9.0}$ IU/ml inoculum
10. $3.1x10^{8.5}$ IU/ml inoculum
11. $3.1x10^{8.0}$ IU/ml inoculum
12. Phosphate buffer pH 5.7

Lanes 13 and 14: RT-PCR positive controls

13. $5x10^{7.0}$ IU/ml inoculum
14. RNAase-free water

Figure A3.16: Infectivity assay results for BPL unspiked 8Y product

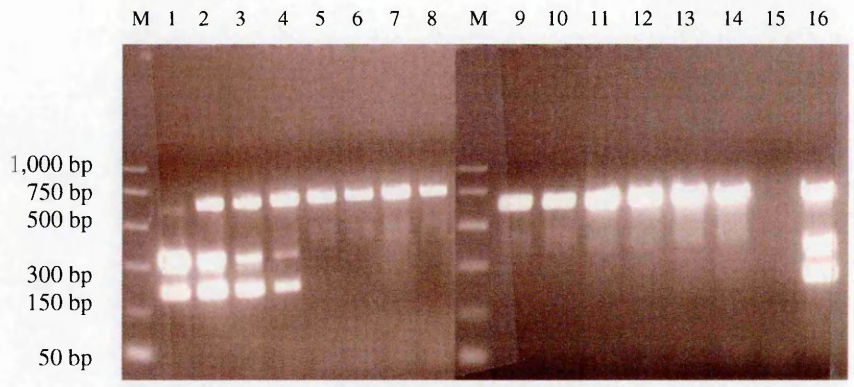

Lane M. PCR markers

Lanes 1 to 8: LP isolate (positive control)

1. $5x10^{8.0}$ IU/ml inoculum
2. $5x10^{7.5}$ IU/ml inoculum
3. $5x10^{7.0}$ IU/ml inoculum
4. $5x10^{6.5}$ IU/ml inoculum
5. $5x10^{6.0}$ IU/ml inoculum
6. $5x10^{5.5}$ IU/ml inoculum
7. $5x10^{5.0}$ IU/ml inoculum
8. Phosphate buffer pH 5.7

Lanes 9 to 16: BPL unspiked 8Y product

9. $3x10^{4.0}$ IU/ml inoculum
10. $3x10^{3.5}$ IU/ml inoculum
11. $3x10^{3.0}$ IU/ml inoculum
12. $3x10^{2.5}$ IU/ml inoculum
13. $3x10^{2.0}$ IU/ml inoculum
14. Phosphate buffer pH 5.7

Lanes 15 and 16: RT-PCR positive controls

17. $5x10^{8.0}$ IU/ml inoculum
18. RNAase-free water

3. Aphios study

- **NIBSC-01**

Figure A3.17: Infectivity assay results for NIBSC-01 "before" (panel A) and CFI-treated #1 samples (panel B)

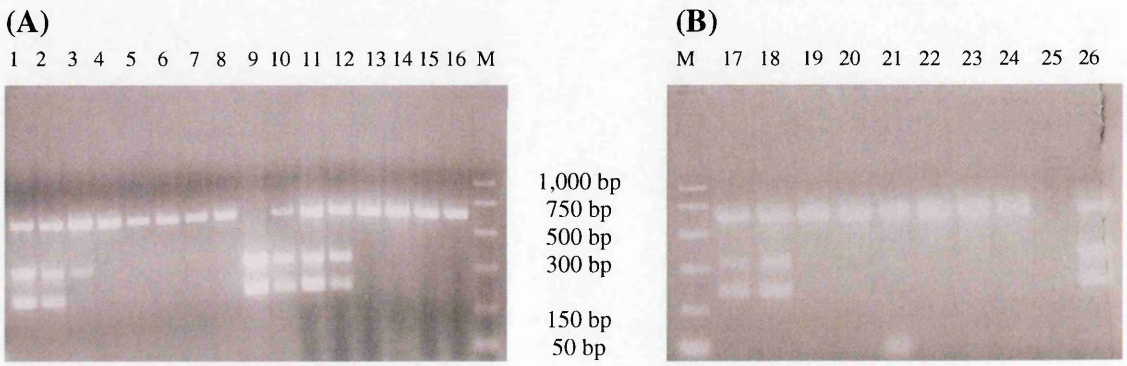

Lane M. PCR markers

Lanes 1 to 8: LP isolate (positive control)

1. $5x10^{7.0}$ IU/ml inoculum
2. $5x10^{6.5}$ IU/ml inoculum
3. $5x10^{6.0}$ IU/ml inoculum
4. $5x10^{5.5}$ IU/ml inoculum
5. $5x10^{5.0}$ IU/ml inoculum
6. $5x10^{4.5}$ IU/ml inoculum
7. $5x10^{4.0}$ IU/ml inoculum
8. Phosphate buffer pH 5.7

Lanes 9 to 16: NIBSC-01 "before"

9. $1x10^{9.0}$ IU/ml inoculum
10. $1x10^{8.5}$ IU/ml inoculum
11. $1x10^{8.0}$ IU/ml inoculum
12. $1x10^{7.5}$ IU/ml inoculum
13. $1x10^{7.0}$ IU/ml inoculum
14. $1x10^{6.5}$ IU/ml inoculum
15. $1x10^{6.0}$ IU/ml inoculum
16. Phosphate buffer pH 5.7

Lanes 17 to 24: NIBSC-01 CFI-treated #1

17. $5x10^{9.0}$ IU/ml inoculum
18. $5x10^{8.5}$ IU/ml inoculum
19. $5x10^{8.0}$ IU/ml inoculum
20. $5x10^{7.5}$ IU/ml inoculum
21. $5x10^{7.0}$ IU/ml inoculum
22. $5x10^{6.5}$ IU/ml inoculum
23. $5x10^{6.0}$ IU/ml inoculum
24. Phosphate buffer pH 5.7

Lanes 25 and 26: RT-PCR positive controls

25. $1x10^{8.0}$ IU/ml inoculum
26. RNAase-free water

Figure A3.18: Infectivity assay results for NIBSC-01 CFI-treated #2 samples

(panels A and B)

(A) **(B)**

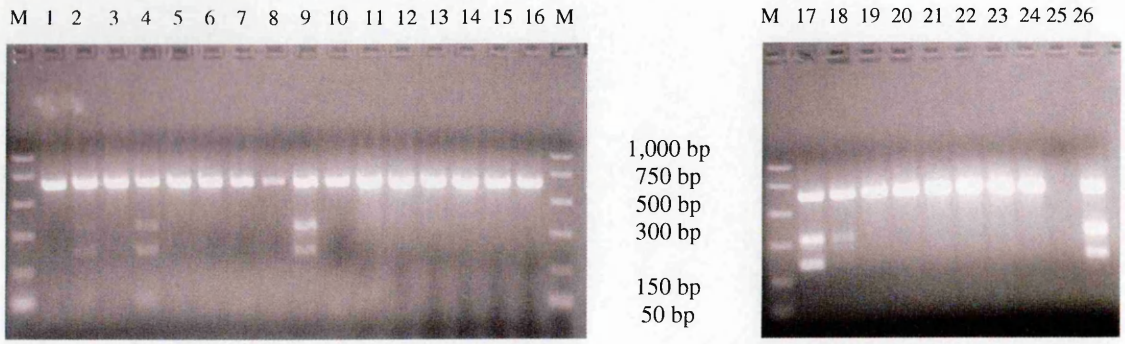

Lane M. PCR markers

Lanes 1 to 8: LP isolate (positive control)

1. $5x10^{7.0}$ IU/ml inoculum
2. $5x10^{6.5}$ IU/ml inoculum
3. $5x10^{6.0}$ IU/ml inoculum
4. $5x10^{5.5}$ IU/ml inoculum
5. $5x10^{5.0}$ IU/ml inoculum
6. $5x10^{4.5}$ IU/ml inoculum
7. $5x10^{4.0}$ IU/ml inoculum
8. Phosphate buffer pH 5.7

Lanes 9 to 16: NIBSC-01 CFI-treated #2

9. $3x10^{9.0}$ IU/ml inoculum
10. $3x10^{8.5}$ IU/ml inoculum
11. $3x10^{8.0}$ IU/ml inoculum
12. $3x10^{7.5}$ IU/ml inoculum
13. $3x10^{7.0}$ IU/ml inoculum
14. $3x10^{6.5}$ IU/ml inoculum
15. $3x10^{6.0}$ IU/ml inoculum
16. Phosphate buffer pH 5.7

Lanes 17 to 24: NIBSC-01 CFI-treated #2

17. $6x10^{9.0}$ IU/ml inoculum
18. $6x10^{8.5}$ IU/ml inoculum
19. $6x10^{8.0}$ IU/ml inoculum
20. $6x10^{7.5}$ IU/ml inoculum
21. $6x10^{7.0}$ IU/ml inoculum
22. $6x10^{6.5}$ IU/ml inoculum
23. $6x10^{6.0}$ IU/ml inoculum
24. Phosphate buffer pH 5.7

Lanes 25 and 26: RT-PCR positive controls

25. RNAase-free water
26. $1x10^{7.0}$ IU/ml inoculum

Figure A3.19: Infectivity assay results for NIBSC-01 CFI-treated #3 (panel A) and "time and temperature" samples (panel B)

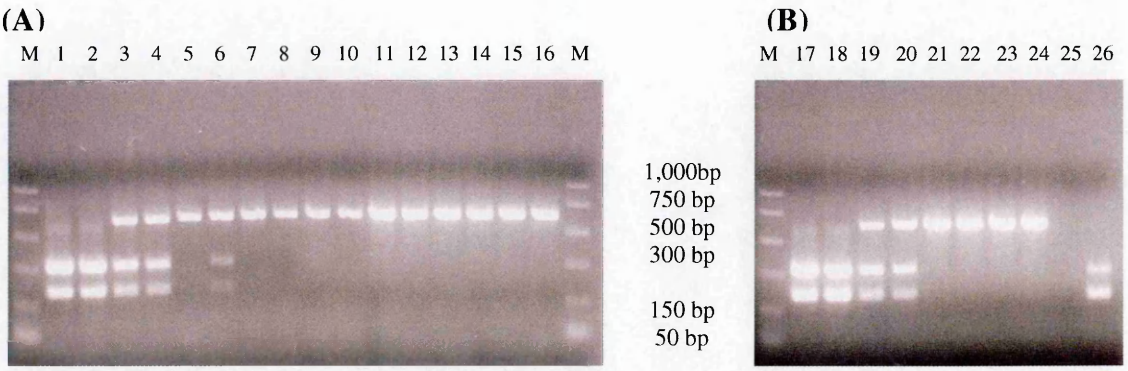

Lane M. PCR markers

Lanes 1 to 8: LP isolate (positive control)

1. $5x10^{7.0}$ IU/ml inoculum
2. $5x10^{6.5}$ IU/ml inoculum
3. $5x10^{6.0}$ IU/ml inoculum
4. $5x10^{5.5}$ IU/ml inoculum
5. $5x10^{5.0}$ IU/ml inoculum
6. $5x10^{4.5}$ IU/ml inoculum
7. $5x10^{4.0}$ IU/ml inoculum
8. Phosphate buffer pH 5.7

Lanes 9 to 16: NIBSC-01 CFI-treated #3

9. $5x10^{9.0}$ IU/ml inoculum
10. $5x10^{8.5}$ IU/ml inoculum
11. $5x10^{8.0}$ IU/ml inoculum
12. $5x10^{7.5}$ IU/ml inoculum
13. $5x10^{7.0}$ IU/ml inoculum
14. $5x10^{6.5}$ IU/ml inoculum
15. $5x10^{6.0}$ IU/ml inoculum
16. Phosphate buffer pH 5.7

Lanes 17 to 24: NIBSC-01 "Time and temperature" controls

17. $5x10^{9.0}$ IU/ml inoculum
18. $5x10^{8.5}$ IU/ml inoculum
19. $5x10^{8.0}$ IU/ml inoculum
20. $5x10^{7.5}$ IU/ml inoculum
21. $5x10^{7.0}$ IU/ml inoculum
22. $5x10^{6.5}$ IU/ml inoculum
23. $5x10^{6.0}$ IU/ml inoculum
24. Phosphate buffer pH 5.7

Lanes 25 and 26: RT-PCR positive

25. RNAase-free water
26. $1x10^{8.0}$ IU/ml inoculum

- **NIBSC-02**

Figure A3.20: Infectivity assay results for NIBSC-02 "before" (panel A) and CFI-treated #1 samples (panel B)

(A) **(B)**

Lane M. PCR markers

Lanes 1 to 8: LP isolate (positive control)

1. $5x10^{7.0}$ IU/ml inoculum
2. $5x10^{6.5}$ IU/ml inoculum
3. $5x10^{6.0}$ IU/ml inoculum
4. $5x10^{5.5}$ IU/ml inoculum
5. $5x10^{5.0}$ IU/ml inoculum
6. $5x10^{4.5}$ IU/ml inoculum
7. $5x10^{4.0}$ IU/ml inoculum
8. Phosphate buffer pH 5.7

Lanes 9 to 16: NIBSC-02 "before"

9. $3x10^{9.0}$ IU/ml inoculum
10. $3x10^{8.5}$ IU/ml inoculum
11. $3x10^{8.0}$ IU/ml inoculum
12. $3x10^{7.5}$ IU/ml inoculum
13. $3x10^{7.0}$ IU/ml inoculum
14. $3x10^{6.5}$ IU/ml inoculum
15. $3x10^{6.0}$ IU/ml inoculum
16. Phosphate buffer pH 5.7

Lanes 17 to 24: NIBSC-02 CFI-treated #1

17. $2x10^{9.0}$ IU/ml inoculum
18. $2x10^{8.5}$ IU/ml inoculum
19. $2x10^{8.0}$ IU/ml inoculum
20. $2x10^{7.5}$ IU/ml inoculum
21. $2x10^{7.0}$ IU/ml inoculum
22. $2x10^{6.5}$ IU/ml inoculum
23. $2x10^{6.0}$ IU/ml inoculum
24. Phosphate buffer pH 5.7

Lanes 25 and 26: RT-PCR positive controls

25. RNAase-free water
26. $1x10^{8.0}$ IU/ml inoculum

Figure A3.21: Infectivity assay results for NIBSC-02 CFI-treated #1 sample (panels A and B)

(A)

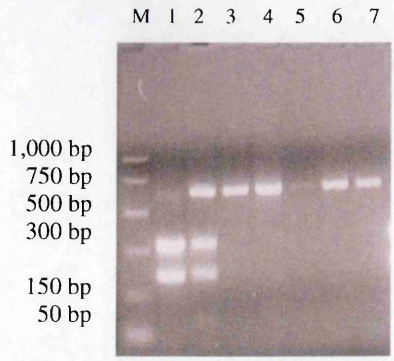

(B)

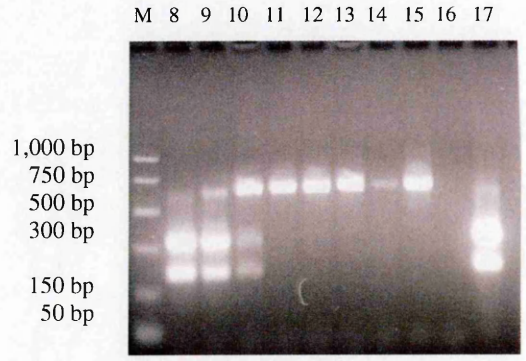

Lane M. PCR markers

Lanes 1 to 8: LP isolate (positive control)

1. $5x10^{7.0}$ IU/ml inoculum
2. $5x10^{6.5}$ IU/ml inoculum
3. $5x10^{5.5}$ IU/ml inoculum
4. $5x10^{5.0}$ IU/ml inoculum
5. $5x10^{4.5}$ IU/ml inoculum
6. $5x10^{4.0}$ IU/ml inoculum
7. Phosphate buffer pH 5.7

Lanes 9 to 16: NIBSC-02 CFI-treated #1

8. $2x10^{9.0}$ IU/ml inoculum
9. $2x10^{8.5}$ IU/ml inoculum
10. $2x10^{8.0}$ IU/ml inoculum
11. $2x10^{7.5}$ IU/ml inoculum
12. $2x10^{7.0}$ IU/ml inoculum
13. $2x10^{6.5}$ IU/ml inoculum
14. $2x10^{6.0}$ IU/ml inoculum
15. Phosphate buffer pH 5.7

Lanes 16 and 17: RT-PCR positive controls

16. RNAase-free water
17. $1x10^{8.0}$ IU/ml inoculum

Figure A3.22: Infectivity assay results for NIBSC-02 CFI-treated #2 sample (panels A and B)

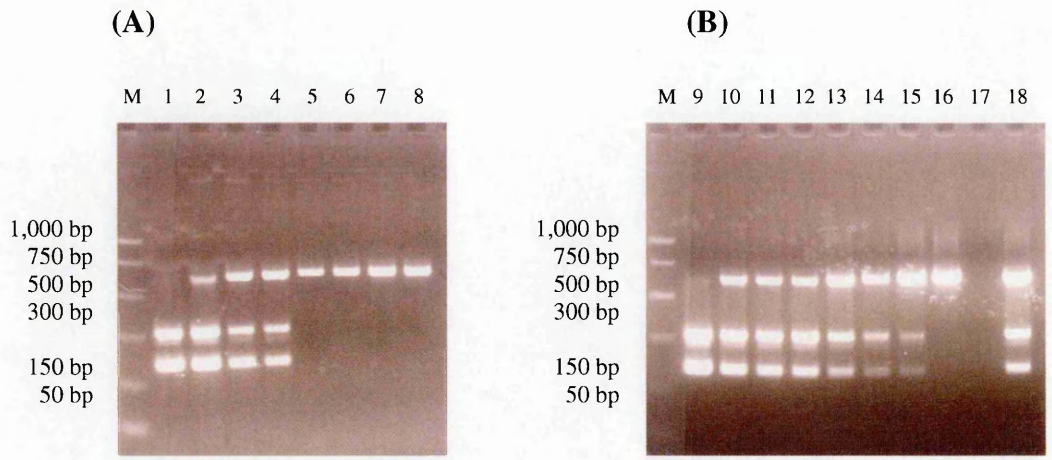

Lane M. PCR markers

Lanes 1 to 8: LP isolate (positive control)

1. $5x10^{7.0}$ IU/ml inoculum
2. $5x10^{6.5}$ IU/ml inoculum
3. $5x10^{6.0}$ IU/ml inoculum
4. $5x10^{5.5}$ IU/ml inoculum
5. $5x10^{5.0}$ IU/ml inoculum
6. $5x10^{4.5}$ IU/ml inoculum
7. $5x10^{4.0}$ IU/ml inoculum
8. Phosphate buffer pH 5.7

Lanes 9 to 16: NIBSC-02 CFI-treated #2

9. $5x10^{9.0}$ IU/ml inoculum
10. $3x10^{8.5}$ IU/ml inoculum
11. $5x10^{8.0}$ IU/ml inoculum
12. $5x10^{7.5}$ IU/ml inoculum
13. $5x10^{7.0}$ IU/ml inoculum
14. $5x10^{6.5}$ IU/ml inoculum
15. $5x10^{6.0}$ IU/ml inoculum
16. Phosphate buffer pH 5.7

Lanes 17 and 18: RT-PCR positive controls

16. RNAase-free water
17. $1x10^{7.0}$ IU/ml inoculum

Figure A3.23: Infectivity assay results for NIBSC-02 CFI-treated #3 (panel A) and "time and temperature" samples (panel B)

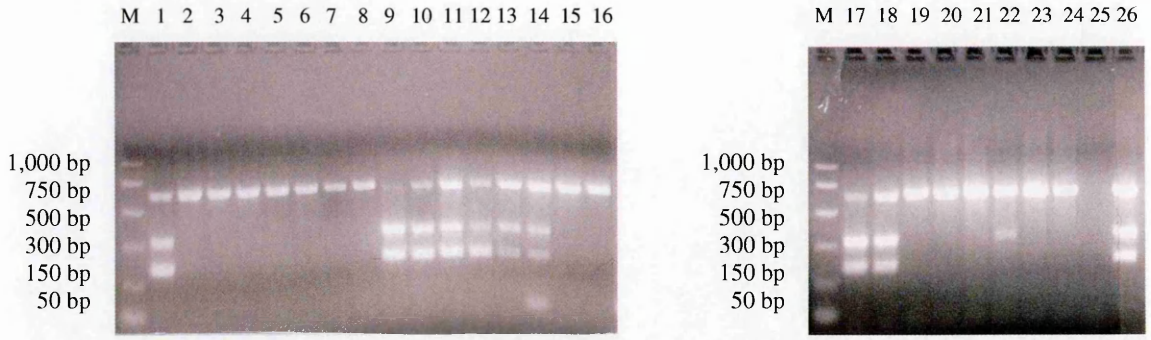

Lane M. PCR markers

Lanes 1 to 8: LP isolate (positive control)

1. $5x10^{7.0}$ IU/ml inoculum
2. $5x10^{6.5}$ IU/ml inoculum
3. $5x10^{6.0}$ IU/ml inoculum
4. $5x10^{5.5}$ IU/ml inoculum
5. $5x10^{5.0}$ IU/ml inoculum
6. $5x10^{4.5}$ IU/ml inoculum
7. $5x10^{4.0}$ IU/ml inoculum
8. Phosphate buffer pH 5.7

Lanes 9 to 16: NIBSC-02 CFI-treated #3

9. $8x10^{9.0}$ IU/ml inoculum
10. $8x10^{8.5}$ IU/ml inoculum
11. $8x10^{8.0}$ IU/ml inoculum
12. $8x10^{7.5}$ IU/ml inoculum
13. $8x10^{7.0}$ IU/ml inoculum
14. $8x10^{6.5}$ IU/ml inoculum
15. $8x10^{6.0}$ IU/ml inoculum
16. Phosphate buffer pH 5.7

Lanes 17 to 24: NIBSC-02 "time and temperature"

17. $7.6x10^{9.0}$ IU/ml inoculum
18. $7.6x10^{8.5}$ IU/ml inoculum
19. $7.6x10^{8.0}$ IU/ml inoculum
20. $7.6x10^{7.5}$ IU/ml inoculum
21. $7.6x10^{7.0}$ IU/ml inoculum
22. $7.6x10^{6.5}$ IU/ml inoculum
23. $7.6x10^{6.0}$ IU/ml inoculum
24. Phosphate buffer pH 5.7

Lanes 25 and 26: RT-PCR positive controls

25. RNAase-free water
26. $1x10^{8.0}$ IU/ml inoculum

- **NIBSC-03**

Figure A3.24: Infectivity assay results for NIBSC-03 "before" and CFI-treated #2 samples

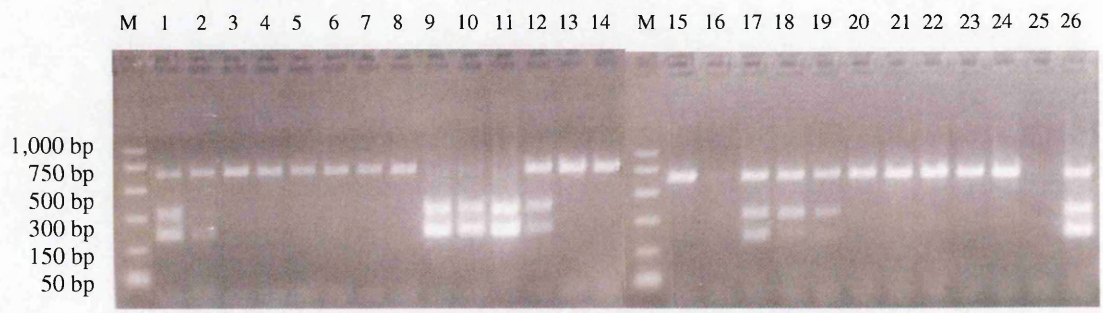

Lane M. PCR markers

Lanes 1 to 8: LP isolate (positive control)

1. $5x10^{7.0}$ IU/ml inoculum
2. $5x10^{6.5}$ IU/ml inoculum
3. $5x10^{6.0}$ IU/ml inoculum
4. $5x10^{5.5}$ IU/ml inoculum
5. $5x10^{5.0}$ IU/ml inoculum
6. $5x10^{4.5}$ IU/ml inoculum
7. $5x10^{4.0}$ IU/ml inoculum
8. Phosphate buffer pH 5.7

Lanes 9 to 16: NIBSC-03 "before"

9. $2x10^{10.0}$ IU/ml inoculum
10. $2x10^{9.5}$ IU/ml inoculum
11. $2x10^{9.0}$ IU/ml inoculum
12. $2x10^{8.5}$ IU/ml inoculum
13. $2x10^{8.0}$ IU/ml inoculum
14. $2x10^{7.5}$ IU/ml inoculum
15. $2x10^{7.0}$ IU/ml inoculum
16. Phosphate buffer pH 5.7

Lanes 17 to 24: NIBSC-03 CFI-treated #2

17. $9x10^{10.0}$ IU/ml inoculum
18. $9x10^{9.5}$ IU/ml inoculum
19. $9x10^{9.0}$ IU/ml inoculum
20. $9x10^{8.5}$ IU/ml inoculum
21. $9x10^{8.0}$ IU/ml inoculum
22. $9x10^{7.5}$ IU/ml inoculum
23. $9x10^{7.0}$ IU/ml inoculum
24. Phosphate buffer pH 5.7

Lanes 25 and 26: RT-PCR positive controls

25. RNAase-free water
26. $1x10^{8.0}$ IU/ml inoculum

Figure A3.25: Infectivity assay results for NIBSC-03 CFI-treated #3 samples

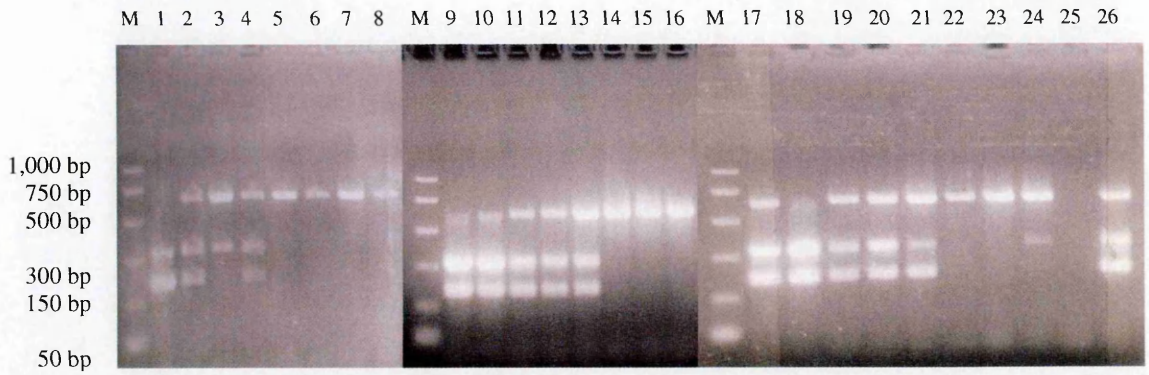

Lane M. PCR markers

Lanes 1 to 8: LP isolate (positive control)

1. $5x10^{7.0}$ IU/ml inoculum
2. $5x10^{6.5}$ IU/ml inoculum
3. $5x10^{6.0}$ IU/ml inoculum
4. $5x10^{5.5}$ IU/ml inoculum
5. $5x10^{5.0}$ IU/ml inoculum
6. $5x10^{4.5}$ IU/ml inoculum
7. $5x10^{4.0}$ IU/ml inoculum
8. Phosphate buffer pH 5.7

Lanes 9 to 16: NIBSC-03 CFI-treated #3

9. $7x10^{10.0}$ IU/ml inoculum
10. $7x10^{9.5}$ IU/ml inoculum
11. $7x10^{9.0}$ IU/ml inoculum
12. $7x10^{8.5}$ IU/ml inoculum
13. $7x10^{8.0}$ IU/ml inoculum
14. $7x10^{7.5}$ IU/ml inoculum
15. $7x10^{7.0}$ IU/ml inoculum
16. Phosphate buffer pH 5.7

Lanes 17 to 24: NIBSC-03 CFI-treated #3

17. $1.7x10^{11.0}$ IU/ml inoculum
18. $1.7x10^{10.5}$ IU/ml inoculum
19. $1.7x10^{10.0}$ IU/ml inoculum
20. $1.7x10^{9.5}$ IU/ml inoculum
21. $1.7x10^{9.0}$ IU/ml inoculum
22. $1.7x10^{8.5}$ IU/ml inoculum
23. $1.7x10^{8.0}$ IU/ml inoculum
24. Phosphate buffer pH 5.7

Lanes 25 and 26: RT-PCR positive controls

25. RNAase-free water
26. $1x10^{8.0}$ IU/ml inoculum

Figure A3.26: Infectivity assay results for NIBSC-03 "time and temperature" sample

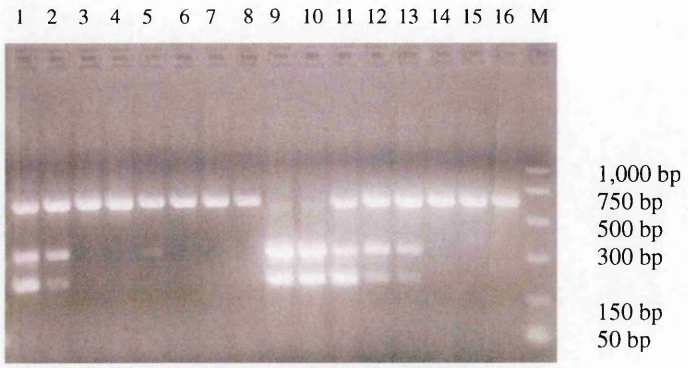

Lane M. PCR markers

Lanes 1 to 8: LP isolate (positive control)

1. $5x10^{7.0}$ IU/ml inoculum
2. $5x10^{6.5}$ IU/ml inoculum
3. $5x10^{6.0}$ IU/ml inoculum
4. $5x10^{5.5}$ IU/ml inoculum
5. $5x10^{5.0}$ IU/ml inoculum
6. $5x10^{4.5}$ IU/ml inoculum
7. $5x10^{4.0}$ IU/ml inoculum
8. Phosphate buffer pH 5.7

Lanes 9 to 16: NIBSC-03 CFI-treated #3

9. $1.7x10^{10.0}$ IU/ml inoculum
10. $1.7x10^{9.5}$ IU/ml inoculum
11. $1.7x10^{9.0}$ IU/ml inoculum
12. $1.7x10^{8.5}$ IU/ml inoculum
13. $1.7x10^{8.0}$ IU/ml inoculum
14. $1.7x10^{7.5}$ IU/ml inoculum
15. $1.7x10^{7.0}$ IU/ml inoculum
16. Phosphate buffer pH 5.7

- **NIBSC-04**

Figure A3.27: Infectivity assay results for NIBSC-04 "before" sample

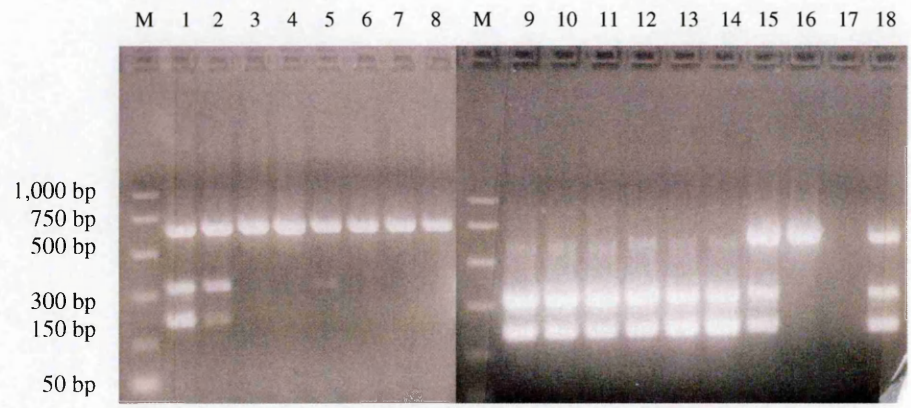

Lane M. PCR markers

Lanes 1 to 8: LP isolate (positive control)

1. $5x10^{7.0}$ IU/ml inoculum
2. $5x10^{6.5}$ IU/ml inoculum
3. $5x10^{6.0}$ IU/ml inoculum
4. $5x10^{5.5}$ IU/ml inoculum
5. $5x10^{5.0}$ IU/ml inoculum
6. $5x10^{4.5}$ IU/ml inoculum
7. $5x10^{4.0}$ IU/ml inoculum
8. Phosphate buffer pH 5.7

Lanes 9 to 16: NIBSC-04 "before"

9. $3x10^{10.0}$ IU/ml inoculum
10. $3x10^{9.5}$ IU/ml inoculum
11. $3x10^{9.0}$ IU/ml inoculum
12. $3x10^{8.5}$ IU/ml inoculum
13. $3x10^{8.0}$ IU/ml inoculum
14. $3x10^{7.5}$ IU/ml inoculum
15. $3x10^{7.0}$ IU/ml inoculum
16. Phosphate buffer pH 5.7

Lanes 17 and 18: RT-PCR positive controls

17. RNAase-free water
18. $1x10^{7.0}$ IU/ml inoculum

Figure A3.28: Infectivity assay results for NIBSC-04 CFI-treated #1 samples

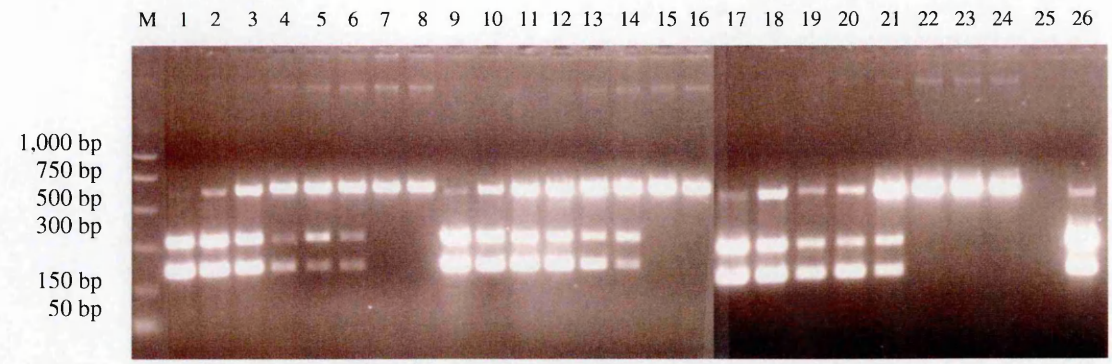

Lane M. PCR markers

Lanes 1 to 8: LP isolate (positive control)

1. $5x10^{8.0}$ IU/ml inoculum
2. $5x10^{7.5}$ IU/ml inoculum
3. $5x10^{7.0}$ IU/ml inoculum
4. $5x10^{6.5}$ IU/ml inoculum
5. $5x10^{6.0}$ IU/ml inoculum
6. $5x10^{5.5}$ IU/ml inoculum
7. $5x10^{5.0}$ IU/ml inoculum
8. Phosphate buffer pH 5.7

Lanes 9 to 16: NIBSC-04 CFI-treated #1

9. $3x10^{8.0}$ IU/ml inoculum
10. $3x10^{7.5}$ IU/ml inoculum
11. $3x10^{7.0}$ IU/ml inoculum
12. $3x10^{6.5}$ IU/ml inoculum
13. $3x10^{6.0}$ IU/ml inoculum
14. $3x10^{5.5}$ IU/ml inoculum
15. $3x10^{5.0}$ IU/ml inoculum
16. Phosphate buffer pH 5.7

Lanes 17 to 24: NIBSC-04 CFI-treated #1

17. $2x10^{8.0}$ IU/ml inoculum
18. $2x10^{7.5}$ IU/ml inoculum
19. $2x10^{7.0}$ IU/ml inoculum
20. $2x10^{6.5}$ IU/ml inoculum
21. $2x10^{6.0}$ IU/ml inoculum
22. $2x10^{5.5}$ IU/ml inoculum
23. $2x10^{5.0}$ IU/ml inoculum
24. Phosphate buffer pH 5.7

Lanes 25 and 26: RT-PCR positive controls

25. RNAase-free water
26. $5x10^{8.0}$ IU/ml inoculum

Figure A3.29: Infectivity assay results for NIBSC-04 CFI-treated #2 sample

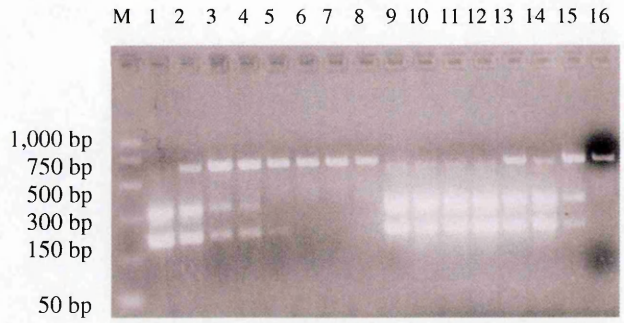

Lane M. PCR markers

Lanes 1 to 8: LP isolate (positive control)

1. $5x10^{7.0}$ IU/ml inoculum
2. $5x10^{6.5}$ IU/ml inoculum
3. $5x10^{6.0}$ IU/ml inoculum
4. $5x10^{5.5}$ IU/ml inoculum
5. $5x10^{5.0}$ IU/ml inoculum
6. $5x10^{4.5}$ IU/ml inoculum
7. $5x10^{4.0}$ IU/ml inoculum
8. Phosphate buffer pH 5.7

Lanes 9 to 16: NIBSC-04 CFI-treated #2

9. $3x10^{10.0}$ IU/ml inoculum
10. $3x10^{9.5}$ IU/ml inoculum
11. $3x10^{9.0}$ IU/ml inoculum
12. $3x10^{8.5}$ IU/ml inoculum
13. $3x10^{8.0}$ IU/ml inoculum
14. $3x10^{7.5}$ IU/ml inoculum
15. $3x10^{7.0}$ IU/ml inoculum
16. Phosphate buffer pH 5.7

Figure A3.30: Infectivity assay results for NIBSC-04 CFI-treated #3 and "time and temperature" samples

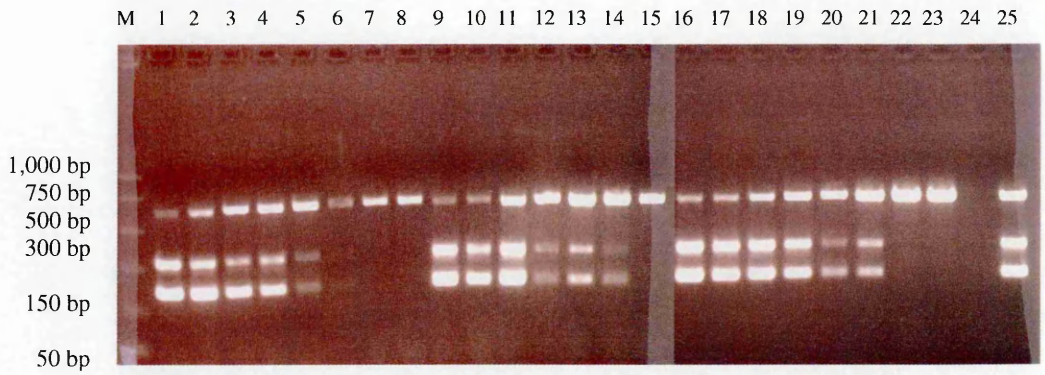

Lane M. PCR markers

Lanes 1 to 8: LP isolate (positive control)

1. $5x10^{8.0}$ IU/ml inoculum
2. $5x10^{7.5}$ IU/ml inoculum
3. $5x10^{7.0}$ IU/ml inoculum
4. $5x10^{6.5}$ IU/ml inoculum
5. $5x10^{6.0}$ IU/ml inoculum
6. $5x10^{5.5}$ IU/ml inoculum
7. $5x10^{5.0}$ IU/ml inoculum
8. Phosphate buffer pH 5.7

Lanes 9 to 15: NIBSC-04 CFI-treated #3

9. $1x10^{8.0}$ IU/ml inoculum
10. $1x10^{7.5}$ IU/ml inoculum
11. $1x10^{7.0}$ IU/ml inoculum
12. $1x10^{6.0}$ IU/ml inoculum
13. $1x10^{5.5}$ IU/ml inoculum
14. $1x10^{5.0}$ IU/ml inoculum
15. Phosphate buffer pH 5.7

Lanes 16 to 24: NIBSC-04 "time and temperature"

17. $3x10^{8.0}$ IU/ml inoculum
18. $3x10^{7.5}$ IU/ml inoculum
19. $3x10^{7.0}$ IU/ml inoculum
20. $3x10^{6.5}$ IU/ml inoculum
21. $3x10^{6.0}$ IU/ml inoculum
22. $3x10^{5.5}$ IU/ml inoculum
23. $3x10^{5.0}$ IU/ml inoculum
24. Phosphate buffer pH 5.7

Lanes 25 and 26: RT-PCR positive controls

25. RNAase-free water
26. $5x10^{7.0}$ IU/ml inoculum

- **NIBSC-05**

Figure A3.31: Infectivity assay results for NIBSC-05 "before" sample

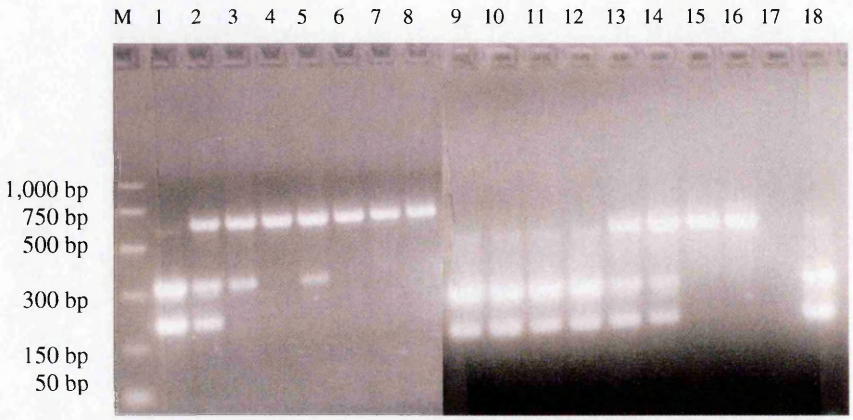

Lane M. PCR markers

Lanes 1 to 8: LP isolate (positive control)

1. $5x10^{8.0}$ IU/ml inoculum
2. $5x10^{7.5}$ IU/ml inoculum
3. $5x10^{7.0}$ IU/ml inoculum
4. $5x10^{6.5}$ IU/ml inoculum
5. $5x10^{6.0}$ IU/ml inoculum
6. $5x10^{5.5}$ IU/ml inoculum
7. $5x10^{5.0}$ IU/ml inoculum
8. Phosphate buffer pH 5.7

Lanes 9 to 16: NIBSC-05 "before"

9. $1x10^{10.0}$ IU/ml inoculum
10. $1x10^{9.5}$ IU/ml inoculum
11. $1x10^{9.0}$ IU/ml inoculum
12. $1x10^{8.5}$ IU/ml inoculum
13. $1x10^{8.0}$ IU/ml inoculum
14. $1x10^{7.5}$ IU/ml inoculum
15. $1x10^{7.0}$ IU/ml inoculum
16. Phosphate buffer pH 5.7

Lanes 17 and 18: RT-PCR positive controls

17. RNAase-free water
18. $1x10^{8.0}$ IU/ml inoculum

Figure A3.32: Infectivity assay results for NIBSC-05 CFI-treated #1 samples

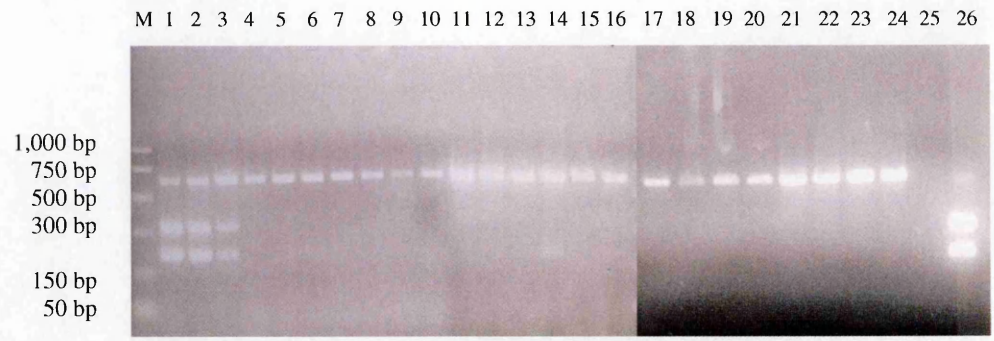

Lane M. PCR markers

Lanes 1 to 8: LP isolate (positive control)

1. $5x10^{8.0}$ IU/ml inoculum
2. $5x10^{7.5}$ IU/ml inoculum
3. $5x10^{7.0}$ IU/ml inoculum
4. $5x10^{6.5}$ IU/ml inoculum
5. $5x10^{6.0}$ IU/ml inoculum
6. $5x10^{5.5}$ IU/ml inoculum
7. $5x10^{5.0}$ IU/ml inoculum
8. Phosphate buffer pH 5.7

Lanes 9 to 16: NIBSC-05 CFI-treated #1

9. $1x10^{10.0}$ IU/ml inoculum
10. $1x10^{9.5}$ IU/ml inoculum
11. $1x10^{9.0}$ IU/ml inoculum
12. $1x10^{8.5}$ IU/ml inoculum
13. $1x10^{8.0}$ IU/ml inoculum
14. $1x10^{7.5}$ IU/ml inoculum
15. $1x10^{7.0}$ IU/ml inoculum
16. Phosphate buffer pH 5.7

Lanes 17 to 24: NIBSC-05 CFI-treated #1

17. $1x10^{10.0}$ IU/ml inoculum
18. $1x10^{9.5}$ IU/ml inoculum
19. $1x10^{9.0}$ IU/ml inoculum
20. $1x10^{8.5}$ IU/ml inoculum
21. $1x10^{8.0}$ IU/ml inoculum
22. $1x10^{7.5}$ IU/ml inoculum
23. $1x10^{7.0}$ IU/ml inoculum
24. Phosphate buffer pH 5.7

Lanes 25 and 26: RT-PCR positive controls

25. RNAase-free water
26. $5x10^{8.0}$ IU/ml inoculum

Figure A3.33: Infectivity assay results for NIBSC-05 CFI-treated #2 samples

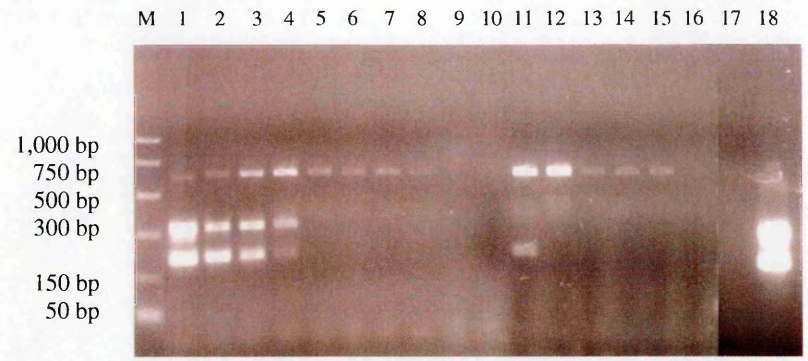

Lane M. PCR markers

Lanes 1 to 8: LP isolate (positive control)

1. $5x10^{8.0}$ IU/ml inoculum
2. $5x10^{7.5}$ IU/ml inoculum
3. $5x10^{7.0}$ IU/ml inoculum
4. $5x10^{6.5}$ IU/ml inoculum
5. $5x10^{6.0}$ IU/ml inoculum
6. $5x10^{5.5}$ IU/ml inoculum
7. $5x10^{5.0}$ IU/ml inoculum
8. Phosphate buffer pH 5.7

Lanes 9 to 16: NIBSC-05 CFI-treated #2

9. $3x10^{8.0}$ IU/ml inoculum
10. $3x10^{7.5}$ IU/ml inoculum
11. $3x10^{7.0}$ IU/ml inoculum
12. $3x10^{6.5}$ IU/ml inoculum
13. $3x10^{6.0}$ IU/ml inoculum
14. $3x10^{5.5}$ IU/ml inoculum
15. $3x10^{5.0}$ IU/ml inoculum
16. Phosphate buffer pH 5.7

Lanes 17 and 18: RT-PCR positive controls

17. RNAase-free water
18. $5x10^{8.0}$ IU/ml inoculum

Figure A3.34: Infectivity assay results for NIBSC-05 CFI-treated #3 samples

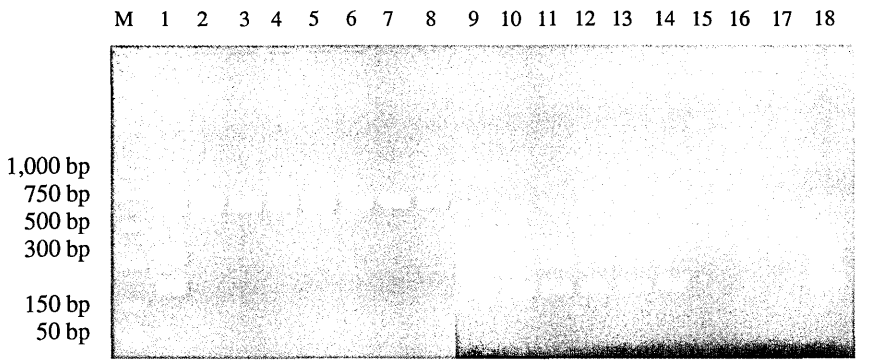

Lane M. PCR markers

Lanes 1 to 8: LP isolate (positive control)

1. $5x10^{7.0}$ IU/ml inoculum
2. $5x10^{6.5}$ IU/ml inoculum
3. $5x10^{6.0}$ IU/ml inoculum
4. $5x10^{5.5}$ IU/ml inoculum
5. $5x10^{5.0}$ IU/ml inoculum
6. $5x10^{4.5}$ IU/ml inoculum
7. $5x10^{4.0}$ IU/ml inoculum
8. Phosphate buffer pH 5.7

Lanes 9 to 16: NIBSC-05 CFI-treated #3

9. $3x10^{9.0}$ IU/ml inoculum
10. $3x10^{8.5}$ IU/ml inoculum
11. $3x10^{8.0}$ IU/ml inoculum
12. $3x10^{7.5}$ IU/ml inoculum
13. $3x10^{7.0}$ IU/ml inoculum
14. $3x10^{6.5}$ IU/ml inoculum
15. $3x10^{6.0}$ IU/ml inoculum
16. Phosphate buffer pH 5.7

Lanes 17 and 18: RT-PCR positive controls

17. RNAase-free water
18. $5x10^{8.0}$ IU/ml inoculum

Figure A3.35: Infectivity assay results for NIBSC-05 "time and temperature" sample

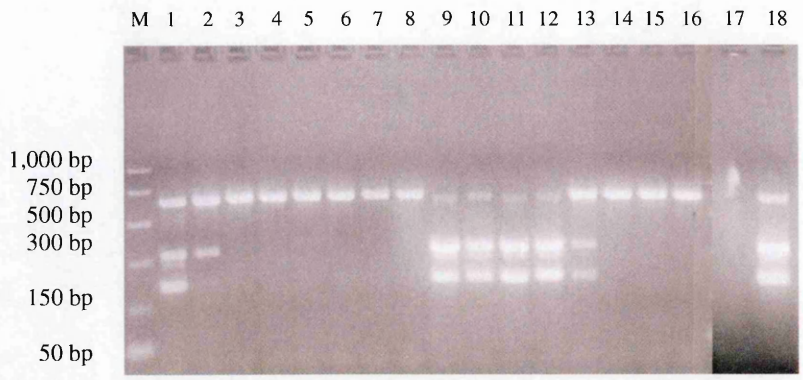

Lane M. PCR markers

Lanes 1 to 8: LP isolate (positive control)

1. $5x10^{7.0}$ IU/ml inoculum
2. $5x10^{6.5}$ IU/ml inoculum
3. $5x10^{6.0}$ IU/ml inoculum
4. $5x10^{5.5}$ IU/ml inoculum
5. $5x10^{5.0}$ IU/ml inoculum
6. $5x10^{4.5}$ IU/ml inoculum
7. $5x10^{4.0}$ IU/ml inoculum
8. Phosphate buffer pH 5.7

Lanes 9 to 16: NIBSC-05 "time and temperature"

9. $5x10^{9.0}$ IU/ml inoculum
10. $5x10^{8.5}$ IU/ml inoculum
11. $5x10^{8.0}$ IU/ml inoculum
12. $5x10^{7.5}$ IU/ml inoculum
13. $5x10^{7.0}$ IU/ml inoculum
14. $5x10^{6.5}$ IU/ml inoculum
15. $5x10^{6.0}$ IU/ml inoculum
16. Phosphate buffer pH 5.7

Lanes 17 and 18: RT-PCR positive controls

17. RNAase-free water
18. $5x10^{8.0}$ IU/ml inoculum

- **NIBSC-06**

Figure A3.36: Infectivity assay results for NIBSC-06 "before" sample

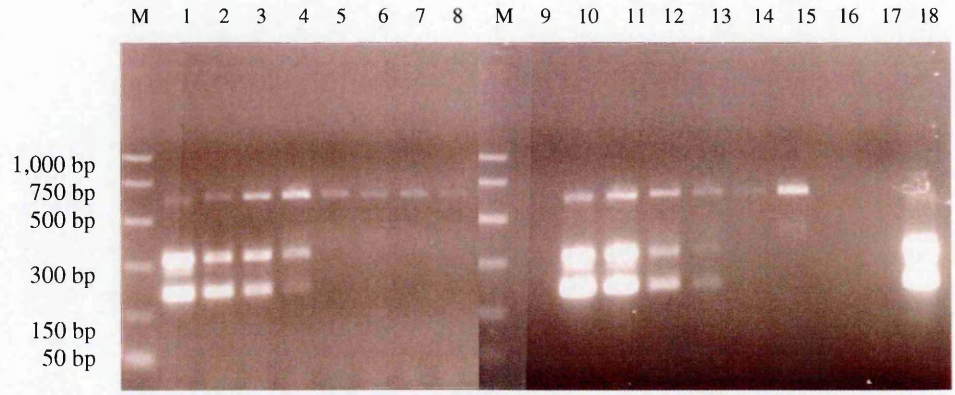

Lane M. PCR markers

Lanes 1 to 8: LP isolate (positive control)

1. $5x10^{8.0}$ IU/ml inoculum
2. $5x10^{7.5}$ IU/ml inoculum
3. $5x10^{7.0}$ IU/ml inoculum
4. $5x10^{6.5}$ IU/ml inoculum
5. $5x10^{6.0}$ IU/ml inoculum
6. $5x10^{5.5}$ IU/ml inoculum
7. $5x10^{5.0}$ IU/ml inoculum
8. Phosphate buffer pH 5.7

Lanes 9 to 16: NIBSC-06 "before"

9. $2x10^{8.0}$ IU/ml inoculum
10. $2x10^{7.5}$ IU/ml inoculum
11. $2x10^{7.0}$ IU/ml inoculum
12. $2x10^{6.5}$ IU/ml inoculum
13. $2x10^{6.0}$ IU/ml inoculum
14. $2x10^{5.5}$ IU/ml inoculum
15. $2x10^{5.0}$ IU/ml inoculum
16. Phosphate buffer pH 5.7

Lanes 17 and 18: RT-PCR positive controls

17. RNAase-free water
18. $5x10^{8.0}$ IU/ml inoculum

Figure A3.37: Infectivity assay results for NIBSC-06 CFI-treated #1 samples

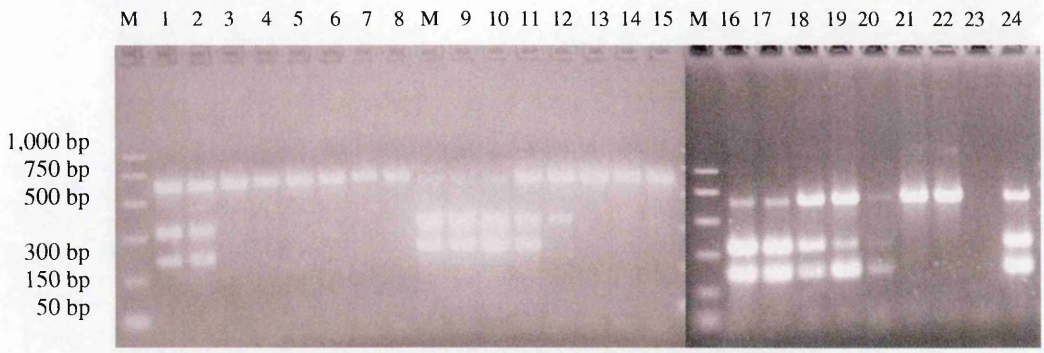

Lane M. PCR markers

Lanes 1 to 8: LP isolate (positive control)

1. $5x10^{7.0}$ IU/ml inoculum
2. $5x10^{6.5}$ IU/ml inoculum
3. $5x10^{6.0}$ IU/ml inoculum
4. $5x10^{5.5}$ IU/ml inoculum
5. $5x10^{5.0}$ IU/ml inoculum
6. $5x10^{4.5}$ IU/ml inoculum
7. $5x10^{4.0}$ IU/ml inoculum
8. Phosphate buffer pH 5.7

Lanes 9 to 16: NIBSC-06 CFI-treated #1

9. $2x10^{9.0}$ IU/ml inoculum
10. $2x10^{8.5}$ IU/ml inoculum
11. $2x10^{8.0}$ IU/ml inoculum
12. $2x10^{7.5}$ IU/ml inoculum
13. $2x10^{7.0}$ IU/ml inoculum
14. $2x10^{6.5}$ IU/ml inoculum
15. $2x10^{6.0}$ IU/ml inoculum
16. Phosphate buffer pH 5.7

Lanes 17 to 24: NIBSC-06 CFI-treated #1

17. $2x10^{9.0}$ IU/ml inoculum
18. $2x10^{8.5}$ IU/ml inoculum
19. $2x10^{8.0}$ IU/ml inoculum
20. $2x10^{7.5}$ IU/ml inoculum
21. $2x10^{7.0}$ IU/ml inoculum
22. $2x10^{6.5}$ IU/ml inoculum
23. $2x10^{6.0}$ IU/ml inoculum
24. Phosphate buffer pH 5.7

Lanes 25 and 26: RT-PCR positive controls

25. RNAase-free water
26. $5x10^{7.0}$ IU/ml inoculum

Figure A3.38: Infectivity assay results for NIBSC-06 CFI-treated #2 samples

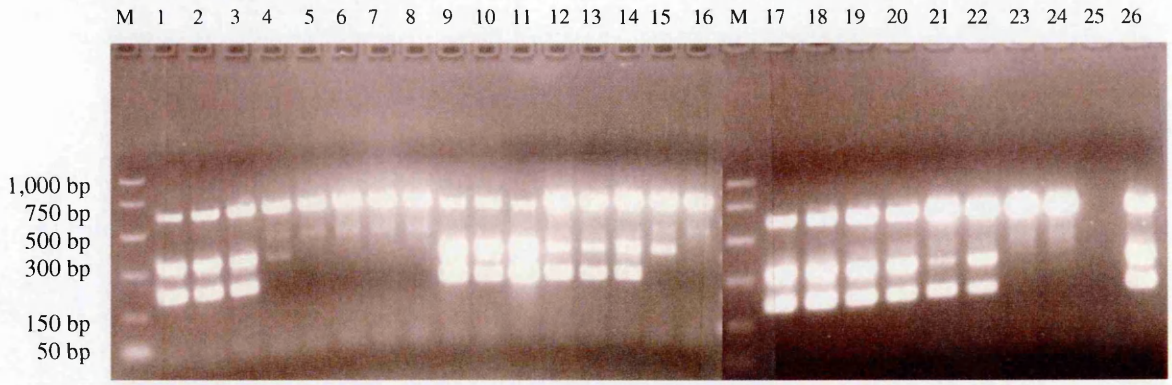

Lane M. PCR markers

Lanes 1 to 8: LP isolate (positive control)

1. $5x10^{8.0}$ IU/ml inoculum
2. $5x10^{7.5}$ IU/ml inoculum
3. $5x10^{7.0}$ IU/ml inoculum
4. $5x10^{6.5}$ IU/ml inoculum
5. $5x10^{6.0}$ IU/ml inoculum
6. $5x10^{5.5}$ IU/ml inoculum
7. $5x10^{5.0}$ IU/ml inoculum
8. Phosphate buffer pH 5.7

Lanes 9 to 16: NIBSC-06 CFI-treated #2

9. $2x10^{8.0}$ IU/ml inoculum
10. $2x10^{7.5}$ IU/ml inoculum
11. $2x10^{7.0}$ IU/ml inoculum
12. $2x10^{6.5}$ IU/ml inoculum
13. $2x10^{6.0}$ IU/ml inoculum
14. $2x10^{5.5}$ IU/ml inoculum
15. $2x10^{5.0}$ IU/ml inoculum
16. Phosphate buffer pH 5.7

Lanes 17 to 24: NIBSC-06 CFI-treated #2

17. $8x10^{7.0}$ IU/ml inoculum
18. $8x10^{6.5}$ IU/ml inoculum
19. $8x10^{6.0}$ IU/ml inoculum
20. $8x10^{5.5}$ IU/ml inoculum
21. $8x10^{5.0}$ IU/ml inoculum
22. $8x10^{4.5}$ IU/ml inoculum
23. $8x10^{4.0}$ IU/ml inoculum
24. Phosphate buffer pH 5.7

Lanes 25 and 26: RT-PCR positive controls

25. RNAase-free water
26. $5x10^{8.0}$ IU/ml inoculum

Figure A3.39: Infectivity assay results for NIBSC-06 CFI-treated "time and temperature" sample

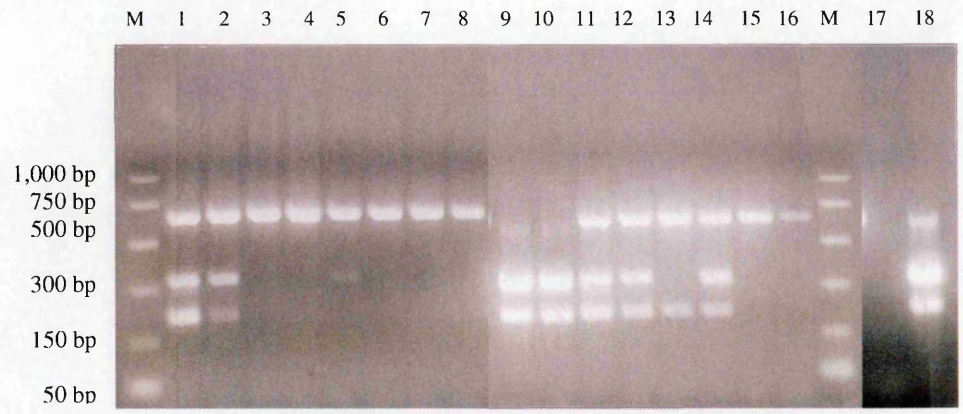

Lane M. PCR markers

Lanes 1 to 8: LP isolate (positive control)

1. $5x10^{7.0}$ IU/ml inoculum
2. $5x10^{6.5}$ IU/ml inoculum
3. $5x10^{6.0}$ IU/ml inoculum
4. $5x10^{5.5}$ IU/ml inoculum
5. $5x10^{5.0}$ IU/ml inoculum
6. $5x10^{4.5}$ IU/ml inoculum
7. $5x10^{4.0}$ IU/ml inoculum
8. Phosphate buffer pH 5.7

Lanes 9 to 16: NIBSC-06 "time and temperature"

9. $2x10^{9.0}$ IU/ml inoculum
10. $2x10^{8.5}$ IU/ml inoculum
11. $2x10^{8.0}$ IU/ml inoculum
12. $2x10^{7.5}$ IU/ml inoculum
13. $2x10^{7.0}$ IU/ml inoculum
14. $2x10^{6.5}$ IU/ml inoculum
15. $2x10^{6.0}$ IU/ml inoculum
16. Phosphate buffer pH 5.7

Lanes 17 and 18: RT-PCR positive controls

17. RNAase-free water
18. $5x10^{8.0}$ IU/ml inoculum

4. Vitex study

Figure A3.40: Infectivity assay results for Vitex TS3A and TS6A samples

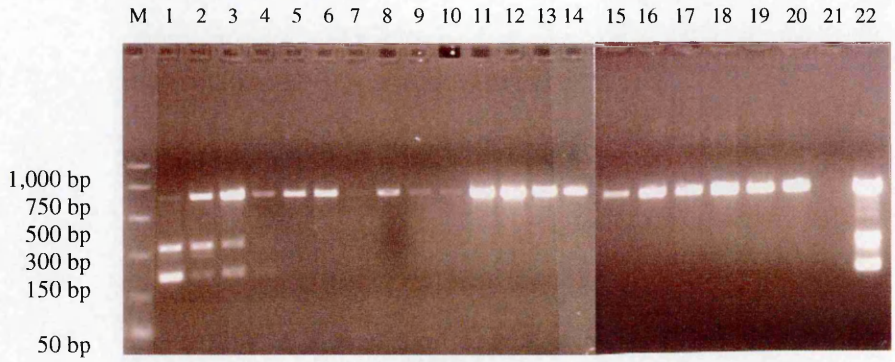

Lane M. PCR markers

Lanes 1 to 8: LP isolate (positive control)

1. $5x10^{8.0}$ IU/ml inoculum
2. $5x10^{7.5}$ IU/ml inoculum
3. $5x10^{7.0}$ IU/ml inoculum
4. $5x10^{6.5}$ IU/ml inoculum
5. $5x10^{6.0}$ IU/ml inoculum
6. $5x10^{5.5}$ IU/ml inoculum
7. $5x10^{5.0}$ IU/ml inoculum
8. Phosphate buffer pH 5.7

Lanes 9 to 14: Vitex TS3A sample

9. $2x10^{7.0}$ IU/ml inoculum
10. $2x10^{6.5}$ IU/ml inoculum
11. $2x10^{6.0}$ IU/ml inoculum
12. $2x10^{5.5}$ IU/ml inoculum
13. $2x10^{5.5}$ IU/ml inoculum
14. Phosphate buffer pH 5.7

Lanes 15 to 20: Vitex TS6A sample

15. $3x10^{6.0}$ IU/ml inoculum
16. $3x10^{5.5}$ IU/ml inoculum
17. $3x10^{5.0}$ IU/ml inoculum
18. $3x10^{4.5}$ IU/ml inoculum
19. $3x10^{4.0}$ IU/ml inoculum
20. Phosphate buffer pH 5.7

Lanes 21 and 22: RT-PCR positive controls

21. $5x10^{8.0}$ IU/ml inoculum
22. RNAase-free water

Figure A3.41: Infectivity assay results for Vitex TS18A, TS22A and PC0A samples

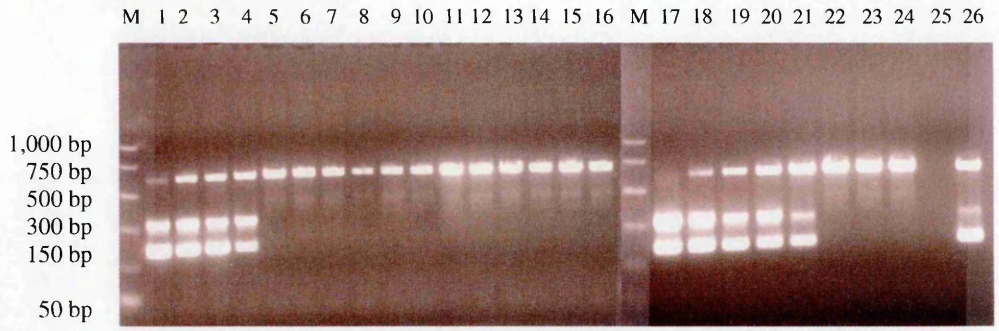

Lane M. PCR markers

Lanes 1 to 8: LP isolate (positive control)

1. $5x10^{8.0}$ IU/ml inoculum
2. $5x10^{7.5}$ IU/ml inoculum
3. $5x10^{7.0}$ IU/ml inoculum
4. $5x10^{6.5}$ IU/ml inoculum
5. $5x10^{6.0}$ IU/ml inoculum
6. $5x10^{5.5}$ IU/ml inoculum
7. $5x10^{5.0}$ IU/ml inoculum
8. Phosphate buffer pH 5.7

Lanes 9 to 12: Vitex TS18A sample

9. $3x10^{4.0}$ IU/ml inoculum
10. $3x10^{3.5}$ IU/ml inoculum
11. $3x10^{3.0}$ IU/ml inoculum
12. Phosphate buffer pH 5.7

Lanes 13 to 16: Vitex TS22A sample

13. $4x10^{3.0}$ IU/ml inoculum
14. $4x10^{2.5}$ IU/ml inoculum
15. $4x10^{2.5}$ IU/ml inoculum
16. Phosphate buffer pH 5.7

Lanes 17 to 24: Vitex PC0A sample

17. $1x10^{8.0}$ IU/ml inoculum
18. $1x10^{7.5}$ IU/ml inoculum
19. $1x10^{7.0}$ IU/ml inoculum
20. $1x10^{6.5}$ IU/ml inoculum
21. $1x10^{6.0}$ IU/ml inoculum
22. $1x10^{5.5}$ IU/ml inoculum
23. $1x10^{5.0}$ IU/ml inoculum
24. Phosphate buffer pH 5.7

Lanes 25 and 26: RT-PCR positive controls

25. $5x10^{7.0}$ IU/ml inoculum
26. RNAase-free water

Figure A3.42: Infectivity assay results for Vitex PC22A and TS3B samples

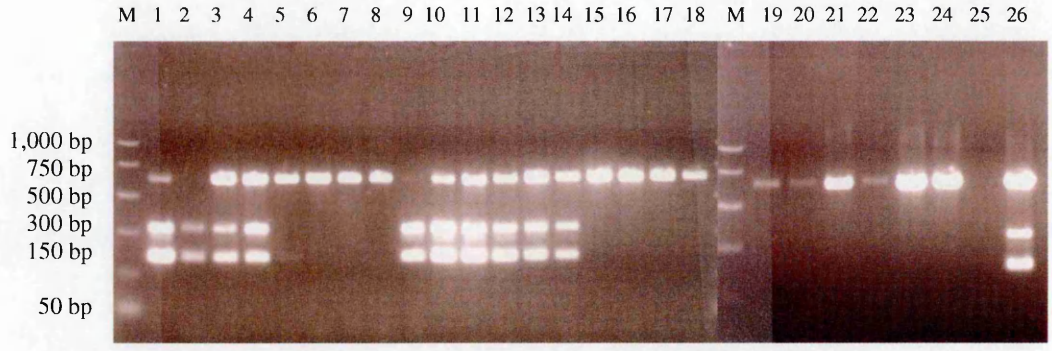

Lane M. PCR markers

Lanes 1 to 8: LP isolate (positive control)

1. $5x10^{8.0}$ IU/ml inoculum
2. $5x10^{7.5}$ IU/ml inoculum
3. $5x10^{7.0}$ IU/ml inoculum
4. $5x10^{6.5}$ IU/ml inoculum
5. $5x10^{6.0}$ IU/ml inoculum
6. $5x10^{5.5}$ IU/ml inoculum
7. $5x10^{5.0}$ IU/ml inoculum
8. Phosphate buffer pH 5.7

Lanes 9 to 18: Vitex PC22A sample

9. $1x10^{9.0}$ IU/ml inoculum
10. $1x10^{8.5}$ IU/ml inoculum
11. $1x10^{8.0}$ IU/ml inoculum
12. $1x10^{7.5}$ IU/ml inoculum
13. $1x10^{7.0}$ IU/ml inoculum
14. $1x10^{6.5}$ IU/ml inoculum
15. $1x10^{6.0}$ IU/ml inoculum
16. $1x10^{5.5}$ IU/ml inoculum
17. $1x10^{5.0}$ IU/ml inoculum
18. Phosphate buffer pH 5.7

Lanes 19 to 24: Vitex TS3B sample

19. $1x10^{5.0}$ IU/ml inoculum
20. $1x10^{4.5}$ IU/ml inoculum
21. $1x10^{4.0}$ IU/ml inoculum
22. $1x10^{3.5}$ IU/ml inoculum
23. $1x10^{3.0}$ IU/ml inoculum
24. Phosphate buffer pH 5.7

Lanes 25 and 26: RT-PCR positive controls

25. $5x10^{8.0}$ IU/ml inoculum
26. RNAase-free water

Figure A3.43: Infectivity assay results for Vitex TS6B, TS18B and TS22B samples

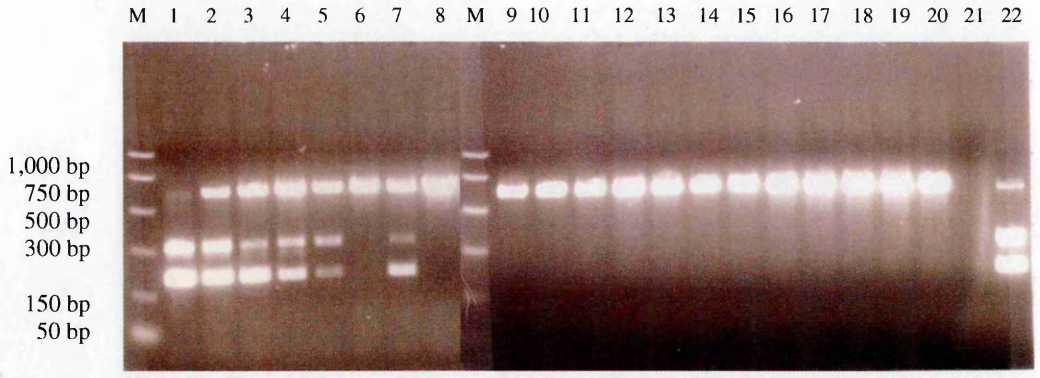

Lane M. PCR markers

Lanes 1 to 8: LP isolate (positive control)

1. $5x10^{8.0}$ IU/ml inoculum
2. $5x10^{7.5}$ IU/ml inoculum
3. $5x10^{7.0}$ IU/ml inoculum
4. $5x10^{6.5}$ IU/ml inoculum
5. $5x10^{6.0}$ IU/ml inoculum
6. $5x10^{5.5}$ IU/ml inoculum
7. $5x10^{5.0}$ IU/ml inoculum
8. Phosphate buffer pH 5.7

Lanes 9 to 12: Vitex TS6B sample

9. $1x10^{4.0}$ IU/ml inoculum
10. $1x10^{3.5}$ IU/ml inoculum
11. $1x10^{3.0}$ IU/ml inoculum
12. Phosphate buffer pH 5.7

Lanes 13 to 16: Vitex TS18B sample

13. neat inoculum
14. $10^{-0.5}$ dilution inoculum
15. $10^{-1.0}$ dilution inoculum
16. Phosphate buffer pH 5.7

Lanes 17 to 20: Vitex TS3B sample

17. neat inoculum
18. $10^{-0.5}$ dilution inoculum
19. $10^{-1.0}$ dilution inoculum
20. Phosphate buffer pH 5.7

Lanes 21 and 22: RT-PCR positive controls

25. $5x10^{8.0}$ IU/ml inoculum
26. RNAase-free water

Figure A3.44: Infectivity assay results for Vitex PC0B sample

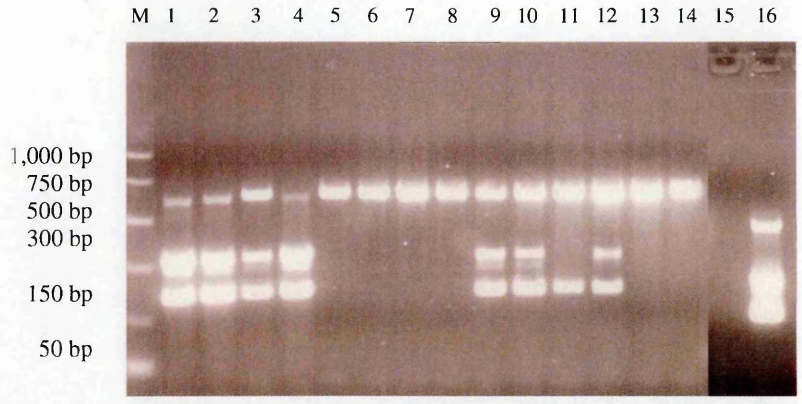

Lane M. PCR markers

Lanes 1 to 8: LP isolate (positive control)

1. $5x10^{8.0}$ IU/ml inoculum
2. $5x10^{7.5}$ IU/ml inoculum
3. $5x10^{7.0}$ IU/ml inoculum
4. $5x10^{6.5}$ IU/ml inoculum
5. $5x10^{6.0}$ IU/ml inoculum
6. $5x10^{5.5}$ IU/ml inoculum
7. $5x10^{5.0}$ IU/ml inoculum
8. Phosphate buffer pH 5.7

Lanes 9 to 14: Vitex PC0B sample

9. $3x10^{7.0}$ IU/ml inoculum
10. $3x10^{6.5}$ IU/ml inoculum
11. $3x10^{6.0}$ IU/ml inoculum
12. $3x10^{5.5}$ IU/ml inoculum
13. $3x10^{5.5}$ IU/ml inoculum
14. Phosphate buffer pH 5.7

Lanes 15 to 20: RT-PCR positive controls

15. $5x10^{8.0}$ IU/ml inoculum
16. RNAase-free water

Figure A3.45: Infectivity assay results for Vitex PC22B and B19 1:20 dilution samples

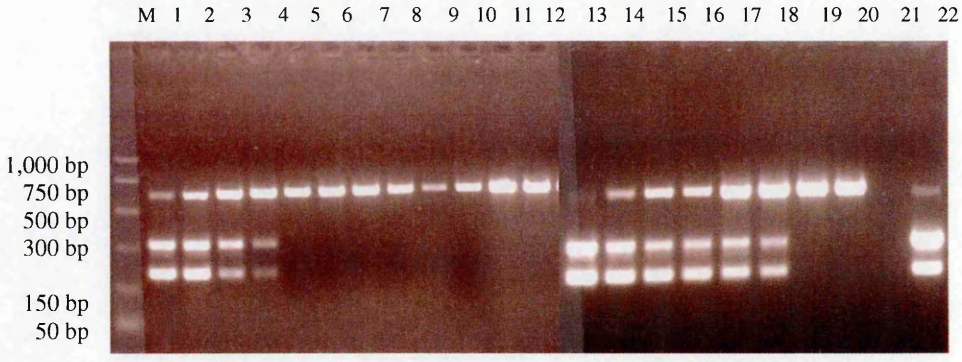

Lane M. PCR markers

Lanes 1 to 8: LP isolate (positive control)

1. $5x10^{8.0}$ IU/ml inoculum
2. $5x10^{7.5}$ IU/ml inoculum
3. $5x10^{7.0}$ IU/ml inoculum
4. $5x10^{6.5}$ IU/ml inoculum
5. $5x10^{6.0}$ IU/ml inoculum
6. $5x10^{5.5}$ IU/ml inoculum
7. $5x10^{5.0}$ IU/ml inoculum
8. Phosphate buffer pH 5.7

Lanes 9 to 12: Vitex PC22B sample

9. $3x10^{7.0}$ IU/ml inoculum
10. $3x10^{6.5}$ IU/ml inoculum
11. $3x10^{6.0}$ IU/ml inoculum
12. Phosphate buffer pH 5.7

Lanes 13 to 20: B19 1:20 dilution

13. $4x10^{8.0}$ IU/ml inoculum
14. $4x10^{7.5}$ IU/ml inoculum
15. $4x10^{7.0}$ IU/ml inoculum
16. $4x10^{6.5}$ IU/ml inoculum
17. $4x10^{6.0}$ IU/ml inoculum
18. $4x10^{5.5}$ IU/ml inoculum
19. $4x10^{5.0}$ IU/ml inoculum
20. Phosphate buffer pH 5.7

Lanes 21 and 22: RT-PCR positive controls

21. $5x10^{8.0}$ IU/ml inoculum
22. RNAase-free water

5. Cerus study

Figure A3.46: Infectivity assay results for Cerus untreated sample

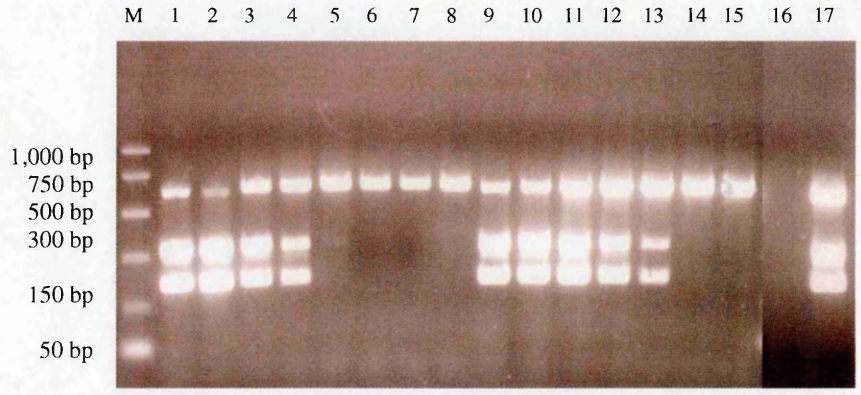

Lane M. PCR markers

Lanes 1 to 8: LP isolate (positive control)

1. $5x10^{8.0}$ IU/ml inoculum
2. $5x10^{7.5}$ IU/ml inoculum
3. $5x10^{7.0}$ IU/ml inoculum
4. $5x10^{6.5}$ IU/ml inoculum
5. $5x10^{6.0}$ IU/ml inoculum
6. $5x10^{5.5}$ IU/ml inoculum
7. $5x10^{5.0}$ IU/ml inoculum
8. Phosphate buffer pH 5.7

Lanes 9 to 15: Cerus untreated

9. $8x10^{6.0}$ IU/ml inoculum
10. $8x10^{5.5}$ IU/ml inoculum
11. $8x10^{5.0}$ IU/ml inoculum
12. $8x10^{4.5}$ IU/ml inoculum
13. $8x10^{4.0}$ IU/ml inoculum
14. $8x10^{3.5}$ IU/ml inoculum
15. Phosphate buffer pH 5.7

Lanes 16 and 17: RT-PCR positive controls

16. $5x10^{8.0}$ IU/ml inoculum
17. RNAase-free water

Figure A3.47: Infectivity assay results for Cerus treated 3J sample

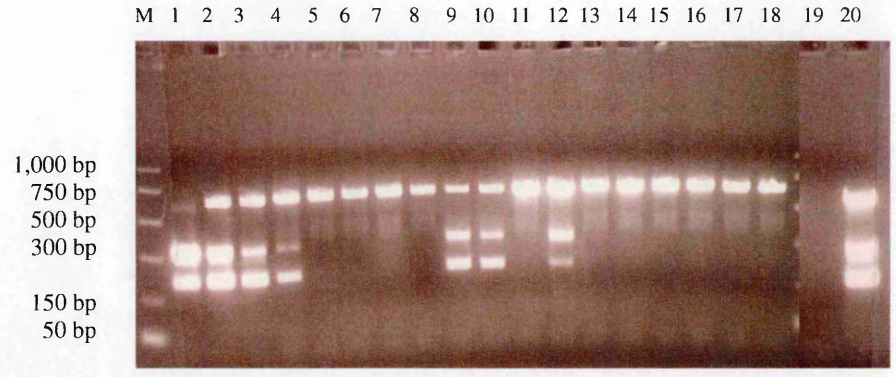

Lane M. PCR markers

Lanes 1 to 8: LP isolate (positive control)

1. $5x10^{8.0}$ IU/ml inoculum
2. $5x10^{7.5}$ IU/ml inoculum
3. $5x10^{7.0}$ IU/ml inoculum
4. $5x10^{6.5}$ IU/ml inoculum
5. $5x10^{6.0}$ IU/ml inoculum
6. $5x10^{5.5}$ IU/ml inoculum
7. $5x10^{5.0}$ IU/ml inoculum
8. Phosphate buffer pH 5.7

Lanes 9 to 18: Cerus treated 3J

9. $2x10^{9.0}$ IU/ml inoculum
10. $2x10^{8.5}$ IU/ml inoculum
11. $2x10^{8.0}$ IU/ml inoculum
12. $2x10^{7.5}$ IU/ml inoculum
13. $2x10^{7.0}$ IU/ml inoculum
14. $2x10^{6.5}$ IU/ml inoculum
15. $2x10^{6.0}$ IU/ml inoculum
16. $2x10^{5.5}$ IU/ml inoculum
17. $2x10^{5.0}$ IU/ml inoculum
18. Phosphate buffer pH 5.7

Lanes 19 and 20: RT-PCR positive controls

19. $5x10^{8.0}$ IU/ml inoculum
20. RNAase-free water